



UNIVERSIDADE DE SÃO PAULO

FACULDADE DE CIÊNCIAS FARMACÊUTICAS DE RIBEIRÃO PRETO

**Development of new selective synthetic methods en route to
privileged scaffolds of pharmaceutical relevance**

**Desenvolvimento de novos métodos sintéticos seletivos visando
estruturas privilegiadas de relevância farmacêutica**

Thiago dos Santos

**Ribeirão Preto
2022**

UNIVERSIDADE DE SÃO PAULO
FACULDADE DE CIÊNCIAS FARMACÊUTICAS DE RIBEIRÃO PRETO

THIAGO DOS SANTOS

**Development of new selective synthetic methods en route to
privileged scaffolds of pharmaceutical relevance**
**Desenvolvimento de novos métodos sintéticos seletivos visando
estruturas privilegiadas de relevância farmacêutica**

Doctoral thesis presented to the Graduate Program of School of Pharmaceutical Sciences of Ribeirão Preto/USP for the degree of Doctor in Sciences.

Concentration Area: Natural and synthetic products.

Supervisor: Prof. Dr. Giuliano Cesar Clososki

Co-supervisor: Prof. Dr. Till Opatz

Versão corrigida da Tese de Doutorado apresentada ao Programa de Pós-Graduação em Ciências Farmacêuticas em 13/01/2022. A versão original encontra-se disponível na Faculdade de Ciências Farmacêuticas de Ribeirão Preto/USP.

Ribeirão Preto
2022

I AUTHORIZE THE REPRODUCTION AND TOTAL OR PARTIAL DISCLOSURE OF THIS WORK, BY ANY CONVENTIONAL OR ELECTRONIC MEANS.

Thiago dos Santos

Development of new selective synthetic methods en route do privileged scaffolds of pharmaceutical relevance. Ribeirão Preto, 2021.

262 p.; 30 cm.

Doctoral thesis presented to the Graduate Program of School of Pharmaceutical Sciences of Ribeirão Preto/USP for the degree of Doctor in Sciences. Concentration Area: Natural and synthetic products.

Supervisor: Prof. Dr. Giuliano Cesar Clososki.

Co-supervisor: Prof. Dr. Till Opatz.

1. Nitriles. 2. Metalation. 3. Building blocks. 4. Glucose. 5. 2,3-dihydroquinazolin-4(1*H*)-ones.

APPROVAL PAGE

Thiago dos Santos

Development of new selective synthetic methods en route to privileged scaffolds of pharmaceutical relevance.

Doctoral thesis presented to the Graduate Program of School of Pharmaceutical Sciences of Ribeirão Preto/USP for the degree of Doctor in Sciences.

Concentration Area: Natural and synthetic products.

Supervisor: Prof. Dr. Giuliano Cesar Clososki.

Co-supervisor: Prof. Dr. Till Opatz.

Approved on:13/01/2022

Examiners

Prof. Dr. _____

Institution: _____ Signature:_____

Prof. Dr. _____

Institution: _____ Signature:_____

Prof. Dr. _____

Institution: _____ Signature:_____

Prof. Dr. _____

Institution: _____ Signature:_____

ACKNOWLEDGMENTS

I am grateful for all the guidance, opportunities, motivational discussions, professional counseling, and support from my supervisor Prof. Dr. Giuliano Cesar Clososki, and co-supervisor Prof. Dr. Till Opatz.

I would like to thank CAPES (Print program - nº 88887.368237/2019-00 and financial code 001) for financing my six-month stay in Mainz (Johannes Gutenberg-Universität Mainz, JGU) in the group of Prof. Dr. Till Opatz, CNPq (fellowship nº 140137/2018-1) for the financial support during my doctorate, and FAPESP.

I thank all the laboratory members I had the chance to meet in Brazil and Germany for the patience, fruitful project discussions, counseling in difficult moments, friendship, great social activities outside the work environment, and the partnership in diverse projects.

I greatly acknowledge the help with HRMS, GC-MS, and NMR analyses from USP and JGU technicians or members including José Carlos Tomaz, Dr. Rodrigo Moreira da Silva, Dr. Norberto Peporine Lopes, Izabel Cristina Casanova Turatti, Dr. Roberto Gomes de Souza Berlinck, Dra. Fabiana Tessari Rodrigues Martinelli, M.S. Vinicius Palaretti, Dr. Johannes C. Liermann (Mainz) and Dr. Christopher Kampf (Mainz).

A very special thanks to my beloved parents and closest friends for their unconditional support throughout my Ph.D. journey.

This study was financed in part by the Coordenação de Aperfeiçoamento de Pessoal de Nível Superior – Brasil (CAPES) – Finance Code 001.

RESUMO

DOS SANTOS, T. **Desenvolvimento de novos métodos sintéticos seletivos visando estruturas privilegiadas de relevância farmacêutica**. 2021. 262f. Tese (Doutorado). Faculdade de Ciências Farmacêuticas de Ribeirão Preto – Universidade de São Paulo, Ribeirão Preto, 2021.

Desde os pioneiros trabalhos de Gilman e Bebb, e Wittig e Furhmann seguidos por importantes contribuições incluindo Snieckus, a metalação *orto*-dirigida (DoM) tem sido empregada na funcionalização de diversos sistemas. Particularmente, os amidetos de 2,2,6,6-tetrametilpiperidil de Knochel e colaboradores apresentam excelente solubilidade em THF e tolerância a grupos funcionais além de boa estabilidade térmica. O grupo ciano é de grande interesse em DoMs seguido do fluoro como destacado no trabalho de Schlosser. Considerando a viabilidade do emprego das bases de Knochel em DoMs e a potencial aplicação de nitrilas fluoradas como blocos construtores, o primeiro projeto compreendeu a metalação regioseletiva e funcionalização de diversas nitrilas fluoradas e posterior aplicação no preparo de 4-aminoquinazolininas. Cerca de 47 nitrilas funcionalizadas (45-90%) foram preparadas via $\text{TMPMgCl}\cdot\text{LiCl}$ ou $(\text{TMP})_2\text{Zn}\cdot 2\text{MgCl}_2\cdot 2\text{LiCl}$ com a exploração de novos e insuficientemente estudados sítios de metalação. Adicionalmente, uma estratégia de difuncionalização foi possível e os blocos construtores funcionalizados aplicados na síntese de relevantes heterociclos. A 2,3-diidroquinazolin-4(1*H*)-ona (DHQ) é uma estrutura privilegiada e presente em várias moléculas bioativas incluindo fármacos e candidatos a fármacos. A glicose, como um recurso renovável, pode ser facilmente obtida de biomassa lignocelulósica e empregada em processos redutivos sob condições alcalinas. O único método direto disponível para a obtenção de DHQs a partir de 2-nitrobenzonitrila demanda excesso de ácido borônico e cobre como catalizador. Assim, o segundo projeto visou o uso de glicose como um agente redutor sustentável em solução aquosa de carbonato de potássio para a síntese de DHQs derivadas da 2-nitrobenzonitrila de maneira *one-pot*. Um protocolo *one-pot* baseado em ciano-hidratação, nitro redução, formação de imina e ciclização empregando glicose em meio aquoso alcalino foi estabelecido fornecendo DHQs em rendimentos de 18-90%. A competição entre a função aldeído da glicose com o carbonílico adicionado não foi verificada e as DHQs podem ser convertidas em suas respectivas quinazolinonas encontrando mais ampla aplicação em química medicinal. Adicionalmente, um estudo de reposicionamento do fármaco Tenofovir foi efetuado.

Palavras-chave: Regioseletividade; Metalação; TMP-bases; Nitrilas; 4-aminoquinazolininas; Glicose; 2,3-diidroquinazolin-4(1*H*)-ona; Eco-friendly; Química Verde.



ABSTRACT

DOS SANTOS, T. **Development of new selective synthetic methods en route to privileged scaffolds of pharmaceutical relevance.** 2021. 262p. Thesis (Doctoral). Faculdade de Ciências Farmacêuticas de Ribeirão Preto – Universidade de São Paulo, Ribeirão Preto, 2021.

Since the pioneering works of Gilman and Bebb, and Wittig and Furhmann accompanied by important contributions including Snieckus, directed *ortho*-metalation reactions (DoM) have found great application in the functionalization of diverse systems. Particularly, the 2,2,6,6-tetramethylpiperidyl bases by Knochel and co-workers show excellent solubility in THF, functional group tolerance, and great stability at room and higher temperatures. The cyano group is of great interest in DoMs followed by fluoro as highlighted by the work of Schlosser. Therefore, considering the feasibility of Knochel bases in DoMs and the potential application of fluorinated nitriles as building blocks, the first project comprised the regioselective metalation-functionalization of diverse fluorinated nitriles and their application in the synthesis of 4-aminoquinazolines. About 47 diverse functionalized nitriles (45-90%) with the exploration of new and scarcely investigated metalation sites were prepared by metalation with $\text{TMPMgCl}\cdot\text{LiCl}$ or $(\text{TMP})_2\text{Zn}\cdot 2\text{MgCl}_2\cdot 2\text{LiCl}$. Besides, a difunctionalization strategy was possible and the building blocks were applied to construct relevant heterocycles. The 2,3-dihydroquinazolin-4(1*H*)-one (DHQ) is a privileged scaffold in a multitude of biologically active molecules including marketed pharmaceuticals and potential drug candidates. Glucose, as a renewable source, can be easily obtained from lignocellulosic biomass and applied in reduction processes under alkaline conditions. The only available method to directly access DHQs from 2-nitrobenzotrile requires an excess of diboronic acid and copper as a catalyst in a water/methanol mixture. Thus, the second project envisioned the use of glucose as an eco-friendly reductant in an aqueous solution of potassium carbonate for the synthesis of DHQs from 2-nitrobenzotrile in a one-pot fashion. A one-pot protocol based on nitrile hydration, nitro-reduction, imine formation, and cyclization with glucose in alkaline water was successfully established affording DHQs in yields 18-90%. No competition of the aldehyde from glucose with the externally added carbonyl compound was verified, and the synthesized DHQs in this work can be further converted to the corresponding quinazolinones finding even wider application in Medicinal Chemistry. Additionally, a study on the repositioning of the drug Tenofovir was performed.

Keywords: Regioselectivity; Metalation; TMP-bases; Nitriles; 4-aminoquinazoline; Glucose; 2,3-dihydroquinazolin-4(1*H*)-one; Eco-friendly; Green Chemistry.



LIST OF FIGURES

Figure 1. Some DMGs explored in the literature.....	01
Figure 2. Developed TMP-bases by Knochel and co-workers.....	03
Figure 3. Some bioactive molecules bearing the cyano group	04
Figure 4. Metalation rates (2,4-difluorophenyl)- 65 , (3,4-difluorophenyl)- 66 , and (3,5-difluorophenyl)trimethylsilane 67	11
Figure 5. Some bioactive 4-aminoquinazolines	12
Figure 6. Some bioactive molecules containing the DHQ core.....	17
Figure 7. Chromatogram for the selective metalation and functionalization of 123b	23
Figure 8. Chromatogram for the selective metalation and functionalization of 123d	28
Figure 9. Expanded ¹ H NMR spectrum of 120a	46
Figure 10. Expanded ¹³ C NMR spectrum of 120a	46
Figure 11. Observation of formate from glucose decomposition for the reaction performed in D ₂ O (Optimized condition, Table 16, entry 6, no benzaldehyde – ¹ H NMR, 400 MHz).....	48
Figure 12. Recorded mass spectra and chromatogram for the optimized conditions (Table 16, entry 6).	50
Figure 13. Docked TDF conformation (triphosphate form) in RdRp (PDB id = 7BV2, 2.50 Å).....	53
Figure 14. Docked TDF conformation (triphosphate form) in RdRp (PDB id = 7BV2, 2.50 Å) in the absence of the Mg atoms.....	53
Figure 15. Mass spectrum of 136	102

LIST OF SCHEMES

Scheme 1. The regioselective magnesiation of methyl benzoate with (TMP) ₂ Mg.....	02
Scheme 2. Employment of TMPMgCl·LiCl in the synthesis of Mepanipyrim	03
Scheme 3. Directed functionalization of cyano-substituted furans and thiophenes plus p <i>K</i> _a values.....	05
Scheme 4. Regioselective functionalization of cyano-substituted indolizines 36 and 39 and p <i>K</i> _a values	06
Scheme 5. Metalation and functionalization of benzonitrile	06
Scheme 6. Regioselective lithiation of pyridines 44a-b and their functionalization	07
Scheme 7. The α-arylation of benzylic nitriles 46a-c with TMPZnCl·LiCl	08
Scheme 8. The regiochemically exhaustive functionalization of 3-fluorophenol by Schlosser and co-workers	09
Scheme 9. Metalation rates (2,4-difluorophenyl)- 65 , (3,4-difluorophenyl)- 66 , and (3,5-difluorophenyl)trimethylsilane 67	10
Scheme 10. The synthesis of 6-methoxy-2-phenylquinazolin-4-amine 77	12
Scheme 11. Some protocols for the synthesis of 4-aminoquinazolines from quinazolinones.	13
Scheme 12. Visible light enabled S _N Ar of 4-mercaptoquinazoline 82 to afford 4-aminoquinazolines 83a-c	14
Scheme 13. Metal-catalyzed synthesis of 4-aminoquinazolines from N-arylamidines ..	14
Scheme 14. Preparation of 4-aminoquinazolines from anthranilonitriles	15
Scheme 15. Synthesis of 4-aminoquinazolines from <i>ortho</i> -halogenated benzonitriles .	16
Scheme 16. Catalyzed synthesis of 2,3-dihydroquinazolin-4(1 <i>H</i>)-ones by SBA-16/GPTMS-TSC-Cu ^I catalyst.....	17
Scheme 17. Synthesis of DHQs from isatoic anhydrides, <i>o</i> -bromobenzonitriles, 2-nitrobenzamides, and 2-amino- benzonitriles or nicotinonitrile.....	18
Scheme 18. Synthetic procedures for the synthesis of DHQs from 2-nitrobenzonitrile.	19
Scheme 19. The main goal from the first project and chosen substrates for study.....	20
Scheme 20. Synthesis of DHQs with glucose as an eco-friendly reductant.....	20



Scheme 21. Synthesis of tetrasubstituted aromatics 126a–b through consecutive metalation-functionalization sequences.....	27
Scheme 22. Synthesis of (<i>E</i>)- <i>N'</i> -(2-cyanophenyl)- <i>N,N</i> -dimethylformimidamide 132	39
Scheme 23. Synthesis of 4-aminoquinazoline 134	40
Scheme 24. Synthesis of 8-(4-methoxyphenyl)-2-(<i>p</i> -tolyl)quinazolin-4-amine 135	41
Scheme 25. Synthesis of 1 <i>H</i> -indazole 137 and dibenzoxazepinamine 138	41
Scheme 26. Nitro reduction pathways	49
Scheme 27. Proposed mechanism for the developed synthesis of DHQs.....	50
Scheme 28. TDF improved synthetic route.....	51

LIST OF TABLES

Table 1. Metalation study of 2-fluorobenzonitrile with TMPMgCl·LiCl.....	22
Table 2. Metalation study of 3-fluorobenzonitrile with TMPMgCl·LiCl.....	23
Table 3. Metalation study of 4-fluorobenzonitrile with TMPMgCl·LiCl	24
Table 4. Metalation sites of 123a–c explored in this work and the literature	25
Table 5. Magnesiumation of 123a–c with TMPMgCl·LiCl followed by trapping with diverse electrophiles.....	26
Table 6. Metalation study of 2,4-difluorobenzonitrile 123d with TMP-bases	28
Table 7. Metalation study of 3,4-difluorobenzonitrile 123e with TMP-bases.....	29
Table 8. Metalation study of 3,5-difluorobenzonitrile 123f with TMP-bases	31
Table 9. Metalation sites of 123d–f explored in this work and the literature.....	32
Table 10. Metalation and functionalization of difluorobenzonitriles 123d–f with TMP-bases.*.....	33
Table 11. Metalation study of 5-fluoropicolinonitrile 123g with TMP-bases	34
Table 12. Metalation study of 2-fluoroisonicotinonitrile 123h with TMP-bases	35
Table 13. Metalation study of 2-fluoronicotinonitrile 123i with TMP-bases.....	37
Table 14. Metalation and functionalization of difluorobenzonitriles 123g–i with TMP-bases.*.....	38
Table 15. Synthesis of 2-aminobenzamide under various conditions	43
Table 16. Optimization of the reaction conditions for the synthesis of 2-phenyl-2,3-dihydroquinazolin-4(1 <i>H</i>)-one	44
Table 17. Synthesis of 2,3-dihydroquinazolin-4(1 <i>H</i>)-ones with the established protocol	47
Table 18. Obtained values of GOLD Fitness for the docking studies.....	52
Table 19. Solvation Gibbs energies (G_{solv}), in Hartree, obtained by PCM/B3LYP/6-311++G(d,p)//B3LYP/6-31+G(d,p) and pK_a values	105

TABLE OF CONTENTS

Resumo	i
Abstract	ii
List of Figures	iii
List of schemes	iv
List of tables	v
1. INTRODUCTION	01
1.1 DIRECTED <i>ORTHO</i> -METALATION	01
1.2 CYANO AND FLUORINE AS DIRECTING GROUPS	03
1.3 4-AMINOQUINAZOLINES: BIOLOGICAL IMPORTANCE AND SYNTHESIS.....	11
1.4 2,3-DIHYDROQUINAZOLIN-4(1 <i>H</i>)-ONES: BIOLOGICAL IMPORTANCE AND SYNTHESIS	16
2. OBJECTIVES	19
3. CHAPTER 01 - REGIOSELECTIVE FUNCTIONALIZATION OF FLUORINATED NITRILES WITH 2,2,6,6-TETRAMETHYLPYPERIDYL BASES	21
3.1 RESULTS AND DISCUSSIONS.....	21
3.1.1 Metalation studies and reaction scope.....	21
3.1.2 Synthesis of 4-aminoquinazolines and other heterocycles as synthetic applications	39
4. CHAPTER 02 - ONE-POT SYNTHESIS OF 2,3-DIHYDROQUINAZOLIN-4(1<i>H</i>)- ONES WITH GLUCOSE AS THE REDUCTANT	42
4.1 RESULTS AND DISCUSSIONS.....	42
5. CHAPTER 03 – TENOFOVIR DISOPROXYL FUMARATE AS A REPOSITIONING STRATEGY TO TACKLE SARS-COV-2	51
6. CONCLUSIONS	54
7. EXPERIMENTAL SECTION	55
7.1 CHAPTER I	55
7.1.1 General considerations.....	55
7.1.1.1 Solvents and reagents.....	55

7.1.1.2 Preparation procedures of the employed TMP-bases and salt solutions.....	56
7.1.1.3 Analytical data and other employed equipment.....	57
7.1.2 General procedures for the functionalization of fluorinated nitriles.....	58
7.1.2.1 Reaction monitoring.....	58
7.1.2.2 General method A (GMA): Standardized procedure for metalation of the studied fluorobenzonitriles with TMPMgCl·LiCl.....	58
7.1.2.2.1 <i>Sequential difunctionalization of 4-fluorobenzonitrile.....</i>	<i>59</i>
7.1.2.2.2 <i>Gram scale synthesis of 2-fluoro-3-(hydroxy(p-tolyl)methyl)benzonitrile (125f).....</i>	<i>59</i>
7.1.2.3 General method B (GMB): Standardized procedure for metalation of the studied difluorobenzonitriles 123d-f with TMPMgCl·LiCl or (TMP) ₂ Zn·2MgCl ₂ ·2LiCl.....	59
7.1.2.4 General method C (GMC): Standardized procedure for metalation of the studied heterocyclic nitriles 123g-i with TMPMgCl·LiCl or (TMP) ₂ Zn·2MgCl ₂ ·2LiCl.....	60
7.1.2.5 Metalation followed by Negishi cross-coupling.....	61
7.1.2.6 Metalation followed by transmetalation with copper salt.....	61
7.1.2.7 Metalation followed by palladium-catalyzed benzylation.....	62
7.1.3 Reaction scope and characterization data.....	62
7.1.4 Examples of synthetic applications of the functionalized nitriles.....	98
7.1.4.1 Synthesis of 4-aminoquinazolines.....	98
7.1.4.1.1 <i>Synthesis of (E)-N'-(2-cyanophenyl)-N,N-dimethylformimidamide 132.....</i>	<i>98</i>
7.1.4.1.2 <i>Synthesis of N-((2-fluoro-4'-methoxy-[1,1'-biphenyl]-3-yl)methyl)-quinazolin-4-amine 134.....</i>	<i>99</i>
7.1.4.1.3 <i>Synthesis of 8-(4-methoxyphenyl)-2-(p-tolyl)quinazolin-4-amine 135.....</i>	<i>101</i>
7.1.4.1.4 <i>Synthesis of 2-phenylquinazolin-4-amine 136.....</i>	<i>102</i>
7.1.4.2 Synthesis of 3-phenyl-1H-indazole-5-carbonitrile (137).....	103
7.1.4.3 Synthesis of 4-(4-methoxyphenyl)dibenzo[b,f][1,4]oxazepin-11-amine (138).....	103
7.1.5 Computational study: pK_a calculations.....	104
7.2 CHAPTER II.....	106
7.2.1 General considerations.....	106
7.2.1.1 Solvents and reagents.....	107



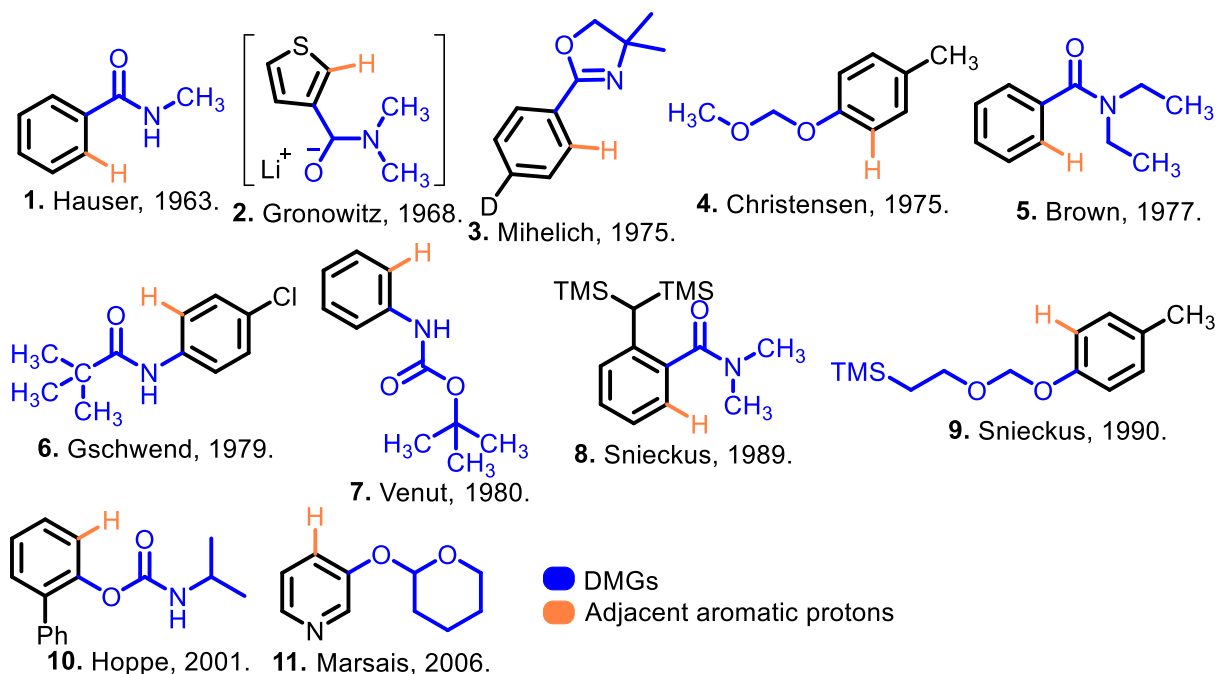
7.2.1.2 Analytical data	107
7.2.2 Developed reactions	108
7.2.2.1 General procedure for the synthesis of 2-aminobenzamide	108
7.2.2.2 General procedure for the synthesis of 2,3-dihydroquinazolin-4(1 <i>H</i>)-ones.....	109
7.2.3 Characterization data of the synthesized	
2,3-dihydroquinazolin-4(1<i>H</i>)-ones.....	109
8. REFERENCES.....	125
APPENDIX A – NMR SPECTRA	145

1. INTRODUCTION

1.1 DIRECTED *ORTHO*-METALATION

The first reports of directed *ortho*-metalation reactions (DoM) come from Gilman and Bebb¹ in 1939 and Wittig and Furhmann² in 1940, the *ortho*-lithiation of methoxy-bearing substrates such as 2-methoxydibenzofuran and anisole with *n*-Butyllithium or phenyl lithium, respectively. The scope of directed *ortho* metalation groups (DMGs) was later expanded³ including the work of Hauser,⁴ Gronowitz,⁵ Gschwend,⁶ Mihelich,⁷ Brown,⁸ Snieckus,⁹ Christensen,¹⁰ Venut,¹¹ Hoppe,¹² Marsais,¹³ and their co-workers (**Figure 1**).

Figure 1. Some DMGs explored in the literature.



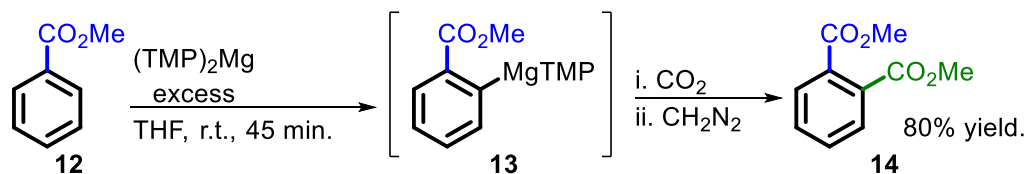
Source: GREEN; CHAUDER; SNEICKUS, 1999;^{3b} MIAH *et al.*, 2018.^{3d}

The *ortho*-directing properties of DMGs can either relate to the establishment of a complex-induced proximity effect (CIPE) with the coordination of a heteroatom to the metal of a base with simultaneous proton transfer (e.g., Lithium in the case of LDA - Lithium diisopropylamide)¹⁴ or the reduction in pK_a for the adjacent aromatic protons through inductive effect.¹⁵

Although lithium bases have been extensively applied to the deprotometalation of aromatic and heteroaromatic systems via DoMs, there are important drawbacks: they normally demand low temperatures or the *in-situ* generation before metalation, and the organolithium intermediates are highly reactive and may lead to side products in the presence of some sensitive groups such as esters.¹⁶

As alternative methods, Hauser and co-workers developed diethyl- and diisopropylaminomagnesium bromides to promote the self-condensation of esters in the synthesis of β -keto esters.¹⁷ In 1989, Eaton, Lee, and Xiong prepared the sterically hindered TMP-bases (2,2,6,6-tetramethylpiperidyl), TMPMgBr, and (TMP)₂Mg, for the *ortho*-magnesiumation of aromatics as depicted in **Scheme 1**.¹⁸ Later, Mulzer and co-workers reported the synthesis of TMPMgCl with the regioselective metalation of pyridinylcarbamates and pyridinecarboxamides.¹⁹

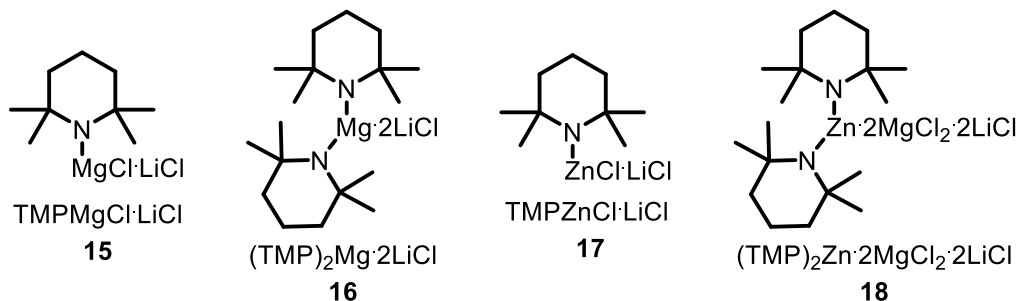
Scheme 1. The regioselective magnesiumation of methyl benzoate with (TMP)₂Mg.



Source: EATON; LEE; XIONG, 1989.¹⁸

However, these magnesium-based bases displayed low solubility in common solvents and needed to be employed in excess (2-12 Equiv.)²⁰ in order to achieve great substrate conversions. To solve such problems, Knochel and co-workers developed the mixed Mg/Li, Zn/Li, and Zn/Mg/Li amides TMPMgCl·LiCl,²⁰ (TMP)₂Mg·2LiCl,²¹ TMPZnCl·LiCl,²² (TMP)₂Zn·2MgCl₂·2LiCl²³ (**Figure 2**) with excellent solubility in THF and functional group tolerance, and great stability at room and higher temperatures. These TMP-bases have been successfully employed for the regioselective magnesiumation and zincation of diverse heteroaromatic and aromatic systems, such as 1,5-naphthyridine scaffold,²⁴ quinolines,²⁵ indolizines,²⁶ oxazolines,^{16b,27} 1,3,4-oxadiazoles and 1,2,4-triazoles,²⁸ 2-pyridones and 2,7-naphthyridones,²⁹ pyrazolo[1,5-*a*]pyridines,³⁰ 2- and 4-pyrones,³¹ pyridines,³² and 1-*H*-imidazo[1,2-*b*]pyrazoles.³³

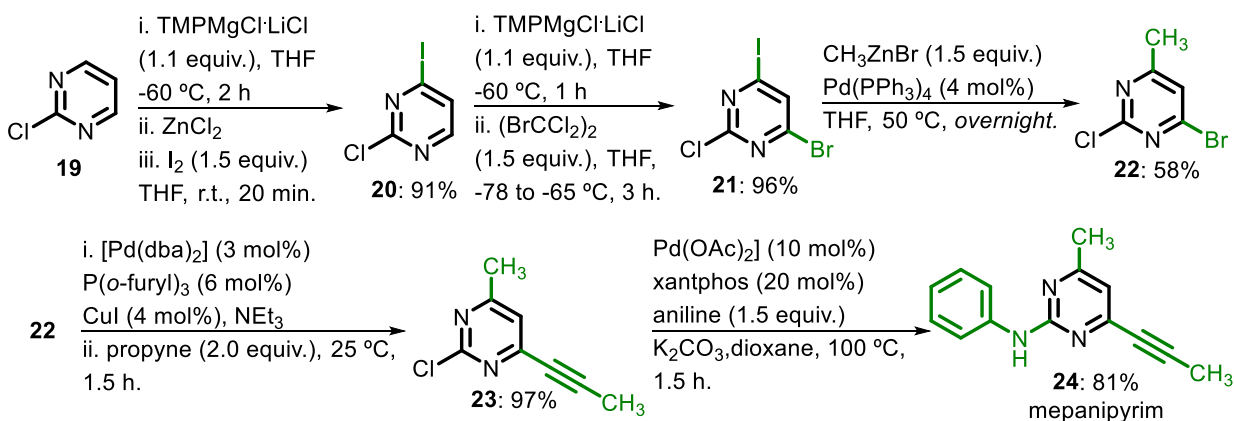
Figure 2. Developed TMP-bases by Knochel and co-workers.



Source: KRASOVSKIY; KRASOVSKAYA; KNOCHEL, 2006;²⁰ CLOSOSKI; ROHBOGNER; KNOCHEL, 2007;²¹ UNSINN; FORD; KNOCHEL, 2013;²² WUNDERLICH; KNOCHEL, 2007.²³

Furthermore, the Knochel bases find direct application in the synthesis of valuable building blocks for the construction of natural products and drugs.³⁴ For example, Mosrin and Knochel obtained the fungicide mepanipyrim (**24**) in 40% overall yield from 2-chloropyrimidine **19** after two consecutive magnesiations with $\text{TMPMgCl}\cdot\text{LiCl}$, followed by a Negishi cross-coupling with CH_3ZnBr , a Sonogashira reaction with propyne, and a Buchwald-Hartwig amination with aniline (**Scheme 2**).³⁵

Scheme 2. Employment of $\text{TMPMgCl}\cdot\text{LiCl}$ in the synthesis of Mepanipyrim.

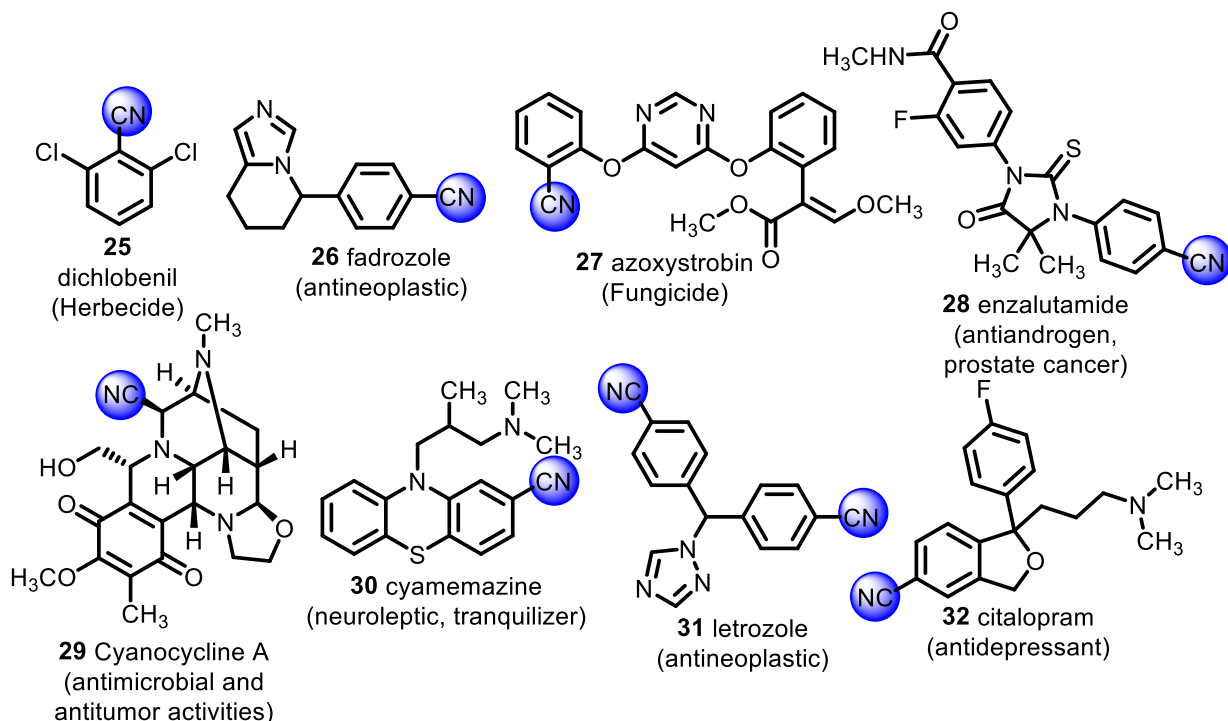


Source: MOSRIN; KNOCHEL, 2009.³⁵

1.2 CYANO AND FLUORINE AS DIRECTING GROUPS

The cyano group is of great interest in organic synthesis and can be easily converted into various functional moieties, such as amines, aldehydes, amides, acids, esters, tetrazoles, triazoles, oxazoles, and thiazoles.³⁶ It is also present in agrochemicals, pharmaceuticals, and natural products as illustrated in **figure 3**.³⁷

Figure 3. Some bioactive molecules bearing the cyano group.

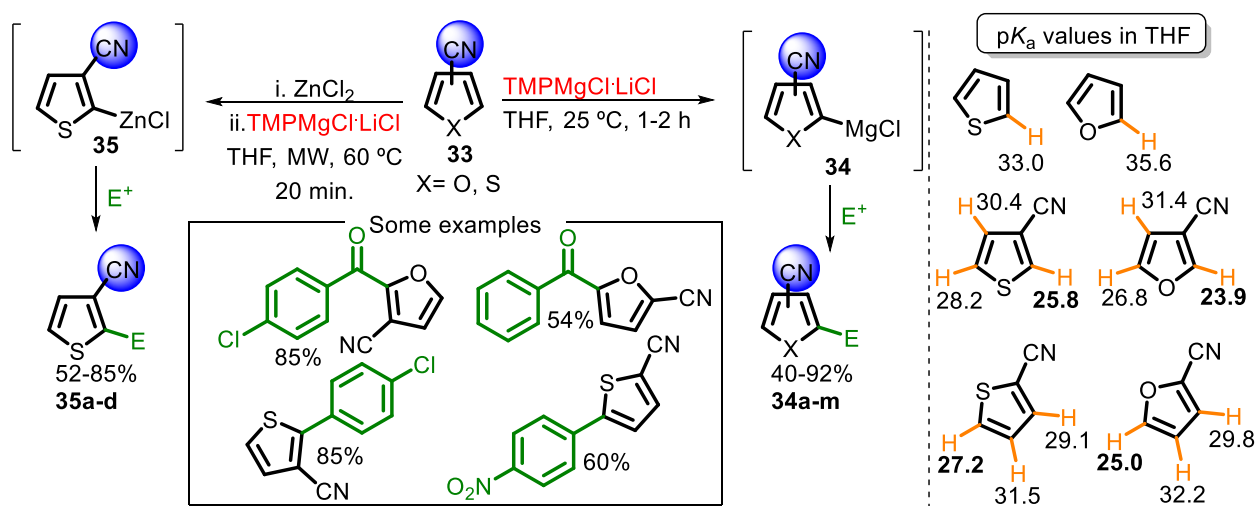


Source: ANBARASAN; SCHAREINA; BELLER, 2011;^{37a} CHAITANYA; ANBARASAN, 2018;^{37b} GRUNDKE; VIERENGEL; OPATZ, 2020.^{37c}

Given the importance of nitriles, DoMs involving the cyano as a directing group (electron-withdrawing effect and coordination properties)³⁸ has become an interesting strategy to access functionalized nitrile-based systems. Our research group has performed the directed metalation of cyano-substituted thiophenes and furans with $\text{TMPMgCl}\cdot\text{LiCl}$ (**Scheme 3**).³⁹ The cyano group led to a decrease in $\text{p}K_{\text{a}}$ ⁴⁰ for C2-H or C5-H in all the studied substrates favoring the deprotonations at these positions. However, the regioselectivity control for thiophene-3-carbonitrile (**35**) was more challenging requiring a pre-complexation with ZnCl_2 followed by the magnesiation at 60

°C in a microwave reactor to avoid a mixture of products, regioisomers, and difunctionalized ones.

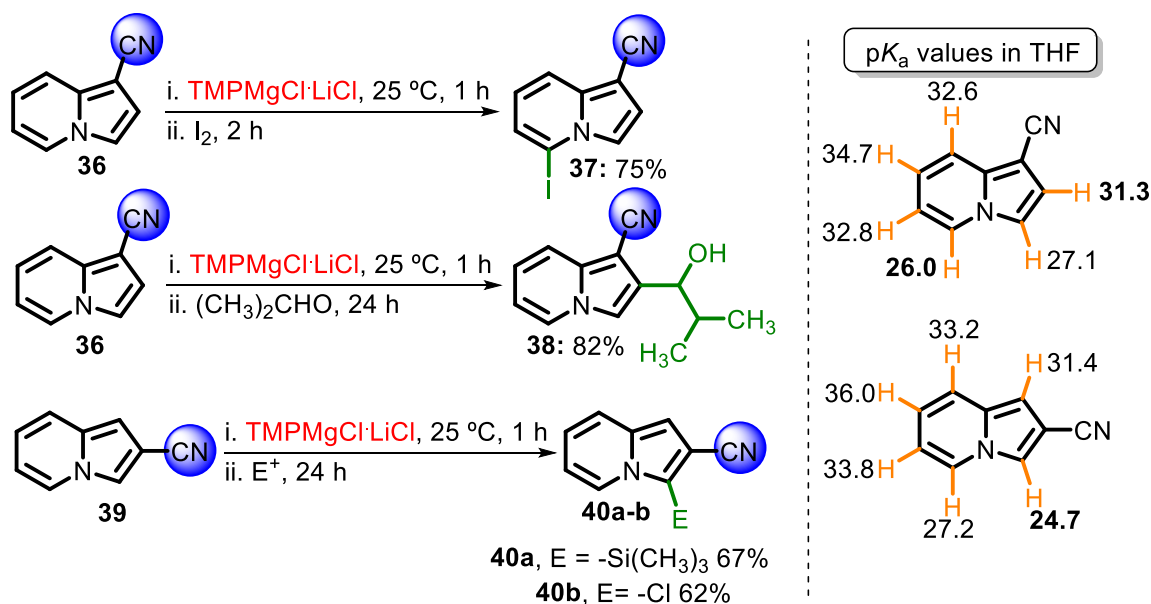
Scheme 3. Directed functionalization of cyano-substituted furans and thiophenes plus pK_a values.



Source: DOS SANTOS *et al.*, 2015;³⁹ FRASER; MANSOUR; SAVARD, 1985.⁴⁰

Additionally, TMPMgCl·LiCl allowed us to access position C2 for 1-cyanoindolizine **36** with isobutyraldehyde and C5 with iodine as the electrophiles, respectively (**Scheme 4**).^{26b} It is expected that the observed regioselectivity for the latter electrophile relies on the disruption of a base-cyano chelate by the generated iodide leading to anion isomerization, C2 to C5. In the case of 2-cyanoindolizine **39**, the metalation took place at C3, the most acidic site.

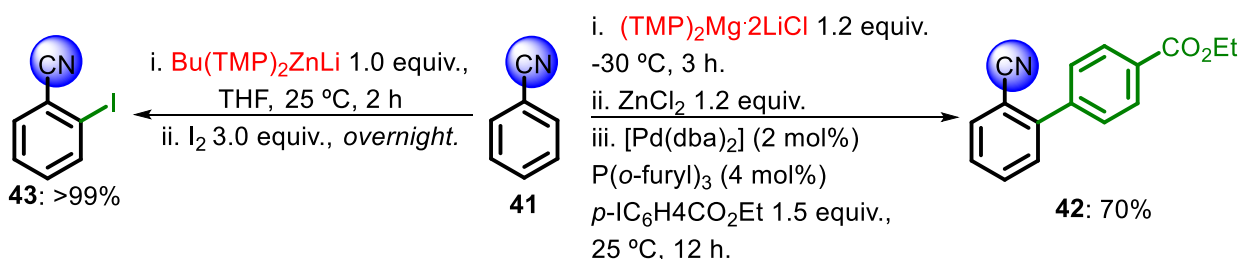
Scheme 4. Regioselective functionalization of cyano-substituted indolizines **36** and **39** and pK_a values.



Source: BERTALLO *et al.*, 2019.^{26b}

Knochel and co-workers have reported the direct magnesiation of benzonitrile (**41**) with the bisamide **16** $(\text{TMP})_2\text{Mg}\cdot 2\text{LiCl}$ at $-30 \text{ }^\circ\text{C}$ for 3 hours with further transmetalation with ZnCl_2 , and a Pd-catalyzed Negishi cross-coupling reaction to afford biaryl **42** in 70%.²¹ The same position, C2, was explored by Mongin and co-workers upon the use of a mixture of $\text{ZnCl}_2\cdot\text{TMEDA}$ ($\text{TMEDA} = N,N,N',N'$ -tetramethylethylenediamine), LiTMP (Lithium 2,2,6,6-tetramethylpiperidide), and $n\text{-BuLi}$ (Butyllithium) to putatively obtain $\text{Bu}(\text{TMP})_2\text{ZnLi}$ in the synthesis of aromatic **43** (Scheme 5).⁴¹

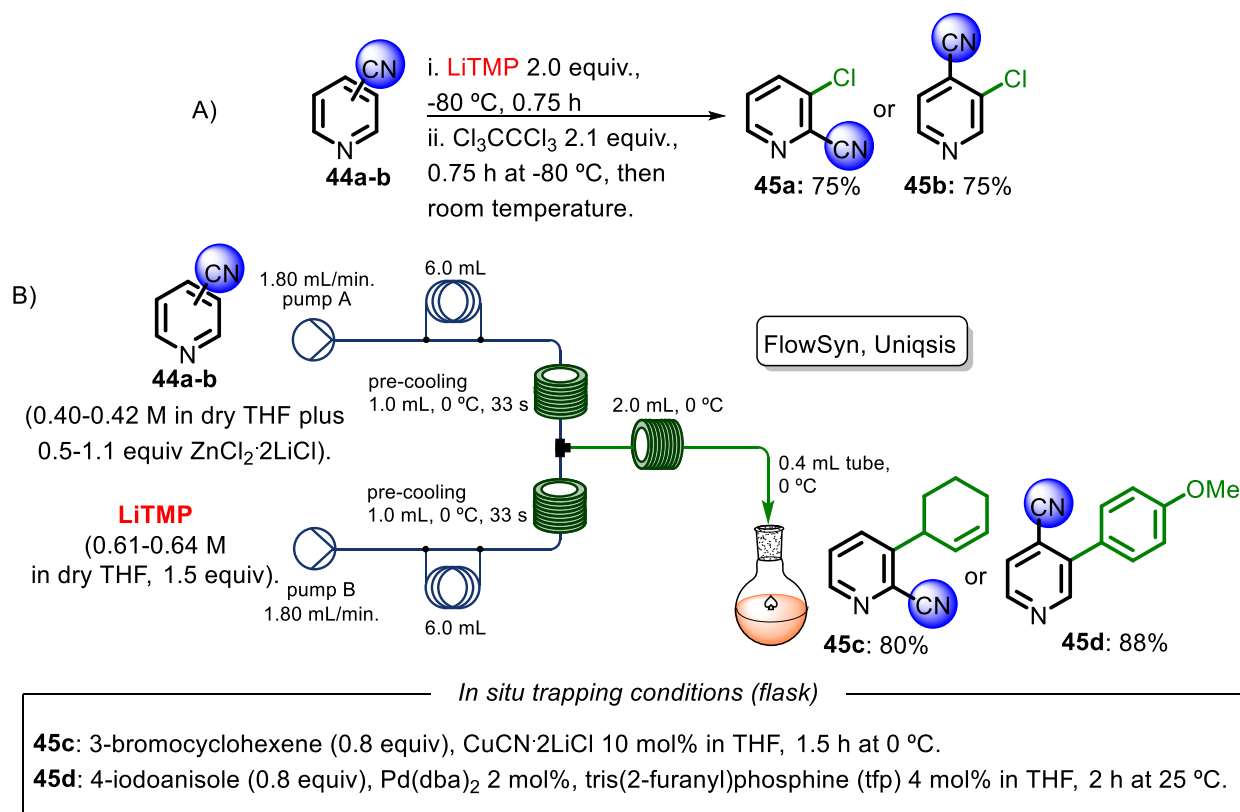
Scheme 5. Metalation and functionalization of benzonitrile.



Source: CLOSOSKI; ROHBOGNER; KNOCHEL, 2007; SNÉGAROFF *et al.*, 2010.⁴¹

Regarding the regioselective metalation of cyano-substituted pyridines, such as 2-cyanopyridine (**44a**) and 4-cyanopyridine (**44b**), Mongin and co-workers applied a mixed lithium-cadmium base, $(\text{TMP})_3\text{CdLi}$, but mixtures of di-, tri-, and four-substituted pyridines were obtained.⁴² LiTMP, differently, can be considered for the regiocontrolled-lithiation under a low temperature of the same substrates affording **45a** and **45b** in 75% yield after reaction with hexachloroethane (**Scheme 6A**).⁴³ Besides, a wise approach developed by Knochel and co-workers, an *in situ* trapping transmetalation via ZnCl_2 , allowed the metalation of **44a-b** to take place at 0 °C (40 s) under flow conditions with the same base resulting in the disubstituted pyridines **45c** and **45d** in great yields (**Scheme 6B**).⁴⁴

Scheme 6. Regioselective lithiation of pyridines **44a-b** and their functionalization.

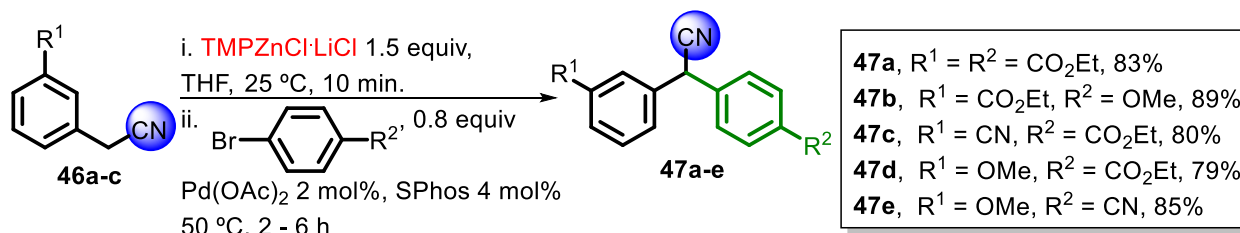


Source: CAILLY; FABIS; RAULT, 2006;⁴³ BECKER; KNOCHEL, 2015.⁴⁴

Expanding the scope of functionalized nitriles via deprotonation, $\text{TMPZnCl}\cdot\text{LiCl}$ was remarkably suitable for the mono- α -arylation of benzylic nitriles at room temperature

even in the presence of *ortho*-directing groups, such as methoxy, cyano, and ethyl ester in the aromatic moiety (**Scheme 7**).⁴⁵

Scheme 7. The α -arylation of benzylic nitriles **46a-c** with TMPZnCl·LiCl.

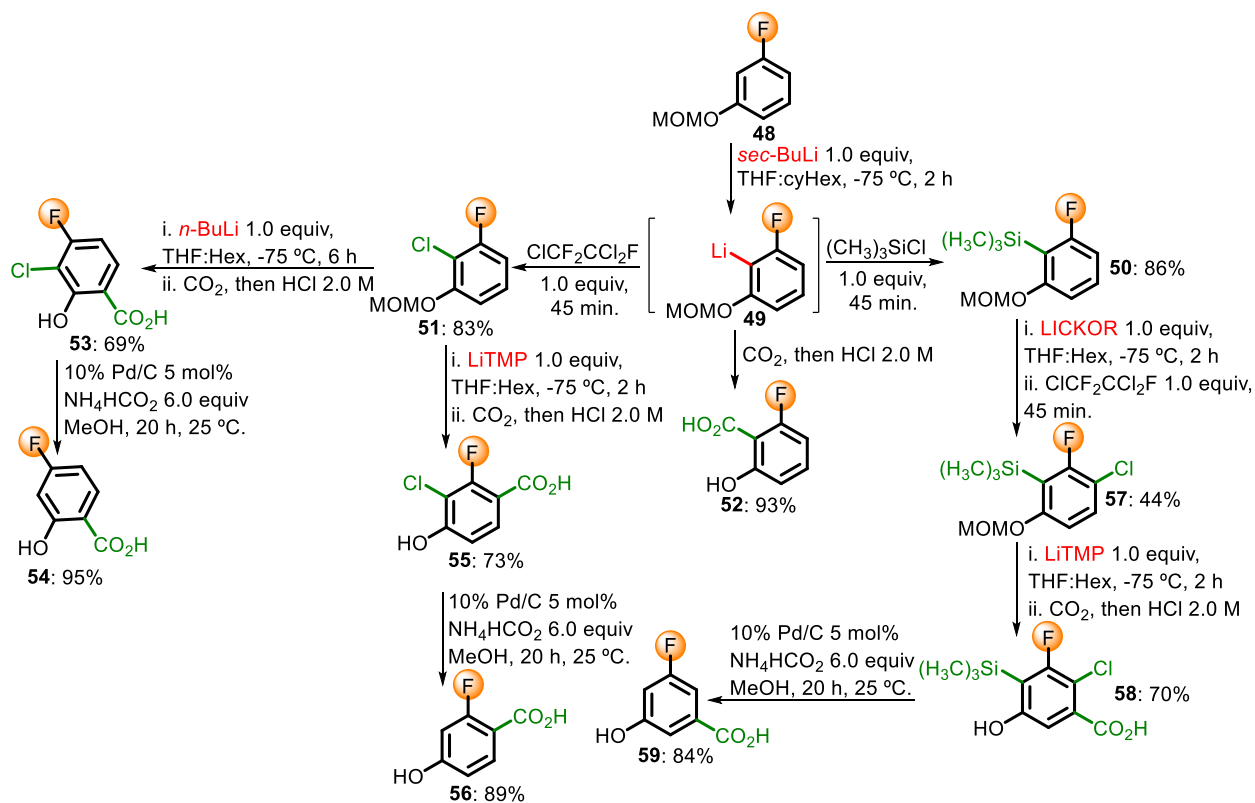


Source: DUEZ *et al.*, 2011.⁴⁵

The fluoro group has been of great importance as an *ortho*-directing group in aromatic and heteroaromatic metalations due to its electron-withdrawing properties.¹⁵ Prof. Dr. Manfred Schlosser has made a huge contribution in this area with the concept of regiochemically exhaustive functionalization of readily available organofluorines to furnish valuable building blocks. For instance, the treatment of the *O*-methoxymethyl-protected 3-fluorophenol **48** with *sec*-Butyllithium afforded the lithiated species **49** which were further reacted with 1,2,2-trichloro-1,2,2-trifluoroethane to obtain **51** (83%), carbon dioxide to synthesize **52** (92%), and chlorotrimethylsilane to prepare **50** (86%) (**Scheme 8**).⁴⁶ Regioselective lithiation of the tri-substituted aromatic **51** by *n*-Butyllithium (position C4) and subsequent carboxylation with deprotection of the phenolic methoxymethyl (MOM) ether under acidic conditions furnished the 3-chloro-4-fluoro-2-hydroxybenzoic acid **53** in 69% yield. Blocking the acidic position C2 in **50** and **51** favored the regioselective metalation with LiTMP and LICKOR at C6 in the synthesis of 3-chloro-2-fluoro-4-hydroxybenzoic acid **55** in 73% and (3-chloro-2-fluoro-6-(methoxymethoxy)phenyl)trimethylsilane **57** in 44%, respectively. LICKOR, also known as Schlosser's base, is comprised of *n*-butyllithium and potassium *tert*-butoxide in a one-to-one ratio. Furthermore, LiTMP was useful to promote the *ortho*-deprotometalation to the chlorine group in **57** giving **58** in 70% after treatment with an excess of carbon dioxide followed by acidic conditions. Therefore, using chlorine and trimethylsilyl groups to switch off metalation positions, or considering directed lithiation with *sec*-BuLi for the MOM ether **48**, all the available functionalization sites were accessed: after removal of

trimethylsilyl group with tetra-butylammonium fluoride and chlorine by catalytic hydrogenation, carboxylic acids derived from 3-fluorophenol, **52**, **54**, **56**, and **59**, were prepared.

Scheme 8. The regiochemically exhaustive functionalization of 3-fluorophenol by Schlosser and co-workers.

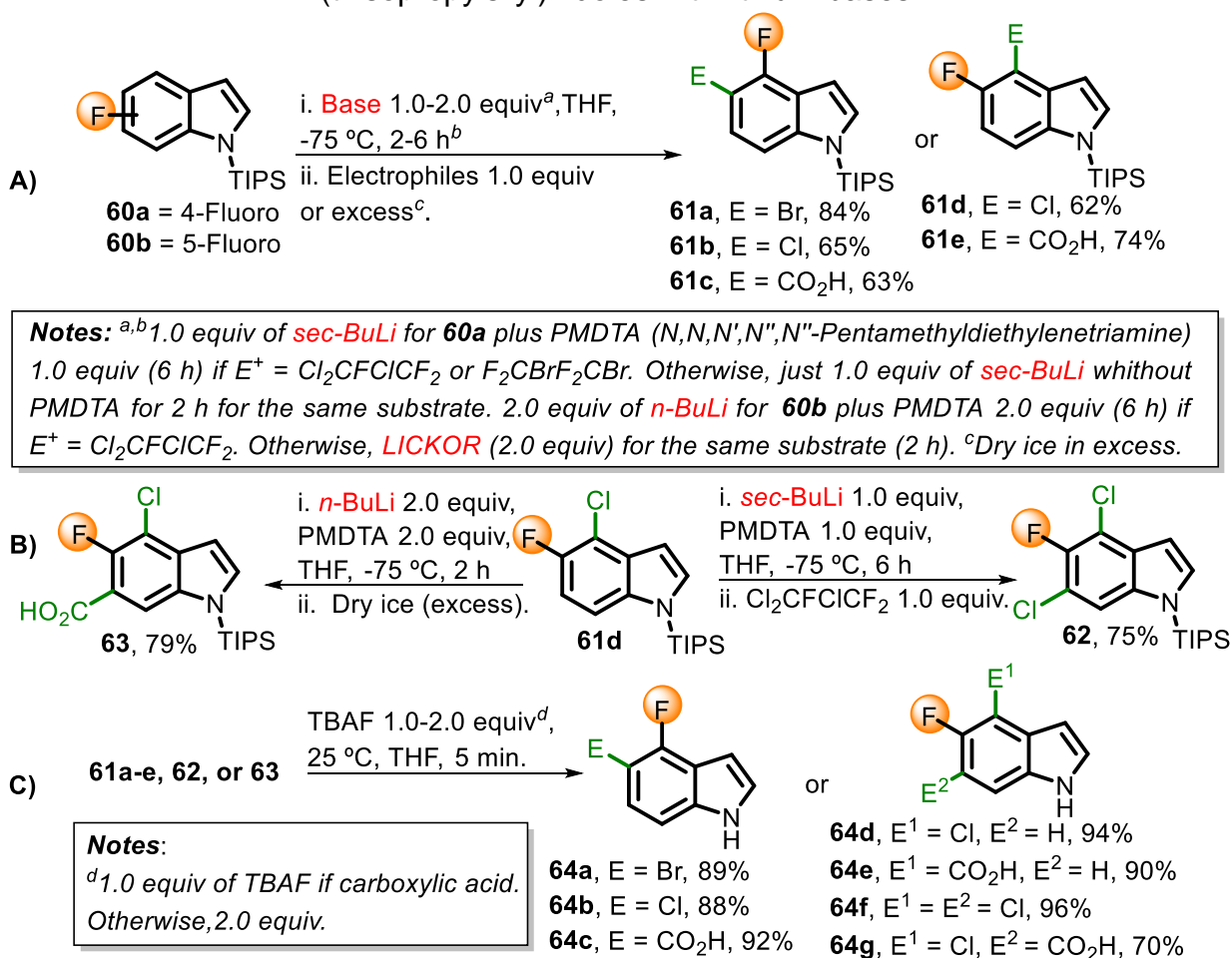


Source: MARZI *et al.*, 2005.⁴⁶

In a similar manner, Schlosser and co-workers have explored the functionalization of fluorinated pyridines (3-fluoropyridine,^{46,47} 2-fluoropyridine, 2,3-difluoropyridine, and 2,5-difluoropyridine,^{47,48} 2,4-difluoropyridine and 2,4,6-trifluoropyridine,^{47,49} 2,6-difluoropyridine,^{47,50} 2,3,5-trifluoropyridine and 3,5-difluoropyridine^{47,51}), phenols (2,4-difluorophenol, 2,5-difluorophenol, 2,3-difluorophenol, 3,5-difluorophenol, 3,4-difluorophenol, 2,4,5-trifluorophenol, and 2,3,4-trifluorophenol),⁵² and indoles.⁵³ For the latter substrate, an interesting strategy was devised in order to avoid metalation at position C2 of the indole system: its nitrogen was protected with a bulky group,

triisopropylsilyl (TIPS). The treatment of 4-fluoro-1-(triisopropylsilyl)indole **60a** with *sec*-BuLi at -75 °C and subsequent trapping with 1,2-dibromo-1,1,2,2-tetrafluoroethane, 1,1,2-trichloro-1,2,2-trifluoroethane or carbon dioxide led to C5-functionalized indoles **61a-c** with yields up to 84%. For 5-fluoro-1-(triisopropylsilyl)indole **60b**, *n*-BuLi and LICKOR were suitable to functionalize C4 position affording **61d** (62%) and **61e** (74%) after chlorination and carboxylation, respectively (**Scheme 9A**). Interestingly, **61d** was subjected to a second metalation with *n*-BuLi or *sec*-BuLi to obtain the tri-substituted indoles **62** and **63** in great yields (**Scheme 9B**). Tetrabutylammonium fluoride was successfully applied to all substrates at 25 °C for 5 minutes to remove the TIPS groups (**Scheme 9C**).⁵³

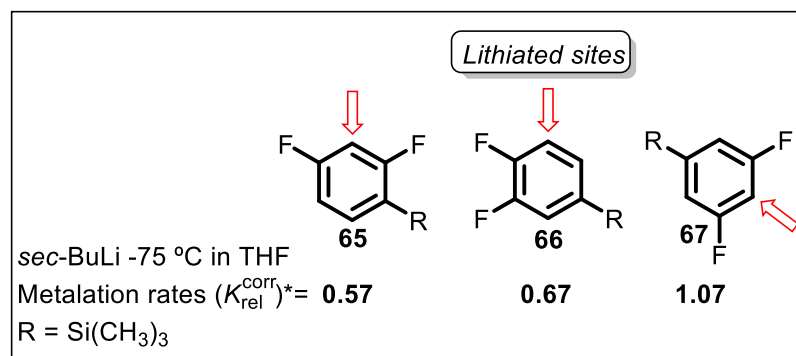
Scheme 9. The metalation and functionalization of 5-fluoro and 4-fluoro -1-(triisopropylsilyl)indoles with lithium bases.



Source: SCHLOSSER; GINANNESCHI; LEROUX, 2006.⁵³

Complementing the study of the influence of a bulky alkyl-silyl group on metalation selectivity for fluorinated compounds, it was found that trimethylsilyl group (TMS) can affect kinetic acidity due to a buttressing effect when occupying a fluoro-neighboring position, and therefore, deprotometalation rates (**Figure 4**). The steric pressure exerted by TMS as pointed by Schlosser is less pronounced in **67** at position C4 because of the *meta* disposition of both fluoro groups. On the other hand, the *meta* position to TMS is available in both **66** and **65** favoring the transmission of the buttressing effect that is greatly enhanced by an adjacent fluoro group in the latter scenario.⁵⁴

Figure 4. Metalation rates (2,4-difluorophenyl)- **65**, (3,4-difluorophenyl)- **66**, and (3,5-difluorophenyl)trimethylsilane **67**.



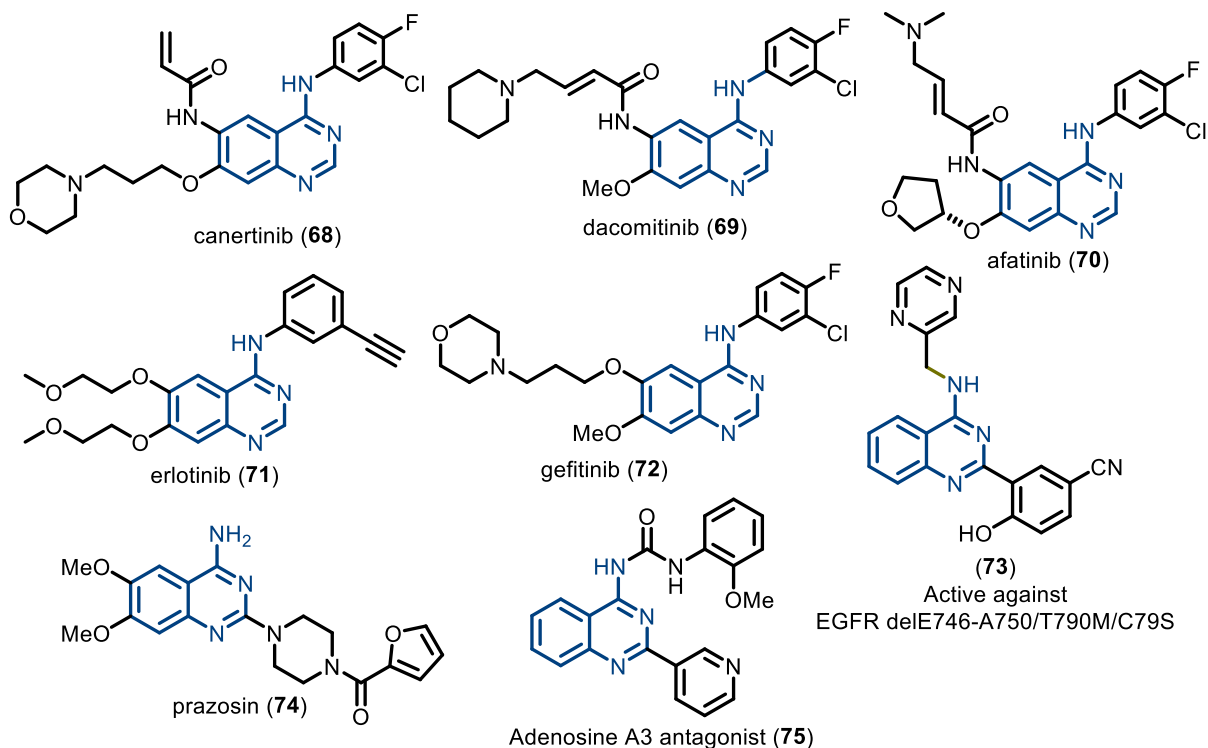
$$*(K_{rel}^{corr}) (= K^{R = Si(CH_3)_3} / K^{R = H}).$$

Source: HEISS *et al.*, 2007.⁵⁴

1.3 4-AMINOQUINAZOLINES: BIOLOGICAL IMPORTANCE AND SYNTHESIS

Heterocyclic systems account for more than 85% of bioactive molecules with special mention to *N*-heterocyclic rings which represent more than 75% of the drugs approved by the FDA (The Food and Drug Administration).⁵⁵ Among them, 4-aminoquinazoline is a privileged scaffold present in bioactive molecules of high pharmaceutical importance, such as the epidermal growth factor receptor (EGFR) inhibitors **68-73**, the antihypertensive agent prazosin **74**, and the human adenosine A₃ receptor antagonist **75** (**Figure 5**).⁵⁶

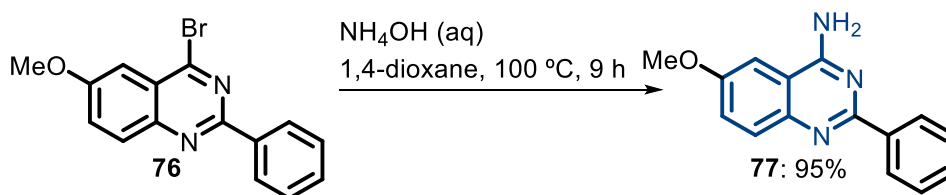
Figure 5. Some bioactive 4-aminoquinazolines.



Source: JIA *et al.*, 2015; CHEN *et al.*, 2018.⁵⁶

Because of their great relevance, preparation protocols to access diverse 4-aminoquinazolines are a prevailing demand. A common method involves the nucleophilic aromatic substitution of 4-haloquinazolines⁵⁷ as verified for the synthesis of **77** in 95% by Ahmad, Hill, and Movassaghi (**Scheme 10**).⁵⁸

Scheme 10. The synthesis of 6-methoxy-2-phenylquinazolin-4-amine **77**.

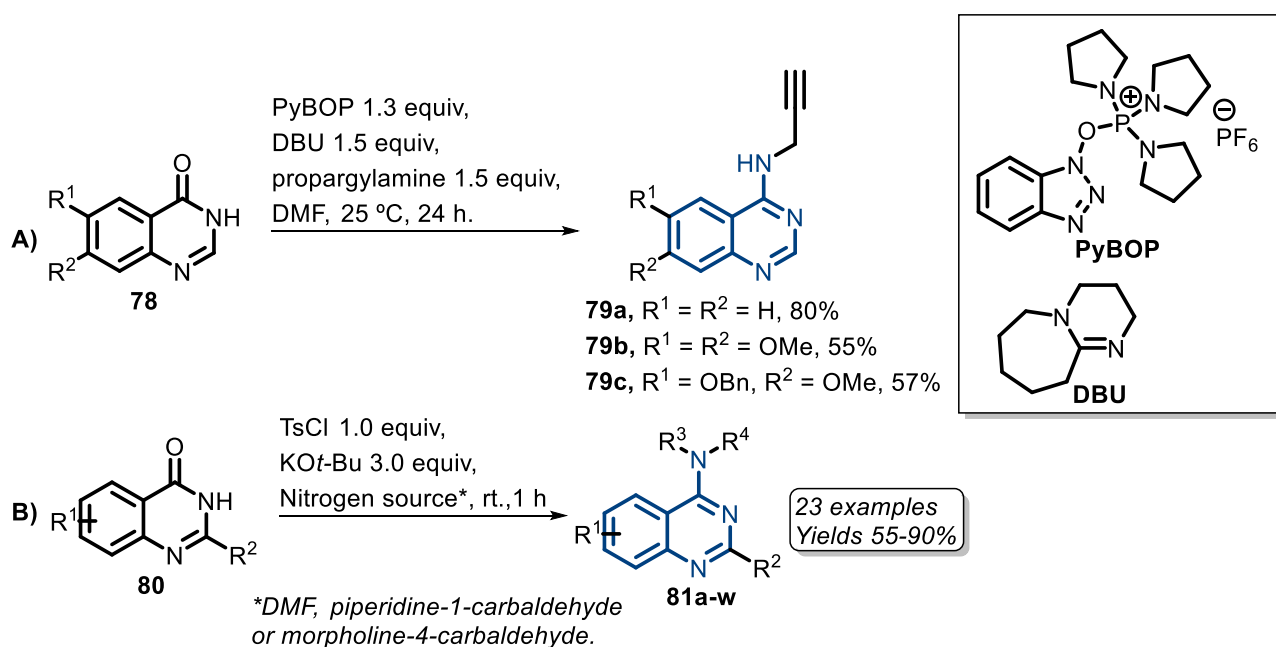


Source: AHMAD; HILL; MOVASSAGHI, 2009.⁵⁸

PyBOP (benzotriazole-1-yl-oxy-tris-pyrrolidino-phosphonium hexafluorophosphate) in the presence of DBU (2,3,4,6,7,8,9,10-octahydropyrimidol[1,2-a]azepine) can be

employed for the *in situ* activation of the carbonyl group of quinazolinones⁵⁹ as in **78** with further substitution by propargylamine in DMF in the synthesis of **79a-c** (**Scheme 11A**).⁶⁰ Another strategy by Peng and co-workers employed 4-toluenesulfonyl chloride in conjunction with potassium *tert*-butoxide in DMF to generate a tosylate intermediate prone to substitution affording 4-dimethylaminoquinazolines **81a-w** (**Scheme 11B**).⁶¹

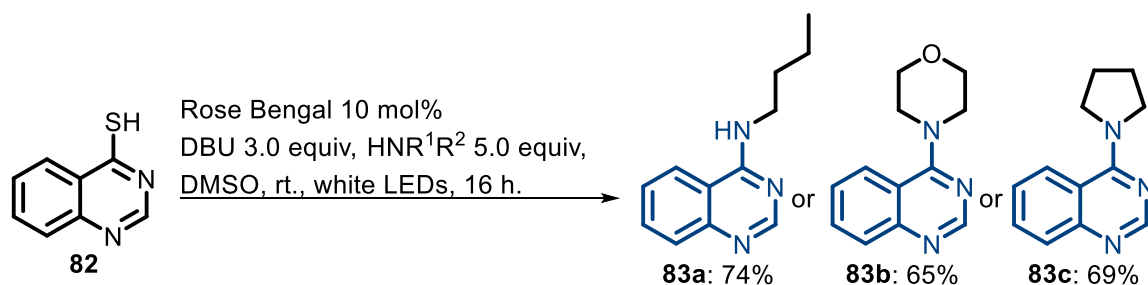
Scheme 11. Some protocols for the synthesis of 4-aminoquinazolines from quinazolinones.



Source: NUNES *et al.*, 2021;⁶⁰ CHEN *et al.*, 2015.⁶¹

In addition to the S_NAr-based protocols, the organic dye Rose Bengal under irradiation of visible light enabled the amination of 4-mercaptoquinazoline **82** with different amines leading to **83a-c** in good yields (**Scheme 12**).⁶²

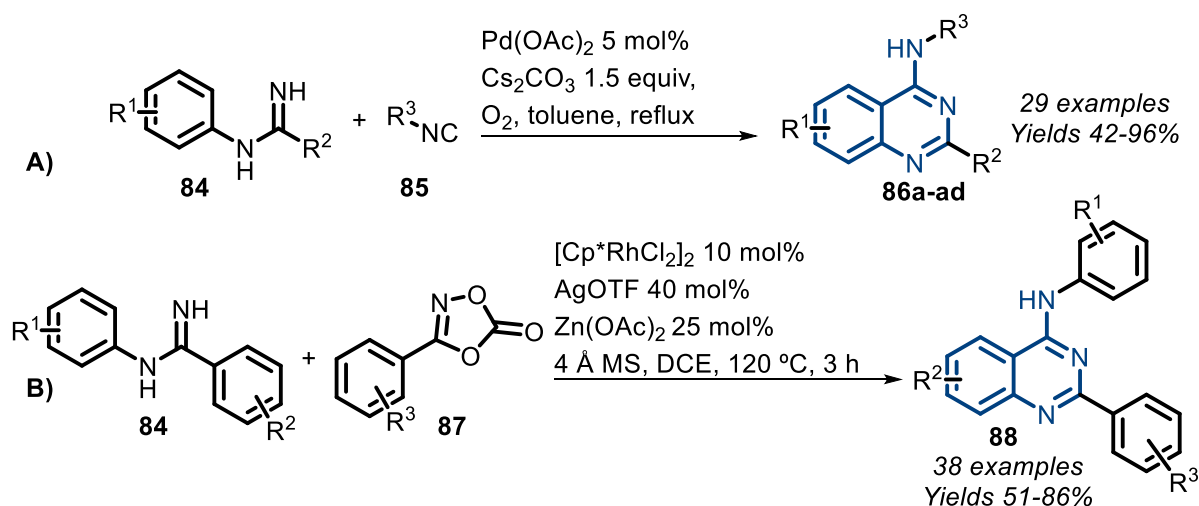
Scheme 12. Visible light enabled S_NAr of 4-mercaptoquinazoline **82** to afford 4-aminoquinazolines **83a-c**.



Source: RATTANANGKOOL; SUKWATTANASINITT; WACHARASINDHU, 2017.⁶²

About the cyclization reactions based on a specific $\text{C}(\text{sp}^2)\text{-H}$ activation bond to access 4-aminoquinazolines, palladium(II) and rhodium(III) have found application in intramolecular C-H amidinations involving isonitrile and 1,4,2-dioxazol-5-ones migratory insertion, respectively. $\text{Pd}(\text{OAc})_2$ with Cs_2CO_3 in toluene under aerobic and reflux conditions catalyzed the conversion of *N*-arylamidines in quinazolines **86a-ad** with yields up to 96% (**Scheme 13A**).⁶³ For the rhodium-catalyzed annulation, $[\text{Cp}^*\text{RhCl}_2]_2$ (pentamethylcyclopentadienyl rhodium dichloride dimer) was used with AgOTf and $\text{Zn}(\text{OAc})_2$ as additives in dichloroethane (DCE) at 120 °C for 3 hours (**Scheme 13B**).⁶⁴

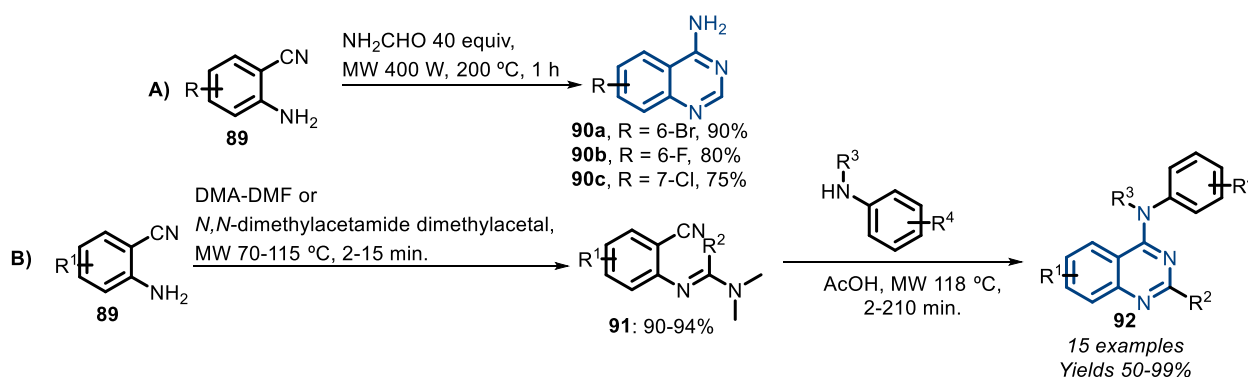
Scheme 13. Metal-catalyzed synthesis of 4-aminoquinazolines from *N*-arylamidines.



Source: WANG *et al.*, 2011;⁶³ REN *et al.*, 2021.⁶⁴

Some other annulation protocols include the use of anthranilonitriles. Loidreau and Besson have applied formamide as an NH_3 and CO source under thermal decomposition in the presence of halogenated anthranilonitriles **89** for the preparation of 4-aminoquinazolines of type **90a-c** in good yields (**Scheme 14A**).⁶⁵ Moreover, anthranilonitriles can be converted into formamidines **91** which under acidic and microwave irradiation conditions react with amines through Dimroth rearrangement to afford 4-aminoquinazolines of type **92** (**Scheme 14B**).⁶⁶

Scheme 14. Preparation of 4-aminoquinazolines from anthranilonitriles.

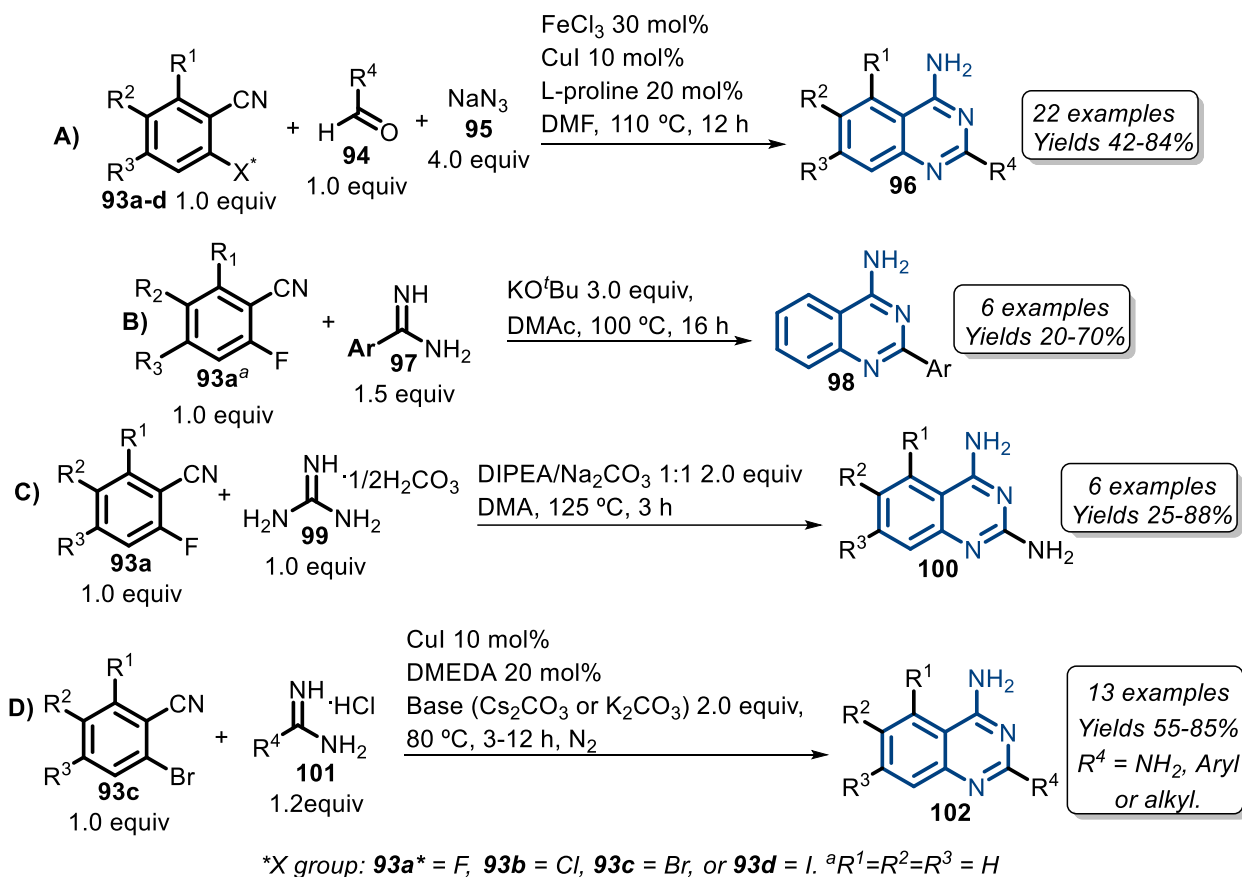


Source: LOIDREAU; BESSON, 2011;⁶⁵ FOU COURT *et al.*, 2010.⁶⁶

Concerning the use of *ortho*-halogenated benzonitriles, distinct protocols have been developed towards the synthesis of 2-substituted 4-aminoquinazolines. For instance, Wu and co-workers devised a domino strategy with consecutive iron-mediated [3+2] cycloaddition, copper-catalyzed $\text{S}_{\text{N}}\text{Ar}$, reduction, cyclization, oxidation, and copper-catalyzed denitrogenation processes for 2-F-, 2-Cl-, 2-Br-, and 2-I-substituted benzonitriles with varied aldehydes and sodium azide as the nitrogen source (**Scheme 15A**).^{56e} Another procedure includes the reaction of amidines with 2-fluorobenzonitriles in the presence of potassium *t*-butoxide at 100 °C for 16 hours by a base-assisted $\text{S}_{\text{N}}\text{Ar}$ followed by the attack of the amino group to the cyano carbon (**Scheme 15B**).⁶⁷ Furthermore, under basic conditions, guanidine salts cyclize well with 2-fluorobenzonitriles at 125 °C in *N,N*-dimethylacetamide (DMAc) (**Scheme 15C**)⁶⁸ and CuI plus *N,N'*-dimethylethylenediamine (DMEDA) is suitable for the Ullmann-type

coupling of 2-bromobenzonitriles with amidine or guanidine salts in DMF at 80 °C (Scheme 15D).⁶⁹

Scheme 15. Synthesis of 4-aminoquinazolines from *ortho*-halogenated benzonitriles.

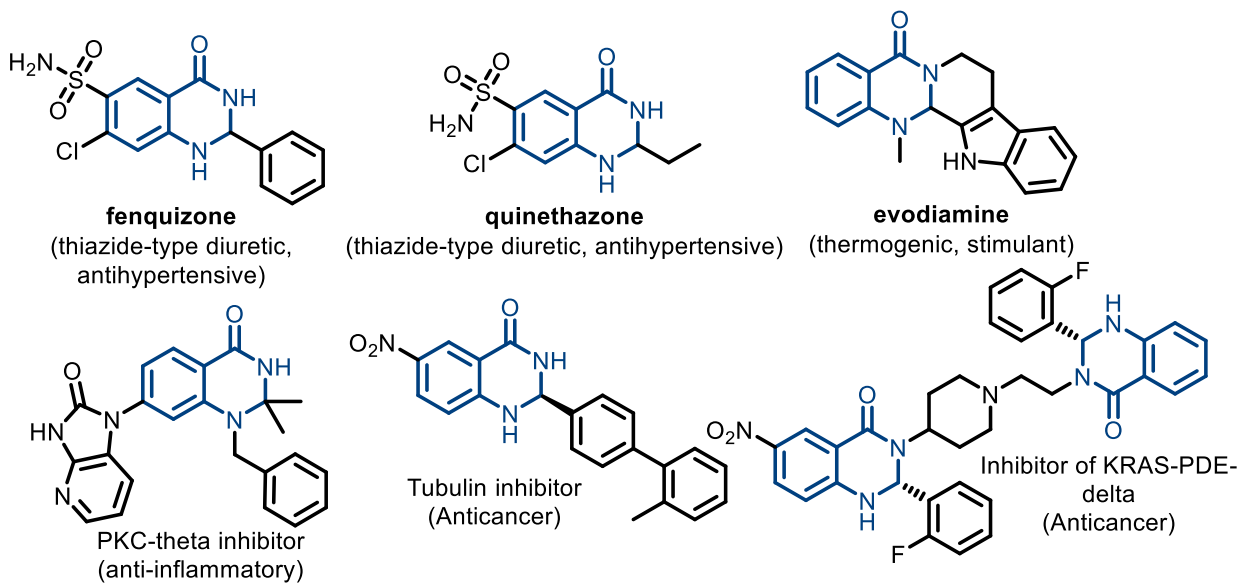


Source JIA *et al.*, 2015;^{56e} FENG; WU, 2015;⁶⁷ SHELKE *et al.*, 2015;⁶⁸ YANG *et al.*, 2010.⁶⁹

1.4 2,3-DIHYDROQUINAZOLIN-4(1H)-ONES: BIOLOGICAL IMPORTANCE AND SYNTHESIS

The 2,3-dihydroquinazolin-4(1H)-one (DHQ), a nitrogen-based heterocycle and a privileged scaffold, is present in a multitude of biologically active molecules including marketed pharmaceuticals and potential drug candidates as depicted in **figure 6**.⁷⁰ Hence, its synthesis mainly targeting 2-substituted derivatives has aroused great interest, and a vast number of synthetic protocols has been reported in the literature.

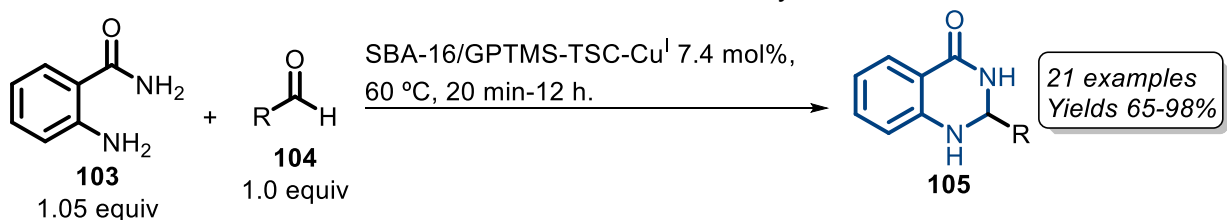
Figure 6. Some bioactive molecules containing the DHQ core.



Source: BADOLATO; AIELLO; NEAMATI, 2018;^{70a} JIANG *et al.*, 2017;^{70d} CHINIGO *et al.*, 2008.^{70b}

The most common synthetic protocols comprise the use of 2-aminobenzamides to construct the central bicyclic ring system.⁷¹ For example, a recent approach by Ghodsinia and co-workers reported the use of the heterogenous catalyst SBA-16/GPTMS-TSC-Cu^I to promote the cyclocondensation of 2-aminobenzamide **103** with aldehydes under solvent-free conditions furnishing twenty-one 2,3-dihydroquinazolin-4(1*H*)-ones in great to excellent yields (**Scheme 16**). For such, mesoporous silica SBA-16 was functionalized by aminated 3-glycidyloxypropyltrimethoxysilane with thiosemicarbazide and further treated with Cu^I.^{71a}

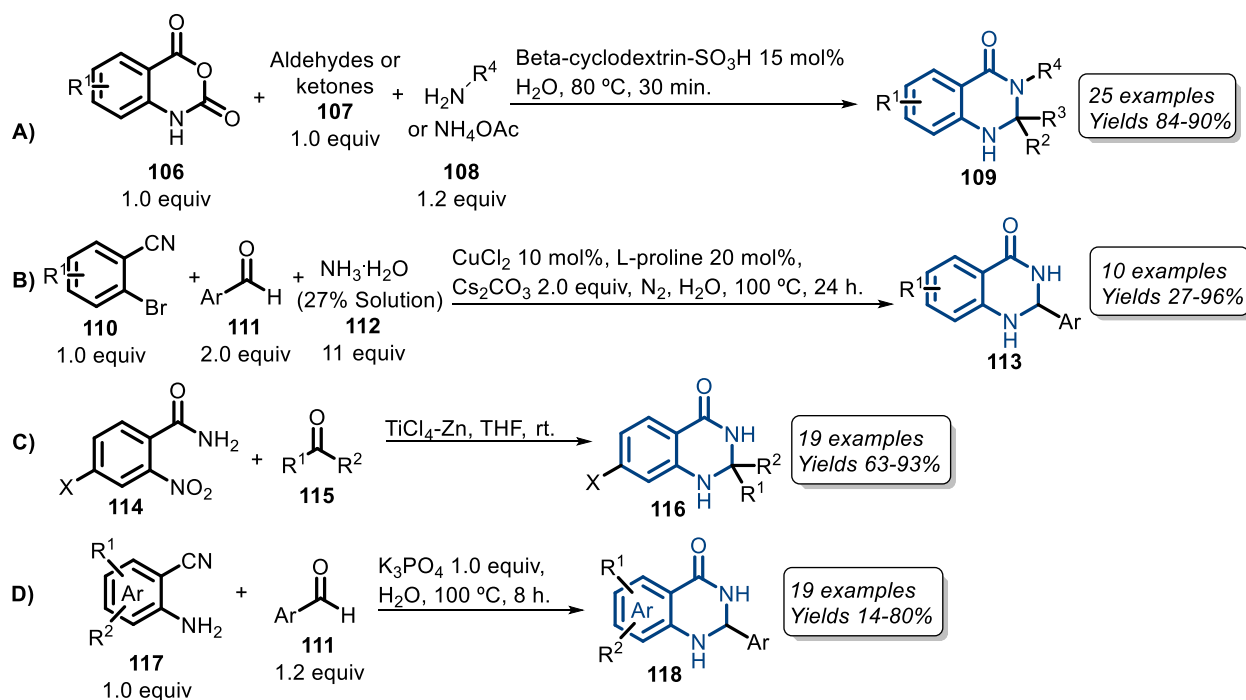
Scheme 16. Catalyzed synthesis of 2,3-dihydroquinazolin-4(1*H*)-ones by SBA-16/GPTMS-TSC-Cu^I catalyst.



Source: ERFAN; AKHLAGHINIA; GHODSINIA, 2020.^{71a}

Other suitable substrates for the synthesis of this scaffold are isatoic anhydrides,⁷² *o*-bromobenzonitriles,⁷³ 2-nitrobenzamides,⁷⁴ and 2-aminobenzonitriles or 2-aminonicotinonitrile.⁷⁵ β -cyclodextrin-SO₃H, a recyclable acid catalyst, applied to the one-pot condensation of isatoic anhydrides **106** with primary amines or ammonium acetate and aldehydes or ketones **107** in aqueous media at 80 °C. Twenty-five 2,3-dihydroquinazolin-4(1*H*)-ones were obtained with yields varying from 84 to 90% (**Scheme 17A**).^{72a} In the case of 2-bromobenzonitriles **110**, their treatment with benzaldehydes and aqueous ammonia under copper catalysis, nitrogen, and basic aqueous conditions gave 2,3-dihydro-2-aryl quinazolin-4(1*H*)-ones with yields up to 96% (**Scheme 17B**).⁷³ Besides, *o*-nitrobenzamides **114** undergo reductive cyclization in the presence of carbonyl compounds with the aid of TiCl₄/Zn in dry THF (**Scheme 17C**),⁷⁴ and 2-aminobenzonitriles **117** favorably react with aromatic aldehydes in K₃PO₄ aqueous solution (**Scheme 17D**).⁷⁵

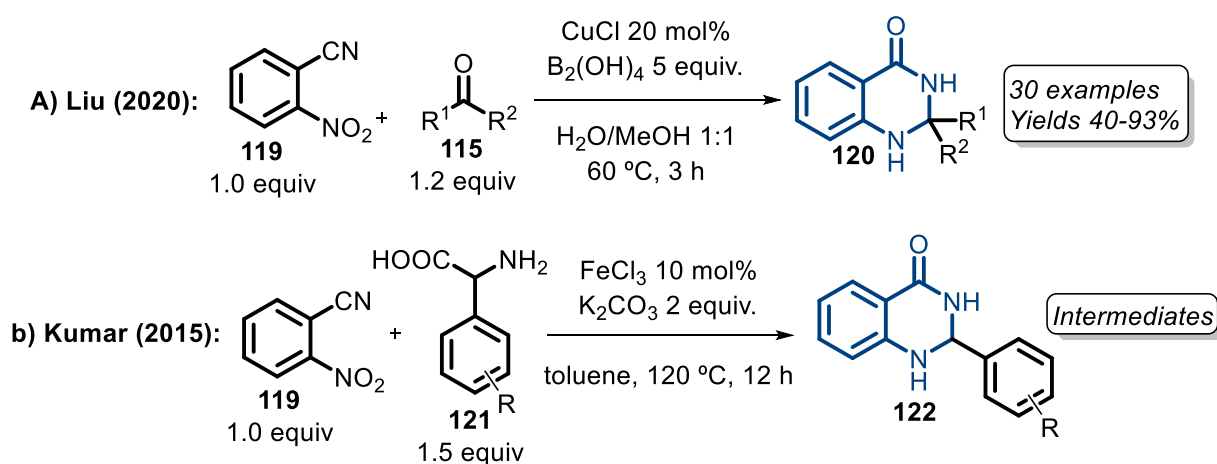
Scheme 17. Synthesis of DHQs from isatoic anhydrides, *o*-bromobenzonitriles, 2-nitrobenzamides, and 2-amino- benzonitriles or nicotinonitrile.



Source: WU *et al.*, 2014;^{72a} LIU *et al.*, 2018;⁷³ SHI *et al.*, 2003;⁷⁴ WU *et al.*, 2014.⁷⁵

Regarding the use of 2-nitrobenzonitrile as a precursor of DHQs, Liu and co-workers have recently reported a combined reduction/hydration/cyclocondensation approach requiring an excess of diboronic acid and copper as a catalyst in a water/methanol mixture.⁷⁶ DHQs were also observed by Kumar and co-workers from the reaction of the same substrate with phenylglycine in the presence of FeCl₃ and K₂CO₃ but only as intermediates.⁷⁷

Scheme 18. Synthetic procedures for the synthesis of DHQs from 2-nitrobenzonitrile.



Source: LIU *et al.*, 2020;⁷⁶ KUMAR *et al.*, 2015.⁷⁷

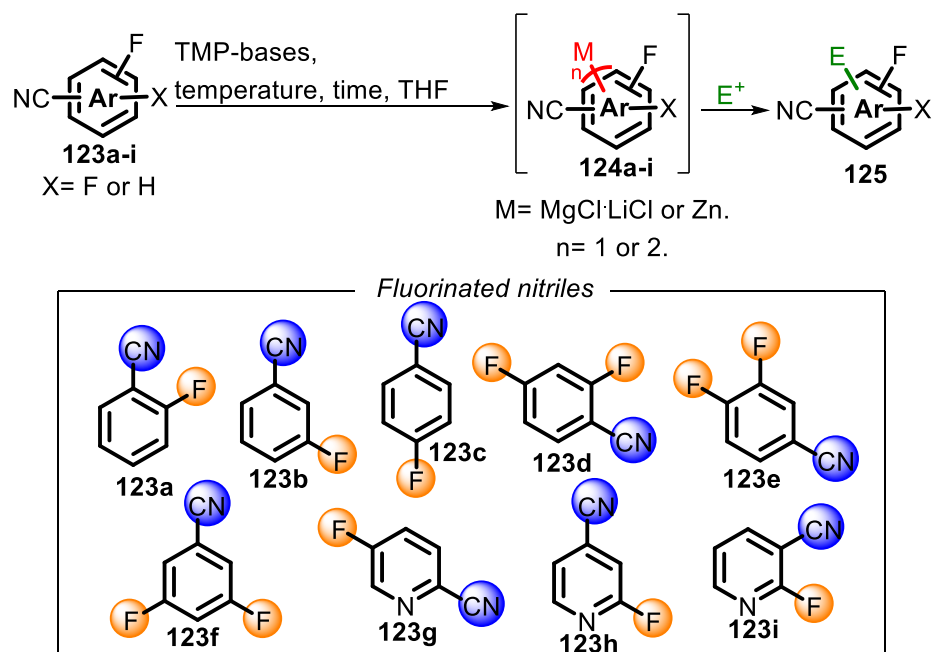
2. OBJECTIVES

In the first project, it was aimed at the regioselective metalation of fluorinated nitriles with 2,2,6,6-tetramethylpiperidyl bases (TMP-bases) to explore new and scarcely investigated metalation positions (**Scheme 19**). The subsequent trapping of the generated aromatic and heteroaromatic organometallic species with diverse electrophiles was investigated to afford functionalized building blocks. Besides, the following specific goals were settled:

- to reproduce the metalation with a TMP-base and further functionalization at gram scale for at least one substrate;
- to study sequential difunctionalization to achieve tetrasubstituted derivatives;

- to exemplify the potential of the functionalized fluorinated nitriles as building blocks in the synthesis of 4-aminoquinazolines and other heterocycles of pharmaceutical importance as synthetic applications.

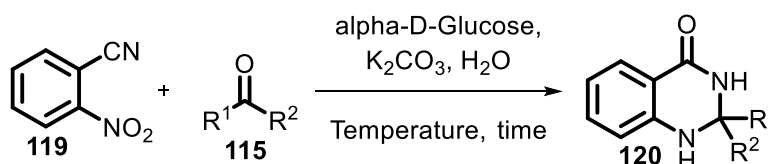
Scheme 19. The main goal from the first project and chosen substrates for study.



Source: The author.

In the second project, it was envisioned the use of glucose as an eco-friendly reductant with an aqueous solution of potassium carbonate for the synthesis of 2,3-dihydroquinazolin-4(1*H*)-ones from 2-nitrobenzonitrile in a one-pot manner (**Scheme 20**). In this scenario, the study of optimal conditions including time and temperature variation, the influence of concentration on reaction outcome, and the scope of carbonyl compounds were planned.

Scheme 20. Synthesis of DHQs with glucose as an eco-friendly reductant.



Source: The author.

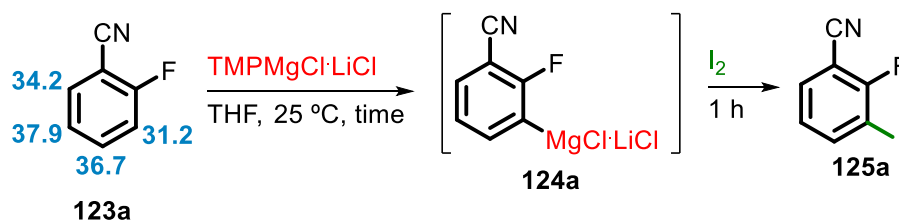
3. CHAPTER 01 - REGIOSELECTIVE FUNCTIONALIZATION OF FLUORINATED NITRILES WITH 2,2,6,6-TETRAMETHYLPYPERIDYL BASES

3.1 RESULTS AND DISCUSSIONS

3.1.1 Metalation studies and reaction scope

As standard procedures regarding characterization, nuclear magnetic resonance spectroscopy (NMR), high-resolution mass spectrometry (HRMS), and gas chromatography-mass spectrometry (GC-MS) analyses plus the determination of melting points were considered for the obtained molecules. Based on the observations for the metalation of the first studied substrate 2-fluorobenzonitrile (**123a**), 1.1 equivalents of the employed TMP-base at room temperature were defined as a reference point for the development of the synthetic protocols. Adjustments involving base equivalent, temperature, type of TMP-base, and transmetalation strategy with ZnCl₂ were made along with the study depending on the reactivity of explored substrates and stability of organometallic intermediates with the observation of side products/regioisomers or degradation.

We initiated our investigation with the selective magnesiation of C3 ($pK_a = 31.2$) for 2-fluorobenzonitrile (**123a**) by TMPMgCl·LiCl. When 1.1 equivalents of the base were employed for 1 hour at 25 °C followed by reaction with molecular iodine as the test electrophile, **125a** was verified at a 6.7:1 ratio (**Table 1, entry 1**). Extending the metalation time to 2 hours did not favor the reaction outcome, but 1.3 equivalents of TMPMgCl·LiCl in 1 hour led to the almost complete substrate-magnesiation affording 2-fluoro-3-iodobenzonitrile **125a** in 96% isolated yield after iodination and purification (**Entries 2 and 3, respectively**).

Table 1. Metalation study of 2-fluorobenzonitrile with TMPMgCl·LiCl.

Entry	TMP-base	Equiv.	Time (h)	123a (%) ^a	125a:123a ratio
1	TMPMgCl·LiCl	1.1	1	13	6.7:1
2	TMPMgCl·LiCl	1.1	2	31	2.2:1
3**	TMPMgCl·LiCl	1.3	1	1	99 ^b :1

^aRemaining starting material: percent composition – Gas chromatography (GC-FID). ^bIsolated Yield = 96%. **Defined as the standard condition.

The reaction regioselectivity can be associated with the NMR data of **125a**: its ¹H spectrum shows two doublets of doublet of doublets (δ 8.01 and 7.61 ppm) with respective coupling constants of ⁴J_{H-F} = 6.0 and 5.8 Hz, ³J_{H-H} = 7.8 and 7.6 Hz, and ⁴J_{H-H} = 1.6 and 1.6 Hz. The triplet-like signal at 7.03 ppm is attributed to C5-H with ³J_{H-H} = 7.8 Hz. Another observation that corroborates with metalation at C3 is the duplet at 82.1 ppm with a characteristic ²J_{C-F} = 24.0 Hz (¹³C NMR spectrum) for the non-hydrogenated carbon C3-I as supported by HSQC analysis (Heteronuclear Single-Quantum Coherence).

TMPMgCl·LiCl was also suitable for the magnesiation of 3-fluorobenzonitrile **123b** (Table 2). The treatment of this benzonitrile with 1.2 equivalents of the base at 25 °C with subsequent iodination afforded almost full conversion and two isomers (Entry 1) (Figure 7). The major one, C2-functionalized, was isolated in 68% yield. The loss in yield throughout purification refers to the challenging separation of the isomers due to similar retention factors on TLC. As an attempt to reduce or eliminate the other isomer, the reaction was both performed at -70 and 0 °C, but no conversion was possible (Entries 2 and 3).

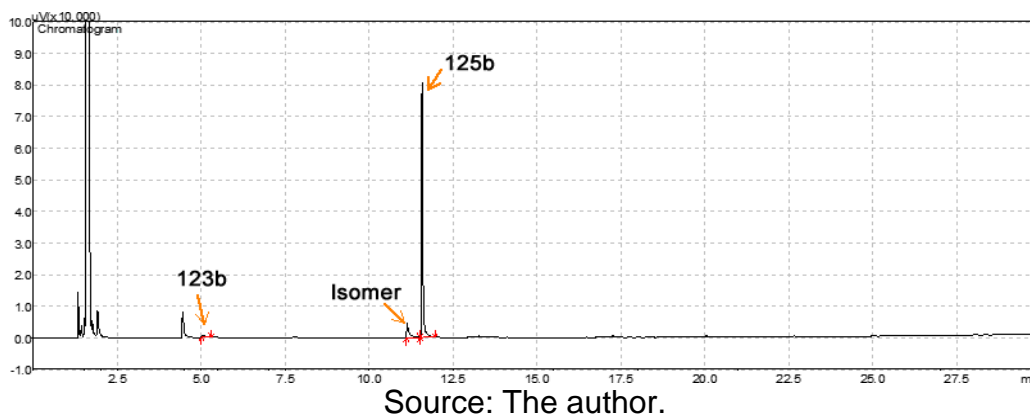
Table 2. Metalation study of 3-fluorobenzonitrile with TMPMgCl·LiCl.

Reaction scheme: 123b (3-fluorobenzonitrile) reacts with TMPMgCl·LiCl in THF at various temperatures and times to form intermediate 124b (magnesium salt). Subsequent reaction with I₂ for 1 hour yields 125b (3-fluoro-4-iodobenzonitrile) and its isomer 125b'.

Entry	Base Equiv.	Time (h)	Temp. (°C)	123b (%) ^a	125b:125b':123b ratio
1**	1.2	0.5	25	2	44:5:1
2	1.2	1	0	>99	-
3	1.3	1	-70	>99	-

^aRemaining starting material: percent composition – Gas chromatography (GC-FID).

^bIsolated Yield = 68%. **Defined as the standard condition.

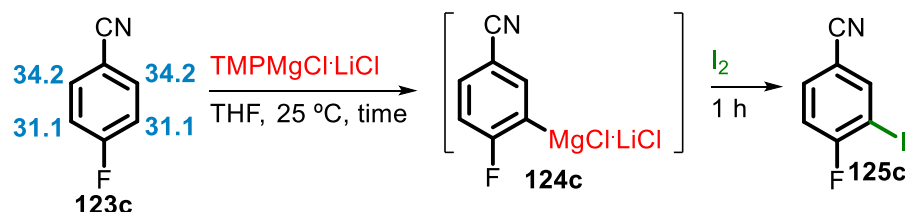
Figure 7. Chromatogram for the selective metalation and functionalization of **123b**.

Analyzing the ¹³C NMR spectrum of **125b**, the duplets at 119.9 ppm (²J_{C-F} = 24.3 Hz) and 87.1 ppm (²J_{C-F} = 29.1 Hz), respectively, are correlated with the two *ortho* carbons to C3-F. While the second signal is attributed to the iodinated carbon (C2-I), the first one refers to C4 whose hydrogen signal appears as a multiplet at 7.31 – 7.25 ppm in the ¹H NMR spectrum. Besides, the two other duplets at 130.8 (J_{C-F} = 8.1 Hz), and 130.4 ppm (J_{C-F} = 3.7 Hz) refer to C5 and C6, respectively. In the case of 3-fluoro-4-iodobenzonitrile, three separated signals should be expected in the ¹H NMR spectrum, two duplets and one triplet.⁷⁸

Complementing the studied group of monofluorinated benzonitriles, 1.3 equivalents of TMPMgCl·LiCl worked well for the practically complete conversion of 4-fluorobenzonitrile

(**123c**) at room temperature (25 °C) furnishing the aromatic **125c** in 82% yield after trapping with I₂ (Table 3, entry 2).

Table 3. Metalation study of 4-fluorobenzonitrile with TMPMgCl·LiCl.



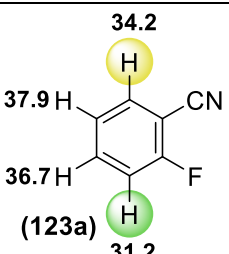
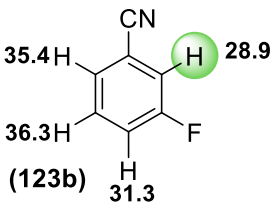
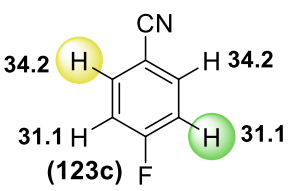
Entry	TMP-base	Equiv.	Time (h)	123c (%) ^a	125c:123c ratio
1	TMPMgCl·LiCl	1.2	1	6	15.7:1
2**	TMPMgCl·LiCl	1.3	1	trace	>99 ^b :1

^aRemaining starting material: percent composition – Gas chromatography (GC-FID). ^bIsolated Yield = 82%. **Defined as the standard condition.

The nitrile **123c** has two adjacent metalation sites to the fluorine group with expected coupling constants of type ²J_{C-F}. For the **125c** ¹³C NMR spectrum, a duplet at 82.3 ppm (²J_{C-F} = 27.3 Hz) is attributed to a non-hydrogenated carbon (HSQC), the iodinated carbon C3. Moreover, its ¹H NMR spectrum shows a doublet of doublets at 8.07 ppm (⁴J_{C-F} = 5.7 Hz and ⁴J_{H-H} = 2.0 Hz) for C2-H. This hydrogen couples with C6-H which is correlated with the doublet of doublet of doublets at 7.65 ppm (³J_{H-H} = 8.5 Hz, ⁴J_{C-F} = 4.6 Hz, and ⁴J_{H-H} = 2.0 Hz). For C5-H, another doublet of doublets is shown at 7.17 ppm (³J_{H-H} = 8.5 Hz and ³J_{C-F} = 7.4 Hz).

Most synthetic strategies concerning the metalation of fluorinated nitriles **123a–c** involve the C2 or C6 positions. About **123b**, Knochel and co-workers were able to directly zincate⁷⁹ and ferrate⁸⁰ the same position achieved with TMPMgCl·LiCl, C2, but longer metalation times were required, 12 and 9 hours, respectively. The regioselective functionalization of C3 has only been accomplished by lithiation with LiTMP⁸² for **123a** and sodiation with *i*Pr₂NNa⁸⁷, lithiation with LDA⁸⁶ or ferration with [(dioxane)_{0.5}NaFe{N(SiMe₃)₂]₃]⁸⁸ for **123c** including important drawbacks, such as long metalation times, need for low or high temperatures, and limited scope (Table 4).

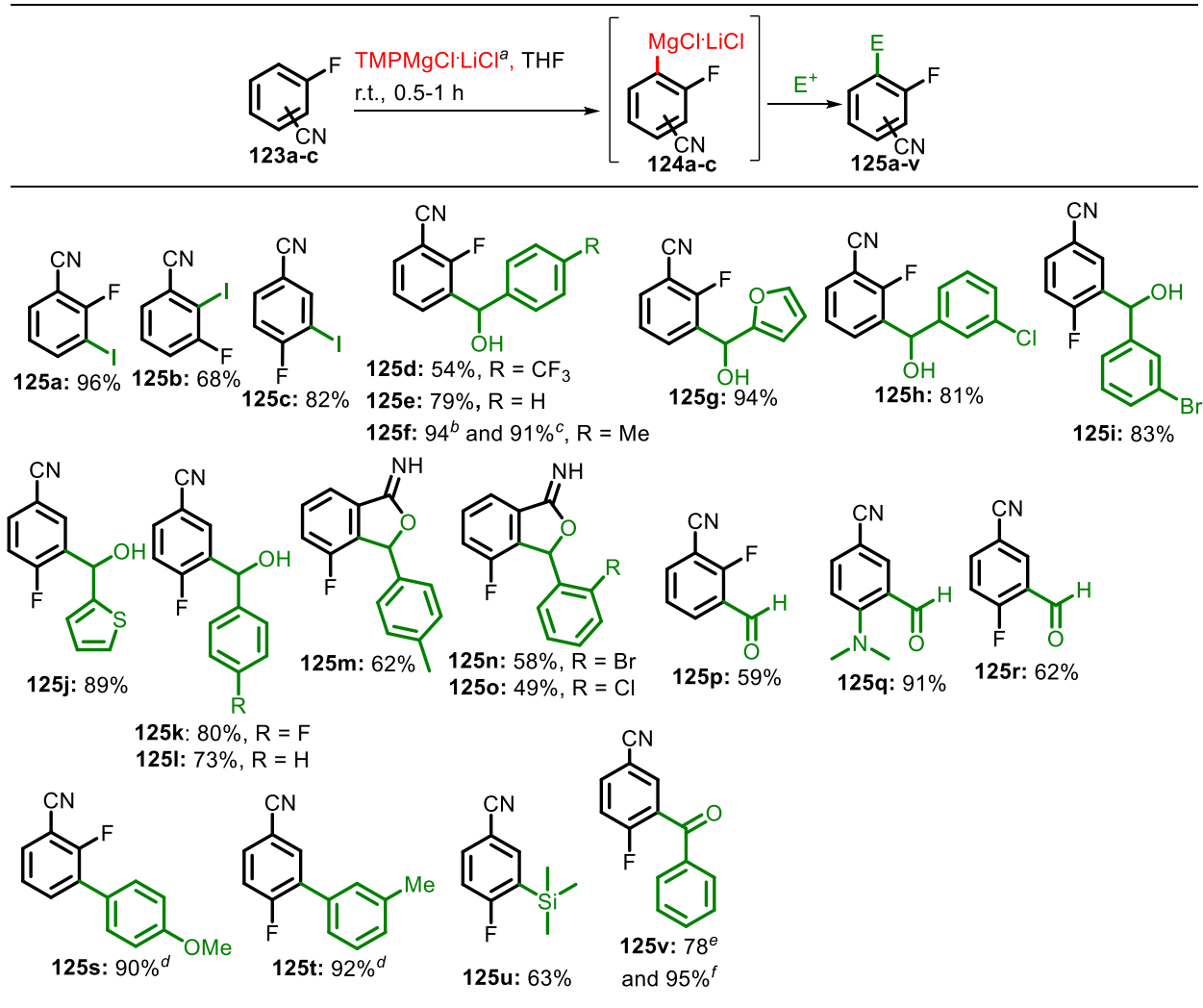
Table 4. Metalation sites of **123a–c** explored in this work and the literature.

Substrates*	H^a	H^b
 <p>(123a)</p>	a. (TMP) ₂ Zn·2MgCl ₂ ·2LiCl, 12 h, 0 °C to rt. ⁷⁹ b. (TMP) ₂ Zn·2MgCl ₂ ·2LiCl, 3 h, 80 °C. ⁸⁰ c. [tBu(<i>i</i> Pr)N] ₂ Zn·2MgCl ₂ ·2LiCl 140 °C, 2 h. ⁸¹	a. LiTMP, -50 °C, 0.5 h. ⁸² b. TMPMgCl·LiCl 1 h, rt. (This work)
 <p>(123b)</p>	-	a. (TMP) ₂ Zn·2MgCl ₂ ·2LiCl, 12 h, 0 °C to r.t. ⁷⁹ b. (TMP) ₂ Fe·2MgCl ₂ ·4LiCl, 25 °C, 9 h. ⁸³ c. TMPMgCl·LiCl 0.5 h, rt. (This work).
 <p>(123c)</p>	a. (TMP) ₂ Zn·2MgCl ₂ ·2LiCl, 3 h, 80 °C. ⁸⁰ b. [tBu(<i>i</i> Pr)N] ₂ Zn·2MgCl ₂ ·2LiCl 100 °C, 2 h. ⁸¹ c. (TMP) ₂ Fe·2MgCl ₂ ·4LiCl, 25 °C, 18 h. ⁸³ d. (TMP) ₂ Mn·2MgCl ₂ ·4LiCl 25 °C, 2 h. ⁸⁴ e. (TMP) ₃ La·3MgCl ₂ ·5LiCl, 0 °C, 1 h. ⁸⁵	a. LDA, -75 °C, 1 h. ⁸⁶ b. <i>i</i> PrNNa (NaDA), 0.5 s, -78 °C (Flow reactor). ⁸⁷ c. [(dioxane) _{0.5} NaFe{N(SiMe ₃) ₂ } ₃], 2 days at 50 °C. ⁸⁸ d. TMPMgCl·LiCl 1 h, rt. (This work).

*pK_a values are listed. ^aYellow = literature. ^bLight-green = both, literature and this work.

With the established optimal conditions for the metalation of nitriles **123a–c**, the reactivity of the derived organomagnesium species were investigated with varied electrophiles (**Table 5**).

Table 5. Magnesiumation of **123a–c** with $\text{TMPMgCl}\cdot\text{LiCl}$ followed by trapping with diverse electrophiles.*



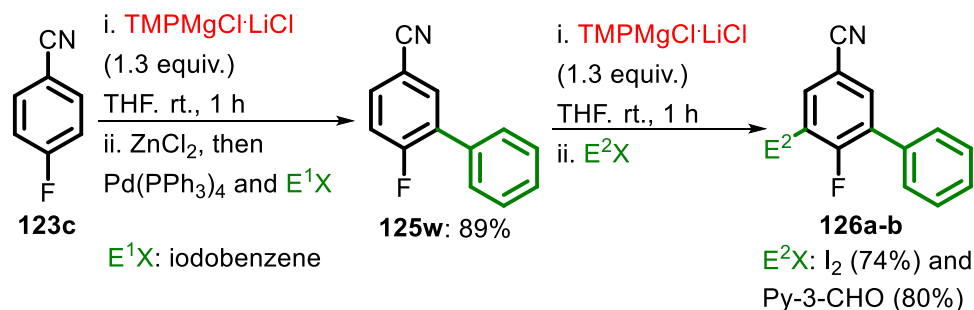
*Isolated yields. ^a1.2 equiv. for **123a** (0.5 h) and 1.3 equiv. for **123b,c** (1 h). ^b0.5 mmol scale. ^c5.5 mmol scale (1.21 g). ^d ZnCl_2 (1 M in THF) followed by Negishi cross-coupling with $\text{Pd}(\text{PPh}_3)_4$. ^eTransmetalation with $\text{CuCl}\cdot 2\text{LiCl}$ (0.5 M in THF) followed by reaction with BzCl . ^f ZnCl_2 (1 M in THF) followed by $\text{Pd}(\text{PPh}_3)_4$ catalyzed benzoylation.

Treating **124a,c** with electron-rich and -deficient aldehydes, provided a library of alcohols (**125d–l**) in yields up to 94%. Notably, the synthesis of **125f** was performed at gram scale without meaningful loss in yield (91%). On the other hand, treatment of the 3-fluorobenzonitrile-derived Grignard species (**124b**) with aldehydes afforded fluorinated isobenzofuran-1(3*H*)-imines **125m–o** in 49–62% yields. Furthermore, while the reaction of **124a** with dimethylformamide provided aldehyde **125p** in 59% yield, **124c** underwent fluorine substitution by the *in situ* generated magnesium dimethylamide and resulted in

tertiary amine **125q** in 91% yield under the same formylation conditions. Nonetheless, when *N*-methylformanilide was employed as the electrophile, aldehyde **125r** was obtained in 62% yield. After transmetalation of **124a,c** with ZnCl_2 and subsequent addition of $\text{Pd}(\text{PPh}_3)_4$ and iodoarenes, Negishi cross-couplings were performed for **125s** and **125t**, in high yields (90% and 92%, respectively). The reaction of **124c** with trimethylsilyl chloride gave the silylated aromatic **125u** in 63% yield. Transmetalation of **124c** with $\text{CuCl}\cdot 2\text{LiCl}$ with the subsequent addition of benzoyl chloride afforded the ketone **125v** in 78% yield. As an alternative, the synthesis of the same ketone was possible by palladium-catalyzed benzoylation with an even higher yield (**125v**: 95%).

Aiming at the synthesis of tetrasubstituted derivatives, the biaryl **125w** was prepared from **123c** and subjected to metalation via the same base, $\text{TMPMgCl}\cdot\text{LiCl}$, to provide **126a–b** in great yields after reaction with I_2 and 3-pyridinecarbaldehyde (**Scheme 21**).

Scheme 21. Synthesis of tetrasubstituted aromatics **126a–b** through consecutive metalation-functionalization sequences.

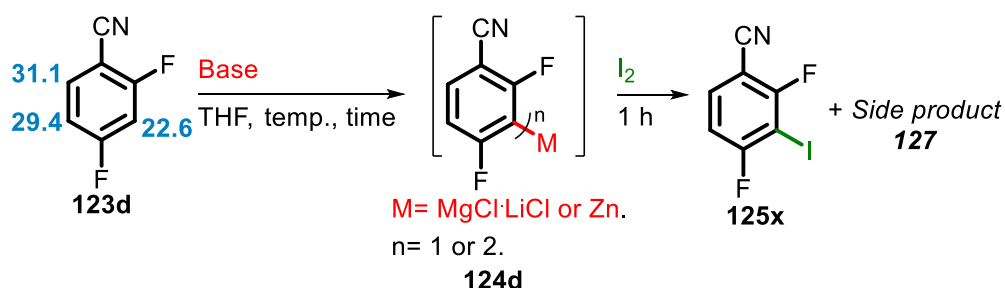


Source: The author.

Considering the suitability of $\text{TMPMgCl}\cdot\text{LiCl}$ in the magnesiation of fluorinated nitriles **123a–c**, this base was then explored for the metalation of nitriles of difficult selectivity control, the difluorinated nitriles **123d–f**. For the metalation of 2,4-difluorobenzonitrile **123d**, increasing the amount of base at 25 °C led to better conversion rates (**Table 6, entries 1–3**). Although 1.3 equivalents of $\text{TMPMgCl}\cdot\text{LiCl}$ afforded the best conversion profile to this point, **125x** was isolated in only 63% (**Entry 3**). Besides the observation of a side product, a putative dimer, the reaction medium always turned black in 1 hour suggesting some sort of degradation not detected by gas

chromatography. To overcome this issue, the reaction was performed at 0 °C instead, leading to the full conversion of **123d** (**Figure 8**) with an isolated yield of 80% for **125x** (**Entry 4**). Notably, (TMP)₂Zn·2MgCl₂·2LiCl allowed the metalation-functionalization of the same position at 25 °C, C3, furnishing **125x** in a higher yield (93%) and establishing a great alternative to the direct zincation of **123d** (**Entry 5**).

Table 6. Metalation study of 2,4-difluorobenzonitrile **123d** with TMP-bases.

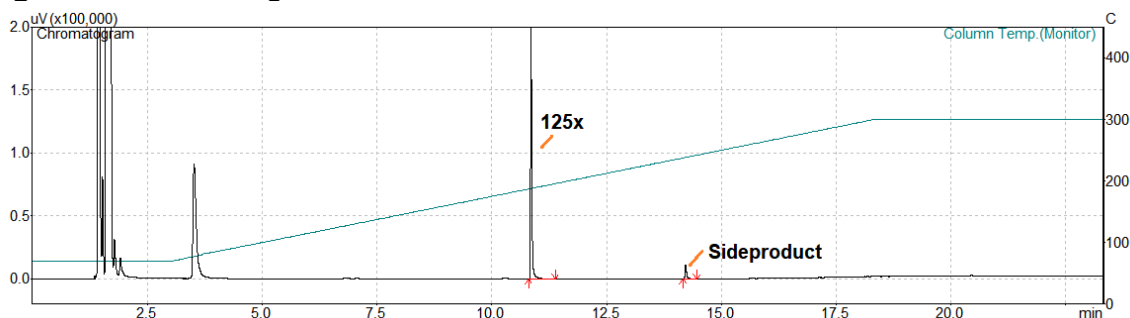


Entry	TMP-base	Equiv.	Time (h)	Temp. (°C)	123d (%) ^a	125x:127:123d ratio
1	TMPMgCl·LiCl	1.04	1	25	16	4.4:0.8:1
2	TMPMgCl·LiCl	1.20	1	25	13	5.7:1:1
3	TMPMgCl·LiCl	1.30	1	25	2	47.5 ^b :1.5:1
4 ^{**}	TMPMgCl·LiCl	1.30	1	0	none	(15.7 ^c :1) ^d
5 ^{**}	(TMP) ₂ Zn·2MgCl ₂ ·2LiCl	0.65	1	25	4	(24 ^e :1) ^f

^aRemaining starting material: percent composition – Gas chromatography (GC-FID).

^bIsolated Yield = 63%. ^cIsolated Yield = 80%. ^dFull conversion. Ratio = 125x:127. ^eIsolated Yield = 93%. ^f125x:123d ratio. No side product was observed. ^{**}Defined as the standard conditions.

Figure 8. Chromatogram for the selective metalation and functionalization of **123d**.

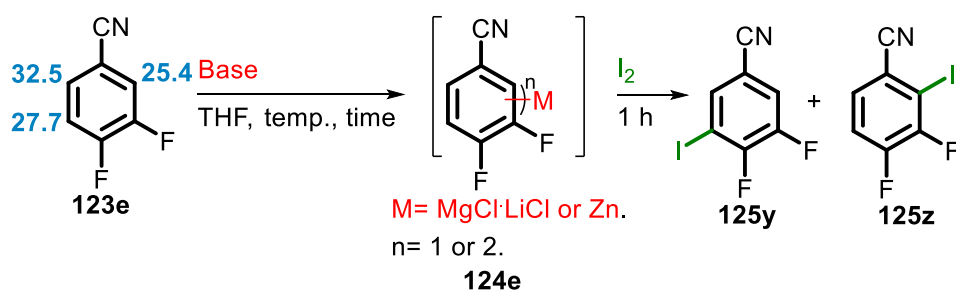


Source: The author.

The ^1H NMR spectrum of **125x** shows a doublet of doublet of doublets at 7.65 ppm with a coupling constant $^3J_{\text{H-H}} = 8.7$ Hz which is consistent with an H-H *ortho* coupling and $^4J_{\text{H-F}} = 7.1$ and 5.7 Hz due to coupling between C6-H and the two fluoro groups (C2-F and C4-F). Besides, $^3J_{\text{H-F}} = 6.8$ Hz and $^5J_{\text{H-F}} = 1.5$ Hz for the doublet of doublet of doublets at 7.02 ppm are compatible with C5-H and the same fluoro groups. The functionalization of C3 is also sustained by the duplet at 72.7 ppm ($^2J_{\text{C-F}} = 30.7$ and 27.9 Hz) which is attributed to the non-hydrogenated carbon C3-I in its ^{13}C NMR spectrum.

When 3,4-difluorobenzonitrile **123e** was treated with 1.2 equivalents of $\text{TMPMgCl}\cdot\text{LiCl}$ at 25 °C, the conversion rate was poor, the reaction medium immediately turned black, and the tetrasubstituted nitrile **125z** was detected (**Table 7, Entry 1**). Interestingly, working at 0 °C afforded the regioisomer **125y** as the major one with a better conversion profile (**Entry 2**). Increasing the base amount to 1.5 equivalents but keeping the temperature led to almost full consumption of the starting material (**Entry 4**). Notwithstanding this result, **125y** was isolated in only 51% yield. As an attempt to surpass this obstacle, the metalation temperature was decreased to -70 °C, but the yield slightly increased to 63% (**Entry 5**). Although no side products were detected by gas chromatography analysis, additional compounds were spotted via TLC. Thinking of it to be a high reactivity-related subject of the generated organomagnesium species even at -70 °C, transmetalation with ZnCl_2 was considered to generate more stable organometallic species. As a result, **125y** was isolated in 75% yield after iodination (**Entry 6**). On the other hand, application of $(\text{TMP})_2\text{Zn}\cdot 2\text{MgCl}_2\cdot 2\text{LiCl}$ at 25 °C exclusively furnished **125z** in 76% with the functionalization of position C2 (**Entry 7**).

Table 7. Metalation study of 3,4-difluorobenzonitrile **123e** with TMP-bases.



Entry	TMP-base	Equiv.	Time (h)	Temp. (°C)	123e (%) ^a	125y:125z:123e ratio
1	TMPMgCl·LiCl	1.20	1	25	88	0.14:1 ^b
2	TMPMgCl·LiCl	1.20	1	0	18	3.8:0.7:1
3	TMPMgCl·LiCl	1.30	1	0	13	5.6:1.1:1
4	TMPMgCl·LiCl	1.50	1	0	2	39 ^c :10:1
5	TMPMgCl·LiCl	1.50	1	-70	2	41.5 ^e :7.5:1
6 ^{d**}	TMPMgCl·LiCl	1.50	1	-70	3	27.7 ^f :4.7:1
7 ^{**}	(TMP) ₂ Zn·2MgCl ₂ ·2LiCl	0.75	1	25	9	0.33:9.7 ^g :1

^aRemaining starting material: percent composition – Gas chromatography (GC-FID). ^b125z:123e ratio. No 125y was verified. ^cIsolated Yield = 51%. ^dAfter metalation at -70 °C, 1.5 equiv. of ZnCl₂ were added to the mixture prior iodination at 25 °C. ^eIsolated yield = 63%. ^fIsolated yield = 75%. ^gIsolated yield = 76%. ^{**}Defined as the standard conditions.

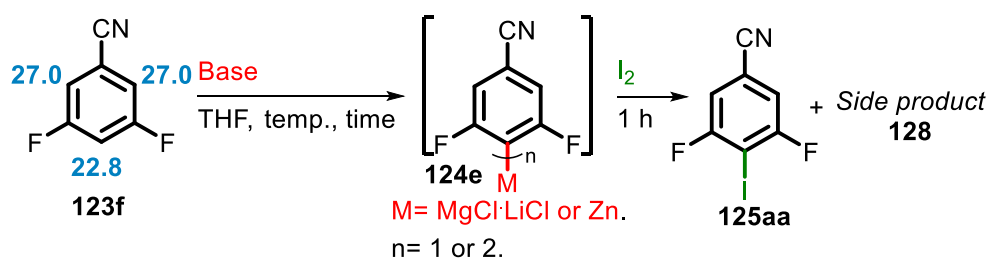
Regarding the ¹H NMR spectrum of **125y**, the coupling constant $J = 1.9$ Hz for both the doublet of triplets at 7.85 ppm and a doublet of doublet of doublets at 7.49 ppm is consistent with a *meta* H-H coupling (⁴ J_{H-H}). For the **125y** ¹³C NMR spectrum, a duplet at 83.7 ppm (² $J_{C-F} = 23.9$ Hz) is attributed to a non-hydrogenated carbon (HSQC), the iodinated carbon C5. Moreover, the coupling constant $J = 20.6$ Hz for the doublet of doublets at 121.6 ppm is characteristic of ² J_{C-F} being correlated with C2-H and C3-E coupling. For the other hydrogenated carbon, C6-H, a doublet of doublets is shown at 138.4 ppm with ³ $J_{C-F} = 4.0$ Hz.

In the case of **125z** ¹H NMR spectrum, the coupling constant $J = 8.8$ Hz for both the doublet of doublet of doublets at 7.40 ppm and the triplet of doublets at 7.29 ppm is compatible with an *ortho* H-H coupling (³ J_{H-H}). Its ¹³C NMR spectrum shows a duplet at 89.1 ppm (d, ² $J_{C-F} = 25.3$ Hz) for C2-I while a doublet of doublets at 118.6 ppm refers to C5-H with a coupling constant ² $J_{C-F} = 18.9$ Hz.

As observed for the metalation of **123e** at 25 °C, the reaction medium for **123f** turned black as soon as TMPMgCl·LiCl was added to the system, and a complex mixture was obtained after transference of I₂ solution in THF (**Table 8, Entry 1**). However, the product **125aa** was detected plus a side product via gas chromatography when **123f** was deprotometalated at 0 °C (**Entry 2**). Then, it was decided to investigate the reaction outcome at a lower temperature (-30 °C) with 1.3

equivalents of the base. Remarkably, under these conditions, no side product was produced and practically full conversion was achieved with an isolated yield for **125aa** of 75% (**Entry 3**). Complementing the metalation strategies towards **123e**, (TMP)₂Zn·2MgCl₂·2LiCl allowed the metalation of the same position, C4, but at 25 °C, furnishing **125aa** in excellent yield (91%) (**Entry 4**).

Table 8. Metalation study of 3,5-difluorobenzonitrile **123f** with TMP-bases.

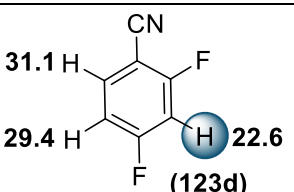
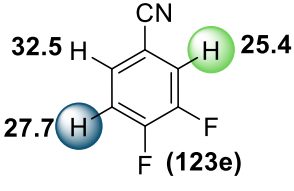
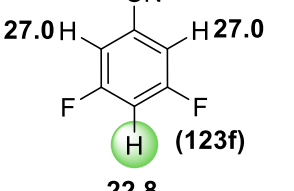


Entry	TMP-base	Equiv.	Time (h)	Temp. (°C)	123f (%) ^a	125aa:128:123f ratio
1	TMPMgCl·LiCl	1.20	1	25	none	*
2	TMPMgCl·LiCl	1.20	1	0	14	2.5:3.6:1
3**	TMPMgCl·LiCl	1.30	1	-30	1	(99 ^b :1) ^c
4**	(TMP) ₂ Zn·2MgCl ₂ ·2LiCl	0.65	1	25	1	(99 ^d :1) ^c

*A complex mixture was obtained. ^aRemaining starting material: percent composition – Gas chromatography (GC-FID). ^bIsolated Yield = 75%. ^c**125aa:123f** ratio. No side product was formed. ^dIsolated Yield = 91%. **Defined as the standard conditions.

The two hydrogens from **125aa** are assigned to a multiplet at 7.20 – 7.16 ppm (¹H NMR spectrum). Although these two hydrogens are chemically equivalent, they can be considered magnetically inequivalent. Therefore, one hydrogen would couple with the other hydrogen (⁴J) in addition to coupling with the different fluorine atoms (³J and ⁵J, respectively). The triplet at 79.1 ppm (²J_{C-F} = 29.4 Hz) stands for C4-I (¹³C NMR spectrum).

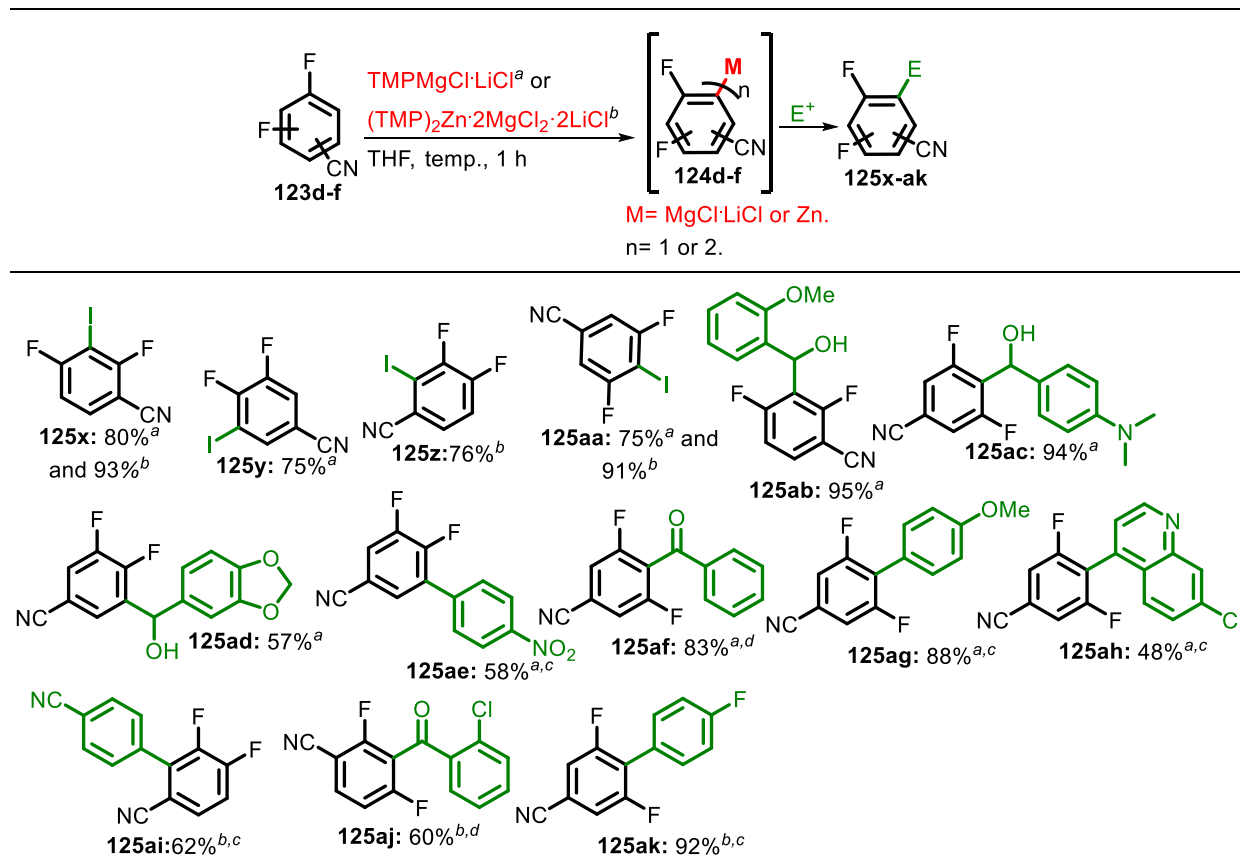
Table 9. Metalation sites of **123d–f** explored in this work and the literature.

Substrates*	H^a	H^b
 <p>31.1 H 29.4 H 22.6 H (123d)</p>	<p>a. TMPMgCl·LiCl 1 h, 0 °C (This work). b. (TMP)₂Zn·2MgCl₂·2LiCl, 1 h, rt. (This work).</p>	-
 <p>32.5 H 27.7 H 25.4 H (123e)</p>	<p>TMPMgCl·LiCl 1 h, -70 °C (This work).</p>	<p>a. TMPZnCl·LiCl, 80 °C, 12 h.⁸⁹ b. (TMP)₂Zn·2MgCl₂·2LiCl, 1 h, r.t. (This work).</p>
 <p>27.0 H 27.0 H 22.8 H (123f)</p>	-	<p>a. LDA, -78 °C, 1 h.⁹⁰ b. TMPMgCl·LiCl 1 h, -30 °C (This work). c. (TMP)₂Zn·2MgCl₂·2LiCl, 1 h, rt. (This work).</p>

*pK_a values are listed. ^aBlue = only this work. ^bLight-green = both, literature and this work.

Regarding the literature, only positions C2 for **123e** and C4 for **123f** have been metalated with **TMPZnCl·LiCl** in 12 h at 80 °C⁸⁹ and by **LDA** in 1 h at -78 °C,⁹⁰ respectively (**Table 9**). As advantages of the developed methodologies over these protocols, **(TMP)₂Zn·2MgCl₂·2LiCl** allows the metalation to be performed in 1 hour at 25 °C, and **TMPMgCl·LiCl** makes it possible to access position C5, a new metalation site for **123e**.

Table 10. Metalation and functionalization of difluorobenzonitriles **123d–f** with TMP-bases.*



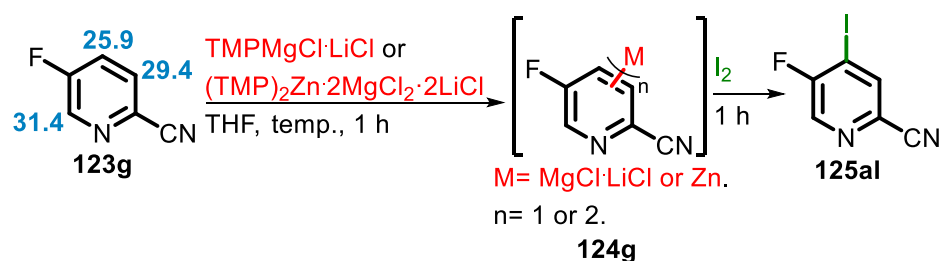
*Isolated yields. ^a1.3 equiv. for both 2,4-difluorobenzonitrile (**123d**) at 0 °C and 3,5-difluorobenzonitrile (**123f**) at -30 °C, and 1.5 equiv. for 3,4-difluorobenzonitrile (**123e**) at -70 °C. ^b0.65 equiv. for both **123d** and **123f**, and 0.75 equiv. for **123e** at room temperature. ^cZnCl₂ (1 M in THF) except for **125ai** followed by Negishi cross-coupling with Pd(PPh₃)₄. ^dZnCl₂ (1 M in THF) except for **125aj** followed by Pd(PPh₃)₄ catalyzed benzylation.

After metalation optimization studies for nitriles **123d–f**, their organomagnesium or organozinc derived species **124d–f** were reacted with diverse electrophiles (**Table 10**). Their treatment with iodine gave iodides **125x–aa** in yields up to 93%. The reaction of the organomagnesium species **124d–f** with 2-methoxybenzaldehyde, 4-(dimethylamino)benzaldehyde, and benzo[*d*][1,3]dioxole-5-carbaldehyde yielded alcohols **125ab–ad** in 57–95% yields. After transmetalation with ZnCl₂, the obtained aromatic zincates were suitable for both palladium-catalyzed Negishi cross-coupling affording systems **125ae**, **125ag**, and **125ah** in 58%, 88%, and 48% yields, respectively, and palladium-catalyzed benzylation leading to **125af** in 83% yield. Moreover, the base (TMP)₂Zn·2MgCl₂·2LiCl was used for the direct zincation at the C2 position of **123e** with

subsequent use in the synthesis of biaryl products **125ai** (62% yield) and **125ak** (92% yield), and the ketone **125aj** (60% yield) under palladium catalysis.

Lastly, the metalation of fluorinated pyridinecarbonitriles **123g–l** was assayed with the TMP-bases successfully employed before. Considering the need for low temperatures in the metalation of deactivated pyridines (e.g. 3-fluoropyridine) by $\text{TMPMgCl}\cdot\text{LiCl}$ ³², it was initially decided to treat 5-fluoropicolinonitrile **123g** with 1.2 equivalents of this base at $-30\text{ }^\circ\text{C}$. Favorably, the aryl iodide **125al** was observed with a tiny amount left of the starting material (**Table 11, Entry 1**). Increasing the base amount to 1.3 equivalents at the same temperature in 1 hour led to the full conversion of nitrile **123g** in the desired product after reaction with iodine (70% isolated yield) (**Entry 2**). When $(\text{TMP})_2\text{Zn}\cdot 2\text{MgCl}_2\cdot 2\text{LiCl}$ was considered at $25\text{ }^\circ\text{C}$, a mixture of **125al** with a side product, a putative regioisomer, was obtained at a 1.3:1 ratio.

Table 11. Metalation study of 5-fluoropicolinonitrile **123g** with TMP-bases.



Entry	TMP-base	Equiv.	Time (h)	Temp. (°C)	123g (%) ^a	125al:123g ratio
1	$\text{TMPMgCl}\cdot\text{LiCl}$	1.20	1	-30	10	9:1
2**	$\text{TMPMgCl}\cdot\text{LiCl}$	1.30	1	-30	none	>99 ^b :1
3	$(\text{TMP})_2\text{Zn}\cdot 2\text{MgCl}_2\cdot 2\text{LiCl}$	0.65	1	25	1	*

^aRemaining starting material: percent composition – Gas chromatography (GC-FID).

^bIsolated Yield = 70%. *Not selective: a mixture of 125al:side product at 1.3:1 ratio was obtained. Not isolated. **Defined as the standard condition.

The deprotometalation for **123g** at 4-position is consistent with the two coupling constants of type $^2J_{\text{C-F}}$ (34.1 Hz for the duplet at 139.1 ppm and 24.8 Hz for the duplet at 93.1 ppm) in its ¹³C NMR spectrum. The first duplet is assigned to C6 and the second one to the halogenated carbon (C4) in **125al**. In the case of a C6

functionalization, a hydrogen-hydrogen coupling ($^3J_{H4-H3}$) and a hydrogen-fluorine coupling ($^3J_{H4-F}$) would be expected with different signals in the 1H NMR spectrum, a possible triplet and a doublet of doublets. Additionally, there are correlations between carbon C4-I and hydrogens C3-H and C6-H which are separated by 2 and 3 bonds, respectively, in the HMBC (Heteronuclear Multiple Bond Correlation) correlation map. In the case of C6 functionalization, these two correlations would probably not be verified.

When 2-fluoroisonicotinonitrile **123h** was treated with 1.3 equiv. of $TMPMgCl \cdot LiCl$ at -30 °C, the reaction medium turned black from the very beginning, and decomposition was observed (**Table 12, entry 1**). Performing the metalation at -70 °C instead led to a light orange colored medium and a mixture of iodide **125am** (57% isolated yield) and a side product (**Entry 2**). Supposing the reaction of organomagnesium species of type **124h** with remaining non-metalated **123h**, transmetalation by $ZnCl_2$ was done after magnesiation at -70 °C (0.5 h) followed by iodination at 25 °C. Surprisingly, no side product was detected under these conditions and more **123h** (percent composition – GC/FID) was left non-functionalized (**Entry 3**). Increasing the base amount to 1.5 and 1.8 equivalents afforded **125am** in 68% and 69%, respectively, with no significant difference (**Entries 4 and 5**). Gratifyingly, 0.9 equiv. of $(TMP)_2Zn \cdot 2MgCl_2 \cdot 2LiCl$ allowed the metalation-functionalization of the same position, C3, but at room temperature furnishing **125am** in 76% after reaction with I_2 .

Table 12. Metalation study of 2-fluoroisonicotinonitrile **123h** with TMP-bases.

The reaction scheme shows 2-fluoroisonicotinonitrile (**123h**) reacting with $TMPMgCl \cdot LiCl$ or $(TMP)_2Zn \cdot 2MgCl_2 \cdot 2LiCl$ in THF at a certain temperature for 1 hour. This forms an intermediate **124h** where the metal M is $MgCl \cdot LiCl$ or Zn , and n is 1 or 2. Subsequent reaction with I_2 for 1 hour yields **125am** and a side product **129**. The 1H NMR chemical shifts for **123h** are 30.6, 25.7, and 35.3 ppm.

Entry	TMP-base	Equiv.	Time (h)	Temp. (°C)	123h (%) ^a	125am:129:123h ratio
1	$TMPMgCl \cdot LiCl$	1.30	1	-30	trace	*
2	$TMPMgCl \cdot LiCl$	1.30	1	-70	8	9.8 ^c :1.8:1

3^b	TMPMgCl·LiCl	1.30	1	-70	29	(2.4:1) ^d
4^b	TMPMgCl·LiCl	1.50	1	-70	26	(2.8 ^e :1) ^d
5^b	TMPMgCl·LiCl	1.80	1	-70	13	(6.7 ^f :1) ^d
6^{**}	(TMP) ₂ Zn·2MgCl ₂ ·2LiCl	0.90	1	25	15	(5.7 ^g :1) ^d

*Decomposition. ^aRemaining starting material: percent composition – Gas chromatography (GC-FID). ^bZnCl₂ 1.3 equiv. (entry 3) or 1.5 equiv. (entries 4 and 5) at -70 °C for 0.5 h after magnesiation. ^cIsolated yield = 57%. ^dRatio = **125am:123h**. No side product was verified. ^eIsolated yield = 68%. ^fIsolated yield = 69%. ^gIsolated yield = 76%. **Defined as the standard condition.

The metalation-functionalization at C3 for **123h** is sustained by the coupling constant $J = 5.0$ Hz which is consistent with an H-H *ortho* coupling between the hydrogens assigned to the doublet of doublets at 8.33 and 7.40 ppm (¹H NMR of **125am**, C6-H and C5-H, respectively). Besides, the duplet at 81.8 Hz in the ¹³C NMR spectrum is attributed with C3-I with a characteristic ²J_{C-F} = 47.1 Hz and there is a correlation between this carbon and hydrogen C5-H over 3 bonds in the HBMC correlation map.

For the metalation of 2-fluoronicotinonitrile **123i**, 1.3 equivalents of TMPMgCl·LiCl was initially employed at -30 °C followed by quenching with I₂. Similar to what was observed for the metalation of **123h**, the reaction medium turned black with a moderate conversion and the observation of a side product in a significant proportion (**Table 13, entry 1**). Increasing the base amount to 1.5 equivalents but working at -70 °C greatly improved the conversion, the reaction color remained light orange, and no side product was produced. After trapping with I₂, the iodide **125an** was isolated in 85% (**Entry 2**). As an attempt to access other metalation sites, **123i** was treated with TMPZnCl·LiCl with no conversion (**Entry 3**). Besides, (TMP)₂Zn·2MgCl₂·2LiCl led to a mixture of **125an** (minor) and a regioisomer (major) at a 1:2.8 ratio (**Entry 4**). Performing the same reaction but at 60 °C in a microwave reactor or at -20°C both for 1 h afforded only traces of **125an** and traces of the regioisomer, respectively (**Entries 5 and 6**).

Table 13. Metalation study of 2-fluoronicotinonitrile **123i** with TMP-bases.

Reaction scheme: **123i** (with ^1H NMR shifts 32.8, 28.9, 35.1) $\xrightarrow{\text{Base, THF, temp., 1 h}}$ **124i** ($M = \text{MgCl}\cdot\text{LiCl}$ or Zn , $n = 1$ or 2) $\xrightarrow{\text{I}_2, 1 \text{ h}}$ **125an** + side product **130**.

Entry	TMP-base	Equiv.	Time (h)	Temp. (°C)	123i (%) ^a	125an:130:123i ratio
1	TMPMgCl·LiCl	1.30	1	-30	30	1.5:0.8:1
2**	TMPMgCl·LiCl	1.50	1	-70	9	(10.1 ^b :1) ^c
3	TMPZnCl·LiCl	1.50	1	25	>99	None ^d
4	(TMP) ₂ Zn·2MgCl ₂ ·2LiCl	0.80	1	25	85	Regioisomers ^e
5	(TMP) ₂ Zn·2MgCl ₂ ·2LiCl	0.80	1	60 ^g	94	(0.06:1) ^c
6	(TMP) ₂ Zn·2MgCl ₂ ·2LiCl	0.80	1	-20	97	Regioisomer ^f

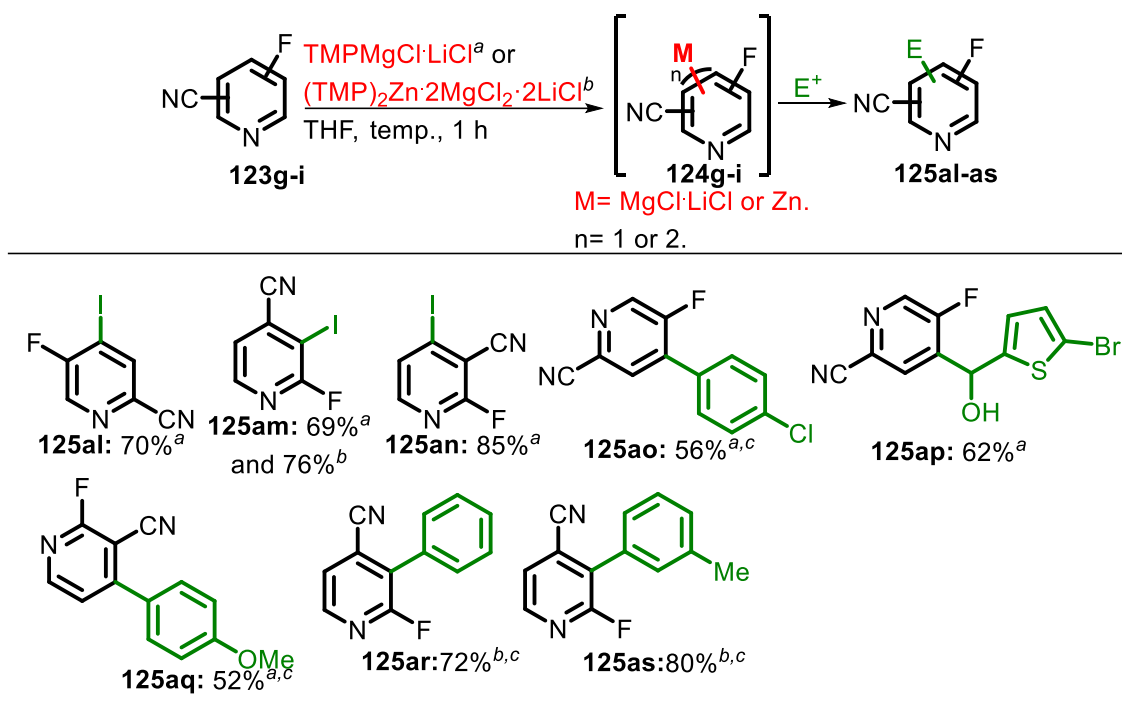
^aRemaining starting material: percent composition – Gas chromatography (GC-FID). ^bIsolated yield = 85%. ^cRatio = **125an:123i**. No side product was verified. ^dNo products were detected. ^eA mixture of regioisomers (Ratio **125an**:regioisomer = 1:2.8) was furnished with a poor conversion rate. ^fThe non-isolated regioisomer was detected (Ratio regioisomer:**123i** = 0.03:1). ^gMicrowave reactor. **Defined as the standard condition.

The ^1H NMR spectrum of **125an** displays two doublets of doublets (8.08 and 7.80 ppm) with a coupling constant $J = 5.3$ Hz, which is suggestive of an *ortho* coupling involving C6-H and C5-H. Concerning its ^{13}C NMR, the duplet at 106.4 ppm ($^2J_{\text{C-F}} = 32.7$ Hz) is assigned to C3-CN which only correlates with C5-H over 3 bonds by HMBC analysis corroborating with the scenario of a C4 metalation-functionalization.

Interestingly, no metalation reports have been found in the literature for the three studied pyridinecarbonitriles **123g-i**. To illustrate the application of the regioselectively generated organomagnesium and organozinc species by the developed metalation protocols, electrophiles including the 5-bromo-2-thiophenecarboxaldehyde and iodoarenes (1-chloro-4-iodobenzene and 4-methoxyiodobenzene) for palladium-catalyzed Negishi cross-couplings were employed in the synthesis of **125ao-aq** (52 - 62%). Moreover, zincates from 2-fluoroisonicotinonitrile **123h** were directly accessed by

(TMP)₂Zn·2MgCl₂·2LiCl at 25 °C in one hour and subsequently used in the preparation of biaryls **125ar,as** in great yields, 72 and 80%, respectively.

Table 14. Metalation and functionalization of difluorobenzonitriles **123g–i** with TMP-bases.*



*Isolated Yields. ^a1.3 equiv. for 5-fluoropicolinonitrile (**123g**) at -30 °C, and 1.5 equiv. at -70 °C for both 2-fluoronicotinonitrile (**123i**) and 2-fluoroisonicotinonitrile (**123h**). ^b(TMP)₂Zn·2MgCl₂·2LiCl (0.9 equiv. for **123h**). ^cZnCl₂ (1 M in THF) followed by Negishi cross-coupling with Pd(PPh₃)₄.

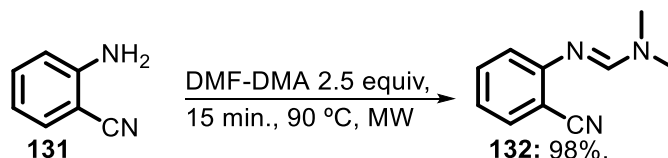
The great influence of electron-withdrawing properties of the fluoro group on the acidity of adjacent aromatic hydrogens for the studied nitriles is noticeable when the predicted pK_a values in THF by DFT (Density-functional theory) calculations are compared to the benzonitrile (Page 99). Interestingly, except for **123e** where the most acidic hydrogen was selectively abstracted by (TMP)₂Zn·2MgCl₂·2LiCl, TMPMgCl·LiCl mostly abstracted the most acidic hydrogens for the other nitriles, which are often located *ortho* to the fluoro group. It is known that this magnesium amide is prone to undergo kinetic driven metalations⁹¹ instead of the thermodynamically based ones observed for the TMP-zinc base TMPZnCl·LiCl.⁹² The thermodynamic control for the deprotonation at C2 in **123e** by (TMP)₂Zn·2MgCl₂·2LiCl can benefit from -CN and -F

electron-withdrawing properties and their effect in acidity and stabilization of the generated anion as noticed by Otsuka and coworkers for the same substrate via $\text{TMPZnCl}\cdot\text{LiCl}$.⁸⁹ Notably, despite the coordinating capability of nitrogen from pyridines to the metal center in $\text{TMPMgCl}\cdot\text{LiCl}$ as explored by Knochel and co-workers,³² the directing properties of fluoro and cyano groups implied the observed regioselectivity for the studied pyridines **123g-i**.

3.1.2 Synthesis of 4-aminoquinazolines and other heterocycles as synthetic applications

Initially, the 2-aminobenzonitrile **131** was reacted with 1,1-dimethoxy-*N,N*-dimethylmethanimine (DMF-DMA) under microwave irradiation for 15 minutes to afford (*E*)-*N'*-(2-cyanophenyl)-*N,N*-dimethylformimidamide **132** in 98% (**Scheme 22**).⁶⁶

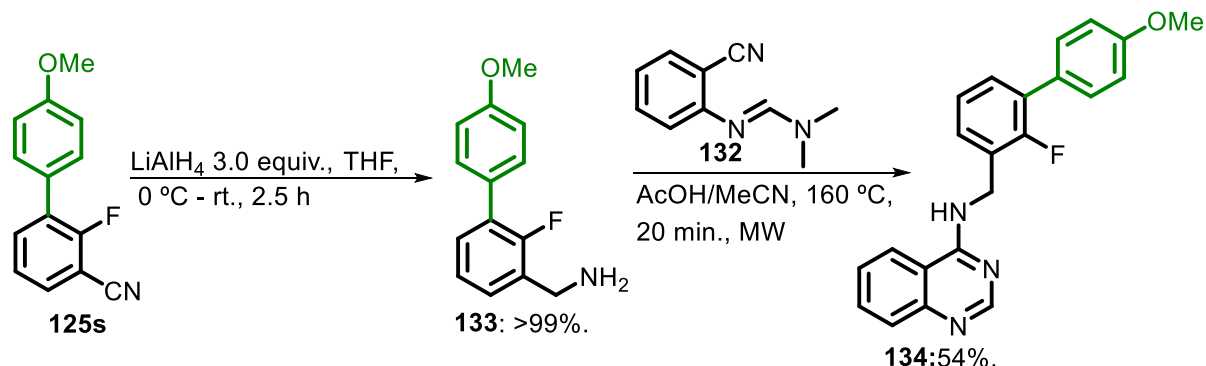
Scheme 22. Synthesis of (*E*)-*N'*-(2-cyanophenyl)-*N,N*-dimethylformimidamide **132**.



Source: The author.

Then, to illustrate the potential application of the functionalized building blocks in the construction of heterocyclic systems of pharmaceutical relevance, a 4-aminoquinazoline, **125s** was reduced to the respective benzylamine **133** in quantitative yield¹²⁷ and subsequently applied without purification to the preparation of *N*-((2-fluoro-4'-methoxy-[1,1'-biphenyl]-3-yl)methyl)quinazolin-4-amine **134** in 54% as a white solid (**Scheme 23**). The desired cyclization through Dimroth rearrangement was performed under microwave irradiation at 160 °C for 20 minutes as an adaptation of the work of Besson and co-workers.⁶⁶

Scheme 23. Synthesis of 4-aminoquinazoline **134**.



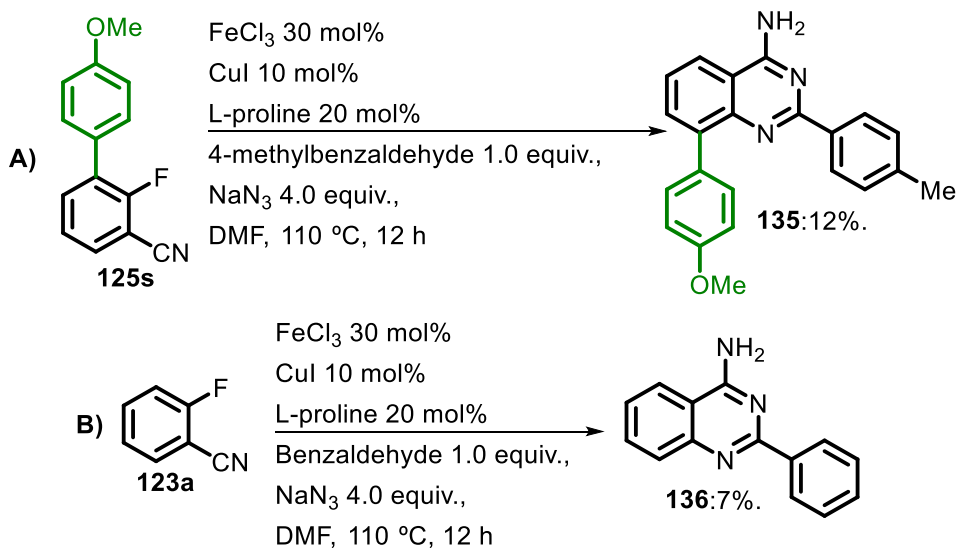
Source: The author.

Besides, based on the successful Fe(III) and Cu(I) catalyzed conversion of 2-fluorobenzonitrile in 2-phenylquinazolin-4-amine by Wu and co-workers,^{56e} their domino protocol was investigated for **125s** with 4-methylbenzaldehyde (**Scheme 24A**). After 12 hours at 110 °C and under air, **135** was spotted via TLC in conjunction with very polar yellow substances (Hexanes:AcOEt 7:3). Unfortunately, **135** was isolated in low yield (12%). The other fractions from column chromatography were sent to NMR analysis but no conclusion was possible about their identity. By facing this matter, it was decided to reproduce the exact reaction done by Wu and co-workers (**Scheme 24B**). However, a low yield (7%) was also obtained for 4-aminoquinazoline **136**.

Trying to reason the observed low yields, it was noticed that the employed DMF by the researchers was distilled from magnesium sulfate before use and, therefore, still contained traces of water. The used DMF, however, was dried with CaH₂, distilled, and stored over 4Å molecular sieves. Since water is expected to aid copper reduction (Cu^{III} to Cu^I) as pointed out by the authors in the general mechanism, this must have been the issue.

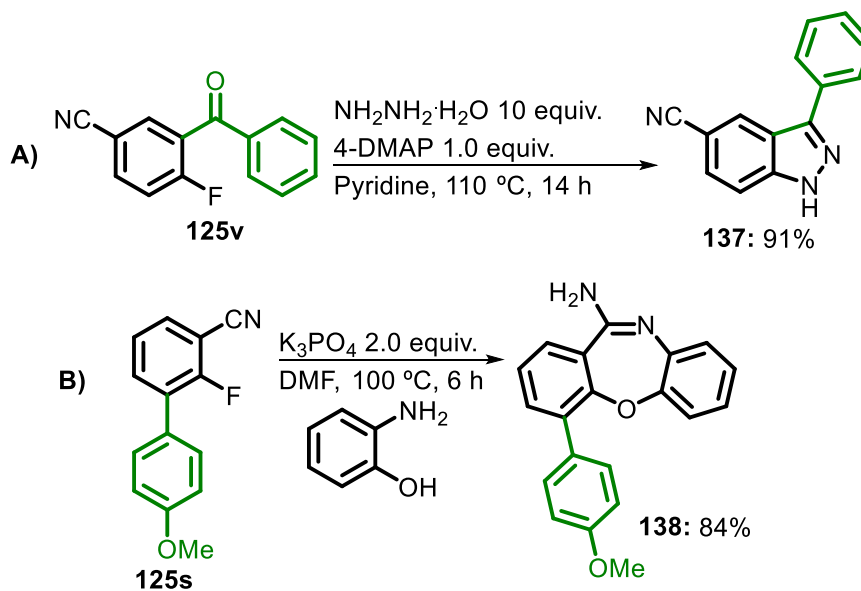
Afterward, DMF was treated as in their procedure and the model reaction (**Scheme 14B**) was repeated. Nonetheless, **136** was furnished in only 10%. An extra attempt was made by adding water to the reaction (3.0 equiv.), but no significant change in yield was observed.

Scheme 24. Synthesis of 8-(4-methoxyphenyl)-2-(*p*-tolyl)quinazolin-4-amine **135**.



Source: The author.

Scheme 25. Synthesis of 1*H*-indazole **137** and dibenzoxazepinamine **138**.



Source: The author.

In addition to the synthesis heterocycles of great interest by employing the functionalized nitriles as building blocks, **125v** and **125s** were applied to the synthesis of 1*H*-indazole **137** and dibenzoxazepinamine **138** in 84% and 91% yields, respectively (**Scheme 25AB**). The indazole core is present in a vast number of bioactive

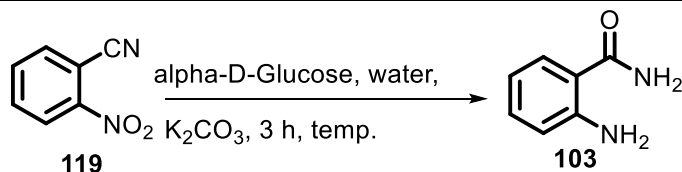
molecules,⁹³ including bendazac and benzydamine.⁹⁴ Besides, the dibenzoxazepinamine scaffold is commonly found in antidepressant pharmaceuticals like loxapine.⁹⁵

Parts of the developed work in Chapter I have been published as “Selective Metalation and Functionalization of Fluorinated Nitriles Using 2,2,6,6-Tetramethylpiperidyl Bases” in *Organic Letters*.⁹⁶

4. CHAPTER 02 - ONE-POT SYNTHESIS OF 2,3-DIHYDROQUINAZOLIN-4(1H)-ONES WITH GLUCOSE AS THE REDUCTANT.

4.1 RESULTS AND DISCUSSIONS

Potassium carbonate, an eco-friendly and inexpensive base,⁹⁷ was chosen together with an aqueous glucose solution (**Table 15**) instead of the often-used strong bases potassium hydroxide and sodium hydroxide in similar reduction processes with this carbohydrate.⁹⁸ Initially, the treatment of **119** with 0.8 mmol (4 equiv.) of the base in 0.8 mL of water at 100 °C led to both nitroreduction and cyano hydration in the formation of 2-aminobenzamide **103** in 79% (**Entry 1**). Decreasing the base excess and changing the amount of glucose (**Entries 2 and 3**) improved the yield albeit running the reaction in air instead of argon did not change the outcome (**Entries 3 and 4**). Notably, by working with more diluted solutions, a higher yield was obtained (**Entries 6 and 7**) unless the amount of glucose was changed to 1 equivalent (**Entry 5**). Running the reaction at 50 °C for three hours or in the absence of glucose only afforded 2-nitrobenzamide (**Entries 8 and 9, respectively**). **Entry 6** was established as the optimum set of conditions providing 2-aminobenzamide in 92% isolated yield.

Table 15. Synthesis of 2-aminobenzamide under various conditions.^a

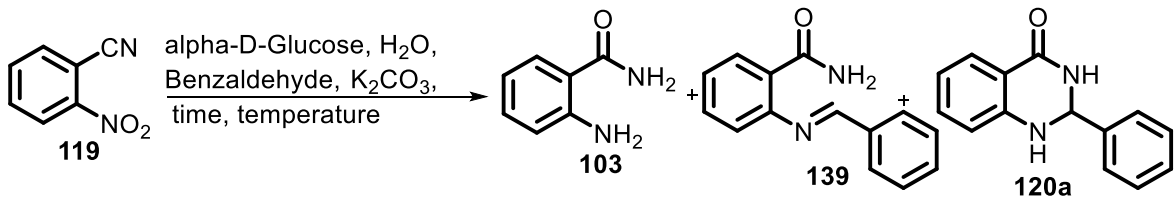
Entry	α -D-glucose	Solvent	Base amount	Yield (%) ^b
1	2 equiv.	0.8 mL	4 equiv.	79
2	1.5 equiv.	0.8 mL	3 equiv.	87
3	2 equiv.	0.8 mL	2 equiv.	91
4 ^c	2 equiv.	0.8 mL	2 equiv.	90
5	1 equiv.	4 mL	2 equiv.	74
6	2 equiv.	4 mL	2 equiv.	94^d
7	2 equiv.	4 mL	4 equiv.	95
8 ^e	2 equiv.	4 mL	4 equiv.	None
9	None	4 mL	2 equiv.	None ^f

^aThe time of 3 h, temperature of 100 °C, air as atmosphere, and 0.2 mmol of 2-nitrobenzonitrile apply for all the reactions unless otherwise stated. ^bDimethyl sulfone was employed as NMR standard for quantification. ^cArgon as atmosphere. ^dIsolated yield: 92%. ^eThe temperature of 50 °C favored the formation of 2-nitrobenzamide (86% yield, NMR quantification after extraction with AcOEt 3·10 mL). ^fOnly 2-nitrobenzamide was observed.

Then, it was speculated if in the presence of benzaldehyde under the established conditions to obtain 2-aminobenzamide, the respective imine would be formed with a subsequent 6-*endo-trig*-cyclization to yield the expected 2,3-dihydroquinazolin-4(1*H*)-one in a one-pot fashion. Gratifyingly, one equivalent of benzaldehyde at 100 °C for 16 hours (**Table 2, entry 1**) afforded 2-phenyl-2,3-dihydroquinazolin-4(1*H*)-one (**120a**) in 55% yield along with 2-aminobenzamide (**103**) (**Table 16**). Increasing the aldehyde amount to 2 equivalents boosted the conversion of **119** in the imine **139** (**Entry 2**). Besides, adjusting the temperature to 120 °C with a slight excess of benzaldehyde improved the yield of **120a** (Entry 3). Keeping this temperature but working with a more concentrated medium also increased yield with the only trace of imine **139** (**Entry 4**). The variation in solvent amount was then investigated with 1.5 equivalents of

benzaldehyde (**Entries 5, 6, and 7**), and 0.8 mL of water was found to be optimal. Lastly, no increase in yield was observed by using 4 equivalents of the base (**Entry 10**), 1.5 equivalents of glucose with 3 equivalents of potassium carbonate (**Entry 9**), or with a reaction time of 24 hours (**Entry 8**). The 2-phenyl-2,3-dihydroquinazolin-4(1*H*)-one **120a** was isolated as a white solid in 75% yield (**Optimized conditions, Entry 6**).

Table 16. Optimization of the reaction conditions for the synthesis of 2-phenyl-2,3-dihydroquinazolin-4(1*H*)-one.^a



Entry	Solvent (H ₂ O)	Temp. (°C)	Benzaldehyde	Time	Yield (%) ^b		
					103	139	120a
1	2 mL	100	1.0 equiv.	16 h	35	**	55
2	2 mL	100	2.0 equiv.	16 h	18	17	54
3	2 mL	120	1.2 equiv.	16 h	13	6	63
4	1 mL	120	1.2 equiv.	16 h	17 (trace)		72
5	1 mL	120	1.5 equiv.	16 h	7	**	75
6	0.8 mL	120	1.5 equiv.	16 h	5	**	78^c
7	0.6 mL	120	1.5 equiv.	16 h	14	**	72
8	0.8 mL	120	1.5 equiv.	24 h	**	**	76
9 ^d	0.8 mL	120	1.5 equiv.	16 h	**	**	77
10 ^e	0.8 mL	120	1.5 equiv.	16 h	**	**	74

^a0.2 mmol equiv. of 2-nitrobenzonitrile, air as atmosphere, α -D-glucose (2 equiv.) and K_2CO_3 (2 equiv.) apply for all the reactions unless otherwise stated. ^bDetermined by ¹H-NMR using dimethyl sulfone as a standard. ^cIsolated yield: 75% (white solid). ^{**}Not detected by ¹H-NMR. ^d α -D-glucose (1.5 equiv.) and K_2CO_3 (3 equiv.) were employed. ^e K_2CO_3 (4 equiv.) was employed.

The next step comprised the investigation of reaction scope including diverse aldehydes and ketones (**Table 17**). Electron-rich aldehydes, 4-substituted

benzaldehydes bearing methyl and methoxy groups afforded DHQs in good yields (**120b**, 77% and **120e**, 75%). 3,4-disubstituted benzaldehydes with similar electronic characteristics as for **120k** (90%) and **120l** (63%), were also tolerated. A lower yield was verified for the three-substituted aldehyde 3,5-bis(benzyloxy)-4-methoxybenzaldehyde for the synthesis of **120r**. For halogenated benzaldehydes (4-Cl-, 4-F-, 3-Br-, 2-I-, and 2,3-dichloro-) low to moderate yields were obtained (**120c,d,f,g,q**, 23–65%). As a synthetic limitation, the reaction with acetophenone did not provide **120s**. However, it worked well for cyclic aliphatic ketones as for cyclohexanone (**120i**, 79%) and cyclopentanone (**120n**, 61%). Extending the scope with heterocyclic aldehydes, the 2-thiophenecarboxaldehyde derivative **120h** was isolated in 59% yield while the expected products from furfural (**120u**) and 2-pyridinecarboxaldehyde (**120t**) were not observed. Furthermore, the developed protocol was suitable for a model aliphatic aldehyde, pentanal, with a moderate yield of 56% (**120j**).

Concerning the characterization of the obtained DHQs, they were subjected to nuclear magnetic resonance spectroscopy (NMR), Infrared spectroscopy, and high-resolution mass spectrometry (HRMS) analyses plus the determination of melting points. To illustrate, for the ^1H NMR data for **120a** (**Figure 9**), a singlet at 5.76 ppm refers to H-2 while the other singlets at 8.29 and 7.11 ppm are attributed to -CONH- and -NH-, respectively. Additionally, a doublet of doublets at 7.61 ppm ($^3J = 7.8$ Hz and $^4J = 1.7$ Hz) is attributed to the aromatic hydrogen H-5, a multiplet from 7.51 to 7.49 ppm to H-2' and H-6', a multiplet from 7.41 to 7.32 to H-3', H-4', and H-5', a doublet of doublets of doublets at 7.24 ppm to H-7 ($^3J = 8.5, 7.1$ Hz and $^4J = 1.7$ Hz), a duplet at 6.75 ppm to H-8 ($^3J = 7.1$ Hz), and a multiplet from 6.69 to 6.65 to H-6. The ^{13}C NMR spectrum of **120a** (**Figure 10**) shows signals at 163.6 and 66.6 ppm for -CONH- and C-2, respectively. The aromatic carbons are correlated with signals from 147.9 to 114.4 ppm. The **120a** IR spectrum shows important absorption bands including the ones at 3302 and 3178 cm^{-1} for -N-H stretching vibrations, at 3131, 3061, and 3035 cm^{-1} for -C-H (aromatic carbons, sp^2 hybridized) stretching vibrations, at 1652 cm^{-1} for -C=O (amide) stretching vibration, at 1610 cm^{-1} for -N-H bending vibration, and at 1507 cm^{-1} for C-C stretching vibration.

Figure 9. Expanded ^1H NMR (400 MHz, $\text{DMSO-}d_6$) spectrum of **120a**.

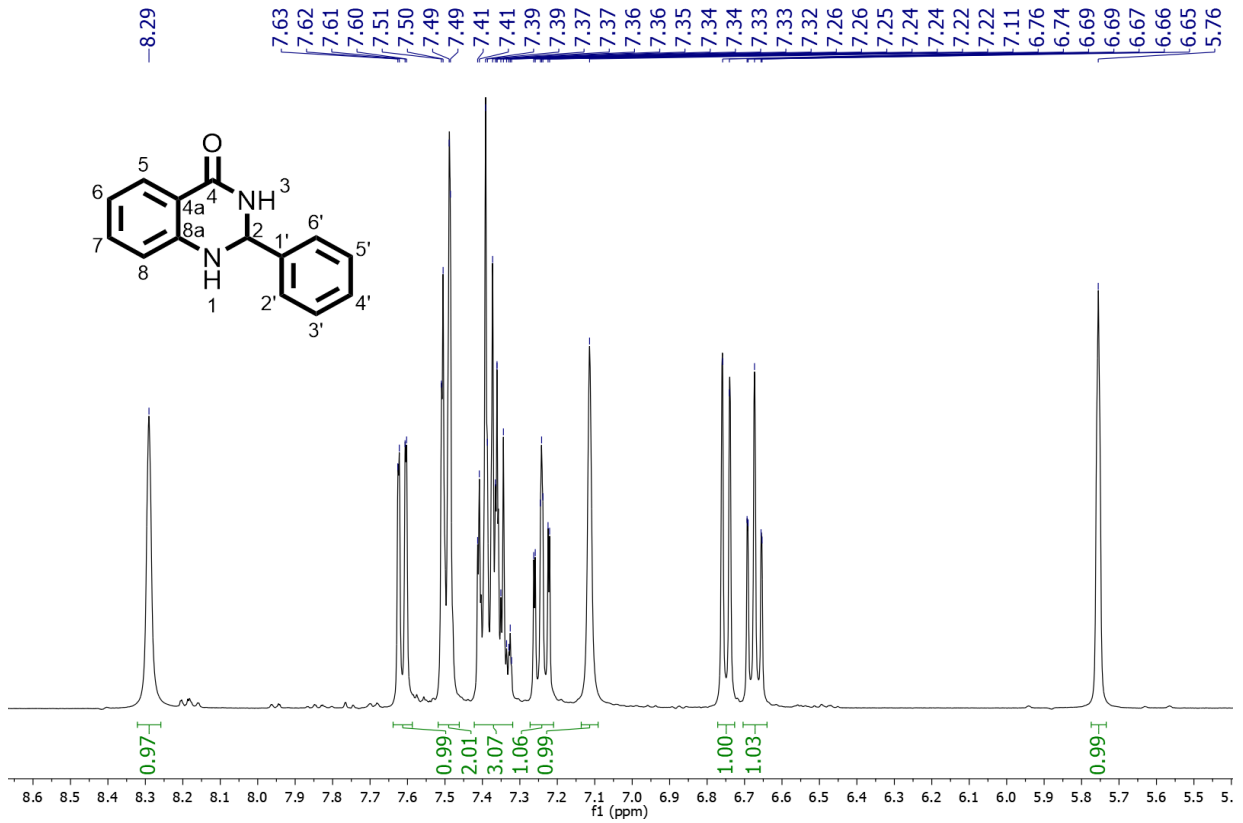


Figure 10. Expanded ^{13}C NMR (101 MHz, $\text{DMSO-}d_6$) spectrum of **120a**.

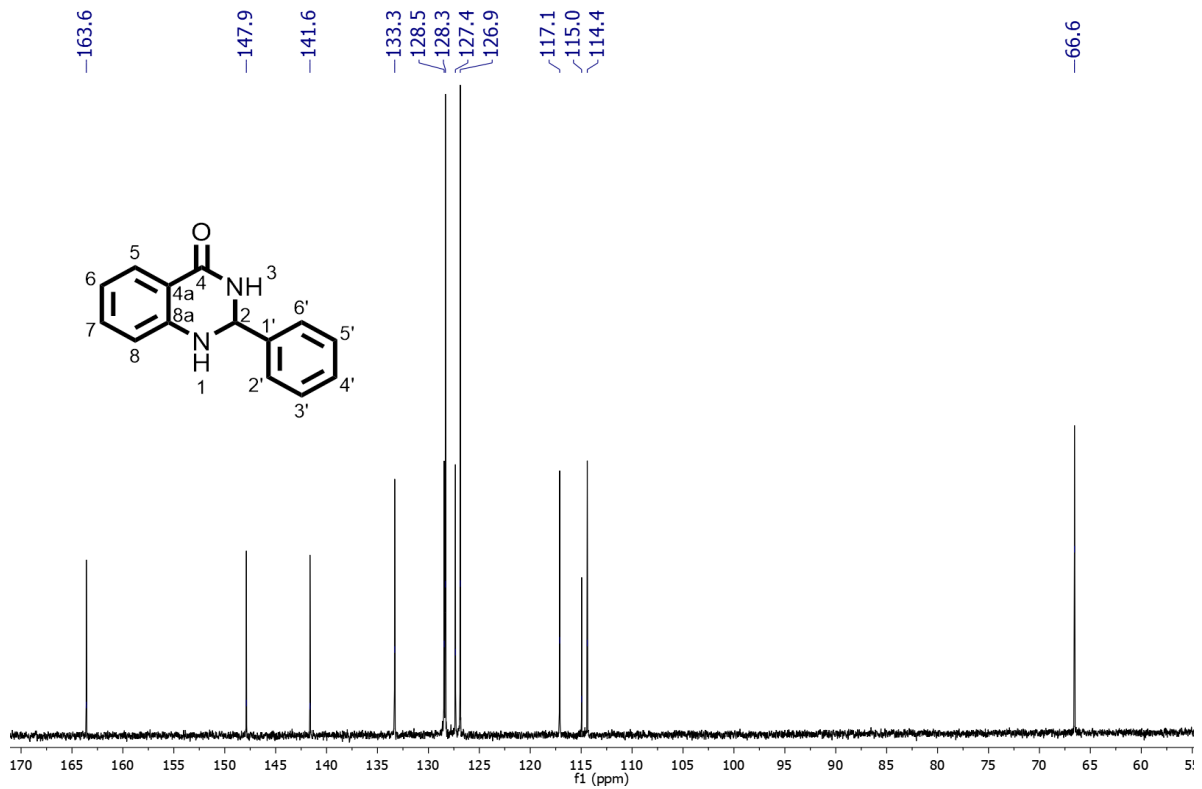
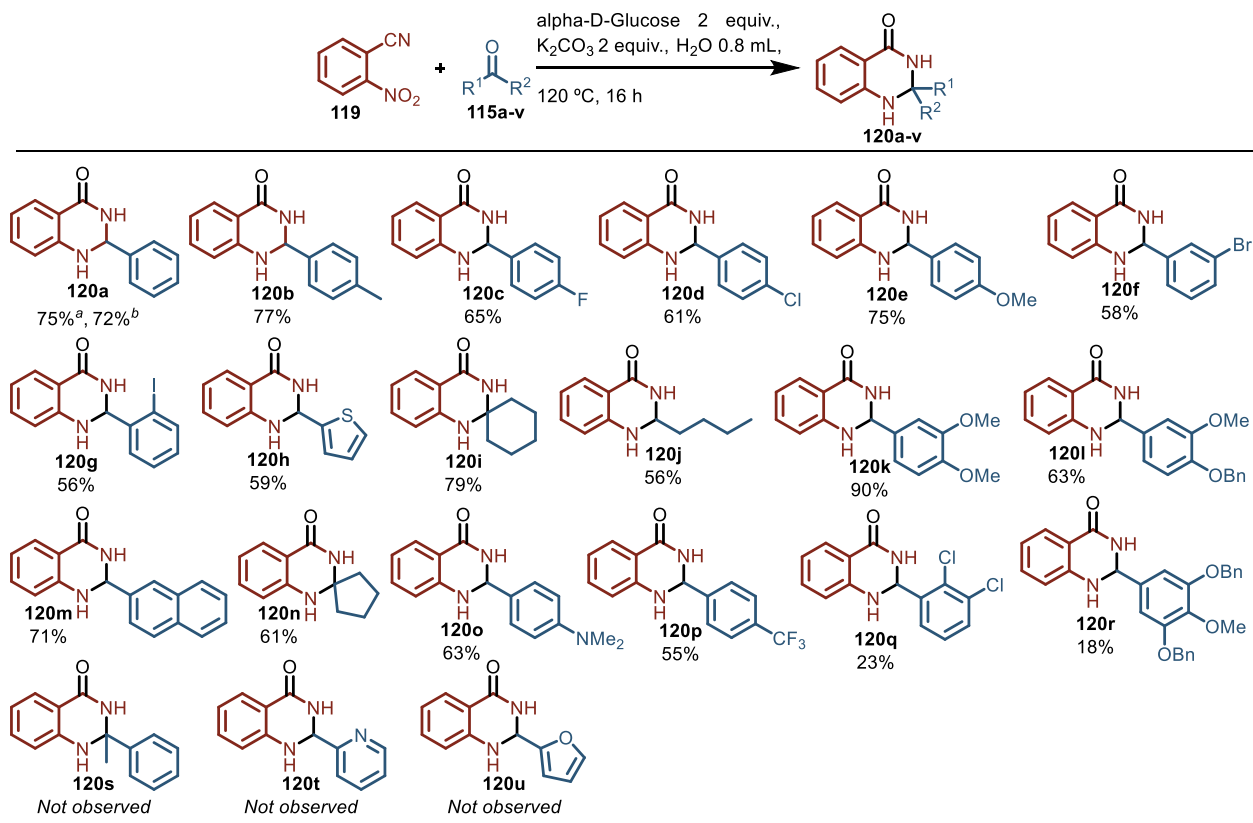
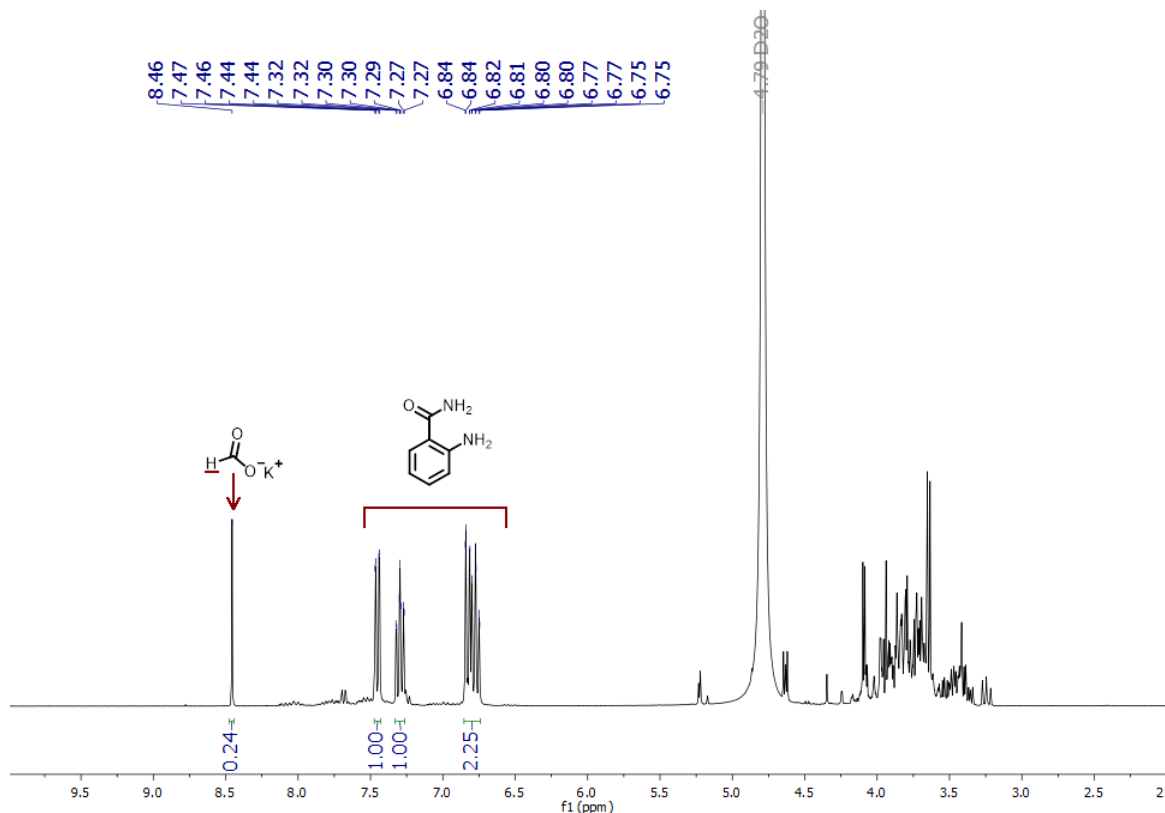


Table 17. Synthesis of 2,3-dihydroquinazolin-4(1*H*)-ones with the established protocol.

Source: The author.

Regarding the mechanism underlying the devised protocol, it is known that glucose under hot alkaline conditions produces reduction equivalents (“H₂”) with the aid of hydroxide anion in its decomposition into carboxylates such as formate, lactate, and glycolate.⁹⁹ The ion hydroxide can be generated by water deprotonation with potassium carbonate as explored by Tu and co-workers in the hydration of diverse nitriles.¹⁰⁰ Interestingly, formate was detected for the reaction performed in D₂O (**Figure 11**). Hence, it is plausible to expect hydroxide anion concomitantly acting on glucose decomposition and nitrile hydration in the preparation of 2-amizobenzamide **103** as observed in this study at temperatures equal to or above 100 °C. The facile hydration of 2-nitrobenzonitrile into 2-nitrobenzamide at 50 °C relies on the strong electron-withdrawing effect of the *ortho*-nitro group.

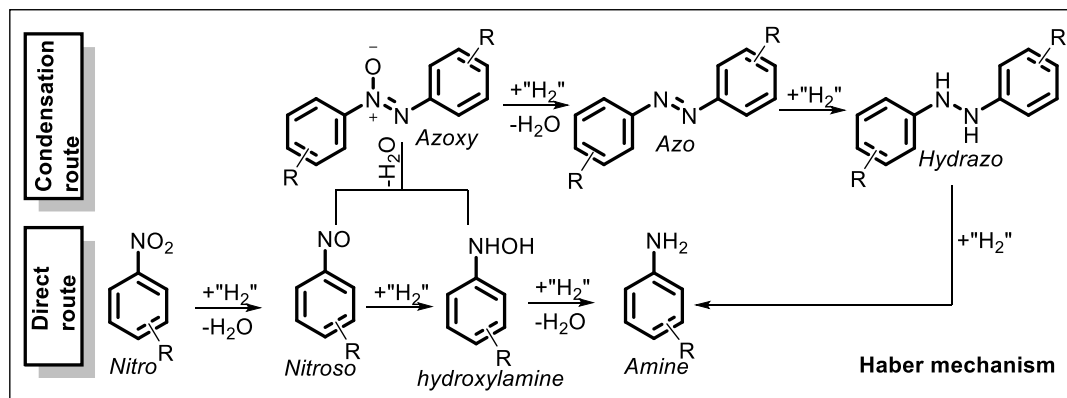
Figure 11. Observation of formate from glucose decomposition for the reaction performed in D₂O (Optimized condition, Table 16, entry 6, no benzaldehyde - ¹H NMR, 400 MHz). In accordance with the literature.¹⁰¹



Source: The author.

The nitro reduction may take two different pathways according to the Haber mechanism (**Scheme 26**),¹⁰² one involving hydroxylamine intermediate and the other one bearing heterodimerization to azoxy and azo compounds under usually high alkaline conditions.^{98c,103} Notably, no azoxy and azo species were verified by Opolonick in the nitro reduction of nitrobenzene with glucose in aqueous potassium carbonate.¹⁰⁴

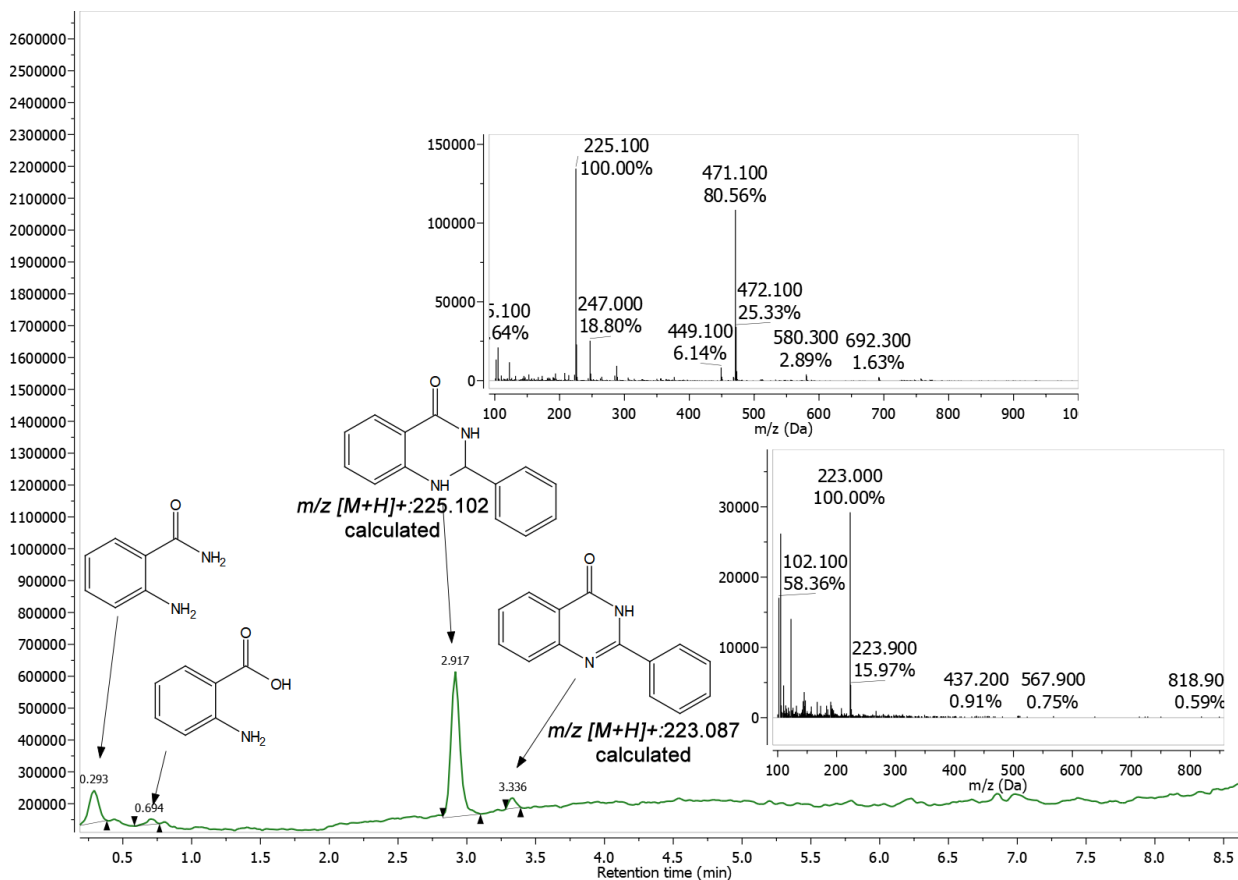
Scheme 26. Nitro reduction pathways.



Source: SERNA; CORMA, 2015.

The synthesis of azoxy compounds can be straightforwardly achieved with the addition of glucose to an aqueous solution of NaOH and the nitro compound. Besides, with the application of a second equivalent of glucose to the same reaction medium, azoxy compounds are converted in respective azo species.^{98c,105} To selectively obtain the hydroxylamine instead, glucose can be employed as the reductant in an enzymatic process with a nitroreductase¹⁰⁶ or in fermentation with baker's yeast.¹⁰⁷ Concerning the potential competing reactions for the synthesis of 2,3-dihydroquinazolin-4(1*H*)-ones in this study, amide hydrolysis leading to carboxylic acid even with potassium carbonate and production of 2-phenylquinazolin-4(3*H*)-ones as verified via HPLC-MS (**Figure 12**) and base-induced reactions¹⁰⁸ of the aldehyde component cannot be ruled out.

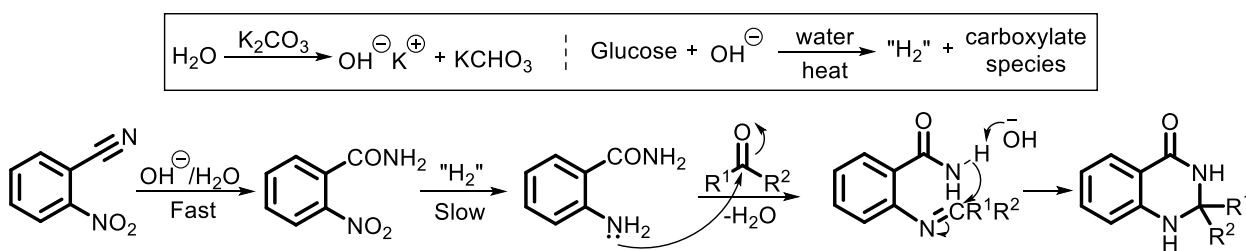
Figure 12. Recorded mass spectra and chromatogram for the optimized conditions (Table 16, entry 6).



Source: The author.

A plausible mechanism is depicted in **scheme 27**. Cyano hydration is the fastest step followed by nitro reduction, imine formation, and cyclization.

Scheme 27. Proposed mechanism for the developed synthesis of DHQs.



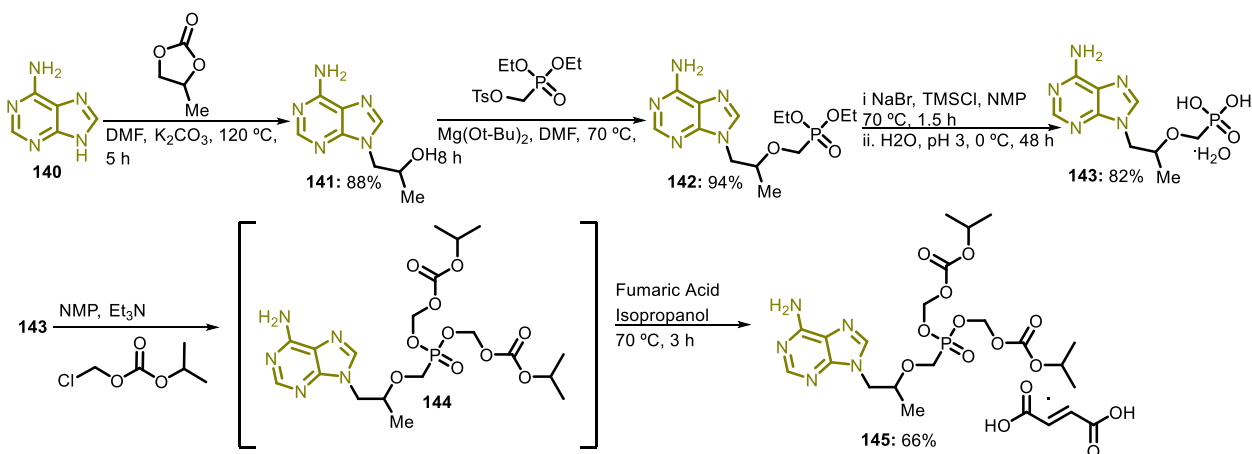
Source: The author.

This work has been published as “Glucose as an Eco-Friendly Reductant in a One-Pot Synthesis of 2,3-Dihydroquinazolin-4(1*H*)-ones” in the *European Journal of Organic Chemistry*.¹⁰⁹

5. CHAPTER 03 – TENOFOVIR DISOPROXIL FUMARATE AS A REPOSITIONING STRATEGY TO TACKLE SARS-COV-2

Considering the SARs-COV-2 related pandemic's huge impact on public health worldwide since the beginning of 2020,¹¹⁰ our research group decided to make efforts in the search for an antiviral agent against this coronavirus using a drug repositioning approach.¹¹¹ Tenofovir disoproxil fumarate (TDF), an antiretroviral pharmaceutical used to treat acquired immune deficiency syndrome (AIDS) and hepatitis B, was synthetically obtained in a scaled-up and improved manner (**Scheme 28**) with *in situ* infrared spectroscopy monitoring and a degradation study. Subsequently, TDF was *in vitro* assayed against SARS-CoV-2 and was able to significantly reduce SARs-COV-2 viral replication (Vero CCL-81 cells were treated with TDF and further incubated with the virus).

Scheme 28. TDF improved synthetic route.



Source: The author.

Inspired by the known mechanism of action of TDF upon HIV (reverse transcriptase inhibition) and the known inhibition of the viral RNA-dependent RNA polymerase from

SARS-CoV-1 by Remdesivir, my contribution to this work relied on the computational prediction of TDF affinity toward SARS-CoV-2 RNA-dependent RNA polymerase (RdRp) as a potential target.¹¹² The molecular docking studies were performed with a cryogenic electron microscopy (cryo-EM) structure of SARS-CoV-2 RdRp (PDB id = 7BV2, 2.50 Å) via GOLD (version 2020.1 CSD release). The cryo-EM structure of SARS-CoV-2 RNA-dependent RNA polymerase was prepared via HERMES (version 2020.1 CSD release): the water molecules and the complex remdesivir-primer were removed, and the hydrogens were added. All located residues within 18 Å via GOLD (version 2020.1 CSD release) were included for the explored binding site. CHEMPLP was chosen as score function, and 50 runs per ligand were performed.

Interestingly, both drugs, TDF and Remdesivir occupied the same region in the RdRp and, therefore, a potential inhibition of this viral enzyme by TDF may not be ruled out and possibly contributed to the observed decline in viral replication. The three magnesium atoms from SARS-CoV-2 RdRp were initially kept for the docking studies given their relevant catalytic activity.¹¹³ It is known that Tenofovir Disoproxil Fumarate undergoes enzymatic phosphorylations after oral administration leading to a triphosphate form.¹¹⁴ This phosphorylated drug structure was correlated with the best predicted affinity towards the binding pocket of SARS-CoV-2 RdRp (**Table 18**) with important interactions involving residues ASN611 and ARG473 for hydrogen bonding (**Figure 13**) and some oxygens from the phosphate groups in distances less than 2.30 Å to the Mg atoms for oxygen-metal coordination. In the absence of the Mg atoms, the predicted affinity greatly decreases even with the possibility of other hydrogen bondings including the residues CYS542, LYS541, ARG473, and LYS471 (**Figure 14**).

Table 18. Obtained values of GOLD Fitness for the docking studies.

Ligand	GOLD Fitness (ChemPLP)	
	The Mg atoms were kept	The Mg atoms were removed
Tenofovir monophosphate	58.8993	-
Tenofovir diphosphate	86.0030	-
Tenofovir triphosphate	93.5799	54.3267

Figure 13. Docked TDF conformation (triphosphate form) in RdRp (PDB id = 7BV2, 2.50 Å).

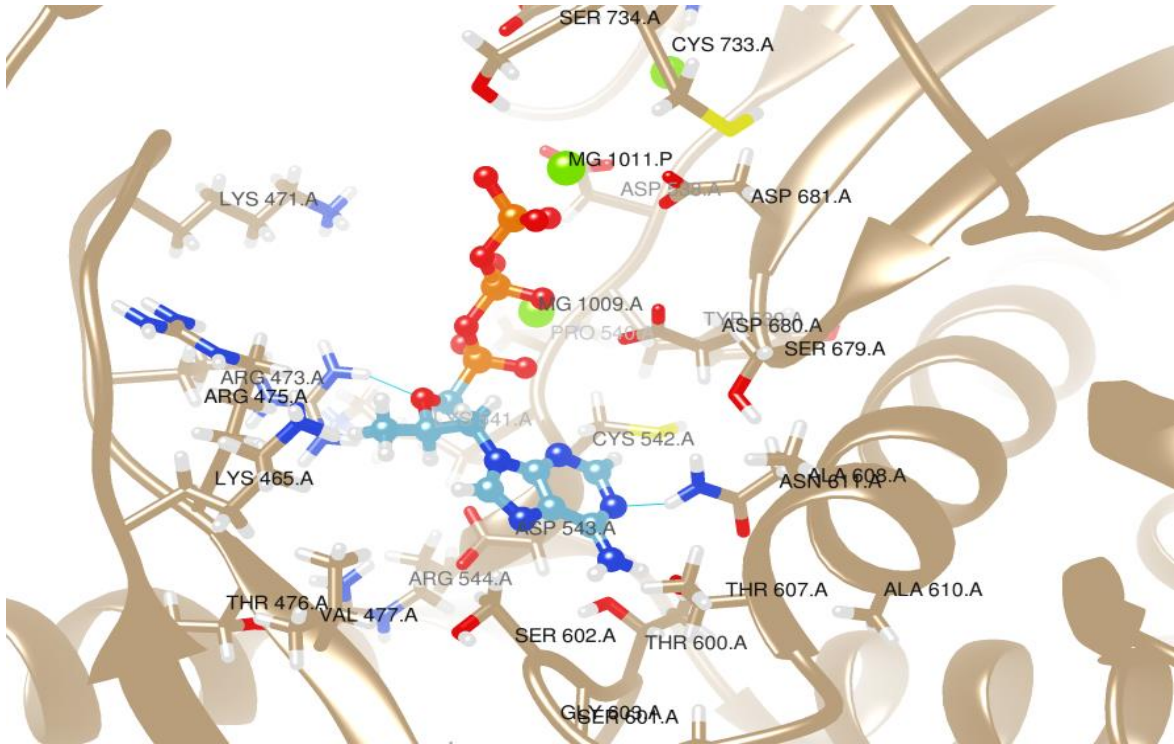
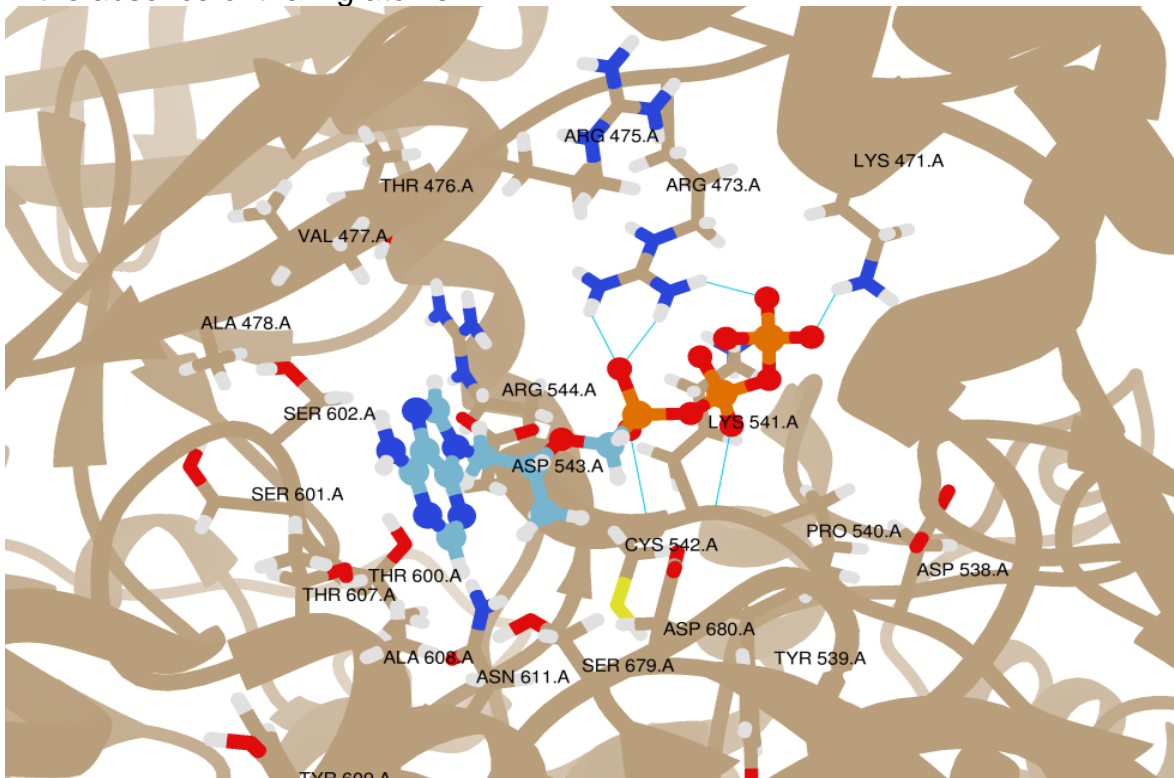


Figure 14. Docked TDF conformation (triphosphate form) in RdRp (PDB id = 7BV2, 2.50 Å) in the absence of the Mg atoms.



This work made it to the cover of the *Journal of the Brazilian Chemical Society* (JBCS) and resulted in an ongoing prospective, randomized, double-blind, placebocontrolled clinical trial coordinated by Dr. Aldo Ângelo Moreira Lima. It was approved by the Brazilian National Research Ethics Commission (no. 34 18262.00.0000.5045) and the ClinicalTrials.gov (NCT04712357) and is being carried out in the city of FortalezaCE, Brazil. Details regarding the employed biological assay, synthetic studies, and computational studies of the developed work (JBCS) can be found via <http://dx.doi.org/10.21577/0103-5053.20200106>.¹¹⁵

6. CONCLUSIONS

About 47 diverse functionalized nitriles with the exploration of new and scarcely investigated metalation sites were prepared in yields ranging from 48 to 95% by metalation with the TMP-bases $\text{TMPMgCl}\cdot\text{LiCl}$ or $(\text{TMP})_2\text{Zn}\cdot 2\text{MgCl}_2\cdot 2\text{LiCl}$. In the case of known metalation positions, this study has greatly contributed to the establishment of shorter metalation times at milder temperatures with a better exploration of reactivity towards varied electrophiles. Favorably, the devised methods proved to be scalable as illustrated by the synthesis of **125f** at a 5.5 mmol scale (91% isolated yield, 1.21 g). The suitability of $\text{TMPMgCl}\cdot\text{LiCl}$ in the difunctionalization of **123c** to access tetrasubstituted derivatives **126a-b** can be viewed as a blueprint for the development of exhaustive functionalization protocols with TMP-bases as wisely explored by prof. Manfred Schlosser with lithium-based bases.

The obtained functionalized fluorinated nitriles can be employed as building blocks in the construction of heterocyclic systems of great pharmaceutical importance as exemplified by the synthesis of 4-aminoquinazolines **134** and **135**, 1*H*-indazole **137**, and dibenzoxazepinamine **138**. Furthermore, the prepared building blocks may find application in the synthesis of other diverse important heterocycles since fluorinated nitriles have been also successfully used to access spiro[indazolo[3,2-*b*]quinazoline-7,3'-indolines,¹¹⁶ indazolo-quinazolinones,¹¹⁷ cyanodibenzo[1,4]dioxines,¹¹⁸ dibenzo[*b,f*][1,4]oxazepines,¹¹⁹ oxazepinones,¹²⁰ 11*H*-pyrido[2,1-*b*]quinazolin-11-ones,¹²¹ and benzo[*d*]imidazo[2,1-*b*]thiazoles.¹²²

In the second work, an environmentally friendly one-pot protocol based on nitrile hydration, nitro-reduction, imine formation, and cyclization with glucose in alkaline water was successfully established affording DHQs in yields 18-90%. As a transition metal-free method, it represents a great and fast alternative to access 2,3-dihydroquinazolin-4(1*H*)-ones from 2-nitrobenzotrile. Moreover, it may ignite the general interest of the research community in applying glucose as a green reductant in the synthesis of other important heterocyclic systems.

Speaking of sustainability, glucose is a relevant renewable resource easily accessible from lignocellulosic biomass through well-established technology and was favorably employed in water as the solvent with potassium carbonate (“potash”, available from plant ashes) as the base. Also important, no competition of the aldehyde from glucose with the externally added carbonyl compound was verified, and the synthesized DHQs in this work can be easily oxidized under eco-friendly conditions to the corresponding quinazolinones¹²³ finding even wider application in medicinal chemistry.

7. EXPERIMENTAL SECTION

7.1 CHAPTER I

7.1.1 General considerations

7.1.1.1 Solvents and reagents

Unless otherwise stated, all the solvents and reagents were obtained from commercial suppliers and used without prior purification. All fluorinated nitriles, salts (ZnCl₂, CuCl, LiCl, NH₄Cl, MgSO₄), *i*-PrMgCl-LiCl, deuterated solvents, TMPH, PdCl₂, PPh₃, and electrophiles were purchased from Merck. All the water-sensitive reactions were carried out with dry solvents under anhydrous conditions and a nitrogen atmosphere. The transference of the dry solvents and air-sensitive reagents was carried out through standard syringe techniques. A saturated sodium thiosulfate solution instead

of NH_4Cl was used for quenching when iodine was employed as the electrophile. $\text{Pd}(\text{PPh}_3)_4$ was prepared according to the literature.¹²⁴

7.1.1.2 Preparation procedures of the employed TMP-bases and salt solutions

TMPMgCl·LiCl: A dry round-bottom flask equipped with a stirring bar was charged with *i*-PrMgCl·LiCl (1.3 M in THF, 14 mmol, 10.77 mL) under N_2 . Then, fresh distilled 2,2,6,6-tetramethylpiperidine (1.05 equiv., 14.7 mmol, 2.48 mL) was added dropwise. The flask was wrapped in aluminum foil, and the reaction was kept at room temperature for 48 hours. The resulting base was titrated with benzoic acid, and 4-(phenylazo)-diphenylamine was used as the indicator (Base concentration range: 0.87 – 1.1 M).

TMPZnCl·LiCl: A dry round-bottom flask equipped with a stirring bar was charged with TMPH (1.1 equiv., 11 mmol, 1.86 mL) and THF (10 mL). This solution was cooled to $-30\text{ }^\circ\text{C}$, and *n*-Buli (2.35 M, 1 equiv., 10 mmol, 4.26 mL) was added dropwise. The reaction was allowed to slowly warm to $-5\text{ }^\circ\text{C}$, and ZnCl_2 (0.99 M solution in THF, 1 equiv., 10 mmol, 10.1 mL) was added dropwise. The resulting solution was stirred at this temperature for 30 minutes and then more 30 minutes at $25\text{ }^\circ\text{C}$ before titration with benzoic acid using 4-(phenylazo)-diphenylamine as an indicator (Base concentration: 0.39 M).

CuCl·2LiCl (0.5 M in THF): A dry round-bottom flask equipped with a magnetic bar was charged with LiCl (0.85 g, 20 mmol) and heated to $140\text{ }^\circ\text{C}$ (oil bath) for 2 hours under vacuum. After cooling to room temperature, CuCl (0.99 g, 10 mmol) was added under nitrogen, and the temperature was adjusted to $140\text{ }^\circ\text{C}$ for 5 h under vacuum. After cooling, the flask was charged with dry THF (20 mL), covered in aluminum foil, and kept under vigorous stirring to obtain a yellow homogenous solution.

ZnCl₂ (1 M in THF): The solution was prepared by drying ZnCl_2 (2.73 g, 20 mmol) at $150\text{ }^\circ\text{C}$ (oil bath) for 5 h under vacuum, which was followed by the addition of dry THF (20 mL) at room temperature and vigorous stirring until all the solids were dissolved.

(TMP)₂Zn·2MgCl₂·2LiCl: A dry round-bottom flask equipped with a stirring bar was charged with ZnCl_2 (1 M, 0.53 equiv., 7.10 mmol, 7.10 mL), and TMPMgCl·LiCl (0.87 M, 13.4 mmol, 15.4 mL) was added dropwise. The flask was wrapped in aluminum foil, and

the reaction was kept at room temperature for 2.5 h. The resulting solution was titrated with benzoic acid, and 4-(phenylazo)-diphenylamine was used as the indicator (Base concentration = 0.29 M).

TMPH: TMPH was stirred overnight with NaOH beads, distilled under reduced pressure, and stored under nitrogen before use.

7.1.1.3 Analytical data and other employed equipment.

Chromatography: Chromatographic purification of the products was performed by flash column chromatography on silica gel (Sigma–Aldrich, particle size 0.040 – 0.063 nm). Thin-layer chromatography (TLC) was carried out on silica plates (TLC Silica 60 F₂₅₄ by Merck). Gas chromatographic investigations were performed on a Shimadzu GC-2014 chromatograph equipped with a capillary column (Restek, RTX-1, 30 m × 0.25 mm) and a flame ionization detector (FID). Nitrogen gas was used as the mobile phase.

NMR spectra: NMR spectra were recorded on a Bruker DRX 400 (¹H-NMR: 400 MHz, ¹³C-NMR: 101 MHz), Bruker DRX 500 (¹H-NMR: 500 MHz, ¹³C-NMR: 126 MHz), or on a Bruker DRX 300 (¹⁹F-NMR: 282 MHz) spectrometer. Chemical shifts are referenced to residual solvent signals (DMSO-*d*₆: 2.50 ppm and 39.52 ppm, and CDCl₃: 7.26 ppm and 77.16 ppm for ¹H-NMR and ¹³C-NMR, respectively), TMS (tetramethylsilane) or using the spectrometer frequency (¹⁹F-NMR, CDCl₃), and reported in parts per million (ppm). Coupling constants (*J*) are reported in Hz, and multiplicities of NMR signals are abbreviated as follows: bs = broad singlet, s = singlet, d = doublet, dd = doublet of doublets, ddd = doublet of doublet of doublets, t = triplet, td = triplet of doublets, dt = doublet of triplets, qd = quartet of doublets, sxt = sextet, m = multiplet and combinations thereof, app = apparent. NMR spectrometry analyses in conjunction with GC-MS and HRMS analyses were used to confirm compound identity. Additionally, we compared the obtained data with the literature for known molecules.

Mass spectra: Mass spectra (MS) were recorded on a Shimadzu GCMS-QP2010 mass spectrometer equipped with a DB-5 MS column from J&W Scientific. Helium was used as the mobile phase, and electron ionization (EI, 70 eV) was the ionization method. High-resolution masses (HRMS) were recorded on a Bruker Daltonics micrOTOF

QII/ESI-TOF with a suitable external calibrant or on a Waters Acquity UPLC H-Class System Xevo G2-XS Q-TOF equipped with an Acquity UPLC BEH C₁₈ column (1.7 μm, 2.1x100 mm).

Melting point: Melting points were determined in open capillary tubes by using a BÜCHI Labortechnik M-560 melting point meter.

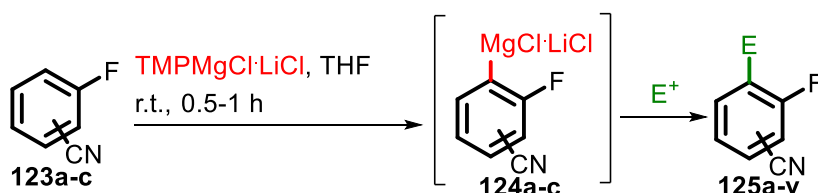
Microwave reactor: Reactions under microwave irradiation were carried out using a dedicated single-mode microwave reactor, a Monowave 300 from Anton-Paar.

7.1.2 General procedures for the functionalization of fluorinated nitriles

7.1.2.1 Reaction monitoring

Metalation of the studied nitriles was monitored by quenching reaction aliquots with an iodine solution in dry THF followed by gas chromatography analysis.

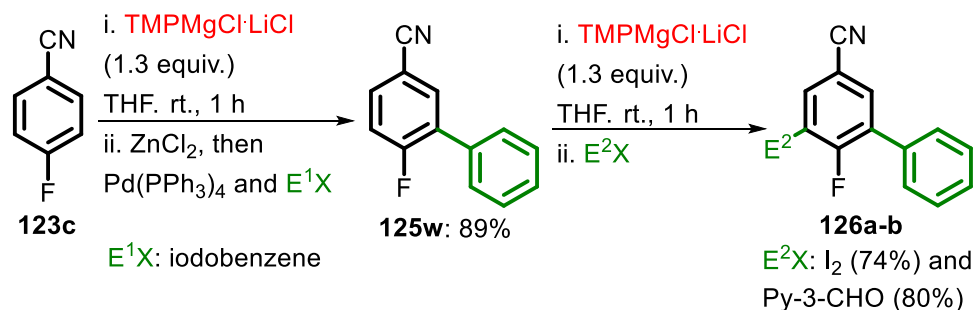
7.1.2.2 General method A (GMA): Standardized procedure for metalation of the studied fluorobenzonitriles with TMPMgCl·LiCl



A dry round-bottom flask flushed with N₂ was charged with the desired fluorobenzonitrile (0.5 mmol, 1 equiv., 0.0606 g) and dry THF (2 mL). The base, TMPMgCl·LiCl (1.3 equiv. for *ortho* **123a** and *para* fluoro-substituted **123c** benzonitriles and 1.2 equiv. for the *meta* one **123b**), was added dropwise, and the reaction was kept at room temperature for 1 h for the first two fluorobenzonitriles and 0.5 h for the latter substrate. The generated organomagnesium species were trapped with an electrophile (1.1 equiv.), and the mixture was allowed to react for 12 h. The reaction was quenched with saturated aqueous NH₄Cl and extracted with ethyl acetate (3x10 mL). The combined organic phases were dried over MgSO₄, filtered, and concentrated under

reduced pressure. The crude product was purified by flash column chromatography (silica gel, hexanes/ethyl acetate).

7.1.2.2.1 Sequential difunctionalization of 4-fluorobenzonitrile

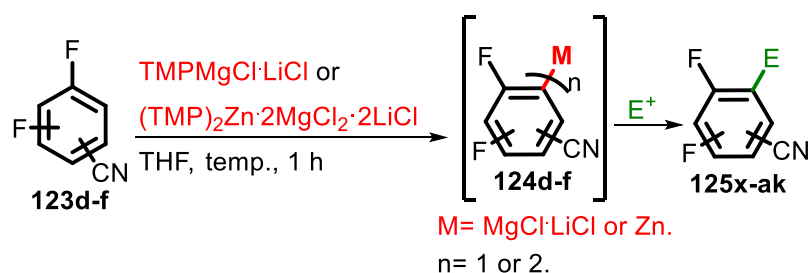


Following **GMA**, **125w** was obtained and employed in the synthesis of **126a-b** via further functionalization via the same TMP-base. The details regarding their characterization and reaction conditions are described in section 6.1.3.

7.1.2.2.2 Gram scale synthesis of 2-fluoro-3-(hydroxy(*p*-tolyl)methyl)benzonitrile (**125f**)

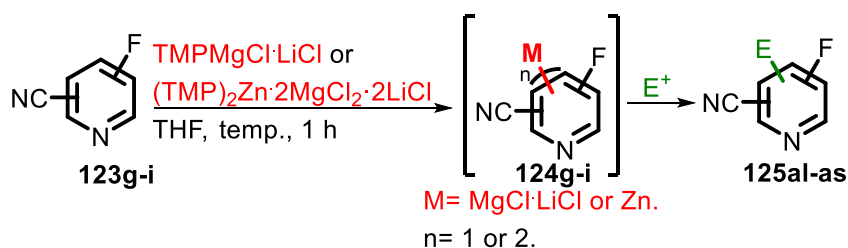
To a dry round-bottom flask flushed with N_2 and charged with 2-fluorobenzonitrile (5.5 mmol, 0.6 mL, 1 equiv.) and dry THF (22 mL), **TMPMgCl·LiCl** (1.3 equiv., 1.09 M, 6.6 mL) was added dropwise, and the reaction was kept at room temperature for 1 h. The generated organomagnesium species were trapped with *p*-tolualdehyde (1.1 equiv., 0.78 mL), and the mixture was allowed to react for 12 h. The reaction was quenched with saturated aqueous NH_4Cl and extracted with ethyl acetate (3×10 mL). The combined organic phases were dried over MgSO_4 , filtered, and concentrated under reduced pressure. Purification was accomplished by flash column chromatography (silica gel, Hexanes/AcOEt 7:3) to afford a white solid (1.21 g, 91% yield).

7.1.2.3 General method B (GMB): Standardized procedure for metalation of the studied difluorobenzonitriles **123d-f** with **TMPMgCl·LiCl** or $(\text{TMP})_2\text{Zn}\cdot 2\text{MgCl}_2\cdot 2\text{LiCl}$



A dry round-bottom flask flushed with N_2 was charged with the desired difluorobenzonitrile (0.5 mmol, 1 equiv., 0.0696 g) and dry THF (2 mL), and the mixture was kept at the specified temperature. The base, $\text{TMPMgCl}\cdot\text{LiCl}$ (1.3 equiv. for 2,4-difluorobenzonitrile and 3,5-difluorobenzonitrile, and 1.5 equiv. for 3,4-difluorobenzonitrile) or $(\text{TMP})_2\text{Zn}\cdot 2\text{MgCl}_2\cdot 2\text{LiCl}$ (0.65 equivalents for 2,4-difluorobenzonitrile and 3,5-difluorobenzonitrile, and 0.75 equivalents for 3,4-difluorobenzonitrile), was added dropwise, and the reaction was kept at the same temperature for 1 h. The generated organomagnesium or organozinc species were trapped with an electrophile (1.1 equiv.), and the mixture was allowed to slowly reach room temperature in the case of the metalations performed under reduced temperature. The reaction was quenched with saturated aqueous NH_4Cl and extracted with ethyl acetate (3×10 mL). The combined organic phases were dried over MgSO_4 , filtered, and concentrated under reduced pressure. The crude product was purified by flash column chromatography (silica gel, hexanes/ethyl acetate).

7.1.2.4 General method C (GMC): Standardized procedure for metalation of the studied heterocyclic nitriles **123g-i** with $\text{TMPMgCl}\cdot\text{LiCl}$ or $(\text{TMP})_2\text{Zn}\cdot 2\text{MgCl}_2\cdot 2\text{LiCl}$



A dry round-bottom flask flushed with N_2 was charged with the desired fluorinated pyridinecarbonitrile (0.5 mmol, 1 equiv., 0.0611 g) and dry THF (2 mL), and the mixture was kept at the specified temperature. The base, $\text{TMPMgCl}\cdot\text{LiCl}$ (1.3 equiv. for 5-

fluoropicolinonitrile **123g**, and 1.5 equiv. for 2-fluoroisonicotinonitrile **123h** and 2-fluoronicotinonitrile **123i**) or $(\text{TMP})_2\text{Zn}\cdot 2\text{MgCl}_2\cdot 2\text{LiCl}$ (0.9 equiv. for 2-fluoroisonicotinonitrile **123h**), was added dropwise, and the reaction was kept at the same temperature for 1 h. The generated organomagnesium or organozinc species were trapped with an electrophile (1.1 equiv.), and the mixture was allowed to slowly reach room temperature in the case of metalation performed under reduced temperature. The reaction was quenched with saturated aqueous NH_4Cl and extracted with ethyl acetate (3×10 mL). The combined organic phases were dried over MgSO_4 , filtered, and concentrated under reduced pressure. The crude product was purified by flash column chromatography (silica gel, hexanes/ethyl acetate). Observation: The base $\text{TMPZnCl}\cdot\text{LiCl}$ (1.5 equivalents) was exclusively investigated for 2-fluoronicotinonitrile **123i** at 25 °C for 1 hour followed by iodination (1.1 equiv. of I_2).

7.1.2.5 Metalation followed by Negishi cross-coupling

After the magnesiation step (**GMA**), a solution of ZnCl_2 (1 M in THF) was added dropwise at room temperature, and the reaction was kept under stirring for 0.5 h. For the direct zincation via **GMB** or **GMC**, the organozinc species were directly considered for the next step. Then, $\text{Pd}(\text{PPh}_3)_4$ (5 mol%) and the desired iodoarene (1.2 equiv.) in THF (1 mL) were transferred, and the reaction was warmed to 50 °C (oil bath) and kept under stirring for 12 h. The reaction was quenched with saturated aqueous NH_4Cl and extracted with ethyl acetate (3×10 mL). The combined organic phases were dried over MgSO_4 , filtered, and concentrated under reduced pressure. The crude product was purified by flash column chromatography (silica gel, hexanes/ethyl acetate).

7.1.2.6 Metalation followed by transmetalation with copper salt

After the magnesiation step (**GMA**), the temperature was set to -40 °C. Then, a solution of $\text{CuCl}\cdot 2\text{LiCl}$ (0.5 M in THF, 1 equiv.) was added, and the reaction was kept at this temperature for 20 min. Next, the temperature was increased to -30 °C, the acyl chloride was added, and the reaction was kept under stirring for 2 h. The reaction was

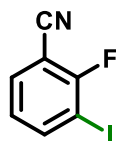
quenched with saturated aqueous NH_4Cl and extracted with ethyl acetate (3×10 mL). The combined organic phases were dried over MgSO_4 , filtered, and concentrated under reduced pressure. The crude product was purified by flash column chromatography (silica gel, hexanes/ethyl acetate).

7.1.2.7 Metalation followed by palladium-catalyzed benzoylation

To the organomagnesium and organozinc species obtained via **GMA**, ZnCl_2 (1 M in THF) was added, and the reaction was kept at room temperature for 20 min. Then, $\text{Pd}(\text{PPh}_3)_4$ (5 mol%) and the desired acyl chloride (1 equiv.) were added. For the direct zincation via **GMB**, the organozinc species were directly employed with the palladium catalyst and an acyl chloride for the benzoylation. After 12 h, the reaction was quenched with saturated aqueous NH_4Cl and extracted with ethyl acetate (3×10 mL). The combined organic phases were dried over MgSO_4 , filtered, and concentrated under reduced pressure. The crude product was purified by flash column chromatography (silica gel, hexanes/ethyl acetate).

7.1.3 Reaction scope and characterization data

1. 2-Fluoro-3-iodobenzonitrile (125a)



2-fluoro-3-iodobenzonitrile was obtained from **123a** via **GMA** using $\text{TMPMgCl}\cdot\text{LiCl}$ (1 M, 1.3 equiv., 0.65 mL) and iodine (1.1 equiv., 0.55 mmol, 139.6 mg). Purification via column chromatography (Hexanes/AcOEt 9.5:0.5) afforded the product as a yellow solid (0.48 mmol, 119.0 mg, 96%). **CAS**: 211943-27-0.

Mp: 44 – 47 °C.

$^1\text{H-NMR}$ (400 MHz, CDCl_3): δ [ppm] = 8.01 (ddd, $J = 7.8, 6.0, 1.6$ Hz, 1H), 7.61 (ddd, $J = 7.6, 5.8, 1.6$ Hz, 1H), 7.03 (t-like, 1H).

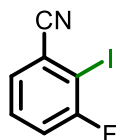
$^{13}\text{C}\{^1\text{H}\}$ NMR (101 MHz, CDCl_3): δ [ppm] = 162.3 (d, $J_{\text{C-F}} = 256.7$ Hz), 144.5, 133.6, 126.3 (d, $J_{\text{C-F}} = 4.3$ Hz) 113.1, 102.1 (d, $J_{\text{C-F}} = 18.3$ Hz), 82.1 (d, $J_{\text{C-F}} = 24.0$ Hz).

^{19}F NMR (282 MHz, CDCl_3): δ [ppm] = -85.98 (t, $J = 5.9$ Hz, 1F).

HRMS (ESI-TOF) m/z : $[\text{M}+\text{Na}]^+$ Calcd for $\text{C}_7\text{H}_3\text{FINNa}$ 269.9186; Found 269.9184.

The reported characterization data is in accordance with the literature.⁸²

2. 3-Fluoro-2-iodobenzonitrile (125b)



3-fluoro-2-iodobenzonitrile was obtained from **123b** via **GMA** using $\text{TMPMgCl}\cdot\text{LiCl}$ (1 M, 1.2 equiv., 0.60 mL) and iodine (1.1 equiv., 0.55 mmol, 139.6 mg). Purification via column chromatography (Hexanes/ AcOEt 9.5:0.5) afforded the product as a yellow solid (0.34 mmol, 84 mg, 68%). **CAS**: 916792-62-6.

Mp: 86 – 88 °C.

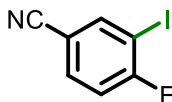
^1H -NMR (400 MHz, CDCl_3): δ [ppm] = 7.49 – 7.43 (m, 2H), 7.31 – 7.25 (m, 1H).

$^{13}\text{C}\{^1\text{H}\}$ NMR (101 MHz, CDCl_3): δ [ppm] = 162.6 (d, $J_{\text{C-F}} = 248.6$ Hz), 130.8 (d, $J_{\text{C-F}} = 8.1$ Hz), 130.4 (d, $J_{\text{C-F}} = 3.7$ Hz), 122.7, 119.9 (d, $J_{\text{C-F}} = 24.3$ Hz), 118.5 (d, $J_{\text{C-F}} = 3.5$ Hz), 87.1 (d, $J_{\text{C-F}} = 29.1$ Hz).

^{19}F NMR (282 MHz, CDCl_3): δ [ppm] = -87.24 – -87.33 (m, 1F).

HRMS (ESI-TOF) m/z : $[\text{M}+\text{H}]^+$ Calcd for $\text{C}_7\text{H}_4\text{FIN}$ 247.9367; Found 247.9366.

3. 4-Fluoro-3-iodobenzonitrile (125c)



4-fluoro-3-iodobenzonitrile was obtained from **123c** via **GMA** using $\text{TMPMgCl}\cdot\text{LiCl}$ (1 M, 1.3 equiv., 0.65 mL) and iodine (1.1 equiv., 0.55 mmol, 139.6 mg). Purification via column chromatography (Hexanes/AcOEt 9.5:0.5) afforded the product as a yellow solid (0.41 mmol, 101.3 mg, 82%). **CAS**: 159719-57-0.

Mp: 55 – 58 °C.

$^1\text{H-NMR}$ (400 MHz, CDCl_3): δ [ppm] = 8.07 (dd, $J = 5.7, 2.0$ Hz, 1H), 7.65 (ddd, $J = 8.5, 4.6, 2.0$ Hz, 1H), 7.17 (dd, $J = 8.5, 7.4$ Hz, 1H).

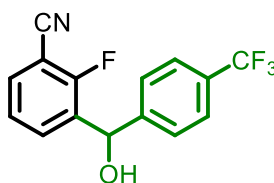
$^{13}\text{C}\{^1\text{H}\}$ NMR (101 MHz, CDCl_3): δ [ppm] = 164.6 (d, $J_{\text{C-F}} = 255.0$ Hz), 143.5, 134.5 (d, $J_{\text{C-F}} = 8.9$ Hz), 116.9, 116.6, 110.5 (d, $J_{\text{C-F}} = 4.1$ Hz), 82.3 (d, $J_{\text{C-F}} = 27.3$ Hz).

^{19}F NMR (282 MHz, CDCl_3): δ [ppm] = -83.16 – -83.23 (m, 1F).

GC-MS (EI, 70 eV) m/z : 246.95 (100%), 120.05 (58%), 100.05 (21%), 93.00 (10%), 247.95 (8%).

The reported characterization data is in accordance with the literature.¹²⁵

4. 2-Fluoro-3-(hydroxy(4-(trifluoromethyl)phenyl)methyl)benzonitrile (**125d**)



2-fluoro-3-(hydroxy(4-(trifluoromethyl)phenyl)methyl)benzonitrile was obtained from **123a** via **GMA** using $\text{TMPMgCl}\cdot\text{LiCl}$ (1 M, 1.3 equiv., 0.65 mL) and 4-(trifluoromethyl)benzaldehyde (1.1 equiv., 0.55 mmol, 75 μL). Purification via column chromatography (Hexanes/AcOEt 8:2) afforded the product as a yellow solid (0.27 mmol, 80 mg, 54%).

Mp: 112 – 114 °C.

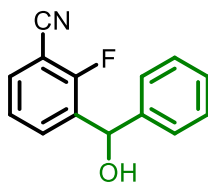
$^1\text{H-NMR}$ (400 MHz, CDCl_3): δ [ppm] = 7.86 – 7.82 (m, 1H), 7.62 (d, $J = 8.2$ Hz, 2H), 7.57 – 7.52 (m, 3H), 7.32 – 7.28 (m, 1H), 6.22 (s, 1H), 2.78 (bs, 1H).

$^{13}\text{C}\{^1\text{H}\}$ NMR (101 MHz, CDCl_3): δ [ppm] = 160.1 (d, $J_{\text{C-F}} = 258.7$ Hz), 145.6, 133.0, 132.8 (d, $J_{\text{C-F}} = 4.6$ Hz), 132.2 (d, $J_{\text{C-F}} = 12.1$ Hz), 130.6 (q, $J_{\text{C-F}} = 32.4$ Hz), 126.7 (2C), 125.9 (q, $J_{\text{C-F}} = 11.6$ Hz, 2C), 125.4 (d, $J_{\text{C-F}} = 4.6$ Hz), 124.1 (q, $J_{\text{C-F}} = 273.3$ Hz), 113.8, 101.8 (d, $J_{\text{C-F}} = 15.3$ Hz), 68.8 (d, $J_{\text{C-F}} = 2.8$ Hz).

^{19}F NMR (282 MHz, CDCl_3): δ [ppm] = -62.62 (s, 3F), -111.78 (t, $J = 6.5$ Hz, 1F).

HRMS (ESI-TOF) m/z : $[\text{M}+\text{H}-\text{H}_2\text{O}]^+$ Calcd for $\text{C}_{15}\text{H}_8\text{F}_4\text{N}$ 278.0587; Found 278.0585.

5. 2-Fluoro-3-(hydroxy(phenyl)methyl)benzonitrile (125e)



2-fluoro-3-(hydroxy(phenyl)methyl)benzonitrile was obtained from **123a** via **GMA** using $\text{TMPMgCl}\cdot\text{LiCl}$ (1 M, 1.3 equiv., 0.65 mL) and benzaldehyde (1.1 equiv., 0.55 mmol, 56 μL). Purification via column chromatography (Hexanes/AcOEt 8:2) afforded the product as a yellow oil (0.40 mmol, 90 mg, 79%).

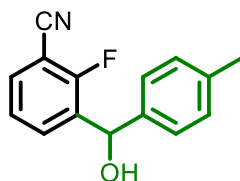
^1H -NMR (400 MHz, CDCl_3): δ [ppm] = δ 7.90 – 7.86 (m, 1H), 7.51 (ddd, $J = 7.7, 6.0, 1.8$ Hz, 1H), 7.38 – 7.25 (m, 6H), 6.13 (s, 1H), 2.67 (s, 1H).

$^{13}\text{C}\{^1\text{H}\}$ NMR (101 MHz, CDCl_3): δ [ppm] = 160.2 (d, $J_{\text{C-F}} = 258.9$ Hz), 141.8, 132.9 (d, $J_{\text{C-F}} = 10.6$ Hz), 132.8 (d, $J_{\text{C-F}} = 4.5$ Hz), 132.5, 128.9 (2C), 128.5, 126.5 (2C), 125.1 (d, $J_{\text{C-F}} = 4.2$ Hz), 114.0, 101.5 (d, $J_{\text{C-F}} = 15.9$ Hz), 69.5 (d, $J_{\text{C-F}} = 2.9$ Hz).

^{19}F NMR (282 MHz, CDCl_3): δ [ppm] = -111.54 (t, $J = 6.6$ Hz, 1F).

HRMS (ESI-TOF) m/z : $[\text{M}+\text{H}-\text{H}_2\text{O}]^+$ Calcd for $\text{C}_{14}\text{H}_9\text{FN}$ 210.0714; Found 210.0711.

6. 2-Fluoro-3-(hydroxy(p-tolyl)methyl)benzonitrile (125f)



2-fluoro-3-(hydroxy(phenyl)methyl)benzonitrile was obtained from **123a** via **GMA** using $\text{TMPMgCl}\cdot\text{LiCl}$ (1 M, 1.3 equiv., 0.65 mL) and 4-methylbenzaldehyde (1.1 equiv., 0.55 mmol, 65 μL). Purification via column chromatography (Hexanes/AcOEt 8:2) afforded the product as a white solid (0.47 mmol, 113.4 mg, 94%).

Mp: 76 – 79 °C.

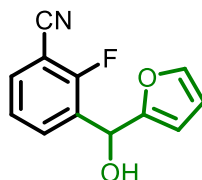
$^1\text{H-NMR}$ (500 MHz, CDCl_3): δ [ppm] = 7.91 – 7.88 (m, 1H), 7.52 – 7.49 (m, 1H), 7.28 – 7.24 (m, 3H), 7.16 (d, $J = 7.9$ Hz, 2H), 6.09 (s, 1H), 2.54 (s, 1H), 2.33 (s, 3H).

$^{13}\text{C}\{^1\text{H}\}$ NMR (126 MHz, CDCl_3): δ [ppm] = 160.2 (d, $J_{\text{C-F}} = 259.0$ Hz), 139.0, 138.4, 133.0 (d, $J_{\text{C-F}} = 11.9$ Hz), 132.7 (d, $J_{\text{C-F}} = 5.0$ Hz), 132.4, 129.6 (2C), 126.4 (2C), 125.0 (d, $J_{\text{C-F}} = 4.3$ Hz), 114.0, 101.6 (d, $J_{\text{C-F}} = 15.7$ Hz), 69.5 (d, $J_{\text{C-F}} = 2.8$ Hz), 21.2.

^{19}F NMR (282 MHz, CDCl_3): δ [ppm] = -111.52 (t, $J = 6.6$ Hz, 1F).

HRMS (ESI-TOF) m/z: $[\text{M}+\text{H}-\text{H}_2\text{O}]^+$ Calcd for $\text{C}_{15}\text{H}_{11}\text{FN}$ 224.0870; Found 224.0869.

7. 2-Fluoro-3-(furan-2-yl(hydroxy)methyl)benzonitrile (125g)



2-fluoro-3-(furan-2-yl(hydroxy)methyl)benzonitrile was obtained from **123a** via **GMA** using $\text{TMPMgCl}\cdot\text{LiCl}$ (1 M, 1.3 equiv., 0.65 mL) and 2-furaldehyde (1.1 equiv., 0.55 mmol, 46 μL). Purification via column chromatography (Hexanes/AcOEt 7:3) afforded the product as an orange oil (0.47 mmol, 103.2 mg, 94%).

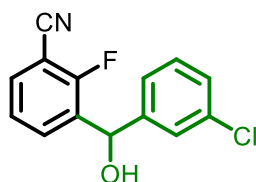
$^1\text{H-NMR}$ (400 MHz, CDCl_3): δ [ppm] = 7.94 – 7.90 (m, 1H), 7.59 (ddd, $J = 7.8, 6.0, 1.8$ Hz, 1H), 7.39 (dd, $J = 1.9, 0.9$ Hz, 1H), 7.31 (t, $J = 7.8$ Hz, 1H), 6.34 (dd, $J = 3.3, 1.9$ Hz, 1H), 6.17 (d, $J = 3.3$ Hz, 1H), 6.14 (s, 1H), 2.86 (s, 1H).

$^{13}\text{C}\{^1\text{H}\}$ NMR (101 MHz, CDCl_3): δ [ppm] = 160.3 (d, $J_{\text{C-F}} = 259.7$ Hz), 153.6, 143.2, 133.5 (d, $J_{\text{C-F}} = 4.7$ Hz), 133.1, 129.9 (d, $J_{\text{C-F}} = 11.6$ Hz), 125.1 (d, $J_{\text{C-F}} = 3.9$ Hz), 113.9, 110.6, 108.1, 101.6 (d, $J_{\text{C-F}} = 15.3$ Hz), 63.4 (d, $J_{\text{C-F}} = 3.3$ Hz).

^{19}F NMR (282 MHz, CDCl_3): δ [ppm] = -112.03 (t, $J = 6.5$ Hz, 1F).

HRMS (ESI-TOF) m/z : $[\text{M}+\text{H}-\text{H}_2\text{O}]^+$ Calcd for $\text{C}_{12}\text{H}_7\text{FNO}$ 200.0506; Found 200.0504.

8. 3-((3-Chlorophenyl)(hydroxy)methyl)-2-fluorobenzonitrile (125h)



3-((3-chlorophenyl)(hydroxy)methyl)-2-fluorobenzonitrile was obtained from **123a** via **GMA** using $\text{TMPMgCl}\cdot\text{LiCl}$ (1 M, 1.3 equiv., 0.65 mL) and 3-chlorobenzaldehyde (1.1 equiv., 0.55 mmol, 62 μL). Purification via column chromatography (Hexanes/ AcOEt 8:2) afforded the product as a yellow oil (0.40 mmol, 106 mg, 81%).

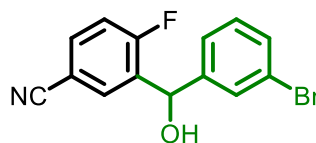
$^1\text{H-NMR}$ (500 MHz, CDCl_3): δ [ppm] = 7.86-7.82 (m, 1H), 7.54 (ddd, $J = 7.8, 6.0, 1.8$ Hz, 1H), 7.38 (s, 1H), 7.31 – 7.24 (m, 4H), 6.11 (s, 1H), 2.79 (s, 1H).

$^{13}\text{C}\{^1\text{H}\}$ NMR (126 MHz, CDCl_3): δ [ppm] = 160.1 (d, $J_{\text{C-F}} = 259.1$ Hz), 143.8, 134.9, 132.9, 132.8 (d, $J_{\text{C-F}} = 4.7$ Hz), 132.3 (d, $J_{\text{C-F}} = 12.0$ Hz), 130.2, 128.6, 126.6, 125.3 (d, $J_{\text{C-F}} = 4.4$ Hz), 124.6, 113.8, 101.7 (d, $J_{\text{C-F}} = 15.9$ Hz), 68.8 (d, $J_{\text{C-F}} = 2.9$ Hz).

^{19}F NMR (282 MHz, CDCl_3): δ [ppm] = -111.67 (t, $J = 6.5$ Hz, 1F).

HRMS (ESI-TOF) m/z : $[\text{M}+\text{H}-\text{H}_2\text{O}]^+$ Calcd for $\text{C}_{14}\text{H}_8\text{ClFN}$ 244.0324; Found 244.0327.

9. 3-((3-Bromophenyl)(hydroxy)methyl)-4-fluorobenzonitrile (125i)



3-((3-bromophenyl)(hydroxy)methyl)-4-fluorobenzonitrile was obtained from **123c** via **GMA** using $\text{TMPMgCl}\cdot\text{LiCl}$ (1 M, 1.3 equiv., 0.65 mL) and 3-bromobenzaldehyde (1.1 equiv., 0.55 mmol, 64 μL). Purification via column chromatography (Hexanes/AcOEt 8:2) afforded the product as a white solid (0.41 mmol, 127.0 mg, 83%).

Mp: 111 – 114 °C.

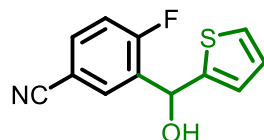
$^1\text{H-NMR}$ (500 MHz, CDCl_3): δ [ppm] = 7.93 (dd, J = 6.6, 2.2 Hz, 1H), 7.59 (ddd, J = 8.5, 4.8, 2.2 Hz, 1H), 7.53 (s, 1H), 7.44 – 7.42 (m, 1H), 7.31 (d, J = 7.7 Hz, 1H), 7.23 (t, J = 7.8 Hz, 1H), 7.13 (t-like, J = 8.5 Hz, 1H), 6.07 (s, 1H), 2.39 (bs, 1H).

$^{13}\text{C}\{^1\text{H}\}$ NMR (126 MHz, CDCl_3): δ [ppm] = 162.0 (d, $J_{\text{C-F}}$ = 256.8 Hz), 144.0, 133.9 (d, $J_{\text{C-F}}$ = 9.7 Hz), 132.7 (d, $J_{\text{C-F}}$ = 14.5 Hz), 132.3 (d, $J_{\text{C-F}}$ = 5.5 Hz), 131.6, 130.5, 129.6, 125.1, 123.1, 118.1, 117.0 (d, $J_{\text{C-F}}$ = 23.3 Hz), 109.1 (d, $J_{\text{C-F}}$ = 3.8 Hz), 68.9 (d, $J_{\text{C-F}}$ = 2.7 Hz).

^{19}F NMR (282 MHz, CDCl_3): δ [ppm] = -107.77 – -107.85 (m, 1F).

HRMS (ESI-TOF) m/z : $[\text{M}+\text{H}]^+$ Calcd for $\text{C}_{14}\text{H}_{10}\text{BrFNO}$ 305.9925; Found 305.9921.

10. 4-Fluoro-3-(hydroxy(thiophen-2-yl)methyl)benzonitrile (**125j**)



4-fluoro-3-(hydroxy(thiophen-2-yl)methyl)benzonitrile was obtained from **123c** via **GMA** using $\text{TMPMgCl}\cdot\text{LiCl}$ (1 M, 1.3 equiv., 0.65 mL) and 2-thiophenecarboxaldehyde (1.1 equiv., 0.55 mmol, 51 μL). Purification via column chromatography (Hexanes/AcOEt 8:2) afforded the product as a yellow solid (0.44 mmol, 104.0 mg, 89%). **CAS:** 2237249-90-8.

Mp: 60 – 62 °C.

$^1\text{H-NMR}$ (500 MHz, CDCl_3): δ [ppm] = 8.01 (dd, $J = 6.7, 2.2$ Hz, 1H), 7.61 (ddd, $J = 8.5, 4.7, 2.2$ Hz, 1H), 7.30 (dd, $J = 4.2, 2.2$ Hz, 1H), 7.14 (dd, $J = 9.4, 8.5$ Hz, 1H), 6.97 – 6.96 (m, 2H), 6.34 (s, 1H), 2.85 (s, 1H).

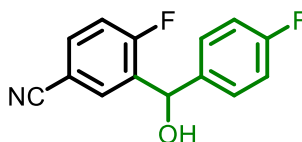
$^{13}\text{C}\{^1\text{H}\}$ NMR (126 MHz, CDCl_3): δ [ppm] = 162.1 (d, $J_{\text{C-F}} = 257.0$ Hz), 145.6, 133.9 (d, $J_{\text{C-F}} = 9.6$ Hz), 132.8 (d, $J_{\text{C-F}} = 14.3$ Hz), 132.2 (d, $J_{\text{C-F}} = 5.3$ Hz), 127.1, 126.2, 125.4, 118.1, 117.0 (d, $J_{\text{C-F}} = 23.2$ Hz), 109.0 (d, $J_{\text{C-F}} = 3.9$ Hz), 65.6 (d, $J_{\text{C-F}} = 3.7$ Hz).

^{19}F NMR (282 MHz, CDCl_3): δ [ppm] = -108.19 – -108.27 (m, 1F).

HRMS (ESI-TOF) m/z : $[\text{M-H}]^-$ Calcd for $\text{C}_{12}\text{H}_7\text{FNOS}$ 232.0238; Found 232.0235.

The reported characterization data is in accordance with the literature.¹²⁶

11. 4-Fluoro-3-((4-fluorophenyl)(hydroxy)methyl)benzonitrile (125k)



4-fluoro-3-((4-fluorophenyl)(hydroxy)methyl)benzonitrile was obtained from **123c** via **GMA** using $\text{TMPMgCl}\cdot\text{LiCl}$ (1 M, 1.3 equiv., 0.65 mL) and 4-fluorobenzaldehyde (1.1 equiv., 0.55 mmol, 59 μL). Purification via column chromatography (Hexanes/ AcOEt 8:2) afforded the product as a white solid (0.40 mmol, 98.1 mg, 80%). **CAS:** 1519447-09-6.

Mp: 82 – 84 $^\circ\text{C}$.

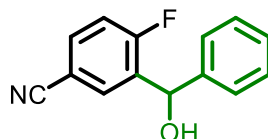
$^1\text{H-NMR}$ (500 MHz, CDCl_3): δ [ppm] = 7.96 (dd, $J = 6.8, 2.2$ Hz, 1H), 7.58 (ddd, $J = 8.5, 4.7, 2.2$ Hz, 1H), 7.35 (dd, $J = 8.5, 5.4$ Hz, 2H), 7.11 (dd, $J = 9.7, 8.5$ Hz, 1H), 7.06 – 7.02 (m, 2H), 6.09 (s, 1H), 2.61 (d, $J = 2.6$ Hz, 1H).

$^{13}\text{C}\{^1\text{H}\}$ NMR (126 MHz, CDCl_3): δ [ppm] = 162.7 (d, $J_{\text{C-F}} = 247.4$ Hz), 162.0 (d, $J_{\text{C-F}} = 256.4$ Hz), 137.6 (d, $J_{\text{C-F}} = 3.1$ Hz), 133.7 (d, $J_{\text{C-F}} = 9.7$ Hz), 133.2 (d, $J_{\text{C-F}} = 14.5$ Hz), 132.1 (d, $J_{\text{C-F}} = 5.6$ Hz), 128.4 (d, $J_{\text{C-F}} = 8.3$ Hz, 2C), 118.2, 117.6, (d, $J_{\text{C-F}} = 23.1$ Hz), 115.9 (d, $J_{\text{C-F}} = 21.9$ Hz, 2C), 109.0 (d, $J_{\text{C-F}} = 3.9$ Hz), 69.0 (d, $J_{\text{C-F}} = 2.8$ Hz).

^{19}F NMR (282 MHz, CDCl_3): δ [ppm] = -107.84 – -107.92 (m, 1F), -113.27 – -113.37 (m, 1F).

HRMS (ESI-TOF) m/z : $[\text{M}+\text{Na}]^+$ Calcd for $\text{C}_{14}\text{H}_9\text{F}_2\text{NNaO}$ 268.0544; Found 268.0546.

12. 4-Fluoro-3-(hydroxy(phenyl)methyl)benzonitrile (125l)



4-fluoro-3-(hydroxy(phenyl)methyl)benzonitrile was obtained from **123c** via **GMA** using $\text{TMPMgCl}\cdot\text{LiCl}$ (1 M, 1.3 equiv., 0.65 mL) and benzaldehyde (1.1 equiv., 0.55 mmol, 56 μL). Purification via column chromatography (Hexanes/ AcOEt 8:2) afforded the product as a white solid (0.36 mmol, 83 mg, 73%). **CAS**: 1499388-65-6.

Mp: 101 – 103 $^\circ\text{C}$.

^1H -NMR (400 MHz, CDCl_3): δ [ppm] = 7.96 (dd, J = 6.8, 2.2 Hz, 1H), 7.56 (ddd, J = 8.5, 4.8, 2.2 Hz, 1H), 7.39 – 7.35 (m, 4H), 7.35 – 7.29 (m, 1H), 7.10 (dd, J = 9.6, 8.5 Hz, 1H), 6.10 (s, 1H), 2.40 (s, 1H).

$^{13}\text{C}\{^1\text{H}\}$ NMR (101 MHz, CDCl_3): δ [ppm] = 162.1 (d, $J_{\text{C-F}}$ = 256.6 Hz), 141.7, 133.5 (d, $J_{\text{C-F}}$ = 9.6 Hz), 133.2 (d, $J_{\text{C-F}}$ = 14.6 Hz), 132.2 (d, $J_{\text{C-F}}$ = 5.6 Hz), 129.0 (2C), 128.5, 126.5 (2C), 118.3, 116.9 (d, $J_{\text{C-F}}$ = 23.3 Hz), 108.8 (d, $J_{\text{C-F}}$ = 3.8 Hz), 69.6 (d, $J_{\text{C-F}}$ = 2.7 Hz).

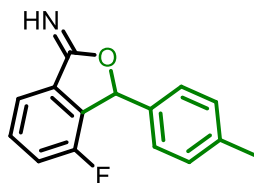
^{19}F NMR (282 MHz, CDCl_3): δ [ppm] = -107.68 – -107.75 (m, 1F).

GC-MS (EI, 70 eV) m/z : 227.00 (100%), 79.05 (96%), 148.00 (68%), 78.05 (37%), 77.00 (37%).

HRMS (ESI-TOF) m/z : $[\text{M}+\text{FA}-\text{H}]^-$ Calcd for $\text{C}_{15}\text{H}_{11}\text{FNO}_3$ 272.0728; Found 272.0701.

The reported characterization data is in accordance with the literature.⁸⁷

13. 4-Fluoro-3-(*p*-tolyl)isobenzofuran-1(3*H*)-imine (125m)



4-fluoro-3-(*p*-tolyl)isobenzofuran-1(3*H*)-imine was obtained from **123b** via **GMA** using $\text{TMPMgCl}\cdot\text{LiCl}$ (1 M, 1.2 equiv., 0.6 mL) and 4-methylbenzaldehyde (1.1 equiv., 0.55 mmol, 65 μL). Purification via column chromatography (Hexanes/AcOEt 8:2) afforded the product as a white solid (0.31 mmol, 75 mg, 62%).

Mp: 121 – 125 °C.

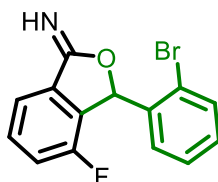
$^1\text{H-NMR}$ (500 MHz, CDCl_3): δ [ppm] = 7.74 (d, J = 6.9 Hz, 1H), 7.49 (td, J = 7.9, 4.5 Hz, 1H), 7.20 – 7.16 (m, 5H), 6.46 (s, 1H), 2.35 (s, 3H).

$^{13}\text{C}\{^1\text{H}\}$ NMR (126 MHz, CDCl_3): δ [ppm] = 157.2 (d, $J_{\text{C-F}}$ = 251.4 Hz), 139.4, 133.6, 133.5 (d, $J_{\text{C-F}}$ = 17.8 Hz), 131.5 (d, $J_{\text{C-F}}$ = 6.3 Hz), 129.6 (2C), 127.1 (2C), 120.0 (2C), 119.1 (d, $J_{\text{C-F}}$ = 19.6 Hz, 2C), 82.9, 21.3.

^{19}F NMR (282 MHz, CDCl_3): δ [ppm] = -118.29 (dd, J = 8.8, 4.6 Hz, 1F).

HRMS (ESI-TOF) m/z : $[\text{M}+\text{H}]^+$ Calcd for $\text{C}_{15}\text{H}_{12}\text{FO}_2$ 243.0816; Found 243.0815. * Under the analysis conditions (MeCN: H_2O mixture, formic acid) the 3-substituted-isobenzofuran-1(3*H*)-imine was converted into the respective isobenzofuran-1(3*H*)-one. The hydrolysis under acidic conditions is already mentioned in the literature.¹²⁷

14. 3-(2-Bromophenyl)-4-fluoroisobenzofuran-1(3*H*)-imine (125n)



3-(2-bromophenyl)-4-fluoroisobenzofuran-1(3*H*)-imine was obtained from **123b** via **GMA** using $\text{TMPMgCl}\cdot\text{LiCl}$ (1 M, 1.2 equiv., 0.6 mL) and 2-bromobenzaldehyde (1.1 equiv.,

0.55 mmol, 64 μ L). Purification via column chromatography (Hexanes/AcOEt 8:2) afforded the product as a yellow solid (0.29 mmol, 89 mg, 58%).

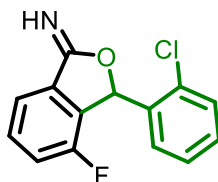
Mp: 112 – 115 °C.

$^1\text{H-NMR}$ (500 MHz, CDCl_3): δ [ppm] = 7.77 (d, $J = 7.6$ Hz, 1H), 7.67 – 7.65 (m, 1H), 7.53 (td, $J = 7.9, 4.5$ Hz, 1H), 7.27 – 7.21 (m, 3H), 6.98 (s, 1H), 6.95 (dd, $J = 7.2, 2.5$ Hz, 1H).

$^{13}\text{C}\{^1\text{H}\}$ NMR (126 MHz, CDCl_3): δ [ppm] = 157.1 (d, $J_{\text{C-F}} = 253.0$ Hz), 135.4, 133.6, 132.6 (d, $J_{\text{C-F}} = 17.9$ Hz), 131.9 (d, $J_{\text{C-F}} = 6.6$ Hz), 131.0, 128.9, 128.1, 124.3, 120.2, 120.1, 119.3 (d, $J_{\text{C-F}} = 19.1$ Hz, 2C), 81.9.

HRMS (ESI-TOF) m/z : $[\text{M}+\text{H}]^+$ Calcd for $\text{C}_{14}\text{H}_9\text{BrFO}_2$ 306.9765; Found 306.9765. * Under the analysis conditions (MeCN: H_2O mixture, formic acid) the 3-substituted-isobenzofuran-1(3*H*)-imine was converted into the respective isobenzofuran-1(3*H*)-one. The hydrolysis under acidic conditions is already mentioned in the literature.¹²⁷

15. 3-(2-Chlorophenyl)-4-fluoroisobenzofuran-1(3*H*)-imine (125o)



3-(2-chlorophenyl)-4-fluoroisobenzofuran-1(3*H*)-imine was obtained from **123b** via **GMA** using $\text{TMPMgCl}\cdot\text{LiCl}$ (1 M, 1.2 equiv., 0.6 mL) and 2-chlorobenzaldehyde (1.1 equiv., 0.55 mmol, 62 μ L). Purification via column chromatography (Hexanes/AcOEt 8:2) afforded the product as a white solid (0.24 mmol, 64 mg, 49%).

Yield: 49% (white solid, 64 mg).

Mp: 110 – 113 °C.

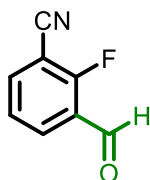
$^1\text{H-NMR}$ (500 MHz, CDCl_3): δ [ppm] = 7.76 (d, $J = 7.6$ Hz, 1H), 7.52 (td, $J = 8.0, 4.5$ Hz, 1H), 7.46 (d, $J = 8.0$ Hz, 1H), 7.32 – 7.29 (m, 1H), 7.23 – 7.20 (m, 2H), 6.99 – 6.97 (m, 2H).

$^{13}\text{C}\{^1\text{H}\}$ NMR (126 MHz, CDCl_3): δ [ppm] = 157.1 (d, $J_{\text{C-F}} = 252.1$ Hz), 134.3, 133.8, 132.5 (d, $J_{\text{C-F}} = 17.7$ Hz), 131.9 (d, $J_{\text{C-F}} = 6.6$ Hz), 130.7, 130.3, 128.7, 127.4, 120.1 (2C), 119.2 (d, $J_{\text{C-F}} = 19.4$ Hz, 2C), 79.5.

HRMS (ESI-TOF) m/z : $[\text{M}+\text{H}]^+$ Calcd for $\text{C}_{14}\text{H}_9\text{ClFO}_2$ 263.0270; Found 263.0266.

*Under the analysis conditions (MeCN: H_2O mixture, formic acid) the 3-substituted-isobenzofuran-1(3*H*)-imine was converted into the respective isobenzofuran-1(3*H*)-one. The hydrolysis under acidic conditions is already mentioned in the literature.¹²⁷

16. 2-Fluoro-3-formylbenzonitrile (125p)



2-fluoro-3-formylbenzonitrile was obtained from **123a** via **GMA** using $\text{TMPMgCl}\cdot\text{LiCl}$ (1 M, 1.3 equiv., 0.65 mL) and *N,N*-dimethylformamide (2.0 equiv., 1.0 mmol, 77 μL). Purification via column chromatography (Hexanes/ AcOEt 8:2) afforded the product as a yellow solid (0.29 mmol, 44 mg, 59%). **CAS:** 1261823-31-7.

Mp: 46 – 48 $^\circ\text{C}$.

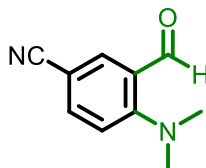
$^1\text{H-NMR}$ (400 MHz, CDCl_3): δ [ppm] = 10.36 (s, 1H), 8.13 (ddd, $J = 7.9, 6.7, 1.9$ Hz, 1H), 7.90 (ddd, $J = 7.8, 6.1, 1.9$ Hz, 1H), 7.44 (t-like, $J = 7, 8$ Hz, 1H).

$^{13}\text{C}\{^1\text{H}\}$ NMR (101 MHz, CDCl_3): δ [ppm] = 184.9 (d, $J_{\text{C-F}} = 6.3$ Hz), 164.9 (d, $J_{\text{C-F}} = 270.0$ Hz), 139.1, 133.5, 125.6 (d, $J_{\text{C-F}} = 4.6$ Hz), 124.8 (d, $J_{\text{C-F}} = 7.4$ Hz), 112.7, 103.2 (d, $J_{\text{C-F}} = 14.9$ Hz).

^{19}F NMR (282 MHz, CDCl_3): δ [ppm] = -116.08 (t, $J = 6.4$ Hz, 1F).

HRMS (ESI-TOF) m/z : $[\text{M}+\text{H}]^+$ Calcd for $\text{C}_8\text{H}_5\text{FNO}$ 150.0350; Found 150.0351.

17. 4-(Dimethylamino)-3-formylbenzonitrile (125q)



4-(dimethylamino)-3-formylbenzonitrile was obtained from **123c** via **GMA** using $\text{TMPMgCl}\cdot\text{LiCl}$ (1 M, 1.3 equiv., 0.65 mL) and *N,N*-dimethylformamide (2.0 equiv., 1.0 mmol, 77 μL). Purification via column chromatography (Hexanes/AcOEt 8:2) afforded the product as a yellow solid (0.45 mmol, 79.3 mg, 91%). **CAS**: 1289200-50-5.

Mp: 62 – 64 °C.

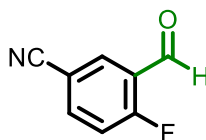
$^1\text{H-NMR}$ (500 MHz, CDCl_3): δ [ppm] = 9.97 (s, 1H), 7.96 (d, $J = 2.2$ Hz, 1H), 7.57 (dd, $J = 8.8, 2.2$ Hz, 1H), 6.97 (d, $J = 8.8$ Hz, 1H), 3.06 (s, 6H).*

$^{13}\text{C}\{^1\text{H}\}$ NMR (126 MHz, CDCl_3): δ [ppm] = 188.2, 155.9, 137.9, 136.6, 124.4, 119.0, 116.9, 101.0, 44.5 (2C).

HRMS (ESI-TOF) m/z : $[\text{M}+\text{H}]^+$ Calcd for $\text{C}_{10}\text{H}_{11}\text{N}_2\text{O}$ 175.0866; Found 175.0863.

*Previously reported in the literature.¹²⁸

18. 4-Fluoro-3-formylbenzonitrile (125r)



4-fluoro-3-formylbenzonitrile was obtained from **123c** via **GMA** using $\text{TMPMgCl}\cdot\text{LiCl}$ (1 M, 1.3 equiv., 0.65 mL) and *N*-methylformanilide (2.0 equiv., 1.0 mmol, 123 μL). Purification via column chromatography (Hexanes/AcOEt 9:1) afforded the product as a white solid (0.31 mmol, 46.2 mg, 62%). **CAS**: 146137-79-3.

Yield: 62% (white solid, 46.2 mg).

Mp: 68 – 71 °C.

¹H-NMR (400 MHz, CDCl₃): δ [ppm] = 10.34 (s, 1H), 8.20 (ddd, *J* = 6.3, 2.3, 0.4 Hz, 1H), 7.91 (ddd, *J* = 8.7, 4.8, 2.3 Hz, 1H), 7.38 – 7.33 (m, 1H).

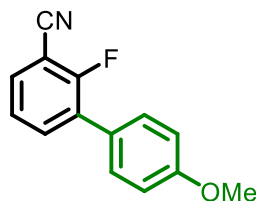
¹³C{¹H} NMR (101 MHz, CDCl₃): δ [ppm] = 185.0 (d, *J* = 6.2 Hz), 166.4 (d, *J*_{C-F} = 267.5 Hz), 139.6 (d, *J*_{C-F} = 10.4 Hz), 133.6 (d, *J*_{C-F} = 3.3 Hz), 125.0 (d, *J*_{C-F} = 9.8 Hz), 118.5 (d, *J*_{C-F} = 22.3 Hz), 117.0, 109.9 (d, *J*_{C-F} = 3.9 Hz).

¹⁹F NMR (282 MHz, CDCl₃): δ [ppm] = -112.19 – -112.27 (m, 1F).

GC-MS (EI, 70 eV) m/z: 148.05 (100%), 149.05 (64%), 120.05 (36%), 94.00 (15%), 100.00 (14%).

The reported characterization data is in accordance with the literature.¹²⁹

19. 2-Fluoro-4'-methoxy-[1,1'-biphenyl]-3-carbonitrile (125s)



After applying **GMA** [TMPMgCl·LiCl (1 M, 1.3 equiv., 0.65 mL)] for **123a** followed by transmetalation with ZnCl₂ (1 M in THF, 1.3 equiv., 0.65 mL), the Negishi cross-coupling was performed using Pd(PPh₃)₄ (5 mol%, 29 mg) and 4-methoxyiodobenzene (1.2 equiv., 0.6 mmol, 140.4 mg) at 50 °C (oil bath). Purification via column chromatography (Hexanes/AcOEt 9:1) afforded the product as a beige solid (0.45 mmol, 102.3 mg, 90%).

Mp: 106 – 108 °C.

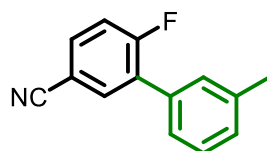
¹H-NMR (500 MHz, CDCl₃): δ [ppm] = 7.66 (t-like, *J* = 7.8 Hz, 1H), 7.55 (t-like, *J* = 7.1 Hz, 1H), 7.47 (d, *J* = 8.5 Hz, 2H), 7.30 (t, *J* = 7.8 Hz, 1H), 7.00 (d, *J* = 8.5 Hz, 2H), 3.86 (s, 3H).

¹³C{¹H} NMR (126 MHz, CDCl₃): δ [ppm] = 160.3 (d, *J*_{C-F} = 259.6 Hz), 160.1, 135.5 (d, *J*_{C-F} = 4.1 Hz), 131.8, 130.3 (d, *J*_{C-F} = 14.0 Hz), 130.2 (d, *J*_{C-F} = 3.1 Hz, 2C), 125.9, 125.1 (d, *J*_{C-F} = 4.3 Hz), 114.4 (2C), 114.3, 102.4 (d, *J*_{C-F} = 17.0 Hz), 55.5.

^{19}F NMR (282 MHz, CDCl_3): δ [ppm] = -111.52 (t, J = 6.6 Hz, 1F).

HRMS (ESI-TOF) m/z : $[\text{M}+\text{H}]^+$ Calcd for $\text{C}_{14}\text{H}_{11}\text{FNO}$ 228.0819; Found 228.0818.

20. 6-Fluoro-3'-methyl-[1,1'-biphenyl]-3-carbonitrile (125t)



After applying **GMA** [TMPMgCl·LiCl (1 M, 1.3 equiv., 0.65 mL)] for **123c** followed by transmetalation with ZnCl_2 (1 M in THF, 1.3 equiv., 0.65 mL), the Negishi cross-coupling was performed using $\text{Pd}(\text{PPh}_3)_4$ (5 mol%, 29 mg) and 1-iodo-3-methylbenzene (1.2 equiv., 0.6 mmol, 77 μL) at 50 °C (oil bath). Purification via column chromatography (Hexanes/AcOEt 9:1) afforded the product as a white solid (0.46 mmol, 97.2 mg, 92%).

CAS: 1267960-92-8.

Mp: 57 – 59 °C.

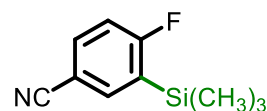
^1H -NMR (500 MHz, CDCl_3): δ [ppm] = 7.66 (dd, J = 7.0, 2.2 Hz, 1H), 7.53 (ddd, J = 8.6, 4.5, 2.2 Hz, 1H), 7.27 (t, J = 7.5 Hz, 1H), 7.23 – 7.21 (m, 2H), 7.18 – 7.14 (m, 2H), 2.33 (s, 3H).

$^{13}\text{C}\{^1\text{H}\}$ NMR (126 MHz, CDCl_3): δ [ppm] = 162.2 (d, $J_{\text{C-F}}$ = 257.7 Hz), 138.7, 135.2 (d, $J_{\text{C-F}}$ = 5.1 Hz), 133.5, 133.1 (d, $J_{\text{C-F}}$ = 9.6 Hz), 131.2 (d, $J_{\text{C-F}}$ = 15.1 Hz), 129.7, 129.6, 128.8, 126.1 (d, $J_{\text{C-F}}$ = 3.0 Hz), 118.2, 117.7 (d, $J_{\text{C-F}}$ = 24.6 Hz), 109.0 (d, $J_{\text{C-F}}$ = 4.0 Hz), 21.5.

^{19}F NMR (282 MHz, CDCl_3): δ [ppm] = -107.55 – -107.64 (m, 1F).

HRMS (ESI-TOF) m/z : $[\text{M}+\text{H}]^+$ Calcd for $\text{C}_{14}\text{H}_{11}\text{FN}$ 212.0870; Found 212.0869.

21. 4-Fluoro-3-(trimethylsilyl)benzonitrile (125u)



4-fluoro-3-(trimethylsilyl)benzotrile was obtained from **123c** via **GMA** using $\text{TMPMgCl}\cdot\text{LiCl}$ (1 M, 1.3 equiv., 0.65 mL) and fresh distilled chlorotrimethylsilane (1.1 equiv., 0.55 mmol, 70 μL). Purification via column chromatography (Hexanes/AcOEt 9:1) afforded the product as a yellow solid (0.31 mmol, 61 mg, 63%).

Mp: 49 – 51 °C.

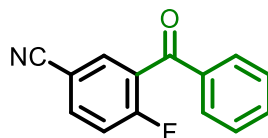
$^1\text{H-NMR}$ (500 MHz, CDCl_3): δ [ppm] = 7.70 (dd, J = 4.9, 2.2 Hz, 1H), 7.68 – 7.64 (m, 1H), 7.08 (t, J = 8.2 Hz, 1H), 0.34 (s, 9H).

$^{13}\text{C}\{^1\text{H}\}$ NMR (126 MHz, CDCl_3): δ [ppm] = 169.5 (d, $J_{\text{C-F}}$ = 250.9 Hz), 140.0 (d, $J_{\text{C-F}}$ = 13.4 Hz), 135.6 (d, $J_{\text{C-F}}$ = 10.0 Hz), 129.1 (d, $J_{\text{C-F}}$ = 32.9 Hz), 118.6, 116.1 (d, $J_{\text{C-F}}$ = 27.9 Hz), 108.7 (d, $J_{\text{C-F}}$ = 3.4 Hz), -1.2 (3C).

^{19}F NMR (282 MHz, CDCl_3): δ [ppm] = -90.55 – -90.61 (m, 1F).

HRMS (ESI-TOF) m/z : $[\text{M}+\text{H}]^+$ Calcd for $\text{C}_{10}\text{H}_{13}\text{FNSi}$ 194.0796; Found 194.0793.

22. 3-Benzoyl-4-fluorobenzotrile (**125v**)



After applying **GMA** [$\text{TMPMgCl}\cdot\text{LiCl}$ (1 M, 1.3 equiv., 0.65 mL)] for **123c** followed by transmetalation with ZnCl_2 (1 M in THF, 1.3 equiv., 0.65 mL), the benzoylation was performed using $\text{Pd}(\text{PPh}_3)_4$ (5 mol%, 29 mg) and benzoyl chloride (1.0 equiv., 0.5 mmol, 58 μL) at room temperature. Purification via column chromatography (Hexanes/AcOEt 9:1) afforded the product as a white solid (0.47 mmol, 107 mg, 95%). Applying **GMA** at the same conditions followed by transmetalation with $\text{CuCl}\cdot 2\text{LiCl}$ (0.5 M in THF, 1 equiv.) at -40 °C and the reaction of organocopper species with benzoyl chloride (1.0 equiv., 0.5 mmol, 58 μL), furnished the same ketone in 78%. **CAS:** 217498-80-1.

Mp: 92 – 95 °C.

¹H-NMR (400 MHz, CDCl₃): δ [ppm] = 7.87 – 7.78 (m, 4H), 7.65 (tt, J = 7.4, 1.2 Hz, 1H), 7.52 – 7.48 (m, 2H), 7.31 (t, J = 8.8 Hz, 1H).

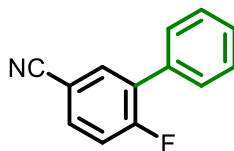
¹³C{¹H} NMR (101 MHz, CDCl₃): δ [ppm] = 190.8, 162.1 (d, J_{C-F} = 261.3 Hz), 136.7 (d, J_{C-F} = 9.5 Hz), 136.3, 135.1 (d, J_{C-F} = 4.4 Hz), 134.2, 129.8 (2C), 128.8 (2C), 128.6 (d, J_{C-F} = 16.3 Hz), 118.0 (d, J_{C-F} = 23.4 Hz), 117.2, 109.3 (d, J_{C-F} = 4.2 Hz).

¹⁹F NMR (282 MHz, CDCl₃): δ [ppm] = -101.35 – -101.42 (m, 1F).

HRMS (ESI-TOF) m/z: [M+Na]⁺ Calcd for C₁₄H₈FNNaO 248.0482; Found 248.0482.

The reported characterization data is in accordance with the literature.¹³⁰

23. 6-Fluoro-[1,1'-biphenyl]-3-carbonitrile (125w)



After applying **GMA** [TMPMgCl-LiCl (1 M, 1.3 equiv., 3.7 mL) and 4-fluorobenzonitrile (**123c**) (1.0 equiv., 2.84 mmol, 344 mg)] followed by transmetalation with ZnCl₂ (1 M in THF, 1.3 equiv., 3.7 mL), the Negishi cross-coupling was performed using Pd(PPh₃)₄ (5 mol%, 164.1 mg) and iodobenzene (1.2 equiv., 3.41 mmol, 0.38 mL) at 50 °C (oil bath). Purification via column chromatography (Hexanes/AcOEt 9:1) afforded the product as a white solid (2.52 mmol, 497 mg, 89%). **CAS:** 1214331-73-3.

Mp: 83 – 84 °C.

¹H-NMR (400 MHz, CDCl₃): δ [ppm] = 7.77 (dd, J = 7.1, 2.2 Hz, 1H), 7.64 (ddd, J = 8.6, 4.5, 2.2 Hz, 1H), 7.53 – 7.42 (m, 5H), 7.27 (app t, J = 8.6 Hz, 1H).

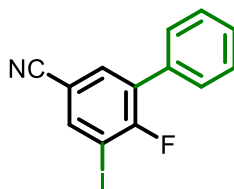
¹³C{¹H} NMR (101 MHz, CDCl₃): δ [ppm] = 162.2 (d, J_{C-F} = 257.9 Hz), 135.2 (d, J_{C-F} = 5.2 Hz), 133.5, 133.2 (d, J_{C-F} = 9.6 Hz), 131.1 (d, J_{C-F} = 15.2 Hz), 129.0 (d, J_{C-F} = 2.9 Hz, 2C), 128.9 (2C), 128.9, 118.2, 117.7 (d, J_{C-F} = 24.6 Hz), 109.1 (d, J_{C-F} = 4.2 Hz).

¹⁹F NMR (282 MHz, CDCl₃): δ [ppm] = -107.71 – -107.79 (m, 1F).

GC-MS (EI, 70 eV) m/z: 197.05 (100%), 196.05 (28%), 198.05 (18%), 169.00 (14%), 170.00 (11%).

The reported characterization data is in accordance with the literature.¹³¹

24. 6-Fluoro-5-iodo-[1,1'-biphenyl]-3-carbonitrile (126a)



6-fluoro-5-iodo-[1,1'-biphenyl]-3-carbonitrile was obtained from **125w** via **GMA** using TMPMgCl·LiCl (1 M, 1.3 equiv., 0.65 mL), 6-fluoro-[1,1'-biphenyl]-3-carbonitrile (1.0 equiv., 0.5 mmol, 99 mg) and iodine (1.1 equiv., 0.55 mmol, 139.6 mg). Purification via column chromatography (Hexanes/AcOEt 9:1) afforded the product as a white solid (0.37 mmol, 119.5 mg, 74%).

Mp: 103 – 105 °C.

¹H-NMR (400 MHz, CDCl₃): δ [ppm] = 8.03 (dd, *J* = 5.1, 2.1 Hz, 1H), 7.71 (dd, *J* = 6.5, 2.1 Hz, 1H), 7.49 – 7.45 (m, 5H).

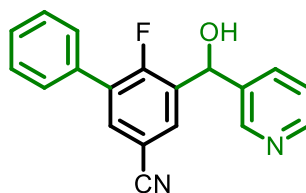
¹³C{¹H} NMR (101 MHz, CDCl₃): δ [ppm] = 161.3 (d, *J*_{C-F} = 255.6 Hz), 141.8 (d, *J*_{C-F} = 3.1 Hz), 135.1 (d, *J*_{C-F} = 4.5 Hz), 133.0 (d, *J*_{C-F} = 1.9 Hz), 131.2 (d, *J*_{C-F} = 17.8 Hz), 129.3, 129.0 (2C), 129.0 (2C), 116.7, 110.6 (d, *J*_{C-F} = 4.7 Hz), 83.4 (d, *J*_{C-F} = 29.3 Hz).

¹⁹F NMR (282 MHz, CDCl₃): δ [ppm] = -86.97 (t, *J* = 5.8 Hz, 1F).

GC-MS (EI, 70 eV) m/z: 322.95 (100%), 195.00 (26%), 169.00 (25%), 323.95 (15%), 195.95 (14%).

HRMS (ESI-TOF) m/z: [M+CH₃OH+H]⁺ Calcd for C₁₄H₁₂FINO 355.9942; Found 355.9950.

25. 6-Fluoro-5-(hydroxy(pyridin-3-yl)methyl)-[1,1'-biphenyl]-3-carbonitrile (126b)



6-fluoro-5-(hydroxy(pyridin-3-yl)methyl)-[1,1'-biphenyl]-3-carbonitrile was obtained from **125w** via **GMA** using $\text{TMPMgCl}\cdot\text{LiCl}$ (1 M, 1.3 equiv., 0.65 mL), 6-fluoro-[1,1'-biphenyl]-3-carbonitrile (1.0 equiv., 0.5 mmol, 99 mg) and 3-pyridinecarboxaldehyde (1.1 equiv., 0.55 mmol, 52 μL). Purification via column chromatography (Hexanes/AcOEt 7:3) afforded the product as a white solid (0.40 mmol, 121.6 mg, 80%).

Mp: 127 – 130 °C.

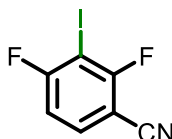
$^1\text{H-NMR}$ (400 MHz, CDCl_3): δ [ppm] = 8.58 (d, J = 1.5 Hz, 1H), 8.42 (dd, J = 4.9, 1.5 Hz, 1H), 8.00 (dd, J = 6.0, 2.1 Hz, 1H), 7.82 (app dt, J = 8.0, 1.9 Hz, 1H), 7.66 (dd, J = 6.8, 2.1 Hz, 1H), 7.46 – 7.39 (m, 5H), 7.35 (dd, J = 8.0, 4.9 Hz, 1H), 6.20 (s, 1H), 5.03 (s, 1H).

$^{13}\text{C}\{^1\text{H}\}$ NMR (101 MHz, CDCl_3): δ [ppm] = 158.8 (d, $J_{\text{C-F}}$ = 257.4 Hz), 147.8, 147.0 (d, $J_{\text{C-F}}$ = 1.7 Hz), 139.1, 135.9, 134.4 (d, $J_{\text{C-F}}$ = 5.1 Hz), 133.2 (d, $J_{\text{C-F}}$ = 16.1 Hz), 133.1, 131.0 (d, $J_{\text{C-F}}$ = 15.5 Hz), 130.6 (d, $J_{\text{C-F}}$ = 5.4 Hz), 129.0 (d, $J_{\text{C-F}}$ = 4.4 Hz, 2C), 129.0, 128.9 (2C), 124.4, 118.1, 109.2 (d, $J_{\text{C-F}}$ = 4.3 Hz), 67.2 (d, $J_{\text{C-F}}$ = 3.8 Hz).

^{19}F NMR (282 MHz, CDCl_3): δ [ppm] = -113.41 (t, J = 6.5 Hz, 1F).

HRMS (ESI-TOF) m/z : $[\text{M}+\text{H}]^+$ Calcd for $\text{C}_{19}\text{H}_{14}\text{FN}_2\text{O}$ 305.1085; Found 305.1070.

26. 2,4-Difluoro-3-iodobenzonitrile (**125x**)



2,4-difluoro-3-iodobenzonitrile was obtained from **123d** via **GMB** using $\text{TMPMgCl}\cdot\text{LiCl}$ (1 M, 1.3 equiv., 0.65 mL) at 0 °C or $(\text{TMP})_2\text{Zn}\cdot 2\text{MgCl}_2\cdot 2\text{LiCl}$ (0.29 M in THF, 0.65 equiv., 1.1 mL) at room temperature followed by trapping with iodine (1.1 equiv., 0.55 mmol,

139.6 mg). Purification via column chromatography (Hexanes/AcOEt 9.7:0.3) afforded the product as a white solid (106 mg - 80%^a and 123.2 mg - 93%^b). **CAS:** 1804885-55-9.

Mp: 58 – 59 °C.

¹H-NMR (400 MHz, CDCl₃): δ [ppm] = 7.65 (ddd, *J* = 8.7, 7.1, 5.7 Hz, 1H), 7.02 (ddd, *J* = 8.7, 6.8, 1.5 Hz, 1H).

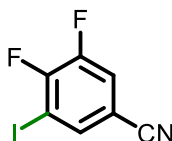
¹³C{¹H} NMR (101 MHz, CDCl₃): δ [ppm] = 165.9 (dd, *J*_{C-F} = 257.2, 5.5 Hz), 164.0 (dd, *J*_{C-F} = 258.2, 6.7 Hz), 134.7 (dd, *J*_{C-F} = 10.3, 1.6 Hz), 112.7 (dd, *J*_{C-F} = 25.6, 3.8 Hz), 112.5 (d, *J*_{C-F} = 3.4 Hz), 98.3 (dd, *J*_{C-F} = 18.2, 4.0 Hz), 72.7 (dd, *J*_{C-F} = 30.7, 27.9 Hz).

¹⁹F NMR (282 MHz, CDCl₃): δ [ppm] = -79.96 – -80.03 (m, 1F), -82.90 (dt, *J* = 6.9, 1.4 Hz, 1F).

GC-MS (EI, 70 eV) m/z: 264.90 (100%), 138.05 (46%), 88.00 (30%), 265.90 (9%), 87.00 (6%).

Note: HRMS analysis of compound **125x** was not possible due to low stability.

27. 3,4-Difluoro-5-iodobenzonitrile (125y)



3,4-difluoro-5-iodobenzonitrile was obtained from **123e** via **GMB** using TMPMgCl·LiCl (1 M, 1.5 equiv., 0.75 mL) at -70 °C followed by transmetalation with ZnCl₂ (1 M in THF, 1.5 equiv., 0.75 mL) during 20 minutes and quenching with iodine (1.1 equiv., 0.55 mmol, 139.6 mg). Purification via column chromatography (Hexanes/AcOEt 9:1) afforded the product as a white solid (0.37 mmol, 99 mg, 75%). **CAS:** 1439903-28-2.

Mp: 71 – 73 °C.

^a Metalation via TMPMgCl·LiCl

^b Metalation via (TMP)₂Zn·2MgCl₂·2LiCl.

$^1\text{H-NMR}$ (400 MHz, CDCl_3): δ [ppm] = 7.85 (dt, $J = 4.7, 1.9$ Hz, 1H), 7.49 (ddd, $J = 8.8, 6.6, 1.9$ Hz, 1H).

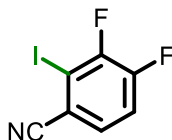
$^{13}\text{C}\{^1\text{H}\}$ NMR (101 MHz, CDCl_3): δ [ppm] = 154.0 (dd, $J_{\text{C-F}} = 256.2, 13.4$ Hz), 149.6 (dd, $J_{\text{C-F}} = 258.2, 15.6$ Hz), 138.4 (dd, $J_{\text{C-F}} = 4.0, 1.4$ Hz), 121.6 (dd, $J_{\text{C-F}} = 20.6, 1.5$ Hz), 115.6, 110.7 (dd, $J_{\text{C-F}} = 8.1, 5.1$ Hz), 83.7 (d, $J_{\text{C-F}} = 23.9$ Hz).

^{19}F NMR (282 MHz, CDCl_3): δ [ppm] = -106.06 – -106.18 (m, 1F), -129.90 – -130.02 (m, 1F).

GC-MS (EI, 70 eV) m/z : 264.90 (100%), 138.00 (56%), 88.05 (31%), 265.90 (9%), 87.00 (8%).

Note: HRMS analysis of compound **125y** was not possible due to low stability.

28. 3,4-Difluoro-2-iodobenzonitrile (**125z**)



3,4-difluoro-2-iodobenzonitrile was obtained from **123e** via **GMB** using $(\text{TMP})_2\text{Zn}\cdot 2\text{MgCl}_2\cdot 2\text{LiCl}$ (0.29 M in THF, 0.75 equiv., 1.3 mL) at room temperature and iodine (1.1 equiv., 0.55 mmol, 139.6 mg). Purification via column chromatography (Hexanes/AcOEt 9.5:0.5) afforded the product as a white solid (0.38 mmol, 101 mg, 76%). **CAS:** 1803847-48-4.

Mp: 67 – 69 °C.

$^1\text{H-NMR}$ (400 MHz, $\text{DMSO-}d_6$): δ [ppm] = 7.47 (ddd, $J = 8.8, 4.6, 1.8$ Hz, 1H), 7.29 (td, $J = 8.8, 7.2$ Hz, 1H).

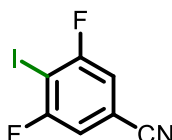
$^{13}\text{C}\{^1\text{H}\}$ NMR (101 MHz, $\text{DMSO-}d_6$): δ [ppm] = 152.4 (dd, $J_{\text{C-F}} = 263.6, 15.1$ Hz), 151.6 (dd, $J_{\text{C-F}} = 250.0, 14.0$ Hz), 131.0 (dd, $J_{\text{C-F}} = 7.6, 4.3$ Hz), 118.6 (dd, $J_{\text{C-F}} = 18.9, 0.9$ Hz), 117.9, 117.8 (dd, $J_{\text{C-F}} = 4.1, 1.3$ Hz), 89.1 (d, $J_{\text{C-F}} = 25.3$ Hz).

^{19}F NMR (282 MHz, CDCl_3): δ [ppm] = -109.65 (ddd, J = 23.0, 7.2, 1.7 Hz, 1F), -123.99 (ddd, J = 23.0, 9.0, 4.6 Hz, 1F).

GC-MS (EI, 70 eV) m/z: 264.90 (100%), 138.05 (50%), 88.05 (33%), 265.90 (9%), 87.00 (7%).

Note: HRMS analysis of compound **125z** was not possible due to low stability.

29. 3,5-Difluoro-4-iodobenzonitrile (**125aa**)



3,5-difluoro-4-iodobenzonitrile was obtained from **123f** via **GMB** using $\text{TMPMgCl}\cdot\text{LiCl}$ (1 M, 1.3 equiv., 0.65 mL) at $-30\text{ }^\circ\text{C}$ or $(\text{TMP})_2\text{Zn}\cdot 2\text{MgCl}_2\cdot 2\text{LiCl}$ (0.29 M in THF, 0.65 equiv., 1.1 mL) at room temperature followed by iodine (1.1 equiv., 0.55 mmol, 139.6 mg). Purification via column chromatography (Hexanes/AcOEt 9:1) afforded the product as a white solid (93 mg - 75%^c and 120.6 mg - 91%^d). **CAS:** 1487337-76-7.

Mp: 127 – 130 $^\circ\text{C}$.

^1H -NMR (400 MHz, CDCl_3): δ [ppm] = 7.20 – 7.16 (m, 2H).

$^{13}\text{C}\{^1\text{H}\}$ NMR (101 MHz, CDCl_3): δ [ppm] = 163.0 (dd, $J_{\text{C-F}}$ = 250.6, 6.3 Hz, 2C), 116.3 (t, $J_{\text{C-F}}$ = 3.4 Hz), 115.2-114.9 (m, 2C), 114.4 (t, $J_{\text{C-F}}$ = 11.1 Hz), 79.1 (t, $J_{\text{C-F}}$ = 29.4 Hz).

^{19}F NMR (282 MHz, CDCl_3): δ [ppm] = -87.41 – -87.47 (m, 2F).

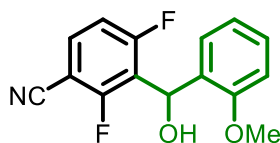
GC-MS (EI, 70 eV) m/z: 264.90 (100%), 138.05 (43%), 88.00 (31%), 265.90 (9%), 87.00 (7%).

The reported characterization data is in accordance with the literature.⁹⁰

30. 2,4-Difluoro-3-(hydroxy(2-methoxyphenyl)methyl)benzonitrile (**125ab**)

^c Metalation via $\text{TMPMgCl}\cdot\text{LiCl}$.

^d Metalation via $(\text{TMP})_2\text{Zn}\cdot 2\text{MgCl}_2\cdot 2\text{LiCl}$.



2,4-difluoro-3-(hydroxy(2-methoxyphenyl)methyl)benzonitrile was obtained from **123d** via **GMB** using $\text{TMPMgCl}\cdot\text{LiCl}$ (1 M, 1.3 equiv., 0.65 mL) at 0 °C and 2-methoxybenzaldehyde (1.1 equiv., 0.55 mmol, 75 mg). Purification via column chromatography (Hexanes/AcOEt 8:2) afforded the product as a white solid (0.47 mmol, 130.7 mg, 95%).

Mp: 120 – 121 °C.

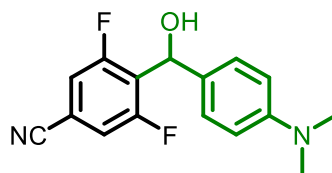
$^1\text{H-NMR}$ (400 MHz, CDCl_3): δ [ppm] = 7.55 – 7.48 (m, 2H), 7.30 (td, J = 8.1, 1.7 Hz, 1H), 7.01 (td, J = 7.5, 0.9 Hz, 1H), 6.97 (td, J = 9.3, 1.3 Hz, 1H), 6.86 (app dd, J = 8.1, 0.7 Hz, 1H), 6.38 (s, 1H), 3.79 (s, 3H), 2.78 (bs, 1H).

$^{13}\text{C}\{^1\text{H}\}$ NMR (101 MHz, CDCl_3): δ [ppm] = 164.0 (dd, $J_{\text{C-F}}$ = 260.7, 8.5 Hz), 162.4 (dd, $J_{\text{C-F}}$ = 262.6, 9.1 Hz), 156.3, 133.3 (dd, $J_{\text{C-F}}$ = 11.6, 2.3 Hz), 129.4, 128.5, 126.8 (t, $J_{\text{C-F}}$ = 2.0 Hz), 120.9 (dd, $J_{\text{C-F}}$ = 16.9, 14.7 Hz), 120.7, 113.6, 113.3 (dd, $J_{\text{C-F}}$ = 24.4, 3.8 Hz), 110.5, 98.3 (dd, $J_{\text{C-F}}$ = 17.0, 3.9 Hz), 64.3 (t, $J_{\text{C-F}}$ = 2.8 Hz), 55.4.

^{19}F NMR (282 MHz, CDCl_3): δ [ppm] = -101.26 – -101.35 (m, 1F), -104.96 (dd, J = 11.2, 7.0 Hz, 1F).

HRMS (ESI-TOF) m/z : $[\text{M}+\text{Na}]^+$ Calcd for $\text{C}_{15}\text{H}_{11}\text{F}_2\text{NNaO}_2$ 298.0650; Found 298.0640.

31.4-((4-(Dimethylamino)phenyl)(hydroxy)methyl)-3,5-difluorobenzonitrilebenzo-nitrile (125ac)



4-((4-(dimethylamino)phenyl)(hydroxy)methyl)-3,5-difluorobenzonitrilebenzonitrile was obtained from **123f** via **GMB** using $\text{TMPMgCl}\cdot\text{LiCl}$ (1 M, 1.3 equiv., 0.65 mL) at -30 °C

and 4-(dimethylamino)benzaldehyde (1.1 equiv., 0.55 mmol, 82 mg) as the electrophile. Purification via column chromatography (Hexanes/AcOEt 8:2) afforded the product as a beige solid (0.47 mmol, 135.5 mg, 94%).

Mp: 150 – 151 °C.

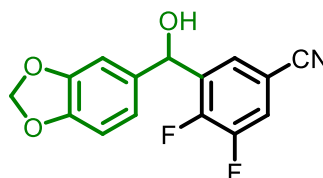
¹H-NMR (400 MHz, CDCl₃): δ [ppm] = 7.24 (app d, *J* = 8.4 Hz, 2H), 7.21 (app d, *J* = 7.7 Hz, 2H), 6.71 (d, *J* = 8.4 Hz, 2H), 6.16 (s, 1H), 2.95 (s, 6H), 2.73 (bs, 1H).

¹³C{¹H} NMR (101 MHz, CDCl₃): δ [ppm] = 160.6 (dd, *J*_{C-F} = 252.4, 9.1 Hz, 2C), 150.4, 126.9 (2C), 126.1 (t, *J*_{C-F} = 16.2 Hz), 116.6 (t, *J*_{C-F} = 3.5 Hz), 116.3 – 116.0 (m, 2C), 112.7 (t, *J*_{C-F} = 12.4 Hz), 112.7 (2C), 111.1, 68.0, 40.7 (2C).

¹⁹F NMR (282 MHz, CDCl₃): δ [ppm] = -110.00 – -110.08 (m, 2F).

HRMS (ESI-TOF) m/z: [M+H]⁺ Calcd for C₁₆H₁₅F₂N₂O 289.1147; Found 289.1135.

32. 3-(Benzo[d][1,3]dioxol-5-yl(hydroxy)methyl)-4,5-difluorobenzonitrile (125ad)



3-(benzo[d][1,3]dioxol-5-yl(hydroxy)methyl)-4,5-difluorobenzonitrile was obtained from **123e** via **GMB** using TMPMgCl·LiCl (1 M, 1.5 equiv., 0.75 mL) at -70 °C and 1,3-benzodioxole-5-carboxaldehyde (1.1 equiv., 0.55 mmol, 82.6 mg) as the electrophile. Purification via column chromatography (Hexanes/AcOEt 8:2) afforded the product as a yellow oil (0.28 mmol, 82.4 mg, 57%).

¹H-NMR (400 MHz, CDCl₃): δ [ppm] = 7.78 – 7.76 (m, 1H), 7.39 (ddd, *J* = 9.1, 6.9, 2.1 Hz, 1H), 6.86 – 6.81 (m, 2H), 6.78 (d, *J* = 7.9 Hz, 1H), 6.03 (s, 1H), 5.96 (d, *J* = 1.4 Hz, 1H), 5.95 (d, *J* = 1.4 Hz, 1H), 2.31 (bs, 1H).

¹³C{¹H} NMR (101 MHz, CDCl₃): δ [ppm] = 150.6 (dd, *J*_{C-F} = 258.6, 12.9 Hz), 150.2 (dd, *J*_{C-F} = 253.4, 13.5 Hz), 148.3, 147.9, 135.8 (d, *J*_{C-F} = 11.2 Hz), 135.2, 127.0 (t, *J*_{C-F} = 3.8

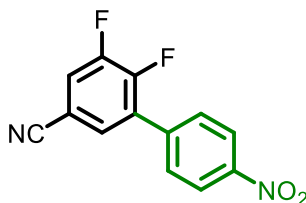
Hz), 120.2 (dd, $J_{C-F} = 20.3, 1.3$ Hz), 120.2 (d, $J_{C-F} = 0.9$ Hz), 117.2, 108.6, 108.6 (dd, $J_{C-F} = 8.1, 5.1$ Hz) 106.9, 101.5, 69.3.

^{19}F NMR (282 MHz, CDCl_3): δ [ppm] = -132.50 (dt, $J = 21.1, 6.2$ Hz, 1F), -134.19 – -134.30 (m, 1F).

GC-MS (EI, 70 eV) m/z: 289.05 (100%), 123.05 (86%), 93.05 (65%), 151.00 (42%), 165.95 (31%).

HRMS (ESI-TOF) m/z: $[\text{M}+\text{FA}-\text{H}]^-$ Calcd for $\text{C}_{16}\text{H}_{10}\text{F}_2\text{NO}_5$ 334.0533; Found 334.0521.

33. 5,6-Difluoro-4'-nitro-[1,1'-biphenyl]-3-carbonitrile (125ae)



5,6-difluoro-4'-nitro-[1,1'-biphenyl]-3-carbonitrile was obtained from **123e** via **GMB** using $\text{TMPMgCl}\cdot\text{LiCl}$ (1 M, 1.5 equiv., 0.75 mL) at -70 °C followed by transmetalation with ZnCl_2 (1 M in THF, 1.5 equiv., 0.75 mL) during 20 minutes and Negishi cross-coupling catalyzed by $\text{Pd}(\text{PPh}_3)_4$ (5 mol%, 29 mg) in the presence of 1-iodo-4-nitrobenzene (1.2 equiv., 0.6 mmol, 149.4 mg) at 50 °C (oil bath). Purification via column chromatography (Hexanes/AcOEt 9:1) afforded the product as an orange solid (0.29 mmol, 75.5 mg, 58%).

Mp: 162 – 164 °C.

^1H -NMR (400 MHz, CDCl_3): δ [ppm] = 8.39 – 8.35 (m, 2H), 7.73 – 7.70 (m, 2H), 7.61 – 7.56 (m, 2H).

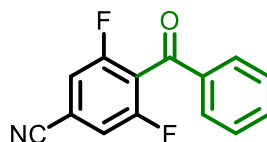
$^{13}\text{C}\{^1\text{H}\}$ NMR (101 MHz, CDCl_3): δ [ppm] = 151.2 (dd, $J_{C-F} = 256.6, 15.8$ Hz), 151.0 (dd, $J_{C-F} = 264.0, 15.8$ Hz), 148.4, 138.7, 130.9 (dd, $J_{C-F} = 11.2, 0.8$ Hz), 130.1 (d, $J_{C-F} = 3.1$ Hz, 2C), 130.0 (t, $J_{C-F} = 3.0$ Hz), 124.3 (2C), 121.4 (dd, $J_{C-F} = 20.0, 2.4$ Hz), 116.6, 109.4 (dd, $J_{C-F} = 8.5, 5.4$ Hz).

GC-MS (EI, 70 eV) m/z: 260.00 (100%), 202.00 (46%), 213.00 (44%), 214.00 (38%), 187.00 (33%).

¹⁹F NMR (282 MHz, CDCl₃): δ [ppm] = -131.74 – -131.85 (m, 1F), -131.93 – -132.05 (m, 1F).

HRMS (ESI-TOF) m/z: [M+CH₃OH+H]⁺ Calcd for C₁₄H₁₁F₂N₂O₃ 293.0732; Found 293.0741.

34. 4-Benzoyl-3,5-difluorobenzonitrile (125af)



4-benzoyl-3,5-difluorobenzonitrile was obtained from **123f** via **GMB** using TMPMgCl-LiCl (1 M, 1.3 equiv., 0.65 mL) at -30 °C followed by transmetalation with ZnCl₂ (1 M in THF, 1.3 equiv., 0.65 mL) for 20 minutes and palladium catalyzed benzoylation using Pd(PPh₃)₄ (5 mol%, 29 mg) and benzoyl chloride (1.0 equiv., 0.5 mmol, 58 μ L) at room temperature. Purification via column chromatography (Hexanes/AcOEt 9:1) afforded the product as a white solid (0.41 mmol, 100.9 mg, 83%).

Mp: 104 – 105 °C.

¹H-NMR (400 MHz, CDCl₃): δ [ppm] = 7.83 (app d, J = 7.7 Hz, 2H), 7.68 (tt, J = 7.1, 1.3 Hz, 1H), 7.55 – 7.50 (m, 2H), 7.37 – 7.32 (m, 2H).

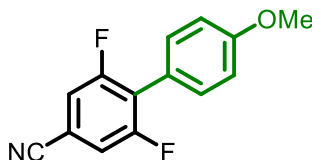
¹³C{¹H} NMR (101 MHz, CDCl₃): δ [ppm] = 186.9, 159.7 (dd, J_{C-F} = 255.5, 8.5 Hz, 2C), 135.9, 135.2, 129.7 (2C), 129.2 (2C), 122.1 (t, J_{C-F} = 22.7 Hz), 116.4 - 116.1 (m, 2C), 116.1 (t, J_{C-F} = 3.5 Hz), 115.5 (t, J_{C-F} = 11.4 Hz).

¹⁹F NMR (282 MHz, CDCl₃): δ [ppm] = -107.68 – -107.73 (m, 2F).

GC-MS (EI, 70 eV) m/z: 105.05 (100%), 243.00 (74%), 77.00 (54%), 165.95 (30%), 51.00 (18%).

HRMS (ESI-TOF) m/z: $[M+CH_3OH+H]^+$ Calcd for $C_{15}H_{12}F_2NO_2$ 276.0831; Found 276.0839.

35. 2,6-Difluoro-4'-methoxy-[1,1'-biphenyl]-4-carbonitrile (125ag)



2,6-difluoro-4'-methoxy-[1,1'-biphenyl]-4-carbonitrile was obtained from **123f** via **GMB** using $TMPMgCl \cdot LiCl$ (1 M, 1.3 equiv., 0.65 mL) at $-30\text{ }^\circ\text{C}$ followed by transmetalation with $ZnCl_2$ (1 M in THF, 1.3 equiv., 0.65 mL) and Negishi cross-coupling catalyzed by $Pd(PPh_3)_4$ (5 mol%, 29 mg) in the presence of 4-methoxyiodobenzene (1.2 equiv., 0.6 mmol, 140.4 mg) at $50\text{ }^\circ\text{C}$ (oil bath). Purification via column chromatography (Hexanes/AcOEt 9:1) afforded the product as a white solid (0.44 mmol, 107.9 mg, 88%).

CAS: 2222566-95-0.

Mp: $150 - 151\text{ }^\circ\text{C}$.

$^1\text{H-NMR}$ (400 MHz, $CDCl_3$): δ [ppm] = 7.44 – 7.39 (m, 2H), 7.33 – 7.26 (m, 2H), 7.03 – 7.00 (m, 2H), 3.87 (s, 3H).

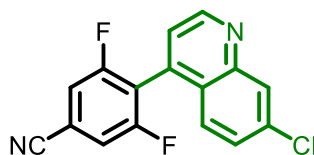
$^{13}\text{C}\{^1\text{H}\}$ NMR (101 MHz, $CDCl_3$): δ [ppm] = 160.5, 160.0 (dd, $J_{C-F} = 251.8, 8.0$ Hz, 2C), 131.6 (t, $J_{C-F} = 2.3$ Hz, 2C), 124.1 (t, $J_{C-F} = 18.3$ Hz), 119.3, 116.9 (t, $J_{C-F} = 3.4$ Hz), 116.2 - 115.9 (m, 2C), 114.2 (2C), 111.7 (t, $J_{C-F} = 12.3$ Hz), 55.5.

^{19}F NMR (282 MHz, $CDCl_3$): δ [ppm] = $-110.59 - -110.66$ (m, 2F).

GC-MS (EI, 70 eV) m/z: 245.05 (100%), 202.00 (59%), 230.00 (25%), 175.95 (19%), 246.05 (17%).

The reported characterization data is in accordance with the literature.¹³²

36. 4-(7-Chloroquinolin-4-yl)-3,5-difluorobenzonitrile (125ah)



4-(7-chloroquinolin-4-yl)-3,5-difluorobenzonitrile was obtained from **123f** via **GMB** using $\text{TMPMgCl}\cdot\text{LiCl}$ (1 M, 1.3 equiv., 0.65 mL) at $-30\text{ }^\circ\text{C}$ followed by transmetalation with ZnCl_2 (1 M in THF, 1.3 equiv., 0.65 mL) and Negishi cross-coupling catalyzed by $\text{Pd}(\text{PPh}_3)_4$ (5 mol%, 29 mg) in the presence of 7-chloro-4-iodoquinoline (1.2 equiv., 0.6 mmol, 173.7 mg) at $50\text{ }^\circ\text{C}$ (oil bath). Purification via column chromatography (Hexanes/AcOEt 8:2) afforded the product as a white solid (0.24 mmol, 72.2 mg, 48%).

Mp: 142 – 144 $^\circ\text{C}$.

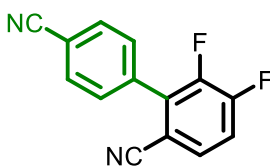
$^1\text{H-NMR}$ (400 MHz, CDCl_3): δ [ppm] = 9.05 (d, $J = 4.5$ Hz, 1H), 8.27 (d, $J = 2.1$ Hz, 1H), 7.53 (dd, $J = 8.9, 2.1$ Hz, 1H), 7.47 – 7.42 (m, 3H), 7.41 (d, $J = 4.5$ Hz, 1H).

$^{13}\text{C}\{^1\text{H}\}$ NMR (101 MHz, CDCl_3): δ [ppm] = 160.1 (dd, $J_{\text{C-F}} = 254.6, 7.2$ Hz, 2C), 150.4, 148.3, 136.6, 134.8, 129.1, 128.8, 126.1, 124.7, 123.0, 119.6 (t, $J_{\text{C-F}} = 20.3$ Hz), 116.4 – 116.1 (m, 2C), 116.2 (t, $J_{\text{C-F}} = 3.4$ Hz), 115.0 (t, $J_{\text{C-F}} = 11.7$ Hz).

^{19}F NMR (282 MHz, CDCl_3): δ [ppm] = -106.24 – -106.30 (m, 2F).

HRMS (ESI-TOF) m/z : $[\text{M}+\text{H}]^+$ Calcd for $\text{C}_{16}\text{H}_8\text{ClF}_2\text{N}_2$ 301.0339; Found 301.0352.

37. 5,6-Difluoro-[1,1'-biphenyl]-2,4'-dicarbonitrile (**125ai**)



5,6-difluoro-[1,1'-biphenyl]-2,4'-dicarbonitrile was obtained from **123e** via **GMB** using $(\text{TMP})_2\text{Zn}\cdot 2\text{MgCl}_2\cdot 2\text{LiCl}$ (0.29 M in THF, 0.75 equiv., 1.3 mL) at room temperature and subsequent Negishi cross-coupling catalyzed by $\text{Pd}(\text{PPh}_3)_4$ (5 mol%, 29 mg) in the presence of 4-iodobenzonitrile (1.2 equiv., 0.6 mmol, 137.4 mg) at $50\text{ }^\circ\text{C}$ (oil bath).

Purification via column chromatography (Hexanes/AcOEt 8:2) afforded the product as a brown solid (0.31 mmol, 74.5 mg, 62%).

Mp: 160 – 162 °C.

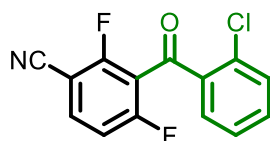
¹H-NMR (400 MHz, DMSO-*d*₆): δ [ppm] = 7.84 (app. d, *J* = 8.6 Hz, 2H), 7.64 – 7.60 (m, 3H), 7.37 (td, *J* = 8.9, 7.3 Hz, 1H).

¹³C{¹H} NMR (101 MHz, DMSO-*d*₆): δ [ppm] = 153.9 (dd, *J*_{C-F} = 260.8, 13.4 Hz), 148.1 (dd, *J*_{C-F} = 253.3, 13.7 Hz), 135.0 (d, *J*_{C-F} = 2.5 Hz), 133.8 (dd, *J*_{C-F} = 14.2, 1.1 Hz), 132.7, 130.7 (d, *J*_{C-F} = 1.9 Hz), 130.6 (dd, *J*_{C-F} = 8.0, 4.8 Hz), 118.5 (d, *J*_{C-F} = 18.6 Hz), 118.2, 116.3 (app. dd, *J*_{C-F} = 3.3, 1.9 Hz), 113.9, 109.2 (app. dd, *J*_{C-F} = 3.7, 2.7 Hz).

¹⁹F NMR (282 MHz, CDCl₃): δ [ppm] = -125.49 (ddd, *J* = 21.7, 9.1, 4.6 Hz, 1F), -136.50 – -136.61 (m, 1F).

HRMS (ESI-TOF) m/z: [M+Na]⁺ Calcd for C₁₄H₇F₂N₂Na 263.0391; Found 263.0389.

38. 3-(2-Chlorobenzoyl)-2,4-difluorobenzonitrile (125aj)



3-(2-chlorobenzoyl)-2,4-difluorobenzonitrile was obtained from **123d** via **GMB** using (TMP)₂Zn·2MgCl₂·2LiCl (0.29 M in THF, 0.65 equiv., 1.1 mL) at room temperature and subsequent palladium-catalyzed benzoylation using Pd(PPh₃)₄ (5 mol%, 29 mg) and 2-chlorobenzoyl chloride (1.0 equiv., 0.5 mmol, 63 μL) at the same temperature. Purification via column chromatography (Hexanes/AcOEt 9:1) afforded the product as a white solid (0.30 mmol, 83.3 mg, 60%).

Mp: 69 – 72 °C.

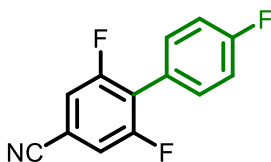
¹H-NMR (400 MHz, DMSO-*d*₆): δ [ppm] = 7.77 (ddd, *J* = 8.7, 7.0, 5.7 Hz, 1H), 7.68 (dd, *J* = 7.7, 1.7 Hz, 1H), 7.53 (ddd, *J* = 8.2, 7.3, 1.7 Hz, 1H), 7.45 (dd, *J* = 8.2, 1.1 Hz, 1H), 7.42 (td, *J* = 7.7, 1.3 Hz, 1H), 7.12 (td, *J* = 8.7, 1.4 Hz, 1H).

$^{13}\text{C}\{^1\text{H}\}$ NMR (101 MHz, DMSO- d_6): δ [ppm] = 185.9, 162.9 (dd, $J_{\text{C-F}} = 264.6, 6.7$ Hz), 161.5 (dd, $J_{\text{C-F}} = 266.4, 7.7$ Hz), 136.7, 136.5 (dd, $J_{\text{C-F}} = 11.1, 1.9$ Hz), 134.2, 132.9, 131.3, 131.1, 127.5, 119.7 (dd, $J_{\text{C-F}} = 19.8, 17.5$ Hz), 113.8 (dd, $J_{\text{C-F}} = 23.2, 4.0$ Hz), 112.6 (d, $J_{\text{C-F}} = 1.2$ Hz), 99.0 (dd, $J_{\text{C-F}} = 16.2, 4.2$ Hz).

^{19}F NMR (282 MHz, CDCl_3): δ [ppm] = -100.10 (td, $J = 8.5, 5.7$ Hz, 1F), -103.68 – -103.74 (m, 1F).

HRMS (ESI-TOF) m/z: $[\text{M}+\text{Na}]^+$ Calcd for $\text{C}_{14}\text{H}_6\text{ClF}_2\text{NNaO}$ 299.9998; Found 300.0022.

39. 2,4',6-Trifluoro-[1,1'-biphenyl]-4-carbonitrile (125ak)



2,4',6-trifluoro-[1,1'-biphenyl]-4-carbonitrile was obtained from **123f** via **GMB** using $(\text{TMP})_2\text{Zn}\cdot 2\text{MgCl}_2\cdot 2\text{LiCl}$ (0.29 M in THF, 0.65 equiv., 1.1 mL) at room temperature and subsequent Negishi cross-coupling catalyzed by $\text{Pd}(\text{PPh}_3)_4$ (5 mol%, 29 mg) in the presence of 4-fluoriodobenzene (1.2 equiv., 0.6 mmol, 69 μL) at 50 $^\circ\text{C}$ (oil bath). Purification via column chromatography (Hexanes/AcOEt 9.5:0.5) afforded the product as a white solid (0.46 mmol, 107.3 mg, 92%).

Mp: 195 – 196 $^\circ\text{C}$.

^1H -NMR (400 MHz, DMSO- d_6): δ [ppm] = 7.47 – 7.44 (m, 2H), 7.35 – 7.29 (m, 2H), 7.22 – 7.17 (m, 2H).

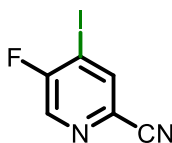
$^{13}\text{C}\{^1\text{H}\}$ NMR (101 MHz, DMSO- d_6): δ [ppm] = 163.4 (d, $J_{\text{C-F}} = 250.1$ Hz), 160.0 (dd, $J_{\text{C-F}} = 252.5, 7.7$ Hz, 2C), 132.2 (dt, $J_{\text{C-F}} = 8.5, 2.1$ Hz, 2C), 123.3 (t, $J_{\text{C-F}} = 18.3$ Hz), 123.1 (d, $J_{\text{C-F}} = 3.4$ Hz), 116.7 (t, $J_{\text{C-F}} = 3.5$ Hz), 116.3 – 115.9 (m, 2C), 116.0 (d, $J_{\text{C-F}} = 21.9$ Hz, 2C), 112.6 (t, $J_{\text{C-F}} = 12.3$ Hz).

^{19}F NMR (282 MHz, CDCl_3): δ [ppm] = -110.32 – -110.39 (m, 2F), -110.98 – -111.07 (m, 1F).

GC-MS (EI, 70 eV) m/z: 233.00 (100%), 234.05 (18%), 213.00 (14%), 232.05 (10%), 116.55 (9%).

HRMS (ESI-TOF) m/z: $[M+CH_3OH+H]^+$ Calcd for $C_{14}H_{11}F_3NO$ 266.0787; Found 266.0797.

40. 5-Fluoro-4-iodopicolinonitrile (125al)



5-fluoro-4-iodopicolinonitrile was obtained from **123g** via **GMC** using $TMPMgCl \cdot LiCl$ (1 M, 1.3 equiv., 0.65 mL) at $-30\text{ }^\circ\text{C}$ and iodine (1.1 equiv., 0.55 mmol, 139.6 mg). Purification via column chromatography (Hexanes/AcOEt 8:2) afforded the product as a white solid (0.35 mmol, 86.8 mg, 70%). **CAS:** 1807159-50-7.

Mp: 130 – 133 $^\circ\text{C}$.

$^1\text{H-NMR}$ (400 MHz, CDCl_3): δ [ppm] = 8.41 (s, 1H), 8.14 (d, $J = 4.6$ Hz, 1H).

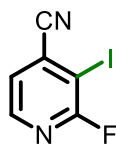
$^{13}\text{C}\{^1\text{H}\}$ NMR (101 MHz, CDCl_3): δ [ppm] = 161.4 (d, $J_{\text{C-F}} = 264.2$ Hz), 139.3 (d, $J_{\text{C-F}} = 5.7$ Hz), 139.1 (d, $J_{\text{C-F}} = 34.1$ Hz), 130.4 (d, $J_{\text{C-F}} = 5.5$ Hz), 115.2, 93.1 (d, $J_{\text{C-F}} = 24.8$ Hz).

^{19}F NMR (282 MHz, CDCl_3): δ [ppm] = -99.10 (d, $J = 4.6$ Hz, 1F).

GC-MS (EI, 70 eV) m/z: 247.95 (100%), 121.00 (51%), 94.00 (24%), 69.00 (12%), 101.00 (8%).

HRMS (ESI-TOF) m/z: $[M+H]^+$ Calcd for $C_6H_3FIN_2$ 248.9320; Found 248.9324.

41. 2-Fluoro-3-iodoisonicotinonitrile (125am)



2-fluoro-3-iodoisonicotinonitrile was obtained from **123h** via **GMC** using $\text{TMPMgCl}\cdot\text{LiCl}$ (1 M, 1.5 equiv., 0.75 mL) at $-70\text{ }^\circ\text{C}$ followed by transmetalation with ZnCl_2 (1 M in THF, 1.5 equiv., 0.75 mL) or $(\text{TMP})_2\text{Zn}\cdot 2\text{MgCl}_2\cdot 2\text{LiCl}$ (0.29 M in THF, 0.9 equiv., 1.5 mL) at room temperature with iodine (1.1 equiv., 0.55 mmol, 139.6 mg) as the electrophile. Purification via column chromatography (Hexanes/AcOEt 9:1) afforded the product as a white solid (85.6 mg - 69%^e and 94.2 mg - 76%^f). **CAS:** 898854-64-3.

Mp: 96 – 97 $^\circ\text{C}$.

$^1\text{H-NMR}$ (400 MHz, CDCl_3): δ [ppm] = 8.33 (dd, $J = 5.0, 0.8$ Hz, 1H), 7.40 (dd, $J = 5.0, 1.0$ Hz, 1H).

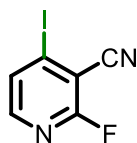
$^{13}\text{C}\{^1\text{H}\}$ NMR (101 MHz, CDCl_3): δ [ppm] = 163.1 (d, $J_{\text{C-F}} = 237.6$ Hz), 148.3 (d, $J_{\text{C-F}} = 14.4$ Hz), 133.2 (d, $J_{\text{C-F}} = 4.2$ Hz), 125.2 (d, $J_{\text{C-F}} = 5.5$ Hz), 116.6 (d, $J_{\text{C-F}} = 4.9$ Hz), 81.8 (d, $J_{\text{C-F}} = 47.1$ Hz).

^{19}F NMR (282 MHz, CDCl_3): δ [ppm] = -48.43 (s, 1F).

GC-MS (EI, 70 eV) m/z: 247.90 (100%), 121.05 (76%), 76.00 (23%), 94.00 (13%), 101.00 (9%).

Note: HRMS analysis of compound **125am** was not possible due to low stability.

42. 2-Fluoro-4-iodonicotinonitrile (**125an**)



2-fluoro-4-iodonicotinonitrile was obtained from **123i** via **GMC** using $\text{TMPMgCl}\cdot\text{LiCl}$ (1 M, 1.5 equiv., 0.75 mL) at $-70\text{ }^\circ\text{C}$ and iodine (1.1 equiv., 0.55 mmol, 139.6 mg) as the

^e Metalation via $\text{TMPMgCl}\cdot\text{LiCl}$.

^f Metalation via $(\text{TMP})_2\text{Zn}\cdot 2\text{MgCl}_2\cdot 2\text{LiCl}$.

electrophile. Purification via column chromatography (Hexanes/AcOEt 8.5:1.5) afforded the product as a white solid (0.42 mmol, 105.4 mg, 85%). **CAS:** 898854-59-6.

Mp: 85 – 86 °C.

¹H-NMR (400 MHz, CDCl₃): δ [ppm] = 8.08 (dd, *J* = 5.3, 0.9 Hz, 1H), 7.80 (dd, *J* = 5.3, 0.9 Hz, 1H).

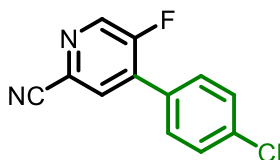
¹³C{¹H} NMR (101 MHz, CDCl₃): δ [ppm] = 163.0 (d, *J*_{C-F} = 251.1 Hz), 150.9 (d, *J*_{C-F} = 15.8 Hz), 132.2 (d, *J*_{C-F} = 4.8 Hz), 114.0, 113.7 (d, *J*_{C-F} = 6.1 Hz), 106.4 (d, *J*_{C-F} = 32.7 Hz).

¹⁹F NMR (282 MHz, CDCl₃): δ [ppm] = -57.27 (s, 1F).

GC-MS (EI, 70 eV) m/z: 247.95 (100%), 121.05 (77%), 76.00 (24%), 94.00 (15%), 75.00 (15%).

Note: HRMS analysis of compound **1125an** was not possible due to low stability.

43. 4-(4-Chlorophenyl)-5-fluoropicolinonitrile (**125ao**)



4-(4-chlorophenyl)-5-fluoropicolinonitrile was obtained from **123g** via **GMC** using TMPMgCl·LiCl (1 M, 1.3 equiv., 0.65 mL) at -30 °C followed by transmetalation with ZnCl₂ (1 M in THF, 1.3 equiv., 0.65 mL) and a Negishi cross-coupling catalyzed by Pd(PPh₃)₄ (5 mol%, 29 mg) in the presence of 1-chloro-4-iodobenzene (1.2 equiv., 0.6 mmol, 143.1 mg) at 50 °C (oil bath). Purification via column chromatography (Hexanes/AcOEt 9:1) afforded the product as a white solid (0.28 mmol, 65.1 mg, 56%).

Mp: 130 – 131 °C.

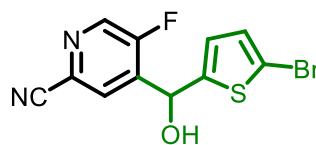
¹H-NMR (400 MHz, CDCl₃): δ [ppm] = 8.63 (d, *J* = 2.2 Hz, 1H), 7.82 (d, *J* = 6.0 Hz, 1H), 7.57 – 7.50 (m, 4H).

$^{13}\text{C}\{^1\text{H}\}$ NMR (101 MHz, CDCl_3): δ [ppm] = 157.7 (d, $J_{\text{C-F}} = 266.8$ Hz), 141.3 (d, $J_{\text{C-F}} = 28.0$ Hz), 136.9, 136.4 (d, $J_{\text{C-F}} = 11.7$ Hz), 130.5 (d, $J_{\text{C-F}} = 5.4$ Hz), 130.2 (d, $J_{\text{C-F}} = 3.7$ Hz, 2C), 129.7 (2C), 129.5 (d, $J_{\text{C-F}} = 2.7$ Hz), 129.3 (d, $J_{\text{C-F}} = 1.8$ Hz), 116.6.

^{19}F NMR (282 MHz, CDCl_3): δ [ppm] = -123.46 – -123.49 (m, 1F).

HRMS (ESI-TOF) m/z : $[\text{M}+\text{H}]^+$ Calcd for $\text{C}_{12}\text{H}_7\text{ClFN}_2$ 233.0277; Found 233.0292.

44. 4-((5-Bromothiophen-2-yl)(hydroxy)methyl)-5-fluoropicolinonitrile (125ap)



4-((5-bromothiophen-2-yl)(hydroxy)methyl)-5-fluoropicolinonitrile was obtained from **123g** via **GMC** using $\text{TMPMgCl}\cdot\text{LiCl}$ (1 M, 1.3 equiv., 0.65 mL) at -30 °C and 5-bromo-2-thiophenecarboxaldehyde (1.1 equiv., 0.55 mmol, 65 μL) as the electrophile. Purification via column chromatography (Hexanes/AcOEt 8:2) afforded the product as a white solid (0.31 mmol, 97.1 mg, 62%).

Mp: 113 – 115 °C.

^1H -NMR (400 MHz, CDCl_3): δ [ppm] = 8.48 (d, $J = 1.1$ Hz, 1H), 8.08 (d, $J = 5.6$ Hz, 1H), 6.92 (d, $J = 3.8$ Hz, 1H), 6.77 (dt, $J = 3.8, 0.7$ Hz, 1H), 6.28 (d, $J = 0.7$ Hz, 1H), 2.53 (bs, 1H).

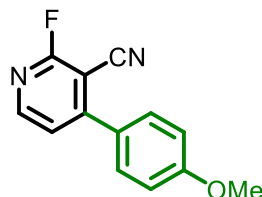
$^{13}\text{C}\{^1\text{H}\}$ NMR (101 MHz, CDCl_3): δ [ppm] = 157.5 (d, $J_{\text{C-F}} = 266.0$ Hz), 145.2, 140.2 (d, $J_{\text{C-F}} = 25.9$ Hz), 140.0 (d, $J_{\text{C-F}} = 12.9$ Hz), 130.4 (d, $J_{\text{C-F}} = 5.2$ Hz), 130.0, 127.0 (d, $J_{\text{C-F}} = 2.8$ Hz), 126.2 (d, $J_{\text{C-F}} = 1.2$ Hz), 116.6, 114.0, 64.9 (d, $J_{\text{C-F}} = 2.5$ Hz).

^{19}F NMR (282 MHz, CDCl_3): δ [ppm] = -122.56 (s, 1F).

GC-MS (EI, 70 eV) m/z : 232.95 (100%), 84.00 (24%), 313.85 (21%), 311.90 (21%), 149.00 (19%).

HRMS (ESI-TOF) m/z : $[\text{M}-\text{H}]^-$ Calcd for $\text{C}_{11}\text{H}_5\text{BrFN}_2\text{OS}$ 310.9295; Found 310.9293.

45. 2-Fluoro-4-(4-methoxyphenyl)nicotinonitrile (125aq)



2-fluoro-4-(4-methoxyphenyl)nicotinonitrile was obtained from **123i** via **GMC** using $\text{TMPMgCl}\cdot\text{LiCl}$ (1 M, 1.5 equiv., 0.75 mL) at $-70\text{ }^\circ\text{C}$ followed by transmetalation with ZnCl_2 (1 M in THF, 1.5 equiv., 0.75 mL) and a Negishi cross-coupling reaction catalyzed by $\text{Pd}(\text{PPh}_3)_4$ (5 mol%, 29 mg) in the presence of 4-methoxyiodobenzene (1.2 equiv., 0.6 mmol, 140.4 mg) at $50\text{ }^\circ\text{C}$ (oil bath). Purification via column chromatography (Hexanes/ AcOEt 8:2) afforded the product as a brown solid (0.26 mmol, 59.3 mg, 52%).

Mp: 136 – 139 $^\circ\text{C}$.

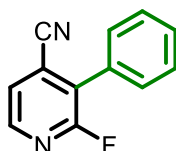
$^1\text{H-NMR}$ (400 MHz, CDCl_3): δ [ppm] = 8.38 (d, $J = 5.3$ Hz, 1H), 7.65 – 7.61 (m, 2H), 7.36 (dd, $J = 5.3, 0.9$ Hz, 1H), 7.08 – 7.04 (m, 2H), 3.89 (s, 3H).

$^{13}\text{C}\{^1\text{H}\}$ NMR (101 MHz, CDCl_3): δ [ppm] = 164.4 (d, $J_{\text{C-F}} = 246.1$ Hz), 161.9, 157.6, 150.8 (d, $J_{\text{C-F}} = 16.1$ Hz), 130.2 (2C), 126.8 (d, $J_{\text{C-F}} = 3.1$ Hz), 121.7 (d, $J_{\text{C-F}} = 4.2$ Hz), 114.9 (2C), 113.1 (d, $J_{\text{C-F}} = 4.5$ Hz), 95.0 (d, $J_{\text{C-F}} = 31.0$ Hz), 55.6.

^{19}F NMR (282 MHz, CDCl_3): δ [ppm] = -60.42 (s, 1F).

HRMS (ESI-TOF) m/z : $[\text{M}+\text{Na}]^+$ Calcd for $\text{C}_{13}\text{H}_9\text{FN}_2\text{NaO}$ 251.0591; Found 251.0584.

46. 2-Fluoro-3-phenylisonicotinonitrile (125ar)



2-fluoro-3-phenylisonicotinonitrile was obtained from **123h** via **GMC** using $(\text{TMP})_2\text{Zn}\cdot 2\text{MgCl}_2\cdot 2\text{LiCl}$ (0.29 M in THF, 0.9 equiv., 1.5 mL) at room temperature and subsequent Negishi cross-coupling catalyzed by $\text{Pd}(\text{PPh}_3)_4$ (5 mol%, 29 mg) in the

presence of iodobenzene (1.2 equiv., 0.6 mmol, 67 μ L) at 50 $^{\circ}$ C (oil bath). Purification via column chromatography (Hexanes/AcOEt 9.5:0.5) afforded the product as a beige solid (0.36 mmol, 71.4 mg, 72%).

Mp: 57 – 58 $^{\circ}$ C.

1 H-NMR (400 MHz, CDCl_3): δ [ppm] = 8.35 (dd, J = 5.1, 1.0 Hz, 1H), 7.56 (dd, J = 5.1, 0.8 Hz, 1H), 7.54 - 7.53 (m, 5H).

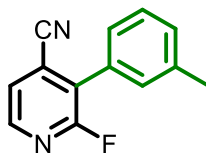
$^{13}\text{C}\{^1\text{H}\}$ NMR (101 MHz, CDCl_3): δ [ppm] = 160.7 (d, $J_{\text{C-F}}$ = 241.7 Hz), 147.2 (d, $J_{\text{C-F}}$ = 15.5 Hz), 130.2, 129.8 (d, $J_{\text{C-F}}$ = 4.6 Hz), 129.7 (d, $J_{\text{C-F}}$ = 1.7 Hz, 2C), 129.0 (2C), 127.4 (d, $J_{\text{C-F}}$ = 33.6 Hz), 124.7 (d, $J_{\text{C-F}}$ = 5.3 Hz), 124.1 (d, $J_{\text{C-F}}$ = 5.6 Hz), 115.4 (d, $J_{\text{C-F}}$ = 5.7 Hz).

^{19}F NMR (282 MHz, CDCl_3): δ [ppm] = -66.01 (s, 1F).

GC-MS (EI, 70 eV) m/z: 198.00 (100%), 197.00 (29%), 199.05 (16%), 171.00 (15%), 151.00 (13%).

HRMS (ESI-TOF) m/z: $[\text{M}+\text{CH}_3\text{OH}+\text{H}]^+$ Calcd for $\text{C}_{13}\text{H}_{12}\text{FN}_2\text{O}$ 231.0928; Found 231.0934.

47. 2-Fluoro-3-(m-tolyl)isonicotinonitrile (125as)



2-fluoro-3-(m-tolyl)isonicotinonitrile was obtained from **123h** via **GMC** using $(\text{TMP})_2\text{Zn}\cdot 2\text{MgCl}_2\cdot 2\text{LiCl}$ (0.29 M in THF, 0.9 equiv., 1.5 mL) at room temperature and subsequent Negishi cross-coupling catalyzed by $\text{Pd}(\text{PPh}_3)_4$ (5 mol%, 29 mg) in the presence of 3-iodotoluene (1.2 equiv., 0.6 mmol, 77 μ L) at 50 $^{\circ}$ C (oil bath). Purification via column chromatography (Hexanes/AcOEt 9.5:0.5) afforded the product as a colorless oil (0.40 mmol, 84.9 mg, 80%).

¹H-NMR (400 MHz, CDCl₃): δ [ppm] = 8.34 (dd, *J* = 5.1, 1.0 Hz, 1H), 7.55 (dd, *J* = 5.1, 0.8 Hz, 1H), 7.44 – 7.40 (m, 1H), 7.33 – 7.32 (m, 3H), 2.44 (s, 3H).

¹³C{¹H} NMR (101 MHz, CDCl₃): δ [ppm] = 160.7 (d, *J*_{C-F} = 241.7 Hz), 147.1 (d, *J*_{C-F} = 15.4 Hz), 138.8, 130.9, 130.2 (d, *J*_{C-F} = 1.7 Hz), 129.7 (d, *J*_{C-F} = 3.9 Hz), 128.9, 127.5 (d, *J*_{C-F} = 33.8 Hz), 126.8 (d, *J*_{C-F} = 1.7 Hz), 124.6 (d, *J*_{C-F} = 5.3 Hz), 124.1 (d, *J*_{C-F} = 5.7 Hz), 115.5 (d, *J*_{C-F} = 5.6 Hz), 21.5.

¹⁹F NMR (282 MHz, CDCl₃): δ [ppm] = -65.90 (s, 1F).

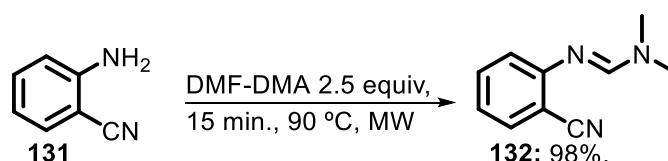
GC-MS (EI, 70 eV) m/z: 212.05 (100%), 211.05 (83%), 184.00 (30%), 185.00 (19%), 165.00 (14%).

HRMS (ESI-TOF) m/z: [M+CH₃OH+H]⁺ Calcd for C₁₄H₁₄FN₂O 245.1085; Found 245.1092.

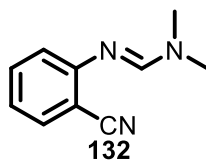
7.1.4 Examples of synthetic applications of the functionalized nitriles

7.1.4.1 Synthesis of 4-aminoquinazolines

7.1.4.1.1 Synthesis of (*E*)-*N'*-(2-cyanophenyl)-*N,N*-dimethylformimidamide **132**



A microwave vessel was charged with 2-aminobenzonitrile (1.0 equiv., 2 mmol, 0.2381 g) and DMF-DMA (2.5 equiv., 5 mmol, 0.67 mL). The reaction was kept at 90 °C for 15 minutes in the microwave reactor. Then, the remaining DMF-DMA was removed under reduced pressure, and the crude material was subjected to column chromatography (hexanes/AcOEt 7:3) to afford (*E*)-*N'*-(2-cyanophenyl)-*N,N*-dimethylformimidamide as a white solid (340 mg, 98%). Note = It only became solid after staying in the freezer overnight followed by drying under high vacuum. **CAS:** 36185-83-8. Procedure according to Besson and co-workers.⁶⁶



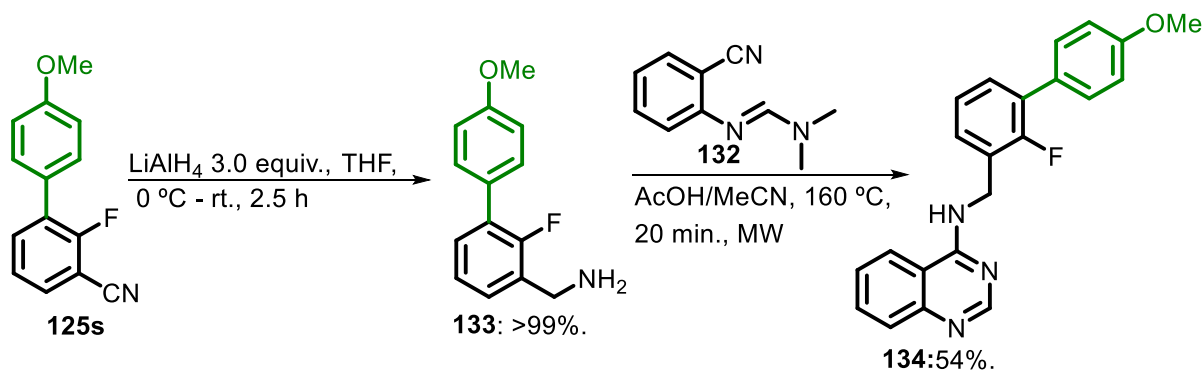
Mp: 40 – 42 °C.

¹H-NMR (400 MHz, CDCl₃): δ [ppm] = 7.57 (s, 1H), 7.51 (dd, *J* = 7.7, 1.6 Hz, 1H), 7.41 – 7.37 (m, 1H), 6.98 (td, *J* = 7.7 Hz, 1H), 6.93 (d, *J* = 8.2 Hz, 1H), 3.07 (s, 3H), 3.06 (s, 3H).

¹³C{¹H} NMR (101 MHz, CDCl₃): δ [ppm] = 155.3, 153.8, 133.5, 133.2, 122.1, 119.9, 118.8, 106.8, 40.4, 34.7.

GC-MS (EI, 70 eV) m/z: 173 (88), 172 (23), 131 (100), 102 (37), 129 (32), 44 (55), 57 (14), 42 (13).

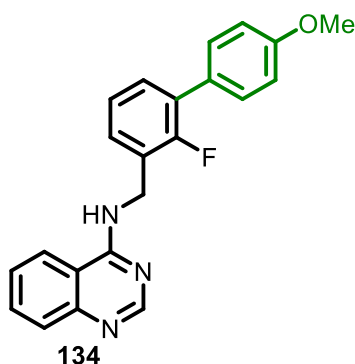
7.1.4.1.2 Synthesis of *N*-((2-fluoro-4'-methoxy-[1,1'-biphenyl]-3-yl)methyl)quinazolin-4-amine **134**



Part A: A solution of 2-fluoro-4'-methoxy-[1,1'-biphenyl]-3-carbonitrile **125s** (1.0 equiv., 0.2 mmol, 0.0454 g) in dry THF (1.5 mL) at 0 °C were gradually transferred to a round-bottom flask charged with LAH (3.0 equiv., 0.6 mmol, 0.0228 g) under nitrogen. The reaction was kept at 0 °C for 1 h and room temperature for 1h30. Then, water (10 mL) was cautiously added to the reaction mixture, and it was extracted with ethyl acetate (3x10 mL). The combined organic phases were dried over MgSO₄, filtered, and concentrated under reduced pressure affording the product as a brown oil in quantitative

yield. The obtained benzylamine⁹ was employed for the next step without further purification. This procedure was adapted from Empfield and co-workers.¹³³

Part B: A solution of (2-fluoro-4'-methoxy-[1,1'-biphenyl]-3-yl)methanamine **133** (1.0 equiv., 0.2 mmol, 0.048 g) in AcOH/MeCN 3:2 (1.2 mL – 0.72 ml of AcOH and 0.48 ml of MeCN) were transferred to a microwave vessel charged with (*E*)-*N*-(2-cyanophenyl)-*N,N*-dimethylformimidamide **132** (0.2 mmol, 0.0346 g). The reaction was kept at 160 °C for 20 minutes. Then, the mixture was cooled and concentrated under reduced pressure prior to purification via column chromatography (Hexanes/AcOEt 6:4). The product was isolated as a white solid (0.039 g, 54% yield). This procedure was adapted from Besson and co-workers.⁶⁶



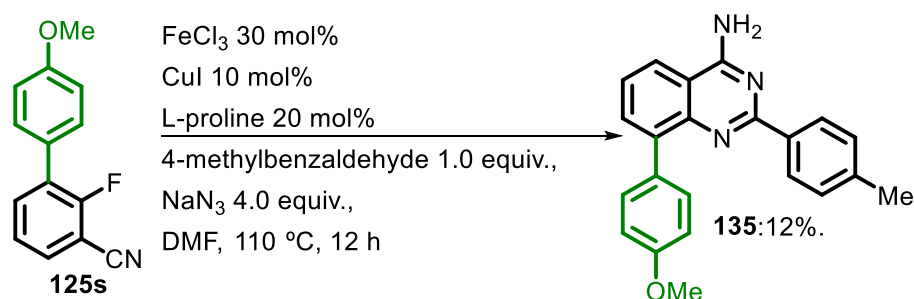
Mp: 155 – 156 °C.

¹H-NMR (400 MHz, DMSO-*d*₆): δ [ppm] = 8.85 (bs, 1H), 8.47 (s, 1H), 8.35 (d, *J* = 8.2 Hz, 1H), 7.80 (t, *J* = 7.5 Hz, 1H), 7.72 (d, *J* = 8.2 Hz, 1H), 7.55 (t, *J* = 7.6 Hz, 1H), 7.50 (d, *J* = 8.5 Hz, 2H), 7.37 (t, *J* = 7.5 Hz, 2H), 7.30 (t, *J* = 7.0 Hz, 1H), 7.18 (t, *J* = 7.6 Hz, 1H), 7.05 (d, *J* = 8.5 Hz, 2H), 4.87 (d, *J* = 5.6 Hz, 2H), 3.80 (s, 3H).

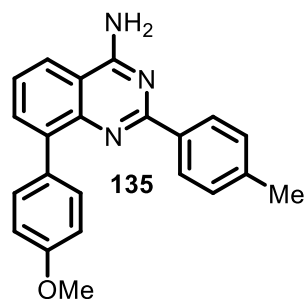
¹³C{¹H} NMR (101 MHz, DMSO-*d*₆): δ [ppm] = 159.3, 158.9, 157.0 (d, *J*_{C-F} = 245.8 Hz), 155.0, 149.1, 132.7, 130.0 (d, *J*_{C-F} = 2.9 Hz, 2C) 129.1 (d, *J*_{C-F} = 2.4 Hz), 127.8 (d, *J*_{C-F} = 21.1 Hz), 127.7 (d, *J*_{C-F} = 3.5 Hz), 127.5, 127.3, 126.6 (d, *J*_{C-F} = 15.8 Hz), 125.8, 124.3 (d, *J*_{C-F} = 3.9 Hz), 122.7, 114.9, 114.0 (2C), 55.1, 37.9 (d, *J*_{C-F} = 5.8 Hz).

HRMS (ESI-TOF) m/z: [M+H]⁺ Calcd for C₂₂H₁₉FN₃O 360.1507; Found 360.1530.

[§] The conversion was confirmed via (GC-MS (EI, 70 eV) m/z: **231 (100)**, 210 (77), 230 (51), 232 (17), 211 (16).

7.1.4.1.3 Synthesis of 8-(4-methoxyphenyl)-2-(*p*-tolyl)quinazolin-4-amine **135**

A vessel was charged with 2-fluoro-4'-methoxy-[1,1'-biphenyl]-3-carbonitrile **125s** (1.0 equiv., 0.3 mmol, 0.0682 g), *p*-Tolualdehyde (1.0 equiv., 0.3 mmol, 0.035 mL), NaN₃ (4.0 equiv., 1.2 mmol, 0.0780 g), FeCl₃ (0.3 equiv., 0.09 mmol, 0.0146 g), CuI (0.1 equiv., 0.03 mmol, 0.0057 g), L-proline (0.2 equiv., 0.06 mmol, 0.0069 g) and dry DMF (1.8 mL). It was sealed under air and kept at 110 °C for 16 h. Then, 20 mL of water was added to the mixture, and it was extracted with EtOAc (3 × 10 mL). The extract was washed with brine (10 mL), dried over anhydrous MgSO₄, and concentrated under reduced pressure (rotary evaporator). Column chromatography (Hexanes/AcOEt 7:3) was performed to afford the desired 4-aminoquinazoline **135** as a white solid (12 mg, 12% yield). Adapted from Wu and co-workers.^{56e}



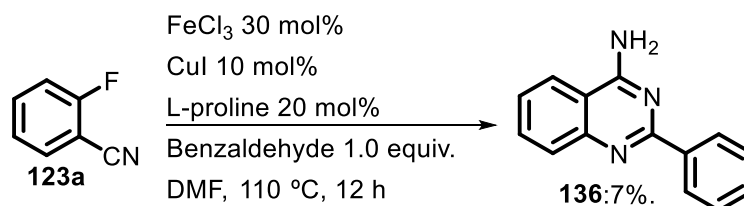
Mp: 253 – 256 °C.

¹H-NMR (400 MHz, CDCl₃): δ [ppm] = 8.33 (d, *J* = 8.2 Hz, 2H), 7.82 – 7.78 (m, 3H), 7.72 (d, *J* = 7.4 Hz, 1H), 7.47 (t-like, *J* = 7.4 Hz, 1H), 7.24 (d, *J* = 8.2 Hz, 2H), 7.06 (d-like, *J* = 8.8 Hz, 2H), 5.85 (s, 2H), 3.92 (s, 3H), 2.40 (s, 3H).

¹³C{¹H} NMR (101 MHz, CDCl₃): δ [ppm] = 161.6, 159.1, 140.3, 139.5, 135.6, 135.4, 133.4, 133.0, 132.1 (2C), 131.1, 129.1 (2C), 128.3 (2C), 125.3, 120.5, 113.4, 113.3 (2C), 55.4, 21.5.

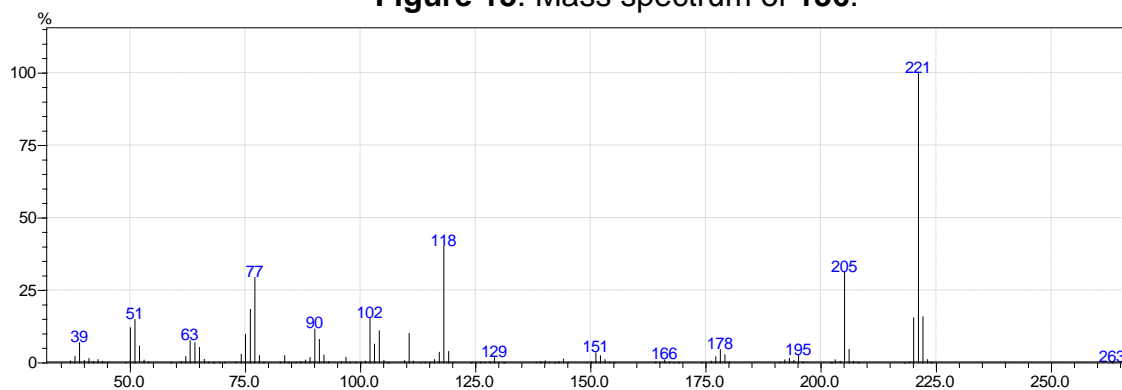
HRMS (ESI-TOF) m/z : $[M+H]^+$ Calcd for $C_{22}H_{20}N_3O$ 342.1601; Found 342.1605.

7.1.4.1.4 Synthesis of 2-phenylquinazolin-4-amine **136**

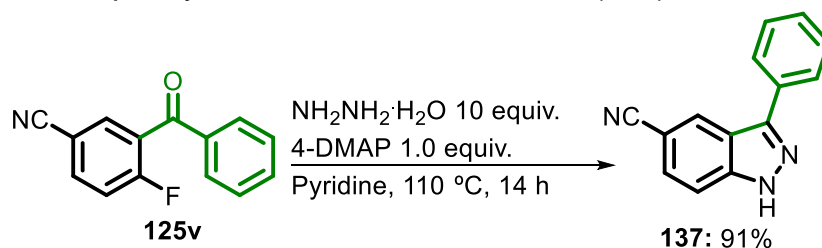


A vessel was charged with 2-fluorobenzonitrile **123a** (1.0 equiv., 0.5 mmol, 0.054 mL), benzaldehyde (1.0 equiv., 0.5 mmol, 0.051 mL), NaN_3 (4.0 equiv., 2.0 mmol, 0.1300 g), $FeCl_3$ (0.3 equiv., 0.15 mmol, 0.0243 g), CuI (0.1 equiv., 0.05 mmol, 0.0095 g), L-proline (0.2 equiv., 0.1 mmol, 0.0115 g) and dry DMF (3.0 mL). It was sealed under air and kept at 110 °C for 16 h. Then, 20 mL of water was added to the mixture, and it was extracted with EtOAc (3 × 10 mL). The extract was washed with brine (10 mL), dried over anhydrous $MgSO_4$, and concentrated under reduced pressure (rotary evaporator). Column chromatography (Hexanes/AcOEt 7:3) was performed to afford the desired 4-aminoquinazoline **136** as a yellow solid (7.7 mg, 7% yield). The product was confirmed via GC-MS analysis: (GC-MS (EI, 70 eV) m/z : **221.10 (100)**, 118.10 (39), 205.10 (30), 77.05 (28), 76 (18) (Figure 15).

Figure 15. Mass spectrum of **136**.



Source: The author.

7.1.4.2 Synthesis of 3-phenyl-1*H*-indazole-5-carbonitrile (**137**)

3-phenyl-1*H*-indazole-5-carbonitrile **137** was prepared according to a modified procedure from Zhu and coworkers.¹³⁴ A mixture of 3-benzoyl-4-fluorobenzonitrile (112.6 mg, 0.5 mmol, 1 equiv.), 4-DMAP (61.1 mg, 0.5 mmol, 1 equiv.), and hydrazine monohydrate (0.24 mL, 5 mmol, 10 equiv.) in pyridine (3.0 mL) was kept at 110 °C (oil bath) for 14 h. Then, water was added (10 mL), and the reaction was extracted with ethyl acetate (3x10 mL). After drying with MgSO_4 , filtration, and concentration under reduced pressure, it was purified by column chromatography (silica gel, hexanes/ethyl acetate 7:3) as a colorless oil (91%, 100 mg). **CAS**: 83684-54-2.

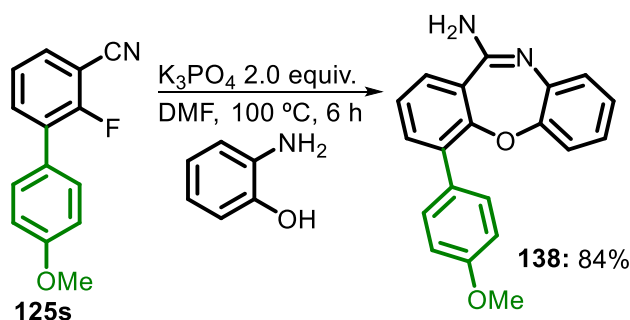
$^1\text{H-NMR}$ (400 MHz, $\text{DMSO-}d_6$): δ [ppm] = 13.77 (s, 1H, $-\text{NH}-$), 8.69 (s, 1H), 8.06 – 8.03 (m, 2H), 7.77 (d, $J = 8.7, 0.8$ Hz, 1H), 7.73 (d, $J = 8.7, 1.3$ Hz, 1H), 7.56 – 7.52 (m, 2H), 7.47 – 7.43 (m, 1H).

$^{13}\text{C}\{^1\text{H}\}$ NMR (101 MHz, $\text{DMSO-}d_6$): δ [ppm] = 144.6, 142.4, 132.4, 129.1 (2C), 128.4, 128.3, 127.8, 127.1 (2C), 119.8, 119.7, 112.2, 103.5.

GC-MS (EI, 70 eV) m/z : 219.05 (100%), 77.00 (26%), 218.05 (22%), 220.05 (18%), 192.00 (15%).

HRMS (ESI-TOF) m/z : $[\text{M-H}]^-$ Calcd for $\text{C}_{14}\text{H}_8\text{N}_3$ 218.0724; Found 218.0704.

7.1.4.3 Synthesis of 4-(4-methoxyphenyl)dibenzo[*b,f*][1,4]oxazepin-11-amine (**138**)



4-(4-methoxyphenyl)dibenzo[*b,f*][1,4]oxazepin-11-amine **138** was prepared according to the procedure of Wu and Feng.¹³⁵ A 5-mL pressure tube equipped with a stirring bar was charged with 2-fluoro-4'-methoxy-[1,1'-biphenyl]-3-carbonitrile (0.5 mmol, 113.6 mg), 2-aminophenol (0.75 mmol, 81.8 mg), K₃PO₄ (2 equiv., 1 mmol, 212.3 mg) and DMF (1 mL). The reaction was kept at 100 °C (oil bath) for 6 h, cooled to room temperature, quenched with distilled water, and extracted with ethyl acetate (3x 10 mL). The combined organic phases were dried with MgSO₄, and the product was purified by column chromatography (ethyl acetate/hexanes = 7:3) as a dark-red oil (84%, 134 mg).

¹H-NMR (400 MHz, DMSO-*d*₆): δ [ppm] = 7.67 (dd, *J* = 7.8, 1.7 Hz, 1H), 7.61 (dd, *J* = 7.8, 1.7 Hz, 1H), 7.44 – 7.40 (m, 2H), 7.35 (t, *J* = 7.8 Hz, 1H), 6.89 – 6.85 (m, 2H), 6.85 – 6.79 (m, 2H), 6.56 (ddd, *J* = 8.8, 6.9, 2.0 Hz, 1H), 6.27 (dd, *J* = 8.2, 1.0 Hz, 1H), 4.34 (bs, 2H), 3.76 (s, 3H).

¹³C{¹H} NMR (101 MHz, DMSO-*d*₆): δ [ppm] = 159.6, 154.2, 146.3, 136.9, 135.8, 132.7, 130.0 (2C), 127.9, 125.8, 123.5, 119.6, 117.4, 115.7, 114.2, 114.1 (2C), 108.6, 55.4.

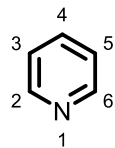
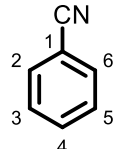
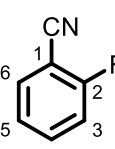
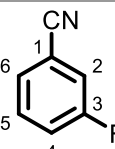
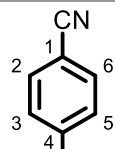
HRMS (ESI-TOF) *m/z*: [M+H]⁺ Calcd for C₂₀H₁₇N₂O₂ 317.1285; Found 317.1268.

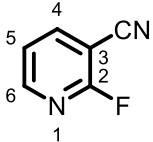
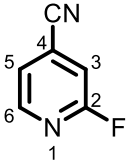
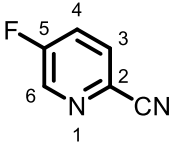
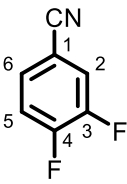
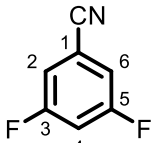
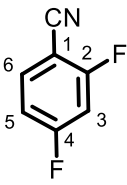
7.1.5 Computational study: p*K*_a calculations

The p*K*_a calculations were performed using hypothetical reactions which combine computational and experimental values, as suggested in some studies.¹³⁶ The deprotonated and neutral compounds had their geometries optimized in B3LYP/6-31+G(d,p) level in Gaussian 03 software.¹³⁷ The vibrational frequencies were calculated

with the same model¹³⁸ where all values were positive, which suggest the minimum in the potential energy surface. The solvent system (THF) was employed using the PCM model¹³⁹ at B3LYP/6-311++G(d,p) and the pyridine was the reference compound to the pK_a value (40.2 in THF).

Table 19 - Solvation Gibbs energies (G_{solv}), in Hartree, obtained by PCM/B3LYP/6-311++G(d,p)//B3LYP/6-31++G(d,p) and pK_a values.

Compound	G_{solv}	pK_a
	Neutral (-248.355300)	H4 = 40.2
	Deprotonated 4 (-247.795888)	
	Neutral (-324.582271)	H2 = 37.4
	Deprotonated 2 (-324.028840)	H3 = 39.8
	Deprotonated 3 (-324.023759)	H4 = 39.9
	Deprotonated 4 (-324.023544)	
	Neutral (-423.846520)	H3 = 31.2
	Deprotonated 3 (-423.306607)	H4 = 36.7
	Deprotonated 4 (-423.294619)	H5 = 37.9
	Deprotonated 5 (-423.292130)	H6 = 34.3
	Deprotonated 6 (-423.299914)	
	Neutral (-423.848337)	H2 = 28.9
	Deprotonated 2 (-423.313463)	H4 = 31.3
	Deprotonated 4 (-423.308176)	H5 = 36.3
	Deprotonated 5 (-423.296727)	H6 = 35.4
	Deprotonated 6 (-423.299267)	
	Neutral (-423.849942)	H2 = 34.2
	Deprotonated 2 (-423.303580)	H3 = 31.1
	Deprotonated 3 (-423.310234)	

	Neutral (-439.893292)	H4 = 28.9
	Deprotonated <u>4</u> (-439.358408)	H5 = 32.8
	Deprotonated <u>5</u> (-439.349881)	H6 = 35.1
	Deprotonated <u>6</u> (-439.344861)	
	Neutral (-439.893001)	H3 = 25.7
	Deprotonated <u>3</u> (-439.365130)	H5 = 30.6
	Deprotonated <u>5</u> (-439.354546)	H6 = 35.3
	Deprotonated <u>6</u> (-439.344165)	
	Neutral (-439.884033)	H3 = 29.4
	Deprotonated <u>3</u> (-439.348086)	H4 = 25.9
	Deprotonated <u>4</u> (-439.355624)	H6 = 31.4
	Deprotonated <u>6</u> (-439.343673)	
	Neutral (-523.108392)	H2 = 25.4
	Deprotonated <u>2</u> (-522.581180)	H5 = 27.7
	Deprotonated <u>5</u> (-522.576255)	H6 = 32.5
	Deprotonated <u>6</u> (-522.565647)	
	Neutral (-523.112559)	H2 = 27.0
	Deprotonated <u>2</u> (-522.581814)	H4 = 22.8
	Deprotonated <u>4</u> (-522.590933)	
	Neutral (-523.112488)	H3 = 22.6
	Deprotonated <u>3</u> (-522.591403)	H5 = 29.4
	Deprotonated <u>5</u> (-522.576637)	H6 = 31.1
	Deprotonated <u>6</u> (-522.572945)	

7.2 CHAPTER II

7.2.1 General considerations

7.2.1.1 Solvents and reagents

Unless otherwise stated, all solvents and reagents were obtained from commercial suppliers and used without prior purification.

7.2.1.2 Analytical data

Chromatography: Chromatographic purification of products was performed as flash column chromatography on silica gel (35–70 μ m, Acros Organics) or with the automatic purification system Isolera Four (Biotage). Thin-layer chromatography (TLC) was carried out on silica plates (TLC Silica 60 F₂₅₄ by Merck).

NMR spectra: NMR spectra were recorded on a Bruker Avance-II (¹H-NMR: 400MHz, ¹³C-NMR: 100.6MHz; ¹⁹F-NMR: 376 MHz) or on a Bruker Avance-III HD (¹H-NMR: 300 MHz, ¹³C-NMR: 75.5 MHz) spectrometer. Chemical shifts are referenced to residual solvent signals (DMSO-*d*₆: 2.50 ppm and 39.52 ppm for ¹H-NMR and ¹³C-NMR respectively) or using the spectrometer frequency (¹⁹F-NMR, DMSO-*d*₆) and reported in parts per million (ppm). Coupling constants (*J*) are reported in Hz, and multiplicities of NMR signals are abbreviated as follows: bs = broad singlet, s = singlet, d = doublet, dd = doublet of doublets, ddd = doublet of doublet of doublets, t = triplet, td = triplet of doublets, m = multiplet and combinations thereof, app = apparent.

Infrared spectra: Infrared (IR) spectra were recorded on an FTIR-spectrometer (Bruker Tensor 27) equipped with a diamond ATR unit and are reported in terms of frequency of absorption ν [cm⁻¹].

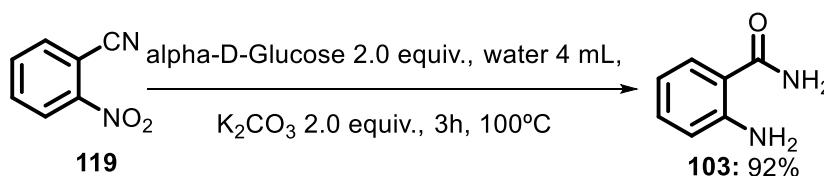
Mass spectra: Electron spray ionization (ESI) mass spectra were recorded on a 1200-series HPLC-system or a 1260-series Infinity II HPLC-system (Agilent-Technologies) with binary pump and integrated diode array detector coupled to an LC/MSDTrap-XTC-mass spectrometer (Agilent-Technologies) or an LC/MSD Infinitylab LC/MSD (G6125BLC/MSD). High-resolution masses were recorded on an Agilent 6545 QTOF instrument with a Lock Spray interface and a suitable external calibrant. Gas chromatographic investigations were carried out using an Agilent 8890 GC gas chromatograph (Agilent Technologies HP 5MS UI GC column (30 m x 0.25 mm x 0.25

μm) and helium as carrier gas with a flow rate of 1.2 mL/min) connected to a 5977 GC/MS detector and evaluated using the Mestrenova software.

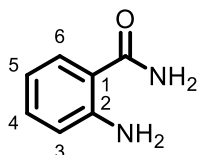
Melting point: Melting points were determined in open capillary tubes using a Krüss-OptronicKSP 1 N thermoelectric melting point meter.

7.2.2 Developed reactions

7.2.2.1 General procedure for the synthesis of 2-aminobenzamide



A test tube was charged with 2-nitrobenzonitrile (0.2 mmol, 1 equiv.), α -D-Glucose (0.4 mmol, 2.0 equiv.), K_2CO_3 (0.4 mmol, 2.0 equiv.) and 4 mL of deionized water and the reaction mixture kept at 100 °C until total consumption of starting material (3h) checked by TLC. After extraction with AcOEt (3x10 mL), the organic phase was concentrated and the product purified by column chromatography ($^{\circ}\text{Hex}:\text{AcOEt}$ 4:6) as a white solid (0.0251 g, 92%). CAS: 88-68-6.



Mp: 110-112 °C.

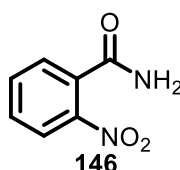
$^1\text{H-NMR}$, COSY (400 MHz, $\text{DMSO-}d_6$): δ [ppm] = δ 7.73 (bs, 1H, $-\text{CONH}_2$), 7.52 (dd, J = 8.1, 1.5 Hz, 1H, H-6), 7.12 (ddd, J = 8.4, 7.1, 1.5 Hz, 1H, H-4), 7.07 (s, 1H, $-\text{CONH}_2$), 6.67 (dd, J = 8.4, 1.2 Hz, 1H, H-3), 6.56 (s, 2H, $-\text{NH}_2$), 6.47 (ddd, J = 8.1, 7.1, 1.2 Hz, 1H, H-5).

$^{13}\text{C-NMR}$, HSQC, HMBC (101 MHz, $\text{DMSO-}d_6$): δ [ppm] = 171.4 ($-\text{CONH}_2$), 150.2 (C-2), 132.0 (C-4), 128.8 (C-6), 116.4 (C-3), 114.4 (C-5), 113.7 (C-1).

GC-MS: m/z (%) = 119.1 (100%), 136.1 (79%) [M].

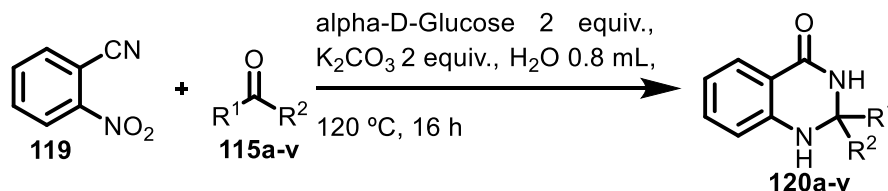
Characterization data in accordance with the literature.¹⁴⁰

When the reaction was performed with Glucose 2 equiv., K₂CO₃ 4 equiv., and 2-nitrobenzamide (0.2 mmol, 1 equiv.) in water (4 mL) at 50 °C for 3h, 2-nitrobenzamide was obtained in 86% yield.



¹H-NMR, COSY (400 MHz, DMSO-*d*₆): δ [ppm] = 8.16 (s, 1H, -CONH₂), 7.99 (dd, *J* = 8.1, 1.2 Hz, 1H, H-6), 7.76 (td, *J* = 7.5, 1.2 Hz, 1H, H-4), 7.69 (s, 1H, -CONH₂), 7.68 – 7.64 (m, 1H, H-5), 7.63 (dd, *J* = 7.5, 1.5 Hz, 1H, H-3). In accordance with the literature.¹⁴¹

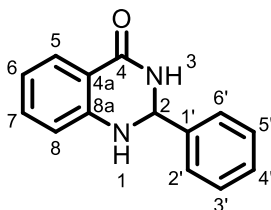
7.2.2.2 General procedure for the synthesis of 2,3-dihydroquinazolin-4(1*H*)-ones



A microwave reaction vial (5 mL, Biotage) was charged with 2-nitrobenzonitrile (0.5 mmol, 1 equiv.), α -D-Glucose (1.0 mmol, 2.0 equiv.), K₂CO₃ (1.0 mmol, 2.0 equiv.), 2.0 mL of deionized water and 1.5 equiv. of the respective aldehyde or ketone. The vial was sealed and the reaction mixture was kept at 120 °C for 16 h under vigorous stirring. After removal of water in vacuo, the crude material was loaded onto silica gel for column chromatography (^cHex:AcOEt 7:3 to 6:4) to afford the desired 2,3-dihydroquinazolin-4(1*H*)-one.

7.2.3 Characterization data of the synthesized 2,3-dihydroquinazolin-4(1*H*)-ones

1. 2-Phenyl-2,3-dihydroquinazolin-4(1*H*)-one (120a)



Yield: 72% (white solid, 0.0809g).

Rf: 0.43 (SiO₂, ^cHex/EtOAc 4:6).

Mp: 218.8 –220.1°C (Lit.: 219 - 223°C).^{71e}

IR (ATR) $\tilde{\nu}$ [cm⁻¹]: 3302, 3178, 3131, 3061, 3035, 1652, 1610, 1507, 1482, 808, 746, 698.

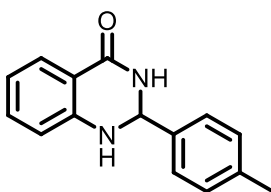
¹H-NMR, COSY (400 MHz, DMSO-*d*₆): δ [ppm] = 8.29 (s, 1H, -CONH-), 7.61 (dd, *J* = 7.8, 1.6 Hz, 1H, H-5), 7.51-7.49 (m, 2H, H-2', H-6'), 7.41 – 7.32 (m, 3H, H-3', H4', H-5'), 7.24 (ddd, *J* = 8.5, 7.1, 1.7 Hz, 1H, H-7), 7.11 (s, 1H, -NH-), 6.75 (d, *J* = 7.1 Hz, 1H, H-8), 6.69-6.65 (m, 1H, H-6), 5.76 (s, 1H, H-2).

¹³C-NMR, HSQC, HMBC (101 MHz, DMSO-*d*₆): δ [ppm] = 163.6 (C-4), 147.9 (C-8a), 141.69 (C-1'), 133.3 (C-7), 128.5 (C-3', C-5'), 128.3 (C-4'), 127.4 (C-5), 126.9 (C-2', C-6'), 117.1 (C-6), 115.0 (C-8), 114.4 (C-4a), 66.6 (C-2).

ESI-MS: (m/z) = 225.1 (100%, [M+H]⁺).

ESI-HRMS (m/z): [M+Na]⁺, calculated for [C₁₄H₁₂N₂ONa]⁺ 247.0842, found 247.0843.

2. 2-(*p*-tolyl)-2,3-dihydroquinazolin-4(1*H*)-one (120b)



Yield: 77% (white solid, 0.0913g).

Rf: 0.41 (SiO₂, ^cHex/EtOAc 4:6).

Mp: 220.4 –222.5°C (Lit.: 221 - 223°C).¹⁴²

IR (ATR) $\tilde{\nu}$ [cm⁻¹]: 3311, 3190, 3132, 3053, 2918, 1670, 1656, 1606, 1506, 1483, 798, 775, 749.

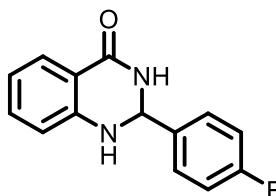
¹H-NMR, COSY (400 MHz, DMSO-*d*₆): δ [ppm] = 8.23 (s, 1H, -CONH-), 7.60 (dd, *J* = 7.8, 1.6 Hz, 1H, H-5), 7.37 (d-like, *J* = 8.0 Hz, 2H, H-2', H-6'), 7.25 – 7.21 (m, 1H, H-7), 7.19 (d-like, *J* = 8 Hz, 2H, H-3', H-5'), 7.05 (s, 1H, -NH-), 6.74 (d, *J* = 7.7 Hz, 1H, H-8), 6.68 – 6.64 (m, 1H, H-6), 5.71 (s, 1H, H-2), 2.29 (s, 3H, -CH₃).

¹³C-NMR, HSQC, HMBC (101 MHz, DMSO-*d*₆): δ [ppm] = 163.6 (C-4), 147.9 (C-8a), 138.7 (C-1'), 137.7 (C-4'), 133.3 (C-7), 128.8 (C-3', C-5'), 127.3 (C-5), 126.8 (C-2', C-6'), 117.1 (C-6), 115.0 (C-8), 114.4 (C-4a), 66.4 (C-2), 20.7 (-CH₃).

ESI-MS: (m/z) = 239.1 (100%, [M+H]⁺).

ESI-HRMS (m/z): [M+Na]⁺, calculated for [C₁₅H₁₄N₂ONa]⁺ 261.0998, found 261.0995.

3. 2-(4-Fluorophenyl)-2,3-dihydroquinazolin-4(1*H*)-one (120c)



Yield: 65% (white solid, 0.0787g).

R_f: 0.43 (SiO₂, ^cHex/EtOAc 4:6).

Mp: 196.2 –198.4°C (Lit.: 198 - 199°C).¹⁴³

IR (ATR) $\tilde{\nu}$ [cm⁻¹]: 3298, 3180, 3125, 3067, 3042, 2936, 1665, 1651, 1604, 1504, 1481, 839, 808, 793, 756.

¹H-NMR, COSY (400 MHz, DMSO-*d*₆): δ [ppm] = 8.29 (s, 1H, -CONH-), 7.62 (dd, *J* = 7.7, 1.6 Hz, 1H, H-5), 7.56-7.51 (m, 2H, H-2', H-6'), 7.27-7.20 (m, 3H, H-7, H-3', H-5'),

7.10 (s, 1H, -NH-), 6.75 (dd, $J = 8.2, 1.0$ Hz, 1H, H-8), 6.70-6.66 (m, 1H, H-6), 5.78 (s, 1H, H-2).

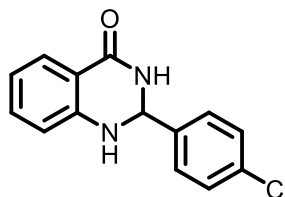
^{13}C -NMR, HSQC, HMBC (101 MHz, DMSO- d_6): δ [ppm] = 163.6 (C-4), 162.1 (C-4', $^1J_{\text{C-F}} = 244.0$ Hz), 147.8 (C-8a), 137.8 (C-1', $^4J_{\text{C-F}} = 2.9$ Hz), 133.4 (C-7), 129.1 (C-2', C-6', $^3J_{\text{C-F}} = 8.3$ Hz), 127.4 (C-5), 117.3 (C-6), 115.1 (C-3', C-5', $^2J_{\text{C-F}} = 21.5$ Hz), 115.0 (C-8), 114.4 (C-4a), 65.9 (C-2).

^{19}F NMR (376 MHz, DMSO- d_6): δ [ppm] = -115.0 (m, F).

ESI-MS: (m/z) = 243.1 (100%, $[\text{M}+\text{H}]^+$).

ESI-HRMS (m/z): $[\text{M}+\text{H}]^+$, calculated for $[\text{C}_{14}\text{H}_{12}\text{FN}_2\text{O}]^+$ 243.0928, found 243.0932.

4. 2-(4-Chlorophenyl)-2,3-dihydroquinazolin-4(1H)-one (120d)



Yield: 61% (white solid, 0.0793g).

R_f: 0.48 (SiO₂, o Hex/EtOAc 4:6).

Mp: 197.0 –199.6°C. (Lit.: 197 - 198°C).¹⁴⁴

IR (ATR) $\tilde{\nu}$ [cm^{-1}]: 3307, 3184, 3129, 3066, 2937, 1666, 1652, 1607, 1506, 1482, 835, 789, 750.

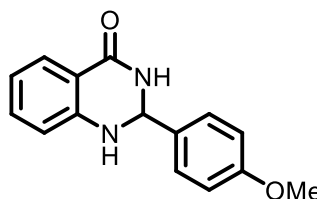
^1H -NMR, COSY (400 MHz, DMSO- d_6): δ [ppm] = 8.34 (s, 1H, -CONH-), 7.61 (dd, $J = 7.7, 1.6$ Hz, 1H, H-5), 7.52 – 7.49 (m, 2H, H-2', H-6'), 7.47 – 7.45 (m, 2H, H-3', H-5'), 7.25 (ddd, $J = 8.7, 7.2, 1.6$ Hz, 1H, H-7), 7.14 (s, 1H, -NH-), 6.75 (dd, $J = 8.7, 1.1$ Hz, 1H, H-8), 6.70-6.66 (m, 1H, H-6), 5.77 (s, 1H, H-2).

¹³C-NMR, HSQC, HMBC (101 MHz, DMSO-*d*₆): δ [ppm] = 163.5 (C-4), 147.7 (C-8a), 140.7 (C-1'), 133.4 (C-7), 133.0 (C-4'), 128.8 (C-3', C-5'), 128.3 (C2', C6'), 127.4 (C-5), 117.3 (C-6), 114.9 (C-8), 114.5 (C-4a), 65.8 (C-2).

ESI-MS: (m/z) = 259.0 (100%, [M+H]⁺).

ESI-HRMS (m/z): [M+H]⁺, calculated for [C₁₄H₁₂ClN₂O]⁺ 259.0633, found 259.0632.

5. 2-(4-Methoxyphenyl)-2,3-dihydroquinazolin-4(1H)-one (120e)



Yield: 75% (white solid, 0.0959g).

Rf: 0.42 (SiO₂, ^cHex/EtOAc 4:6).

Mp: 187.4 –189.2°C. (Lit.: 185 - 187°C).¹⁴⁵

IR (ATR) $\tilde{\nu}$ [cm⁻¹]: 3297, 3176, 3013, 2832, 1651, 1608, 1590, 1504, 1483, 834, 793, 753.

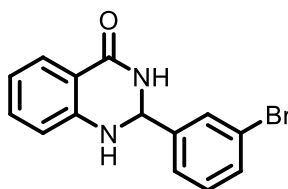
¹H-NMR, COSY (400 MHz, DMSO-*d*₆): δ [ppm] = 8.19 (s, 1H, -CONH-), 7.61 (dd, *J* = 7.8, 1.6 Hz, 1H), 7.44 – 7.40 (m, 2H, H-2', H-6'), 7.24 (ddd, *J* = 8.2, 7.2, 1.6 Hz, 1H, H-7), 7.01 (s, 1H, -NH-), 6.96 – 6.93 (m, 2H, H-3', H5'), 6.74 (dd, *J* = 8.2, 1.0 Hz, 1H), 6.69 – 6.65 (m, 1H), 5.71 (s, 1H, H-2), 3.75 (s, 3H, -OMe).

¹³C-NMR, HSQC, HMBC (101 MHz, DMSO-*d*₆): δ [ppm] = 163.7 (C-4), 159.4 (C-4'), 148.0 (C-8a), 133.5 (C-7), 133.2 (C-1'), 128.2 (C-2', C-6'), 127.3 (C-5), 117.1 (C-6), 115.0 (C-8), 114.4 (C-4a), 113.6 (C-3', C-5'), 66.3 (C-2), 55.2 (-OMe).

ESI-MS: (m/z) = 255.1 (100%, [M+H]⁺).

ESI-HRMS (m/z): [M+Na]⁺, calculated for [C₁₅H₁₄N₂O₂Na]⁺ 277.0947, found 277.0950.

6. 2-(3-Bromophenyl)-2,3-dihydroquinazolin-4(1H)-one (120f)



Yield: 58% (white solid, 0.0875g).

Rf: 0.42 (SiO₂, ^cHex/EtOAc 4:6).

Mp: 176.4 –178.8°C. (Lit.: 184 - 185°C).¹⁴⁶

IR (ATR) $\tilde{\nu}$ [cm⁻¹]: 3275, 3177, 3056, 1646, 1612, 1509, 1474, 745, 696, 679.

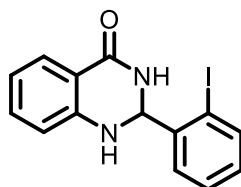
¹H-NMR, COSY (400 MHz, DMSO-*d*₆): δ [ppm] = 8.39 (s, 1H, -CONH-), 7.67 (t, *J* = 1.9 Hz, 1H, H-2'), 7.60 (dd, *J* = 7.8, 1.6 Hz, 1H, H-5), 7.54 (ddd, *J* = 7.9, 2.1, 1.0 Hz, 1H, H-4'), 7.48 (d, *J* = 7.8 Hz, 1H, H-6'), 7.35 (t, *J* = 7.8 Hz, 1H, H-5'), 7.25 (ddd, *J* = 8.8, 7.2, 1.6 Hz, 1H, H-7), 7.21 (s, 1H, -NH-), 6.77 – 6.75 (m, 1H, H-8), 6.70 – 6.66 (m, 1H, H-6), 5.77 (s, 1H, H-2).

¹³C-NMR, HSQC, HMBC (101 MHz, DMSO-*d*₆): δ [ppm] = 163.4 (C-4), 147.5 (C-8a), 144.6 (C-1'), 133.5 (C-7), 131.2 (C-6'), 130.6 (C-5'), 129.7 (C-2'), 127.4 (C-5), 125.8 (C-4'), 121.6 (C-3'), 117.3 (C-6), 114.9 (C-8), 114.5 (C-4a), 65.5 (C-2).

ESI-MS: (*m/z*) = 303.0 (100%, [M+H]⁺).

ESI-HRMS (*m/z*): [M+H]⁺, calculated for [C₁₄H₁₂BrN₂O]⁺ 303.0128, found 303.0128.

7. 2-(2-Iodophenyl)-2,3-dihydroquinazolin-4(1H)-one (120g)



Yield: 56% (white solid, 0.0989g).

Rf: 0.55 (SiO₂, ^cHex/EtOAc 4:6).

Mp: 178.4 –179.4°C.

IR (ATR) $\tilde{\nu}$ [cm⁻¹]: 3299, 3177, 3050, 2923, 2848, 1652, 1630, 1611, 1508, 1486, 1443, 745.

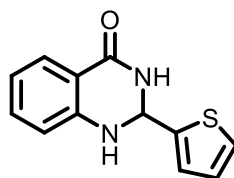
¹H-NMR, COSY (400 MHz, DMSO-*d*₆): δ [ppm] = 8.17 (s, 1H, -CONH-), 7.90 (dd, *J* = 7.9, 1.2 Hz, 1H, H-3'), 7.67 (dd, *J* = 7.8, 1.7 Hz, 1H, H-5), 7.66 (dd, *J* = 7.7, 1.7 Hz, 1H, H-6'), 7.47 (app-td, *J* = 7.7, 1.2 Hz, 1H, H-5'), 7.27 (ddd, *J* = 8.8, 7.1, 1.7 Hz, 1H, H-7), 7.18 – 7.14 (m, 1H, H-4'), 6.96 (bs, 1H, -NH-), 6.77 (app-d, *J* = 8.8 Hz, 1H, H-8), 6.75 – 6.71 (m, 1H, H-6), 5.96 (s, 1H, H-2).

¹³C-NMR, HSQC, HMBC (101 MHz, DMSO-*d*₆): δ [ppm] = 163.6 (C-4), 147.9 (C-8a), 141.5 (C-1'), 139.3 (C-3'), 133.4 (C-7), 131.0 (C-4'), 129.0 (C-6'), 128.7 (C-5'), 127.4 (C-5), 117.6 (C-6), 114.8 (C-8), 114.6 (C-4a), 99.0 (C-2'), 71.7 (C-2).

ESI-MS: (m/z) = 351.0 (100%, [M+H]⁺).

ESI-HRMS (m/z): [M+Na]⁺, calculated for [C₁₄H₁₁IN₂ONa]⁺ 372.9808, found 372.9812.

8. 2-(Thiophen-2-yl)-2,3-dihydroquinazolin-4(1H)-one (120h)



Yield: 59% (white solid, 0.0676g).

Rf: 0.33 (SiO₂, ^cHex/EtOAc 4:6).

Mp: 198.9 –201.1°C. (Lit.: 210 - 212°C).¹⁴⁷

IR (ATR) $\tilde{\nu}$ [cm⁻¹]: 3292, 3171, 3058, 2935, 1651, 1608, 1516, 1487, 1439, 763, 710, 683.

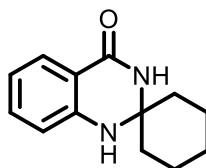
¹H-NMR, COSY (400 MHz, DMSO-*d*₆): δ [ppm] = 8.45 (s, 1H, -CONH-), 7.62 (dd, *J* = 7.7, 1.6 Hz, 1H, H-5), 7.45 (dd, *J* = 5.0, 1.3 Hz, 1H, H-3'), 7.28 – 7.24 (m, 2H, -NH-, H-7), 7.13 (d, *J* = 3.5 Hz, 1H, H-5'), 6.98 (dd, *J* = 5.0, 3.5 Hz, 1H, H-4'), 6.76 (d, 1H, *J* = 8.0 Hz, H-8), 6.70 (t, 1H, *J* = 7.7 Hz, H-6), 6.02 (s, 1H, H-2).

¹³C-NMR, HSQC, HMBC (101 MHz, DMSO-*d*₆): δ [ppm] = 163.1 (C-4), 147.2 (C-8a), 146.4 (C-2'), 133.4 (C-7), 127.3 (C-5), 126.5 (C-4'), 125.9 (C-3'), 125.7 (C-5'), 117.5 (C-6), 115.1 (C-8), 114.7 (C-4a), 62.6 (C-2).

ESI-MS: (m/z) = 231.0 (100%, [M+H]⁺).

ESI-HRMS (m/z): [M+Na]⁺, calculated for [C₁₂H₁₀N₂OSNa]⁺ 253.0406, found 253.0409.

9. 1'*H*-spiro[cyclohexane-1,2'-quinazolin]-4'(3'*H*)-one (120i)



Yield: 79% (white solid, 0.0856g).

R_f: 0.29 (SiO₂, ^cHex/EtOAc 4:6).

Mp: 220.8 – 223.1°C. (Lit.: 223 - 224°C).¹⁴⁸

IR (ATR) $\tilde{\nu}$ [cm⁻¹]: 3366, 3169, 3024, 2936, 2923, 2851, 1645, 1608, 1503, 1482, 754.

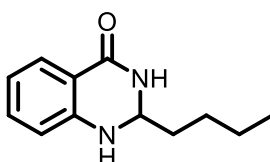
¹H-NMR, COSY (400 MHz, DMSO-*d*₆): δ [ppm] = 7.92 (s, 1H, -CONH-), 7.56 (dd, *J* = 7.7, 1.6 Hz, 1H, H-5'), 7.21 (ddd, *J* = 8.3, 7.2, 1.6 Hz, 1H, H-7'), 6.80 (d, *J* = 8.3 Hz, 1H, H-8'), 6.63 – 6.59 (m, 2H, -NH-, H-6'), 1.76 – 1.73 (m, 2H, -CH₂-), 1.63 – 1.53 (m, 6H, -CH₂-), 1.45 – 1.23 (m, 2H, -CH₂-).

¹³C-NMR, HSQC, HMBC (101 MHz, DMSO-*d*₆): δ [ppm] = 163.2 (C-4'), 146.8, (C-8a'), 133.1 (C-7'), 127.1 (C-5'), 116.5 (C-6'), 114.6 (C-8'), 114.4 (C-4a'), 67.8 (C-1), 37.2 (-CH₂-), 24.6 (-CH₂-), 20.9 (-CH₂-).

ESI-MS: (m/z) = 217.1 (100%, $[M+H]^+$).

ESI-HRMS (m/z): $[M+Na]^+$, calculated for $[C_{13}H_{16}N_2ONa]^+$ 239.1155, found 239.1156.

10. 2-Butylquinazolin-4(3H)-one (120j)



Yield: 56% (white solid, 0.0598g).

Rf: 0.32 (SiO_2 , n Hex/EtOAc 4:6).

Mp: 142.4 – 144.4°C. (Lit.: 144 - 146°C).¹⁴⁹

IR (ATR) $\tilde{\nu}$ [cm^{-1}]: 3339, 3296, 3189, 3069, 2970, 2921, 2855, 1643, 1610, 1501, 1483, 758.

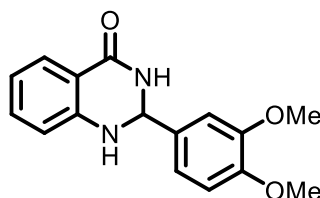
1H -NMR, COSY (400 MHz, DMSO- d_6): δ [ppm] = 7.88 (s, 1H, -CONH-), 7.57 (dd, J = 7.7, 1.6 Hz, 1H, H-5), 7.24-7.20 (m, 1H, H-7), 6.72 (d, J = 7.9 Hz, 1H, H-8), 6.66 – 6.63 (m, 1H, H-6), 6.56 (s, 1H, -NH-), 4.68 (t, 1H, J = 5.2 Hz, H-2), 1.65 – 1.60 (m, 2H, H-1'), 1.43 – 1.35 (m, 2H, H-2'), 1.33 – 1.24 (m, 2H, H-3'), 0.88 (t, J = 7.2 Hz, 3H, H-4').

^{13}C -NMR, HSQC, HMBC (101 MHz, DMSO- d_6): δ [ppm] = 163.9 (C-4), 148.5 (C-8a), 133.0 (C-7), 127.3 (C-5), 116.9 (C-6), 115.0 (C-8), 114.4 (C-4a), 64.4 (C-2), 34.7 (C-1'), 25.4 (C-2'), 22.1 (C-3'), 13.9 (C-4').

ESI-MS: (m/z) = 205.1 (100%, $[M+H]^+$).

ESI-HRMS (m/z): $[M+Na]^+$, calculated for $[C_{12}H_{16}N_2ONa]^+$ 227.1155, found 227.1159.

11. 2-(3,4-Dimethoxyphenyl)-2,3-dihydroquinazolin-4(1H)-one (120k)



Yield: 90% (white solid, 0.1276g).

Rf: 0.18 (SiO₂, ^cHex/EtOAc 4:6).

Mp: 212.6 –214.8°C. (Lit.: 212 - 214°C).¹⁵⁰

IR (ATR) $\tilde{\nu}$ [cm⁻¹]: 3354, 3333, 3177, 2967, 2935, 2836, 1667, 1609, 1497, 1481, 1460, 1142, 1017, 769, 755.

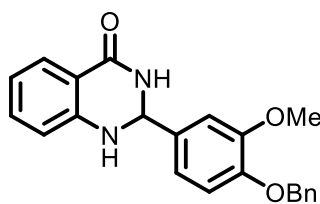
¹H-NMR, COSY (400 MHz, DMSO-*d*₆): δ [ppm] = 8.18 (s, 1H, -CONH-), 7.62 (dd, *J* = 7.8, 1.6 Hz, 1H, H-5), 7.24 (ddd, *J* = 8.8, 7.2, 1.6 Hz, 1H, H-7), 7.13 (d, *J* = 2.0 Hz, 1H, H-2'), 7.01 – 6.98 (m, 2H, -NH-, H-6'), 6.94 (d, *J* = 8.3 Hz, 1H, H-5'), 6.75 (d, 1H, *J* = 8.8 Hz, H-8), 6.70 – 6.66 (m, 1H, H-6), 5.70 (s, 1H, H-2), 3.75 (d, 6H, -(OCH₃)₂).

¹³C-NMR, HSQC, HMBC (101 MHz, DMSO-*d*₆): δ [ppm] = 163.7 (C-4), 149.0 (C-4'), 148.6 (C-3'), 148.1(C-8a), 133.6 (C-7), 133.2 (C-1'), 127.3 (C-5), 119.2 (C-6'), 117.1 (C-6), 115.1 (C-8), 114.4 (C-4a), 111.3 (C-5'), 110.6 (C-2'), 66.5 (C-2), 55.6 (-OCH₃), 55.5 (-OCH₃).

ESI-MS: (m/z) = 285.1 (100%, [M+H]⁺).

ESI-HRMS (m/z): [M+Na]⁺, calculated for [C₁₆H₁₆N₂O₃Na]⁺ 307.1053, found 307.1057.

12. 2-(4-(Benzyloxy)-3-methoxyphenyl)-2,3-dihydroquinazolin-4(1H)-one (120I)



Yield: 63% (white solid, 0.1130g).

Rf: 0.35 (SiO₂, ^cHex/EtOAc 4:6).

Mp: 155.1 –156.2°C.

IR (ATR) $\tilde{\nu}$ [cm⁻¹]: 3361, 3174, 3079, 3060, 2913, 2869, 1655, 1611, 1503, 1485, 1467, 1138, 747.

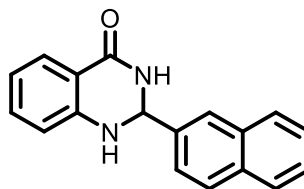
¹H-NMR, COSY (400 MHz, DMSO-*d*₆): δ [ppm] = 8.18 (s, 1H, -CONH-), 7.62 (dd, *J* = 7.8, 1.6 Hz, 1H, H-5), 7.45 – 7.30 (m, 5H, -OBn, H_{Ar}), 7.24 (ddd, *J* = 8.1, 7.2, 1.6 Hz, 1H, H-7), 7.16 (d, *J* = 1.9 Hz, 1H, H-2'), 7.04 – 7.02 (m, 2H, -NH-, H-5'), 6.97 (dd, *J* = 8.3, 1.9 Hz, 1H, H-6'), 6.75 (d, *J* = 8.1 Hz, 1H, H-8), 6.70 – 6.66 (m, 1H, H-6), 5.69 (s, 1H, H-2), 5.09 (s, 2H, -CH₂-), 3.78 (s, 3H, -OCH₃).

¹³C-NMR, HSQC, HMBC (101 MHz, DMSO-*d*₆): δ [ppm] = 163.7 (C-4), 149.0 (C-3'), 148.1 (C-4'), 147.9 (C-8a), 137.1 (-OBn, C_{Ar}), 134.0 (C-1'), 133.2(C-7), 128.4 (-OBn, C_{HAr}), 127.8 (-OBn, C_{HAr}), 127.7 (-OBn, C_{HAr}), 127.3 (C-5), 119.2 (C-6'), 117.1 (C-6), 115.1 (C-8), 114.4 (C-4a), 113.0 (C-5'), 110.9 (C-2'), 69.8 (-CH₂-), 66.5 (C-2), 55.6 (-OCH₃).

ESI-MS: (m/z) = 361.2 (100%, [M+H]⁺).

ESI-HRMS (m/z): [M+H]⁺, calculated for [C₂₂H₂₁N₂O₃]⁺ 361.1547, found 361.1552.

13. 2-(Naphthalen-2-yl)-2,3-dihydroquinazolin-4(1*H*)-one (120m)



Yield: 71% (white solid, 0.1329g).

Rf: 0.45 (SiO₂, ^cHex/EtOAc 4:6).

Mp: 201.4 –202.4°C. (Lit.: 224 - 225°C).¹⁵¹

IR (ATR) $\tilde{\nu}$ [cm⁻¹]: 3279, 3182, 3051, 3021, 1660, 1646, 1607, 1508, 1484, 1440, 1297, 742.

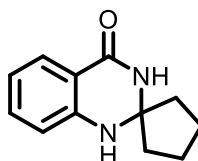
¹H-NMR, COSY (400 MHz, DMSO-*d*₆): δ [ppm] = 8.38 (s, 1H, -CONH-), 7.96 – 7.91 (m, 4H, H-1', H-4', H-8', H-5'), 7.71 (dd, *J* = 8.6, 1.7 Hz, 1H, H-3'), 7.65 (dd, *J* = 7.7, 1.6 Hz, 1H, H-5), 7.56 – 7.51 (m, 2H, H-6', H-7'), 7.26 (ddd, *J* = 8.2, 7.2, 1.6 Hz, 1H, H-7), 7.20 (s, 1H, -NH-), 6.77 (dd, *J* = 8.2, 1.0 Hz, 1H, H-8), 6.71 – 6.67 (m, 1H, H-6), 5.94 (s, 1H, H-2).

¹³C-NMR, HSQC, HMBC (101 MHz, DMSO-*d*₆): δ [ppm] = 163.6 (C-4), 147.9 (C-8a), 138.9 (C-2'), 133.4 (C-7), 133.0 (C-8a'), 132.5 (C-4a'), 128.1 (C-8'), 128.0 (C-5'), 127.6 (4'), 127.4 (C-5), 126.4 (C-6'), 126.4 (C7'), 125.9 (C-1'), 124.9 (C-3'), 117.2 (C-6), 115.0 (C-8), 114.4 (C-4a), 66.8 (C-2).

ESI-MS: (m/z) = 275.1 (100%, [M+H]⁺).

ESI-HRMS (m/z): [M+Na]⁺, calculated for [C₁₈H₁₄N₂ONa]⁺ 297.0998, found 297.1000.

14. 1'*H*-spiro[cyclopentane-1,2'-quinazolin]-4'(3'*H*)-one (120n)



Yield: 61% (white solid, 0.0619).

R_f: 0.23 (SiO₂, ^cHex/EtOAc 4:6).

Mp: 252.0 – 253.4°C. (Lit.: 254 - 256°C).¹⁵²

IR (ATR) $\tilde{\nu}$ [cm⁻¹]: 3289, 3162, 3001, 2972, 2941, 2877, 1635, 1613, 1542, 1516, 1459, 803, 779, 751.

¹H-NMR, COSY (400 MHz, DMSO-*d*₆): δ [ppm] = 8.09 (s, 1H, -CONH-), 7.57 (dd, *J* = 7.7, 1.6 Hz, 1H, H-5'), 7.21 (ddd, *J* = 8.2, 7.3, 1.6 Hz, 1H, H-7'), 6.74 (s, 1H, -NH-), 6.69

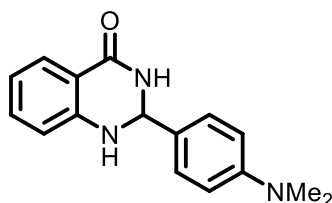
(d, $J = 8.2$ Hz, 1H, H-8'), 6.64 – 6.60 (m, 1H, H-6'), 1.82 – 1.75 (m, 4H, -CH₂-), 1.69 – 1.63 (m, 4H, -CH₂-).

¹³C-NMR, HSQC, HMBC (101 MHz, DMSO-*d*₆): δ [ppm] = 163.4 (C-4'), 147.5 (C-8a'), 133.0 (C-7'), 127.2 (C-5'), 116.5 (C-6'), 114.6 (C-8'), 114.3 (C-4a'), 77.1 (C-1), 22.0 (4C, -CH₂-).

ESI-MS: (m/z) = 203.1 (100%, [M+H]⁺).

ESI-HRMS (m/z): [M+Na]⁺, calculated for [C₁₂H₁₄N₂ONa]⁺ 225.0998, found 225.1000.

15. 2-(4-(Dimethylamino)phenyl)-2,3-dihydroquinazolin-4(1*H*)-one (120o)



Yield: 63% (white solid, 0.0848g).

R_f: 0.30 (SiO₂, ^cHex/EtOAc 4:6).

Mp: 200.1 – 201.6°C. (Lit.: 201 - 203°C).¹⁵³

IR (ATR) $\tilde{\nu}$ [cm⁻¹]: 3291, 3187, 3052, 3031, 2980, 2891, 2803, 1665, 1650, 1609, 1509, 1483, 1436, 817, 798, 749, 730.

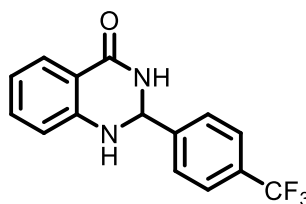
¹H-NMR, COSY (400 MHz, DMSO-*d*₆): δ [ppm] = 8.07 (s, 1H, -CONH-), 7.61 (dd, $J = 7.8, 1.6$ Hz, 1H, H-5), 7.30 (d-like, $J = 8.8$ Hz, 2H, H-2', H-6'), 7.22 (ddd, $J = 8.1, 7.2, 1.6$ Hz, 1H, H-7), 6.92 (s, 1H, -NH-), 6.74 – 6.70 (m, 3H, H-8, H-3', H-5'), 6.68 – 6.64 (m, 1H, H-6), 5.63 (s, 1H, H-2), 2.88 (s, 6H, -N(CH₃)₂).

¹³C-NMR, HSQC, HMBC (101 MHz, DMSO-*d*₆): δ [ppm] = 163.8 (C-4), 150.7 (C-4'), 148.2 (C-8a), 133.1 (C-7), 128.6 (C-1'), 127.7 (C-2', C-6'), 127.3 (C-5), 116.9 (C-6), 115.0 (C-8), 114.4 (C-4a), 111.9 (C-3', C-5'), 66.6 (C-2), 40.2 – 39.0 (-N(CH₃)₂).

ESI-MS: (m/z) = 268.1 (100%, [M+H]⁺).

ESI-HRMS (m/z): $[M+Na]^+$, calculated for $[C_{16}H_{17}N_3ONa]^+$ 290.1264, found 290.1267.

16. 2-(4-(Trifluoromethyl)phenyl)-2,3-dihydroquinazolin-4(1H)-one (120p)



Yield: 55% (white solid, 0.0798g).

Rf: 0.49 (SiO₂, ^cHex/EtOAc 7:3).

Mp: 191.8 –194.1°C. (Lit.: 193 - 195°C).¹⁵⁴

IR (ATR) $\tilde{\nu}$ [cm⁻¹]: 3297, 3184, 1666, 1651, 1613, 1514, 1487, 1325, 1129, 1163, 852, 797, 759.

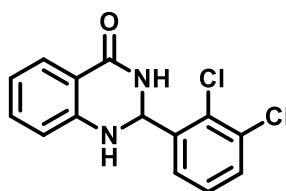
¹H-NMR, COSY (300 MHz, DMSO-*d*₆): δ [ppm] = 8.44 (s, 1H, -CONH-), 7.78 (d-like, J = 8.3 Hz, 2H, H-3', H-5'), 7.70 (d-like, J = 8.3 Hz, 2H, H-2', H-6'), 7.61 (dd, J = 7.8, 1.6 Hz, 1H, H-5), 7.28 – 7.23 (m, 2H, H-7, -NH-), 6.76 (d, J = 8.0 Hz, 1H, H-8), 6.69 (t, J = 7.8 Hz, 1H, H-6), 5.86 (s, 1H, H-2).

¹³C-NMR, HSQC, HMBC (75 MHz, DMSO-*d*₆): δ [ppm] = 163.4 (C-4), 147.5 (C-8a), 146.4 (C-1'), 133.5 (C-7), 129.0 (q, ² J_{C-F} = 32.0 Hz, C-4'), 127.7 (C-2', C6'), 127.4 (C-5), 124.2 (q, ¹ J_{C-F} = 272.2 Hz, -CF₃), 125.4 (q, ³ J_{C-F} = 3.6 Hz, C-3', C-5'), 117.4 (C-6), 114.9 (C-8), 114.5 (C-4a), 65.7 (C-2).

ESI-MS: (m/z) = 293.1 (100%, $[M+H]^+$).

ESI-HRMS (m/z): $[M+H]^+$, calculated for $[C_{15}H_{12}F_3N_2O]^+$ 293.0896, found 293.0898.

17. 2-(2,3-Dichlorophenyl)-2,3-dihydroquinazolin-4(1H)-one (120q)



Yield: 23% (white solid, 0.0331g).

Rf: 0.45 (SiO₂, ^cHex/EtOAc 1:1).

Mp: 227.3 –228.9°C. (Lit.: 232 - 233°C).¹⁵⁵

IR (ATR) $\tilde{\nu}$ [cm⁻¹]: 3274, 1656, 1613, 1509, 1487, 1449, 1415, 1381, 1325, 1158, 755, 715.

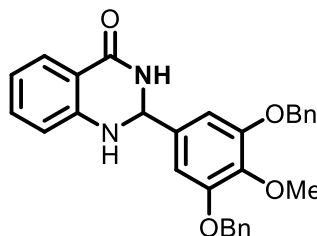
¹H-NMR, COSY (300 MHz, DMSO-*d*₆): δ [ppm] = 8.27 (s, 1H, -CONH-), 7.68 – 7.64 (m, 2H, H-5, H-4'), 7.61 (dd, *J* = 7.9, 1.5 Hz, 1H, H-6'), 7.42 (t, *J* = 7.9 Hz, 1H, H-5'), 7.27 (ddd, *J* = 8.2, 7.2, 1.6 Hz, 1H, H-7), 7.08 (s, 1H, -NH-), 6.77 – 6.69 (m, 2H, H-6, H-8), 6.18 (appt, *J* = 1.9 Hz, 1H, H-2).

¹³C-NMR, HSQC, HMBC (75 MHz, DMSO-*d*₆): δ [ppm] = 163.5 (C-4), 147.4 (C-8a), 140.6 (C-1'), 133.6 (C-7), 132.0 (C-3'), 130.6 (C-4'), 129.9 (C-2'), 128.4 (C-5'), 127.4 (C-5), 127.2 (C-6'), 117.6 (C-6), 114.6 (C-8), 114.6 (C-4a), 64.3 (C-2).

ESI-MS: (m/z) = 293.1 (100%, [M+H]⁺).

ESI-HRMS (m/z): [M+Na]⁺, calculated for [C₁₄H₁₀Cl₂N₂O]⁺ 315.0062, found 315.0062.

18. 2-(3,5-Bis(benzyloxy)-4-methoxyphenyl)-2,3-dihydroquinazolin-4(1H)-one (120r)



Yield: 18% (oil, 0.0410g).

Rf: 0.41 (SiO₂, ^cHex/EtOAc 1:1).

IR (ATR) $\tilde{\nu}$ [cm⁻¹]: 3418, 2255, 1657, 1615, 1503, 1488, 1440, 1236, 1049, 1025, 1004, 824, 762, 700.

¹H-NMR, COSY (300 MHz, DMSO-*d*₆): δ [ppm] = 8.24 (s, 1H, -CONH-), 7.64 (dd, *J* = 7.8, 1.6 Hz, 1H, H-5), 7.47 – 7.33 (m, 10H, -OBn, H_{Ar}), 7.27 (ddd, *J* = 8.5, 7.4, 1.6 Hz, 1H, H-7), 7.08 (s, 1H, -NH-), 7.00 (s, 2H, H-2', H-6'), 6.78 (app-d, *J* = 8.5 Hz, 1H, H-8), 6.73 – 6.68 (m, 1H, H-6), 5.69 (s, 1H, H-2), 5.09 (s, 4H, -CH₂-), 3.70 (s, 3H, -OCH₃).

¹³C-NMR, HSQC, HMBC (75 MHz, DMSO-*d*₆): δ [ppm] = 163.7 (C-4), 152.0 (C-5', C-3'), 147.9 (C-8a), 138.5 (C-4'), 136.9 (2C, -OBn, C_q), 136.9 (C-1'), 133.4 (C-7), 128.5 (4C, -OBn, CH_{Ar}), 127.9 (2C, -OBn, CH_{Ar}), 127.7 (4C, -OBn, CH_{Ar}), 127.4 (C-5), 117.3 (C-6), 115.0 (C-8), 114.5 (C-4a), 106.2 (C-2', C-6'), 70.2 (2C, -CH₂-), 66.7 (C-2), 60.1 (-OCH₃).

ESI-MS: (m/z) = 467.2 (100%, [M+H]⁺).

ESI-HRMS (m/z): [M+H]⁺, calculated for [C₂₉H₂₇N₂O₄]⁺ 467.1966, found 467.1964.

8. References

1. GILMAN, H.; BEBB, R. L. Relative Reactivities of Organometallic Compounds. XX. *Metalation. **Journal of the American Chemical Society**, v. 61, n. 1, p. 109–112, 1939.
2. WITTIG, G.; FUHRMANN, G. Über das Verhalten der halogenierten Anisole gegen Phenyl-lithium (V. Mitteil. über die Reaktionsweise des Phenyl-lithiums). **Berichte der deutschen chemischen Gesellschaft (A and B Series)**, v. 73, n. 11, p. 1197–1218, 1940.
3. a) SLOCUM, D. W.; SUGARMAN, D. I. Directed metalation. **Advances in Chemistry**, n. 130, 222–247, 1974. b) GREEN, L.; CHAUDER, B.; SNIECKUS, V. The directed ortho metalation - Cross-coupling symbiosis in heteroaromatic synthesis. **Journal of Heterocyclic Chemistry**, v. 36, n. 6, p. 1453–1468, 1999. c) HARTUNG, C. G.; SNIECKUS, V. The Directed *ortho* Metalation Reaction— A Point of Departure for New Synthetic Aromatic Chemistry. **Modern Arene Chemistry**. Weinheim, FRG: Wiley-VCH Verlag GmbH & Co. KGaA, 2002. p. 330–367. d) MIAH, M. A. J.; SIBI, M. P.; CHATTOPADHYAY, S.; FAMILONI, O. B.; SNIECKUS, V. Directed *ortho* -Metalation of *O*-Aryl *N,N*-Dialkylcarbamates: Methodology, Anionic *ortho* -Fries Rearrangement, and Lateral Metalation. **European Journal of Organic Chemistry**, v. 2018, n. 4, p. 440–446, 2018.
4. PUTERBAUGH, W. H.; HAUSER, C. R. Metalation of *N*-Methylbenzamide with Excess *n*-Butyllithium. Condensations with Electrophilic Compounds to Form *ortho* Derivatives. Cyclizations. **The Journal of Organic Chemistry**, v. 29, n. 4, p. 853–856, 1964.
5. MICHAEL, U.; GRONOWITZ, S. A Simple One-Pot Procedure for the Synthesis of Certain Substituted Thiophene Aldehydes and Ketones. **Acta Chemica Scandinavica**, v. 22, p. 1353–1355, 1968.
6. FUHRER, W.; GSCHWEND, H. W. Ortho Functionalization of Aromatic Amines: Ortho Lithiation of *N*-Pivaloylanilines. **The Journal of Organic Chemistry**, v. 44, n. 7, p. 1133–1136, 1979.
7. MEYERS, A. I.; MIHELICH, E. D. Oxazolines. XVII. Regioselective Metalation of 2-Aryl Oxazolines. Route to Polydeuteriobenzoic Acids. **The Journal of Organic Chemistry**, v. 40, n. 21, p. 3158–3159, 1975.
8. BEAK, P.; BROWN, R. A. The Ortho Lithiation of Tertiary Benzamides. **The Journal of Organic Chemistry**, v. 42, n. 10, p. 1823–1824, 1977.
9. a) MILLS, R. J.; TAYLOR, N. J.; SNIECKUS, V. Directed Ortho Metalation of *N,N*-Diethylbenzamides. Silicon Protection of Ortho Sites and the *o*-Methyl Group. **The**

- Journal of Organic Chemistry**, v. 54, n. 18, p. 4372–4385, 1989. b) SENGUPTA, S.; SNIECKUS, V. The 2-(Trimethylsilyl)Ethoxymethoxy (OSEM) Directed Ortho Metalation Group. New Regiospecific Synthetic Routes to Substituted Benzenes and Pyridines. **Tetrahedron Letters**, v. 31, n. 30, p. 4267–4270, 1990.
10. CHRISTENSEN, H. Preparation of Salicylaldehydes via the Ortho-Lithio Derivatives of Methoxymethyl-Protected Phenols. **Synthetic Communications**, v. 5, n. 1, p. 65–78, 1975.
11. MUCHOWSKI, J. M.; VENUTI, M. C. Ortho Functionalization of N-(Tert-Butoxycarbonyl)Aniline. **The Journal of Organic Chemistry**, v. 45, n. 23, p. 4798–4801, 1980.
12. KAUCH, M.; HOPPE, D. Synthesis of substituted phenols by directed *ortho*-lithiation of in situ *N*-silyl-protected *O*-aryl *N*-monoalkylcarbamates. **Canadian Journal of Chemistry**, v. 79, n. 11, p. 1736–1746, 2001.
13. AZZOUZ, R.; BISCHOFF, L.; FRUIT, C.; MARSAIS, F. *O*-Tetrahydropyran-2-yloxy (*O*-THP) as an *ortho*-Directing Group in the Lithiation of Pyridines. **Synlett**, v. 2006, n. 12, p. 1908–1912, 2006.
14. WHISLER, M. C.; MACNEIL, S.; SNIECKUS, V.; BEAK, P. Beyond Thermodynamic Acidity: A Perspective on the Complex-Induced Proximity Effect (CIPE) in Deprotonation Reactions. **Angewandte Chemie International Edition**, v. 43, n. 17, p. 2206–2225, 2004.
15. a) BRIDGES, A. J.; LEE, A.; MADUAKOR, E. C.; SCHWARTZ, C. E. Fluorine as an *ortho*-directing group in aromatic metalation: Generality of the reaction and the high position of fluorine in the Dir-Met potency scale. **Tetrahedron Letters**, v. 33, n. 49, p. 7495–7498, 1992. b) KLIS, T.; LULINSKI, S.; SERWATOWSKI, J. Remote-Substituent-Directed Metalations of Arenes. **Current Organic Chemistry**, v. 12, n. 17, p. 1479–1501, 2008. c) TOUDIC, F.; TURCK, A.; PLÉ, N.; QUÉGUINER, G.; DARABANTU, M.; LEQUEUX, T.; POMMELET, J. C. Relative *ortho*-directing power of fluorine, chlorine and methoxy group for the metalation reaction in the diazine series. Diazines XXXV. **Journal of Heterocyclic Chemistry**, v. 40, n. 5, p. 855–860, 2003.
16. a) HAAG, B.; MOSRIN, M.; ILA, H.; MALAKHOV, V.; KNOCHER, P. Regio- and Chemoselective Metalation of Arenes and Heteroarenes Using Hindered Metal Amide Bases. **Angewandte Chemie International Edition**, v. 50, n. 42, p. 9794–9824, 2011. b) BOZZINI, L. A.; DOS SANTOS, T.; MURIE, V. E.; DE MELLO, M. B. M.; VESSECCHI, R.; CLOSOSKI, G. C. Regioselective Functionalization of Ester-, Amide-, Carbonate-, and Carbamate-Substituted 2-Phenyl-2-oxazolines with Mixed Lithium–

Magnesium Amides. **The Journal of Organic Chemistry**, v. 86, n. 1, p. 1204–1215, 2021.

17. a) HAUSER, C. R.; WALKER, H. G. Condensation of Certain Esters by Means of Diethylaminomagnesium Bromide. **Journal of the American Chemical Society**, v. 69, n. 2, p. 295–297, 1947. b) FROSTICK, F. C.; HAUSER, C. R. Condensations of Esters by Diisopropylaminomagnesium Bromide and Certain Related Reagents. **Journal of the American Chemical Society**, v. 71, n. 4, p. 1350–1352, 1949.

18. EATON, P. E.; LEE, C. H.; XIONG, Y. Magnesium amide bases and amido-Grignards. Ortho magnesiation. **Journal of the American Chemical Society**, v. 111, n. 20, p. 8016–8018, 1989.

19. SCHLECKER, W.; HUTH, A.; OTTOW, E.; MULZER, J. Regioselective Metalation of Pyridinylcarbamates and Pyridinecarboxamides with (2,2,6,6-Tetramethylpiperidino)magnesium Chloride. **The Journal of Organic Chemistry**, v. 60, n. 26, p. 8414–8416, 1995.

20. KRASOVSKIY, A.; KRASOVSKAYA, V.; KNOCHEL, P. Mixed Mg/Li Amides of the Type $R_2NMgCl \cdot LiCl$ as Highly Efficient Bases for the Regioselective Generation of Functionalized Aryl and Heteroaryl Magnesium Compounds. **Angewandte Chemie International Edition**, v. 45, n. 18, p. 2958–2961, 2006.

21. CLOSOSKI, G. C.; ROHBOGNER, C. J.; KNOCHEL, P. Direct Magnesiation of Polyfunctionalized Arenes and Heteroarenes Using $(TMP)_2Mg \cdot 2LiCl$. **Angewandte Chemie International Edition**, v. 46, n. 40, p. 7681–7684, 2007.

22. UNSINN, A.; FORD, M. J.; KNOCHEL, P. New Preparation of $TMPZnCl \cdot LiCl$ by Zn Insertion into $TMPCl$. Application to the Functionalization of Dibromodiazines. **Organic Letters**, v. 15, n. 5, p. 1128–1131, 2013.

23. WUNDERLICH, S. H.; KNOCHEL, P. $(TMP)_2Zn \cdot 2MgCl_2 \cdot 2LiCl$: A Chemoselective Base for the Directed Zincation of Sensitive Arenes and Heteroarenes. **Angewandte Chemie International Edition**, v. 46, n. 40, p. 7685–7688, 2007.

24. BALKENHOHL, M.; GREINER, R.; MAKAROV, I. S.; HEINZ, B.; KARAGHIOSOFF, K.; ZIPSE, H.; KNOCHEL, P. Zn-, Mg-, and Li-TMP Bases for the Successive Regioselective Metalations of the 1,5-Naphthyridine Scaffold (TMP=2,2,6,6-Tetramethylpiperidyl). **Chemistry - A European Journal**, v. 23, n. 53, p. 13046–13050, 2017.

25. a) ROHBOGNER, C. J.; WIRTH, S.; KNOCHEL, P. Phosphorodiamidate-Directed Metalation of *N*-Heterocycles using Mg- and Zn-TMP Bases. **Organic Letters**, v. 12, n. 9, p. 1984–1987, 2010. b) MURIE, V. E.; NISHIMURA, R. H. V.; ROLIM, L. A.;

VESSECCHI, R.; LOPES, N. P.; CLOSOSKI, G. C. Base-Controlled Regioselective Functionalization of Chloro-Substituted Quinolines. **The Journal of Organic Chemistry**, v. 83, n. 2, p. 871–880, 2018. c) MURIE, V. E.; NICOLINO, P. V.; DOS SANTOS, T.; GAMBACORTA, G.; NISHIMURA, R. H. V.; PEROVANI, I. S.; FURTADO, L. C.; COSTA-LOTUFO, L. V.; MORAES DE OLIVEIRA, A.; VESSECCHI, R.; BAXENDALE, I. R.; CLOSOSKI, G. C. Synthesis of 7-Chloroquinoline Derivatives Using Mixed Lithium-Magnesium Reagents. **The Journal of Organic Chemistry**, v. 86, n. 19, p. 13402–13419, 2021.

26. a) AMARAL, M. F. Z. J.; BAUMGARTNER, A. A.; VESSECCHI, R.; CLOSOSKI, G. C. Directed Metalation of 1-Ester-Substituted Indolizines: Base/Electrophile-Controlled Regioselective Functionalization. **Organic Letters**, v. 17, n. 2, p. 238–241, 2015. b) BERTALLO, C. R. d. S.; ARROIO, T. R.; TOLEDO, M. F. Z. J.; SADLER, S. A.; VESSECCHI, R.; STEEL, P. G.; CLOSOSKI, G. C. C-H Activation/Metalation Approaches for the Synthesis of Indolizine Derivatives: C-H Activation/Metalation Approaches for the Synthesis of Indolizine Derivatives. **European Journal of Organic Chemistry**, v. 2019, n. 31–32, p. 5205–5213, 2019.

27. BOZZINI, L. A.; BATISTA, J. H. C.; DE MELLO, M. B. M.; VESSECCHI, R.; CLOSOSKI, G. C. Selective functionalization of cyano-phenyl-2-oxazolines using TMPMgCl·LiCl. **Tetrahedron Letters**, v. 58, n. 44, p. 4186–4190, 2017.

28. SCHWÄRZER, K.; TÜLLMANN, C. P.; GRASSL, S.; GÓRSKI, B.; BROCKLEHURST, C. E.; KNOCHEL, P. Functionalization of 1,3,4-Oxadiazoles and 1,2,4-Triazoles via Selective Zincation or Magnesiation Using 2,2,6,6-Tetramethylpiperidyl Bases. **Organic Letters**, v. 22, n. 5, p. 1899–1902, 2020.

29. ZIEGLER, D. S.; GREINER, R.; LUMPE, H.; KQIKU, L.; KARAGHIOSOFF, K.; KNOCHEL, P. Directed Zincation or Magnesiation of the 2-Pyridone and 2,7-Naphthyridone Scaffold Using TMP Bases. **Organic Letters**, v. 19, n. 21, p. 5760–5763, 2017.

30. BALKENHOHL, M.; SALGUES, B.; HIRAI, T.; KARAGHIOSOFF, K.; KNOCHEL, P. Regioselective Metalation and Functionalization of the Pyrazolo[1,5-a]pyridine Scaffold Using Mg- and Zn-TMP Bases. **Organic Letters**, v. 20, n. 10, p. 3114–3118, 2018.

31. ZIEGLER, D.; KLIER, L.; MÜLLER, N.; KARAGHIOSOFF, K.; KNOCHEL, P. Directed Zincation or Magnesiation of 2- and 4-Pyrones and Their Derivatives. **Synthesis**, v. 50, n. 22, p. 4383–4394, 2018.

32. BALKENHOHL, M.; KNOCHEL, P. Regioselective C–H Activation of Substituted Pyridines and other Azines using Mg- and Zn-TMP-Bases. **SynOpen**, v. 02, n. 01, p. 78–95, 2018.

33. SCHWÄRZER, K.; ROUT, S. K.; BESSINGER, D.; LIMA, F.; BROCKLEHURST, C. E.; KARAGHIOSOFF, K.; BEIN, T.; KNOCHEL, P. Selective functionalization of the 1*H*-imidazo[1,2-*b*]pyrazole scaffold. A new potential non-classical isostere of indole and a precursor of push–pull dyes. **Chemical Science**, v. 12, n. 39, p. 12993–13000, 2021.
34. NISHIMURA, R. H. V.; VAZ, A. D. L. L.; BOZZINI, L. A.; MURIE, V. E.; CLOSOSKI, G. C. Recent applications of magnesium- and Zinc-TMP amides in the synthesis of bioactive targets. **Tetrahedron**, v. 75, n. 4, p. 464–474, 2019.
35. MOSRIN, M.; KNOCHEL, P. Regio- and Chemoselective Metalation of Chloropyrimidine Derivatives with $\text{TMPMgCl}\cdot\text{LiCl}$ and $\text{TMP}_2\text{Zn}\cdot 2\text{MgCl}_2\cdot 2\text{LiCl}$. **Chemistry - A European Journal**, v. 15, n. 6, p. 1468–1477, 2009.
36. a) ZHENG, S.; YU, C.; SHEN, Z. Ethyl Cyanoacetate: A New Cyanating Agent for the Palladium-Catalyzed Cyanation of Aryl Halides. **Organic Letters**, v. 14, n. 14, p. 3644–3647, 2012. b) ROKADE, B. V.; MALEKAR, S. K.; PRABHU, K. R. A novel oxidative transformation of alcohols to nitriles: an efficient utility of azides as a nitrogen source. **Chemical Communications**, v. 48, n. 44, p. 5506–5508, 2012.
37. a) ANBARASAN, P.; SCHAREINA, T.; BELLER, M. Recent developments and perspectives in palladium-catalyzed cyanation of aryl halides: synthesis of benzonitriles. **Chemical Society Reviews**, v. 40, n. 10, p. 5049–5067, 2011. b) CHAITANYA, M.; ANBARASAN, P. Recent developments and applications of cyanamides in electrophilic cyanation. **Organic & Biomolecular Chemistry**, v. 16, n. 39, p. 7084–7103, 2018. c) GRUNDKE, C.; VIERENGEL, N.; OPATZ, T. α -Aminonitriles: From Sustainable Preparation to Applications in Natural Product Synthesis. **The Chemical Record**, vol. 20, n. 9, p. 989–1016, 2020. d) YANG, X.; FLEMING, F. F. C- and N-Metalated Nitriles: The Relationship between Structure and Selectivity. **Accounts of Chemical Research**, v. 50, n. 10, p. 2556–2568, 2017.
38. CLEGG, W.; DALE, S. H.; HEVIA, E.; HOGG, L. M.; HONEYMAN, G. W.; MULVEY, R. E.; O'HARA, C. T.; RUSSO, L. Structurally Defined Reactions of Sodium TMP–Zincate with Nitrile Compounds: Synthesis of a Salt-Like Sodium Sodiumdzincate and Other Unexpected Ion-Pair Products. **Angewandte Chemie International Edition**, v. 47, n. 4, p. 731–734, 2008.
39. DOS SANTOS, F.; BATISTA, J.; VESSECCHI, R.; CLOSOSKI, G. Directed Functionalization of Cyano-Substituted Furans and Thiophenes with $\text{TMPMgCl}\cdot\text{LiCl}$. **Synlett**, v. 26, n. 20, p. 2795–2800, 2015.
40. FRASER, R. R.; MANSOUR, T. S.; SAVARD, S. Acidity measurements in THF. V. Heteroaromatic compounds containing 5-membered rings. **Canadian Journal of Chemistry**, v. 63, n. 12, p. 3505–3509, 1985.

41. SNÉGAROFF, K.; KOMAGAWA, S.; CHEVALLIER, F.; GROS, P. C.; GOLHEN, S.; ROISNEL, T.; UCHIYAMA, M.; MONGIN, F. Deprotonative Metalation of Substituted Benzenes and Heteroaromatics Using Amino/Alkyl Mixed Lithium-Zinc Combinations. **Chemistry - A European Journal**, v. 16, n. 27, p. 8191–8201, 2010.
42. BENTABED-ABABSA, G.; CHEIKH SID ELY, S.; HESSE, S.; NASSAR, E.; CHEVALLIER, F.; NGUYEN, T. T.; DERDOUR, A.; MONGIN, F. Direct Metalation of Heteroaromatic Esters and Nitriles Using a Mixed Lithium–Cadmium Base. Subsequent Conversion to Dipyridopyrimidinones. **The Journal of Organic Chemistry**, v. 75, n. 3, p. 839–847, 2010.
43. CAILLY, T.; FABIS, F.; RAULT, S. A new, direct, and efficient synthesis of benzonaphthyridin-5-ones. **Tetrahedron**, v. 62, n. 25, p. 5862–5867, 2006.
44. BECKER, M. R.; KNOCHEL, P. Practical Continuous-Flow Trapping Metalations of Functionalized Arenes and Heteroarenes Using TMPLi in the Presence of Mg, Zn, Cu, or La Halides. **Angewandte Chemie International Edition**, v. 54, n. 42, p. 12501–12505, 2015.
45. DUEZ, S.; BERNHARDT, S.; HEPPEKAUSEN, J.; FLEMING, F. F.; KNOCHEL, P. Pd-Catalyzed α -Arylation of Nitriles and Esters and γ -Arylation of Unsaturated Nitriles with TMPZnCl·LiCl. **Organic Letters**, v. 13, n. 7, p. 1690–1693, 2011.
46. MARZI, E.; BOBBIO, C.; COTTET, F.; SCHLOSSER, M. Converting Core Compounds into Building Blocks: The Concept of Regiochemically Exhaustive Functionalization. **European Journal of Organic Chemistry**, v. 2005, n. 10, p. 2116–2123, 2005.
47. SCHLOSSER, M.; MONGIN, F. Pyridine elaboration through organometallic intermediates: regiochemical control and completeness. **Chemical Society Reviews**, v. 36, n. 7, p. 1161–1172, 2007.
48. BOBBIO, C.; SCHLOSSER, M. Selective Functionalization of 2-Fluoropyridine, 2,3-Difluoropyridine, and 2,5-Difluoropyridine at Each Vacant Position. **The Journal of Organic Chemistry**, v. 70, n. 8, p. 3039–3045, 2005.
49. SCHLOSSER, M.; RAUSIS, T.; BOBBIO, C. Rerouting Nucleophilic Substitution from the 4-Position to the 2- or 6-Position of 2,4-Dihalopyridines and 2,4,6-Trihalopyridines: The Solution to a Long-Standing Problem. **Organic Letters**, v. 7, n. 1, p. 127–129, 2005.
50. SCHLOSSER, M.; RAUSIS, T. The Structural Proliferation of 2,6-Difluoropyridine through Organometallic Intermediates. **European Journal of Organic Chemistry**, v. 2004, n. 5, p. 1018–1024, 2004.

51. BOBBIO, C.; RAUSIS, T.; SCHLOSSER, M. Removal of Fluorine from and Introduction of Fluorine into Polyhalopyridines: An Exercise in Nucleophilic Heteroaryl Substitution. **Chemistry - A European Journal**, v. 11, n. 6, p. 1903–1910, 2005.
52. MARZI, E.; GORECKA, J.; SCHLOSSER, M. The Regioexhaustive Functionalization of Difluorophenols and Trifluorophenols Through Organometallic Intermediates. **Synthesis**, v. 2004, n. 10, p. 1609–1618, 2004.
53. SCHLOSSER, M.; GINANNESCHI, A.; LEROUX, F. In Search of Simplicity and Flexibility: A Rational Access to Twelve Fluoroindolecarboxylic Acids. **European Journal of Organic Chemistry**, v. 2006, n. 13, p. 2956–2969, 2006.
54. HEISS, C.; MARZI, E.; MONGIN, F.; SCHLOSSER, M. Remote Trimethylsilyl Groups Interfering with the ortho Deprotonation of Fluoroarenes and Chloroarenes. **European Journal of Organic Chemistry**, v. 2007, n. 4, p. 669–675, 2007.
55. a) HERAVI, M. M.; ZADSIRJAN, V. Prescribed drugs containing nitrogen heterocycles: an overview. **RSC Advances**, v. 10, n. 72, p. 44247–44311, 2020. b) KERRU, N.; GUMMIDI, L.; MADDILA, S.; GANGU, K. K.; JONNALAGADDA, S. B. A Review on Recent Advances in Nitrogen-Containing Molecules and Their Biological Applications. **Molecules**, v. 25, n. 8, p. 1909, 2020.
56. a) GUNDLA, R.; KAZEMI, R.; SANAM, R.; MUTTINENI, R.; SARMA, J. A. R. P.; DAYAM, R.; NEAMATI, N. Discovery of Novel Small-Molecule Inhibitors of Human Epidermal Growth Factor Receptor-2: Combined Ligand and Target-Based Approach. **Journal of Medicinal Chemistry**, v. 51, n. 12, p. 3367–3377, 2008. b) ZAYED, M.; IHMAID, S.; AHMED, H.; EL-ADL, K.; ASIRI, A.; OMAR, A. Synthesis, Modelling, and Anticonvulsant Studies of New Quinazolines Showing Three Highly Active Compounds with Low Toxicity and High Affinity to the GABA-A Receptor. **Molecules**, v. 22, n. 2, p. 188, 2017. c) CHEN, L.; FU, W.; ZHENG, L.; LIU, Z.; LIANG, G. Recent Progress of Small-Molecule Epidermal Growth Factor Receptor (EGFR) Inhibitors against C797S Resistance in Non-Small-Cell Lung Cancer: Miniperspective. **Journal of Medicinal Chemistry**, v. 61, n. 10, p. 4290–4300, 2018. d) PARK, H.; JUNG, H.-Y.; MAH, S.; HONG, S. Discovery of EGF Receptor Inhibitors That Are Selective for the d746 - 750/T790M/C797S Mutant through Structure-Based de Novo Design. **Angewandte Chemie International Edition**, v. 56, n. 26, p. 7634–7638, 2017. e) JIA, F.-C.; ZHOU, Z.-W.; XU, C.; CAI, Q.; LI, D.-K.; WU, A.-X. Expedient Synthesis of 2-Phenylquinazolin-4-amines via a Fe/Cu Relay-Catalyzed Domino Strategy. **Organic Letters**, v. 17, n. 17, p. 4236–4239, 2015. f) DAS, D.; HONG, J. Recent advancements of 4-aminoquinazoline derivatives as kinase inhibitors and their applications in medicinal chemistry. **European Journal of Medicinal Chemistry**, v. 170, p. 55–72, 2019.

57. a) ZHOU, Z.; HE, J.; YANG, F.; PAN, Q.; YANG, Z.; ZHENG, P.; XU, S.; ZHU, W. Design, synthesis and evaluation of anti-proliferative activity of 2-aryl-4-aminoquinazoline derivatives as EGFR inhibitors. **Bioorganic Chemistry**, v. 112, p. 104848, 2021. b) LIU, F.; HUAI, Z.; XIA, G.; SONG, L.; LI, S.; XU, Y.; HONG, K.; YAO, M.; LIU, G.; HUANG, Y. Synthesis and antitumor activity of novel 6,7,8-trimethoxy N-aryl-substituted-4-aminoquinazoline derivatives. **Bioorganic & Medicinal Chemistry Letters**, v. 28, n. 14, p. 2561–2565, 2018. c) YADAV, M. R.; GRANDE, F.; CHOUHAN, B. S.; NAIK, P. P.; GIRIDHAR, R.; GAROFALO, A.; NEAMATI, N. Cytotoxic potential of novel 6,7-dimethoxyquinazolines. **European Journal of Medicinal Chemistry**, v. 48, n.6, p. 231–243, 2012. d) WEI, X.-W.; YUAN, J.-M.; HUANG, W.-Y.; CHEN, N.-Y.; LI, X.-J.; PAN, C.-X.; MO, D.-L.; SU, G.-F. 2-Styryl-4-aminoquinazoline derivatives as potent DNA-cleavage, p53-activation and in vivo effective anticancer agents. **European Journal of Medicinal Chemistry**, v. 186, p. 111851, 2020. e) UEHLING, D. E.; JOSEPH, B.; CHUNG, K. C.; ZHANG, A. X.; LER, S.; PRAKESCH, M. A.; PODA, G.; GROULEFF, J.; AMAN, A.; KIYOTA, T.; LEUNG-HAGESTEIJN, C.; KONDA, J. D.; MARCELLUS, R.; GRIFFIN, C.; SUBRAMANIAM, R.; ABIBI, A.; STRATHDEE, C. A.; ISAAC, M. B.; AL-AWAR, R.; TIEDEMANN, R. E. Design, Synthesis, and Characterization of 4-Aminoquinazolines as Potent Inhibitors of the G Protein-Coupled Receptor Kinase 6 (GRK6) for the Treatment of Multiple Myeloma. **Journal of Medicinal Chemistry**, v. 64, n. 15, p. 11129–11147, 2021.
58. AHMAD, O. K.; HILL, M. D.; MOVASSAGHI, M. Synthesis of Densely Substituted Pyrimidine Derivatives. **The Journal of Organic Chemistry**, v. 74, n. 21, p. 8460–8463, 2009.
59. WAN, Z.-K.; WACHARASINDHU, S.; BINNUN, E.; MANSOUR, T. An Efficient Direct Amination of Cyclic Amides and Cyclic Ureas. **Organic Letters**, v. 8, n. 11, p. 2425–2428, 2006.
60. NUNES, P. S. G.; DA SILVA, G.; NASCIMENTO, S.; MANTOANI, S. P.; DE ANDRADE, P.; BERNARDES, E. S.; KAWANO, D. F.; LEOPOLDINO, A. M.; CARVALHO, I. Synthesis, biological evaluation and molecular docking studies of novel 1,2,3-triazole-quinazolines as antiproliferative agents displaying ERK inhibitory activity. **Bioorganic Chemistry**, v. 113, p. 104982, 2021.
61. CHEN, X.; YANG, Q.; ZHOU, Y.; DENG, Z.; MAO, X.; PENG, Y. Synthesis of 4-(Dimethylamino)quinazoline via Direct Amination of Quinazolin-4(3H)-one Using N,N-Dimethylformamide as a Nitrogen Source at Room Temperature. **Synthesis**, v. 47, n. 14, p. 2055–2062, 2015.
62. RATTANANGKOOL, E.; SUKWATTANASINITT, M.; WACHARASINDHU, S. Organocatalytic Visible Light Enabled S_NAr of Heterocyclic Thiols: A Metal-Free

Approach to 2-Aminobenzoxazoles and 4-Aminoquinazolines. **The Journal of Organic Chemistry**, v. 82, n. 24, p. 13256–13262, 2017.

63. WANG, Y.; WANG, H.; PENG, J.; ZHU, Q. Palladium-Catalyzed Intramolecular C(sp²)-H Amidation by Isonitrile Insertion Provides Direct Access to 4-Aminoquinazolines from *N*-Arylamidines. **Organic Letters**, v. 13, n. 17, p. 4604–4607, 2011.

64. REN, J.; HUANG, Y.; PI, C.; CUI, X.; WU, Y. Rhodium(III)-catalyzed [4 + 2] annulation of *N*-arylbenzamidines with 1,4,2-dioxazol-5-ones: Easy access to 4-aminoquinazolines via highly selective C-H bond activation. **Chinese Chemical Letters**, v. 32, n. 8, p. 2592–2596, 2021.

65. LOIDREAU, Y.; BESSON, T. Microwave-assisted thermal decomposition of formamide: a tool for coupling a pyrimidine ring with an aromatic partner. **Tetrahedron**, v. 67, n. 26, p. 4852–4857, 2011.

66. FOUCOURT, A.; DUBOUILH-BENARD, C.; CHOSSON, E.; CORBIÈRE, C.; BUQUET, C.; IANNELLI, M.; LEBLOND, B.; MARSAIS, F.; BESSON, T. Microwave-accelerated Dimroth rearrangement for the synthesis of 4-anilino-6-nitroquinazolines. Application to an efficient synthesis of a microtubule destabilizing agent. **Tetrahedron**, v. 66, n. 25, p. 4495–4502, 2010.

67. FENG, J.-B.; WU, X.-F. Synthesis of quinazolinimines and quinazolinamines from 2-fluorobenzonitriles under catalyst-free conditions. **Organic & Biomolecular Chemistry**, v. 13, n. 43, p. 10656–10662, 2015.

68. SHELKE, N. B.; GHORPADE, R.; PRATAP, A.; TAK, V.; ACHARYA, B. N. S_NAr reaction in aqueous medium in the presence of mixed organic and inorganic bases. **RSC Advances**, v. 5, n. 39, p. 31226–31230, 2015.

69. YANG, X.; LIU, H.; FU, H.; QIAO, R.; JIANG, Y.; ZHAO, Y. Efficient Copper-Catalyzed Synthesis of 4-Aminoquinazoline and 2,4-Diaminoquinazoline Derivatives. **Synlett**, v. 2010, n. 01, p. 101–106, 2010.

70. a) BADOLATO, M.; AIELLO, F.; NEAMATI, N. 2,3-Dihydroquinazolin-4(1*H*)-one as a privileged scaffold in drug design. **RSC Advances**, v. 8, n. 37, p. 20894–20921, 2018. b) CHINIGO, G. M.; PAIGE, M.; GRINDROD, S.; HAMEL, E.; DAKSHANAMURTHY, S.; CHRUSZCZ, M.; MINOR, W.; BROWN, M. L. Asymmetric Synthesis of 2,3-Dihydro-2-arylquinazolin-4-ones: Methodology and Application to a Potent Fluorescent Tubulin Inhibitor with Anticancer Activity. **Journal of Medicinal Chemistry**, v. 51, n. 15, p. 4620–4631, 2008. c) HEMALATHA, K.; MADHUMITHA, G. Synthetic strategy with representation on mechanistic pathway for the therapeutic applications of dihydroquinazolinones. **European Journal of Medicinal Chemistry**, v. 123, p. 596–

630, 2016. d) JIANG, Y.; ZHUANG, C.; CHEN, L.; LU, J.; DONG, G.; MIAO, Z.; ZHANG, W.; LI, J.; SHENG, C. Structural Biology-Inspired Discovery of Novel KRAS–PDE δ Inhibitors. **Journal of Medicinal Chemistry**, v. 60, n. 22, p. 9400–9406, 2017.

71. a) ERFAN, M. A.; AKHLAGHINIA, B.; GHODSINIA, S. S. E. An Efficient Green Protocol for Synthesis of 2,3-Dihydroquinazolin-4(1*H*)-ones Using SBA-16/GPTMS-TSC-Cu^I under Solvent-Free Conditions. **ChemistrySelect**, v. 5, n. 7, p. 2306–2316, 2020. b) GONG, W.; CHEN, X.; JIANG, H.; CHU, D.; CUI, Y.; LIU, Y. Highly Stable Zr(IV)-Based Metal–Organic Frameworks with Chiral Phosphoric Acids for Catalytic Asymmetric Tandem Reactions. **Journal of the American Chemical Society**, v. 141, n. 18, p. 7498–7508, 2019. c) HEIDARI, L.; SHIRI, L. CoFe₂O₄@SiO₂-CPTES-Guanidine-Cu(II): A novel and reusable nanocatalyst for the synthesis of 2,3-dihydroquinazolin-4(1*H*)-ones and polyhydroquinolines and oxidation of sulfides: nanocatalyst. **Applied Organometallic Chemistry**, v. 33, n. 3, p. e4636, 2019. d) HONJO, T.; PHIPPS, R. J.; RAUNIYAR, V.; TOSTE, F. Dean. A Doubly Axially Chiral Phosphoric Acid Catalyst for the Asymmetric Tandem Oxyfluorination of Enamides. **Angewandte Chemie International Edition**, v. 51, n. 38, p. 9684–9688, 2012. e) TRAN, P. H.; THI BUI, T.-P.; BACH LAM, X.-Q.; THI NGUYEN, X.-T. Synthesis of benzo[4,5]imidazo[1,2-*a*]pyrimidines and 2,3-dihydroquinazolin-4(1*H*)-ones under metal-free and solvent-free conditions for minimizing waste generation. **RSC Advances**, v. 8, n. 63, p. 36392–36399, 2018. f) GHOSH, S. K.; NAGARAJAN, R. Deep eutectic solvent mediated synthesis of quinazolinones and dihydroquinazolinones: synthesis of natural products and drugs. **RSC Advances**, v. 6, n. 33, p. 27378–27387, 2016. g) PRAKASH, M.; KESAVAN, V. Highly Enantioselective Synthesis of 2,3-Dihydroquinazolinones through Intramolecular Amidation of Imines. **Organic Letters**, v. 14, n. 7, p. 1896–1899, 2012. h) LUO, Y.; WU, Y.; WANG, Y.; SUN, H.; XIE, Z.; ZHANG, W.; GAO, Z. Ethanol promoted titanocene Lewis acid catalyzed synthesis of quinazoline derivatives. **RSC Advances**, v. 6, n. 70, p. 66074–66077, 2016. i) SAFARI, J.; GANDOMI-RAVANDI, S. Silver decorated multi-walled carbon nanotubes as a heterogeneous catalyst in the sonication of 2-aryl-2,3-dihydroquinazolin-4(1*H*)-ones. **RSC Adv.**, v. 4, n. 23, p. 11654–11660, 2014. j) WATSON, A. J. A.; MAXWELL, A. C.; WILLIAMS, J. M. J. Ruthenium-catalysed oxidative synthesis of heterocycles from alcohols. **Org. Biomol. Chem.**, v. 10, n. 2, p. 240–243, 2012. k) SHARMA, M.; PANDEY, S.; CHAUHAN, K.; SHARMA, D.; KUMAR, B.; CHAUHAN, P. M. S. Cyanuric Chloride Catalyzed Mild Protocol for Synthesis of Biologically Active Dihydro/Spiro Quinazolinones and Quinazolinone-glycoconjugates. **The Journal of Organic Chemistry**, v. 77, n. 2, p. 929–937, 2012. l) HUANG, D.; LI, X.; XU, F.; LI, L.; LIN, X. Highly Enantioselective Synthesis of Dihydroquinazolinones Catalyzed by SPINOL-Phosphoric Acids. **ACS Catalysis**, v. 3, n. 10, p. 2244–2247, 2013. m) PARIYAR, G. C.; MITRA, B.; MUKHERJEE, S.; GHOSH, P. Ascorbic Acid as an Efficient Organocatalyst

for the Synthesis of 2-Substituted-2,3-dihydroquinazolin-4(1*H*)-one and 2-Substituted Quinazolin-4(3*H*)-one in Water. **ChemistrySelect**, v. 5, n. 1, p. 104–108, 2020.

72. a) WU, J.; DU, X.; MA, J.; ZHANG, Y.; SHI, Q.; LUO, L.; SONG, B.; YANG, S.; HU, D. Preparation of 2,3-dihydroquinazolin-4(1*H*)-one derivatives in aqueous media with β -cyclodextrin-SO₃H as a recyclable catalyst. **Green Chem.**, v. 16, n. 6, p. 3210–3217, 2014. b) CHEN, J.; WU, D.; HE, F.; LIU, M.; WU, H.; DING, J.; SU, W. Gallium(III) triflate-catalyzed one-pot selective synthesis of 2,3-dihydroquinazolin-4(1*H*)-ones and quinazolin-4(3*H*)-ones. **Tetrahedron Letters**, v. 49, n. 23, p. 3814–3818, 2008. c) CHEN, Y.; SHAN, W.; LEI, M.; HU, L. Thiamine hydrochloride (VB1) as an efficient promoter for the one-pot synthesis of 2,3-dihydroquinazolin-4(1*H*)-ones. **Tetrahedron Letters**, v. 53, n. 44, p. 5923–5925, 2012.

73. LIU, Z.; ZENG, L.-Y.; LI, C.; YANG, F.; QIU, F.; LIU, S.; XI, B. “On-Water” Synthesis of Quinazolinones and Dihydroquinazolinones Starting from *o*-Bromobenzonitrile. **Molecules**, v. 23, n. 9, p. 2325, 2018.

74. SHI, D.; RONG, L.; WANG, J.; ZHUANG, Q.; WANG, X.; HU, H. Synthesis of quinazolin-4(3*H*)-ones and 1,2-dihydroquinazolin-4(3*H*)-ones with the aid of a low-valent titanium reagent. **Tetrahedron Letters**, v. 44, n. 15, p. 3199–3201, 2003.

75. WU, X-F.; OSCHATZ, S.; BLOCK, A.; SPANNENBERG, A.; LANGER, P. Base mediated synthesis of 2-aryl-2,3-dihydroquinazolin-4(1*H*)-ones from 2-aminobenzonitriles and aromatic aldehydes in water. **Organic & Biomolecular Chemistry**, v. 12, n. 12, p. 1865, 2014.

76. LIU, Q.; SUI, Y.; ZHANG, Y.; ZHANG, K.; CHEN, Y.; ZHOU, H. Copper-Catalyzed One-Pot Synthesis of 2,3-Dihydroquinazolin-4(1*H*)-ones from 2-Nitrobenzonitriles and Carbonyl Compounds Mediated by Diboronic Acid in Methanol–Water. **Synlett**, v. 31, n. 03, p. 275–279, 2020.

77. KUMAR, M.; RICHA; SHARMA, S.; BHATT, V.; KUMAR, N. Iron(III) Chloride-Catalyzed Decarboxylative-Deaminative Functionalization of Phenylglycine: A Tandem Synthesis of Quinazolinones and Benzimidazoles. **Advanced Synthesis & Catalysis**, v. 357, n. 13, p. 2862–2868, 2015.

78. GHARAT, L. A.; MUTHUKA-MAN, N.; PISAL, D.; KHAIRATKAR-JOSHI, N.; SHAH, D. M.; KADAM, S. R. **Alkyne compounds as s-nitrosogluthathione reductase inhibitors**. Applicant: Glenmark Pharmaceuticals S.A. WO2016055947 (A1). International Publication Date: 14. Apr. 2016.

79. HAMMANN, J. M.; HAAS, D.; KNOCHEL, P. Cobalt-Catalyzed Negishi Cross-Coupling Reactions of (Hetero)Arylzinc Reagents with Primary and Secondary Alkyl

Bromides and Iodides. **Angewandte Chemie International Edition**, v. 54, n. 15, p. 4478–4481, 2015.

80. WUNDERLICH, S.; KNOCHEL, P. High Temperature Metalation of Functionalized Aromatics and Heteroaromatics using $(\text{TMP})_2\text{Zn}\cdot 2\text{MgCl}_2\cdot 2\text{LiCl}$ and Microwave Irradiation. **Organic Letters**, v. 10, n. 20, p. 4705–4707, 2008.

81. ROHBOGNER, C. J.; WUNDERLICH, S. H.; CLOSOSKI, G. C.; KNOCHEL, P. New Mixed Li/Mg and Li/Mg/Zn Amides for the Chemoselective Metallation of Arenes and Heteroarenes. **European Journal of Organic Chemistry**, v. 2009, n. 11, p. 1781–1795, 2009.

82. EASTWOOD, P. R.; GONZALEZ RODRIGUEZ, J.; GIULIO MATASSA, V. **New substituted indolin-2-one derivatives and their use as p39 mitogen-activated kinase inhibitors**. Applicant: Laboratorios Almirall, S.A. U.S. Patent WO2009132774A1. Publication Date: 14. Nov. 2009.

83. WUNDERLICH, S. H.; KNOCHEL, P. Preparation of Functionalized Aryl Iron (II) Compounds and a Nickel-Catalyzed Cross-Coupling with Alkyl Halides. **Angewandte Chemie International Edition**, v. 48, n. 51, p. 9717–9720, 2009.

84. WUNDERLICH, S.; BRESSER, T.; DUNST, C.; MONZON, G.; KNOCHEL, P. Efficient Preparation of Polyfunctional Organometallics via Directed *ortho*-Metalation. **Synthesis**, v. 2010, n. 15, p. 2670–2678, 2010.

85. WUNDERLICH, S. H.; KNOCHEL, P. Atom-Economical Preparation of Aryl- and Heteroaryl-Lanthanum Reagents by Directed *ortho*-Metalation by Using $\text{tmp}_3[\text{La}]$. **Chemistry - A European Journal**, v. 16, n. 11, p. 3304–3307, 2010.

86. OWTON, W. M. Synthesis of substituted 3-trifluoromethylbenzo[*b*]thiophenes. **Tetrahedron Letters**, v. 44, n. 38, p. 7147–7149, 2003.

87. WEIDMANN, N.; KETELS, M.; KNOCHEL, P. Sodiation of Arenes and Heteroarenes in Continuous Flow. **Angewandte Chemie International Edition**, v. 57, n. 33, p. 10748–10751, 2018.

88. MADDOCK, L. C. H.; NIXON, T.; KENNEDY, A. R.; PROBERT, M. R.; CLEGG, W.; HEVIA, E. Utilising Sodium-Mediated Ferration for Regioselective Functionalisation of Fluoroarenes via C–H and C–F Bond Activations. **Angewandte Chemie International Edition**, v. 57, n. 1, p. 187–191, 2018.

89. OTSUKA, S.; YORIMITSU, H.; OSUKA, A. Palladium-Catalyzed Zinc-Amide-Mediated C-H Arylation of Fluoroarenes and Heteroarenes with Aryl Sulfides. **Chemistry - A European Journal**, v. 21, n. 42, p. 14703–14707, 2015.

90. HUANG, Y.; CAI, Z.; LI, S.; NABULSI, N. CARSON, R. **Radiolabeled pharmaceuticals and methods of making and using same**. Applicant: Yale University, New Haven, CT 06510 (US). U.S. Patent WO 2018/152339 A1. Publication Date: 25. Dec. 2019.
91. KREMSMAIR, A.; HARENBERG, J. H.; SCHWÄRZER, K.; HESS, A.; KNOCHEL, P. Preparation and reactions of polyfunctional magnesium and zinc organometallics in organic synthesis. **Chemical Science**, v. 12, n. 17, p. 6011–6019, 2021.
92. BALKENHOHL, M.; JANGRA, H.; MAKAROV, I. S.; YANG, S.-M.; ZIPSE, H.; KNOCHEL, P. A Predictive Model Towards Site-Selective Metalations of Functionalized Heterocycles, Arenes, Olefins, and Alkanes using TMPZnCl·LiCl. **Angewandte Chemie International Edition**, v. 59, n. 35, p. 14992–14999, 2020.
93. a) GAIKWAD, D. D.; CHAPOLIKAR, A. D.; DEVKATE, C. G.; WARAD, K. D.; TAYADE, A. P.; PAWAR, R. P.; DOMB, A. J. Synthesis of indazole motifs and their medicinal importance: An overview. **European Journal of Medicinal Chemistry**, v. 90, p. 707–731, 2015. b) TOMASSI, S.; LATEGAHN, J.; ENGEL, J.; KEUL, M.; TUMBRINK, H. L.; KETZER, J.; MÜHLENBERG, T.; BAUMANN, M.; SCHULTZ-FADEMRECHT, C.; BAUER, S.; RAUH, D. Indazole-Based Covalent Inhibitors to Target Drug-Resistant Epidermal Growth Factor Receptor. **Journal of Medicinal Chemistry**, v. 60, n. 6, p. 2361–2372, 2017. c) DONG, J.; ZHANG, Q.; WANG, Z.; HUANG, G.; LI, S. Recent Advances in the Development of Indazole-based Anticancer Agents. **ChemMedChem**, v. 13, n. 15, p. 1490–1507, 2018.
94. ZHANG, S.-G.; LIANG, C.-G.; ZHANG, W.-H. Recent Advances in Indazole-Containing Derivatives: Synthesis and Biological Perspectives. **Molecules**, v. 23, n. 11, p. 2783, 2018.
95. FENG, J.-B.; WU, X.-F. Base-promoted synthesis of dibenzoxazepinamines and quinazolinimines under metal-free conditions. **Green Chemistry**, v. 17, n. 9, p. 4522–4526, 2015.
96. DOS SANTOS, T.; ORENHA, H. P.; MURIE, V. E.; VESSECCHI, R.; CLOSOSKI, G. C. Selective Metalation and Functionalization of Fluorinated Nitriles Using 2,2,6,6-Tetramethylpiperidyl Bases. **Organic Letters**, v. 23, n. 19, p. 7396–7400, 2021.
97. HENDERSON, R. K.; HILL, A. P.; REDMAN, A. M.; SNEDDON, H. F. Development of GSK's acid and base selection guides. **Green Chemistry**, v. 17, n. 2, p. 945–949, 2015.
98. a) CHANDNA, N.; KAUR, F.; KUMAR, S.; JAIN, N. Glucose promoted facile reduction of azides to amines under aqueous alkaline conditions. **Green Chemistry**, v. 19, n. 18, p. 4268–4271, 2017. b) ORLANDI, M.; BRENNAN, D.; HARMS, R.; JOST, S.;

BENAGLIA, M. Recent Developments in the Reduction of Aromatic and Aliphatic Nitro Compounds to Amines. **Organic Process Research & Development**, v. 22, n. 4, p. 430–445, 2018. c) GALBRAITH, H. W.; DEGERING, E. F.; HITCH, E. F. The Alkaline Reduction of Aromatic Nitro Compounds with Glucose. **Journal of the American Chemical Society**, v. 73, n. 3, p. 1323–1324, 1951.

99. ELLIS, A. V.; WILSON, M. A. Carbon Exchange in Hot Alkaline Degradation of Glucose. **The Journal of Organic Chemistry**, v. 67, n. 24, p. 8469–8474, 2002.

100. TU, T.; WANG, Z.; LIU, Z.; FENG, X.; WANG, Q. Efficient and practical transition metal-free catalytic hydration of organonitriles to amides. **Green Chemistry**, v. 14, n. 4, p. 921, 2012.

101. FULMER, G. R.; MILLER, A. J. M.; SHERDEN, N. H.; GOTTLIEB, H. E.; NUDELMAN, A.; STOLTZ, B. M.; BERCAW, J. E.; GOLDBERG, K. I. NMR Chemical Shifts of Trace Impurities: Common Laboratory Solvents, Organics, and Gases in Deuterated Solvents Relevant to the Organometallic Chemist. **Organometallics**, v. 29, n. 9, p. 2176–2179, 2010.

102. SERNA, P.; CORMA, A. Transforming Nano Metal Nonselective Particulates into Chemoselective Catalysts for Hydrogenation of Substituted Nitrobenzenes. **ACS Catalysis**, v. 5, n. 12, p. 7114–7121, 2015.

103. SONG, J.; HUANG, Z.-F.; PAN, L.; LI, K.; ZHANG, X.; WANG, L.; ZOU, J.-J. Review on selective hydrogenation of nitroarene by catalytic, photocatalytic and electrocatalytic reactions. **Applied Catalysis B: Environmental**, v. 227, p. 386–408, 2018.

104. OPOLONICK, N. Reduction of Nitrobenzene with Dextrose in Alkaline Solutions. **Industrial & Engineering Chemistry**, v. 27, n. 9, p. 1045–1046, 1935.

105. MUKHERJEE, P. S.; DAS, N.; KRYSCHENKO, Y. K.; ARIF, A. M.; STANG, P. J. Design, Synthesis, and Crystallographic Studies of Neutral Platinum-Based Macrocycles Formed via Self-Assembly. **Journal of the American Chemical Society**, v. 126, n. 8, p. 2464–2473, 2004.

106. NGUYEN-TRAN, H.-H.; ZHENG, G.-W.; QIAN, X.-H.; XU, J.-H. Highly selective and controllable synthesis of arylhydroxylamines by the reduction of nitroarenes with an electron-withdrawing group using a new nitroreductase BaNTR1. **Chemical Communications**, v. 50, n. 22, p. 2861, 2014.

107. LI, F.; CUI, J.; QIAN, X.; ZHANG, R. A novel strategy for the preparation of arylhydroxylamines: chemoselective reduction of aromatic nitro compounds using bakers' yeast. **Chemical Communications**, no. 20, p. 2338–2339, 2004.

108. GEISSMAN, T. A. The Cannizzaro Reaction. *In*: JOHN WILEY & SONS, INC. (ed.). **Organic Reactions**. Hoboken, NJ, USA: John Wiley & Sons, Inc., 2011. p. 94–113. Available at: <https://onlinelibrary.wiley.com/doi/10.1002/0471264180.or002.03>. Accessed on: 11 Nov. 2021.
109. DOS SANTOS, T.; GRUNDKE, C.; LUCAS, T.; GROSSMANN, L.; CLOSOSKI, G. C.; OPATZ, T. Glucose as an Eco-Friendly Reductant in a One-Pot Synthesis of 2,3-Dihydroquinazolin-4(1*H*)-ones. **European Journal of Organic Chemistry**, v. 2020, n. 41, p. 6429–6432, 2020.
110. WU, Z.; JIN, Q.; WU, G.; LU, J.; LI, M.; GUO, D.; LAN, K.; FENG, L.; QIAN, Z.; REN, L.; TAN, W.; XU, W.; YANG, W.; WANG, J.; WANG, C. SARS-CoV-2's origin should be investigated worldwide for pandemic prevention. **The Lancet**, v. 398, n. 10308, p. 1299–1303, 2021.
111. PUSHPAKOM, S.; IORIO, F.; EYERS, P. A.; ESCOTT, K. J.; HOPPER, S.; WELLS, A.; DOIG, A.; GUILLIAMS, T.; LATIMER, J.; MCNAMEE, C.; NORRIS, A.; SANSEAU, P.; CAVALLA, D.; PIRMOHAMED, M. Drug repurposing: progress, challenges and recommendations. **Nature Reviews Drug Discovery**, v. 18, n. 1, p. 41–58, 2019.
112. BEIGEL, J. H.; TOMASHEK, K. M.; DODD, L. E.; MEHTA, A. K.; ZINGMAN, B. S.; KALIL, A. C.; HOHMANN, E.; CHU, H. Y.; LUETKEMEYER, A.; KLINE, S.; LOPEZ DE CASTILLA, D.; FINBERG, R. W.; DIERBERG, K.; TAPSON, V.; HSIEH, L.; PATTERSON, T. F.; PAREDES, R.; SWEENEY, D. A.; SHORT, W. R.; LANE, H. C. Remdesivir for the Treatment of Covid-19 - Final Report. **New England Journal of Medicine**, v. 383, n. 19, p. 1813–1826, 2020.
113. YIN, Wanchao; MAO, Chunyou; LUAN, Xiaodong; SHEN, Dan-Dan; SHEN, Qingya; SU, Haixia; WANG, Xiaoxi; ZHOU, Fulai; ZHAO, Wenfeng; GAO, Minqi; CHANG, Shenghai; XIE, Yuan-Chao; TIAN, Guanghui; JIANG, He-Wei; TAO, Sheng-Ce; SHEN, Jingshan; JIANG, Yi; JIANG, Hualiang; XU, Yechun; ... XU, H. Eric. Structural basis for inhibition of the RNA-dependent RNA polymerase from SARS-CoV-2 by remdesivir. **Science**, v. 368, n. 6498, p. 1499–1504, 2020.
114. KEARNEY, Brian P; FLAHERTY, John F; SHAH, Jaymin. Tenofovir Disoproxil Fumarate: Clinical Pharmacology and Pharmacokinetics. **Clinical Pharmacokinetics**, v. 43, n. 9, p. 595–612, 2004.
115. CLOSOSKI, G.; SOLDI, R.; DA SILVA, R.; GUARATINI, T.; LOPES, J.; PEREIRA, P.; LOPES, J.; DOS SANTOS, T.; MARTINS, R.; COSTA, C.; DE CARVALHO, A.;

DASILVA, L.; ARRUDA, E.; LOPES, N. Tenofovir Disoproxil Fumarate: New Chemical Developments and Encouraging in vitro Biological Results for SARS-CoV-2. **Journal of the Brazilian Chemical Society**, v. 31, n. 8, 1552-1556, 2020.

116. BALWE, S. G.; LIM, K. T.; CHO, B. G.; JEONG, Y. T. One-pot four-component domino reaction for the synthesis of bifunctionalized spiro[indazolo[3,2- b]quinazoline-7,3'-indoline hybrids: A green approach. **Synthetic Communications**, v. 49, n. 4, p. 602–610, 2019.

117. PALANIRAJA, J.; ROOPAN, S. M. Iodine-mediated synthesis of indazoloquinazolinones via a multi-component reaction. **RSC Advances**, v. 5, n. 12, p. 8640–8646, 2015.

118. EASTMOND, G. C.; PAPROTNY, J.; STEINER, A.; SWANSON, L. Synthesis of cyanodibenzo[1,4]dioxines and their derivatives by cyano-activated fluoro displacement reactions. **New Journal of Chemistry**, v. 25, n. 3, p. 379–384, 2001.

119. HU, F.; LIU, H.; JIA, J.; MA, C. Transition-metal-free synthesis of indole-fused dibenzo[b,f][1,4]oxazepines via Smiles rearrangement. **Organic & Biomolecular Chemistry**, v. 14, n. 47, p. 11076–11079, 2016.

120. LIU, Y.; CHU, C.; HUANG, A.; ZHAN, C.; MA, Y.; MA, C. Regioselective Synthesis of Fused Oxazepinone Scaffolds through One-Pot Smiles Rearrangement Tandem Reaction. **ACS Combinatorial Science**, v. 13, n. 5, p. 547–553, 2011.

121. SEN, T.; NEOG, K.; SARMA, S.; MANNA, P.; DEKA BORUAH, H. P.; GOGOI, P.; SINGH, A. K. Efflux pump inhibition by 11H-pyrido[2,1-b]quinazolin-11-one analogues in mycobacteria. **Bioorganic & Medicinal Chemistry**, v. 26, n. 17, p. 4942–4951, 2018.

122. ZHANG, X.; JIA, J.; MA, C. A one-pot regioselective synthesis of benzo[d]imidazo[2,1-b]thiazoles. **Organic & Biomolecular Chemistry**, v. 10, n. 39, p. 7944, 2012.

123. MORADI, S.; SHOKRI, Z.; GHORASHI, N.; NAVAAEE, A.; ROSTAMI, A. Design and synthesis of a versatile cooperative catalytic aerobic oxidation system with co-immobilization of palladium nanoparticles and laccase into the cavities of MCF. **Journal of Catalysis**, v. 382, p. 305–319, 2020.

124. COULSON, D. R.; SATEK, L. C.; GRIM, S. O. **Tetrakis(Triphenylphosphine)Palladium(0)**. In *Inorganic Syntheses*; Cotton, F. A., Ed.; John Wiley & Sons, Inc.: Hoboken, NJ, USA, 2007; pp 121–124.

125. CHAMBERS, R. D.; SKINNER, C. J.; ATHERTON, M. J.; MOILLIET, J. S. Elemental fluorine. Part 4. Use of elemental fluorine for the halogenation of aromatics. **Journal of the Chemical Society, Perkin Transactions 1**, n. 14, p. 1659–1664, 1996.
126. BENISCHKE, A. D.; ANTHORE-DALION, L.; KOHL, F.; KNOCHEL, P. Synthesis of Polyfunctionalized Triaryllanthanum Reagents by Using Ph₃La and Related Species as Exchange Reagents. **Chemistry - A European Journal**, v. 24, n. 43, p. 11103–11109, 2018.
127. KOBAYASHI, K.; MATSUMOTO, K.; KONISHI, H. An Efficient Synthesis of 3-Substituted 3H-Isobenzofuran-1-ylidenamines by the Reaction of 2-Cyanobenzaldehydes with Organolithiums and Their Conversion into Isobenzofuran-1(3H)-ones. **HETEROCYCLES**, v. 83, n. 1, p. 99–106, 2011.
128. BOUGERET, C.; GUILLOU, C.; ROULEAU, J.; RIVOLLIER, J.; CARNIATO, D. **New derivatives of indole for the treatment of cancer, viral infections and lung diseases**. Applicants: Biokinesis, Paris (FR); Centre National De Larecherche Scientifioue, Paris (FR). U.S. patent US 2015/0307450 A1. Publication Date: 29. Oct. 2015.
129. BHAGWAT, S. S.; SATOH, Y.; SAKATA, S. T.; BUHR, C. A.; ALBERS, R.; SAPIENZA, J.; PLANTEVIN, V.; CHAO, Q.; SAHASRABUDHE, K.; FERRI, R.; NARLA, R. K. **Indazole compounds, compositions thereof and methods of treatment therewith**. Applicant: Signal Pharmaceuticals LLC. U.S. patent, US 2005/0009876 A1. Publication Date: 13. Jan. 2005.
130. ISHIHARA, S.; SAITO, F.; MASUKO, H.; KOUNO, K. **Ileum type bile acid transporter inhibitor**. Applicant: SANKYO CO LTD. Japan patent JP2000178188. Publication Date: 27. Jun. 2000.
131. DANZ, M.; ZINK, D. **Organic molecules for use in organic optoelectronic devices**. Applicant: CYNORA GMBH (DE/DE). German Patent WO 2017/005698 A1. Publication Date: 12. Jan. 2017.
132. LUO, Z.-J.; ZHAO, H.-Y.; ZHANG, X. Highly Selective Pd-Catalyzed Direct C–F Bond Arylation of Polyfluoroarenes. **Organic Letters**, v. 20, n. 9, p. 2543–2546, 2018.
133. FOCKEN, T.; BURFORD, K.; GRIMWOOD, M. E.; ZENOVA, A.; ANDREZ, J.-C.; GONG, W.; WILSON, M.; TARON, M.; DECKER, S.; LOFSTRAND, V.; CHOWDHURY, S.; SHUART, N.; LIN, S.; GOODCHILD, S. J.; YOUNG, C.; SORIANO, M.; TARI, P. K.; WALDBROOK, M.; NELKENBRECHER, K.; KWAN, R.; LINDGREN, A.; DE BOER, G.; LEE, S.; SOJO, L.; DEVITA, R. J.; COHEN, C. J.; WESOLOWSKI, S. S.; JOHNSON, J. P.; DEHNHARDT, C. M.; EMPFIELD, J. R. Identification of CNS-Penetrant Aryl

Sulfonamides as Isoform-Selective Nav1.6 Inhibitors with Efficacy in Mouse Models of Epilepsy. **Journal of Medicinal Chemistry**, v. 62, n. 21, p. 9618–9641, 2019.

134. LEI, N.-P.; FU, Y.-H.; ZHU, X.-Q. Elemental step thermodynamics of various analogues of indazolium alkaloids to obtaining hydride in acetonitrile. **Organic & Biomolecular Chemistry**, v. 13, n. 47, p. 11472–11485, 2015.

135. FENG, J.-B.; WU, X.-F. Base-promoted synthesis of dibenzoxazepinamines and quinazolinimines under metal-free conditions. **Green Chemistry**, v. 17, n. 9, p. 4522–4526, 2015.

136. CASASNOVAS, R.; ORTEGA-CASTRO, J.; FRAU, J.; DONOSO, J.; MUÑOZ, F. Theoretical pK_a calculations with continuum model solvents, alternative protocols to thermodynamic cycles. **International Journal of Quantum Chemistry**, v. 114, n. 20, p. 1350–1363, 2014.

137. FRISCH, M. J.; TRUCKS, G. W.; SCHLEGEL, H. B.; SCUSERIA, G. E.; ROBB, M. A.; CHEESEMAN, J. R.; MONTGOMERY, JR., J. A.; VREVEN, T.; KUDIN, K. N.; BURANT, J. C.; MILLAM, J. M.; IYENGAR, S. S.; TOMASI, J.; BARONE, V.; MENNUCCI, B.; COSSI, M.; SCALMANI, G.; REGA, N.; PETERSSON, G. A.; NAKATSUJI, H.; HADA, M.; EHARA, M.; TOYOTA, K.; FUKUDA, R.; HASEGAWA, J.; ISHIDA, M.; NAKAJIMA, T.; HONDA, Y.; KITAO, O.; NAKAI, H.; KLENE, M.; LI, X.; KNOX, J. E.; HRATCHIAN, H. P.; CROSS, J. B.; BAKKEN, V.; ADAMO, C.; JARAMILLO, J.; GOMPERS, R.; STRATMANN, R. E.; YAZYEV, O.; AUSTIN, A. J.; CAMMI, R.; POMELLI, C.; OCHTERSKI, J. W.; AYALA, P. Y.; MOROKUMA, K.; VOTH, G. A.; SALVADOR, P.; DANNENBERG, J. J.; ZAKRZEWSKI, V. G.; DAPPRICH, S.; DANIELS, A. D.; STRAIN, M. C.; FARKAS, O.; MALICK, D. K.; RABUCK, A. D.; RAGHAVACHARI, K.; FORESMAN, J. B.; ORTIZ, J. V.; CUI, Q.; BABOUL, A. G.; CLIFFORD, S.; CIOSLOWSKI, J.; STEFANOV, B. B.; LIU, G.; LIASHENKO, A.; PISKORZ, P.; KOMAROMI, I.; MARTIN, R. L.; FOX, D. J.; KEITH, T.; AL-LAHAM, M. A.; PENG, C. Y.; NANAYAKKARA, A.; CHALLACOMBE, M.; GILL, P. M. W.; JOHNSON, B.; CHEN, W.; WONG, M. W.; GONZALEZ, C.; POPLE, J. A.; *Gaussian 03*, Gaussian, Inc., Wallingford CT, 2004.

138. BECKE, A. D. Density-functional exchange-energy approximation with correct asymptotic behavior. **Physical Review A**, v. 38, n. 6, p. 3098–3100, 1988.

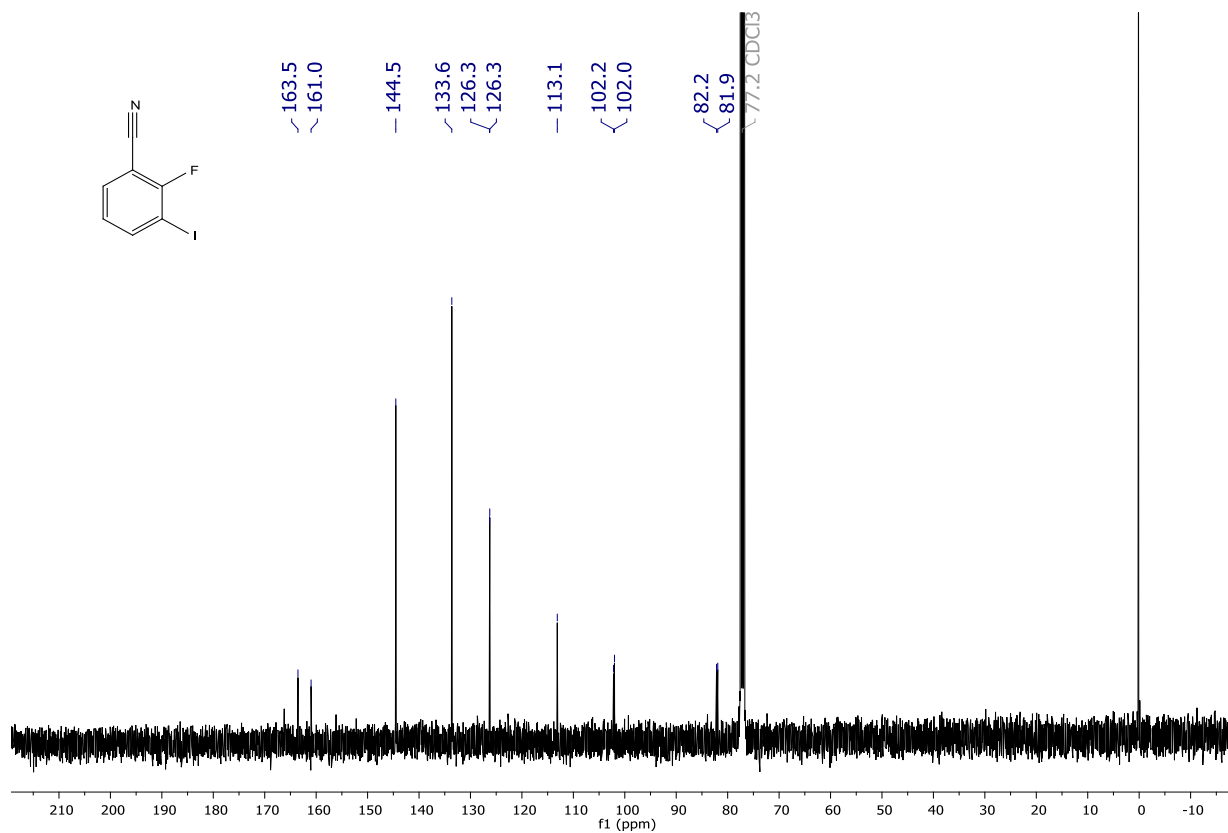
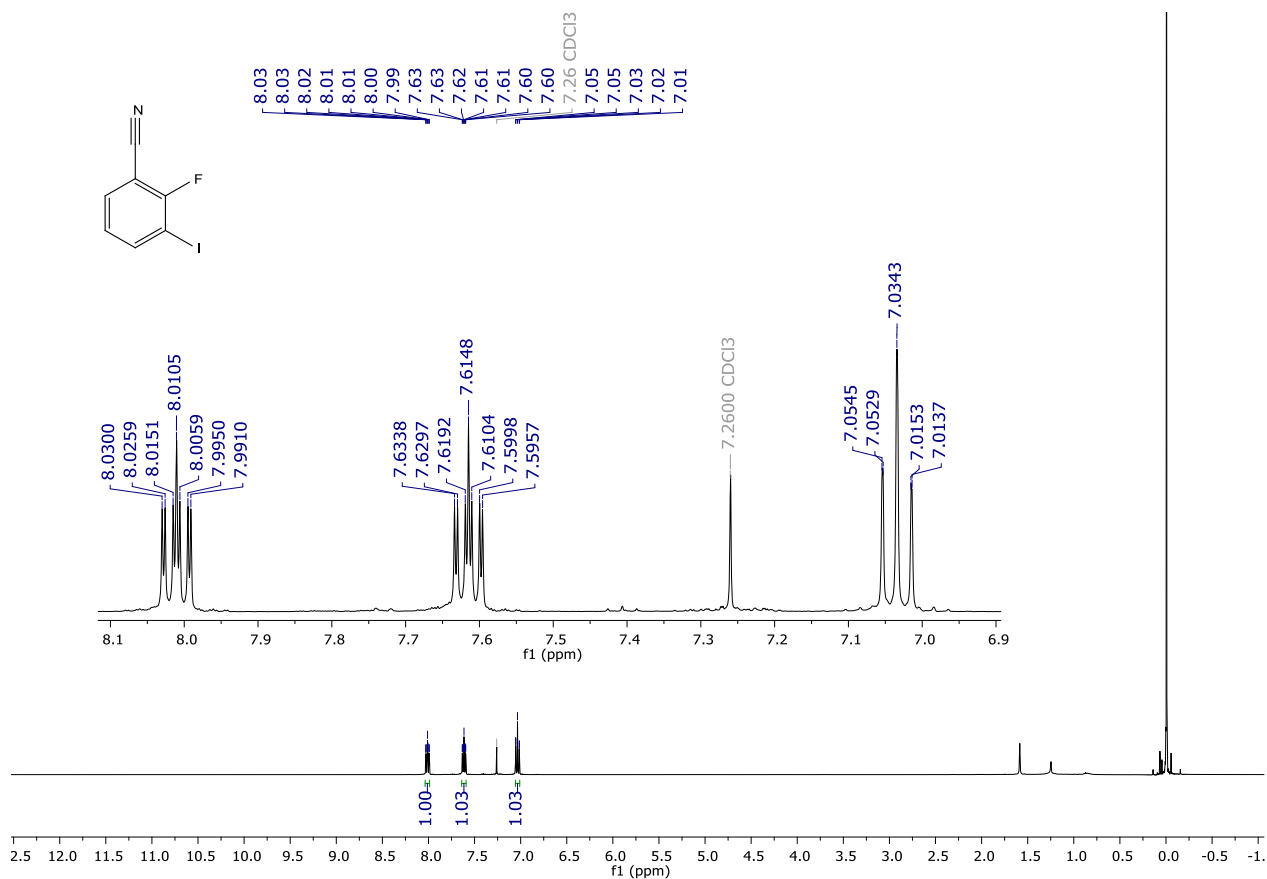
139. BARONE, V. Vibrational zero-point energies and thermodynamic functions beyond the harmonic approximation. **The Journal of Chemical Physics**, v. 120, n. 7, p. 3059–3065, 2004.

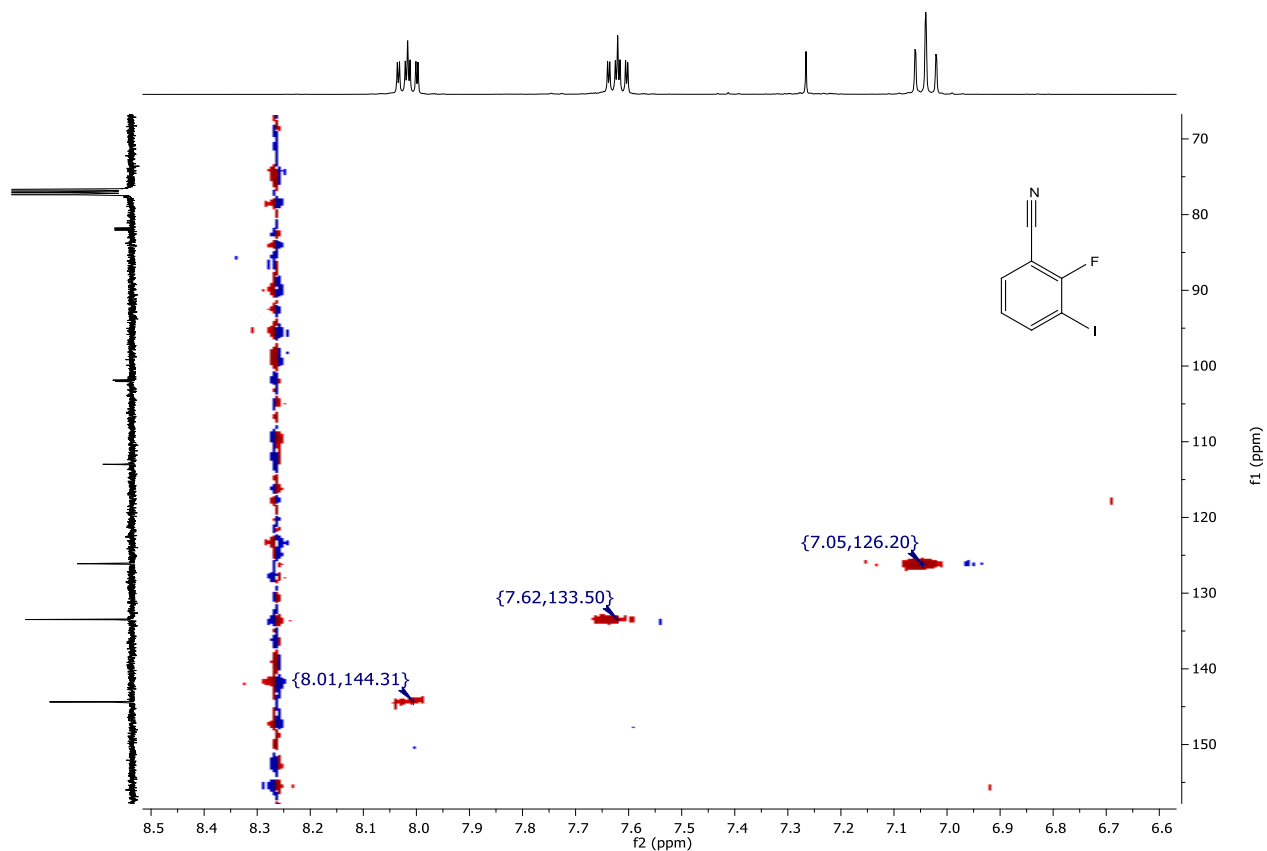
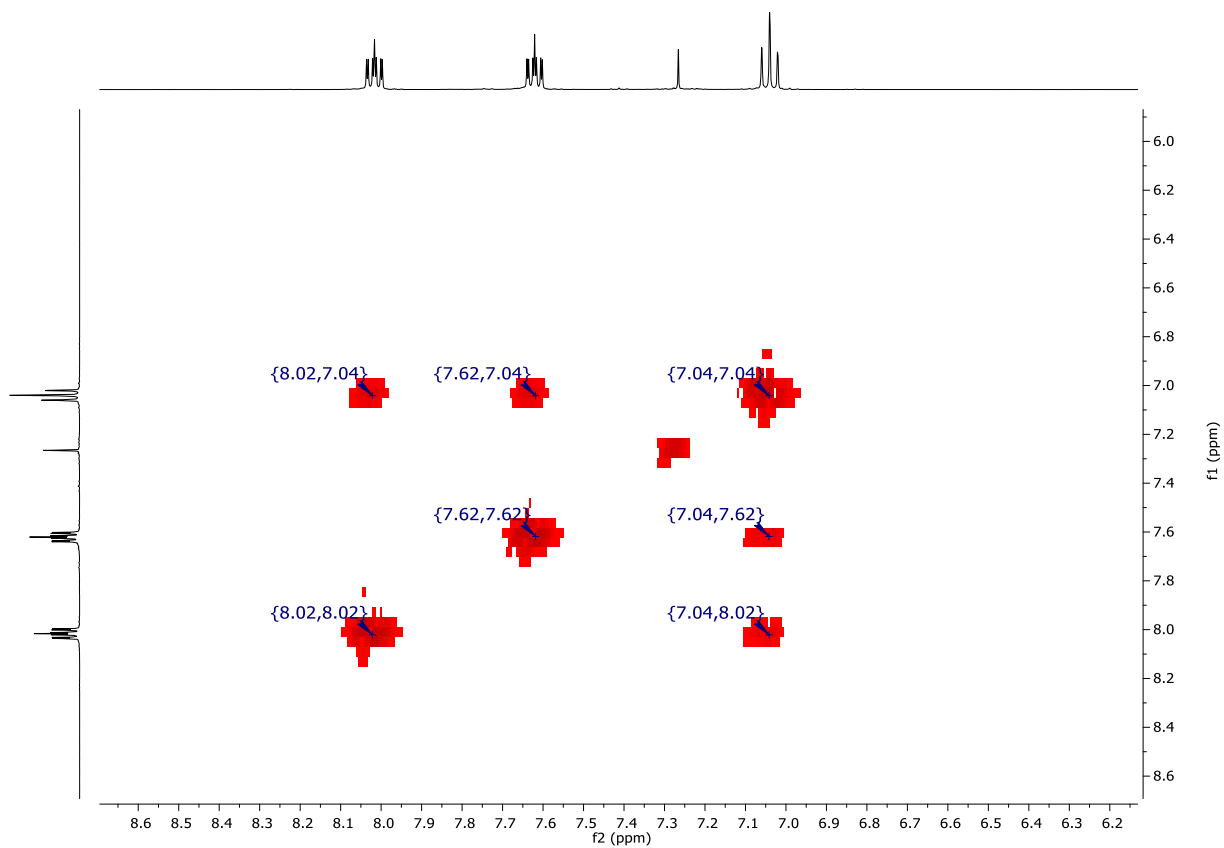
140. ZHANG, S.; TAN, Z.; XIONG, B.; JIANG, H. F.; ZHANG, M. Transition-metal-catalyst-free synthesis of anthranilic acid derivatives by transfer hydrogenative coupling

- of 2-nitroaryl methanols with alcohols/amines. **Organic & Biomolecular Chemistry**, v. 16, n. 4, p. 531–535, 2018.
141. ZHANG, Z.; ZHENG, D.; WAN, Y.; ZHANG, G.; BI, J.; LIU, Q.; LIU, T.; SHI, L. Selective Cleavage of Inert Aryl C–N Bonds in *N*-Aryl Amides. **The Journal of Organic Chemistry**, v. 83, n. 3, p. 1369–1376, 2018.
142. GAO, L.; JI, H.; RONG, L.; TANG, D.; ZHA, Y.; SHI, Y.; TU, S. An efficient synthesis of 2,3-dihydroquinazolin-4(1*H*)-one derivatives under catalyst-free and solvent-free conditions. **Journal of Heterocyclic Chemistry**, v. 48, n. 4, p. 957–960, 2011.
143. TAMADDON, F.; POURAMINI, F. Amberlyst A26 OH as a Recyclable Catalyst for Hydration of Nitriles and -Water-Based Synthesis of 4(1*H*)-Quinazolinones from 2-Aminobenzonitrile and Carbonyl Compounds. **Synlett**, v. 25, n. 08, p. 1127–1131, 2014.
144. DUTTA, A.; DAMARLA, K.; KUMAR, A.; SAIKIA, P. J.; SARMA, D. Gemini basic ionic liquid as bi-functional catalyst for the synthesis of 2,3-dihydroquinazolin-4(1*H*)-ones at room temperature. **Tetrahedron Letters**, v. 61, n. 10, p. 151587, 2020.
145. HAJJAMI, M.; GHORBANI, F.; YOUSOFVAND, Z. Copper(I) complex of 1,3-DimethylBarbituric acid modified SBA-15 and its catalytic role for the synthesis of 2,3-Dihydroquinazolin-4(1*H*)-ones and Imidazoles. **Applied Organometallic Chemistry**, v. 31, n. 12, p. e3843, 2017.
146. KHOSHNAVAZI, R.; BAHRAMI, L.; HAVASI, F. Organic–inorganic hybrid polyoxometalate and its graphene oxide–Fe₃O₄ nanocomposite, synthesis, characterization and their applications as nanocatalysts for the Knoevenagel condensation and the synthesis of 2,3-dihydroquinazolin-4(1*H*)-ones. **RSC Advances**, v. 6, n. 103, p. 100962–100975, 2016.
147. KATLA, R.; CHOWRASIA, R.; DA SILVA, C.; DE OLIVEIRA, A.; DOS SANTOS, B.; DOMINGUES, N. Recyclable [Ce(I-Pro)₂]₂ (Oxa) used as Heterogeneous Catalyst: One-Pot Synthesis of 2,3-Dihydroquinazolin-4(1*H*)-ones in Ethanol. **Synthesis**, v. 49, n. 23, p. 5143–5148, 2017.
148. HU, B.-Q.; WANG, L.-X.; YANG, L.; XIANG, J.-F.; TANG, Y.-L. Copper-Catalyzed Intramolecular C–C Bond Cleavage to Construct 2-Substituted Quinazolinones: C–C Bond Cleavage to Construct 2-Substituted Quinazolinones. **European Journal of Organic Chemistry**, v. 2015, n. 20, p. 4504–4509, 2015.
149. CAI, G.; XU, X.; LI, Z.; LU, P.; WEBER, W. P. A one-pot synthesis of 2-aryl-2,3-dihydro-4(1*H*)-quinazolinones by use of samarium iodide. **Journal of Heterocyclic Chemistry**, v. 39, n. 6, p. 1271–1272, 2002.

150. GHORBANI-CHOGHAMARANI, A.; AZADI, G. Synthesis, characterization, and application of Fe₃O₄-SA-PPCA as a novel nanomagnetic reusable catalyst for the efficient synthesis of 2,3-dihydroquinazolin-4(1*H*)-ones and polyhydroquinolines. **RSC Advances**, v. 5, n. 13, p. 9752–9758, 2015.
151. DEVI, J.; KALITA, S. J.; DEKA, D. C. Expeditious synthesis of 2,3-dihydroquinazolin-4(1*H*)-ones in aqueous medium using thiamine hydrochloride (VB₁) as a mild, efficient, and reusable organocatalyst. **Synthetic Communications**, v. 47, n. 17, p. 1601–1609, 2017.
152. RAMBABU, D.; KIRAN KUMAR, S.; YOGI SREENIVAS, B.; SANDRA, S.; KANDALE, A.; MISRA, P.; BASAVESWARA RAO, M.V.; PAL, M. Ultrasound-based approach to spiro-2,3-dihydroquinazolin-4(1*H*)-ones: their in vitro evaluation against chorismate mutase. **Tetrahedron Letters**, v. 54, n. 6, p. 495–501, 2013.
153. TAMADDON, F.; KAZEMIVARNAMKHASTI, M. T. Self-Assembled Nanoliposomes of Phosphatidylcholine: Bridging the Gap between Organic and Aqueous Media for a Green Synthesis of Hydroquinazolinones. **Synlett**, v. 27, n. 17, p. 2510–2514, 2016.
154. SAFAEI, H. R.; SHEKOUHY, M.; SHAFIEE, V.; DAVOODI, M. Glycerol based ionic liquid with a boron core: A new highly efficient and reusable promoting medium for the synthesis of quinazolinones. **Journal of Molecular Liquids**, v. 180, p. 139–144, 2013.
155. ROSTAMIZADEH, S.; AMANI, A.; MAHDAVINIA, G.; SEPEHRIAN, H.; EBRAHIMI, S. Synthesis of Some Novel 2-Aryl-Substituted 2,3-Dihydroquinazolin-4(1*H*)-ones under Solvent-Free Conditions Using MCM-41-SO₃H as a Highly Efficient Sulfonic Acid. **Synthesis**, v. 2010, n. 08, p. 1356–1360, 2010.

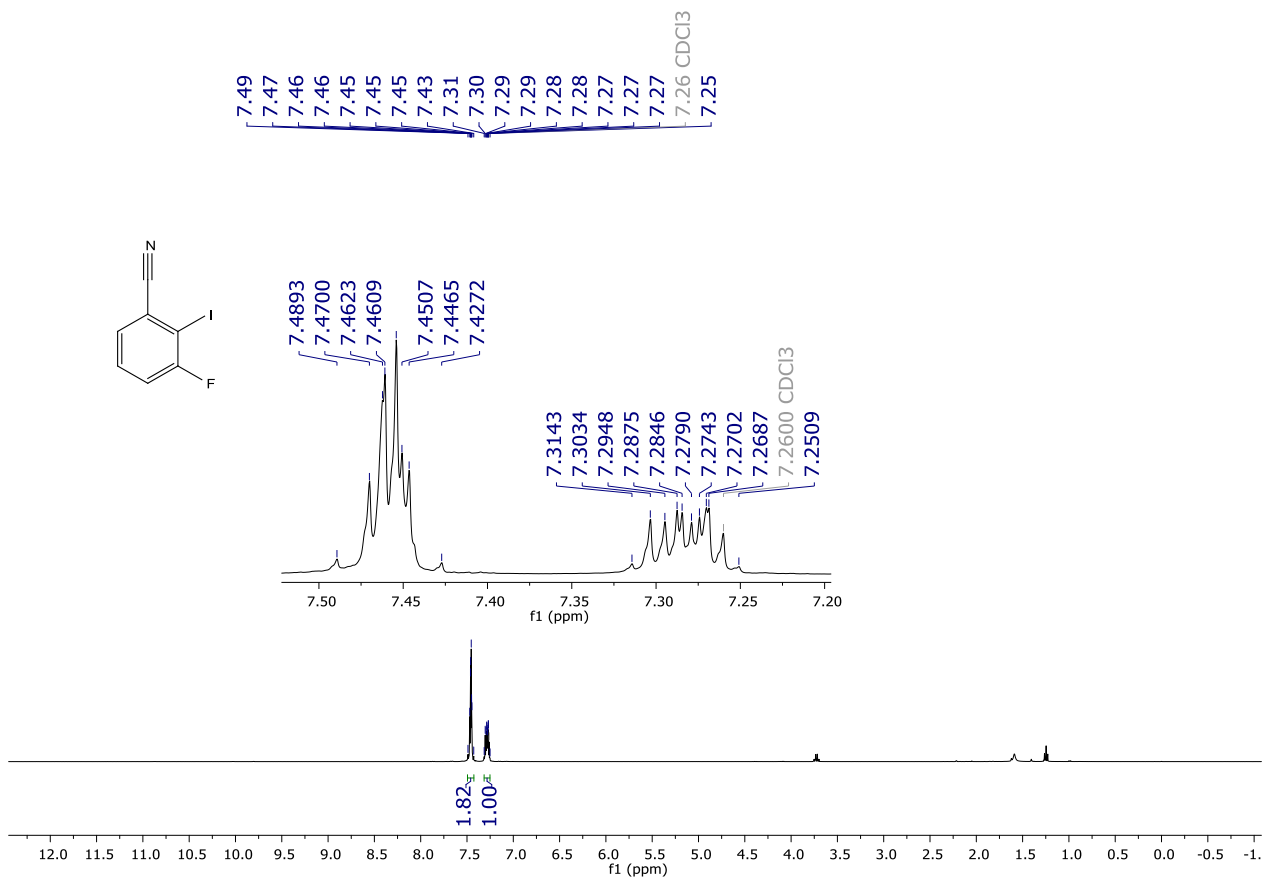
APPENDIX A - NMR SPECTRA



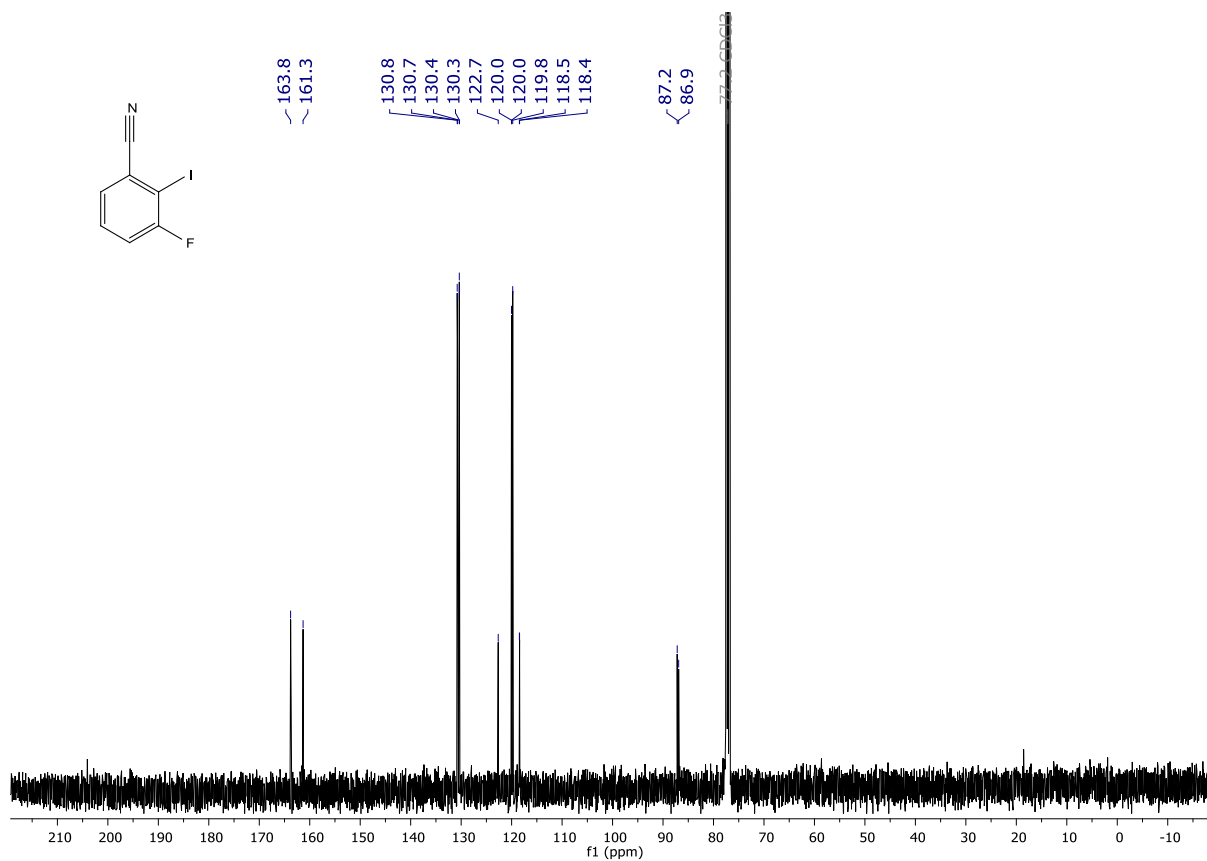
HSQC correlation map of **125a** (400 and 101 MHz, CDCl₃).COSY correlation map of **125a** (101 MHz, CDCl₃).



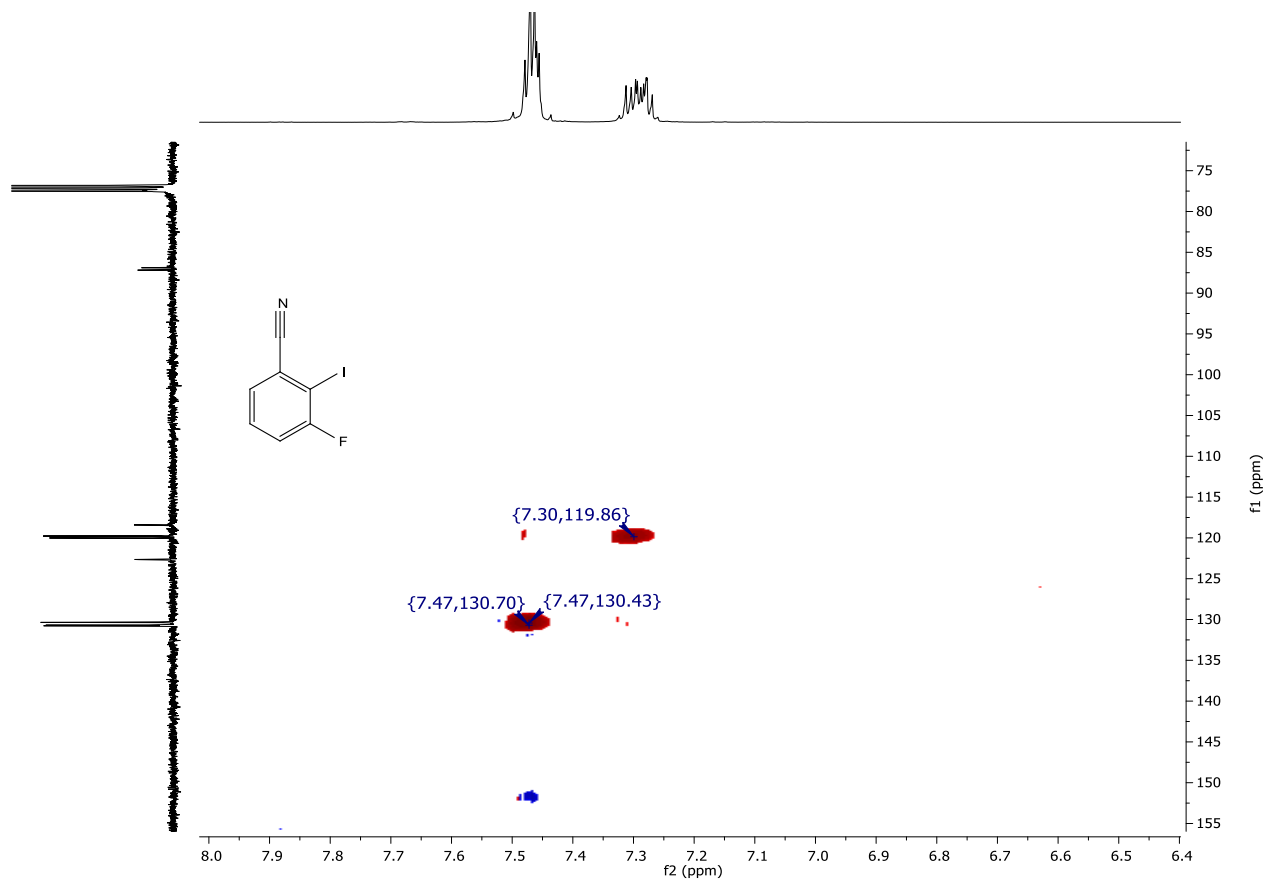
¹⁹F NMR (282 MHz, CDCl₃) spectrum of **125a**.



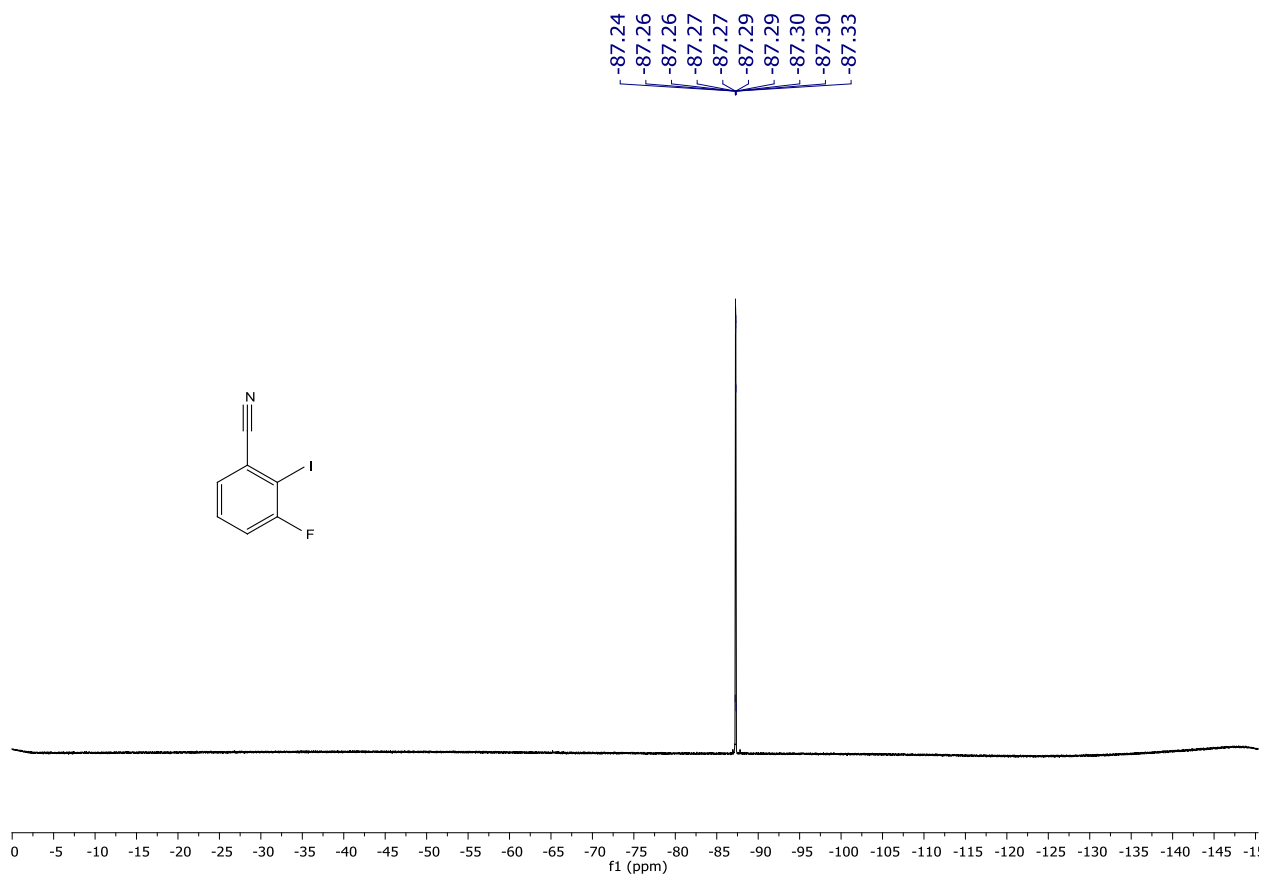
¹H NMR (400 MHz, CDCl₃) spectrum of **125b**.



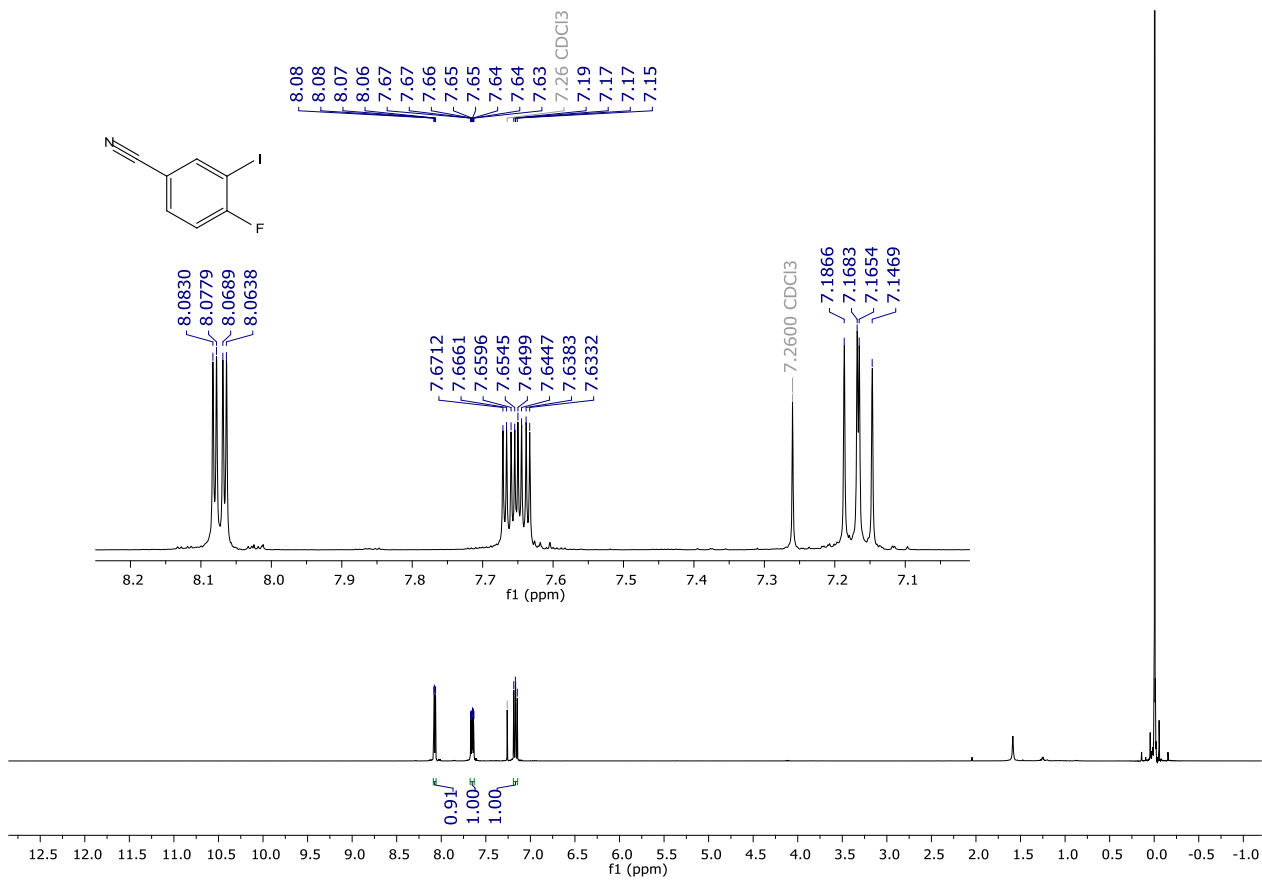
$^{13}\text{C}\{^1\text{H}\}$ NMR (101 MHz, CDCl_3) spectrum of **125b**.



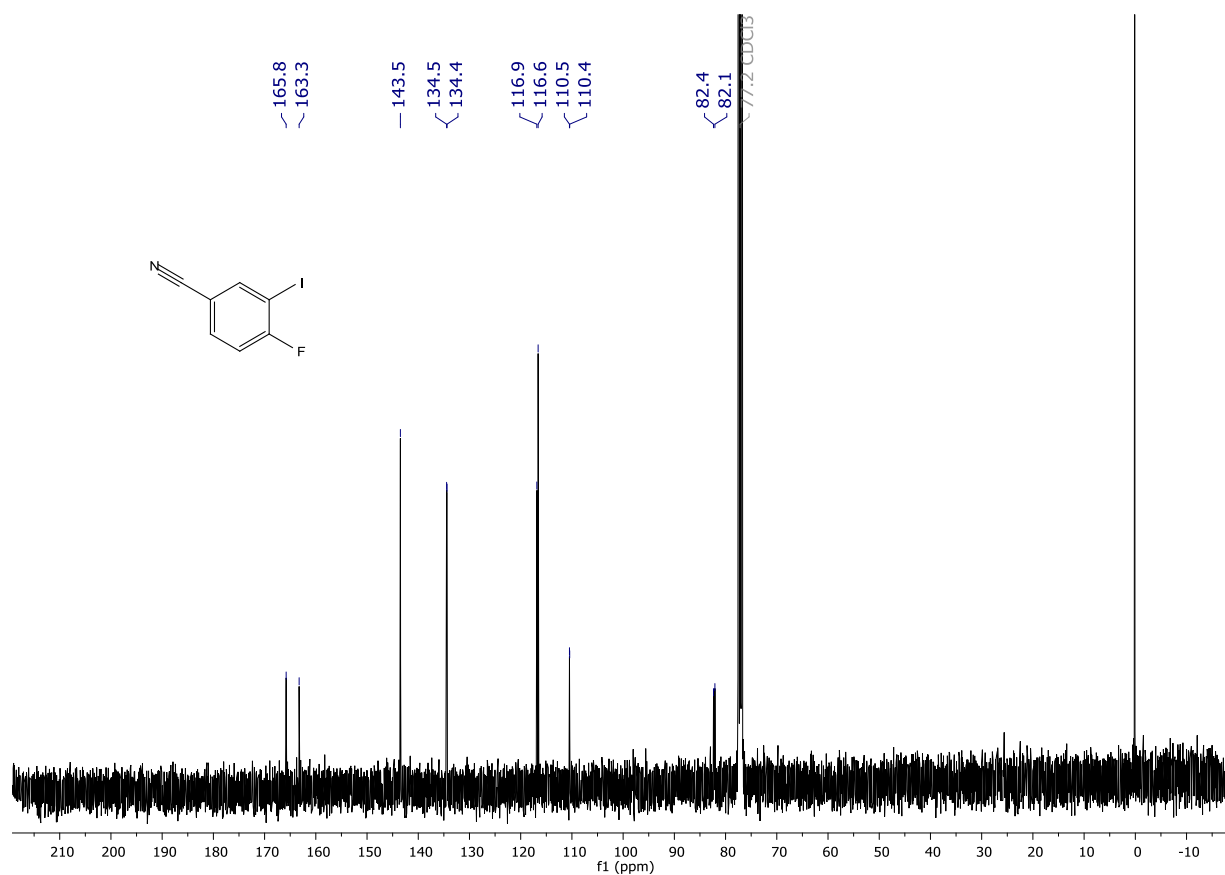
HSQC correlation map of **125b** (400 and 101 MHz, CDCl_3).



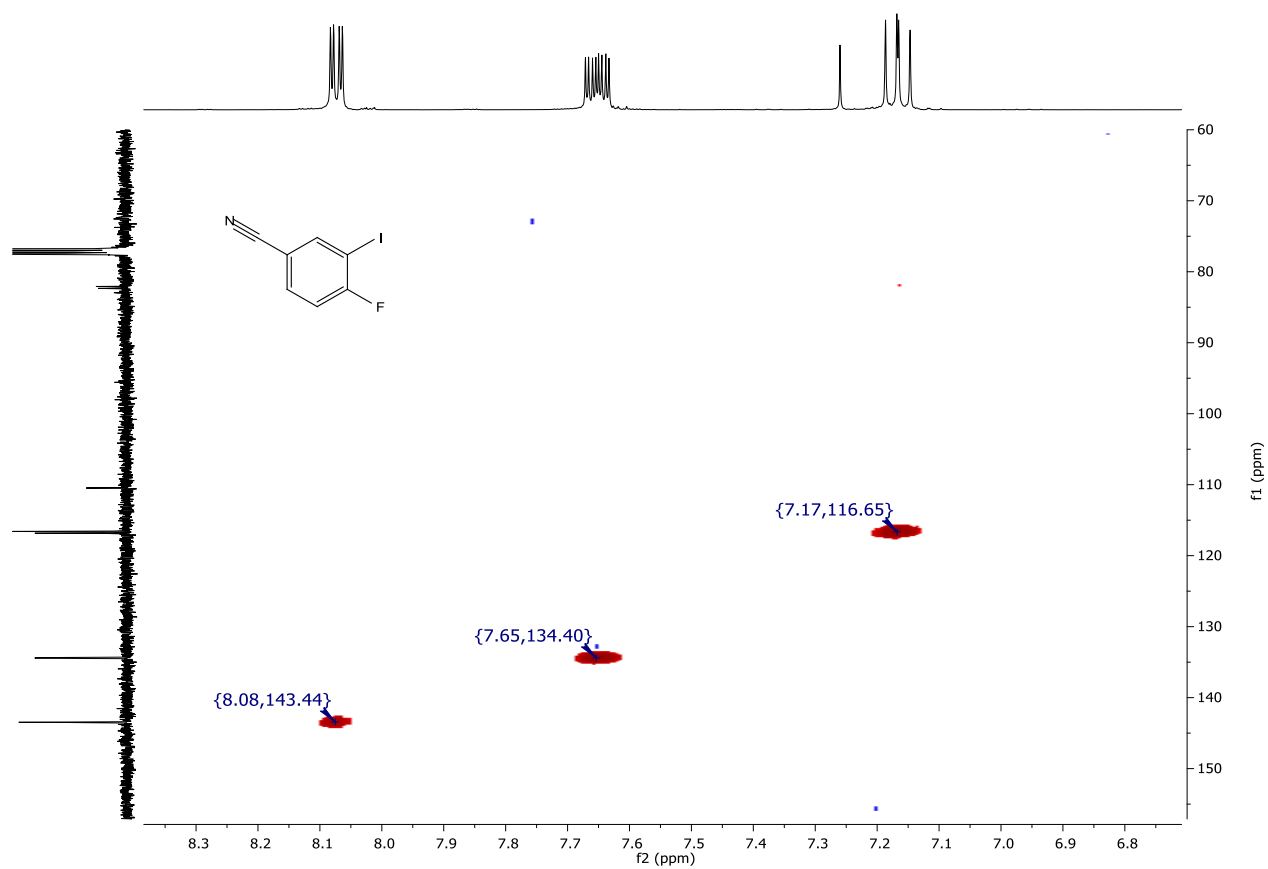
^{19}F NMR (282 MHz, CDCl_3) spectrum of **125b**.



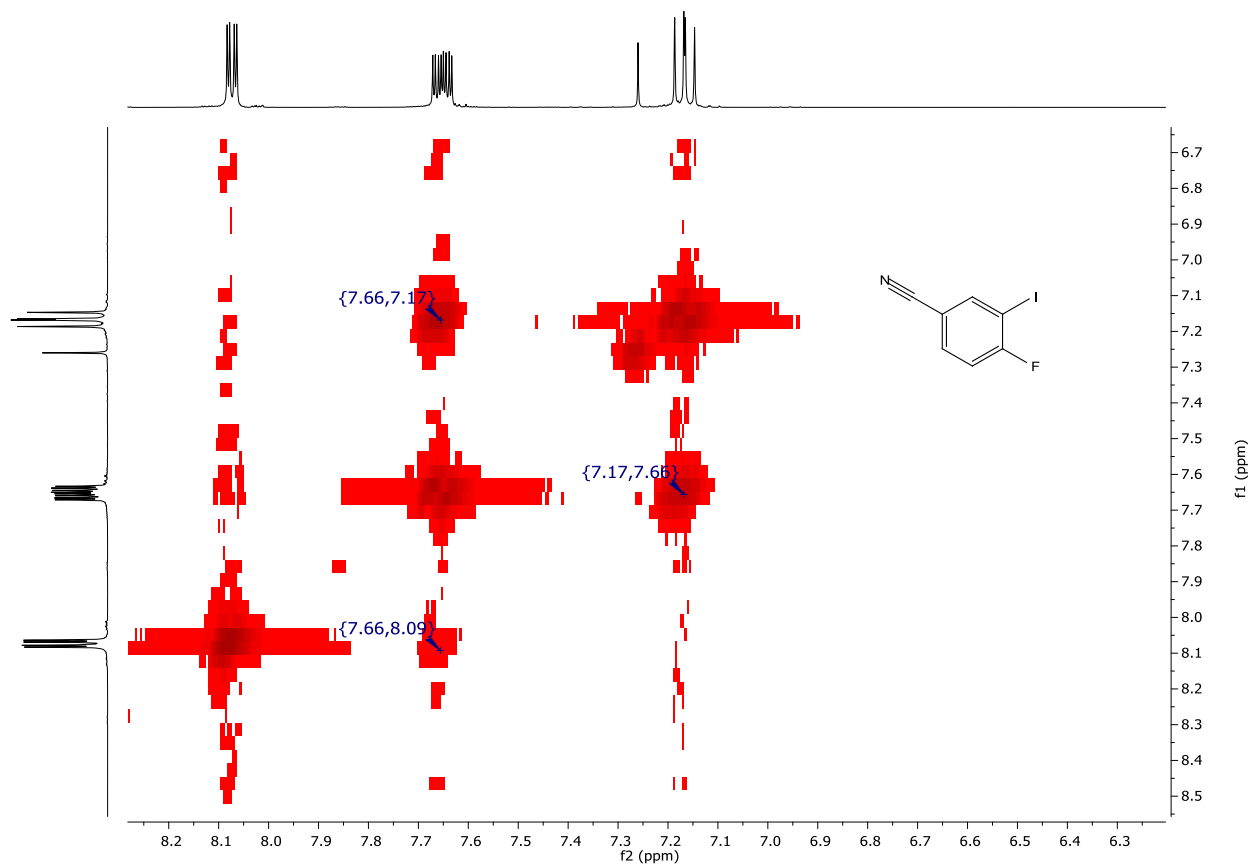
^1H NMR (400 MHz, CDCl_3) spectrum of **125c**.



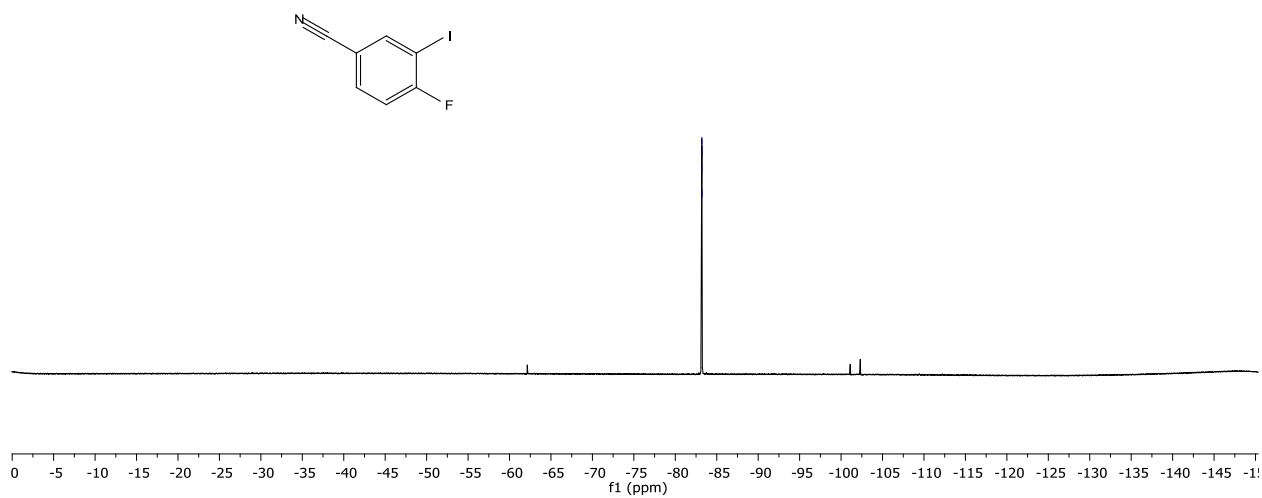
$^{13}\text{C}\{^1\text{H}\}$ NMR (101 MHz, CDCl_3) spectrum of **125c**.

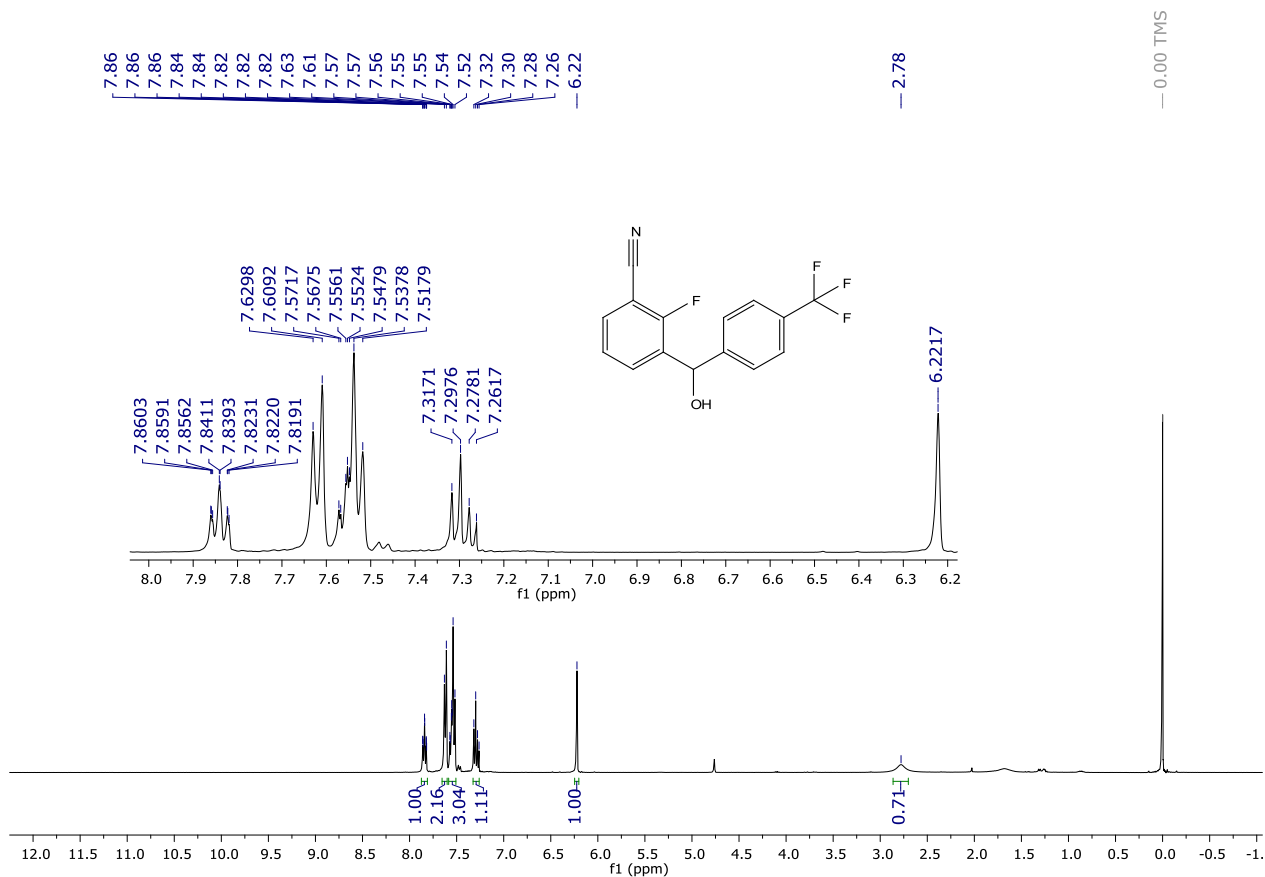


HSQC correlation map of **125c** (400 and 101 MHz, CDCl_3).

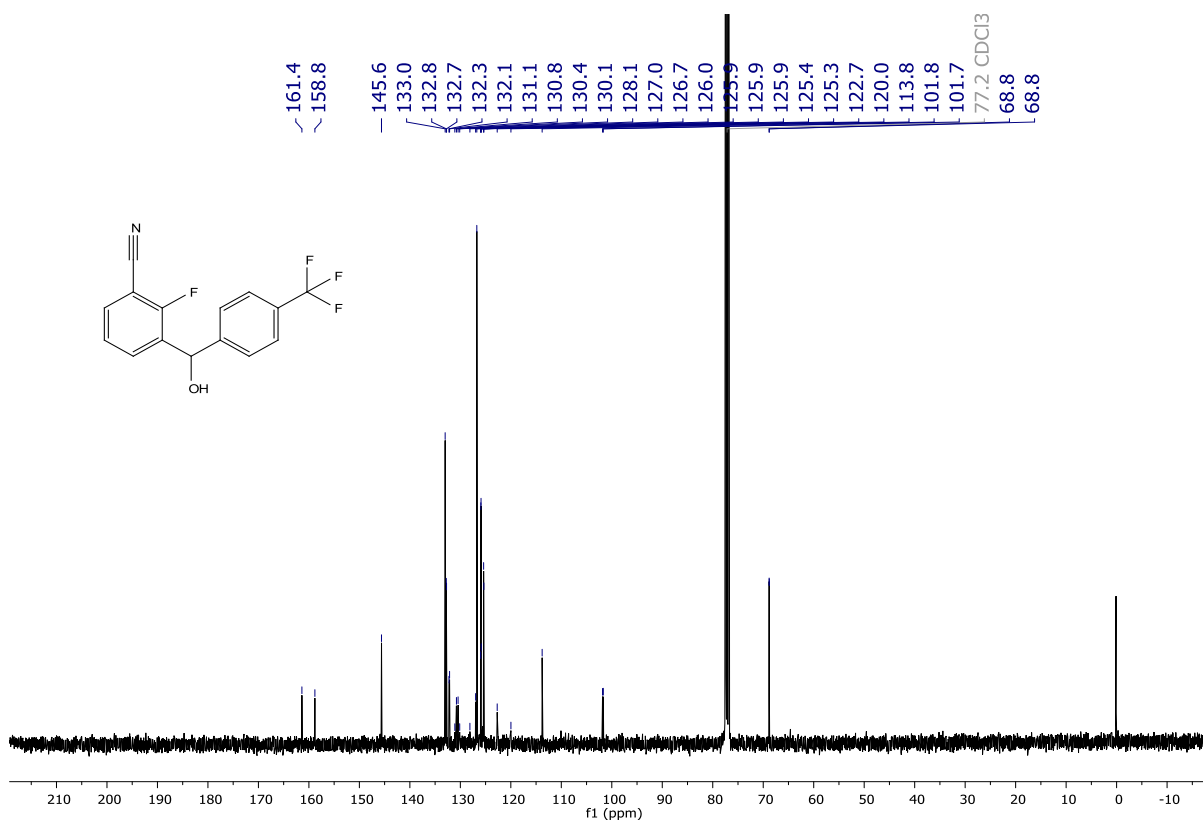
COSY correlation map of **125c** (101 MHz, CDCl_3).

-83.16
-83.18
-83.18
-83.19
-83.20
-83.21
-83.21
-83.23

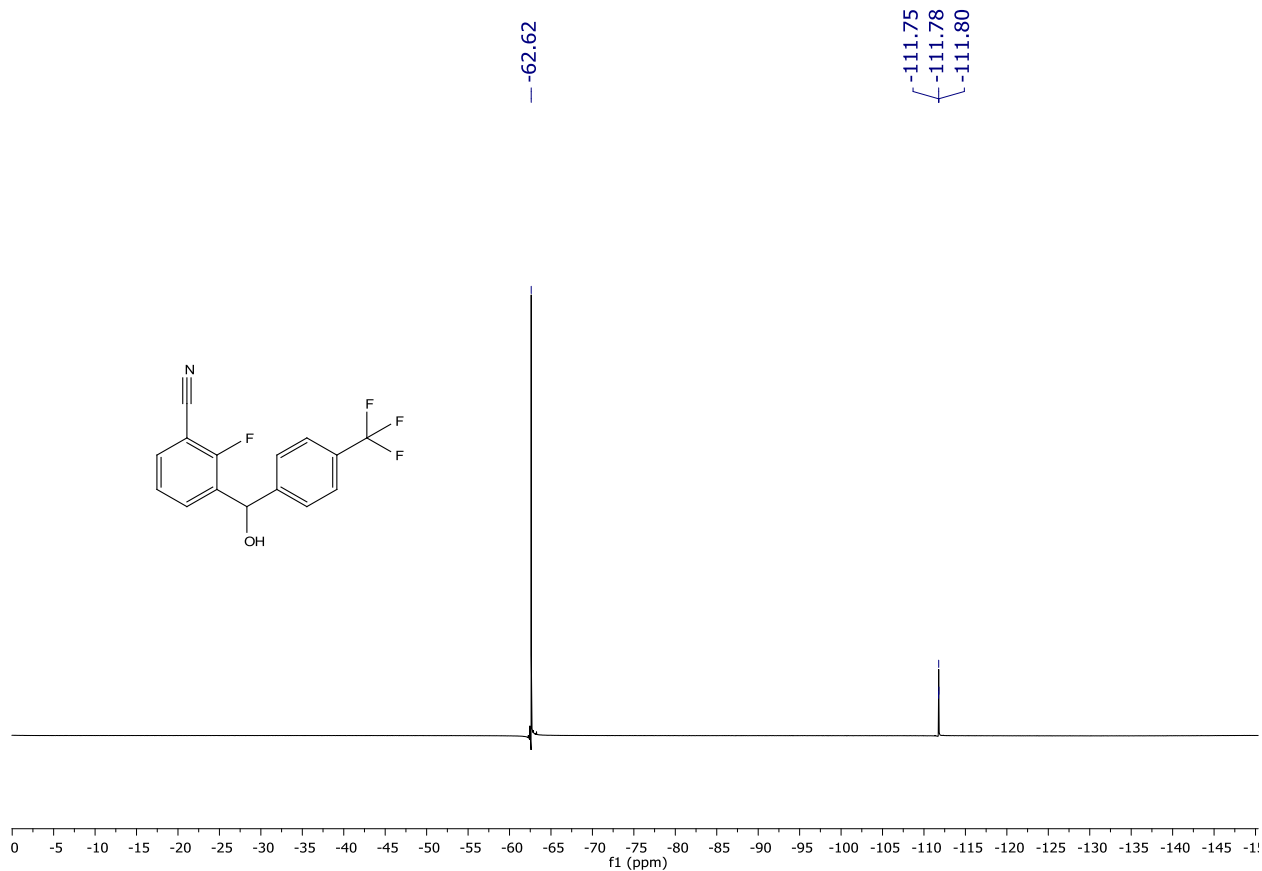
 ^{19}F NMR (282 MHz, CDCl_3) spectrum of **125c**.



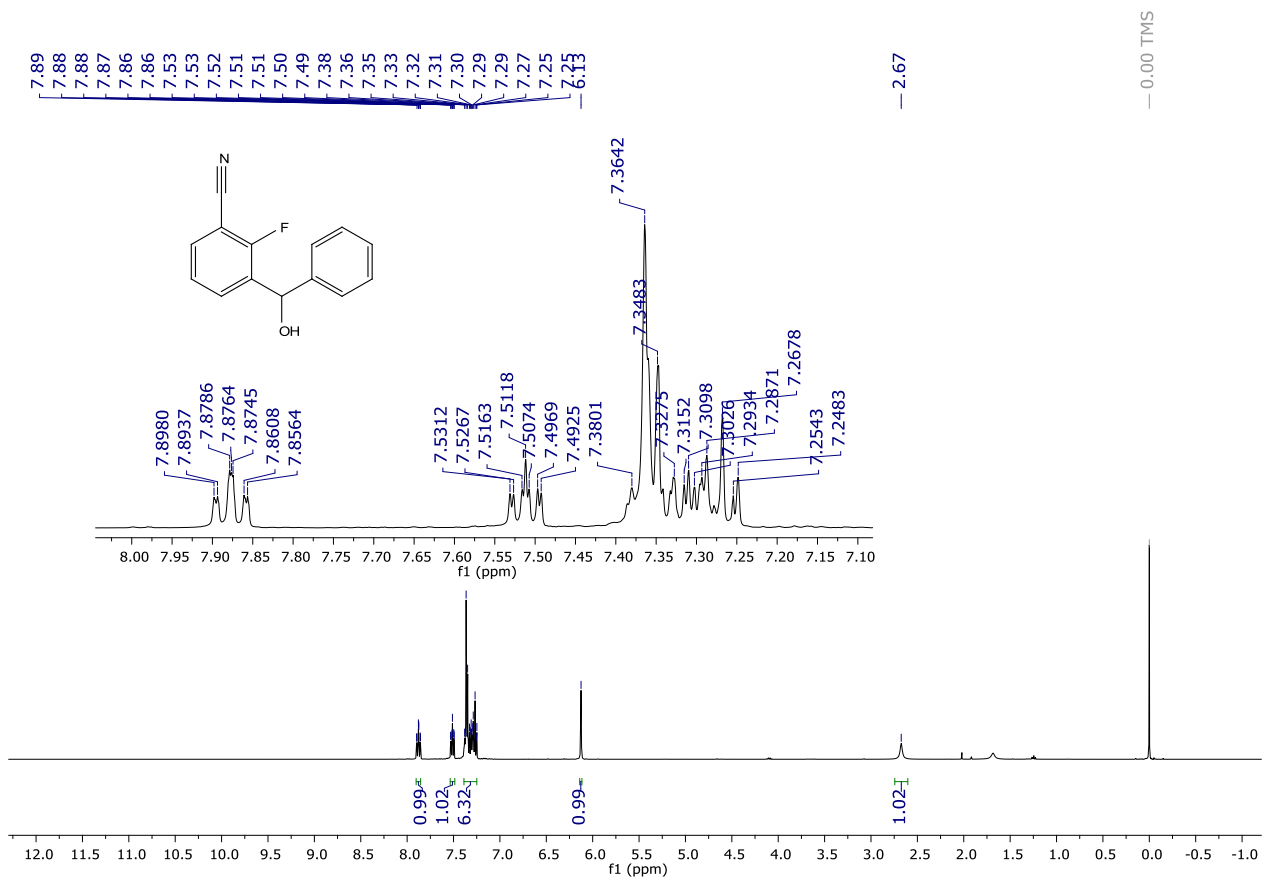
¹H NMR (400 MHz, CDCl₃) spectrum of 125d.



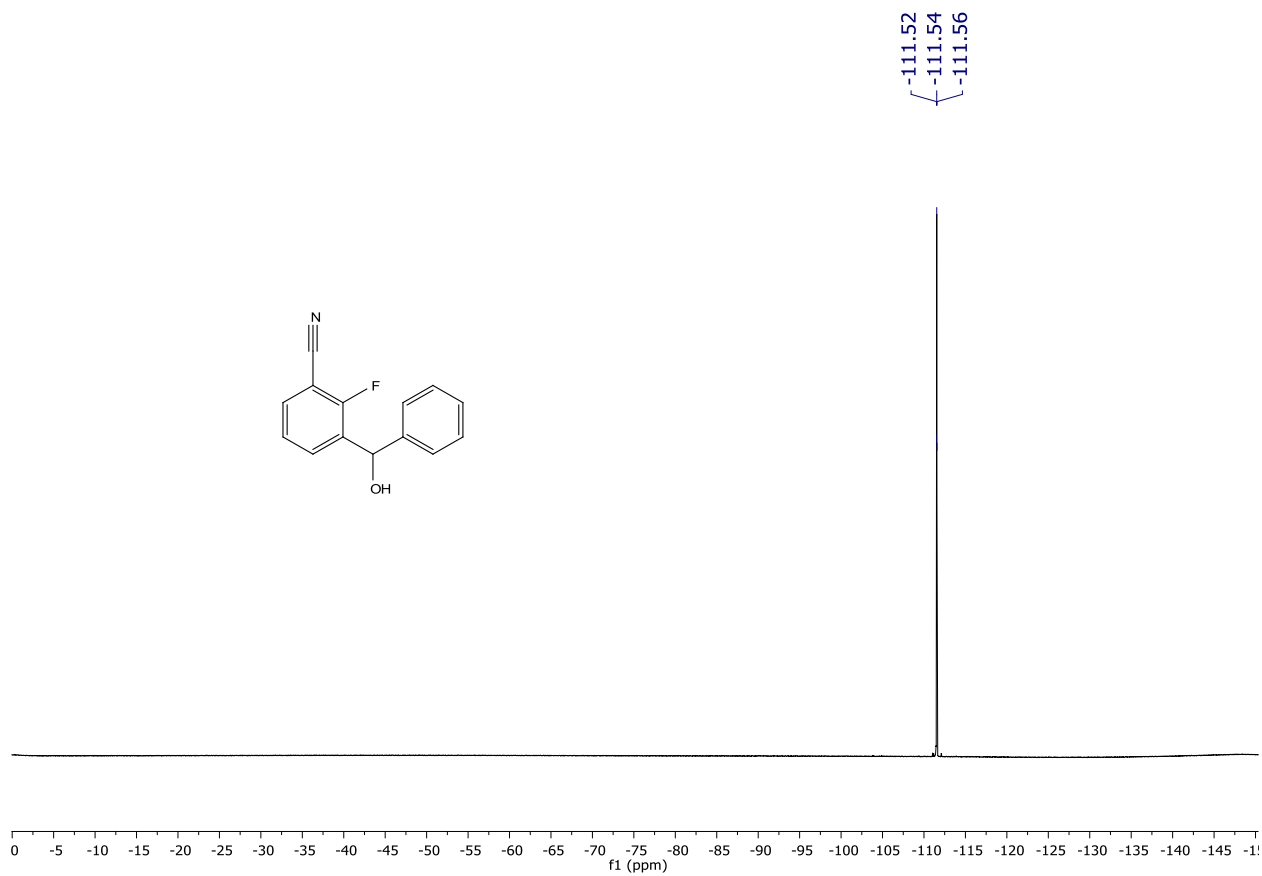
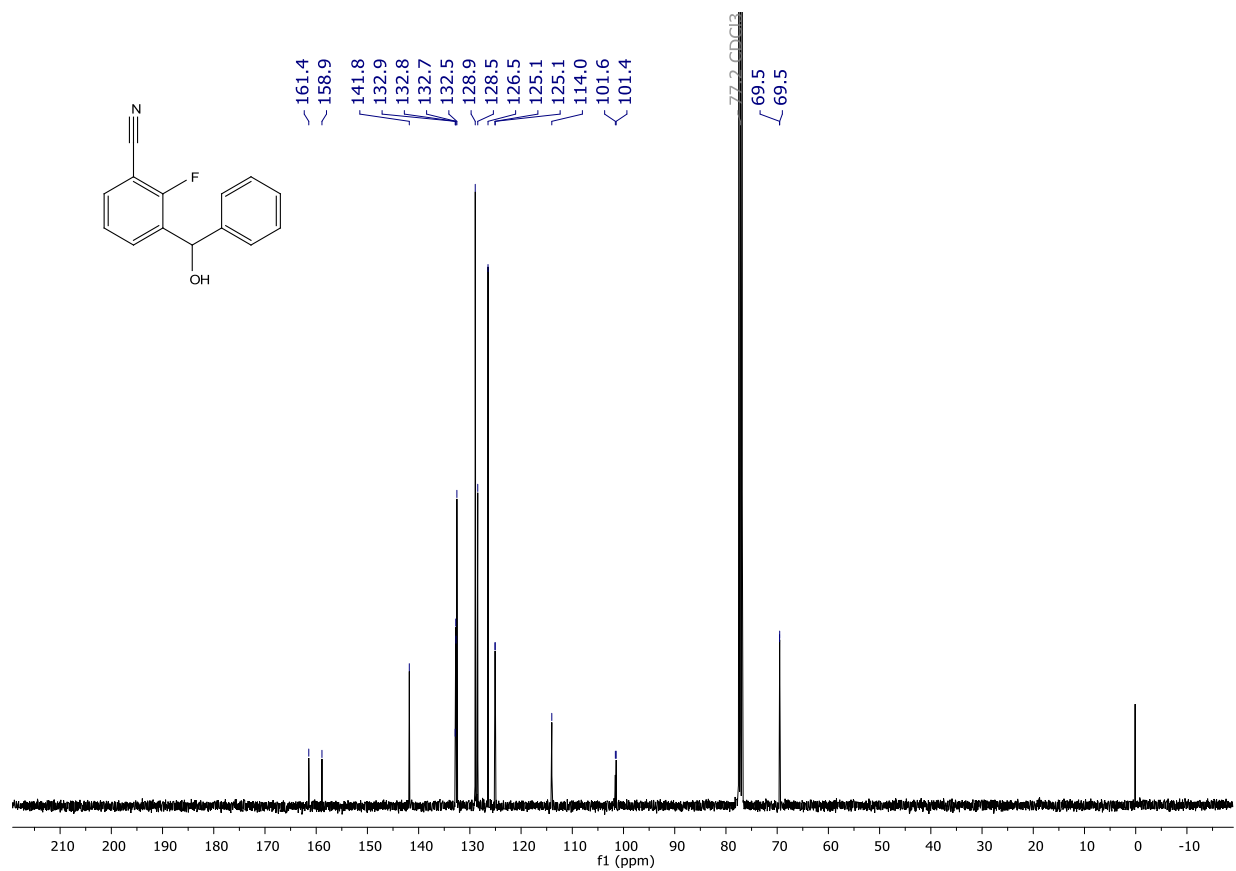
¹³C{¹H} NMR (101 MHz, CDCl₃) spectrum of 125d.



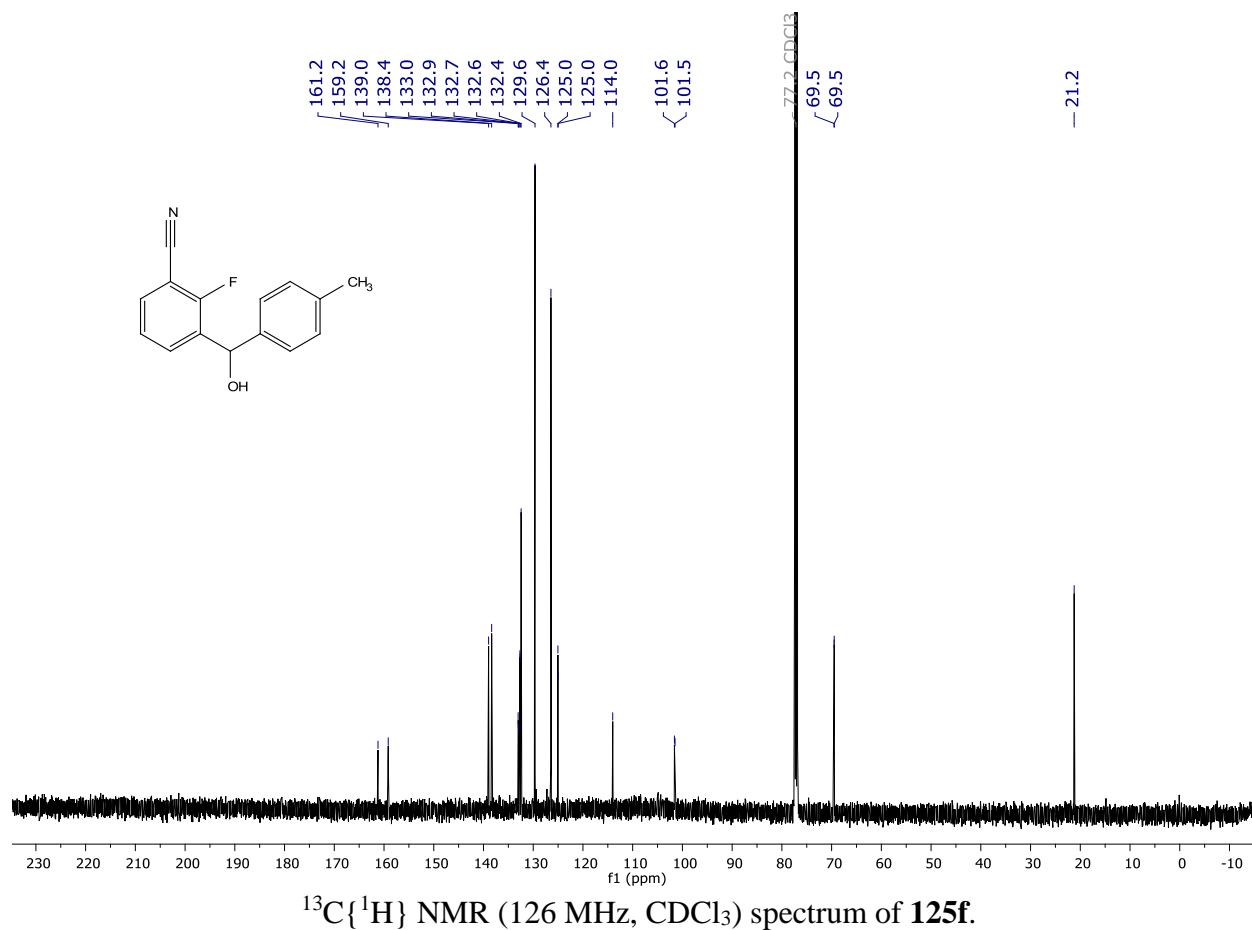
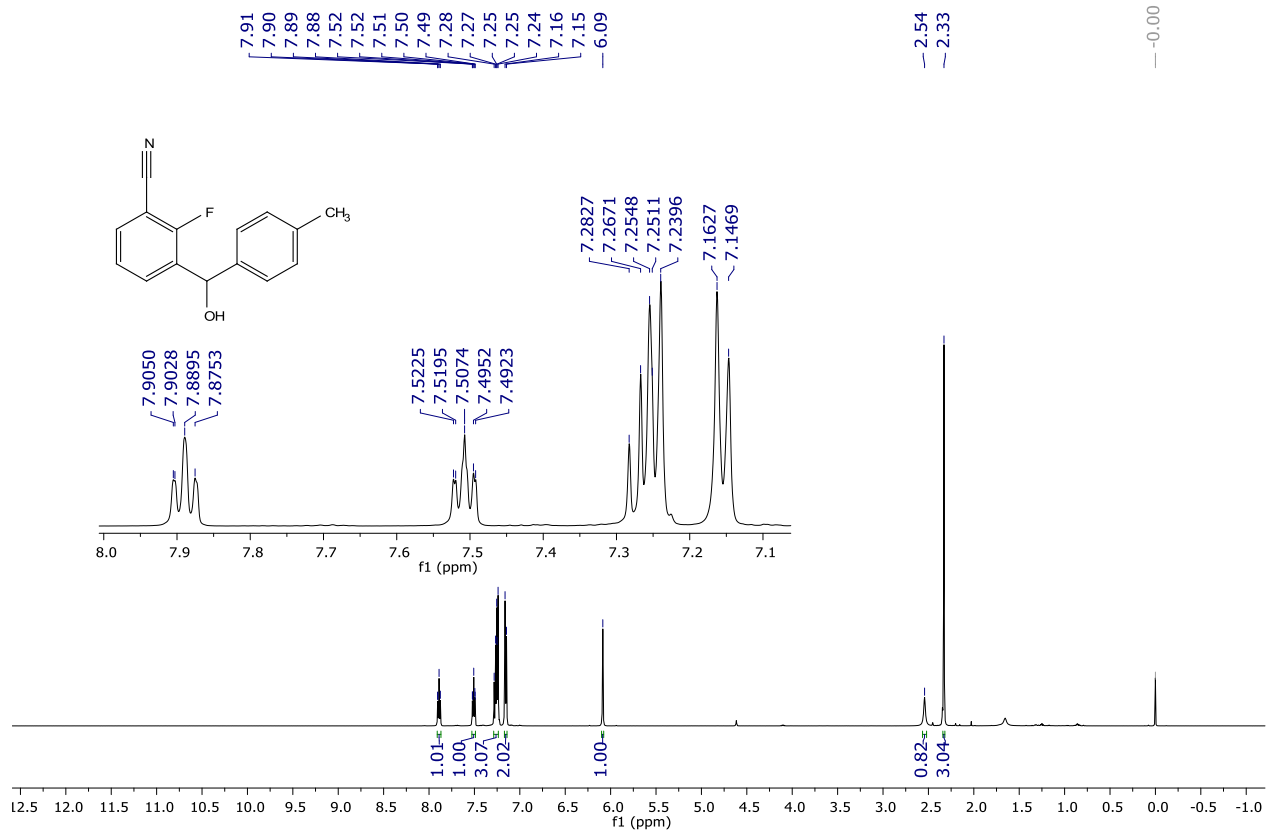
^{19}F NMR (282 MHz, CDCl_3) spectrum of **125d**.

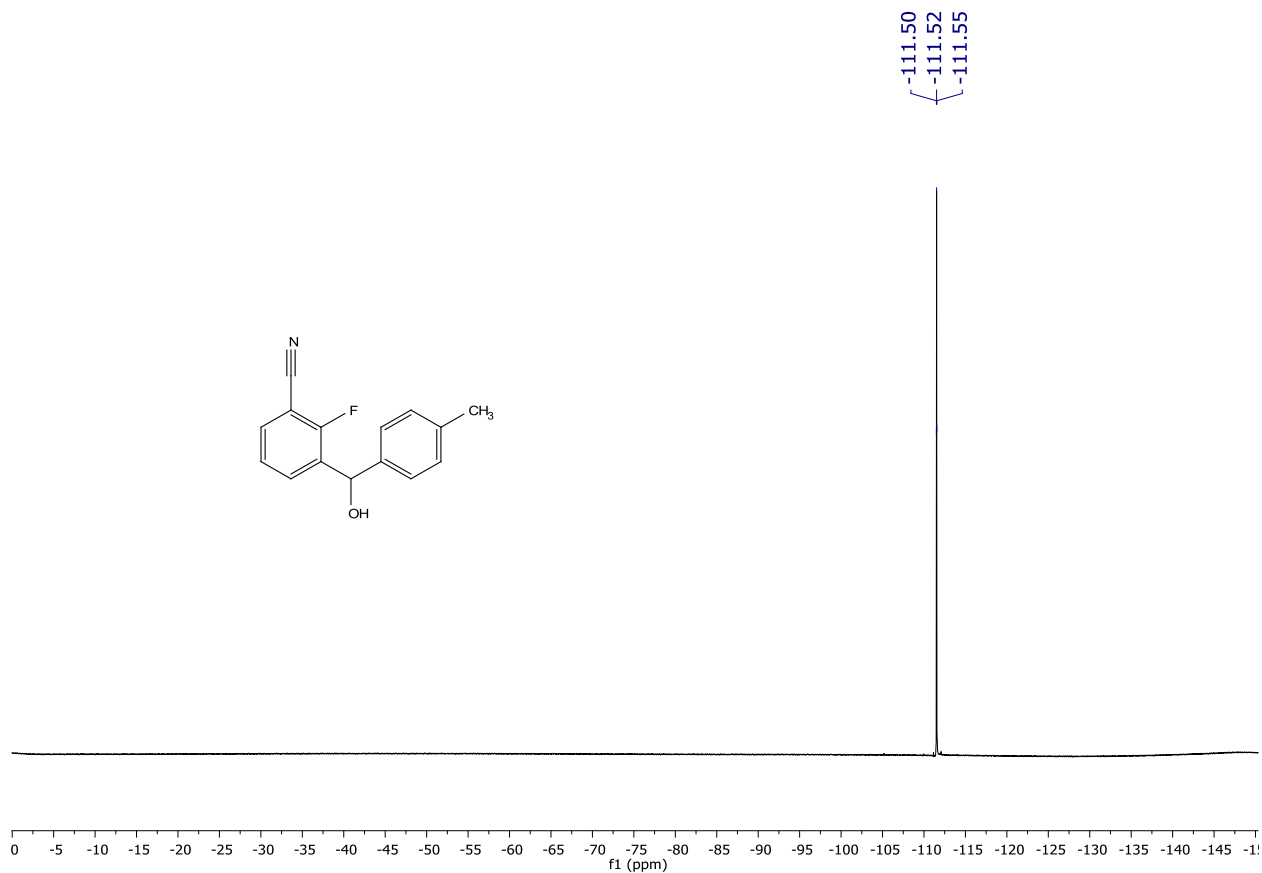


^1H NMR (400 MHz, CDCl_3) spectrum of **125e**.

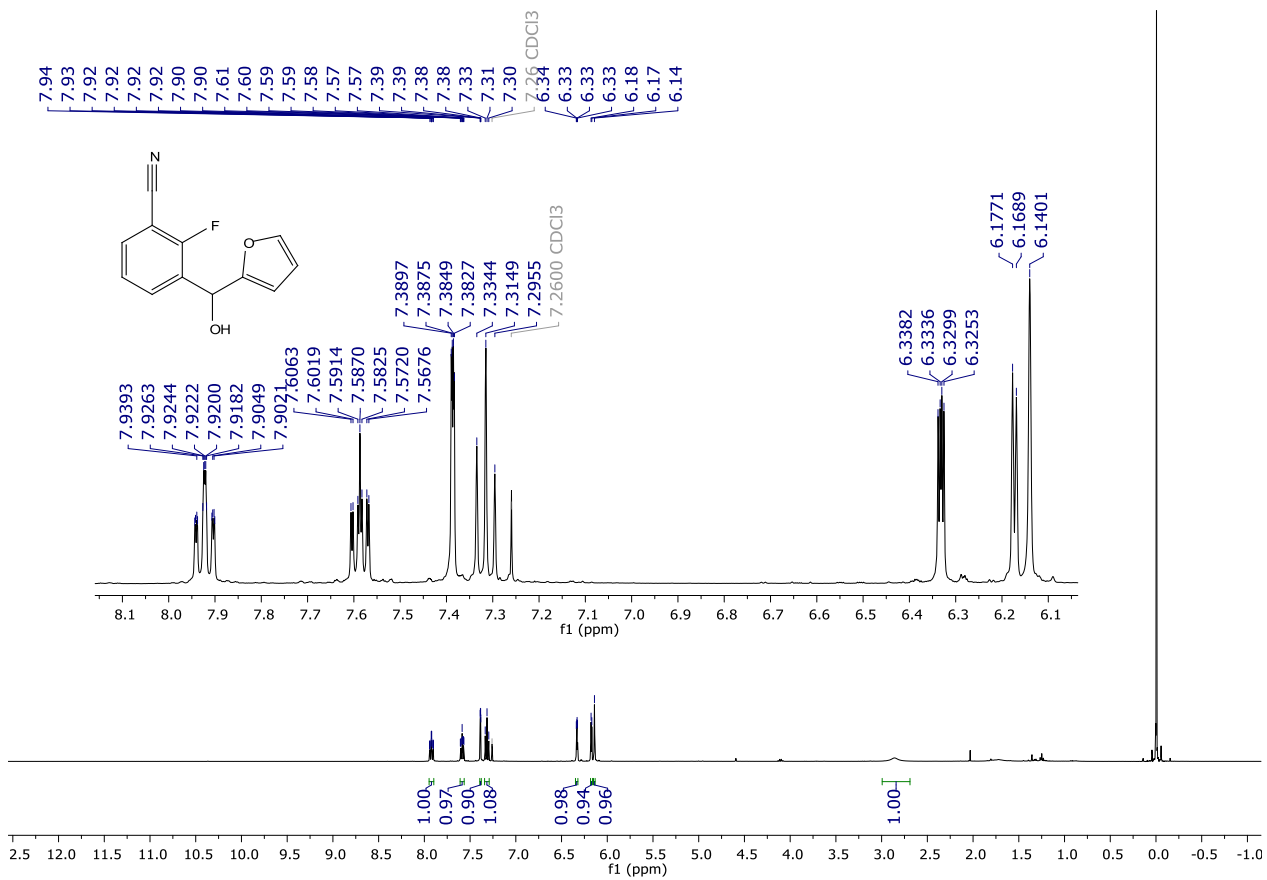


^{19}F NMR (282 MHz, CDCl_3) spectrum of **125e**.

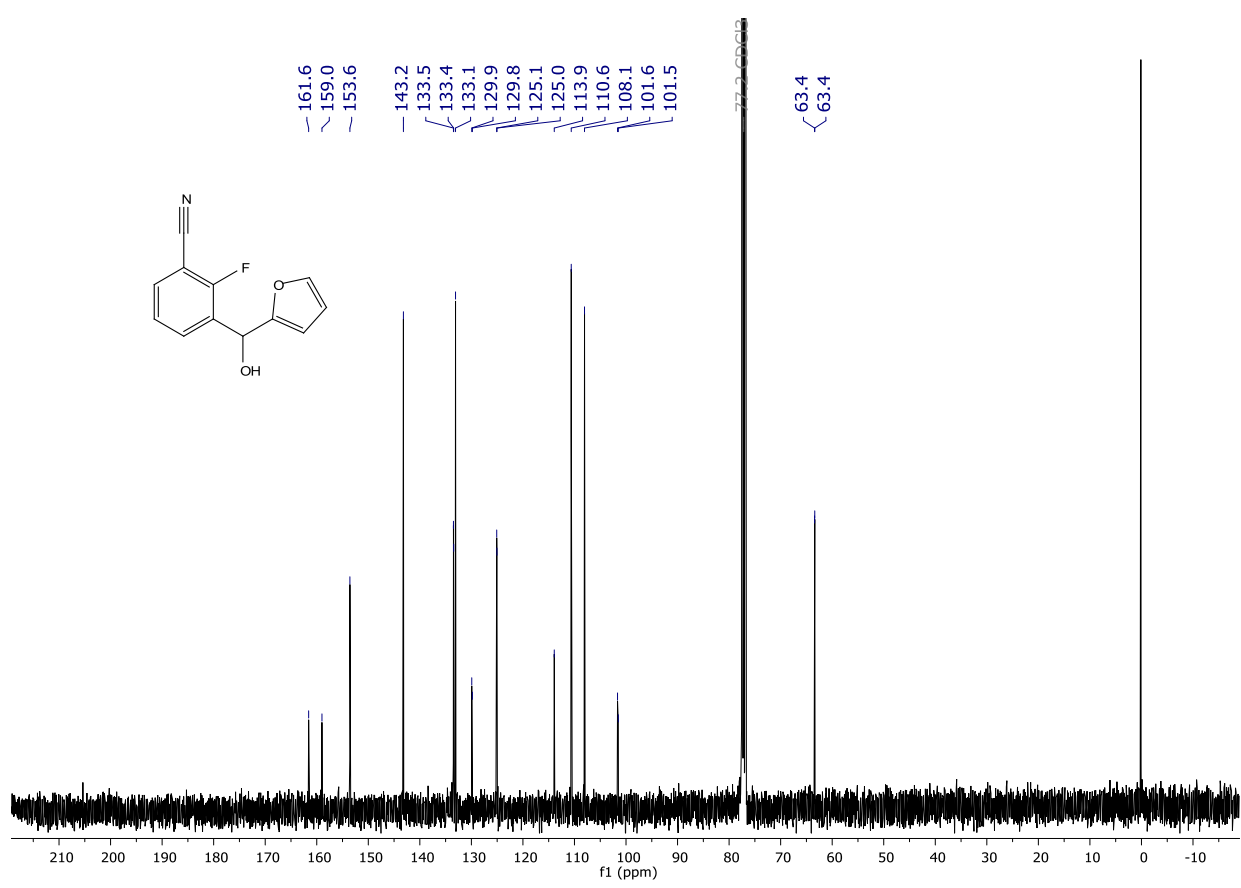




^{19}F NMR (282 MHz, CDCl_3) spectrum of **125f**.

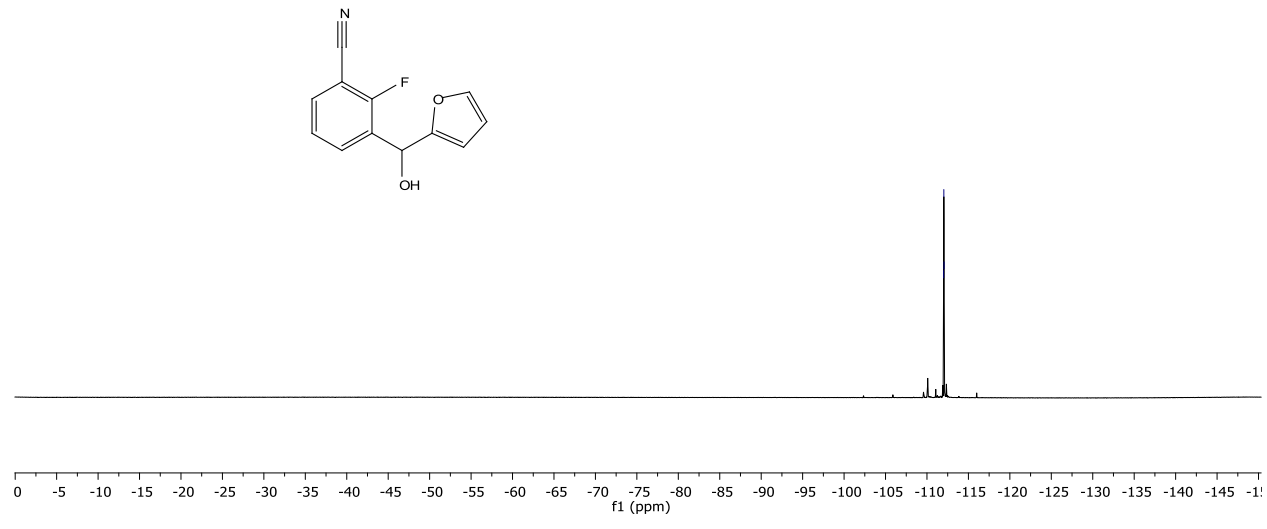


^1H NMR (400 MHz, CDCl_3) spectrum of **125g**.

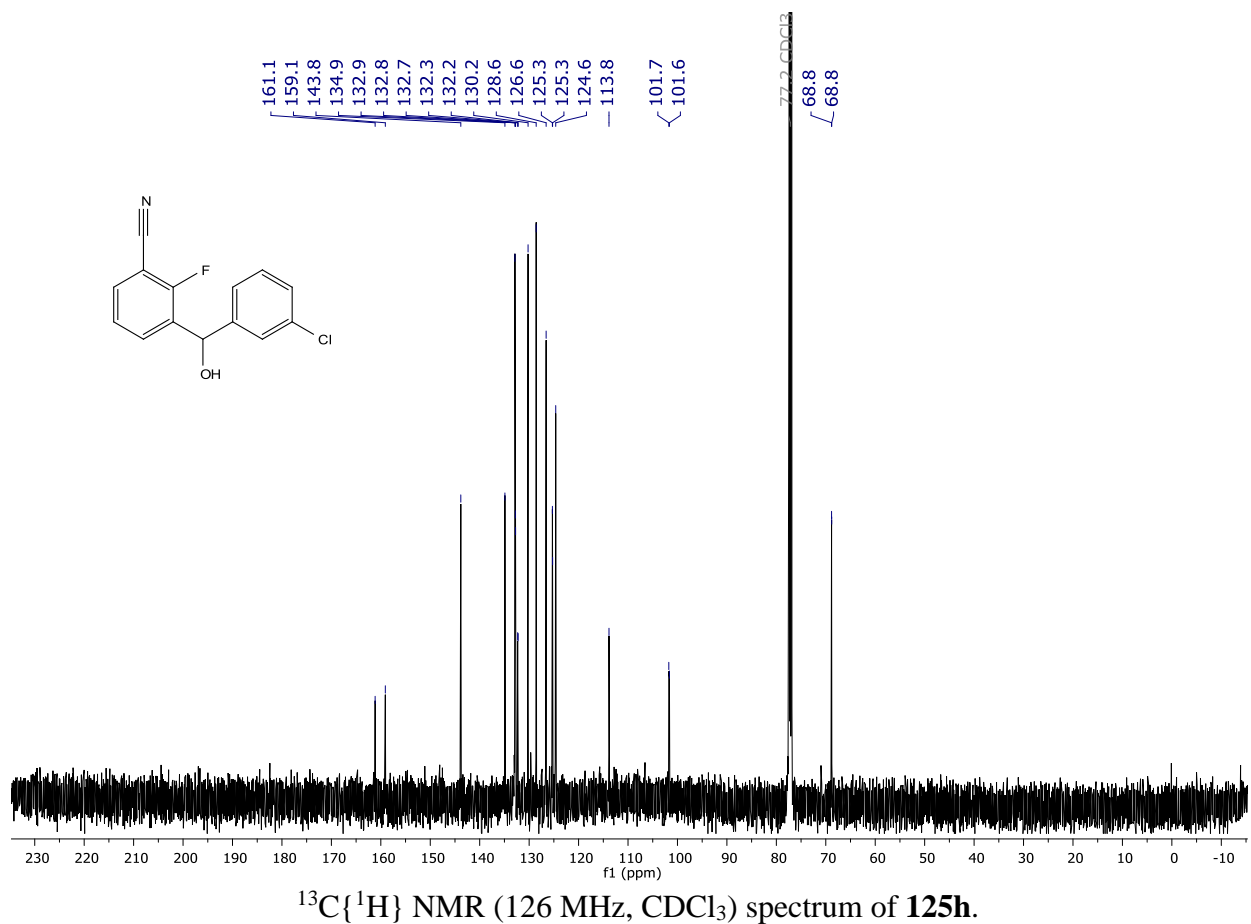
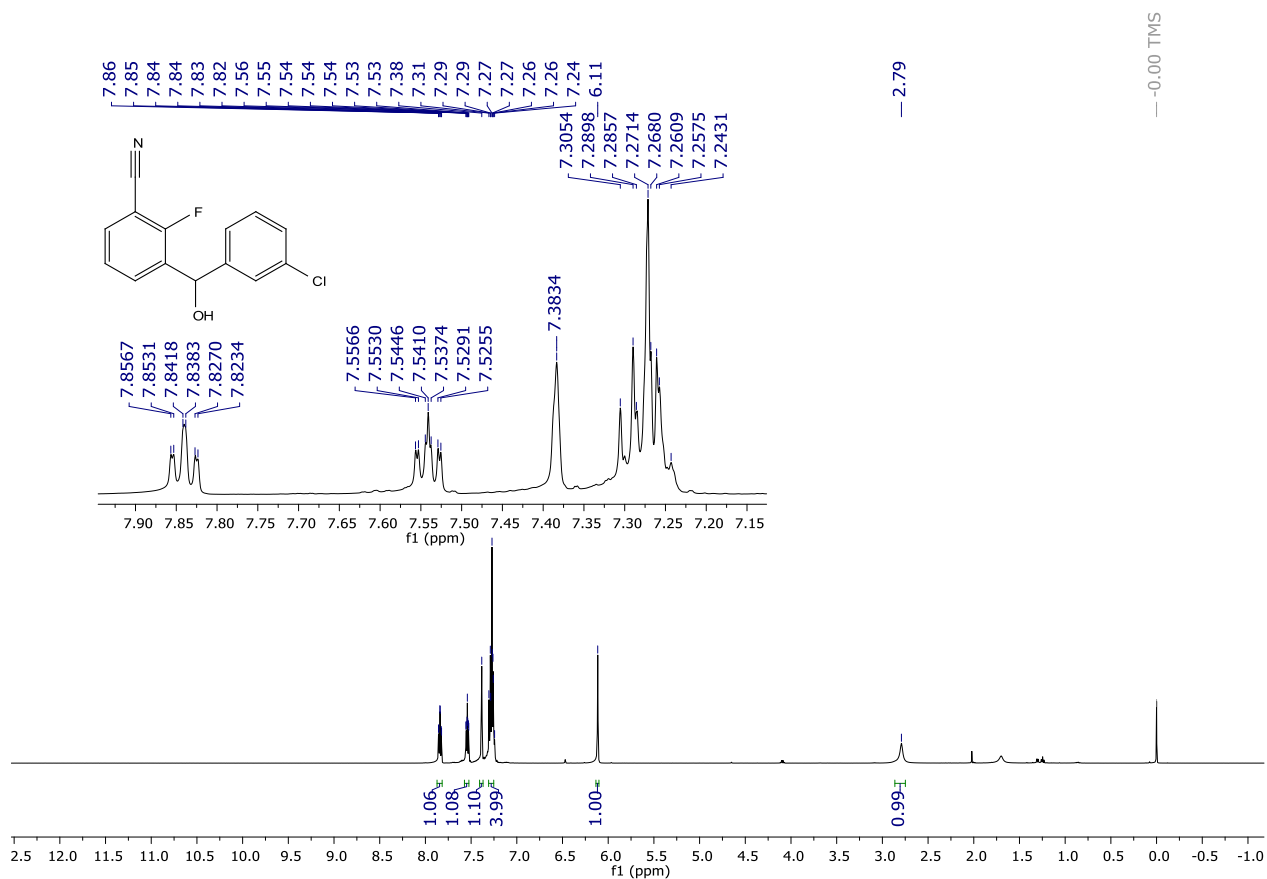


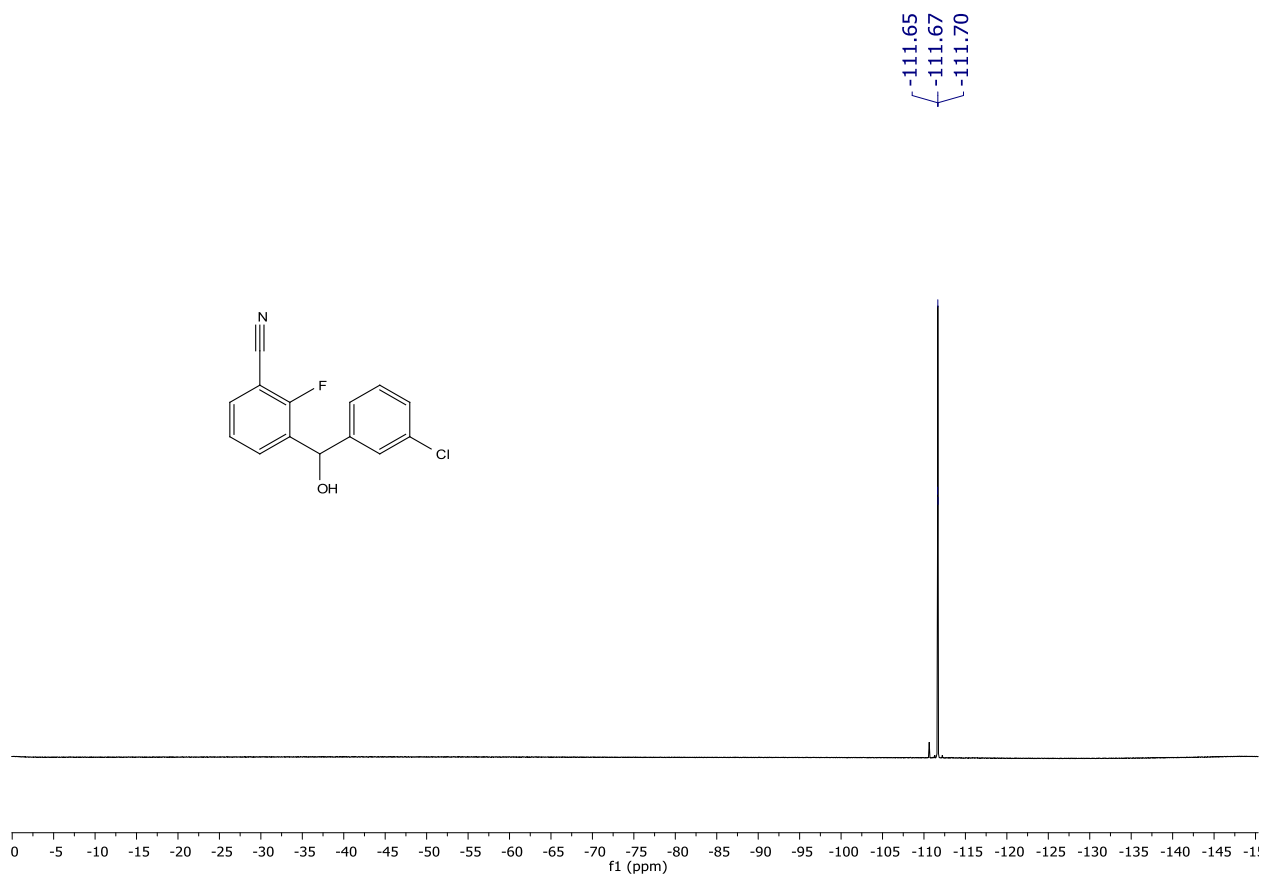
¹³C{¹H} NMR (101 MHz, CDCl₃) spectrum of **125g**.

-112.01
-112.03
-112.06

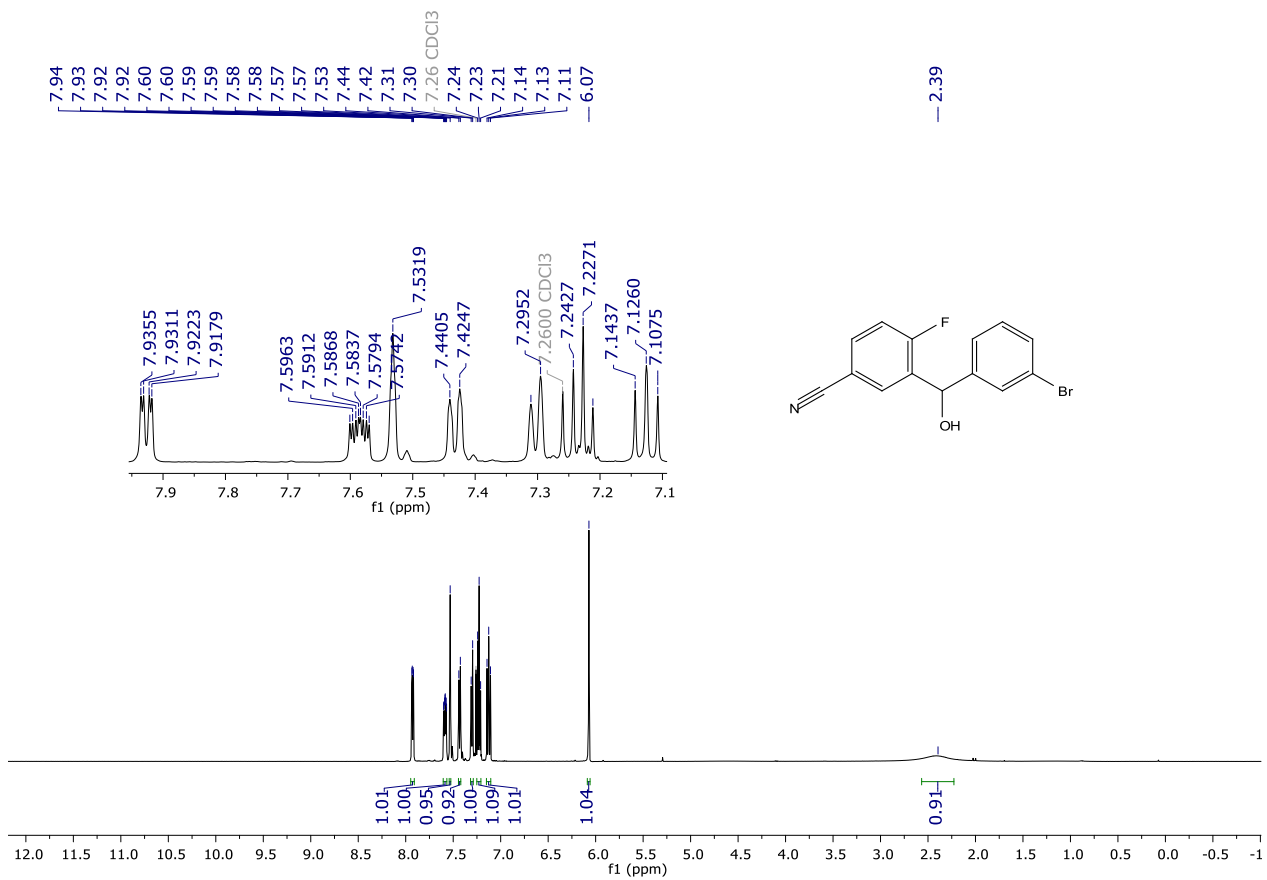


¹⁹F NMR (282 MHz, CDCl₃) spectrum of **125g**.

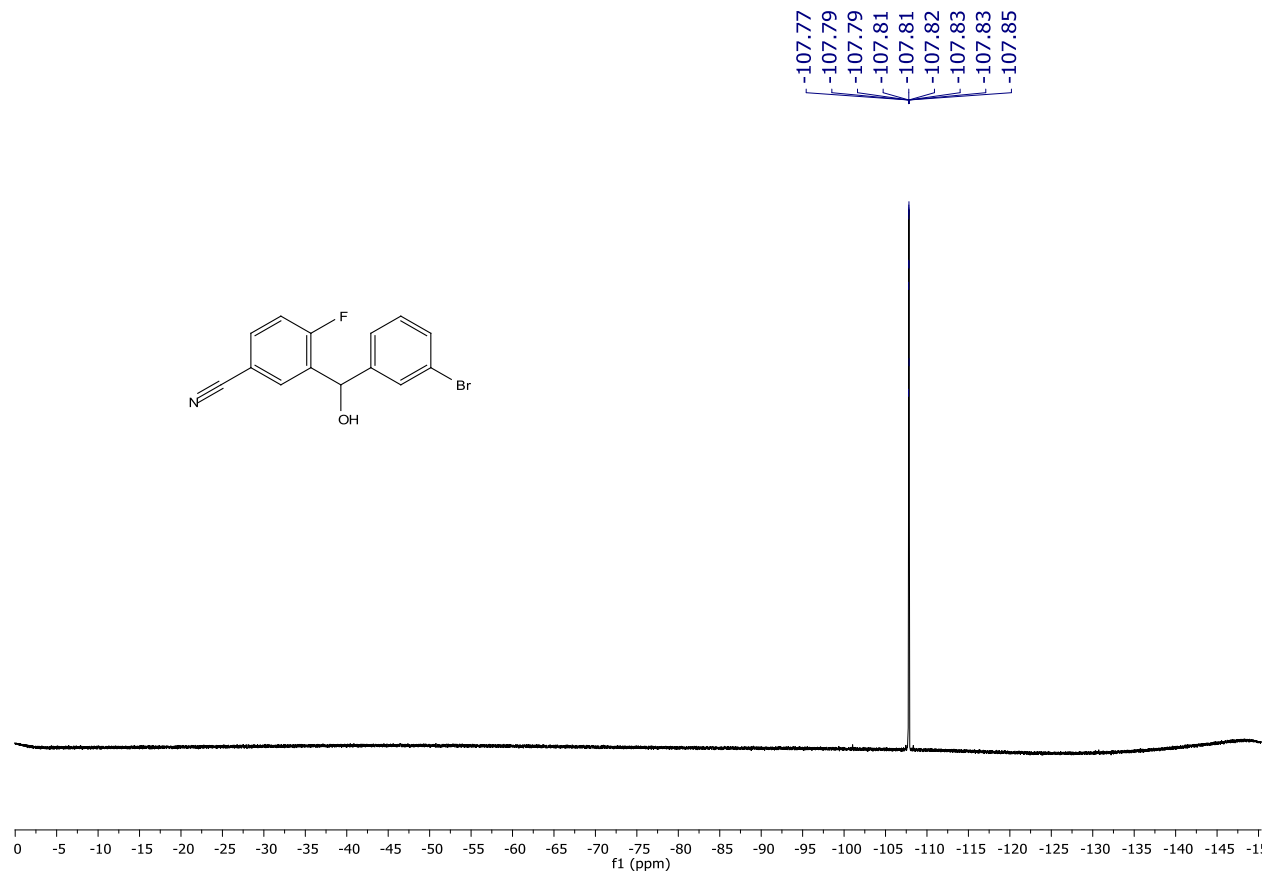
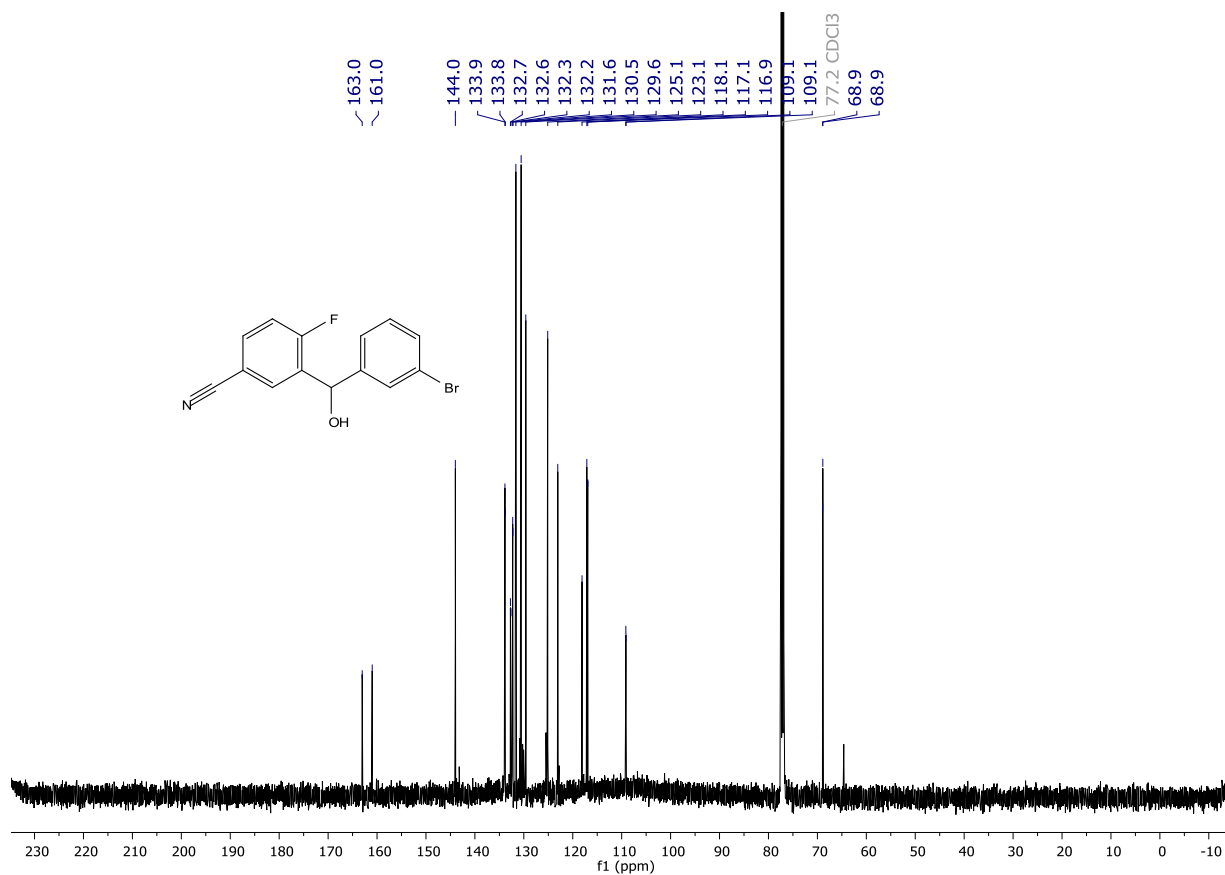


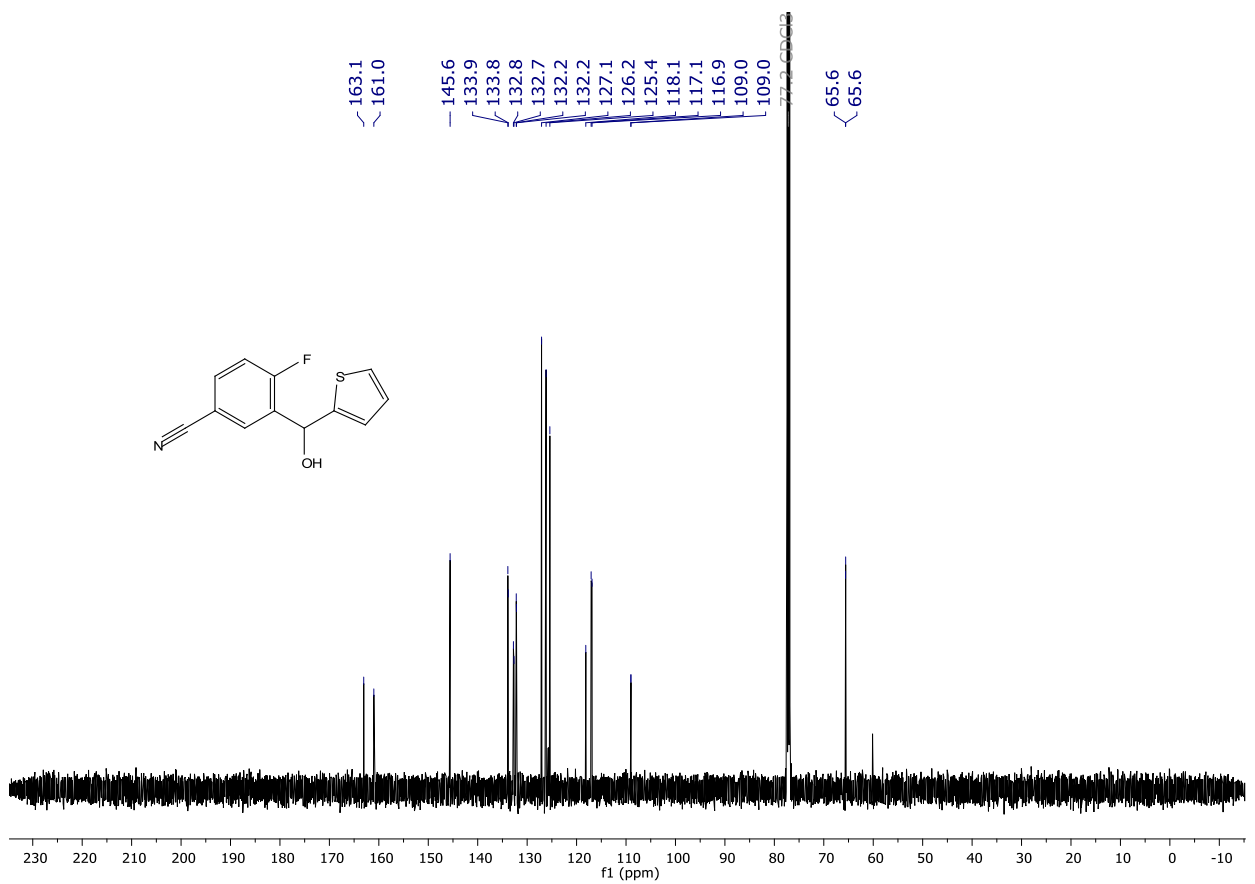
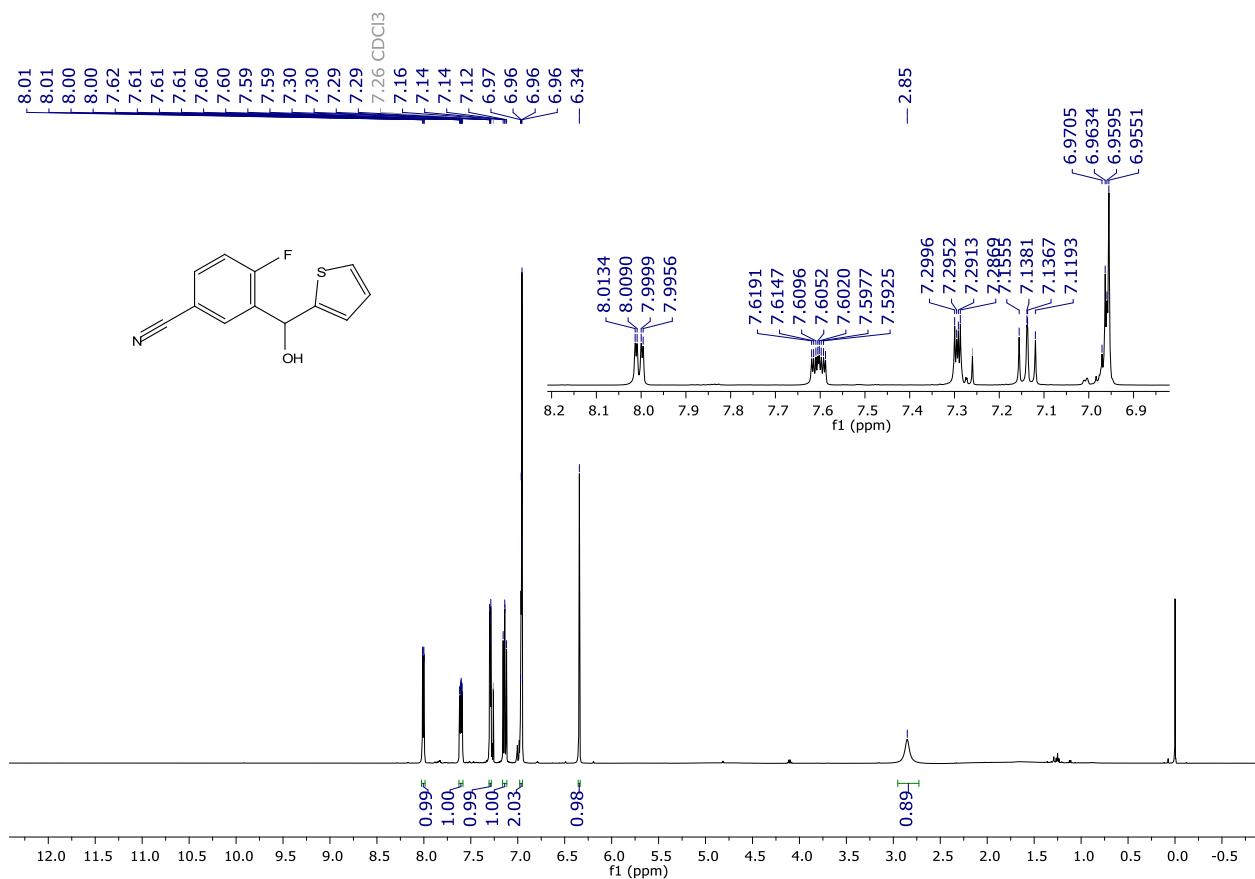


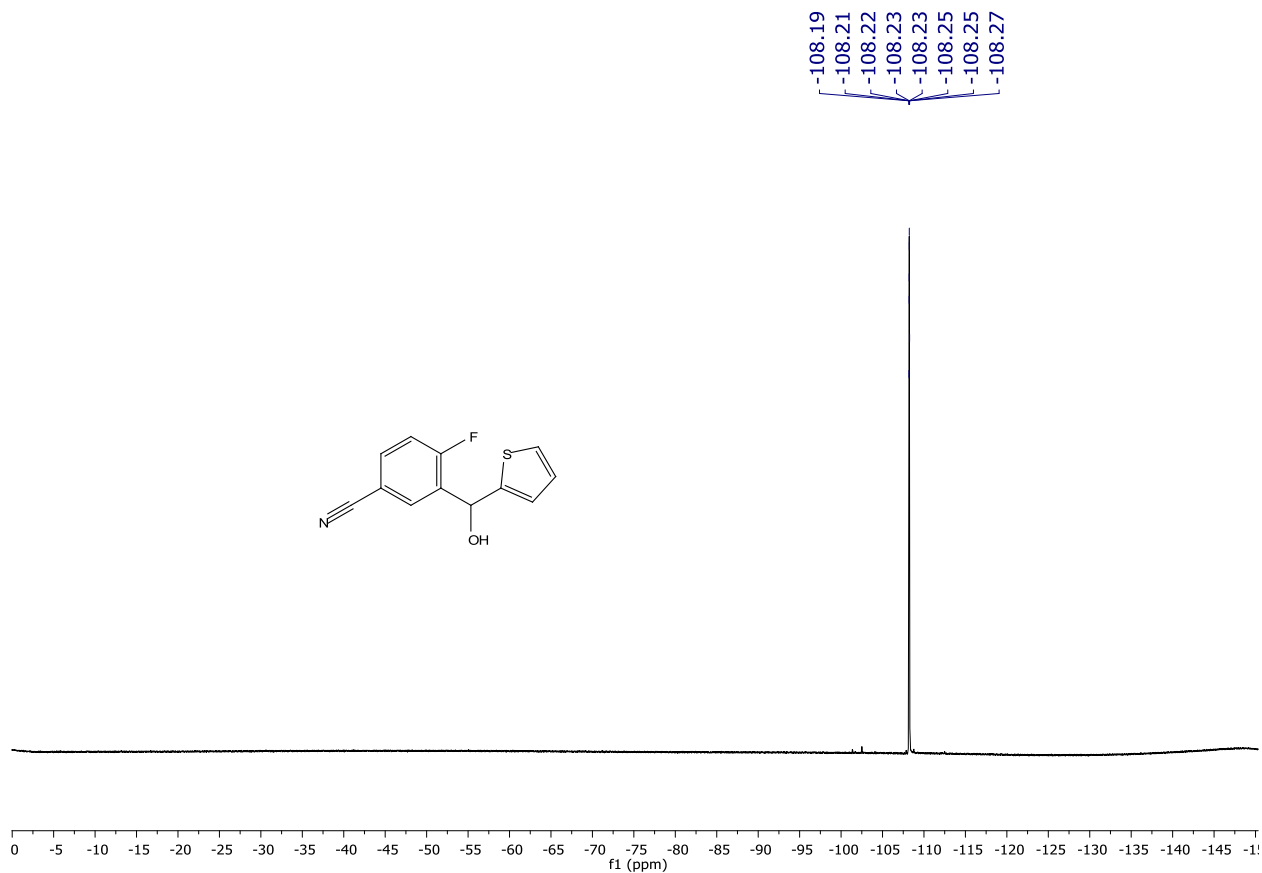
^{19}F NMR (282 MHz, CDCl_3) spectrum of **125h**.



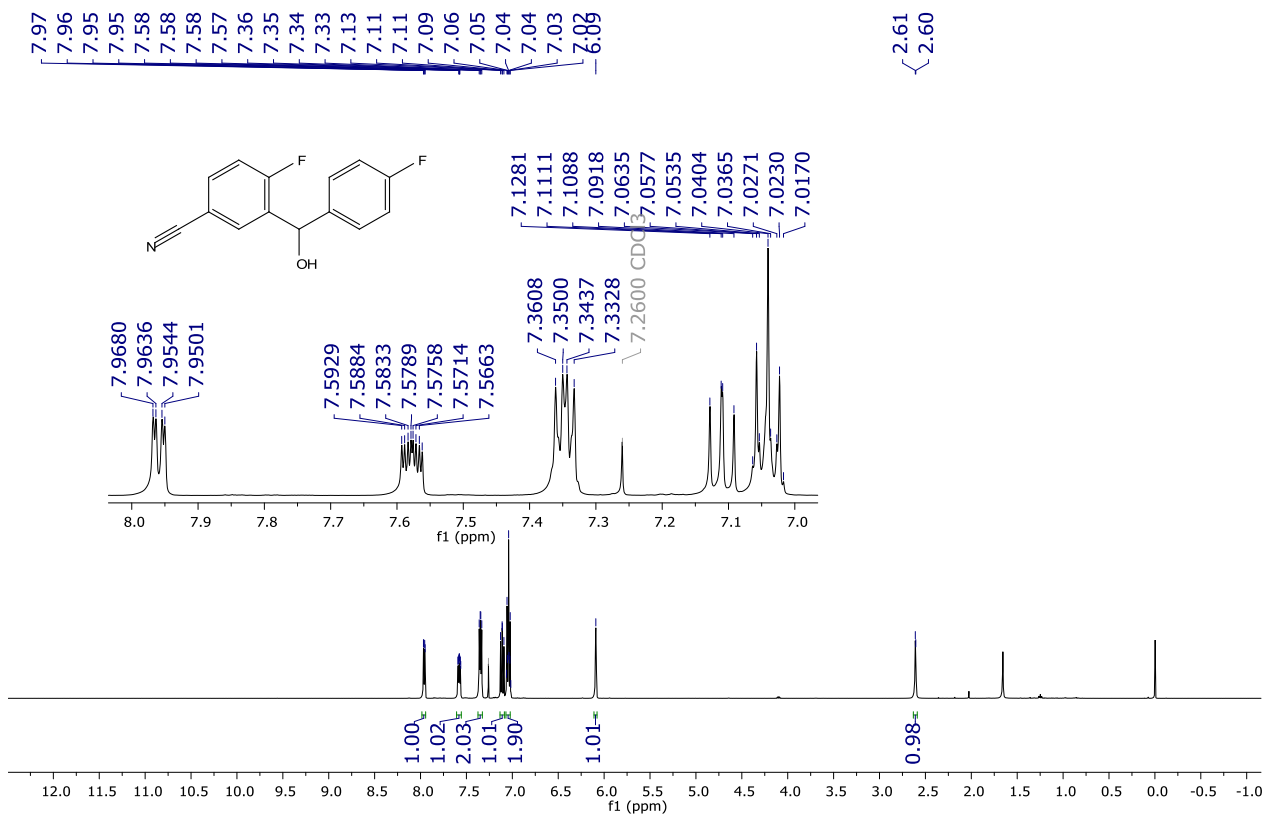
^1H NMR (500 MHz, CDCl_3) spectrum of **125i**.



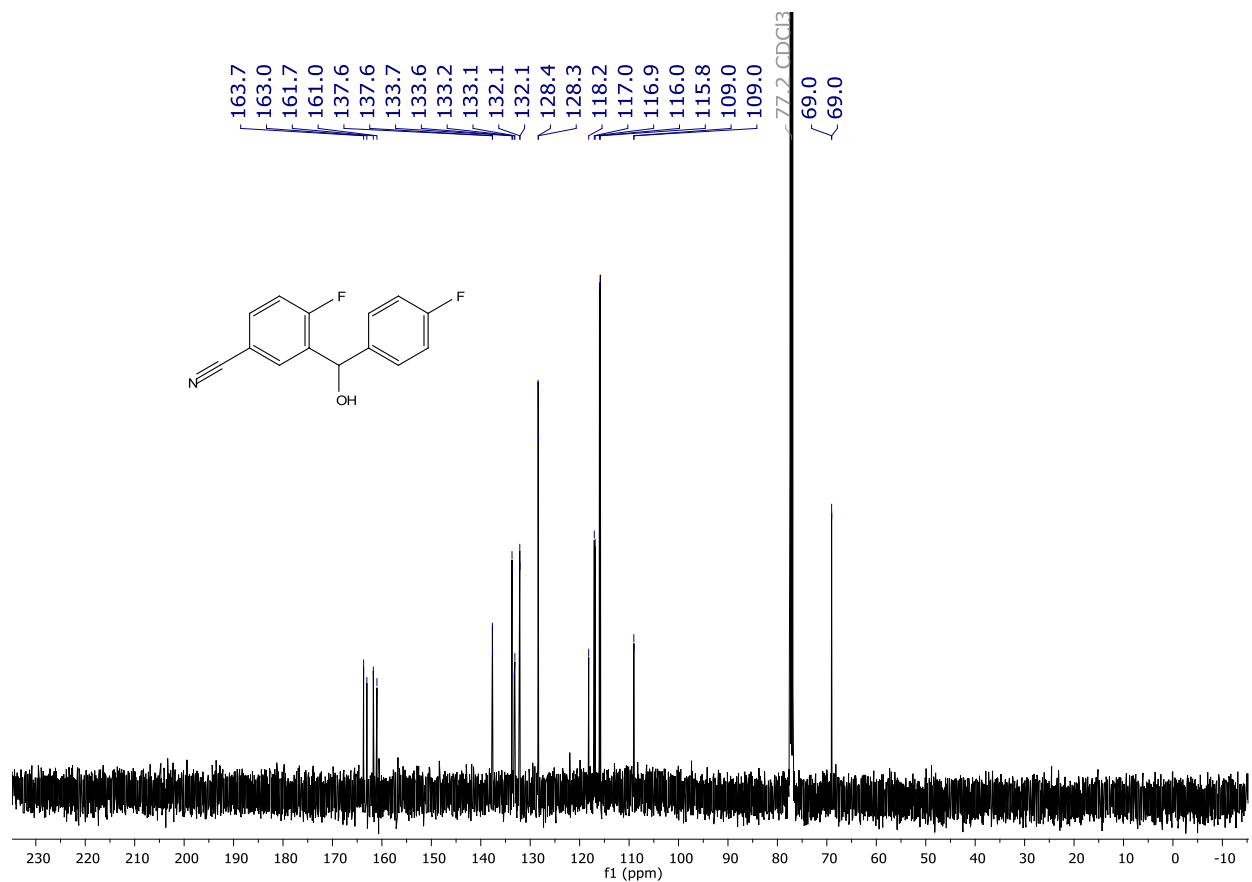




^{19}F NMR (282 MHz, CDCl_3) spectrum of **125j**.



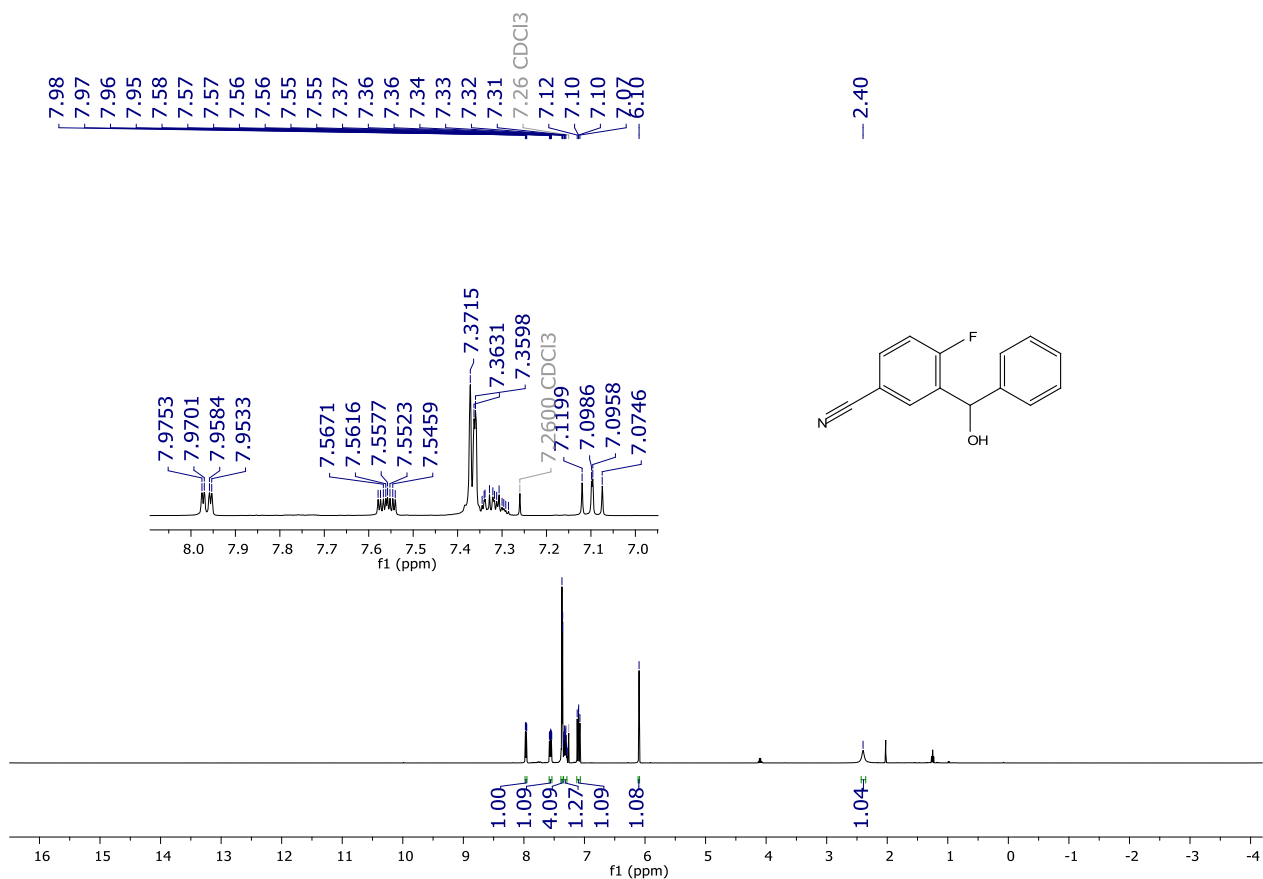
^1H NMR (500 MHz, CDCl_3) spectrum of **125k**.



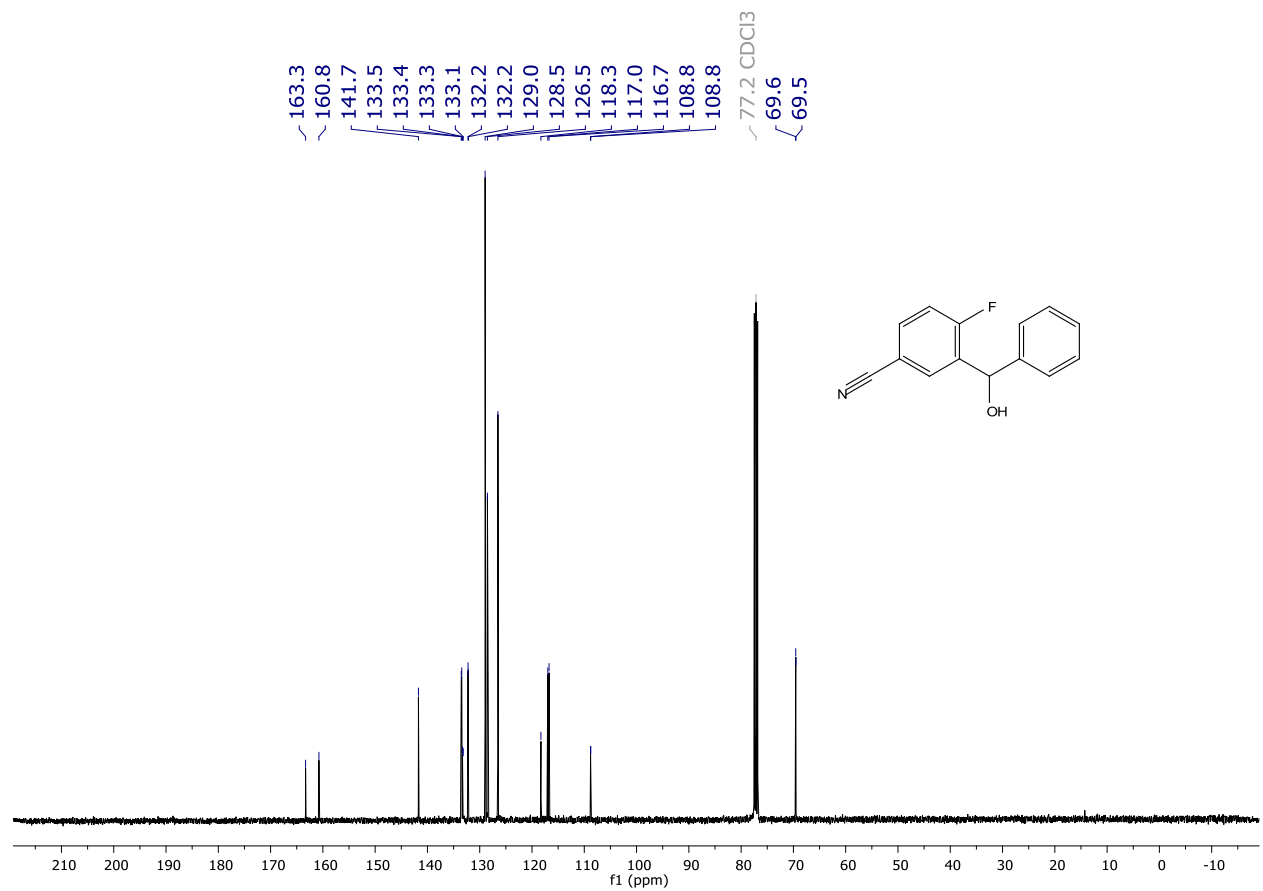
¹³C{¹H} NMR (126 MHz, CDCl₃) spectrum of **125k**.



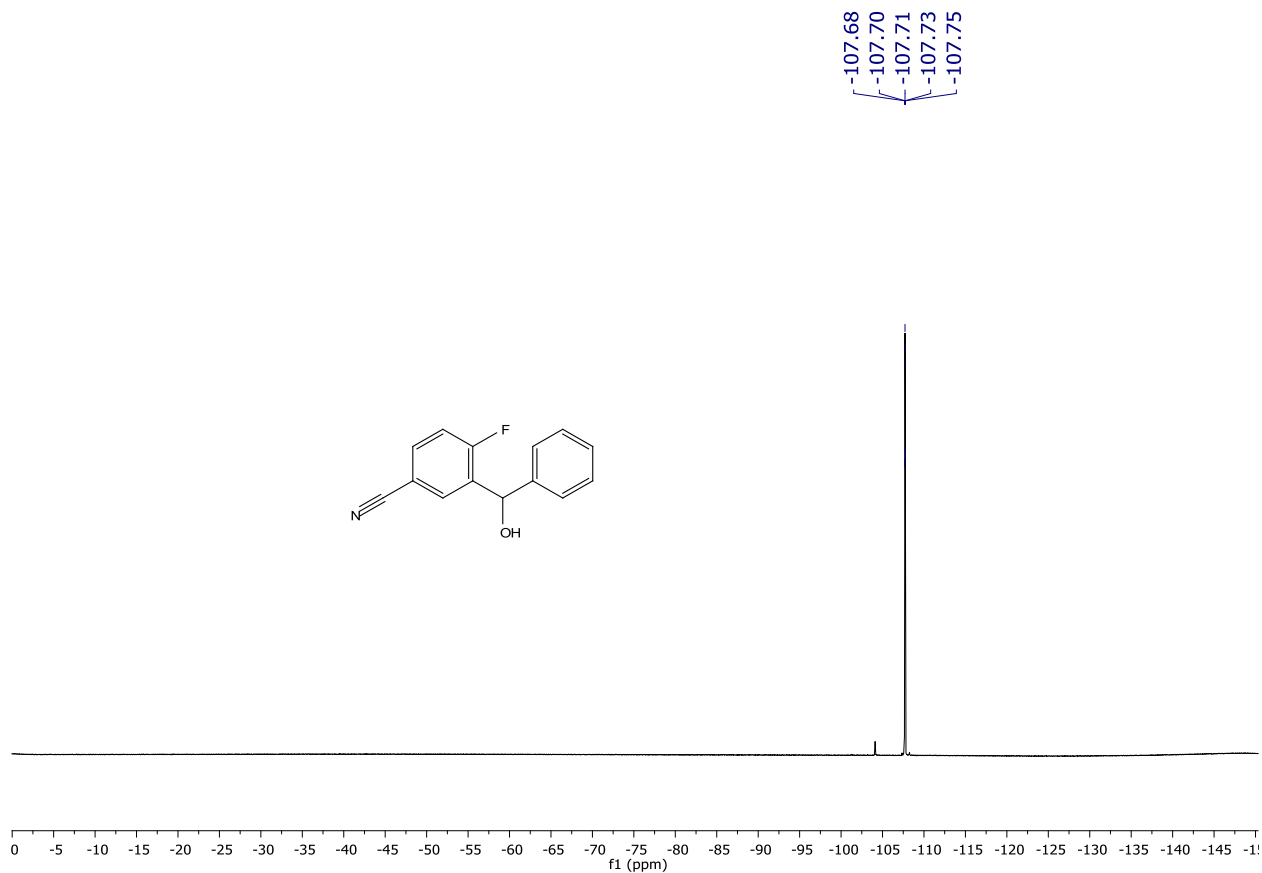
¹⁹F NMR (282 MHz, CDCl₃) spectrum of **125k**.



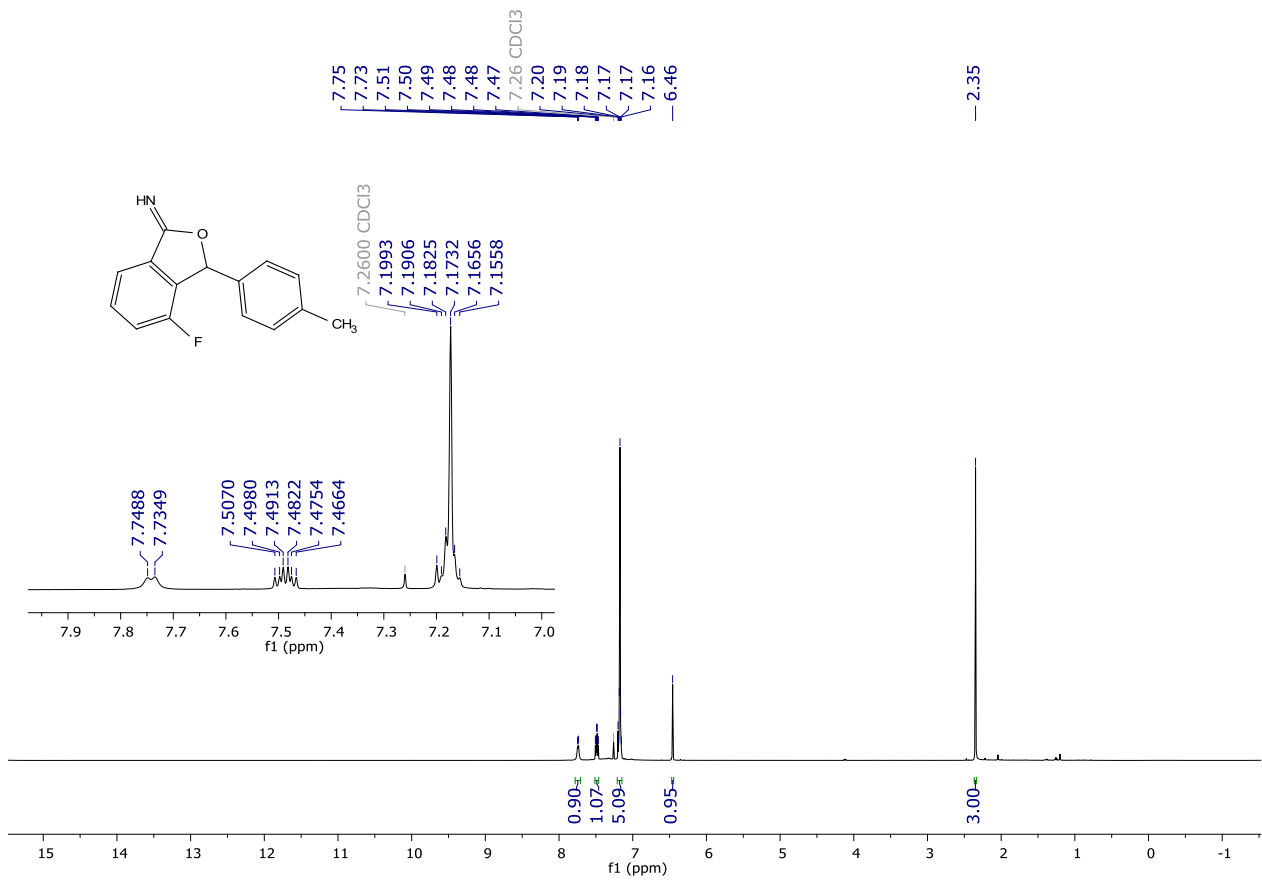
¹H NMR (400 MHz, CDCl₃) spectrum of **125l**.



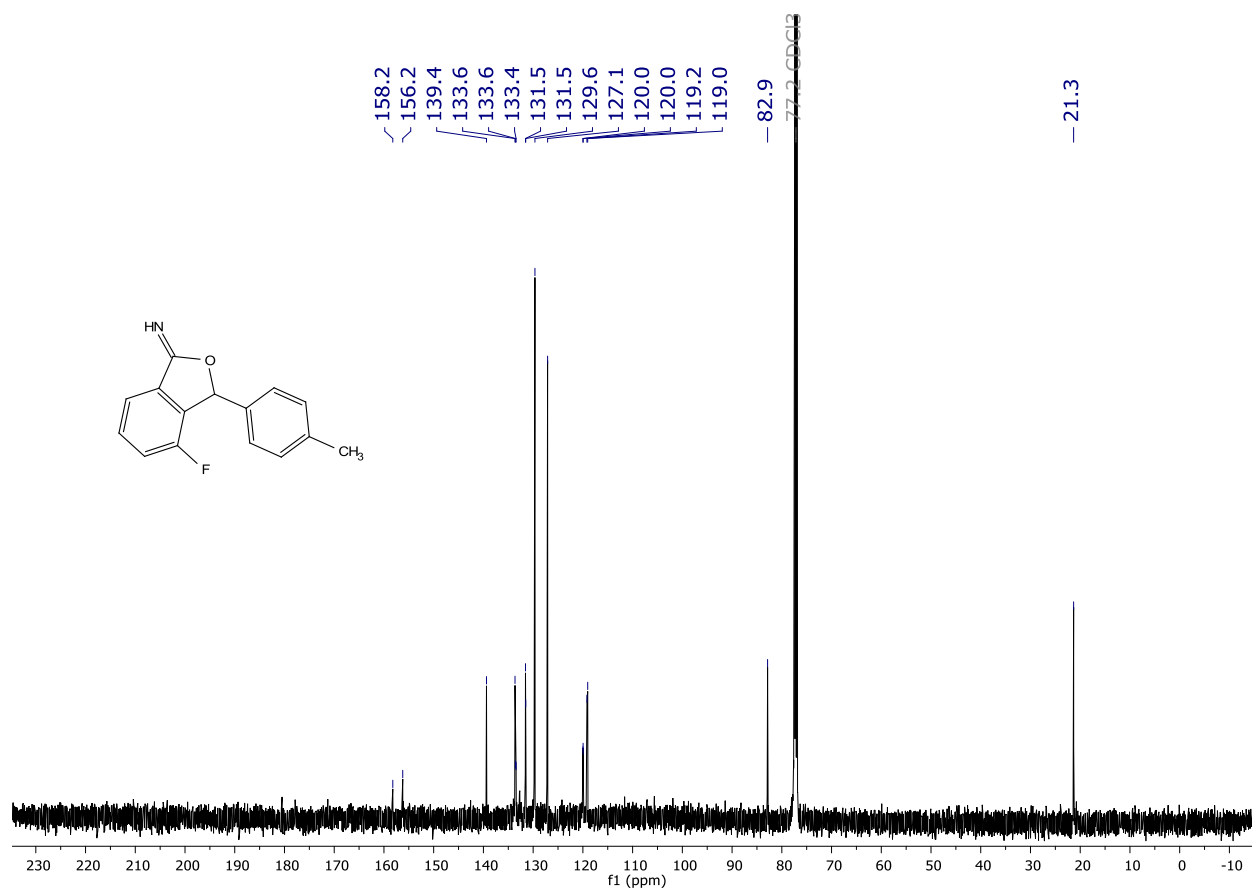
¹³C{¹H} NMR (101 MHz, CDCl₃) spectrum of **125l**.



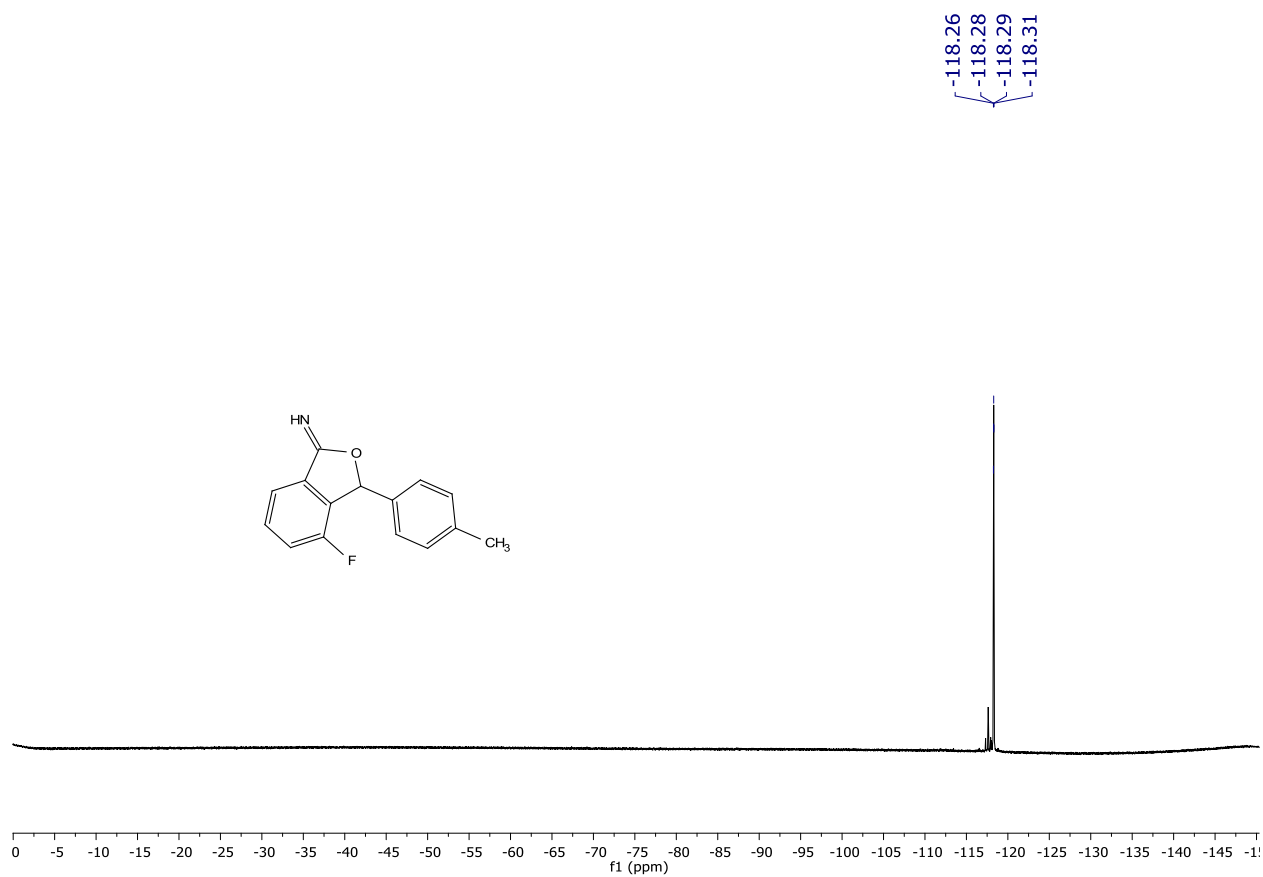
^{19}F NMR (282 MHz, CDCl_3) spectrum of **125l**.



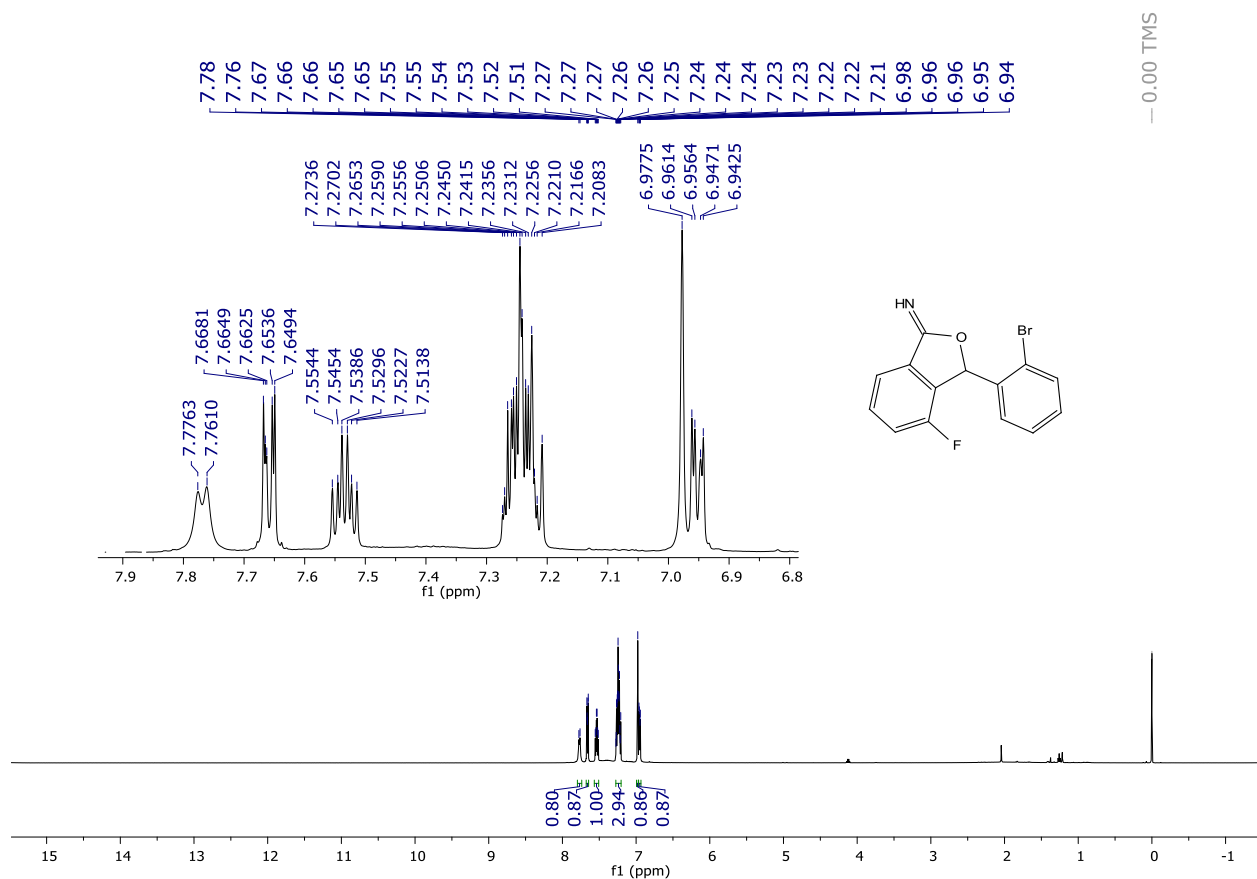
^1H NMR (500 MHz, CDCl_3) spectrum of **125m**.



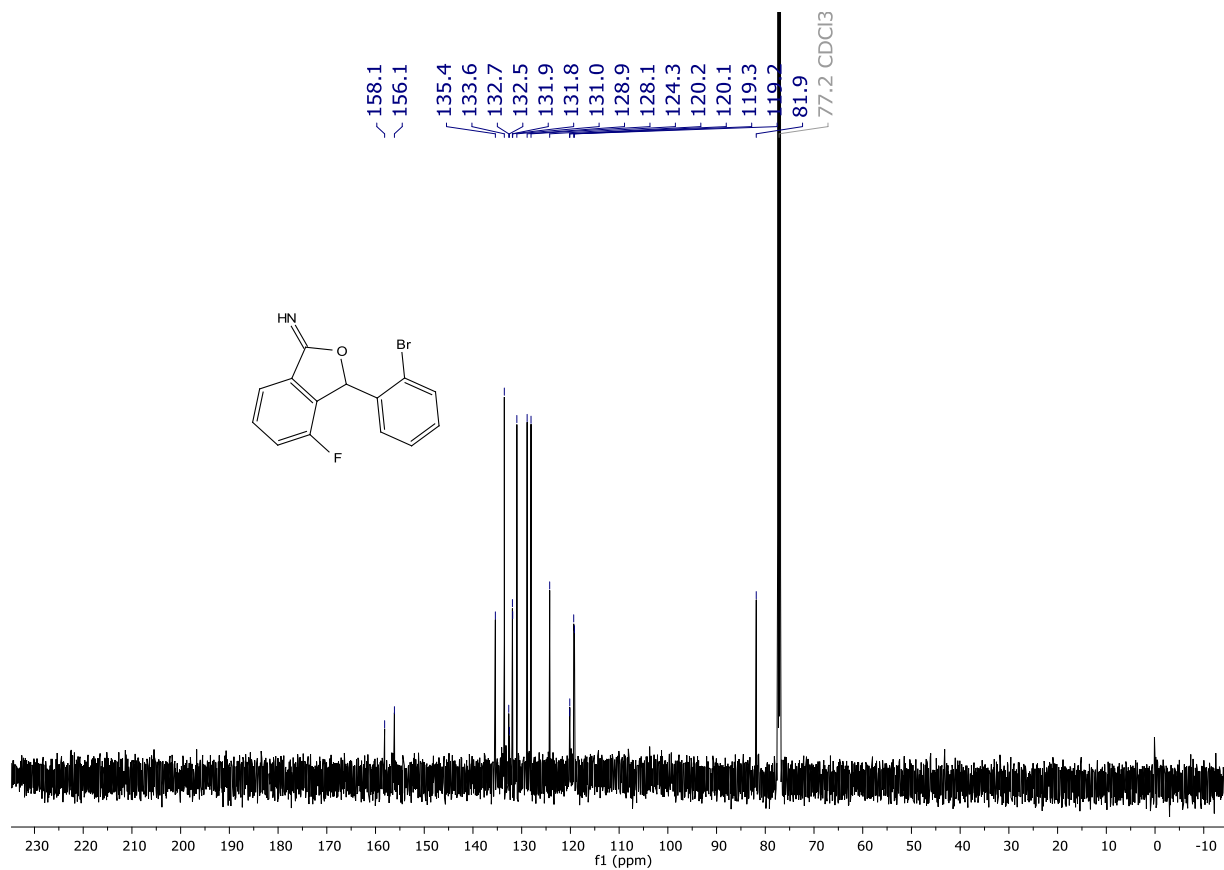
¹³C{¹H} NMR (126 MHz, CDCl₃) spectrum of **125m**.



¹⁹F NMR (282 MHz, CDCl₃) spectrum of **125m**.

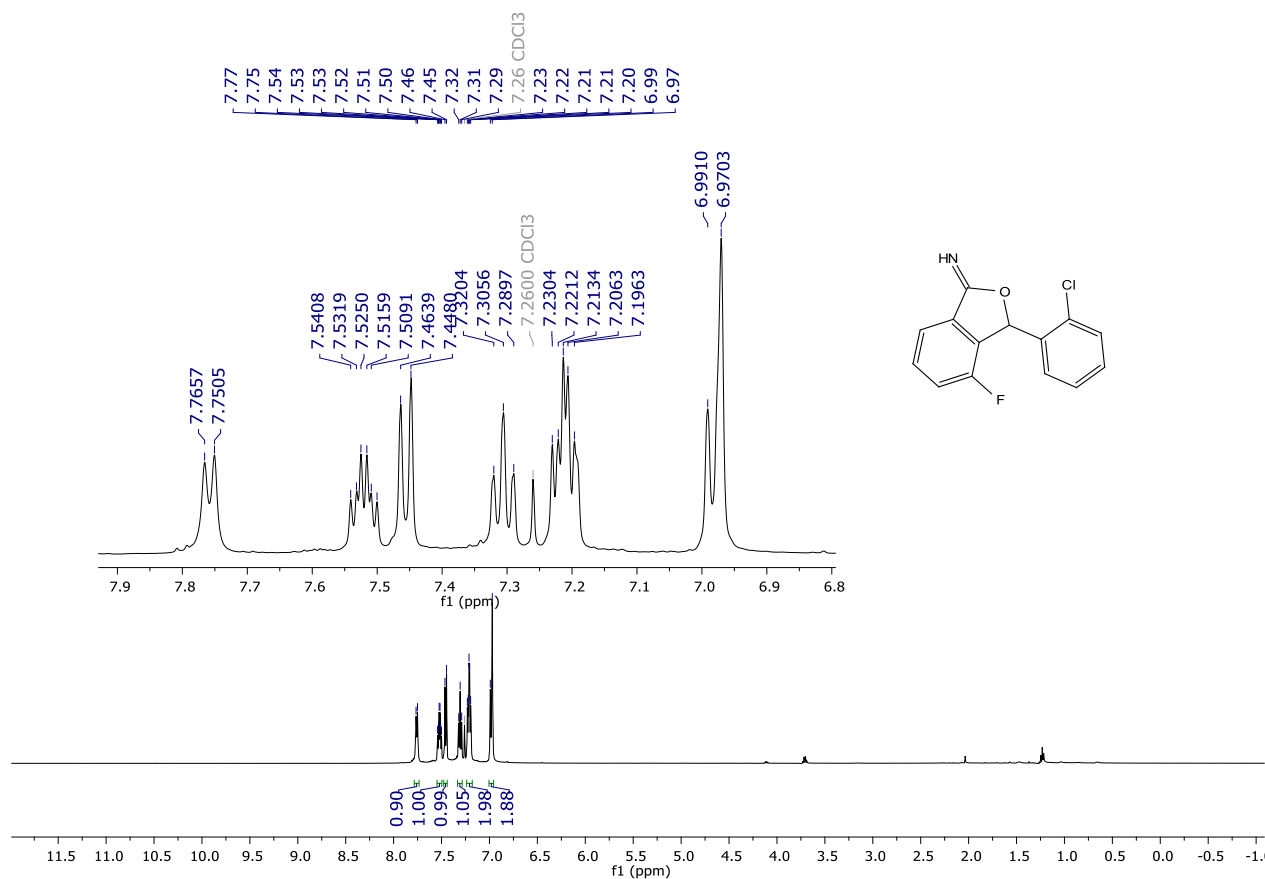


¹H NMR (500 MHz, CDCl₃) spectrum of **125n**.

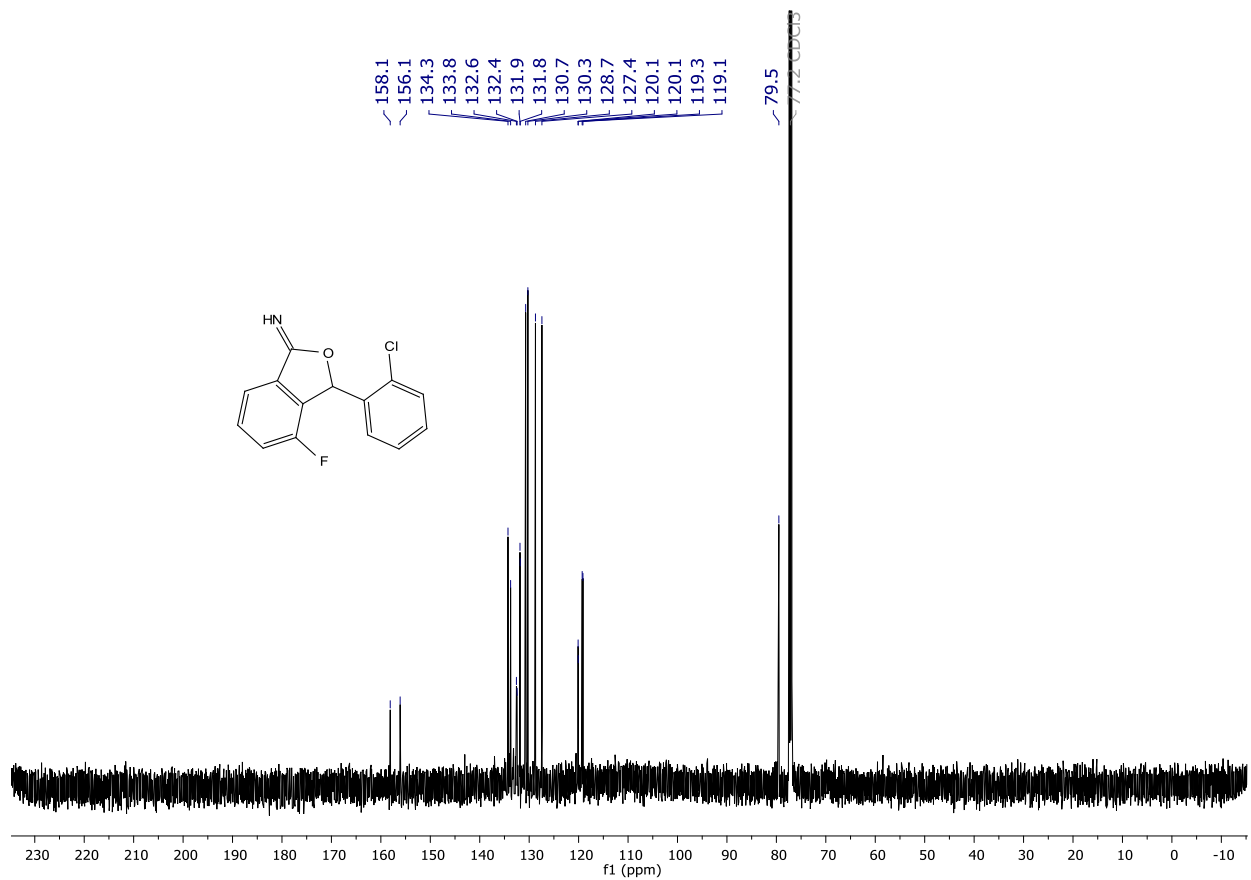


¹³C{¹H} NMR (126 MHz, CDCl₃) spectrum of **125n**.

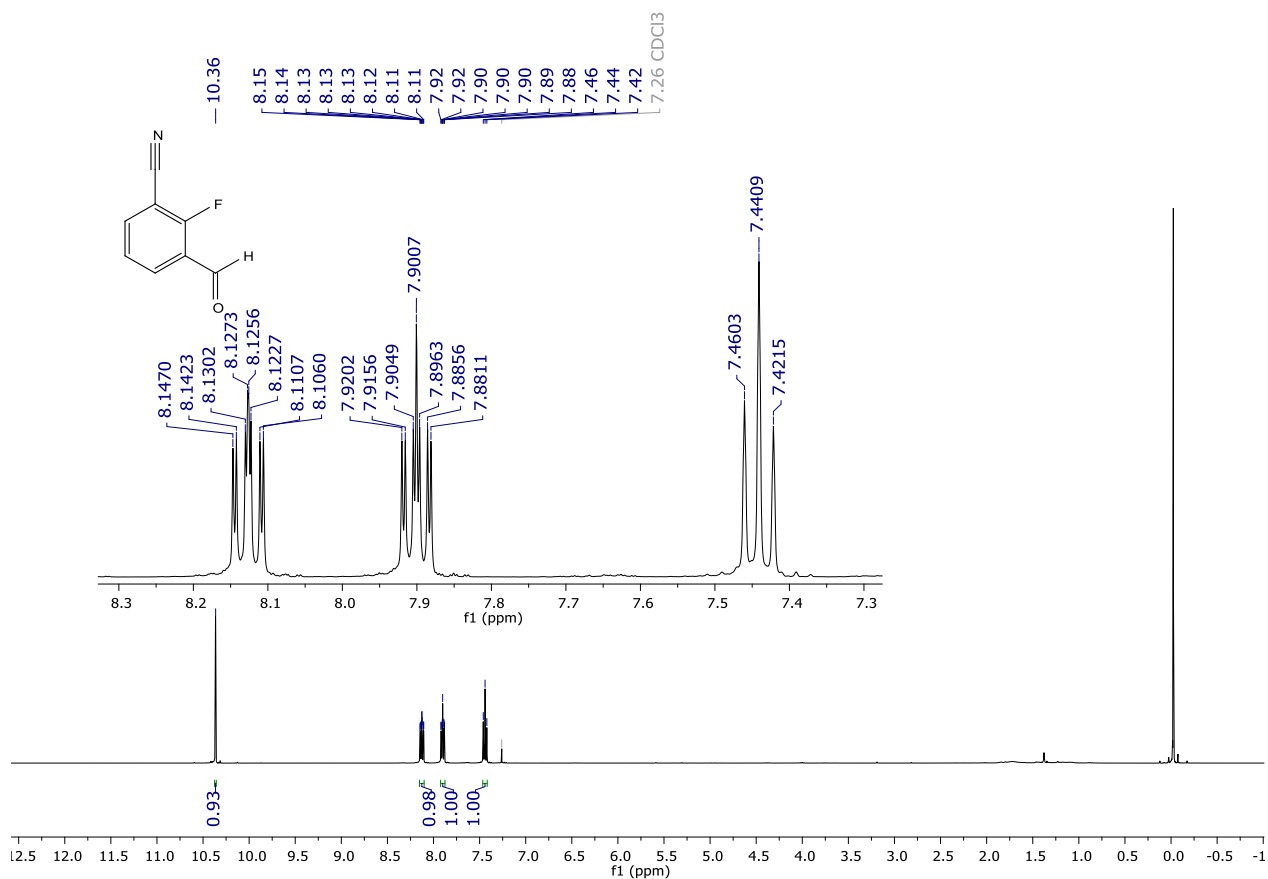
— 0.00 TMS



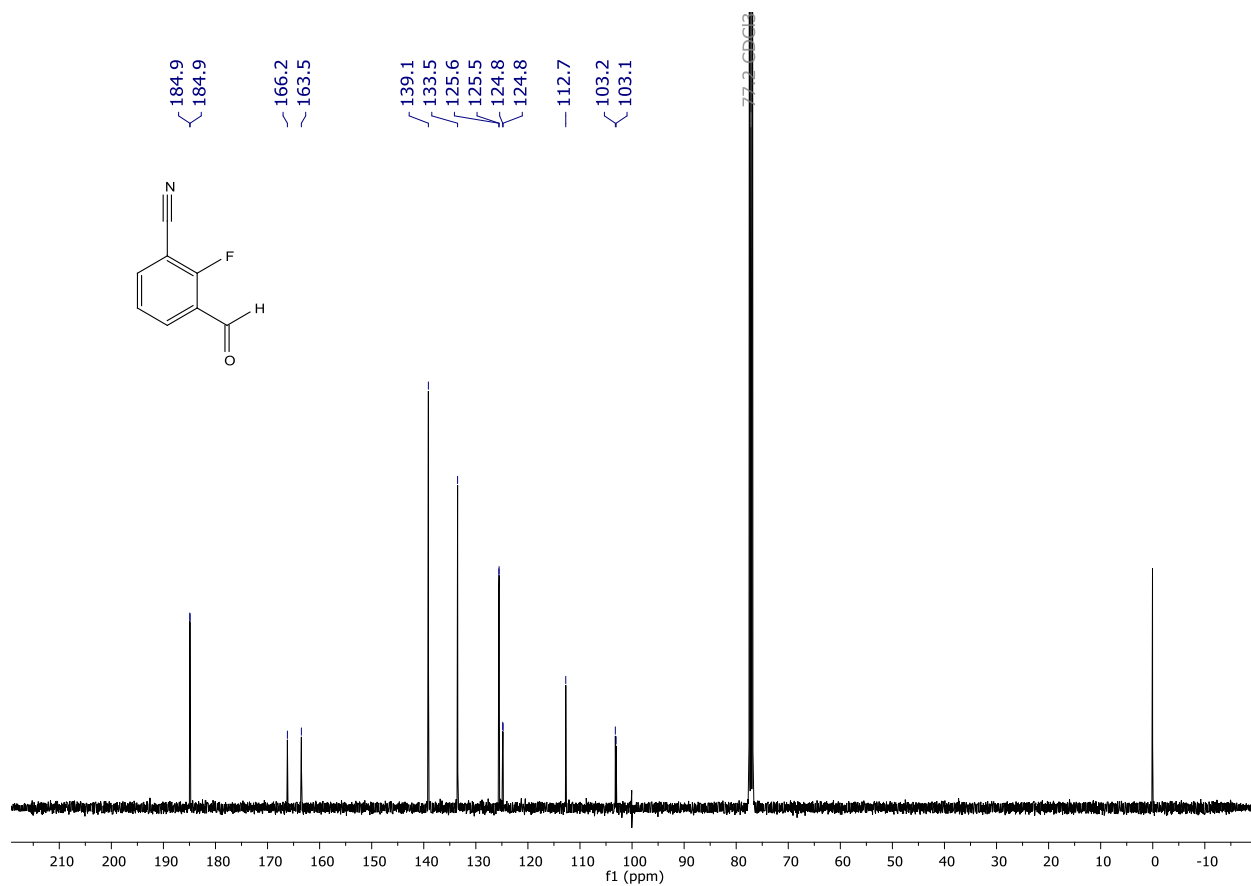
^1H NMR (500 MHz, CDCl_3) spectrum of **125o**.



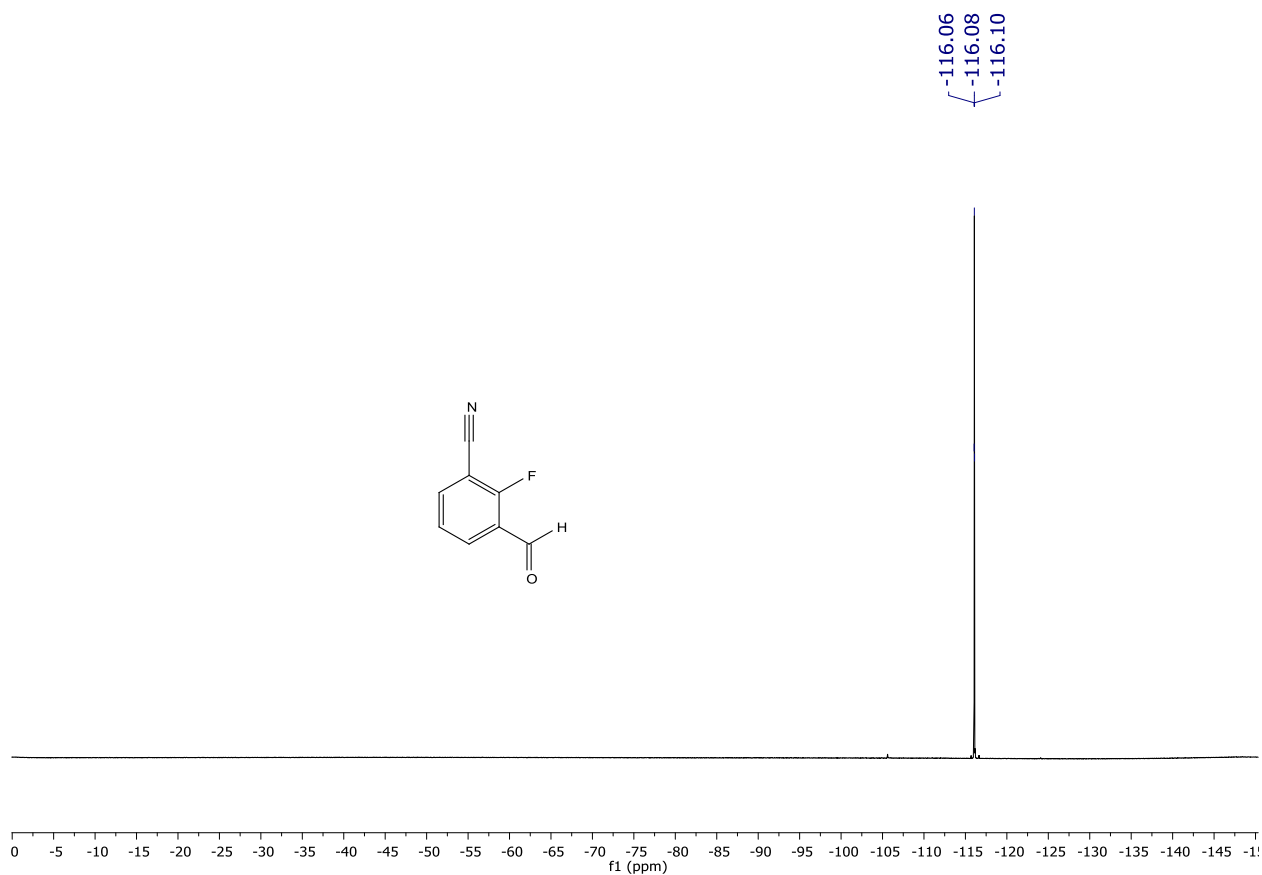
$^{13}\text{C}\{^1\text{H}\}$ NMR (126 MHz, CDCl_3) spectrum of **125o**.



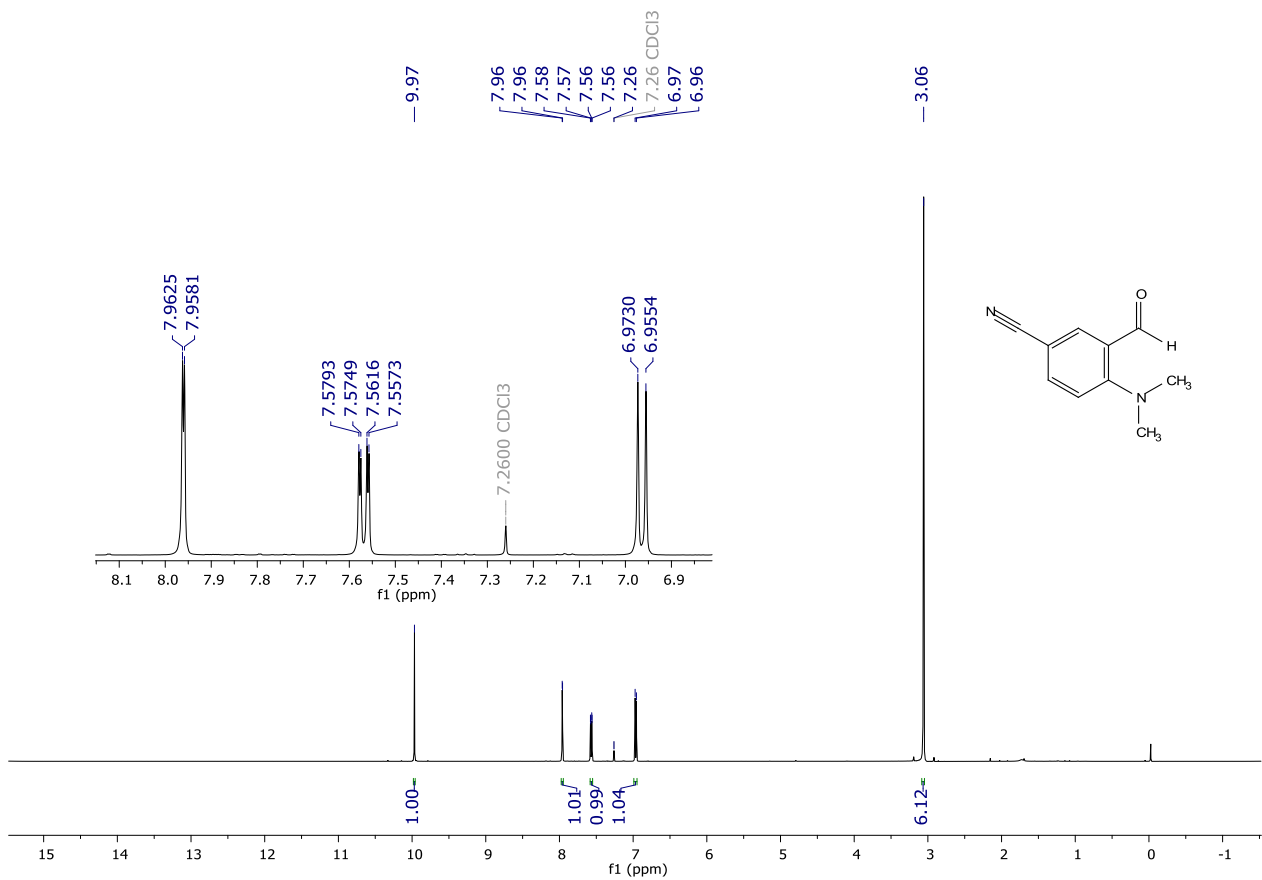
¹H NMR (400 MHz, CDCl₃) spectrum of 125p.



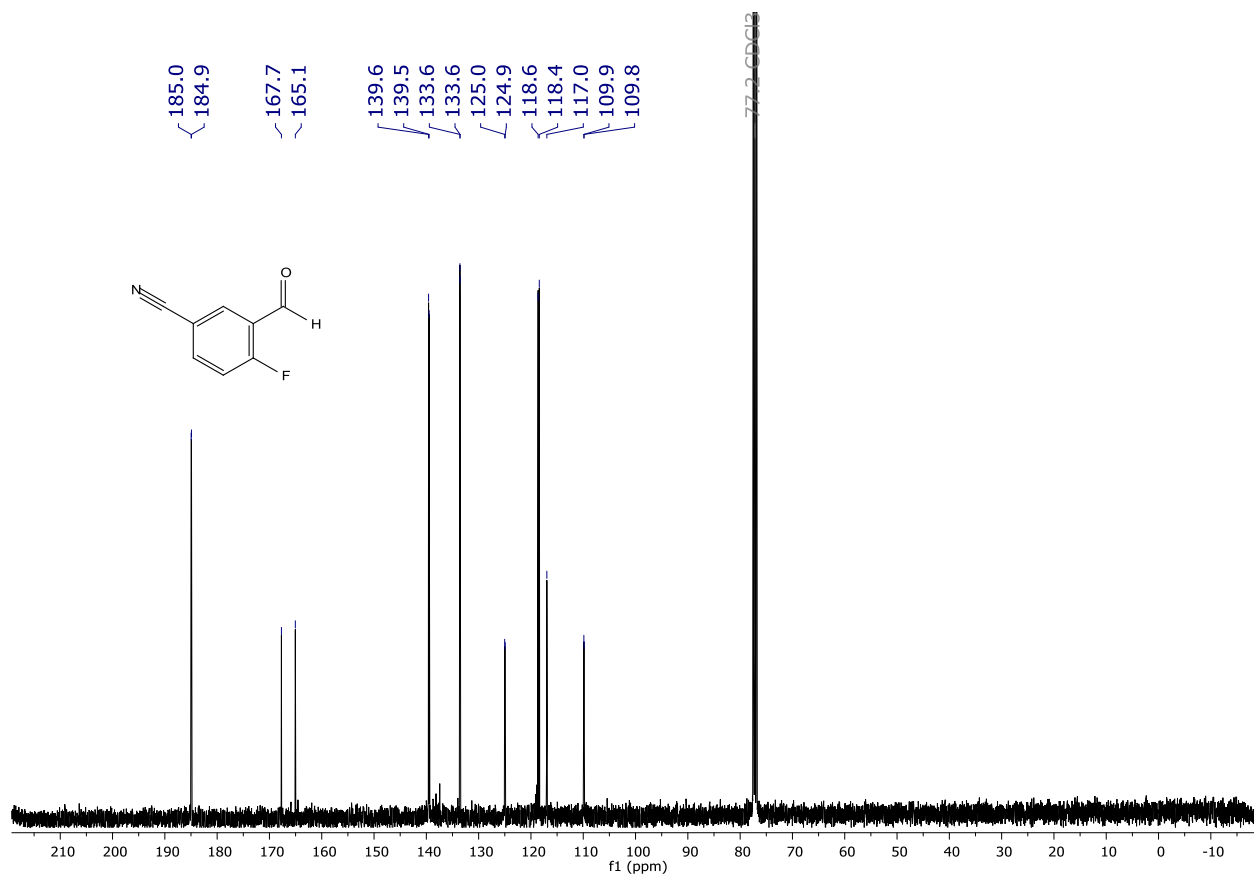
¹³C{¹H} NMR (101 MHz, CDCl₃) spectrum of 125p.



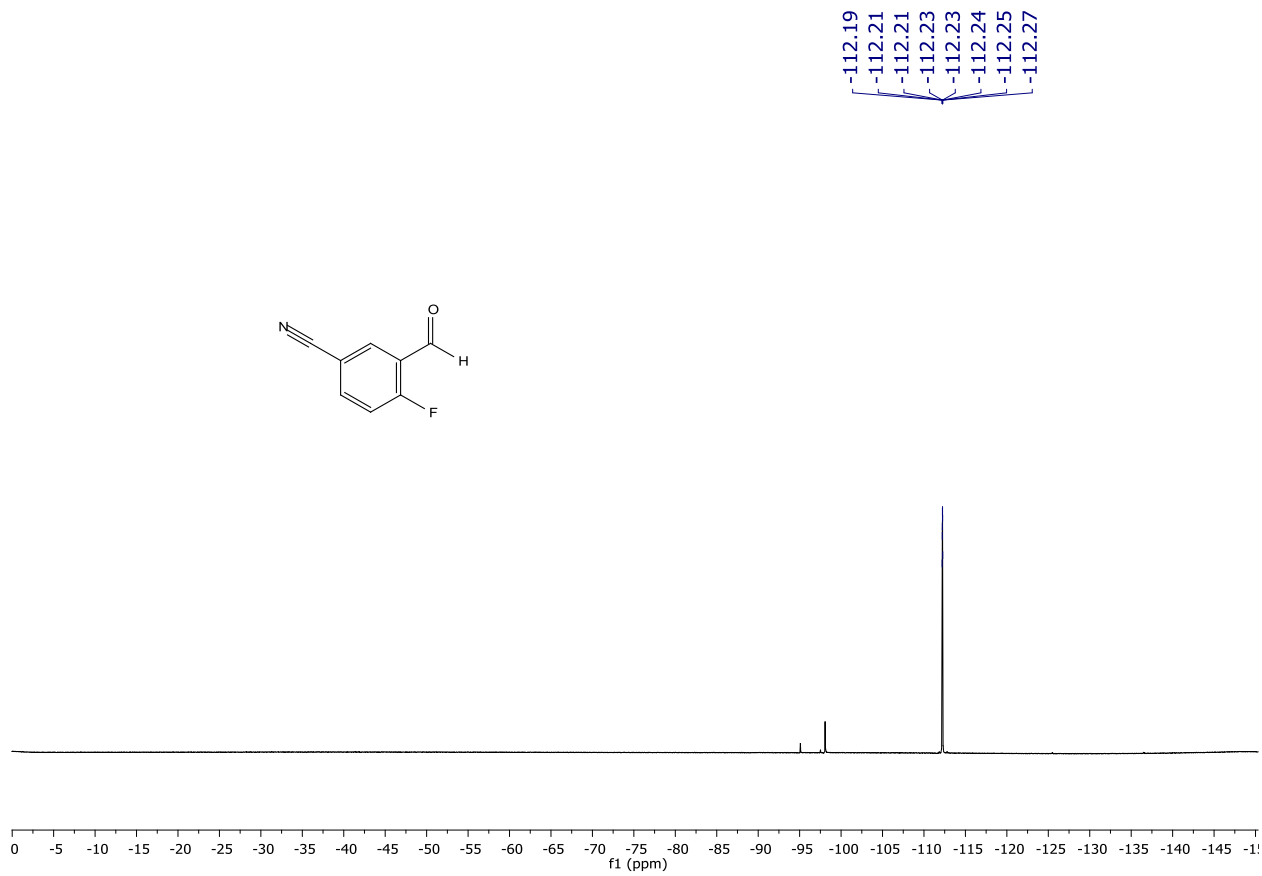
¹⁹F NMR (282 MHz, CDCl₃) spectrum of **125p**.



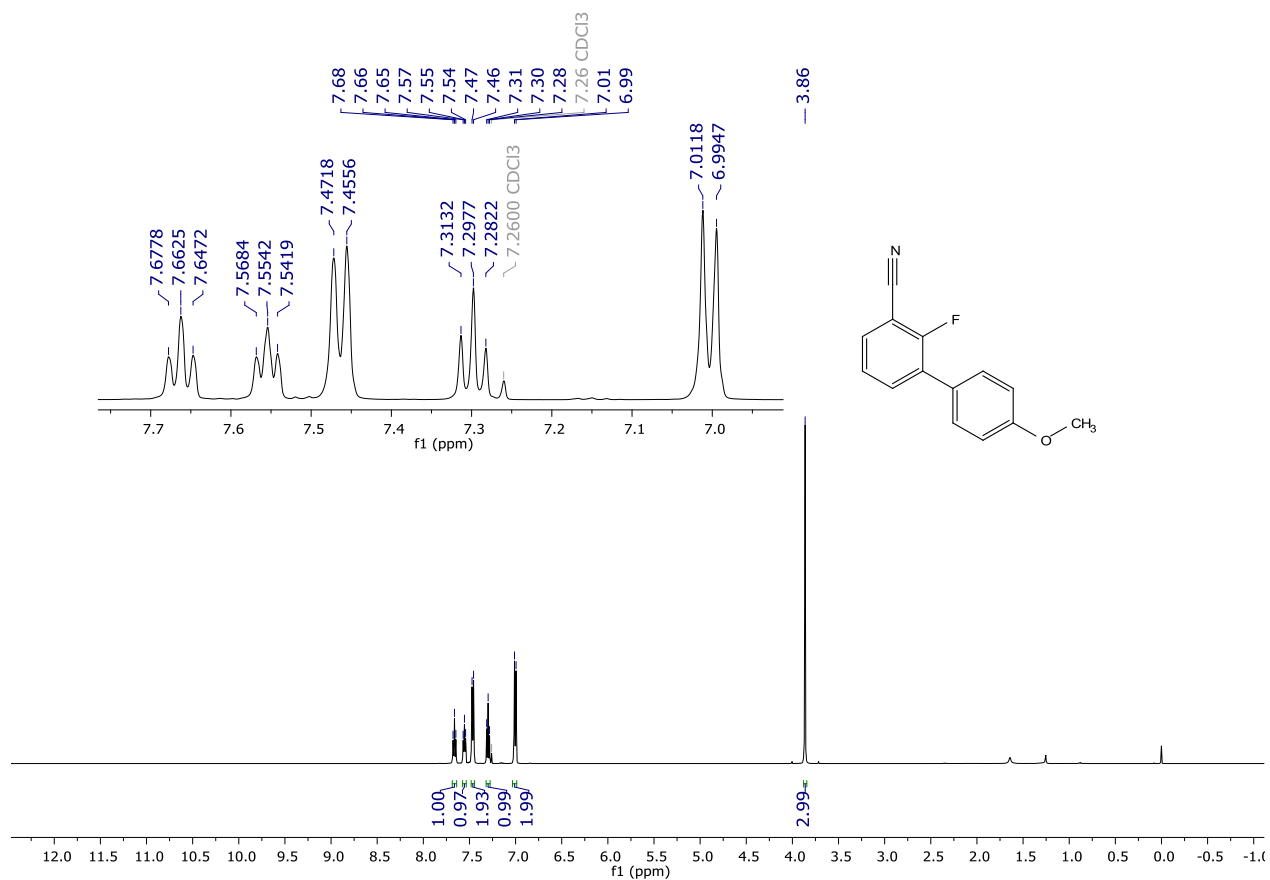
¹H NMR (500 MHz, CDCl₃) spectrum of **125q**.



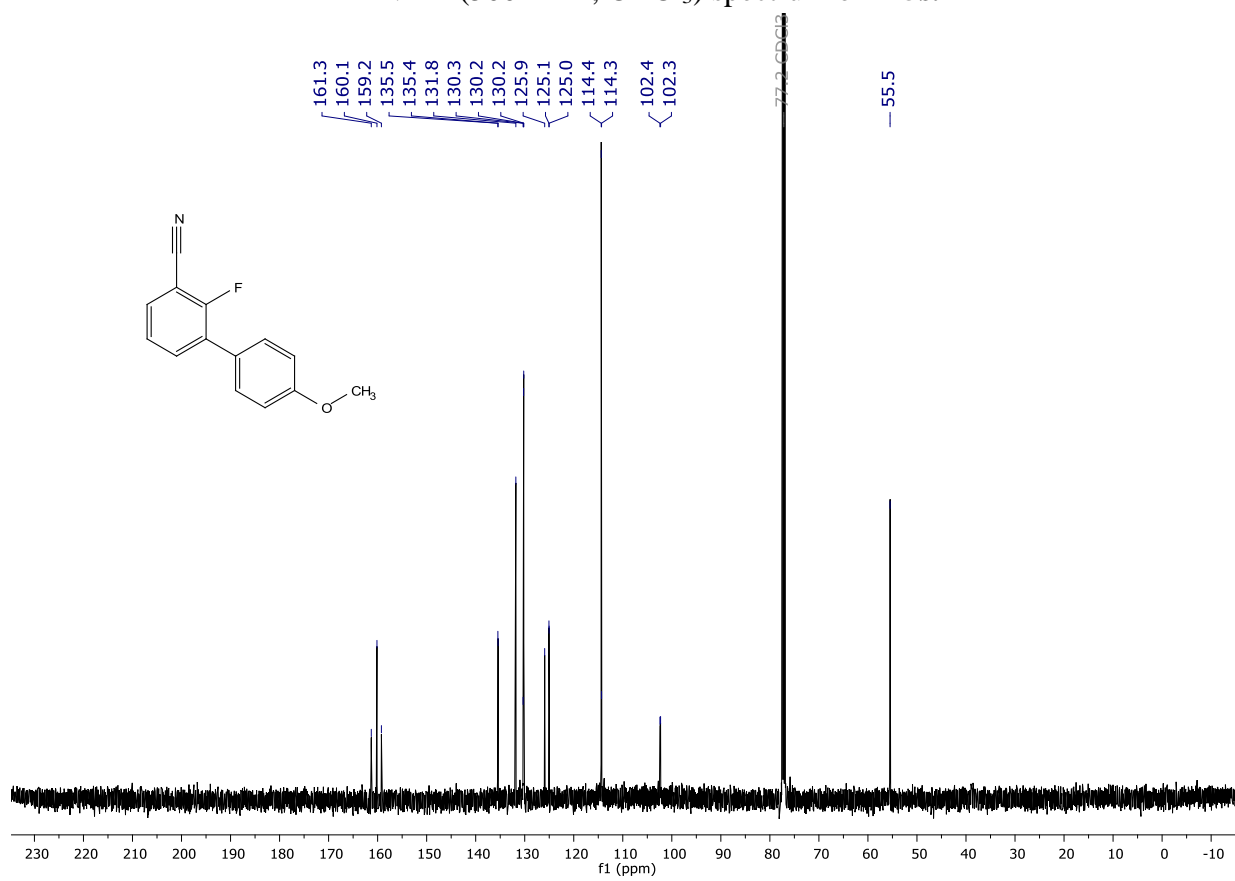
$^{13}\text{C}\{^1\text{H}\}$ NMR (101 MHz, CDCl_3) spectrum of **125r**.



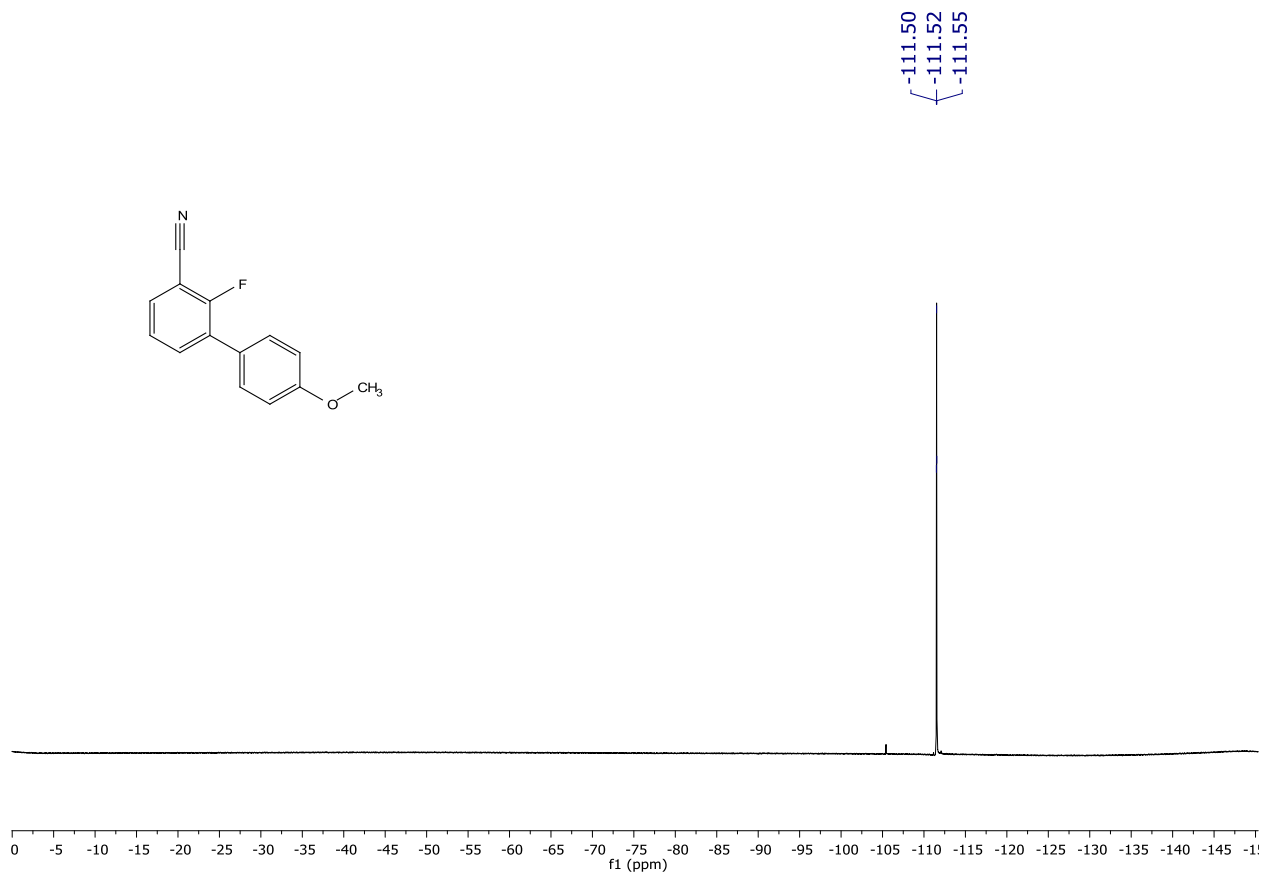
^{19}F NMR (282 MHz, CDCl_3) spectrum of **125r**.



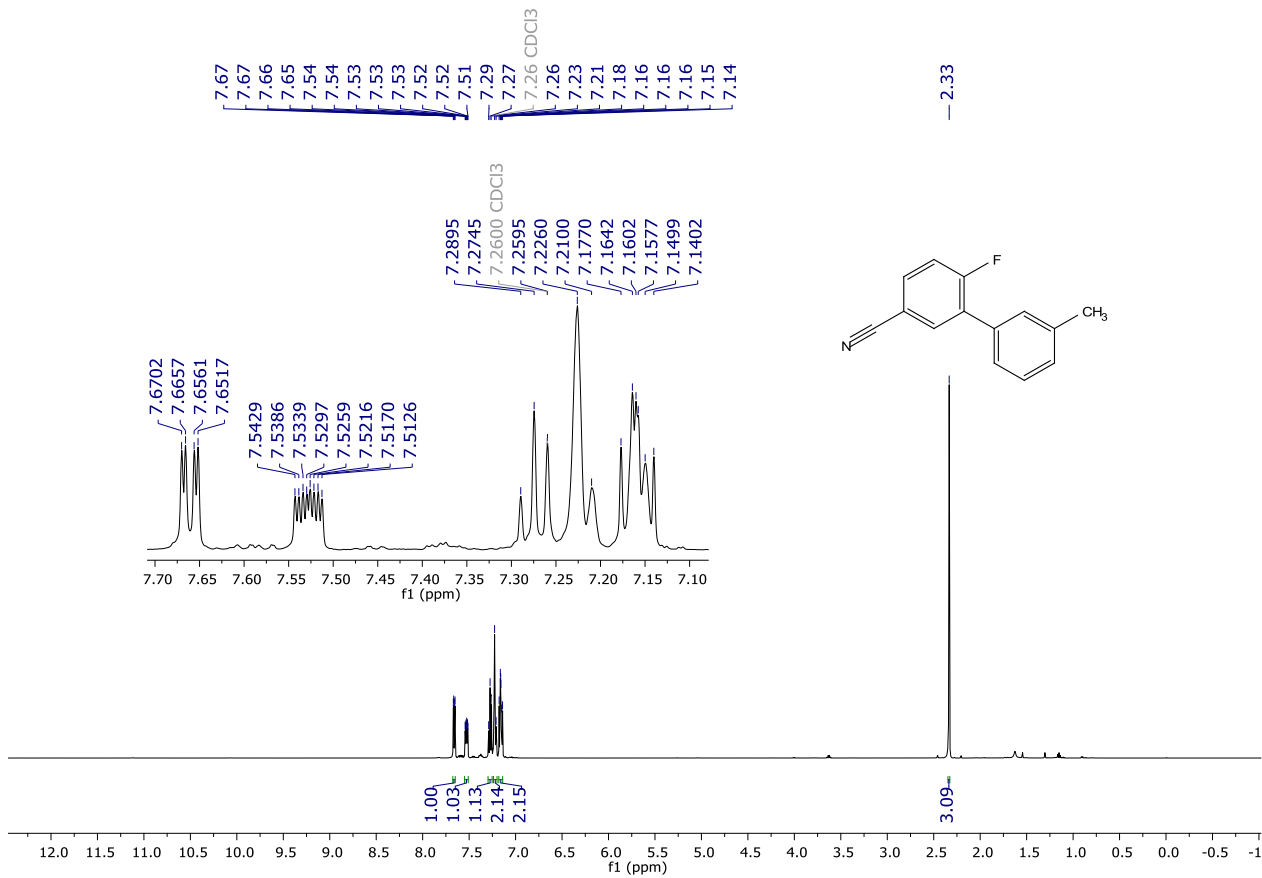
^1H NMR (500 MHz, CDCl_3) spectrum of **125s**.



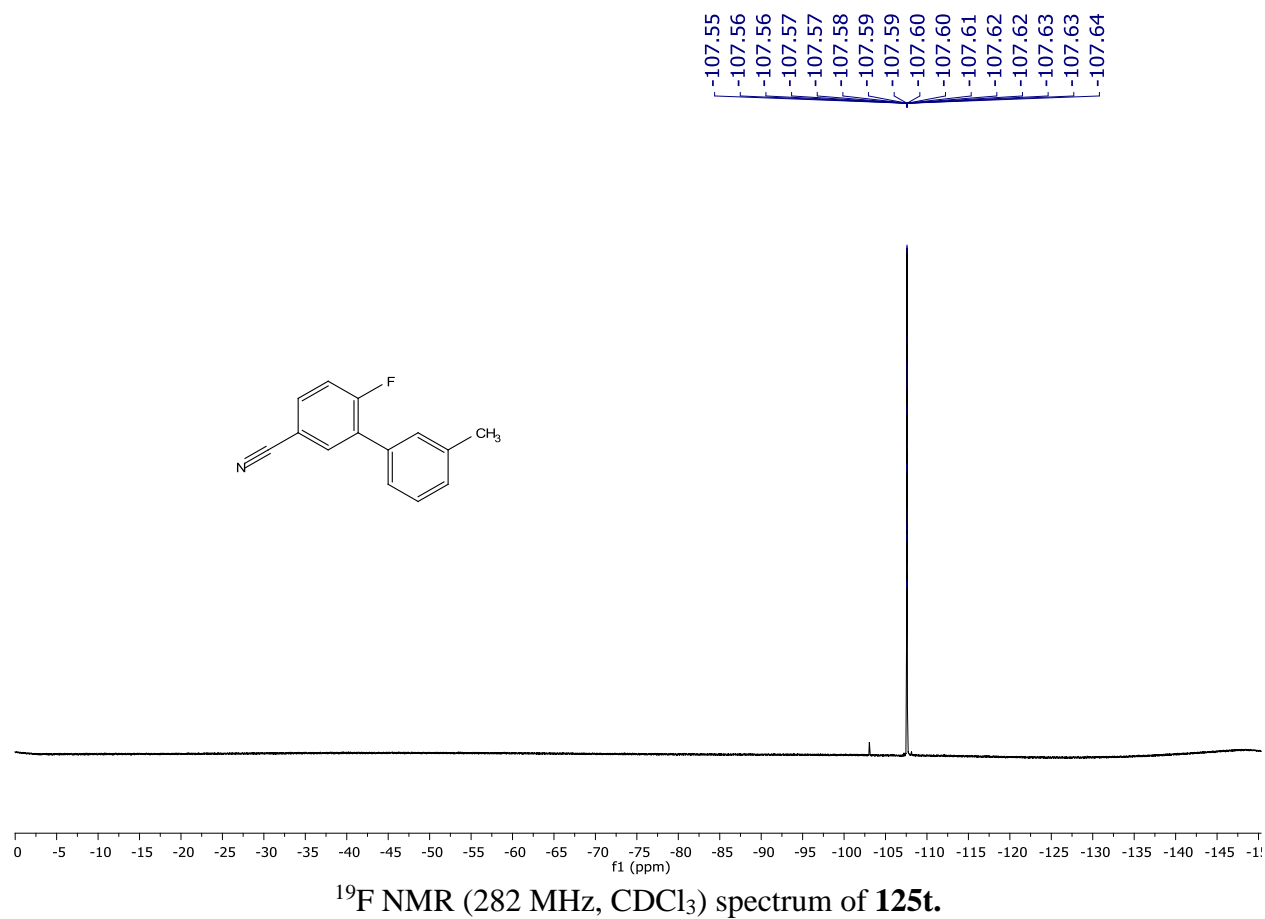
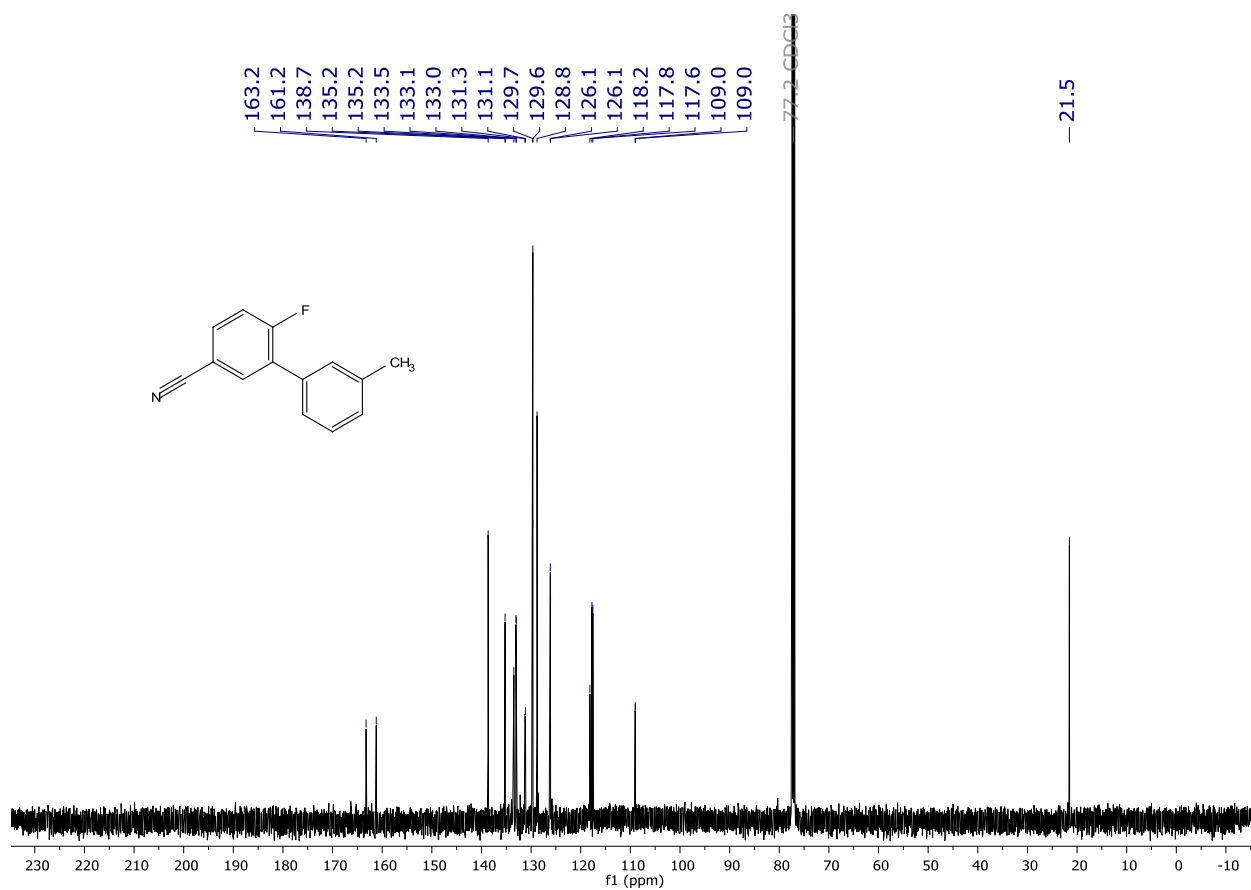
$^{13}\text{C}\{^1\text{H}\}$ NMR (126 MHz, CDCl_3) spectrum of **125s**.

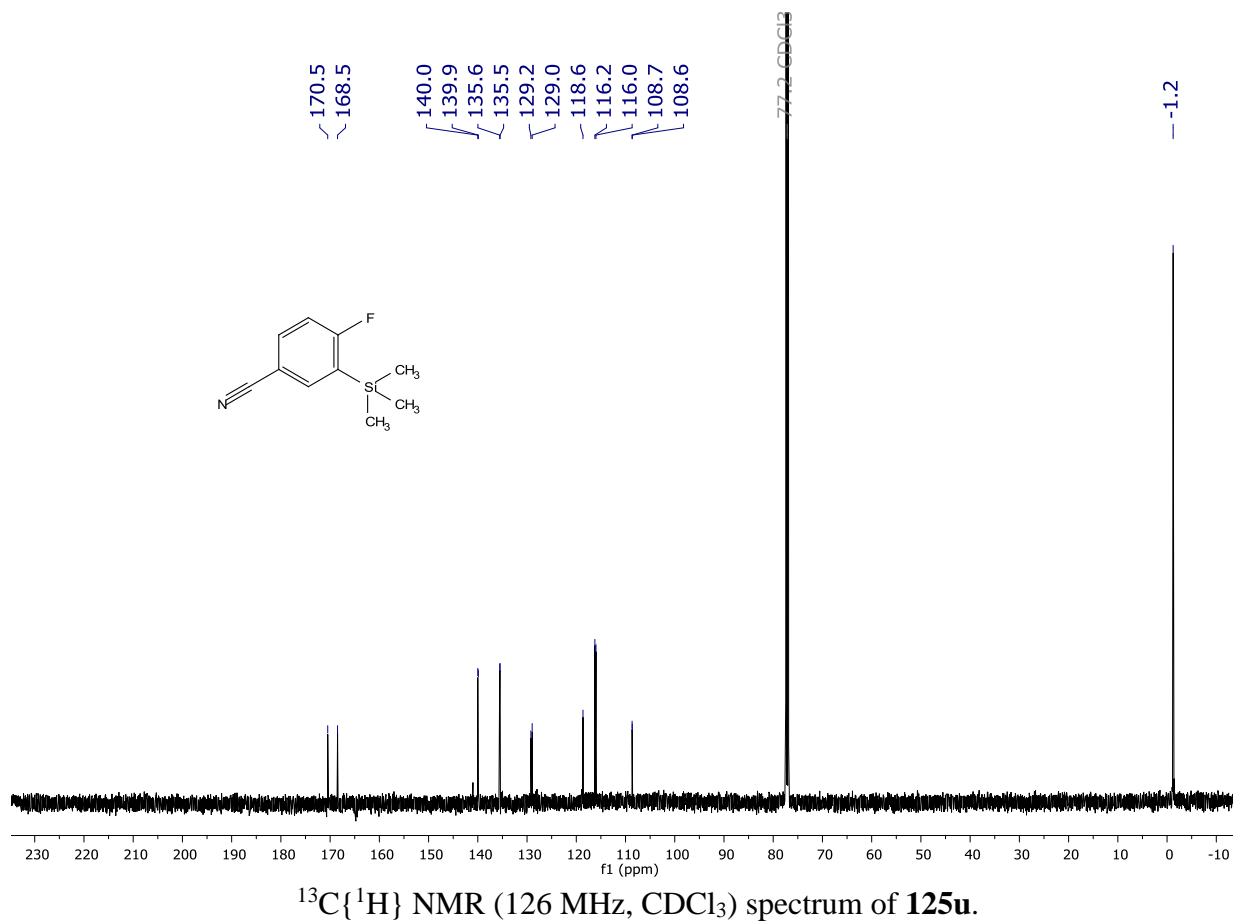
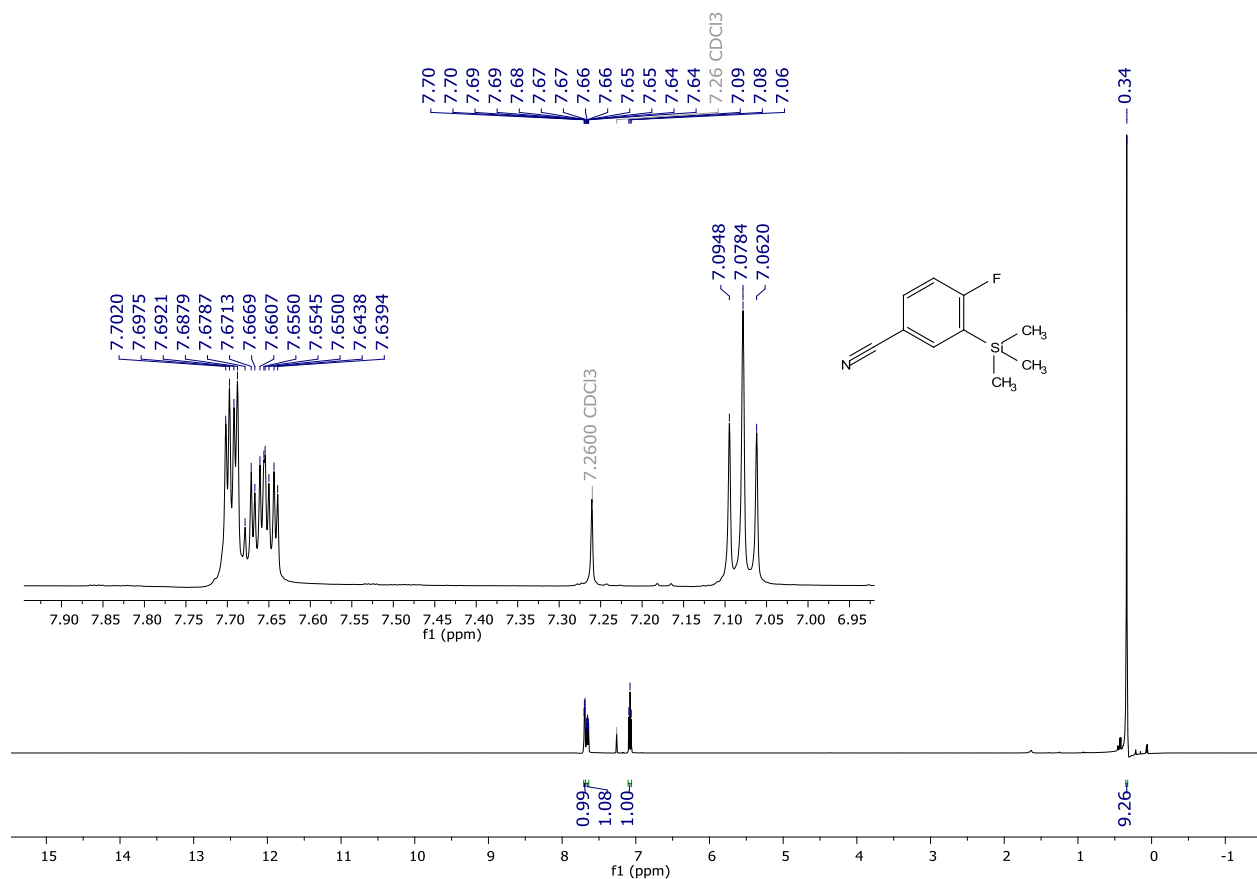


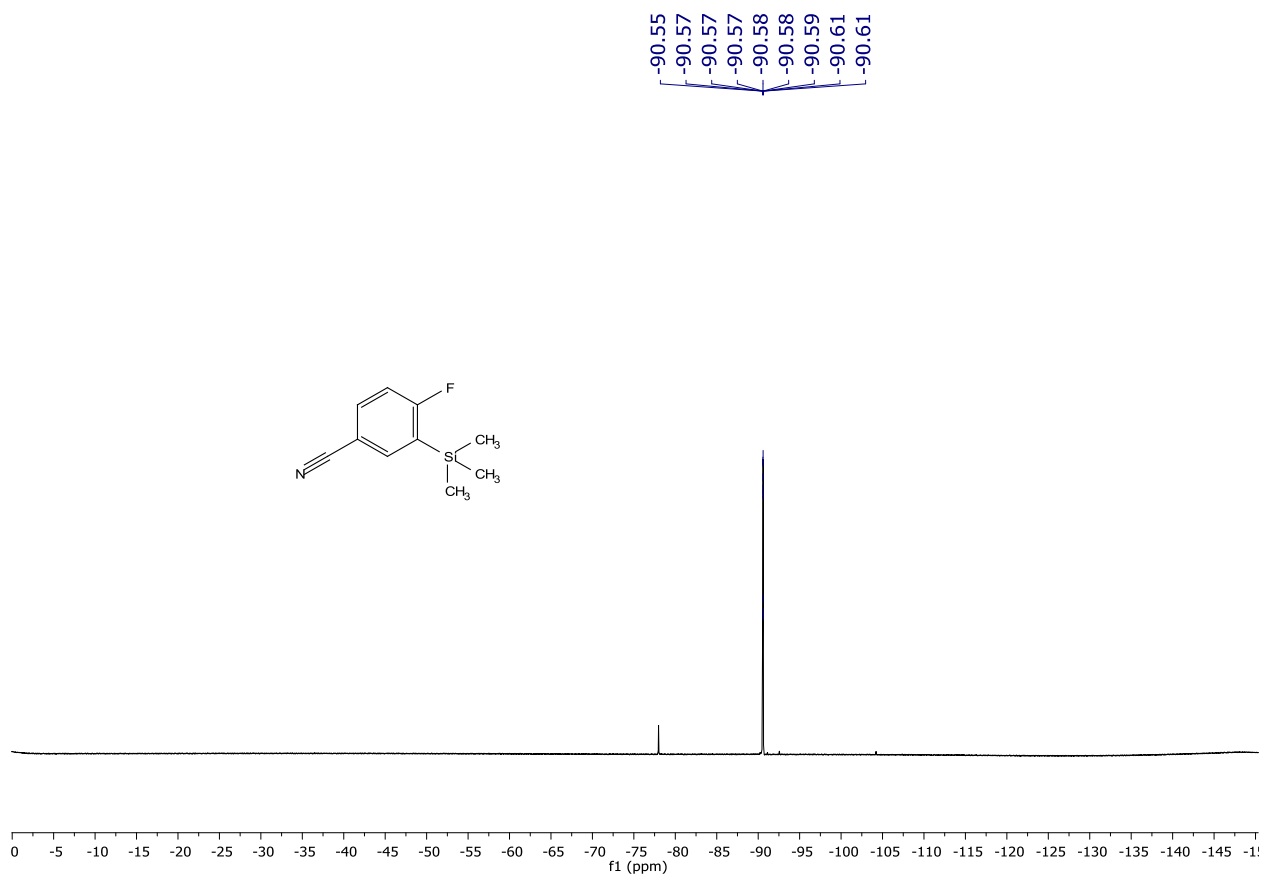
^{19}F NMR (282 MHz, CDCl_3) spectrum of **125s**.



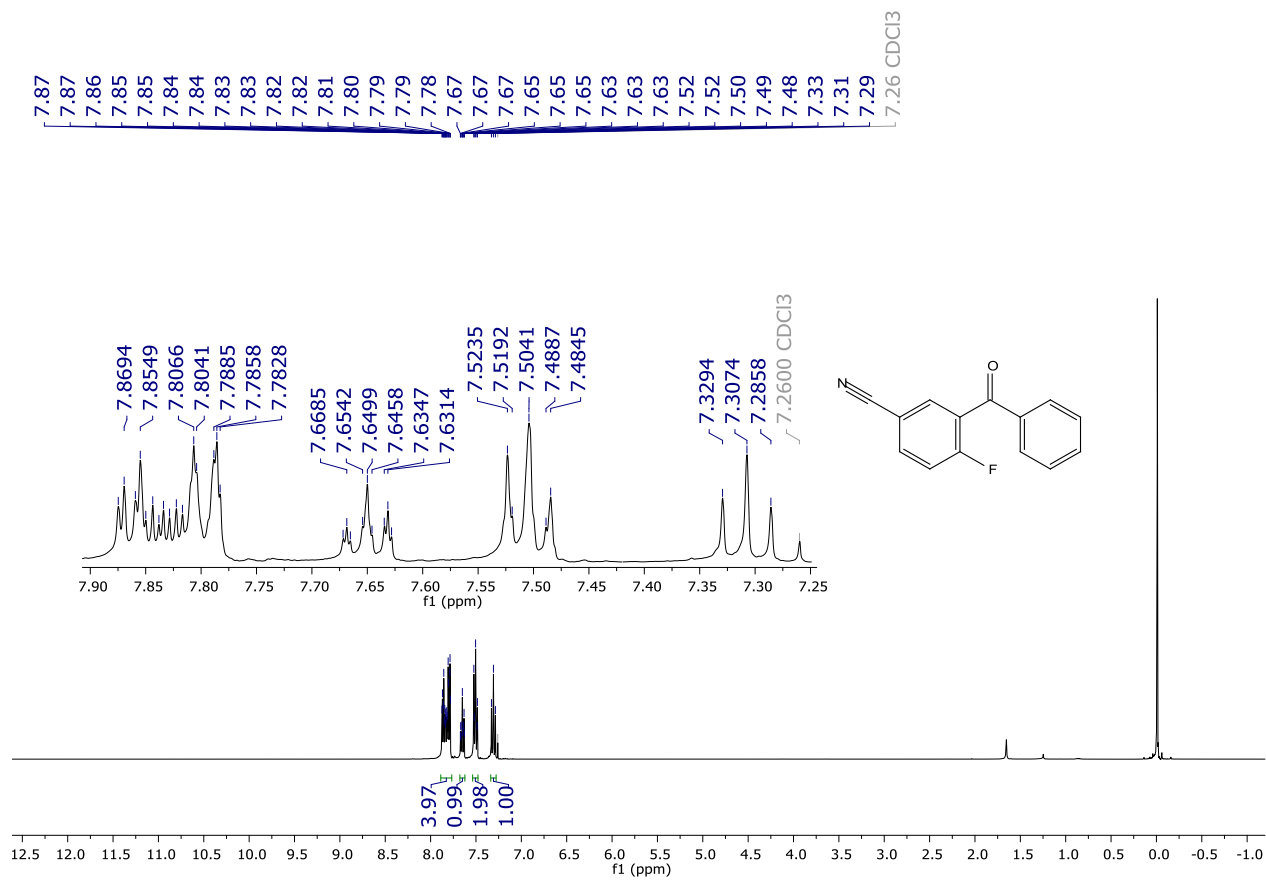
^1H NMR (500 MHz, CDCl_3) spectrum of **125t**.



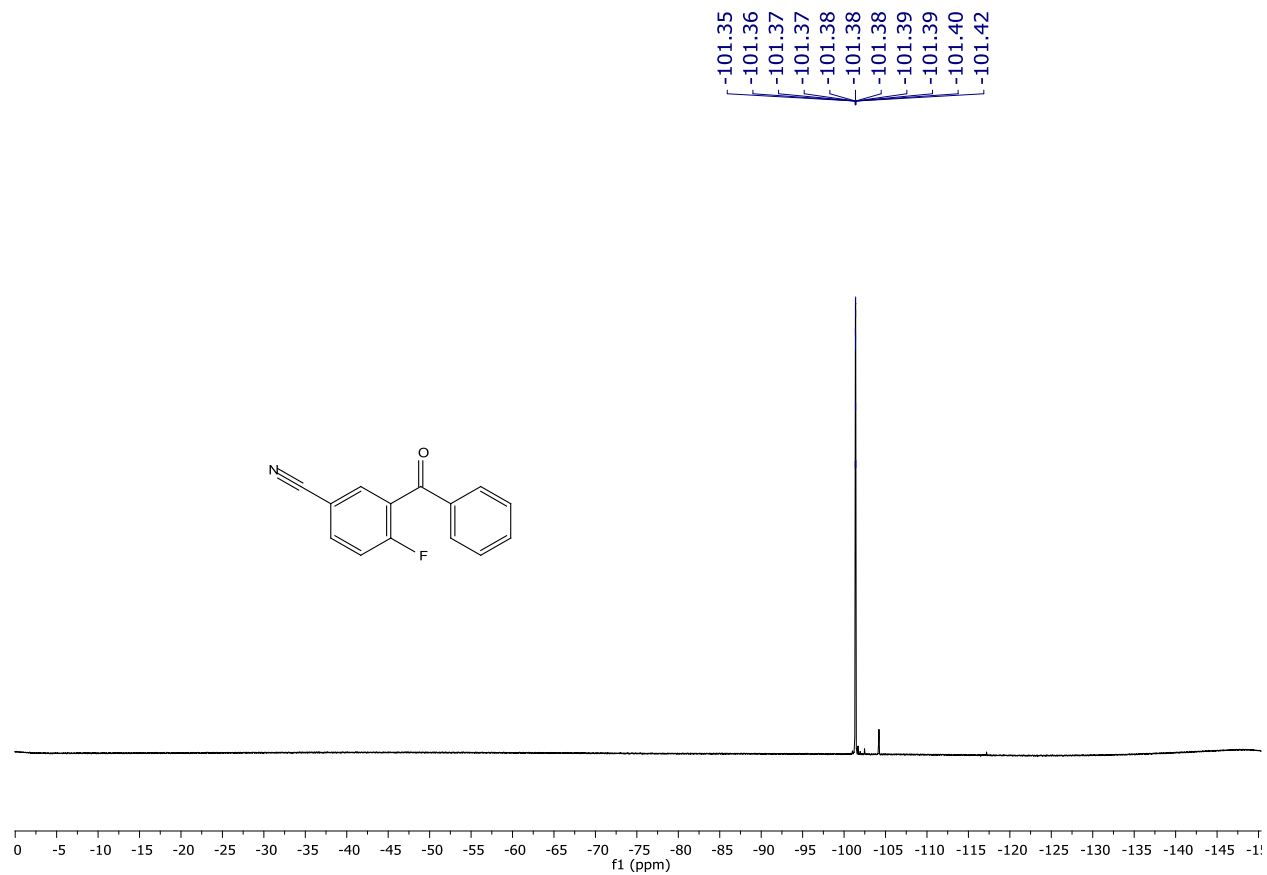
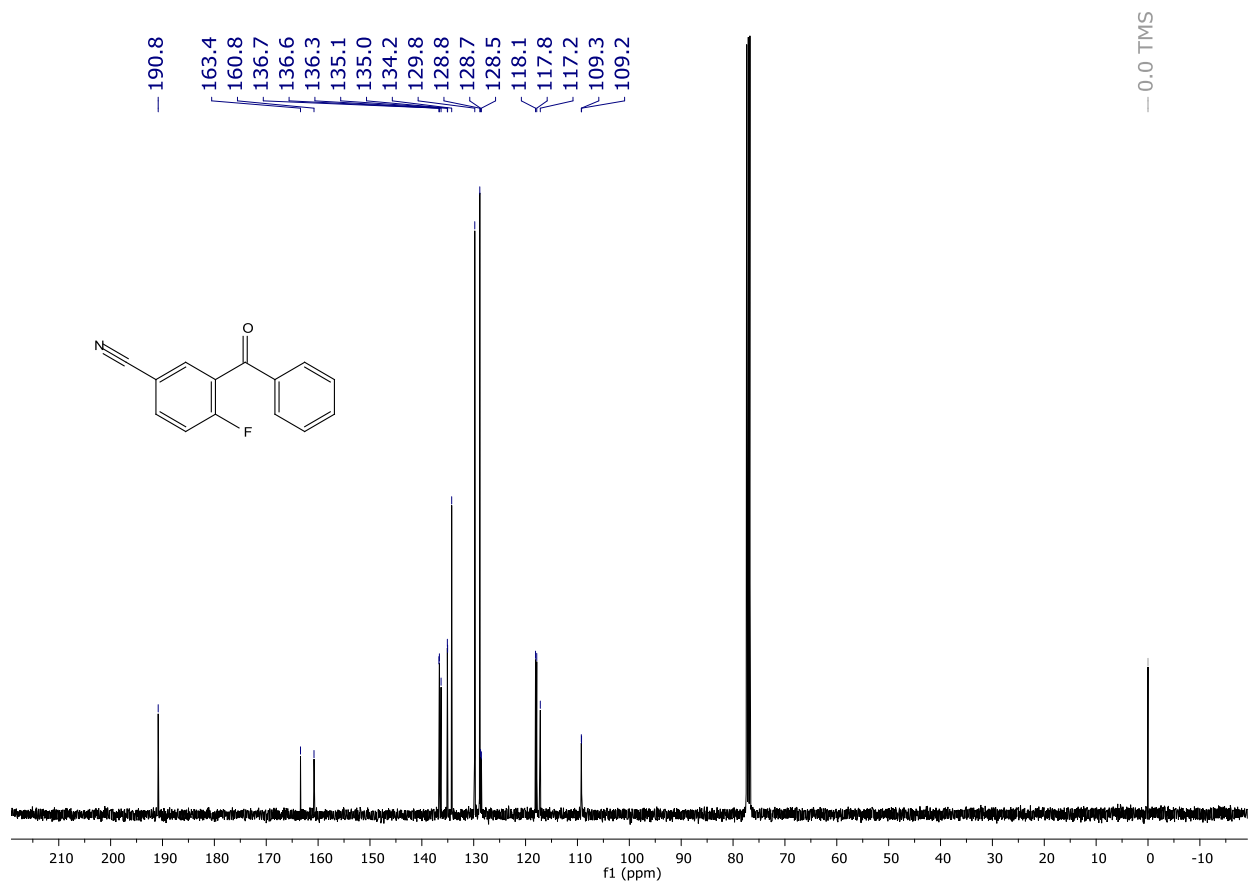


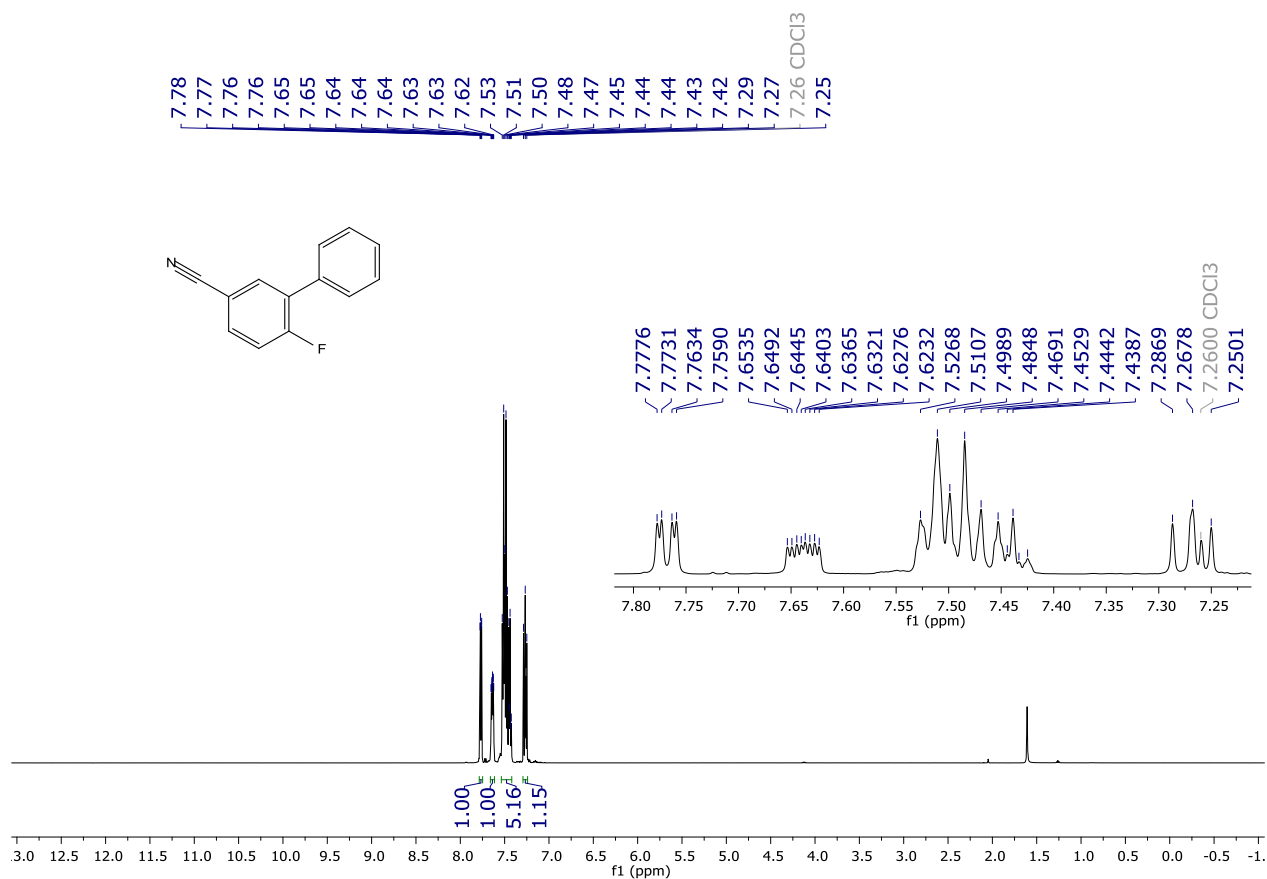


^{19}F NMR (282 MHz, CDCl_3) spectrum of **125u**.

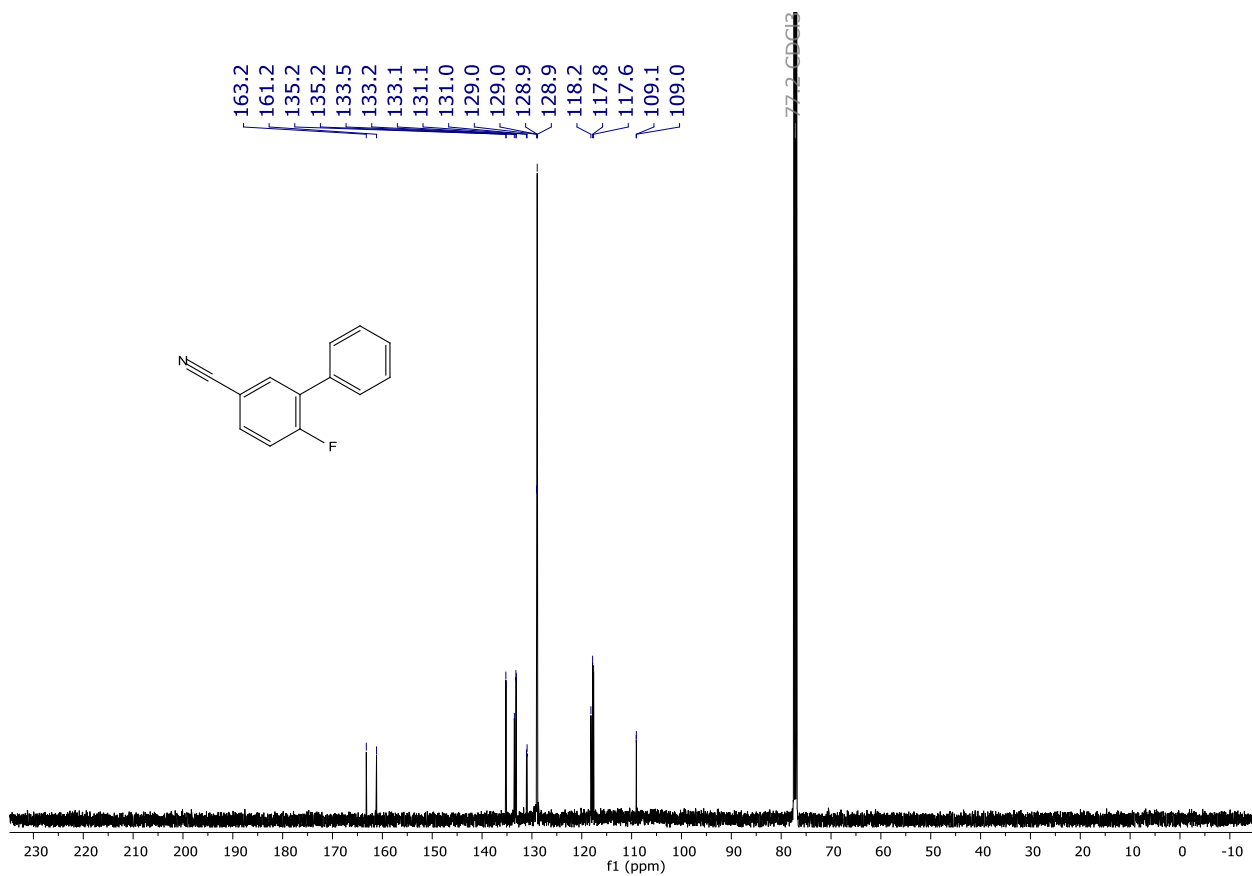


^1H NMR (400 MHz, CDCl_3) spectrum of **125v**.

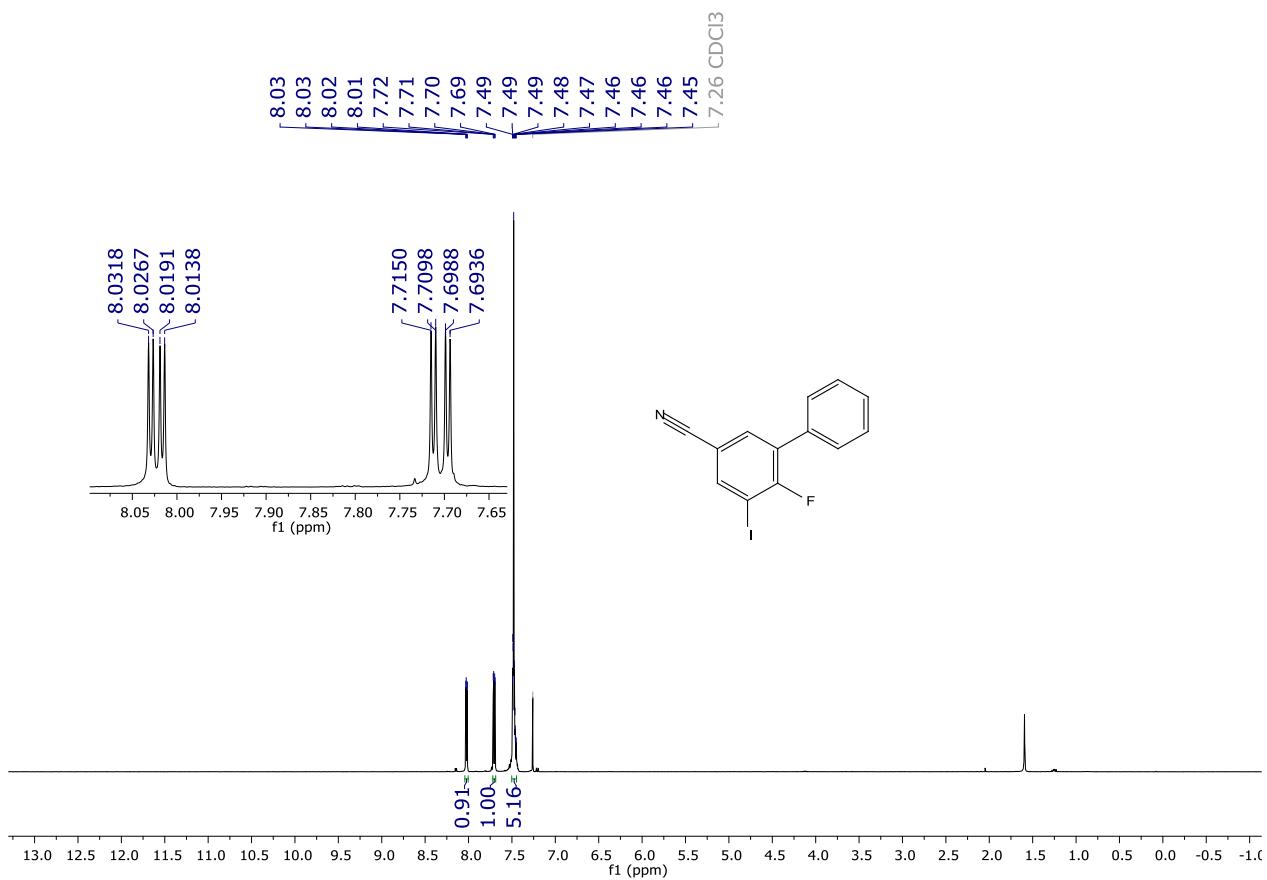
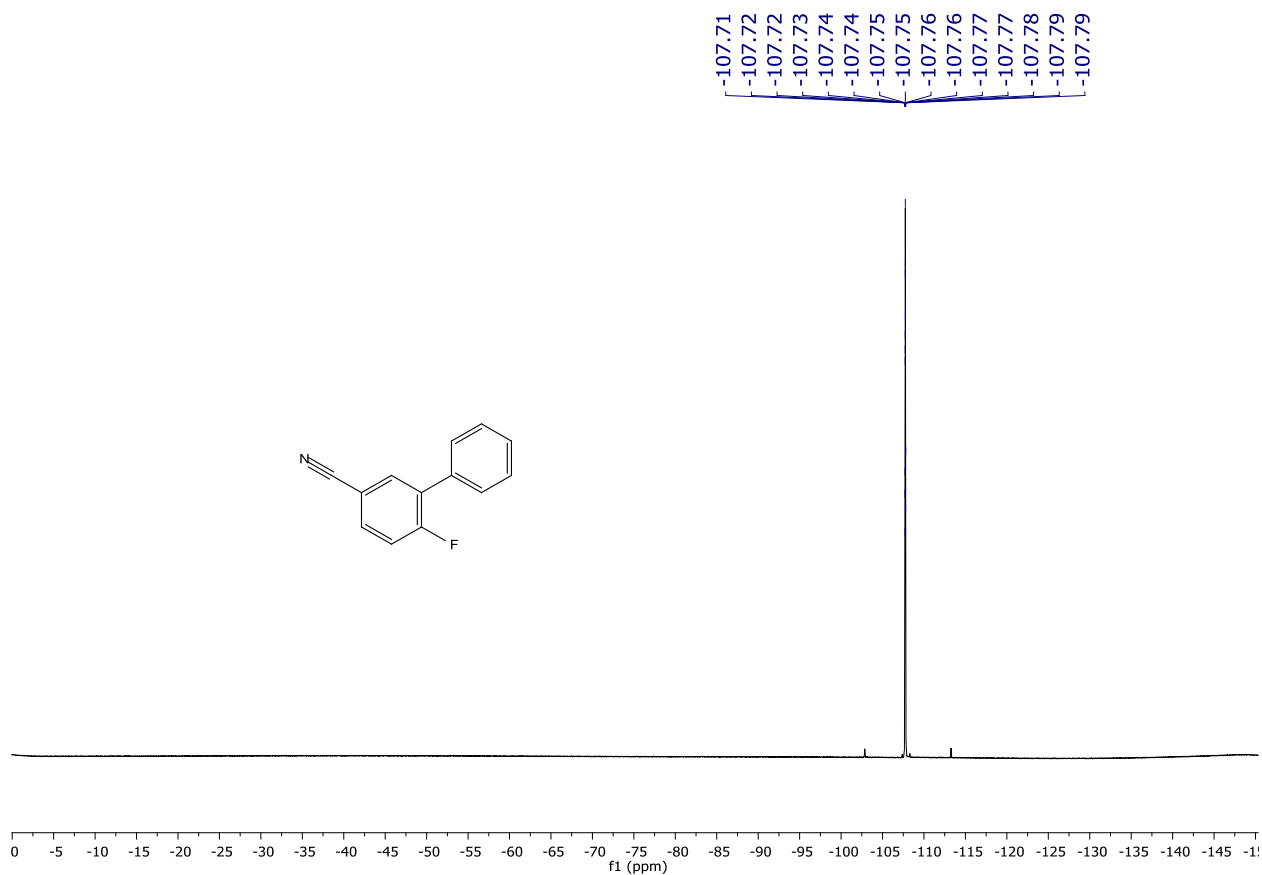




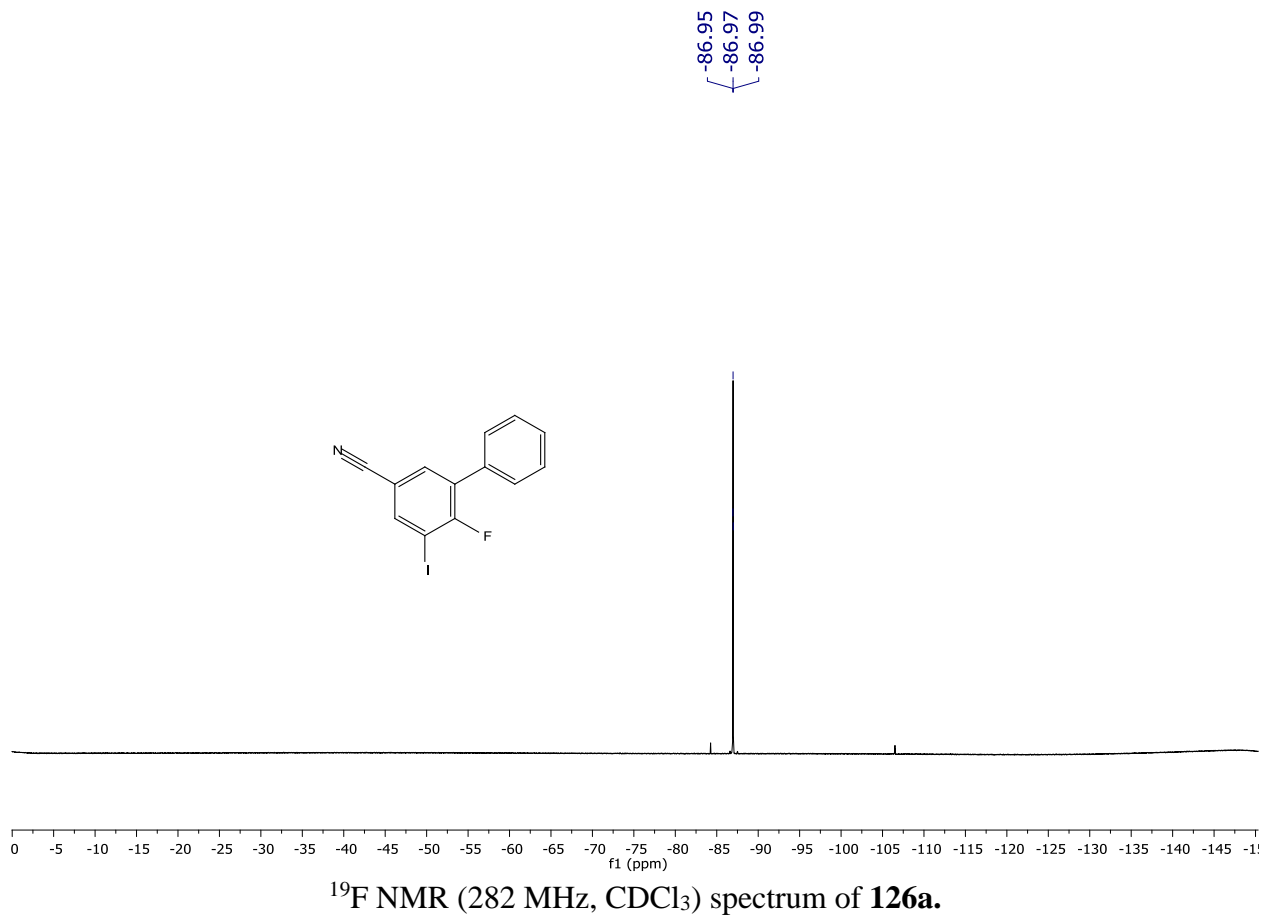
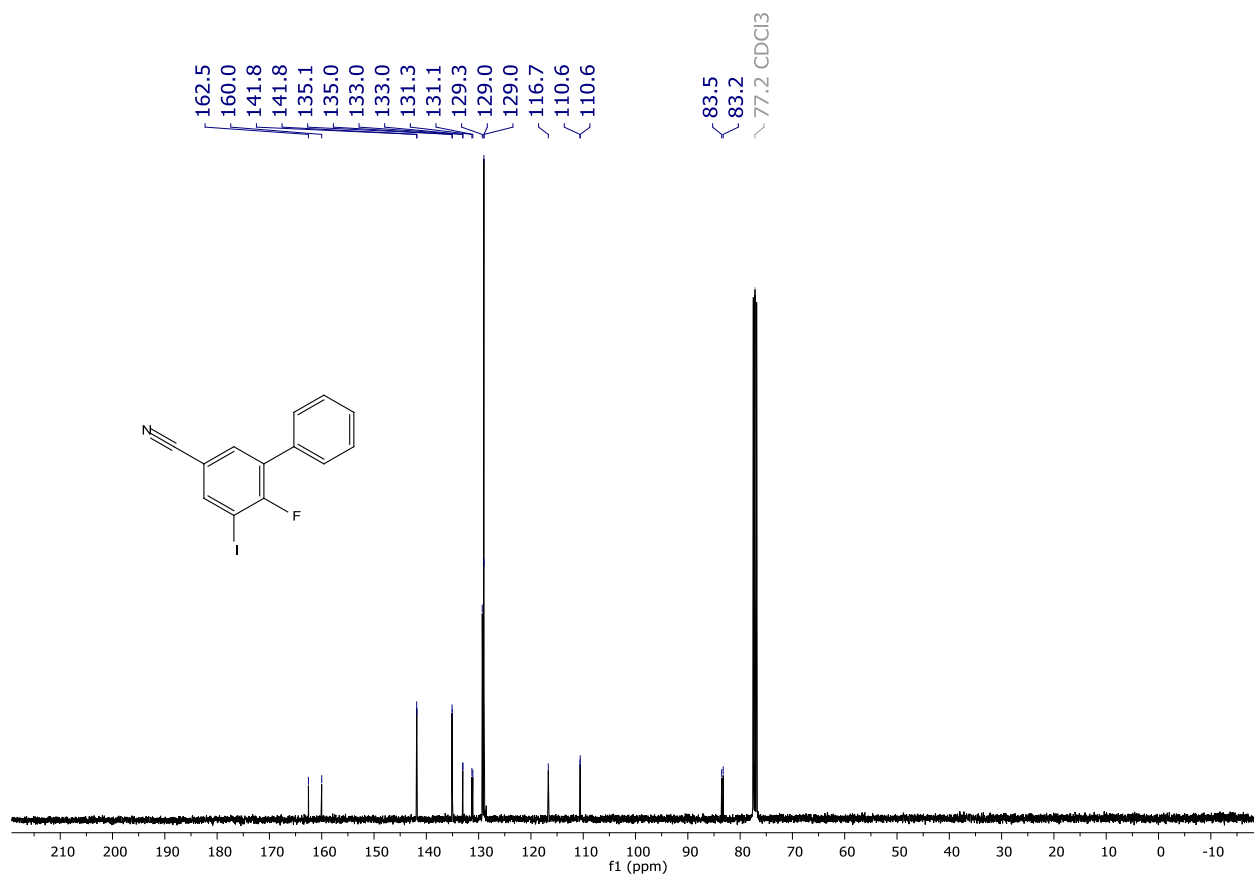
$^1\text{H NMR}$ (400 MHz, CDCl_3) spectrum of **125w**.

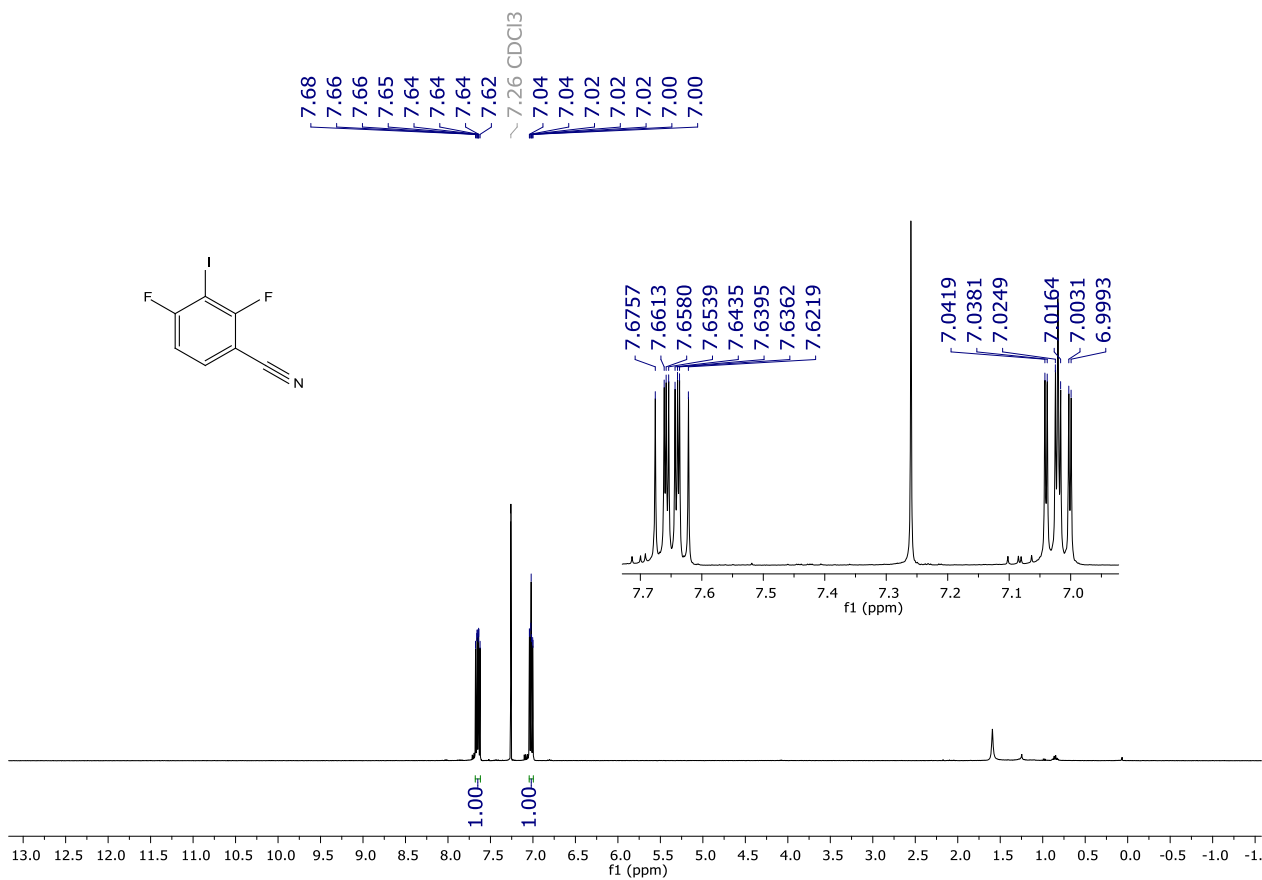
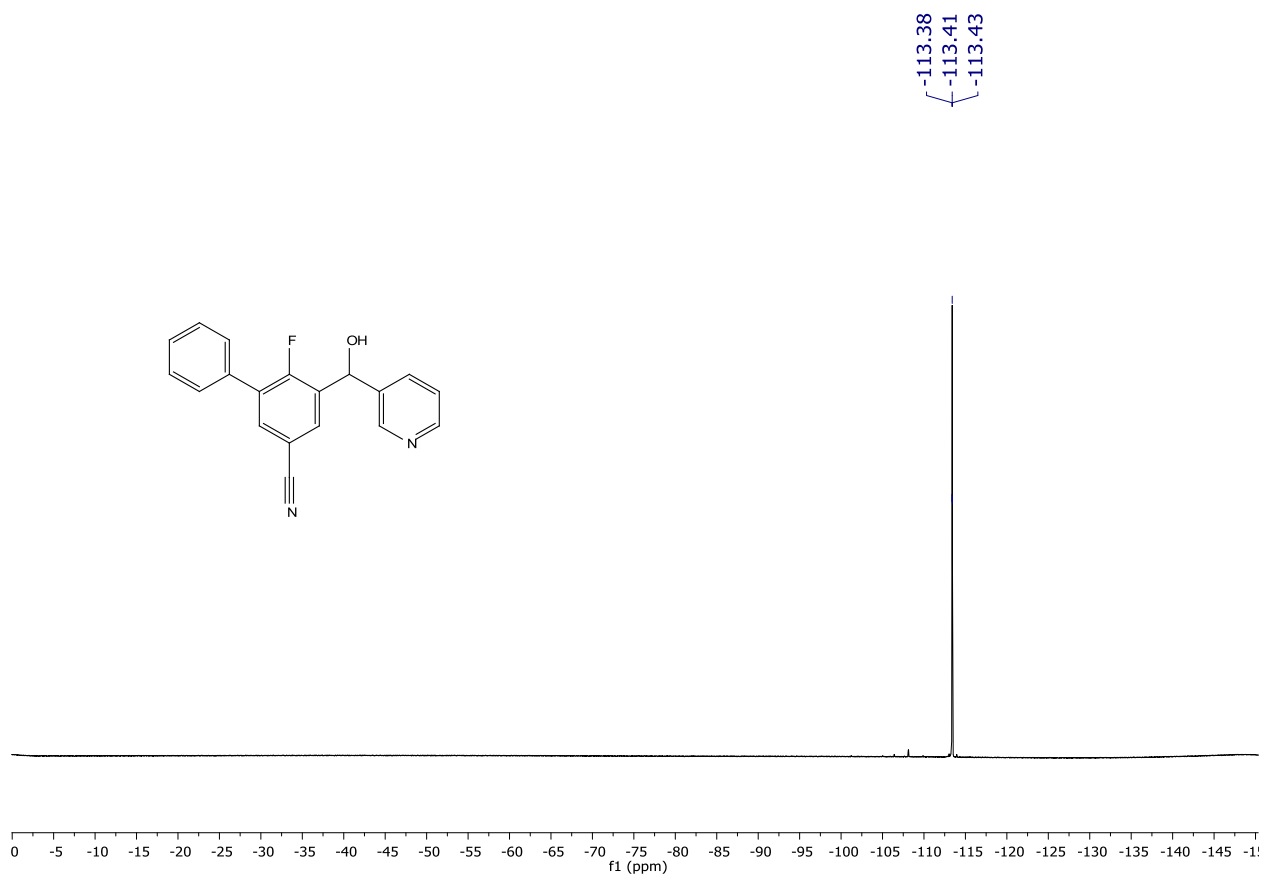


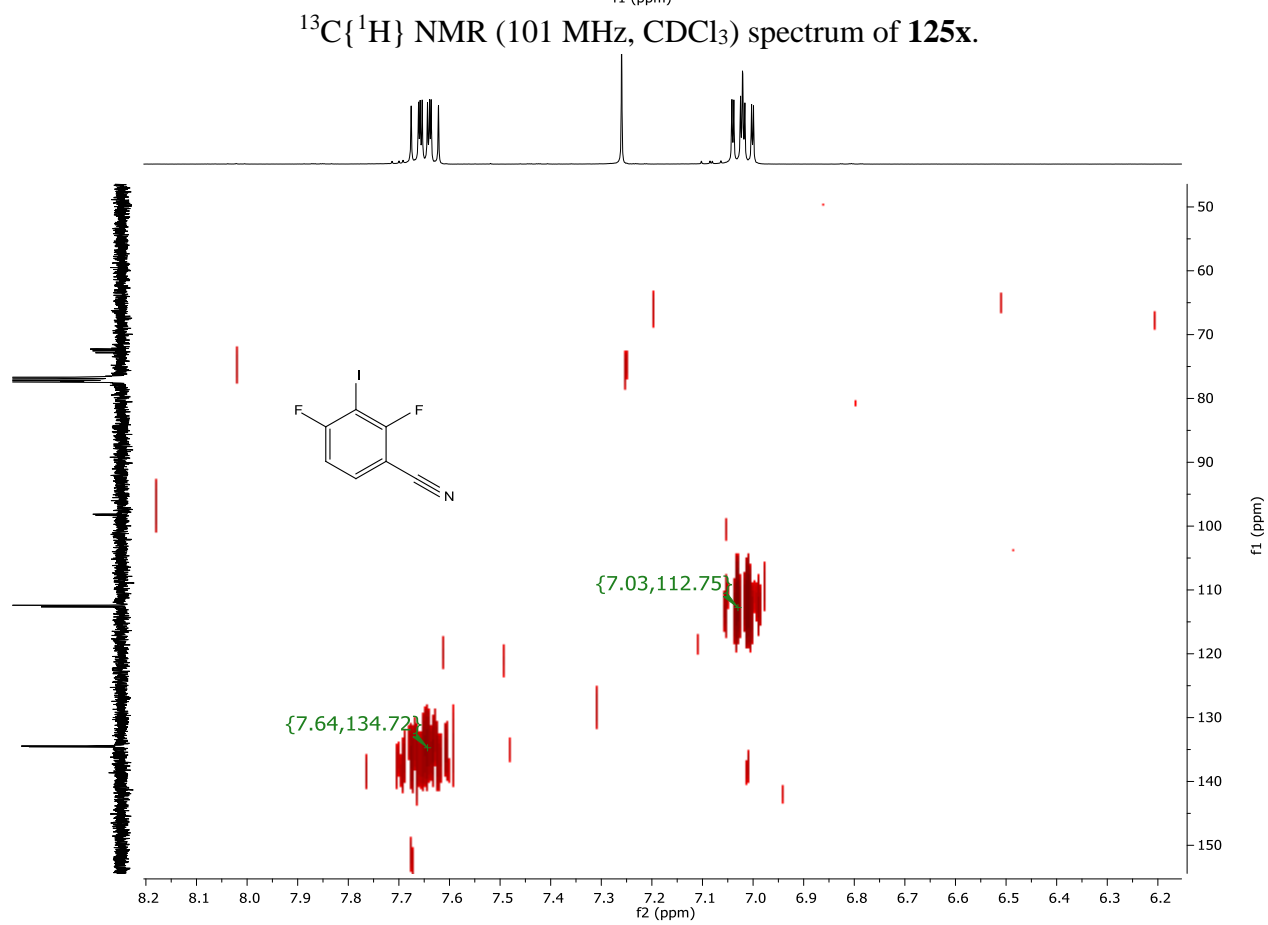
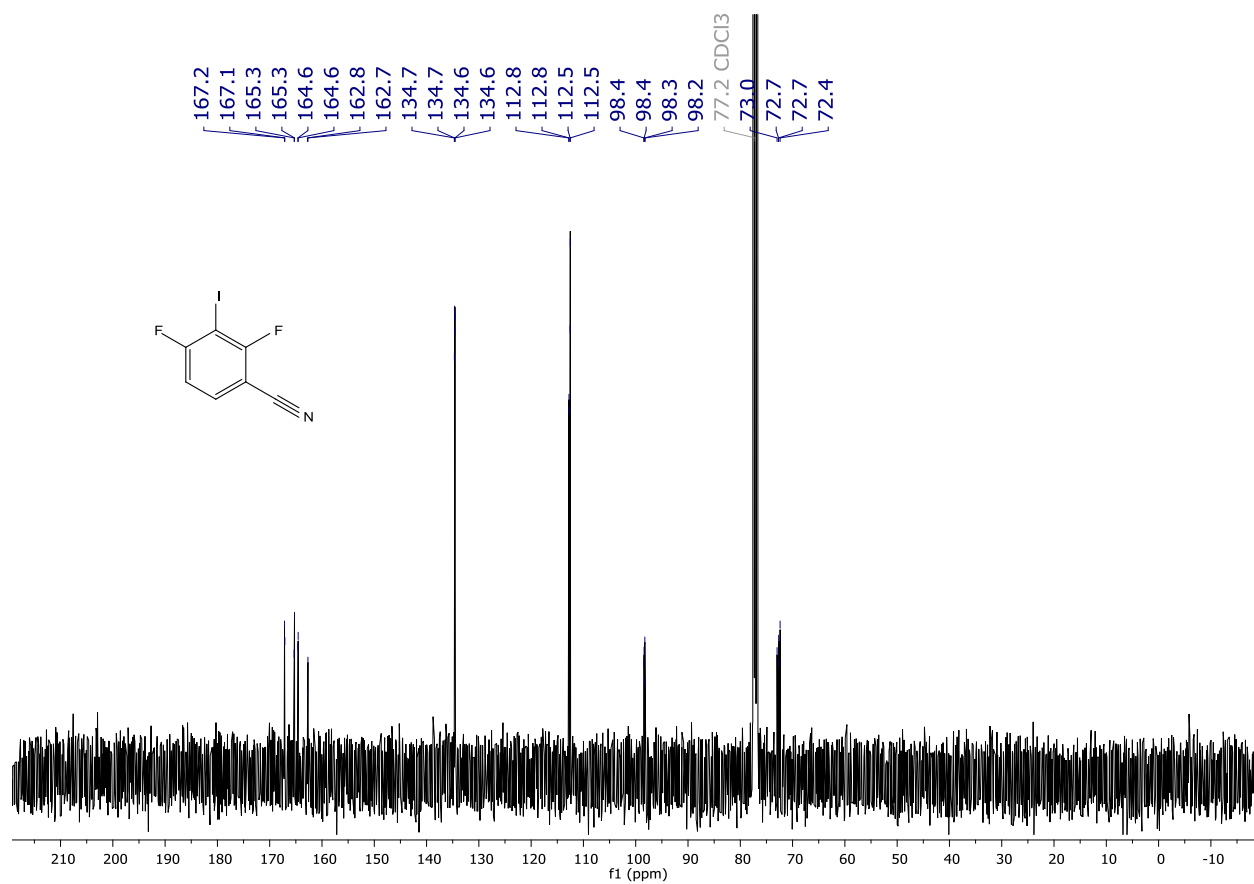
$^{13}\text{C}\{^1\text{H}\}$ NMR (101 MHz, CDCl_3) spectrum of **125w**.



^1H NMR (400 MHz, CDCl_3) spectrum of **126a**.

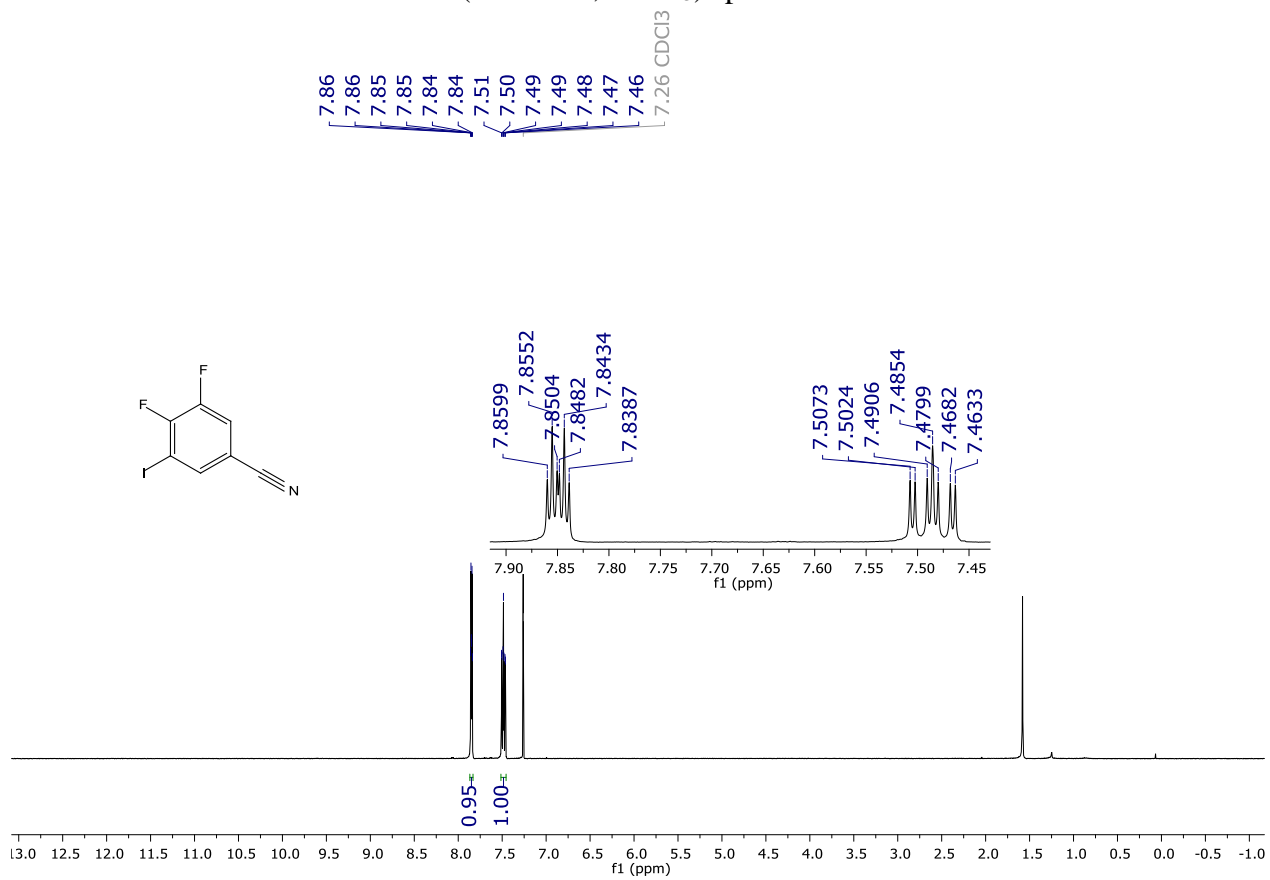




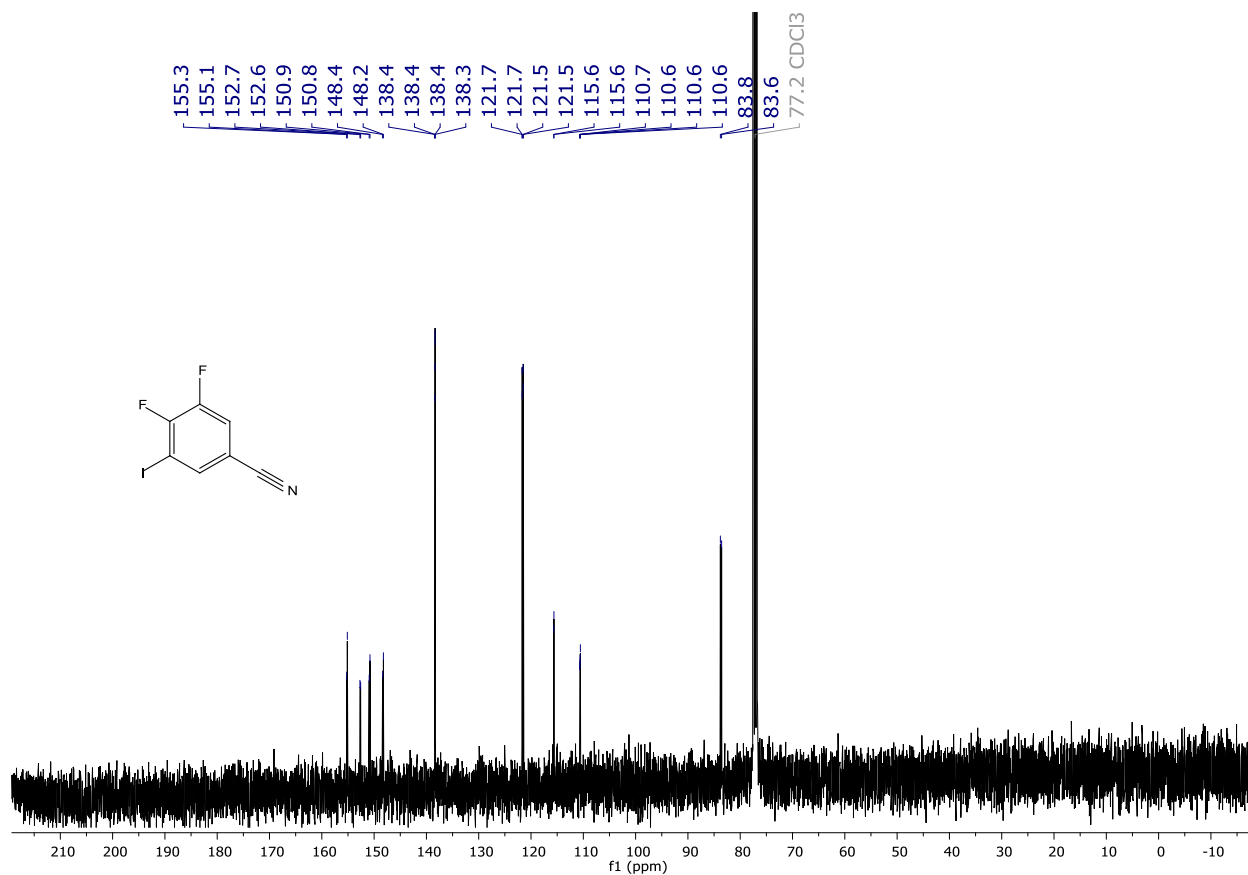
HSQC correlation map of **125x** (400 and 101 MHz, CDCl_3).



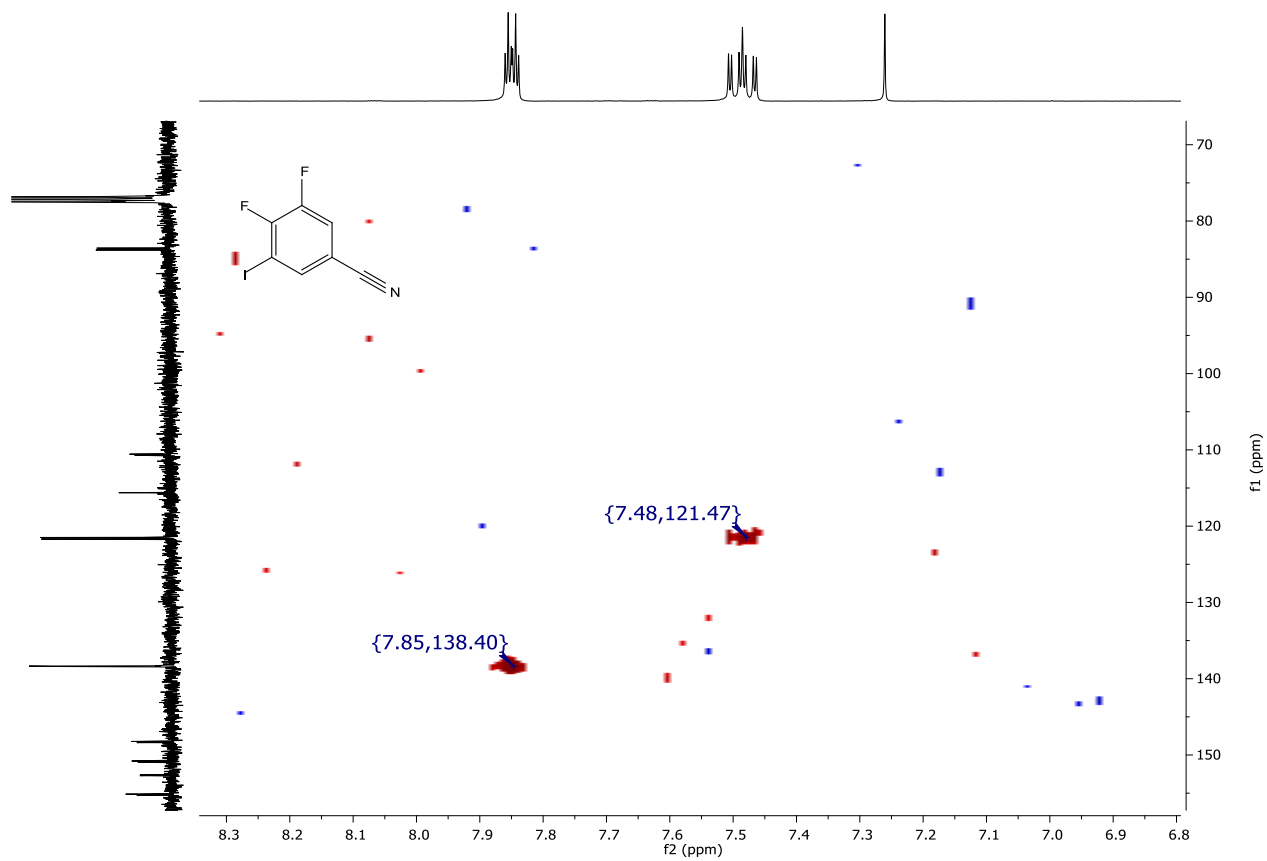
^{19}F NMR (282 MHz, CDCl_3) spectrum of **125x**.



^1H NMR (400 MHz, CDCl_3) spectrum of **125y**.



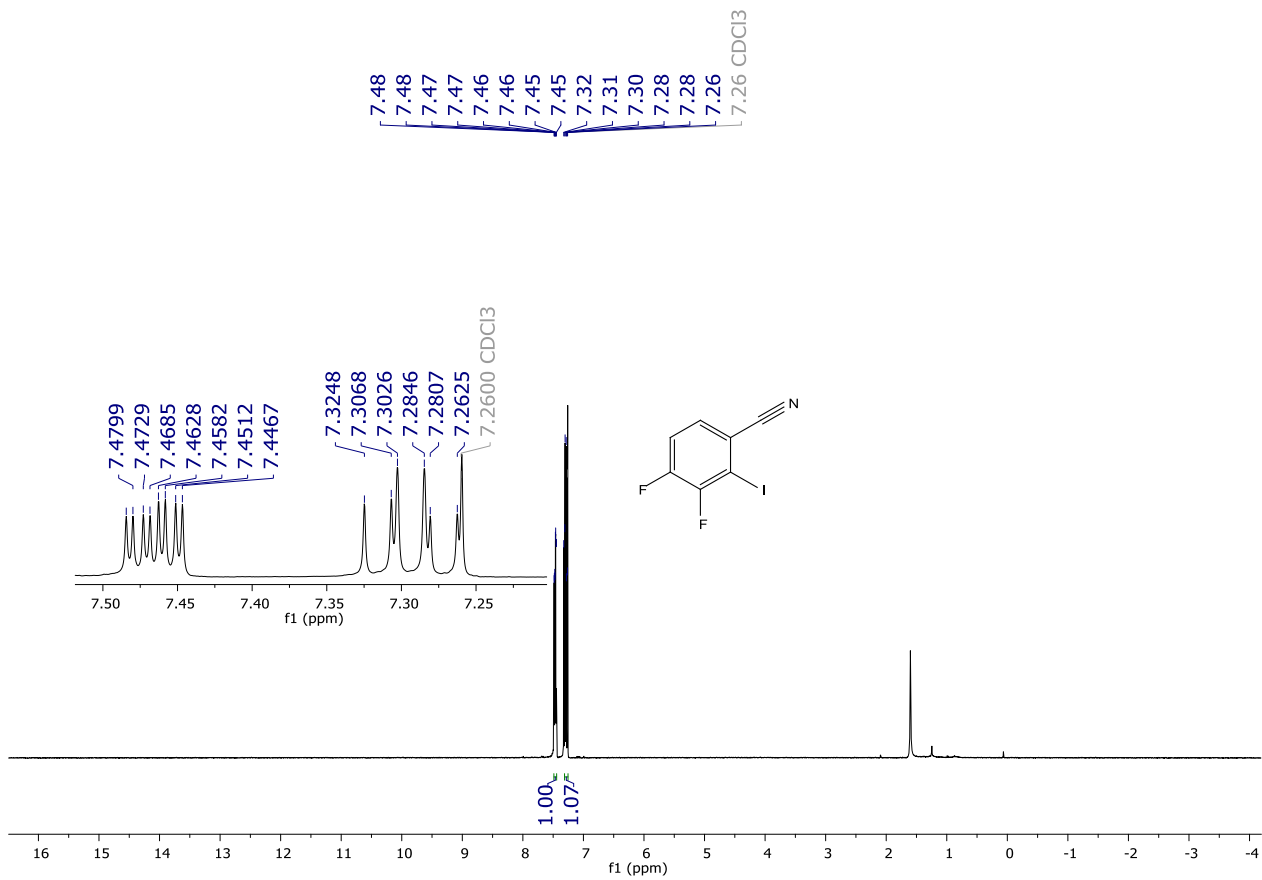
$^{13}\text{C}\{^1\text{H}\}$ NMR (101 MHz, CDCl_3) spectrum of **25y**.



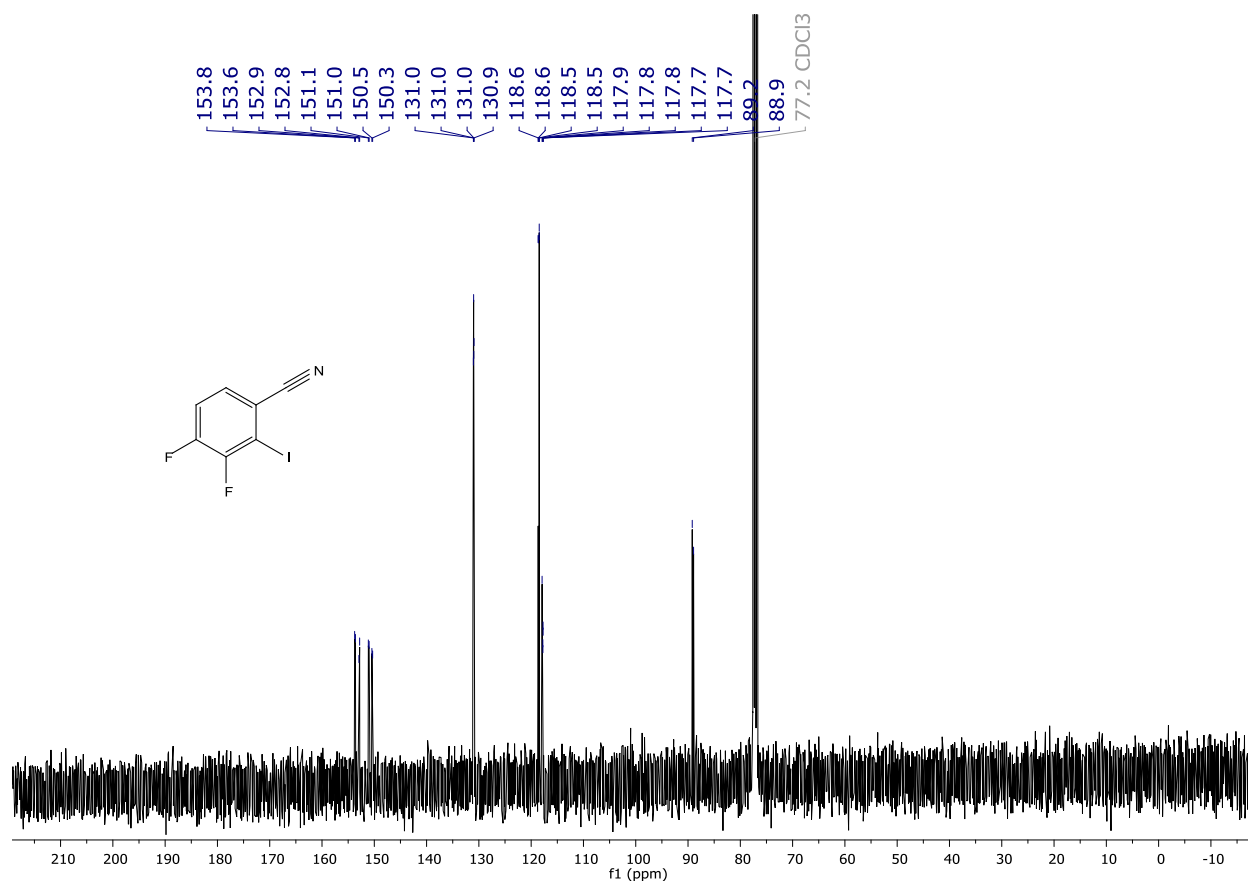
HSQC correlation map of **25y** (400 and 101 MHz, CDCl_3).



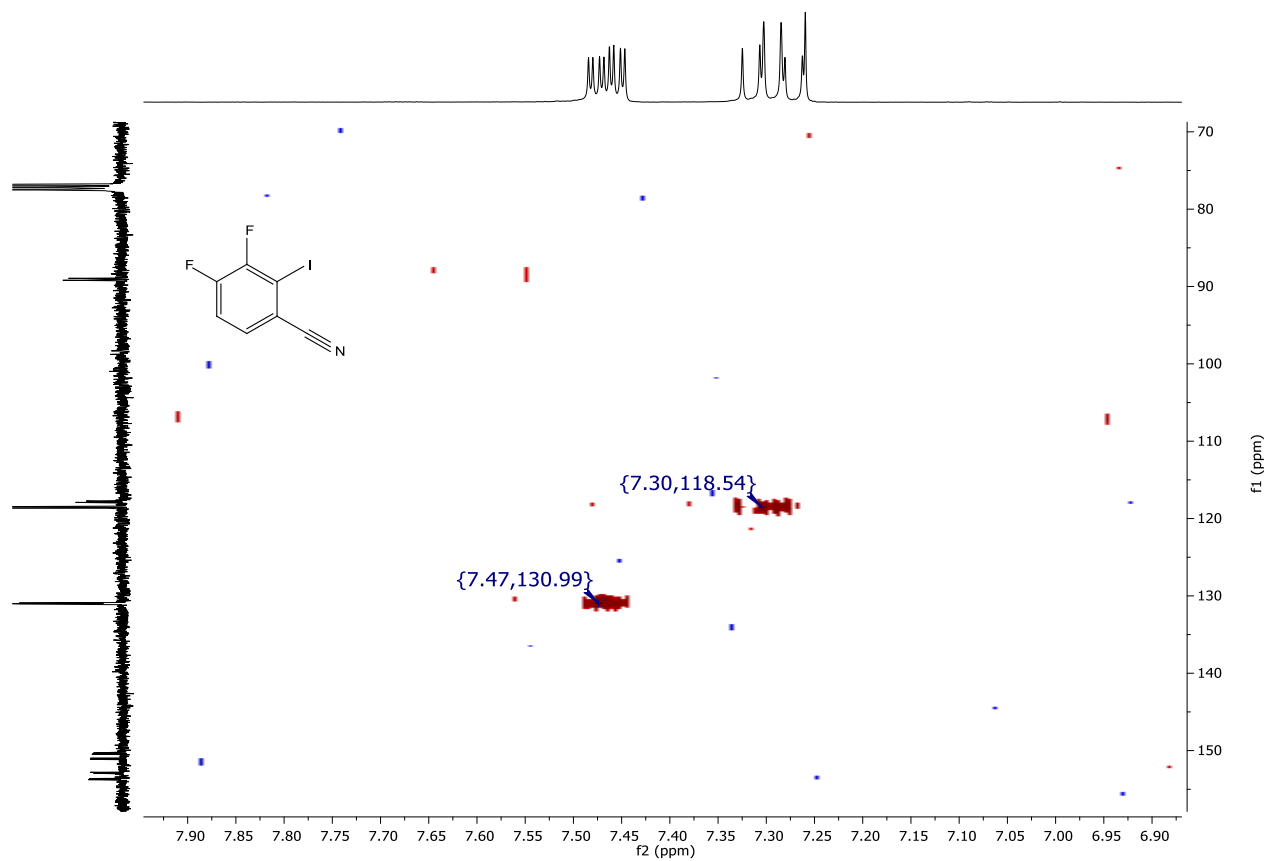
¹⁹F NMR (282 MHz, CDCl₃) spectrum of **125y**.



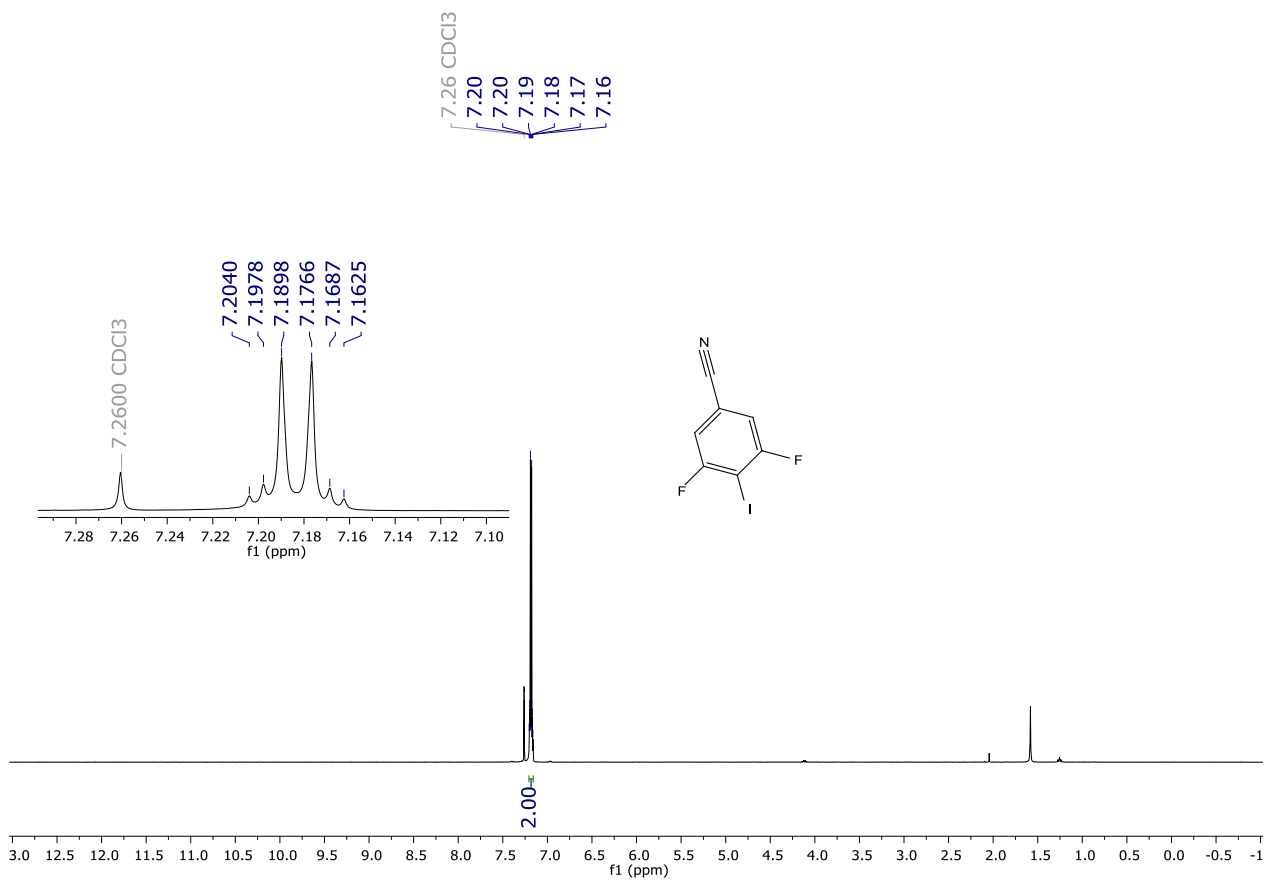
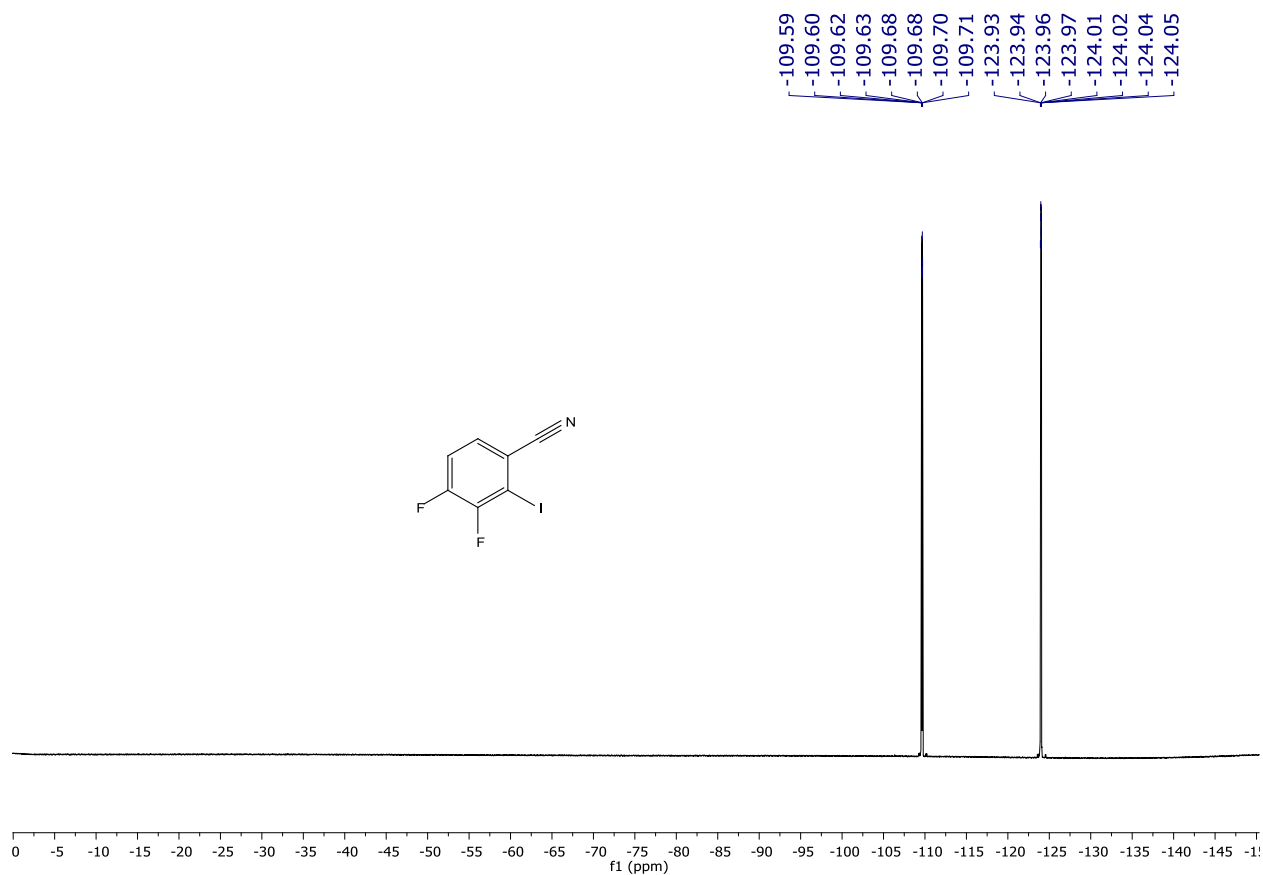
¹H NMR (400 MHz, CDCl₃) spectrum of **125z**.



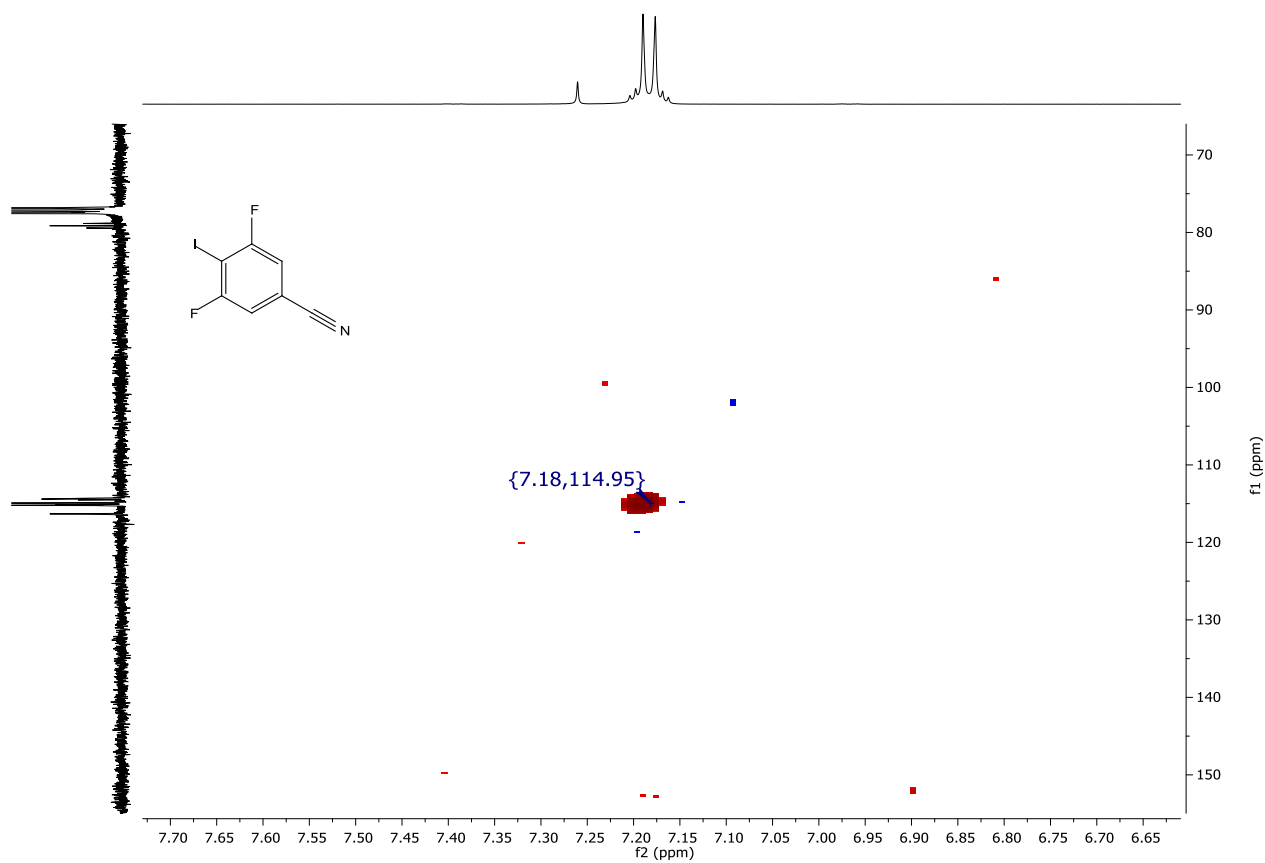
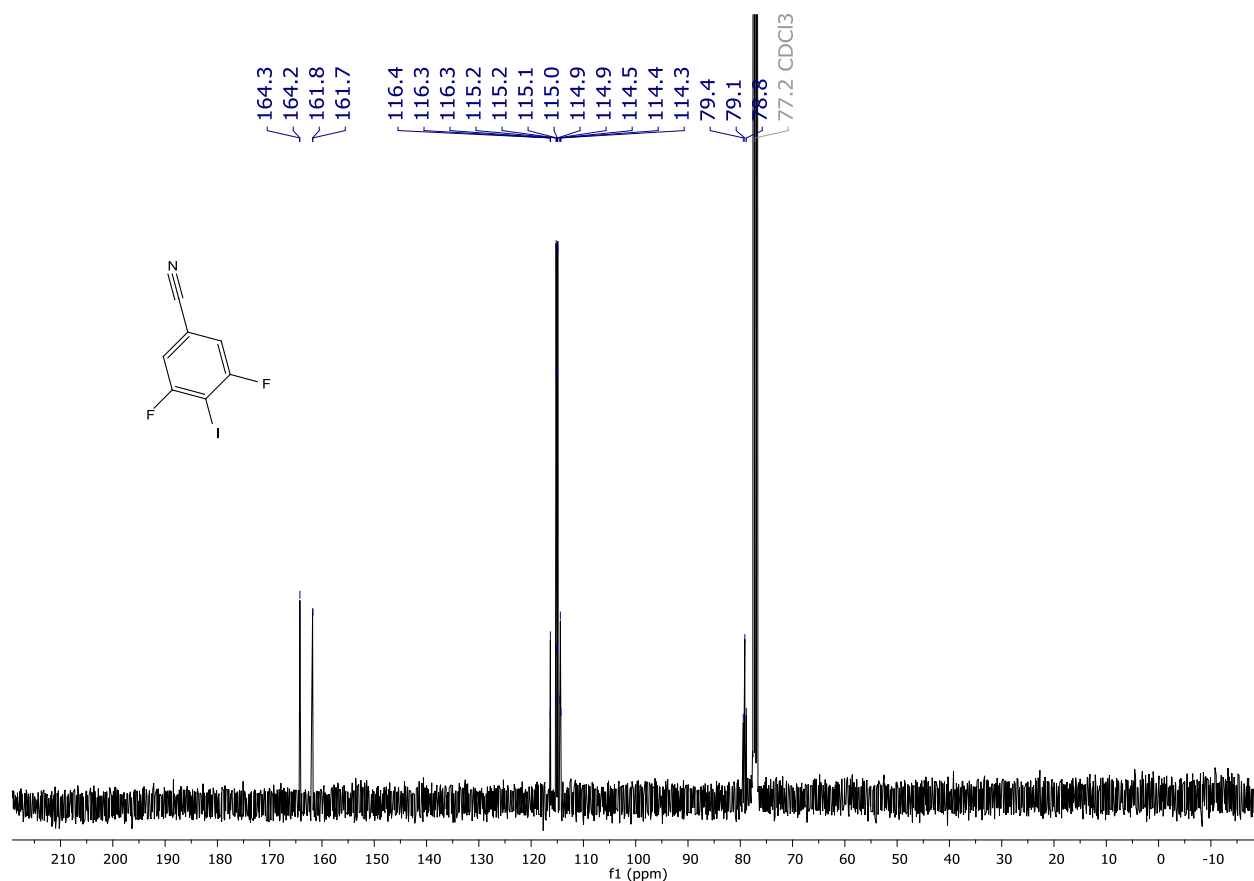
$^{13}\text{C}\{^1\text{H}\}$ NMR (101 MHz, CDCl_3) spectrum of **125z**.

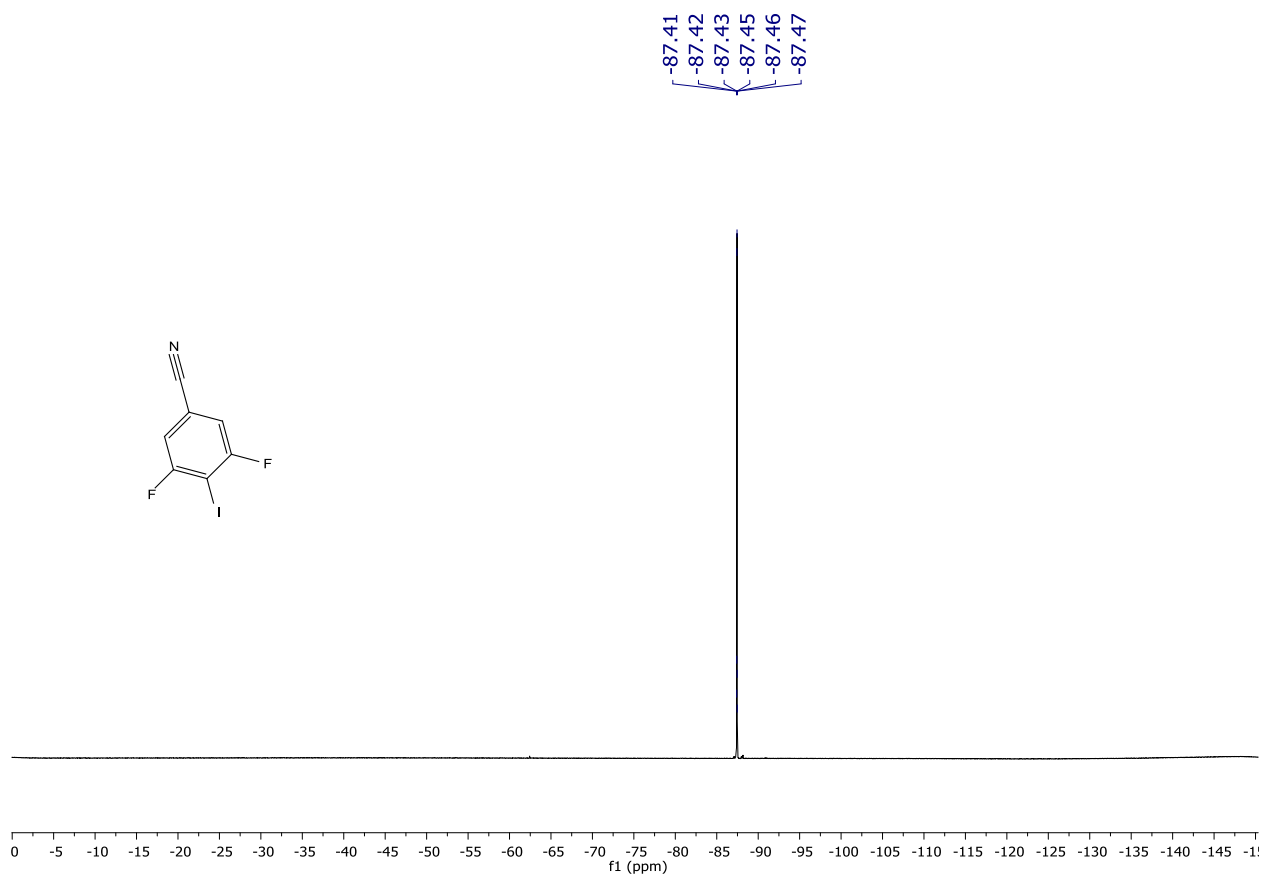


HSQC correlation map of **125z** (400 and 101 MHz, CDCl_3).

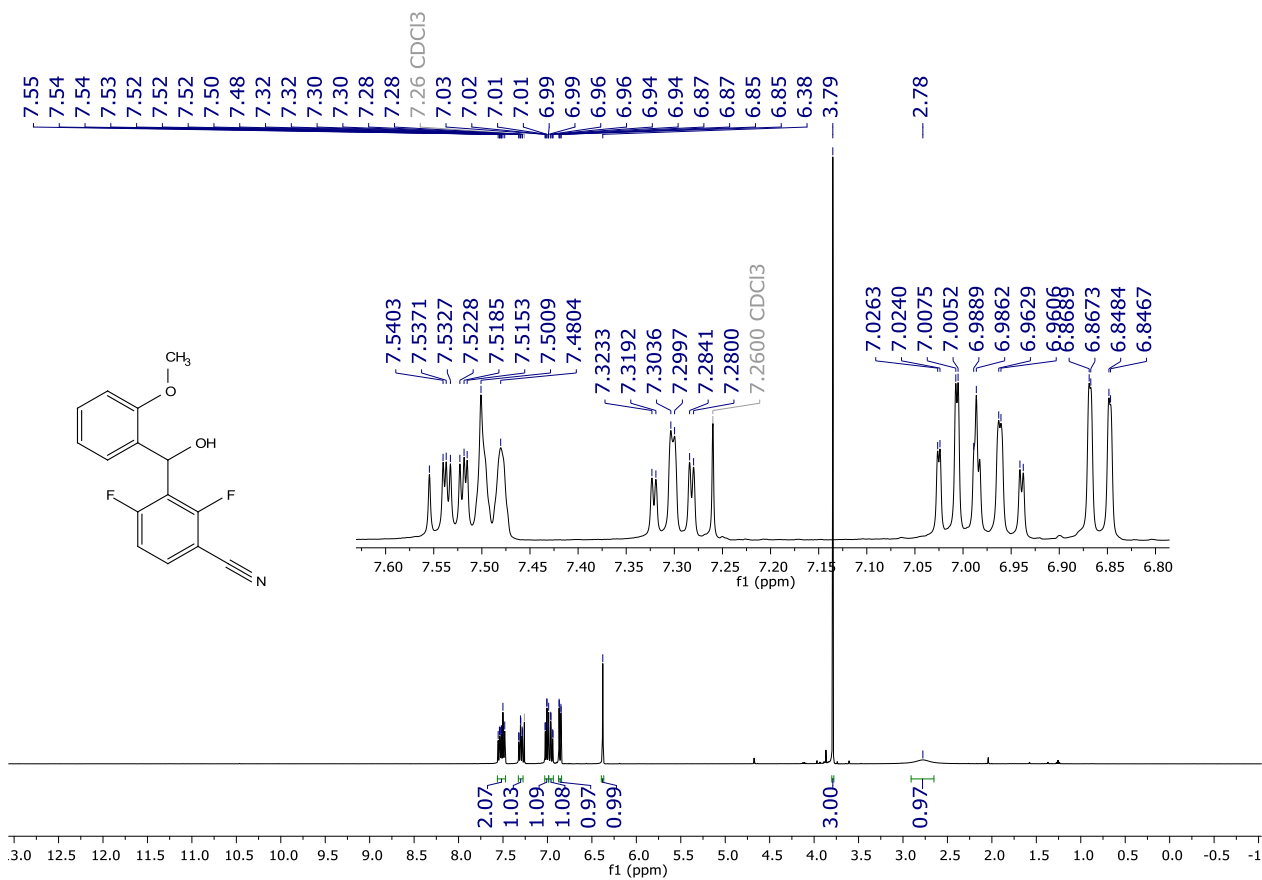


^1H NMR (400 MHz, CDCl_3) spectrum of **125aa**.

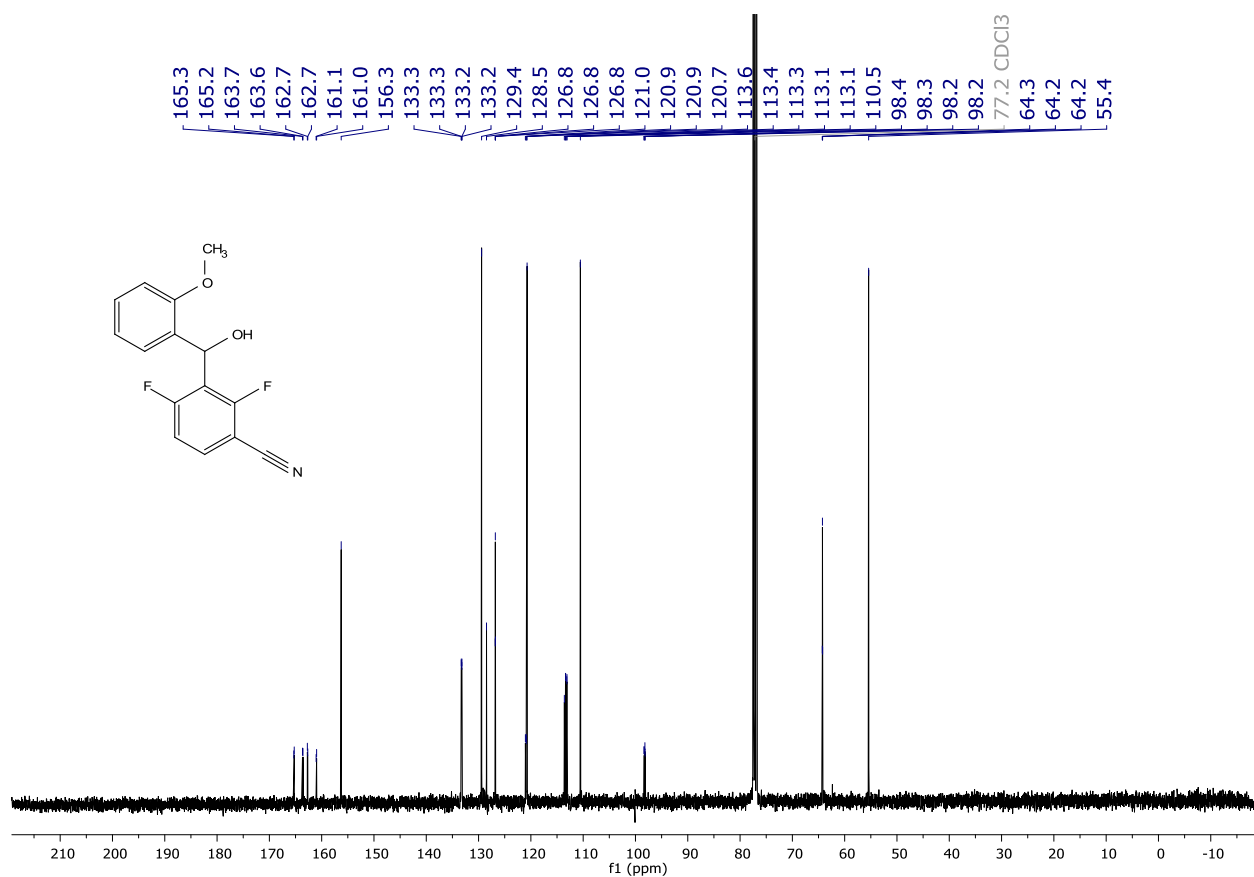
HSQC correlation map of **125aa** (400 and 101 MHz, CDCl_3).



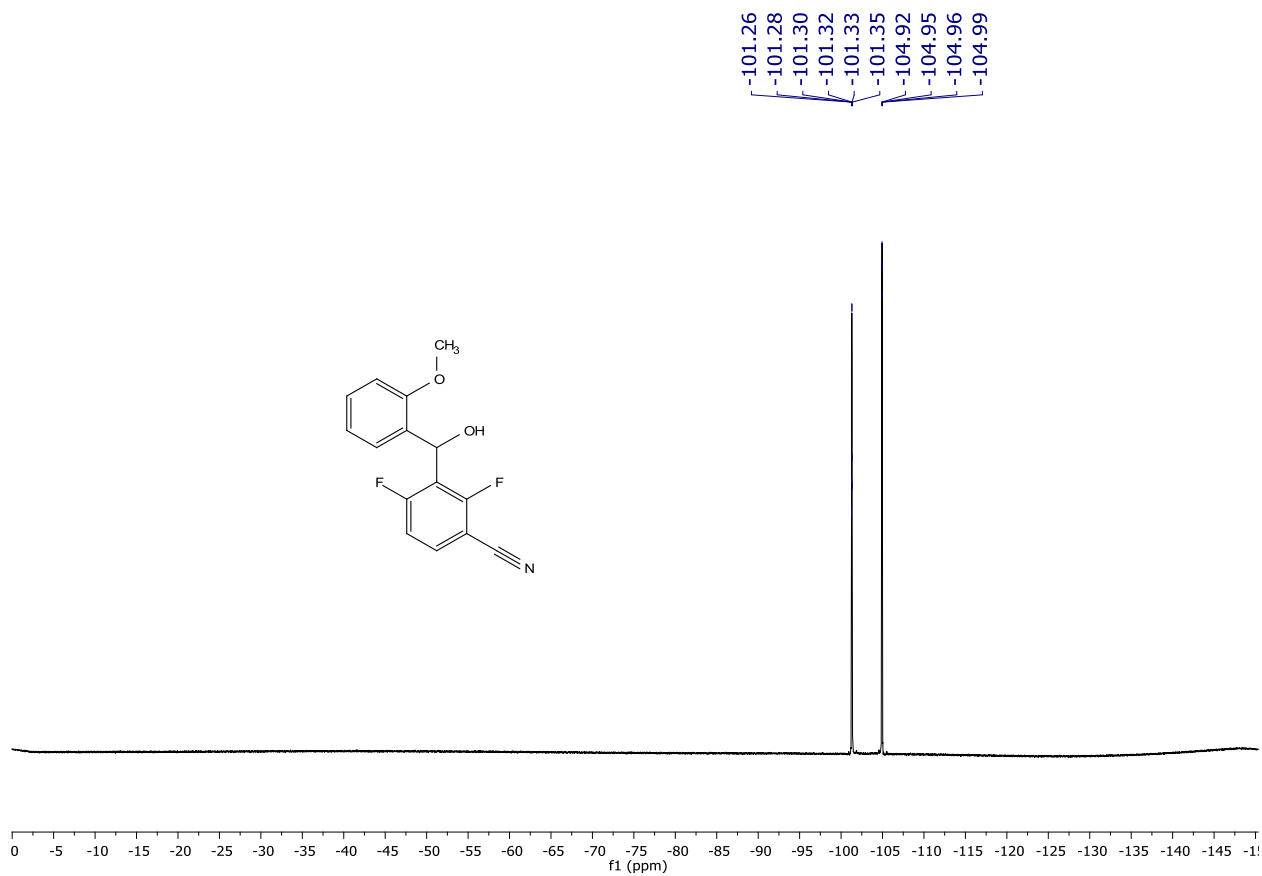
^{19}F NMR (282 MHz, CDCl_3) spectrum of **125aa**.



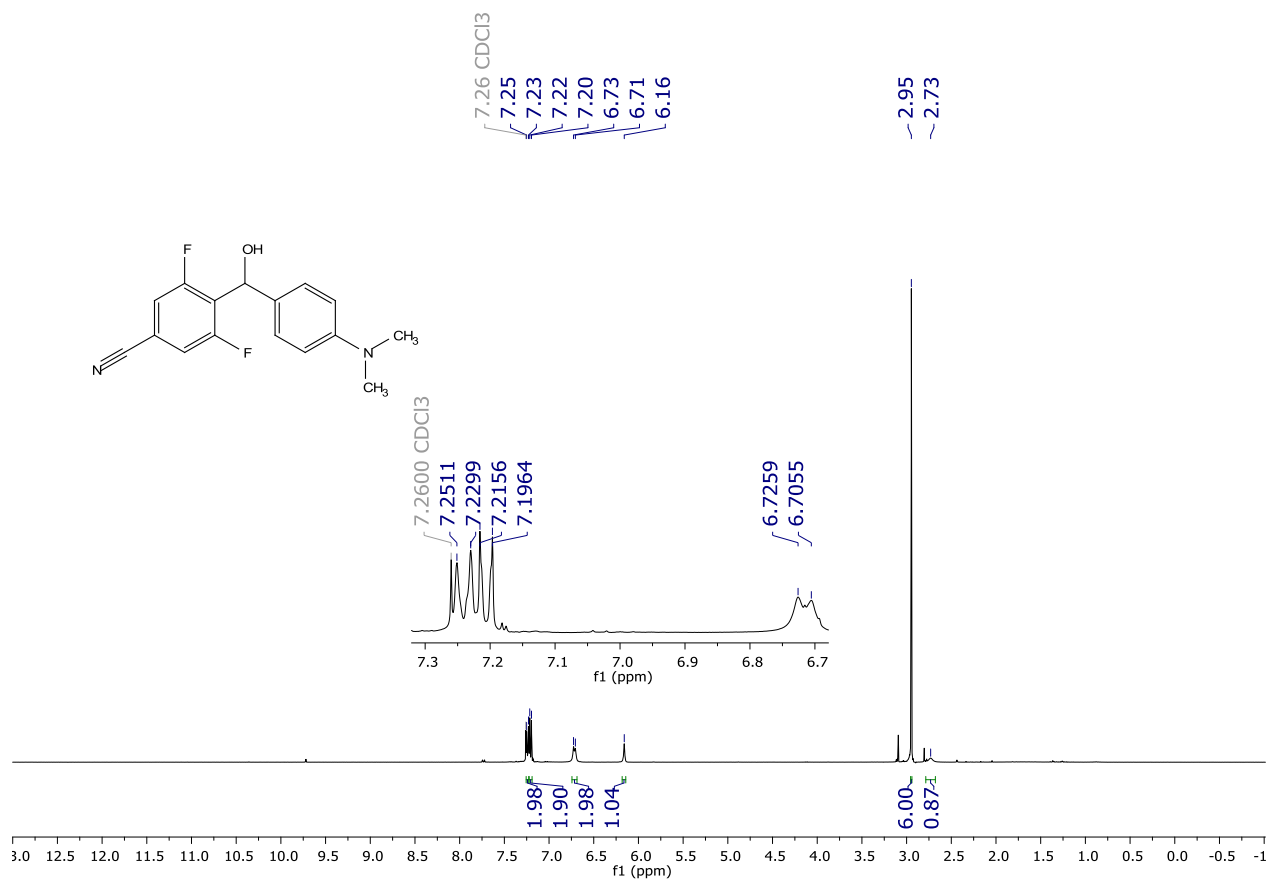
^1H NMR (400 MHz, CDCl_3) spectrum of **125ab**.



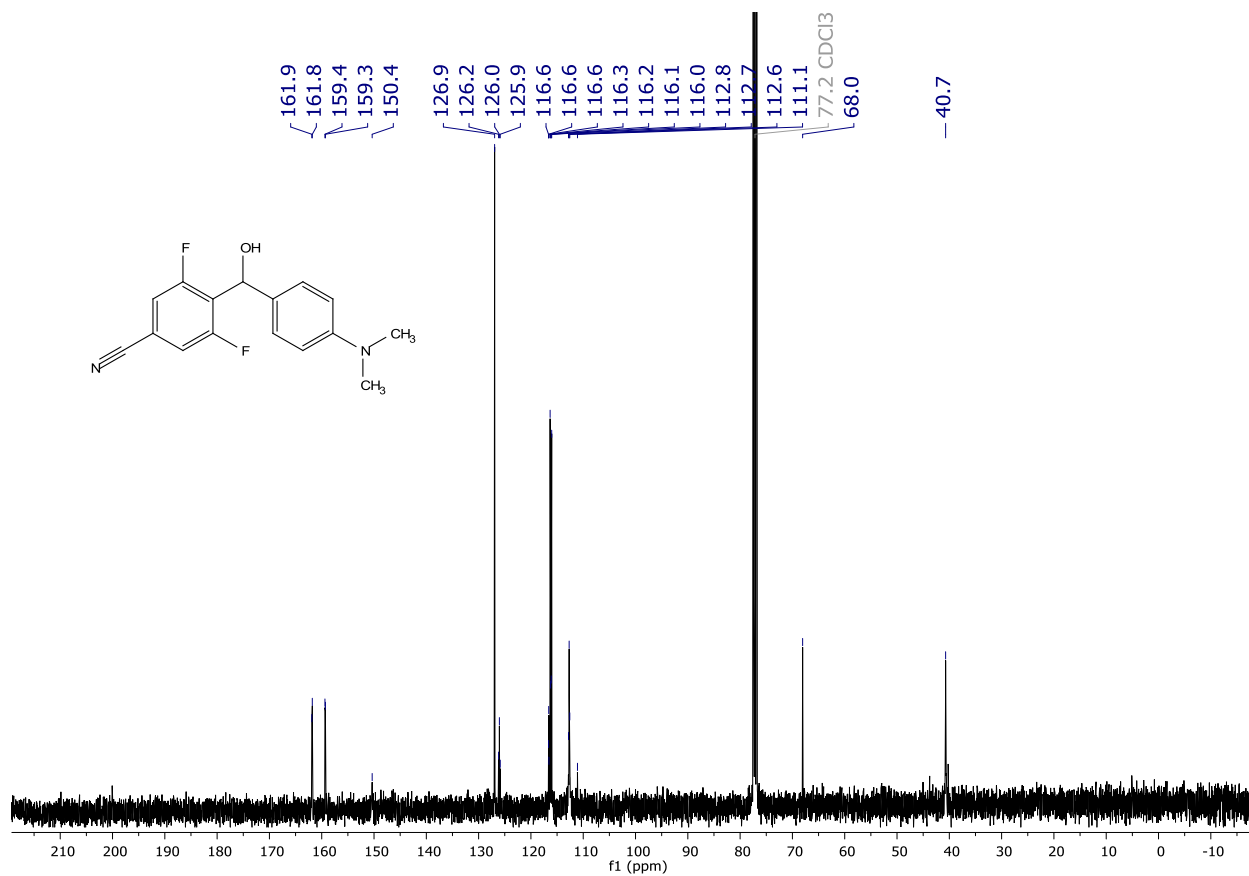
¹³C{¹H} NMR (101 MHz, CDCl₃) spectrum of **125ab**.



¹⁹F NMR (282 MHz, CDCl₃) spectrum of **125ab**.



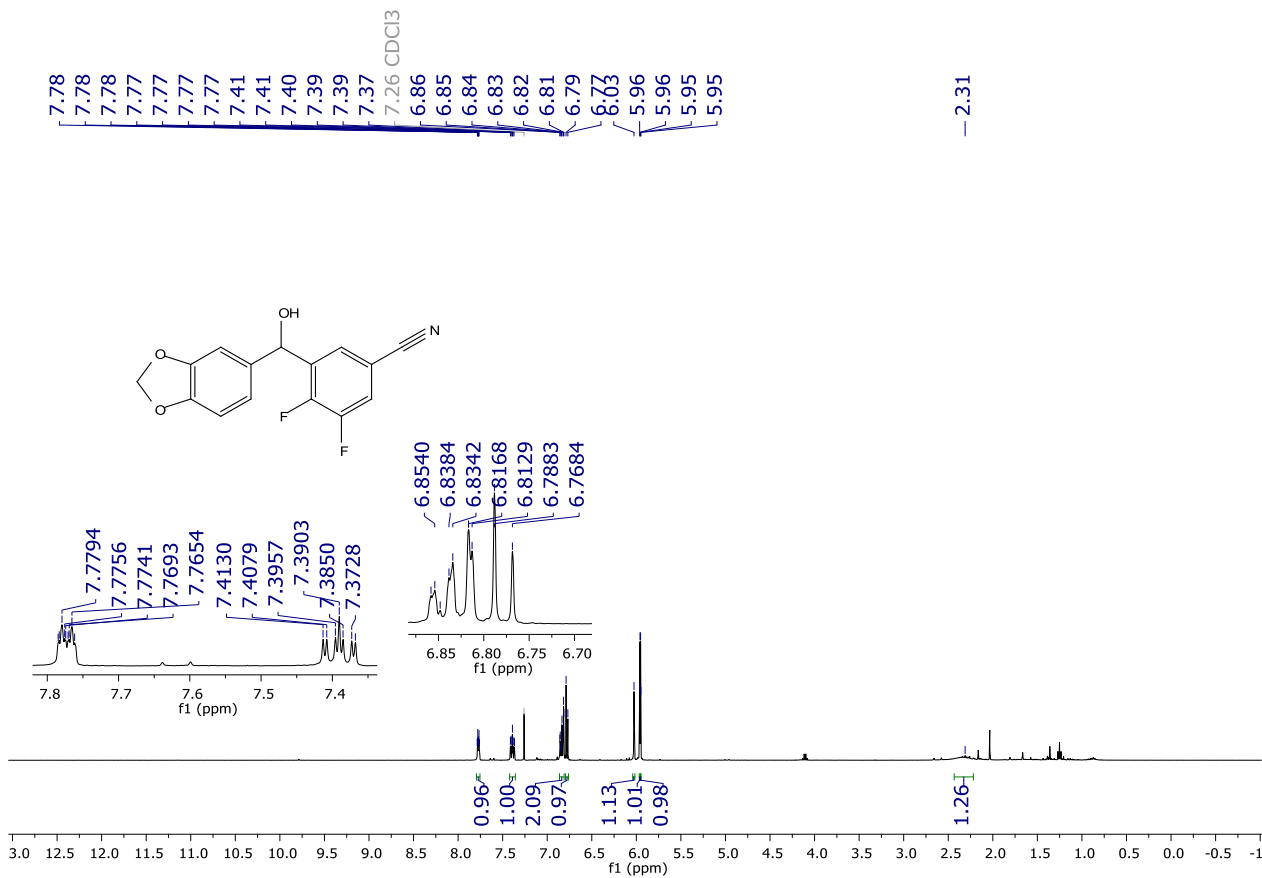
¹H NMR (400 MHz, CDCl₃) spectrum of **125ac**.



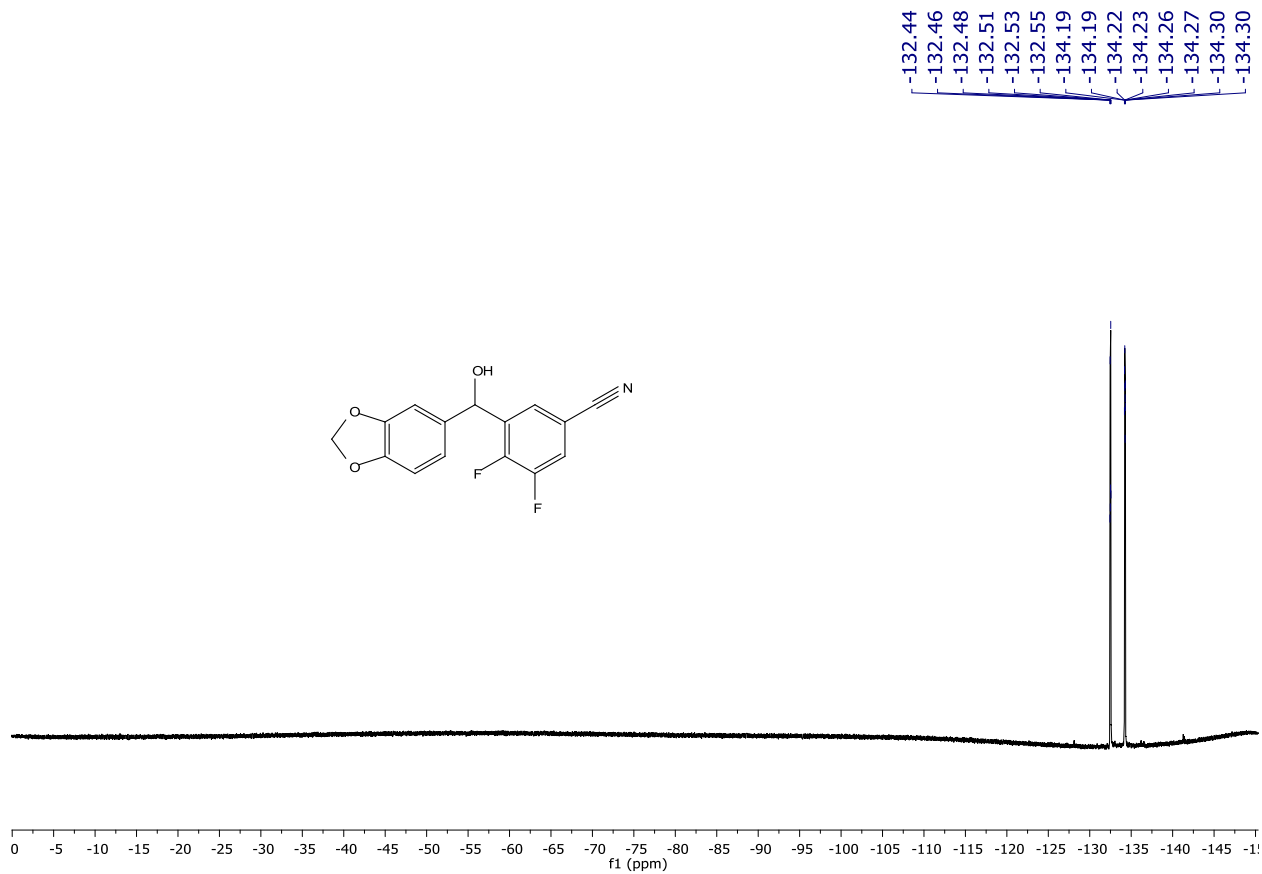
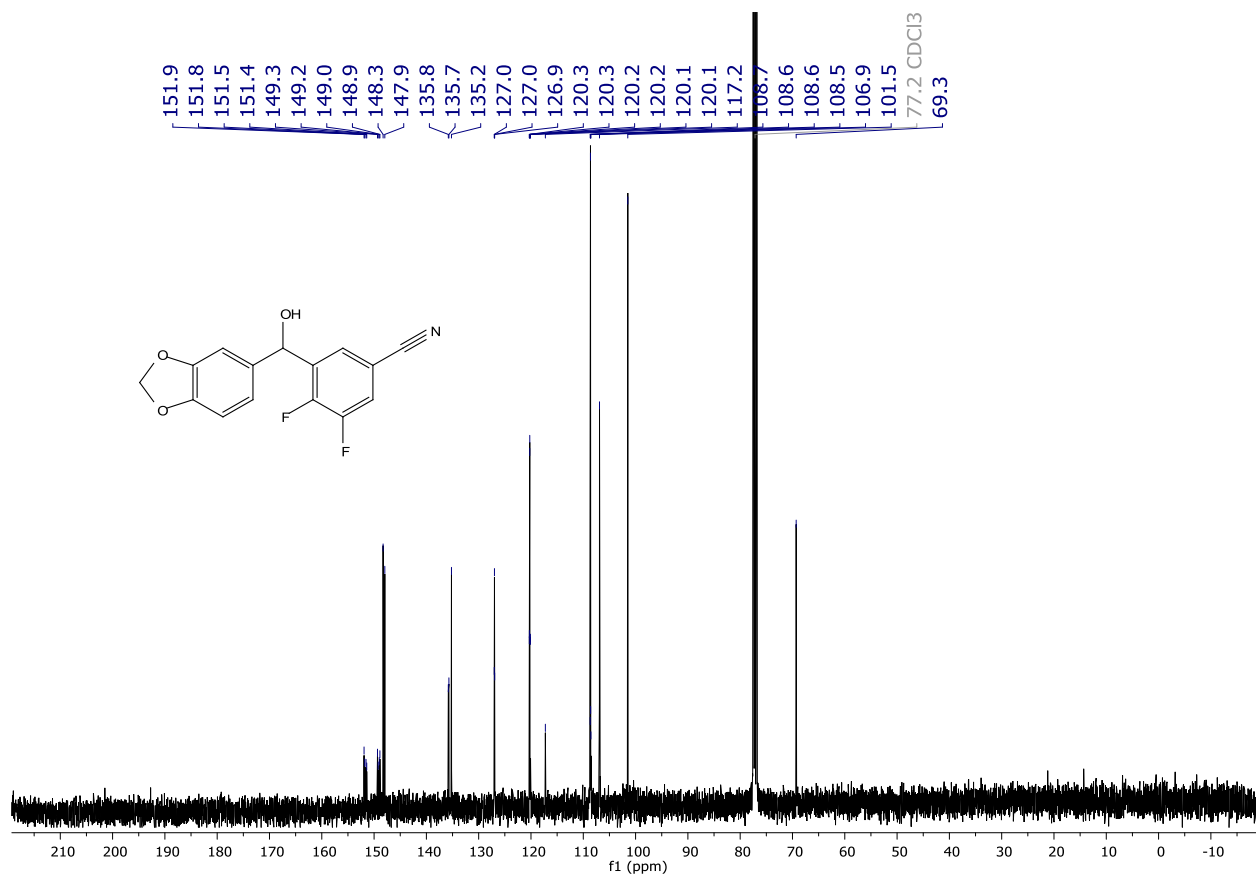
¹³C{¹H} NMR (101 MHz, CDCl₃) spectrum of **125ac**.

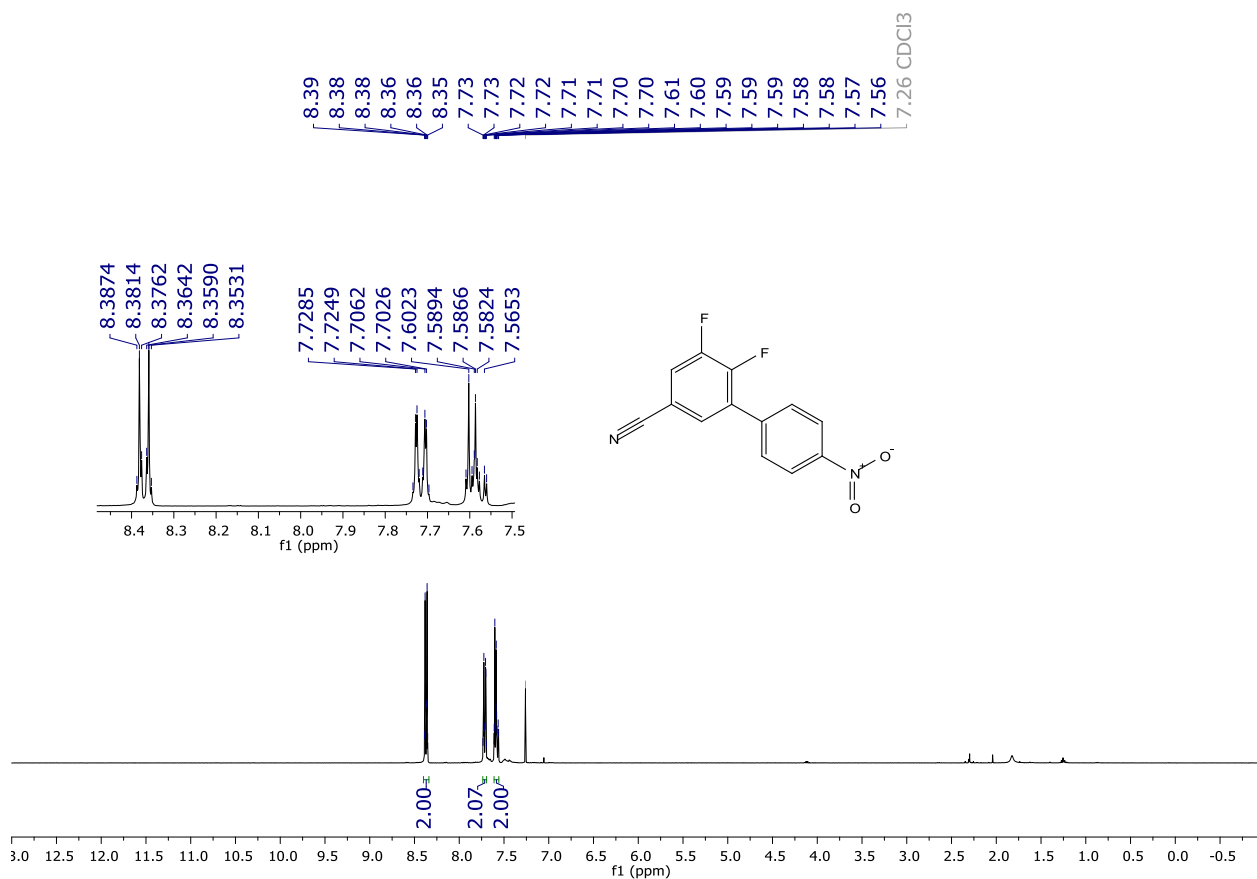


^{19}F NMR (282 MHz, CDCl_3) spectrum of **125ac**.

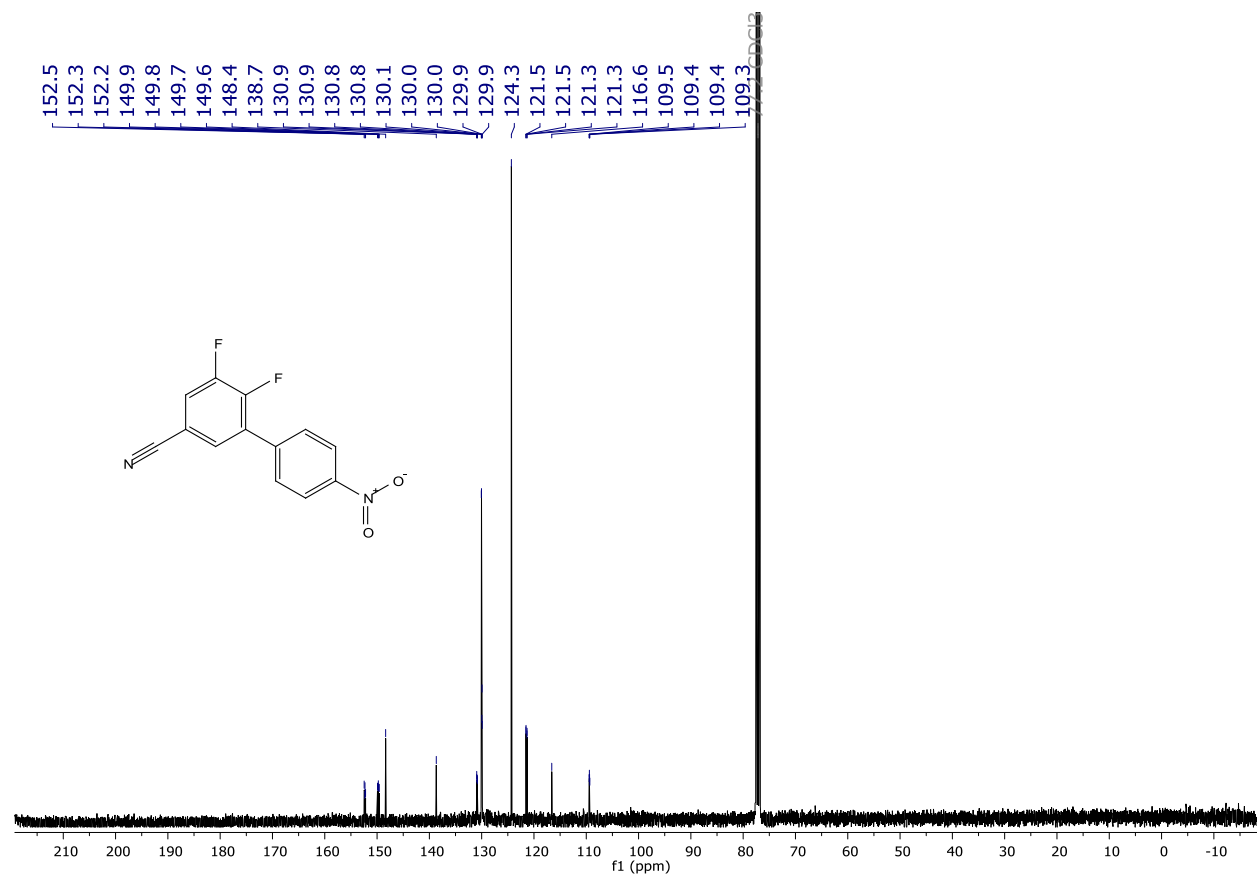


^1H NMR (400 MHz, CDCl_3) spectrum of **125ad**.

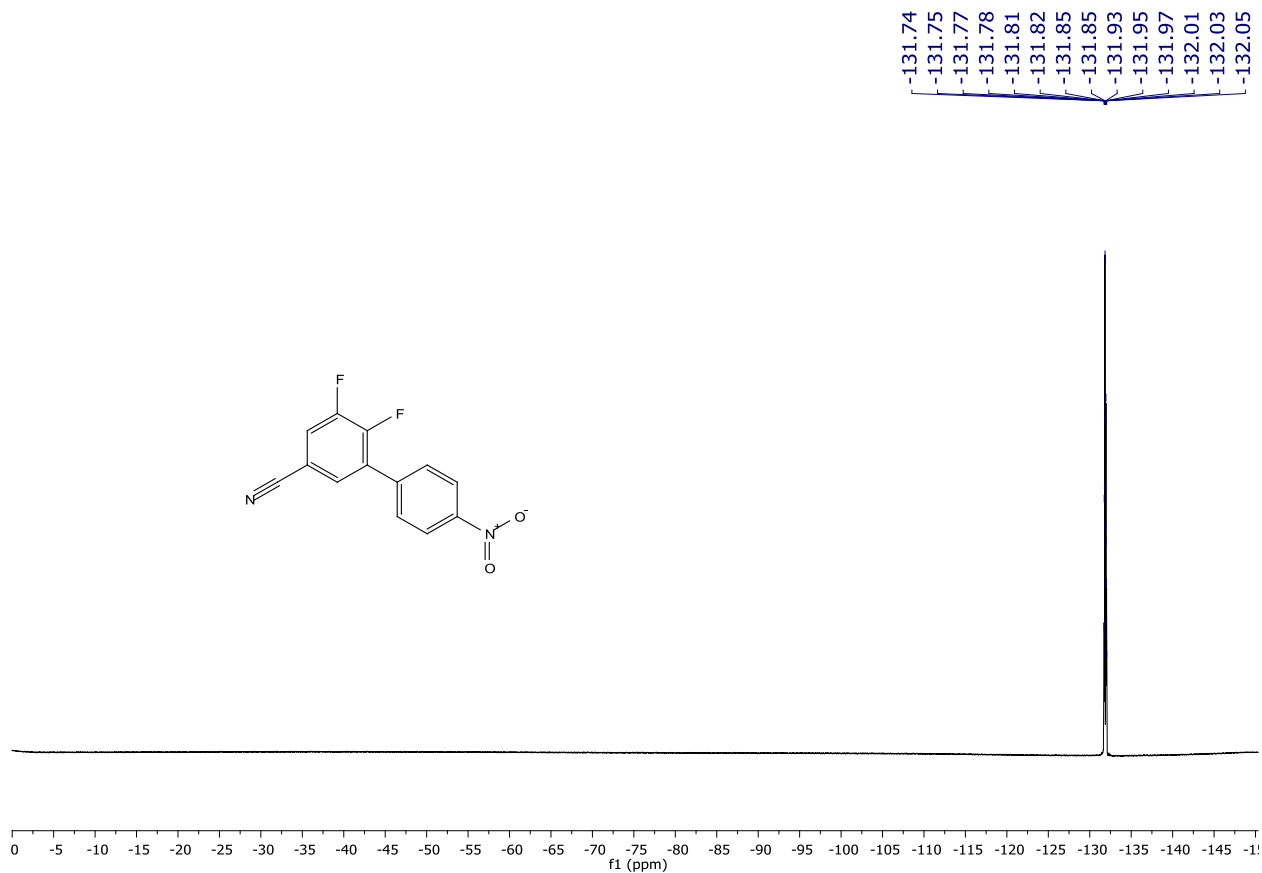




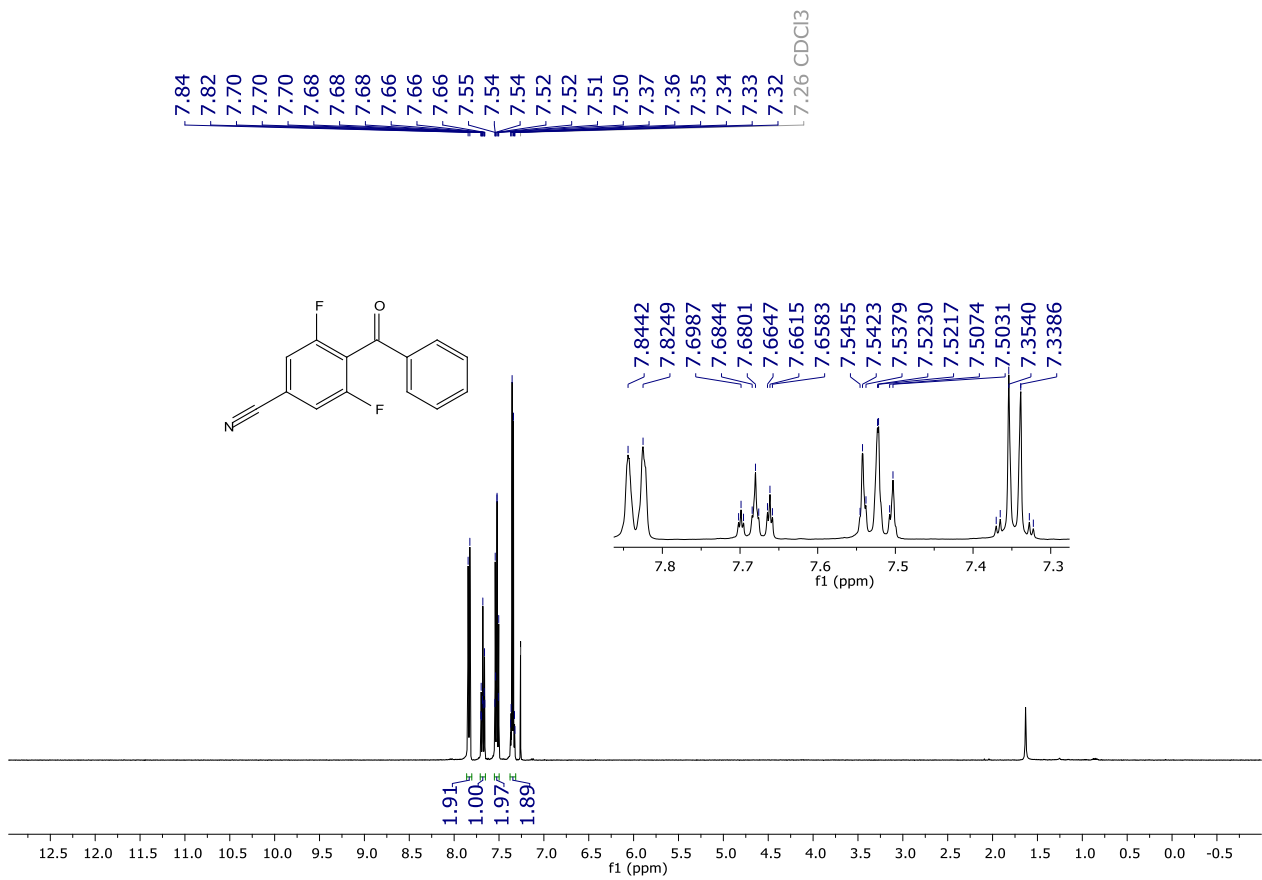
¹H NMR (400 MHz, CDCl₃) spectrum of **125ae**.



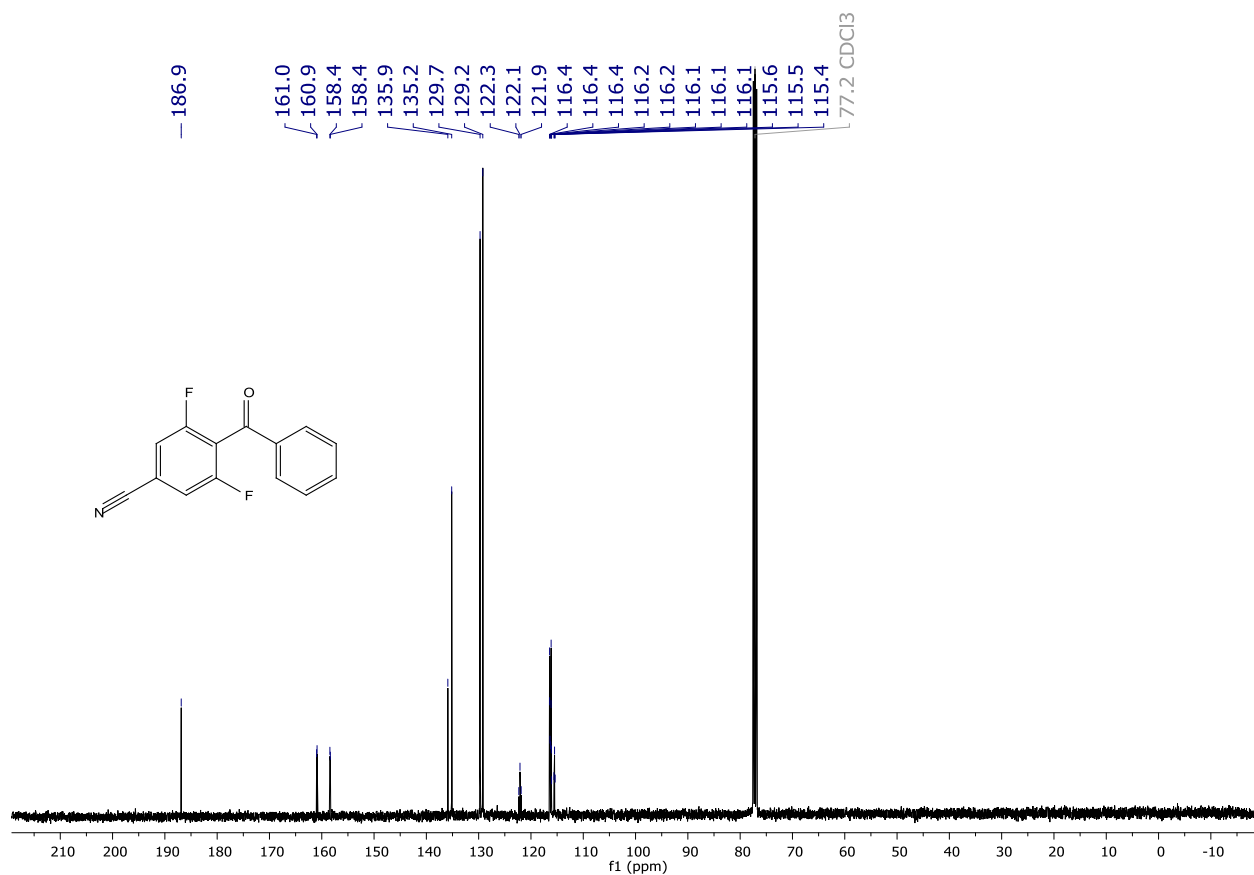
¹³C{¹H} NMR (101 MHz, CDCl₃) spectrum of **125ae**.



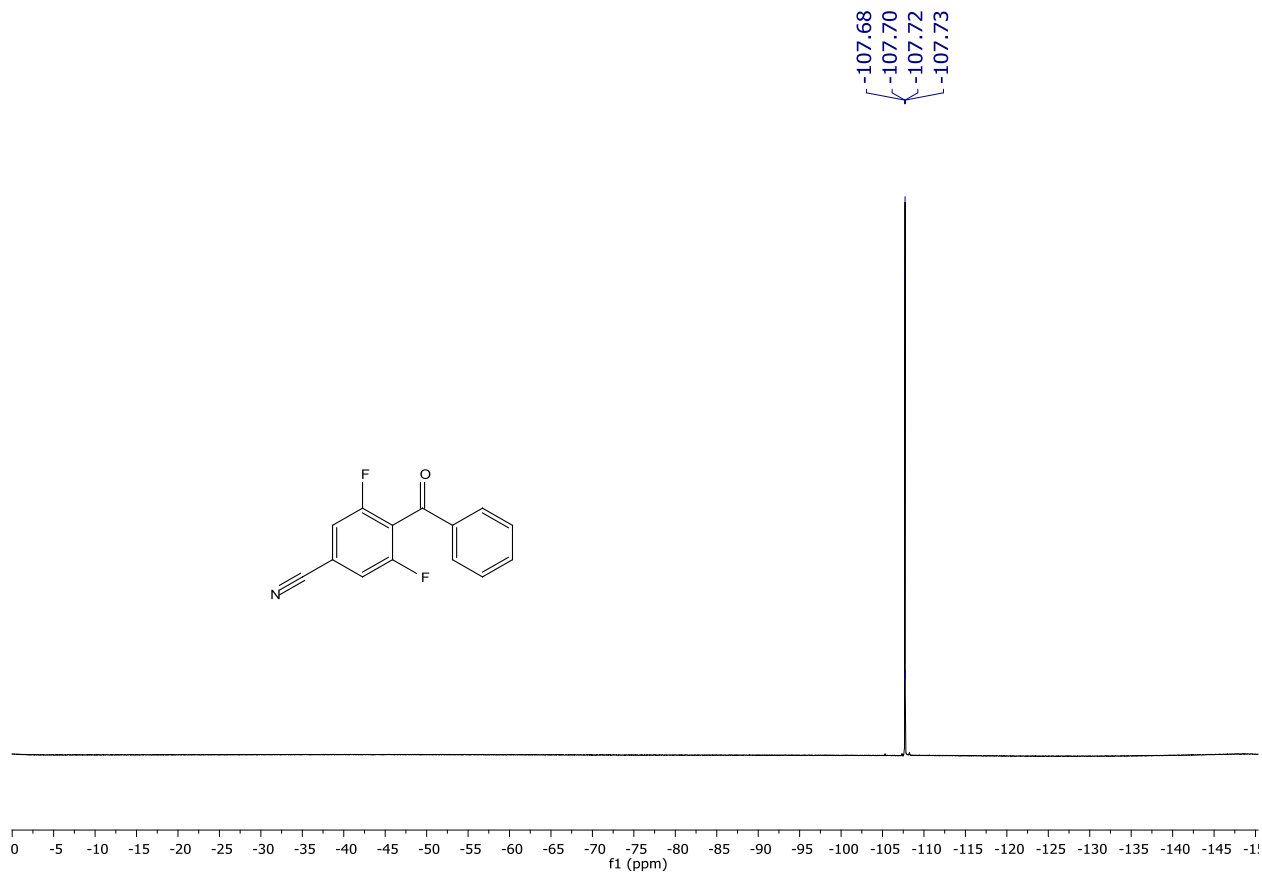
¹⁹F NMR (282 MHz, CDCl₃) spectrum of 125ae.



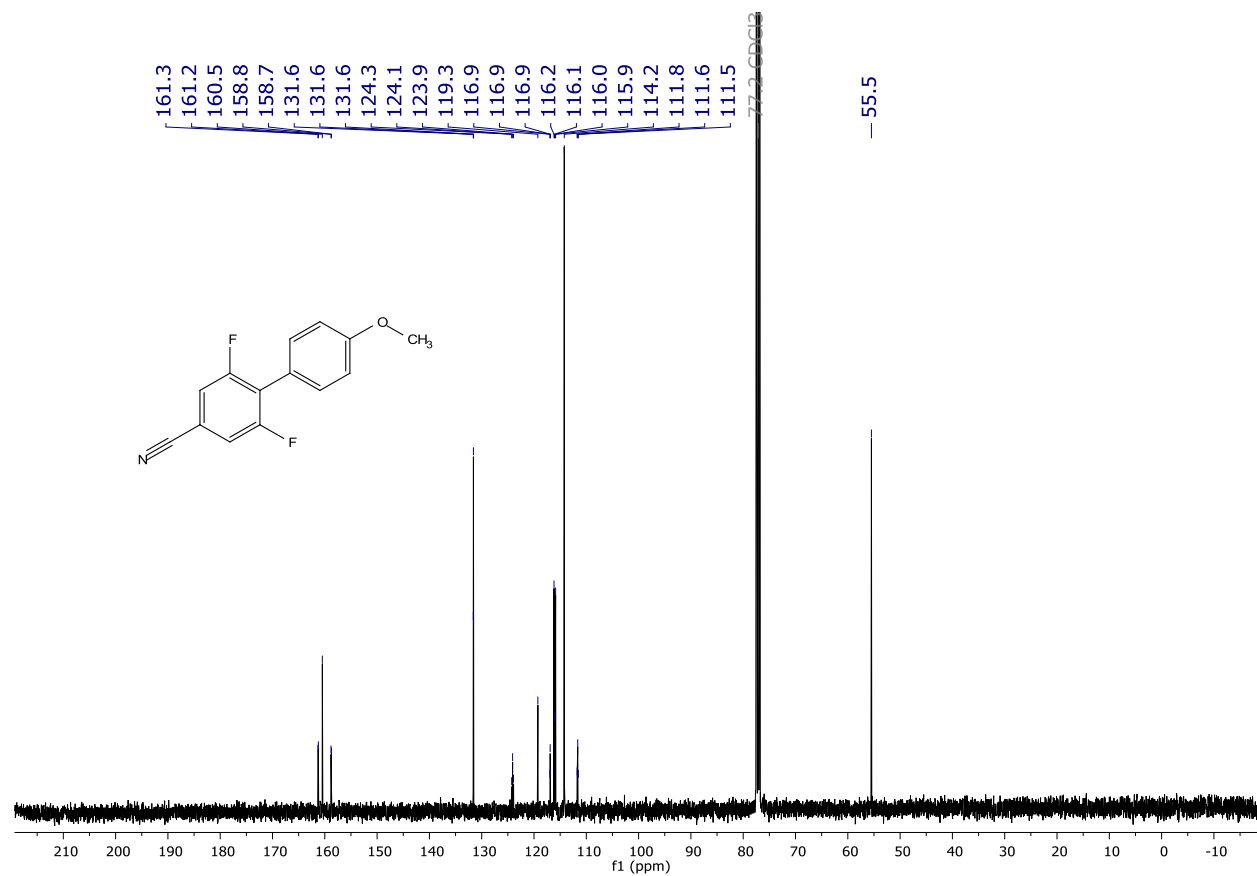
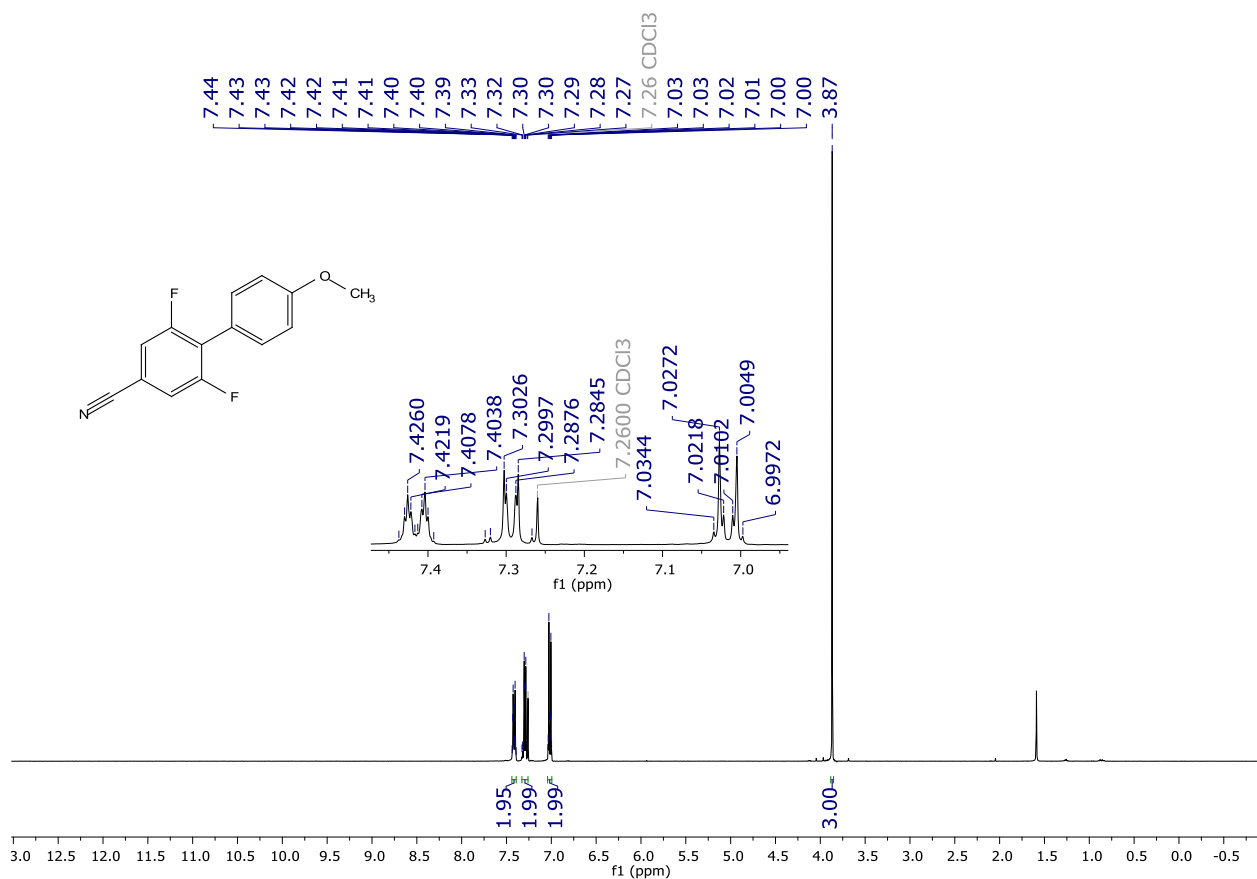
¹H NMR (400 MHz, CDCl₃) spectrum of 125af.

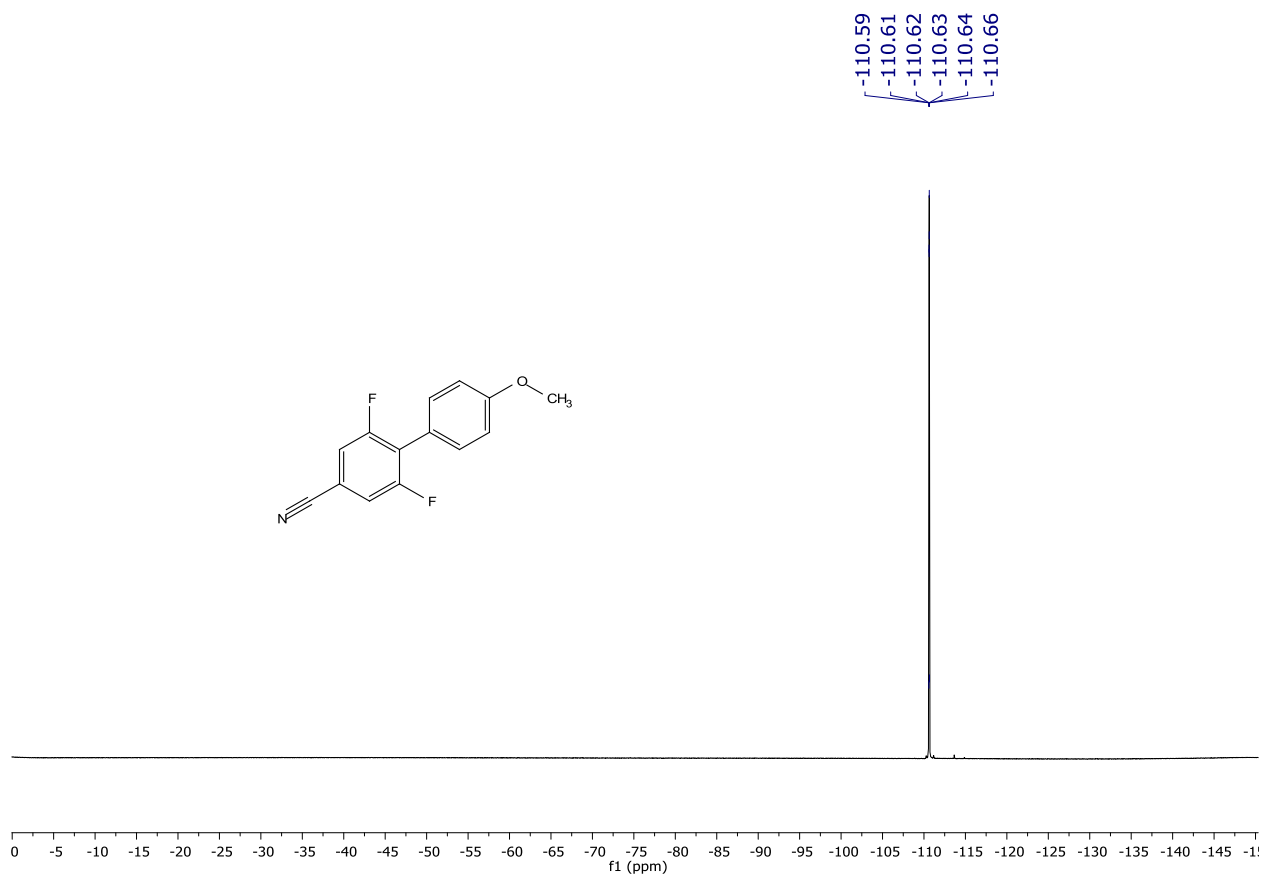


$^{13}\text{C}\{^1\text{H}\}$ NMR (101 MHz, CDCl_3) spectrum of **125af**.

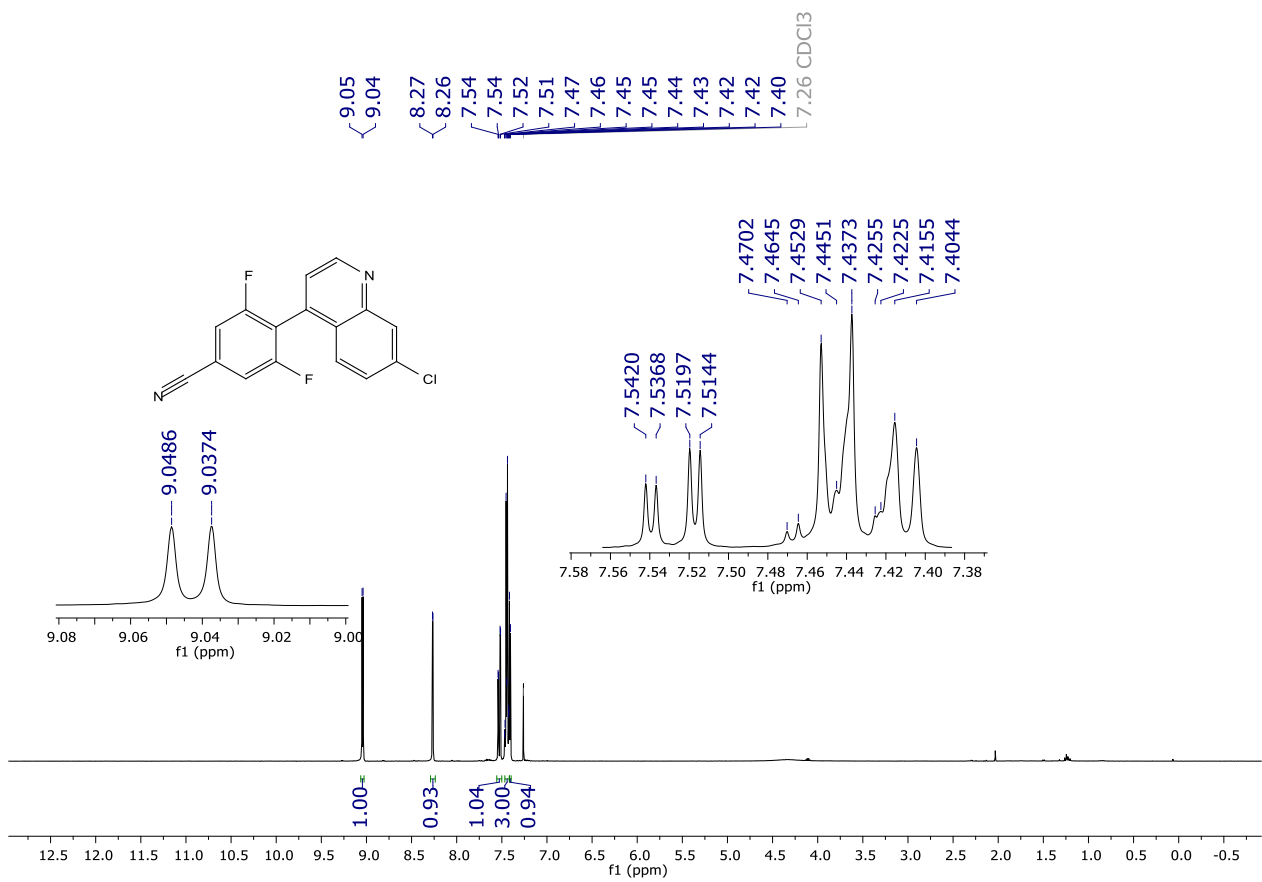


^{19}F NMR (282 MHz, CDCl_3) spectrum of **125af**.

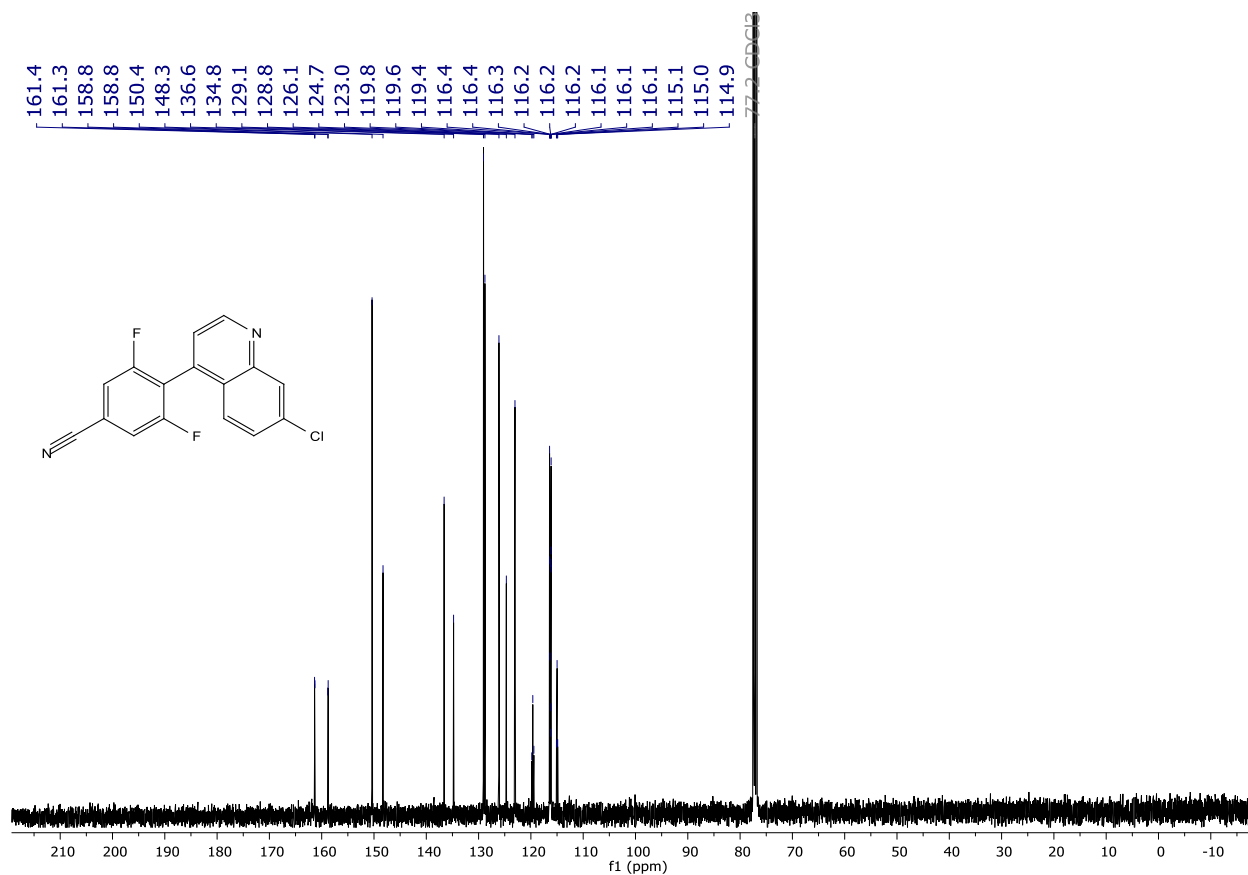




^{19}F NMR (282 MHz, CDCl_3) spectrum of **125ag**.

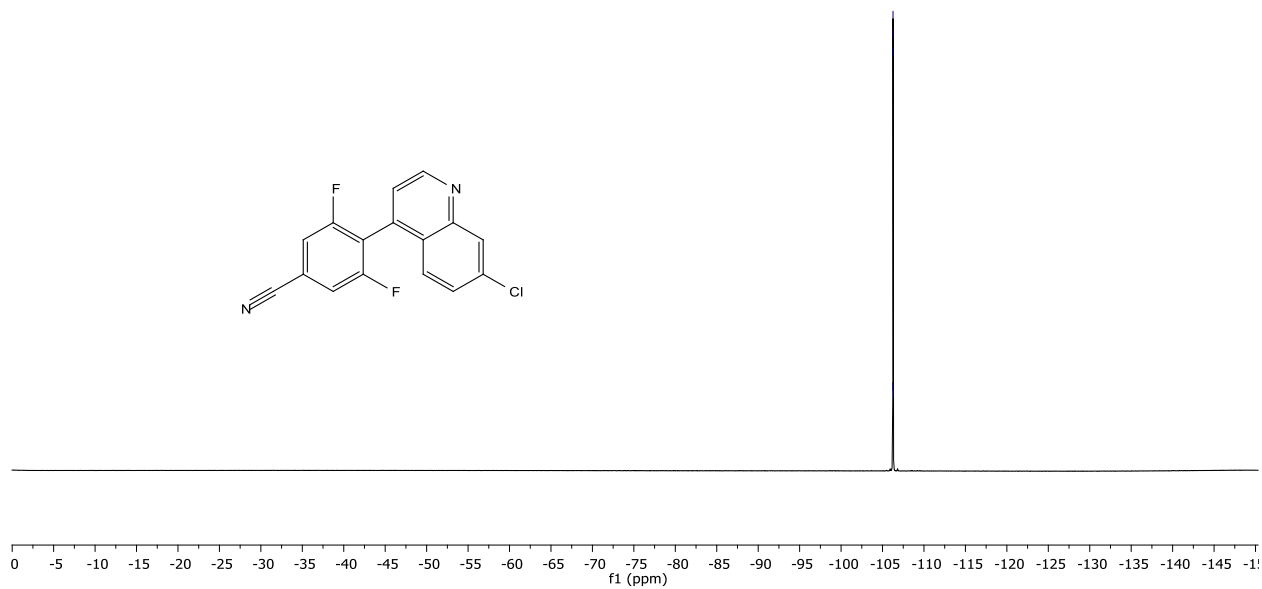


^1H NMR (400 MHz, CDCl_3) spectrum of **125ah**.

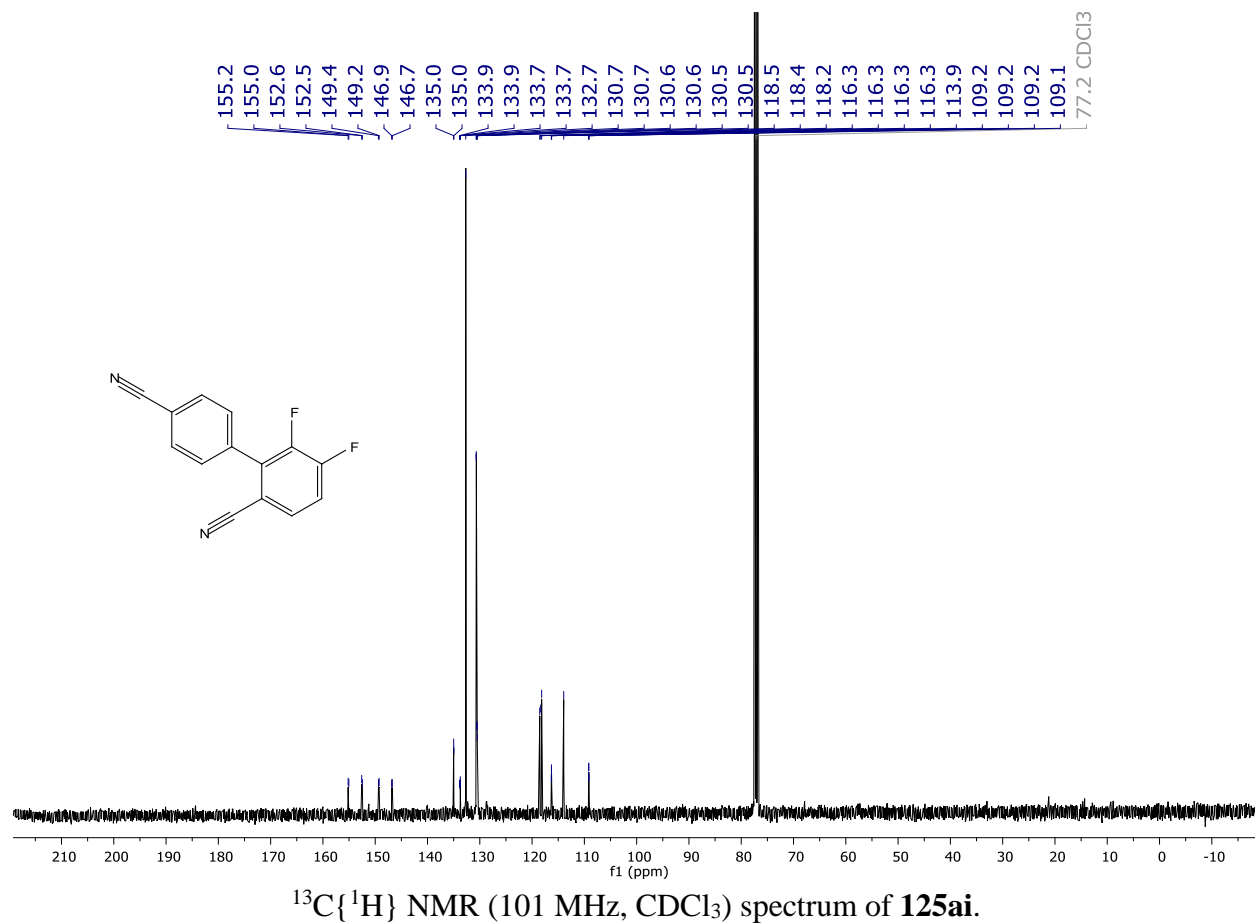
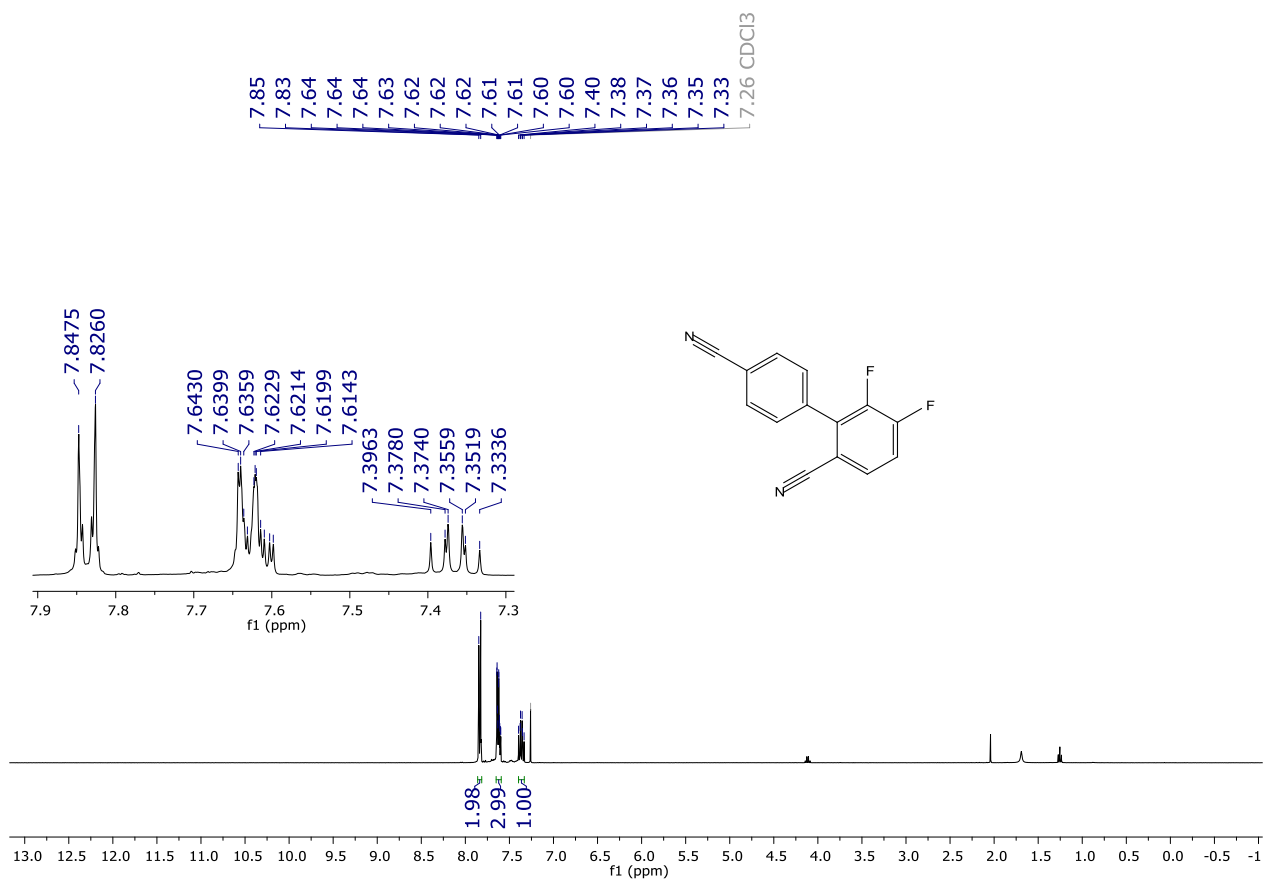


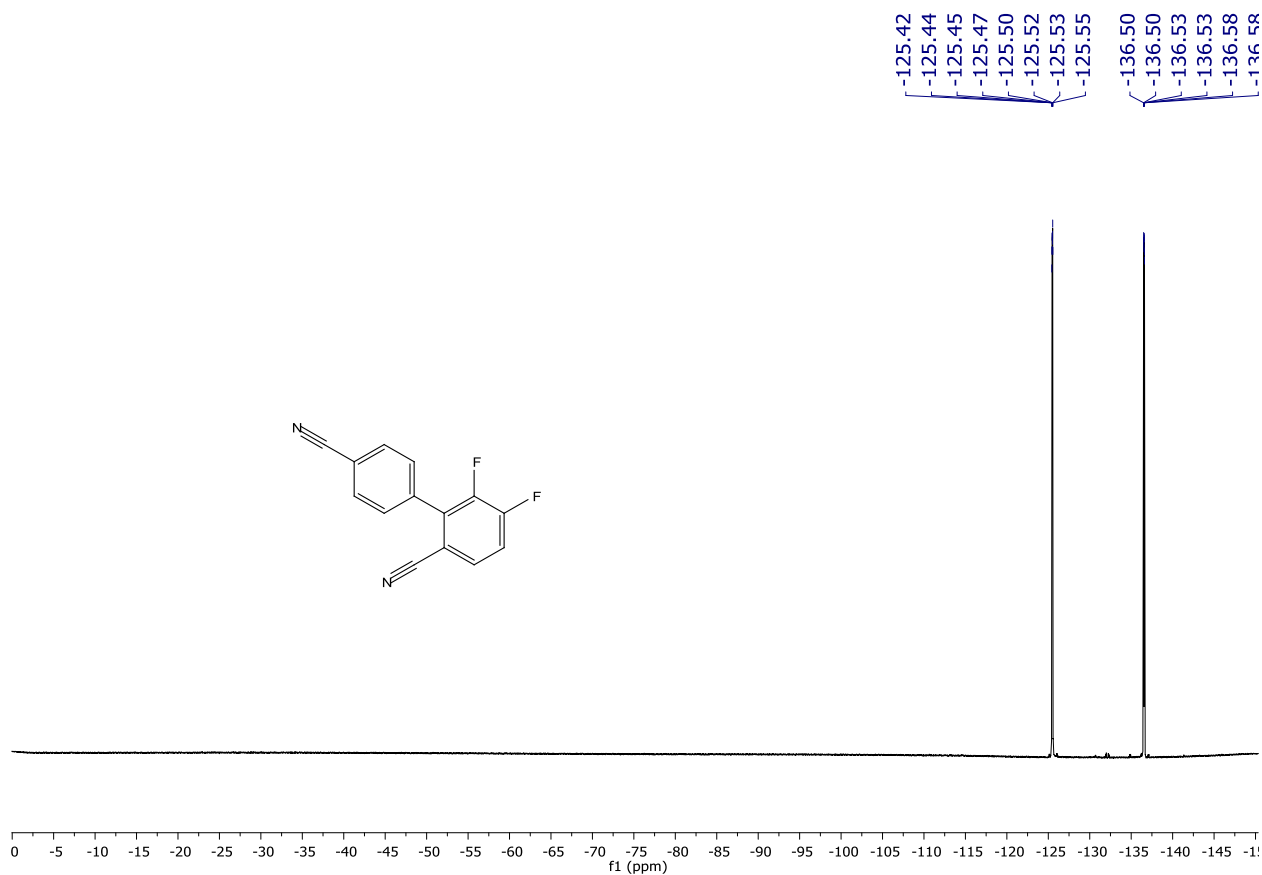
$^{13}\text{C}\{^1\text{H}\}$ NMR (101 MHz, CDCl_3) spectrum of **125ah**.

-106.24
-106.27
-106.28
-106.29
-106.30

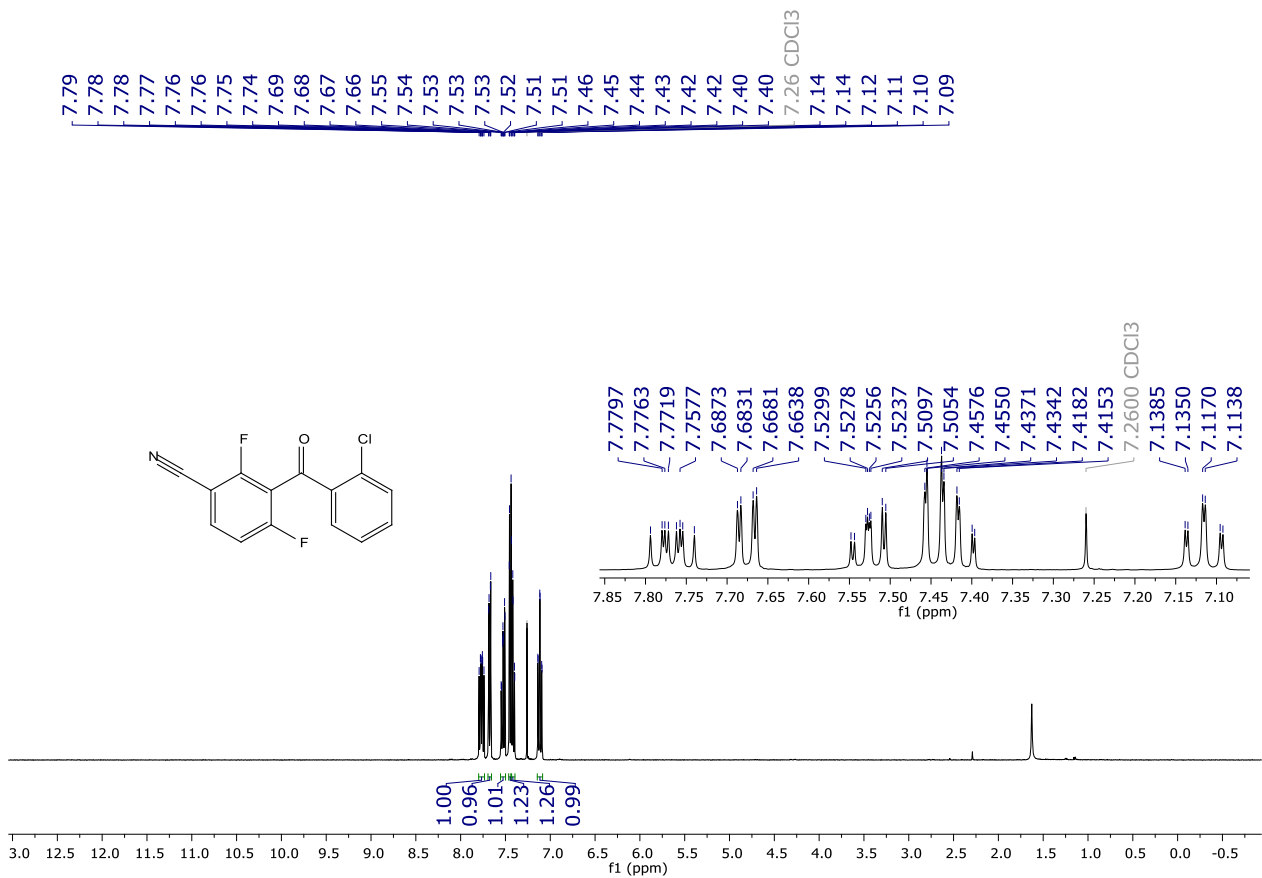


^{19}F NMR (282 MHz, CDCl_3) spectrum of **125ah**.

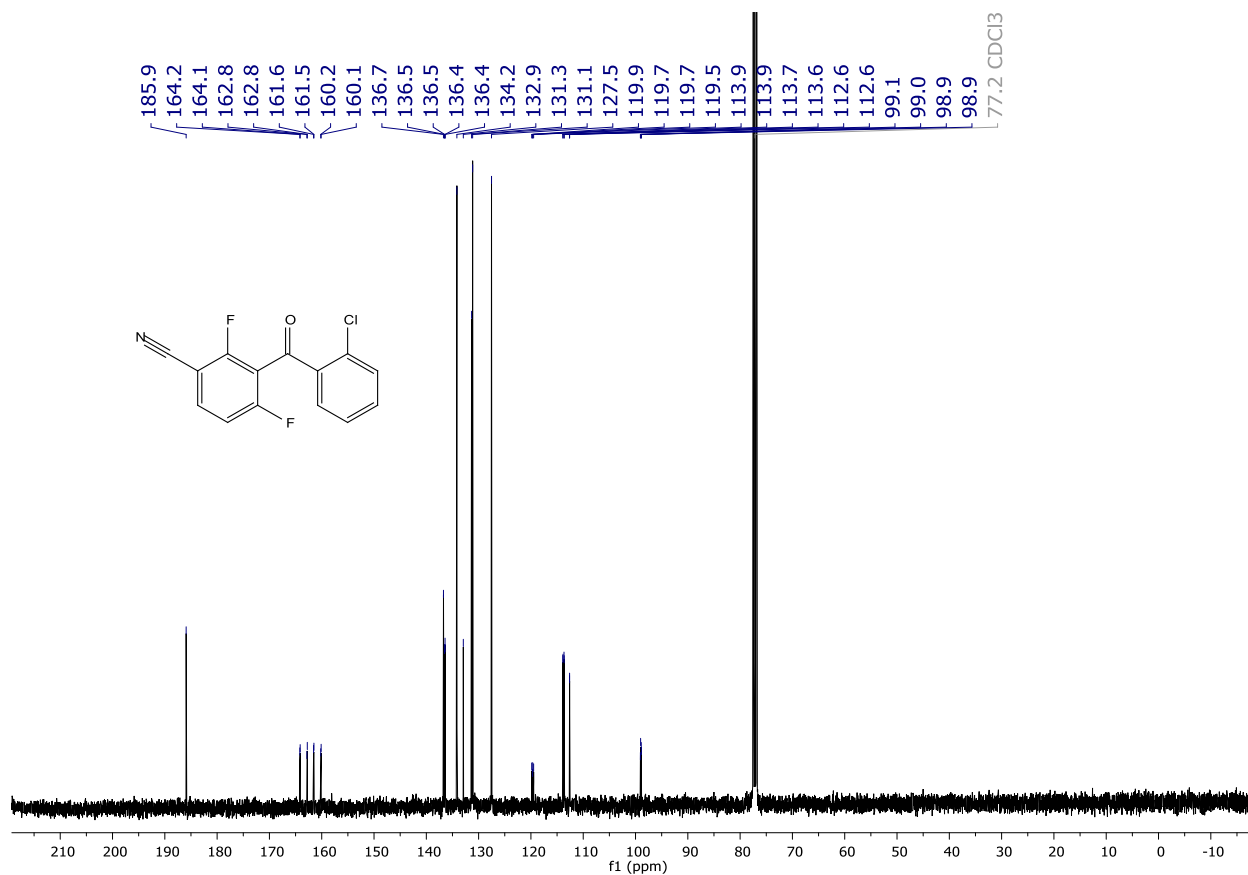




^{19}F NMR (282 MHz, CDCl_3) spectrum of **125ai**.



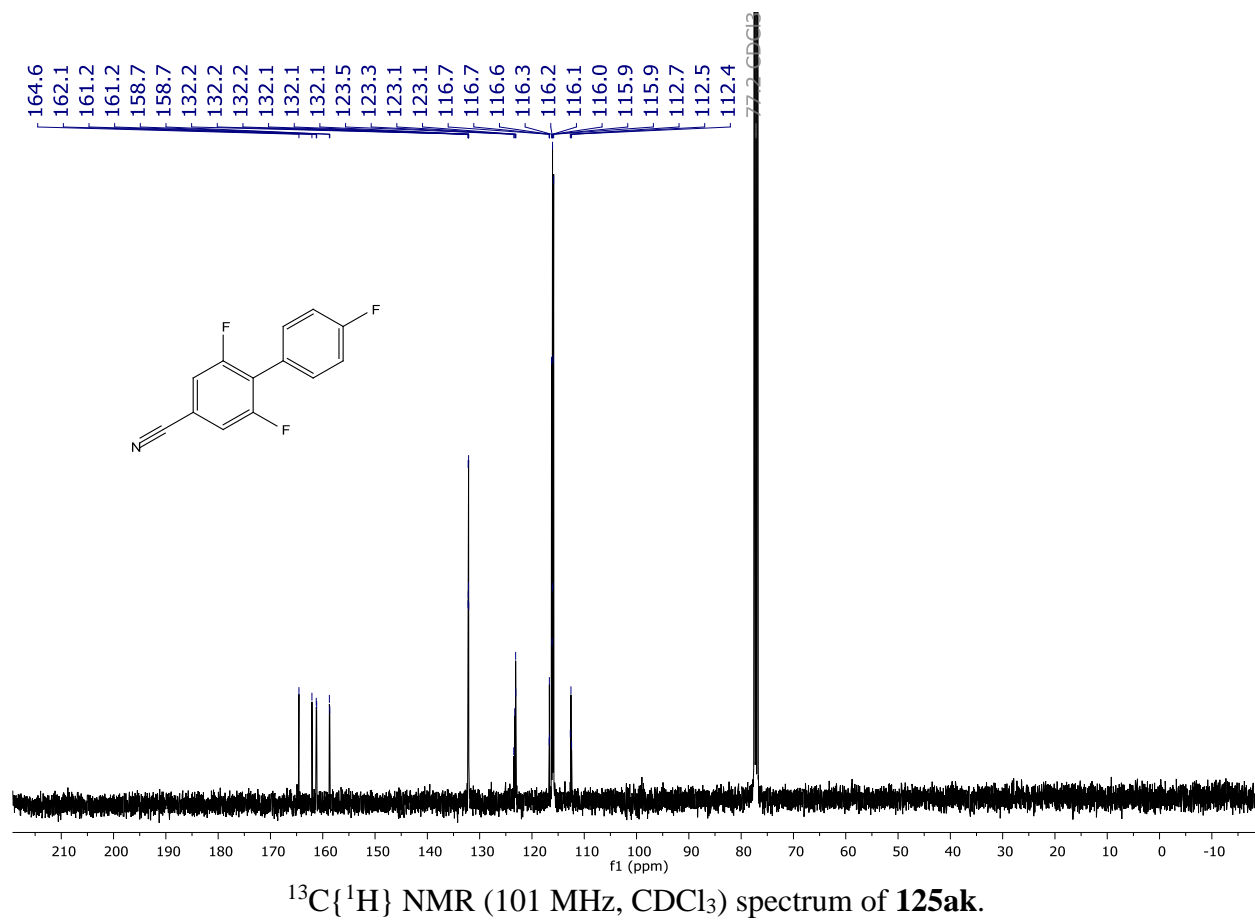
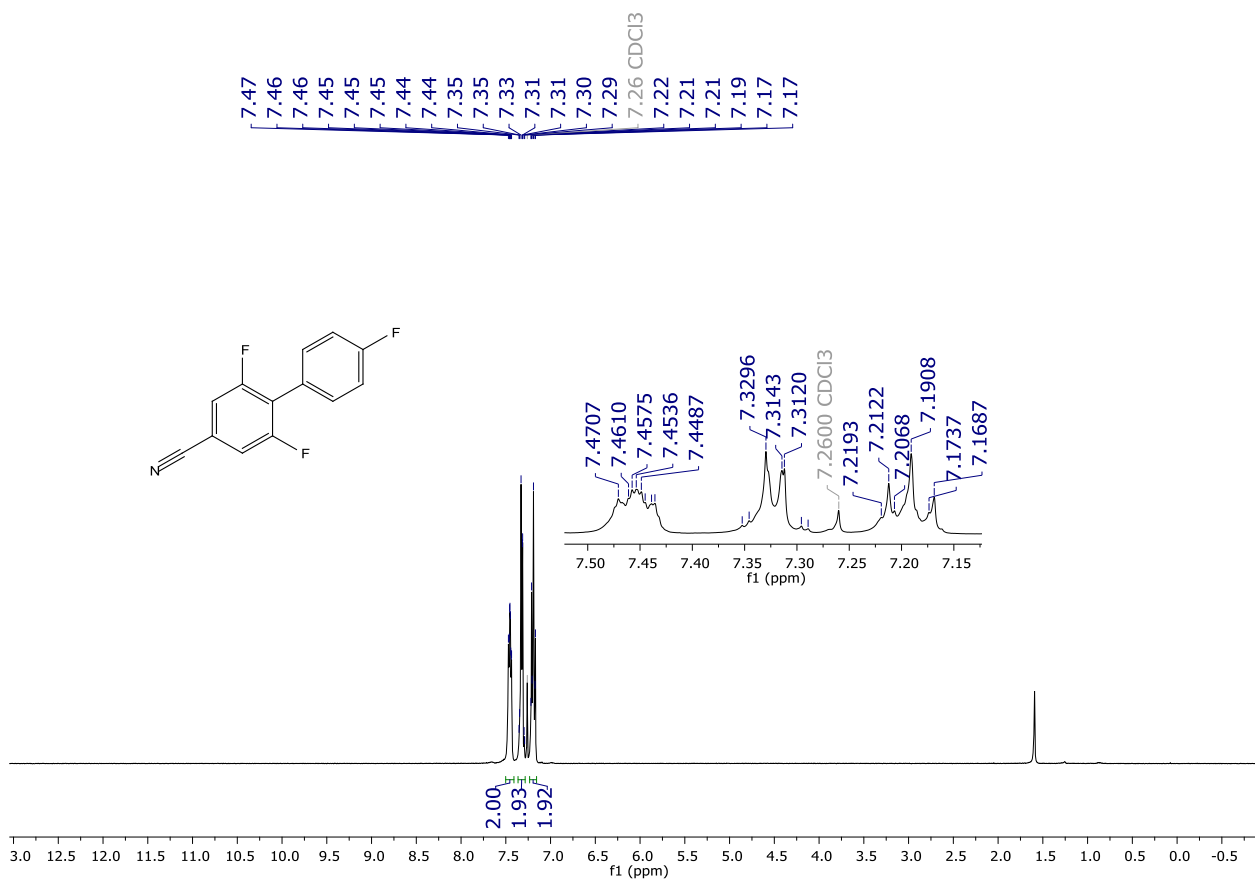
^1H NMR (400 MHz, CDCl_3) spectrum of **125aj**.

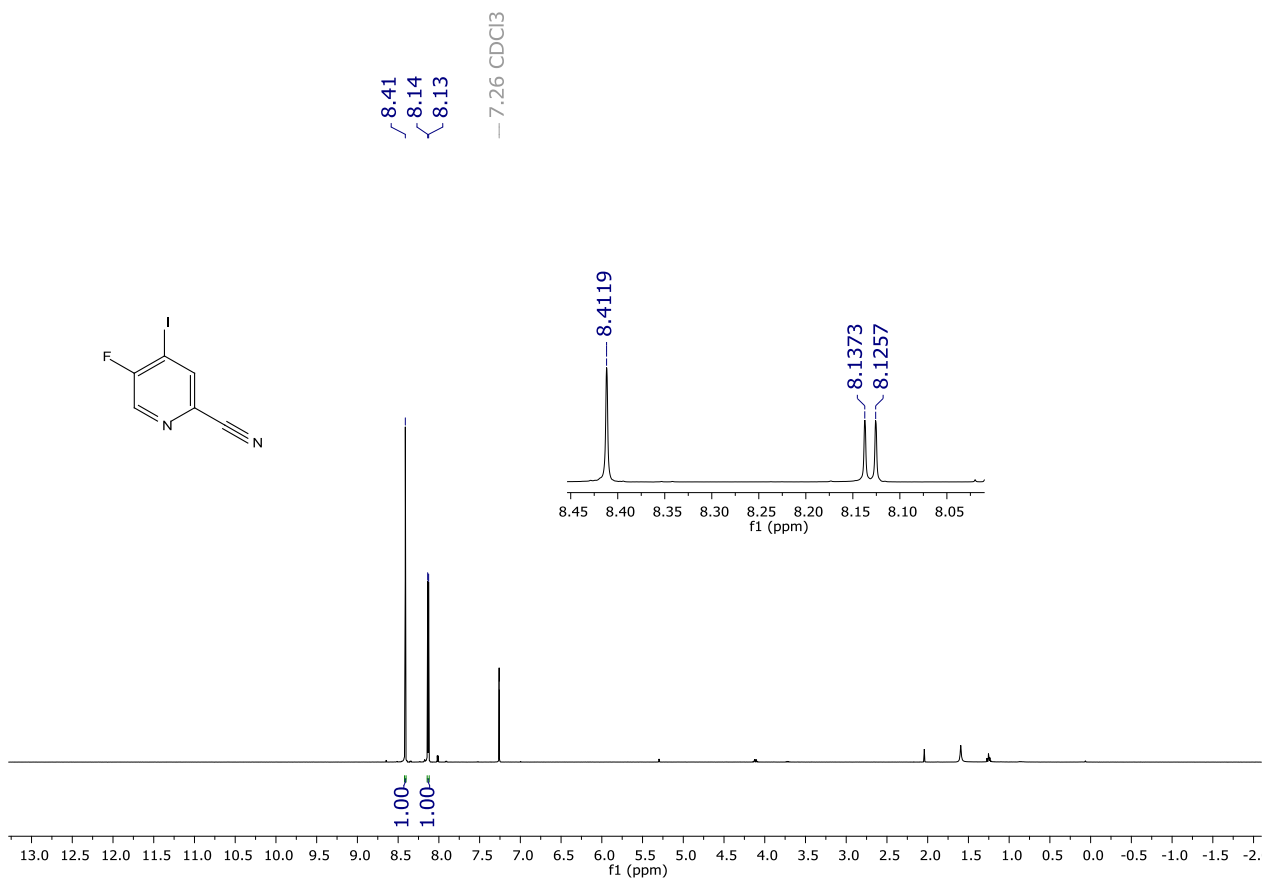
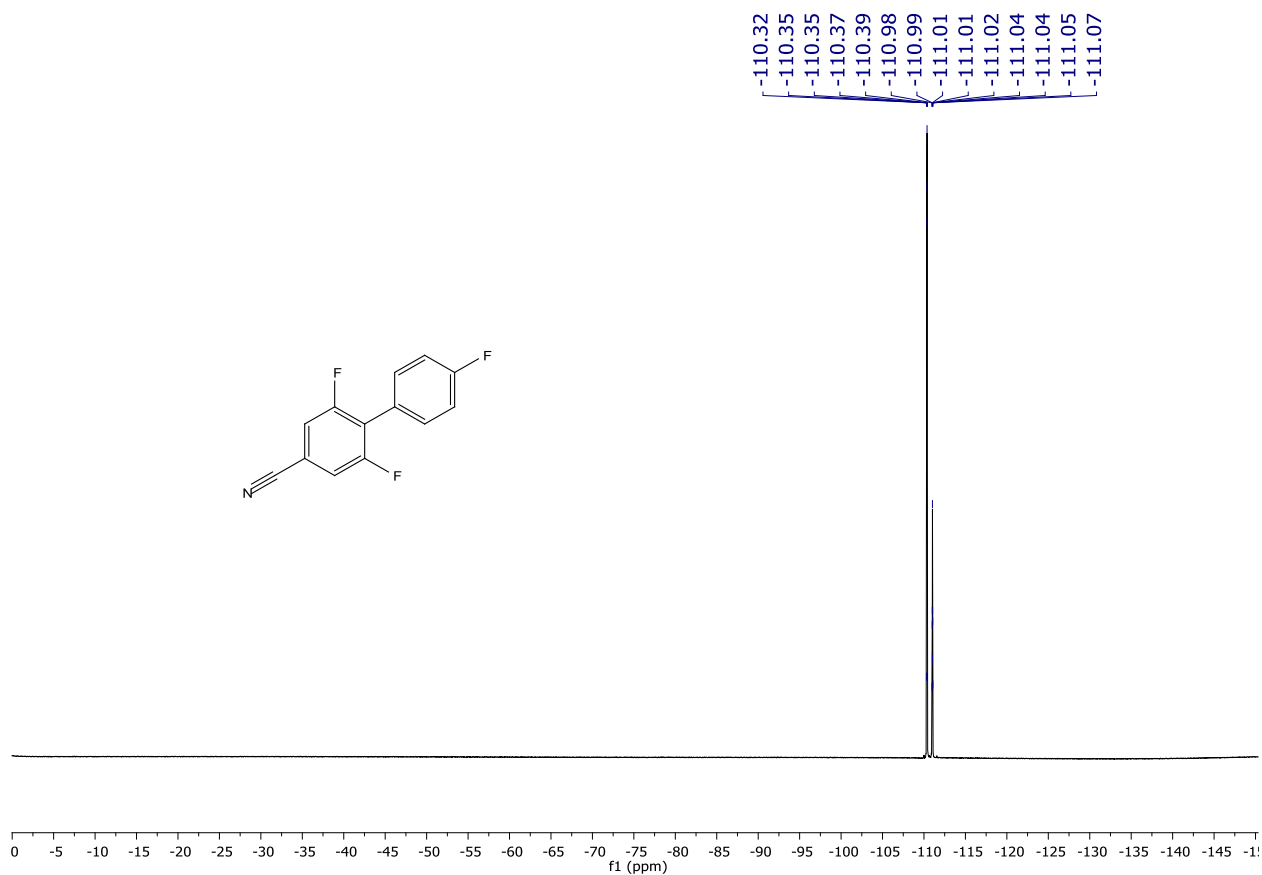


$^{13}\text{C}\{^1\text{H}\}$ NMR (101 MHz, CDCl_3) spectrum of **125aj**.

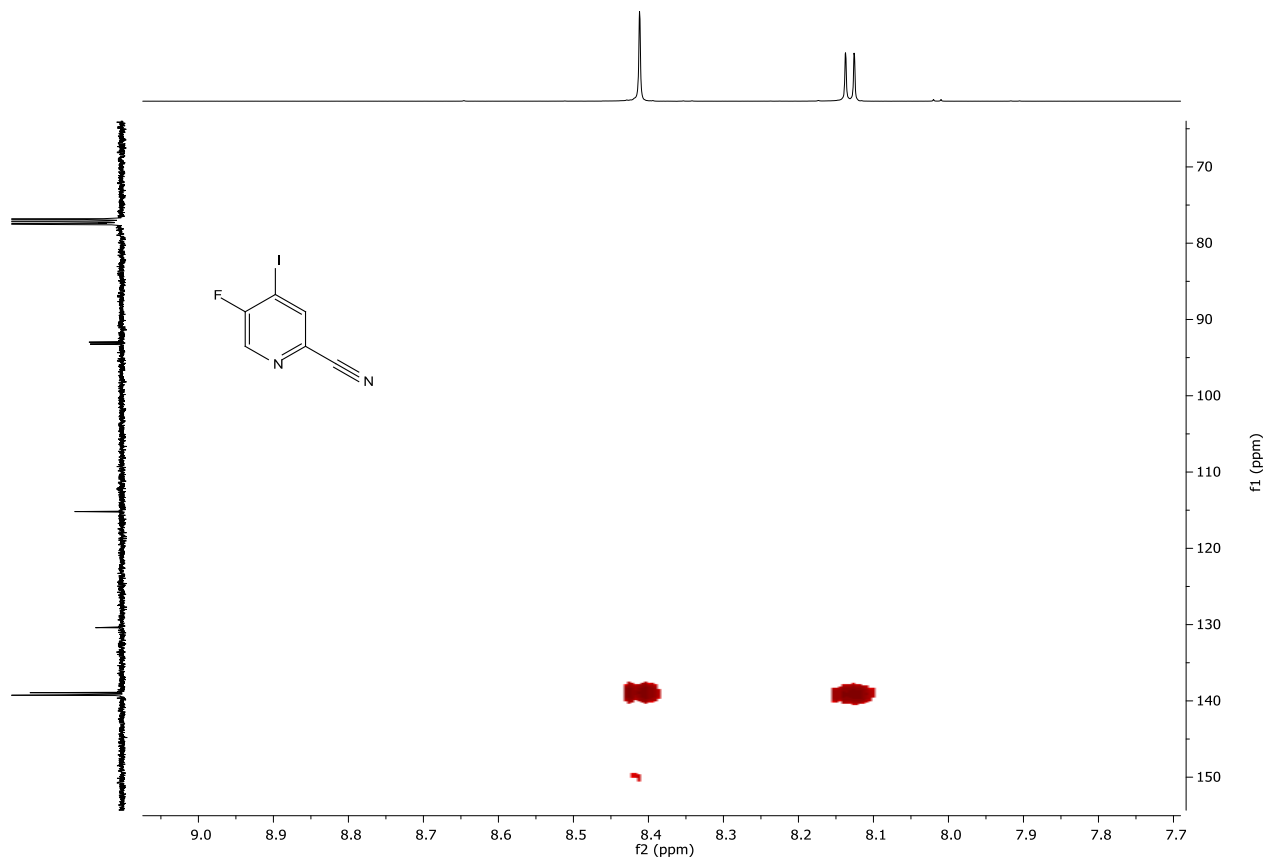
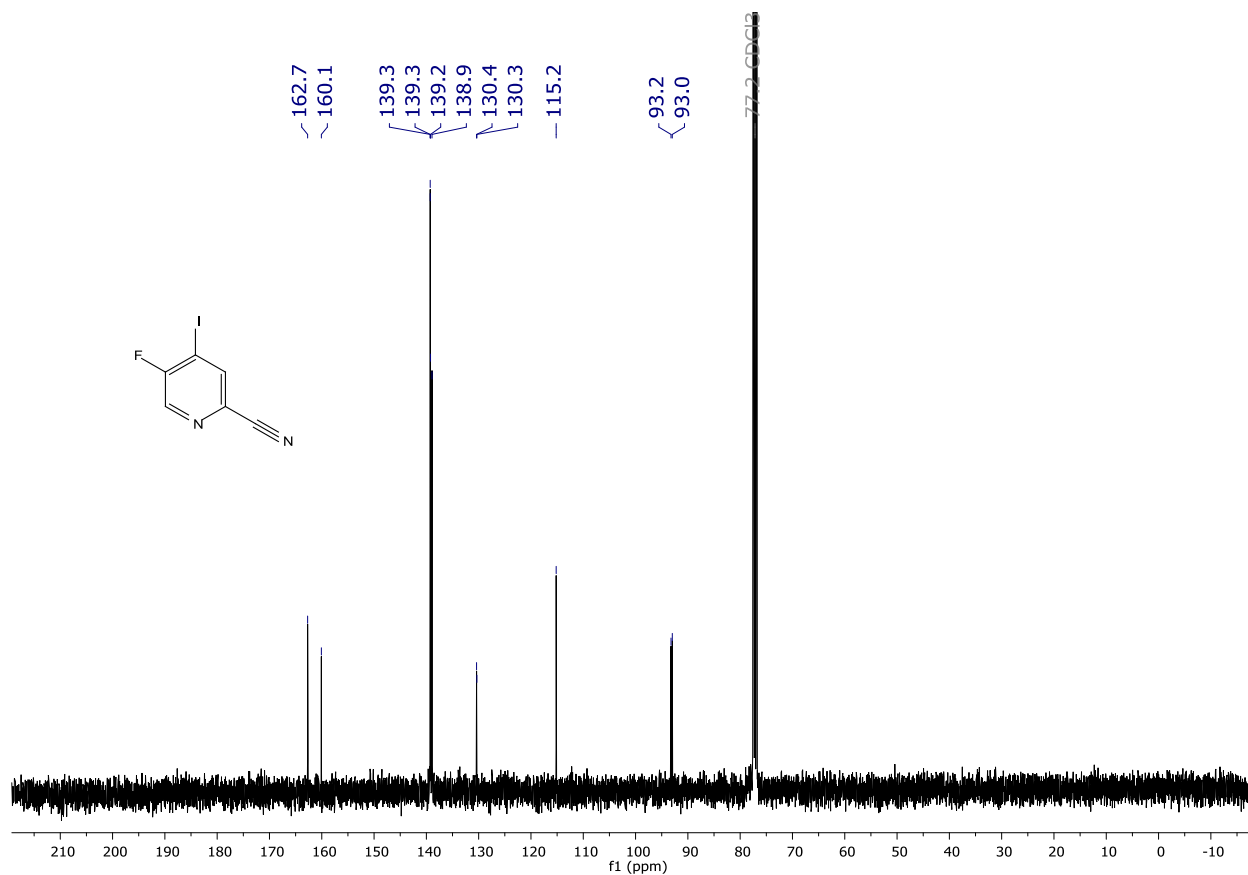


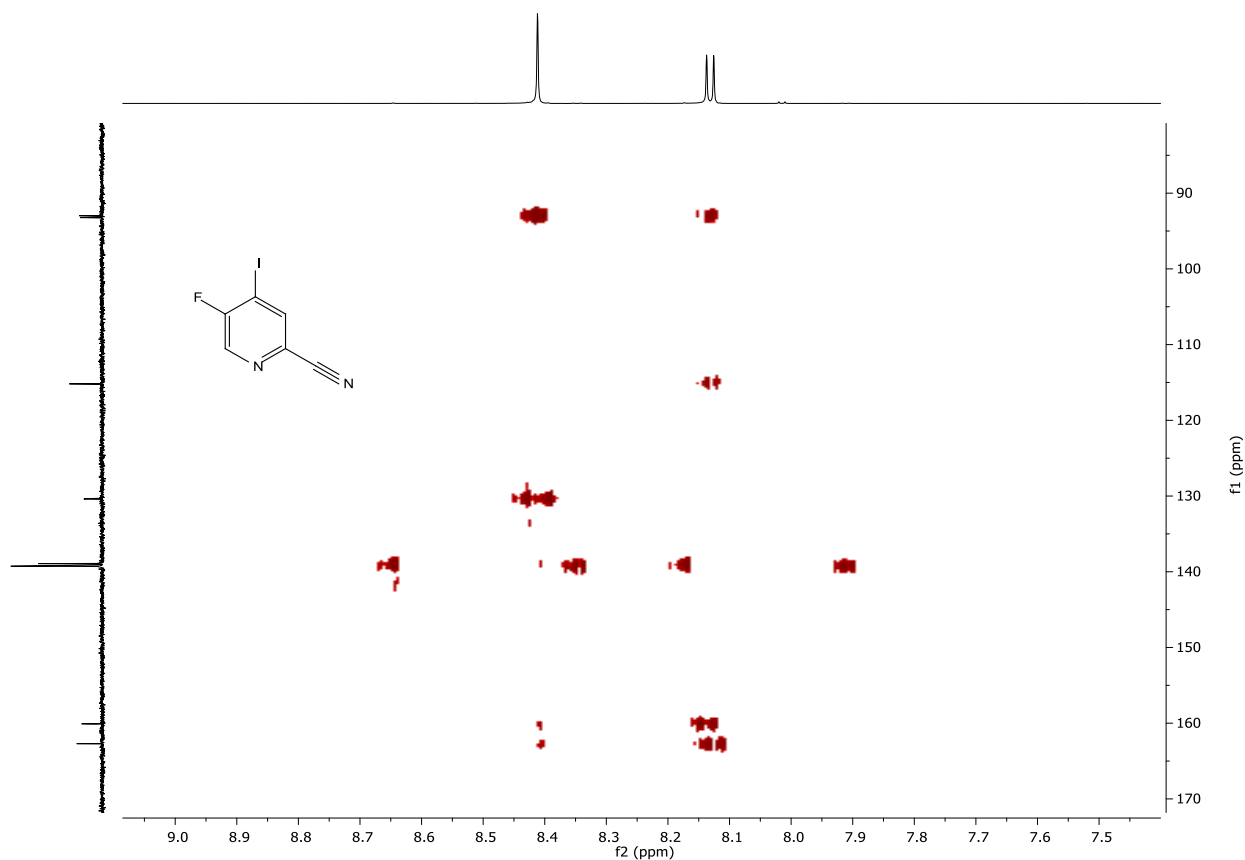
^{19}F NMR (282 MHz, CDCl_3) spectrum of **125aj**.





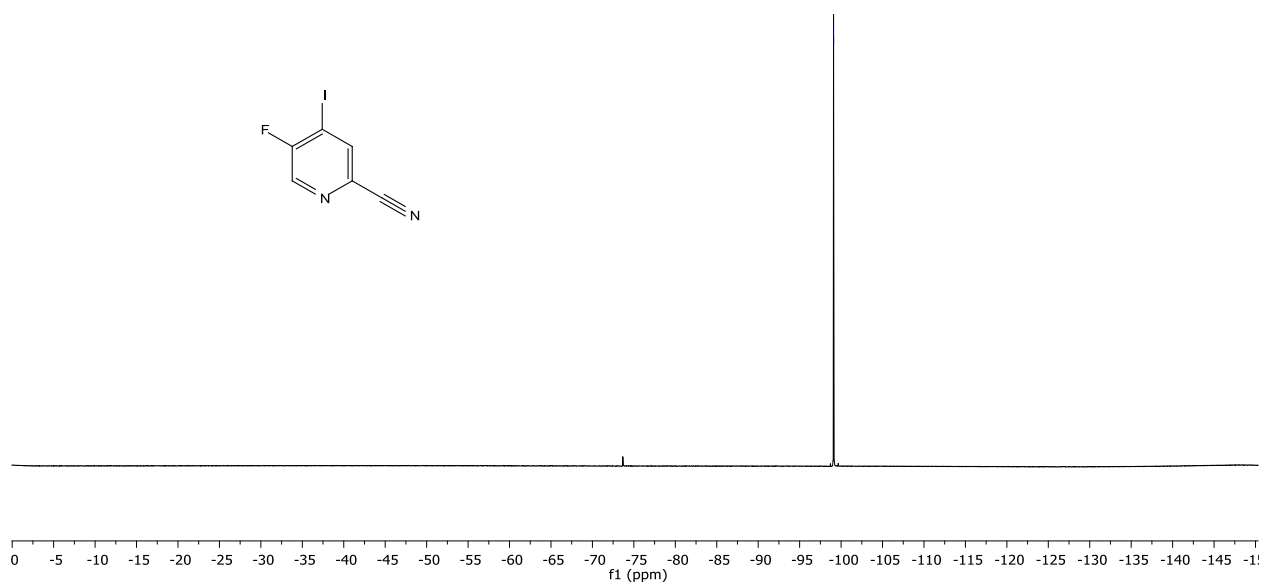
^1H NMR (400 MHz, CDCl_3) spectrum of **125al**.

HSQC correlation map of **125al** (400 and 101 MHz, CDCl_3).

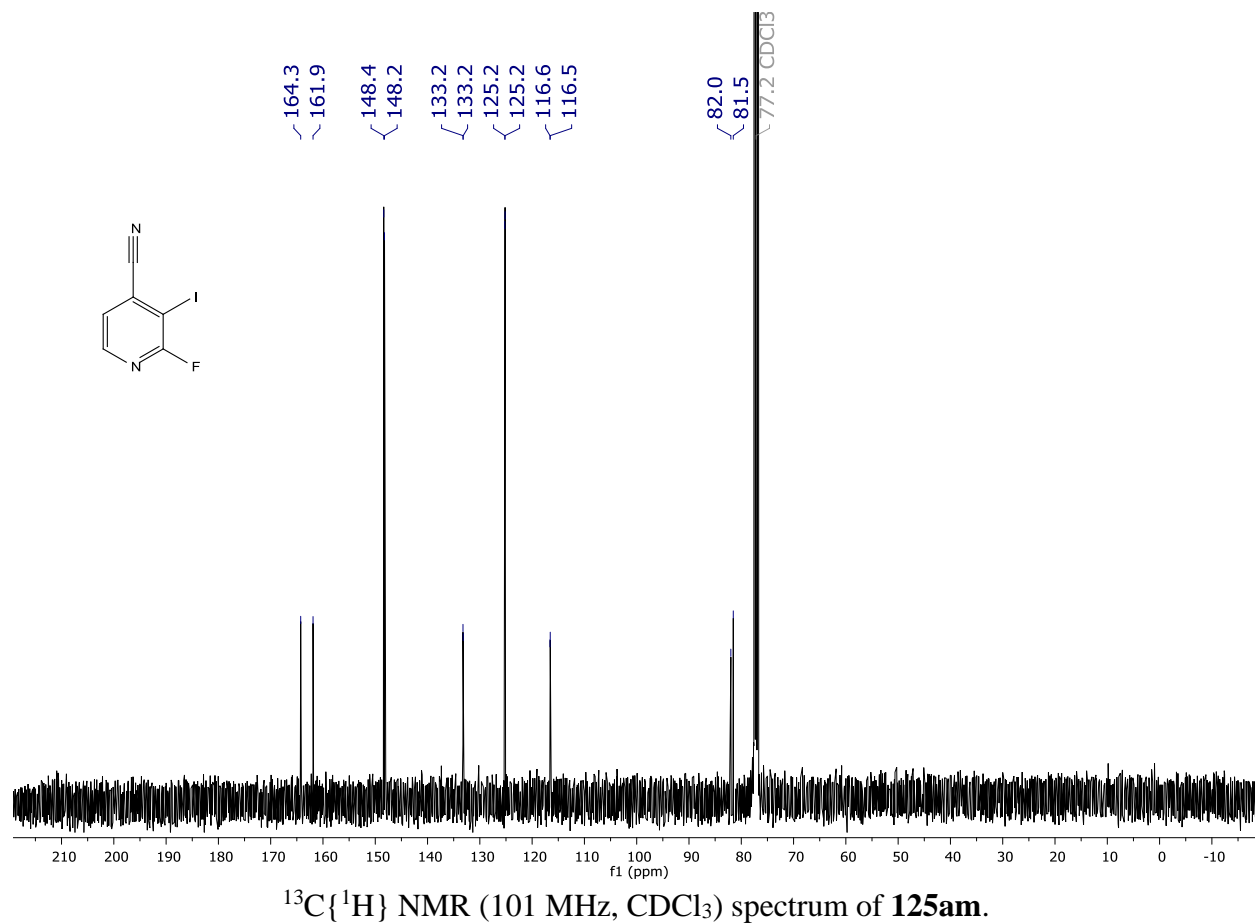
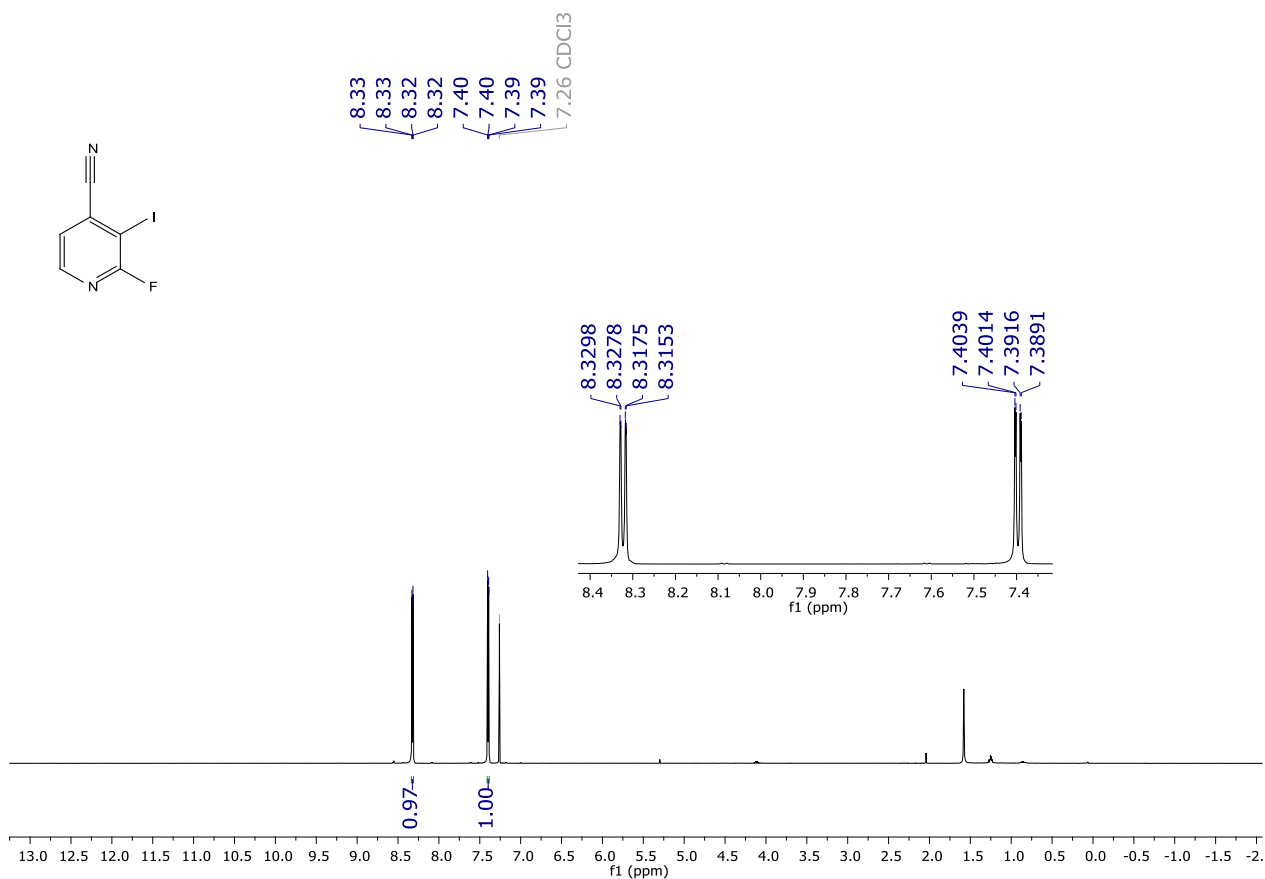


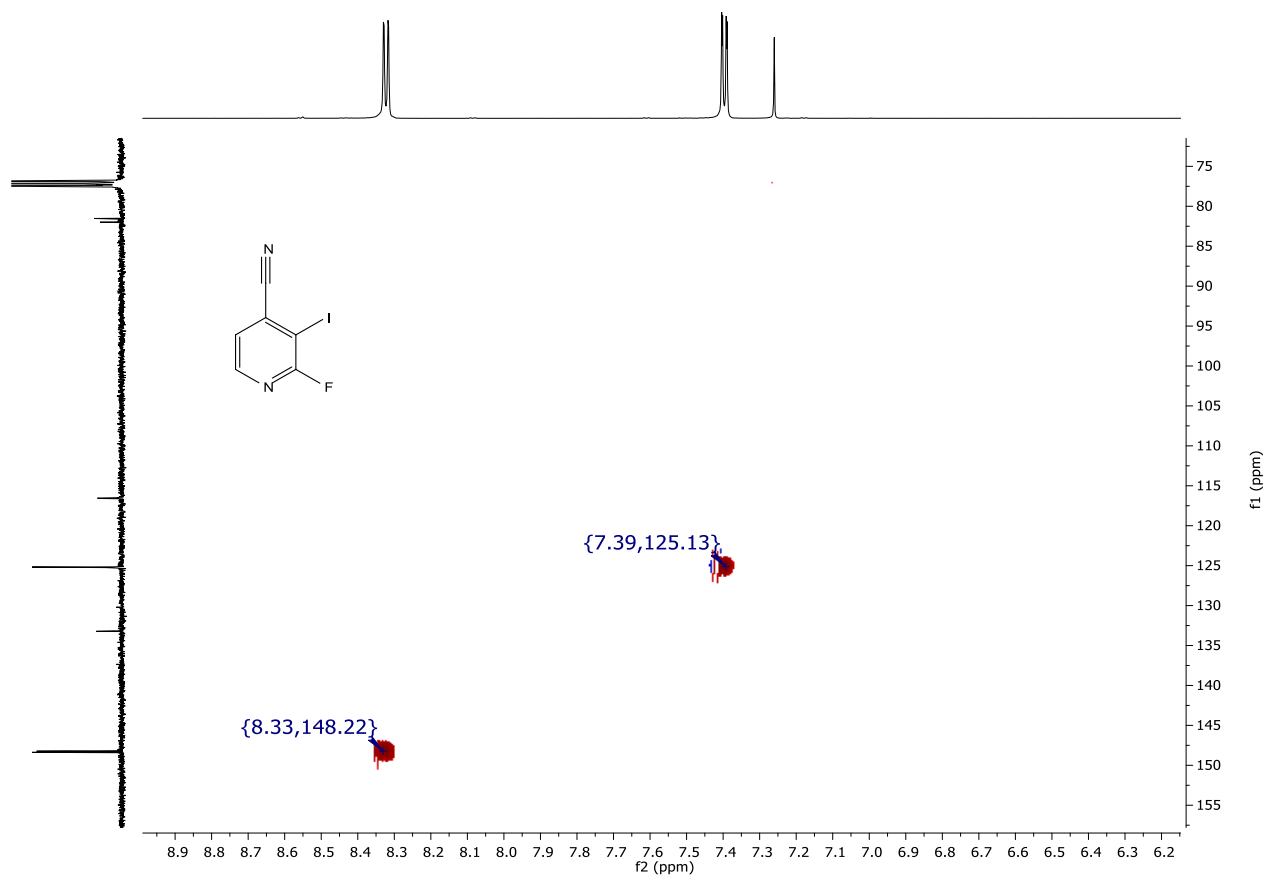
HMBC correlation map of **125al** (400 and 101 MHz, CDCl₃).

-99.09
-99.11

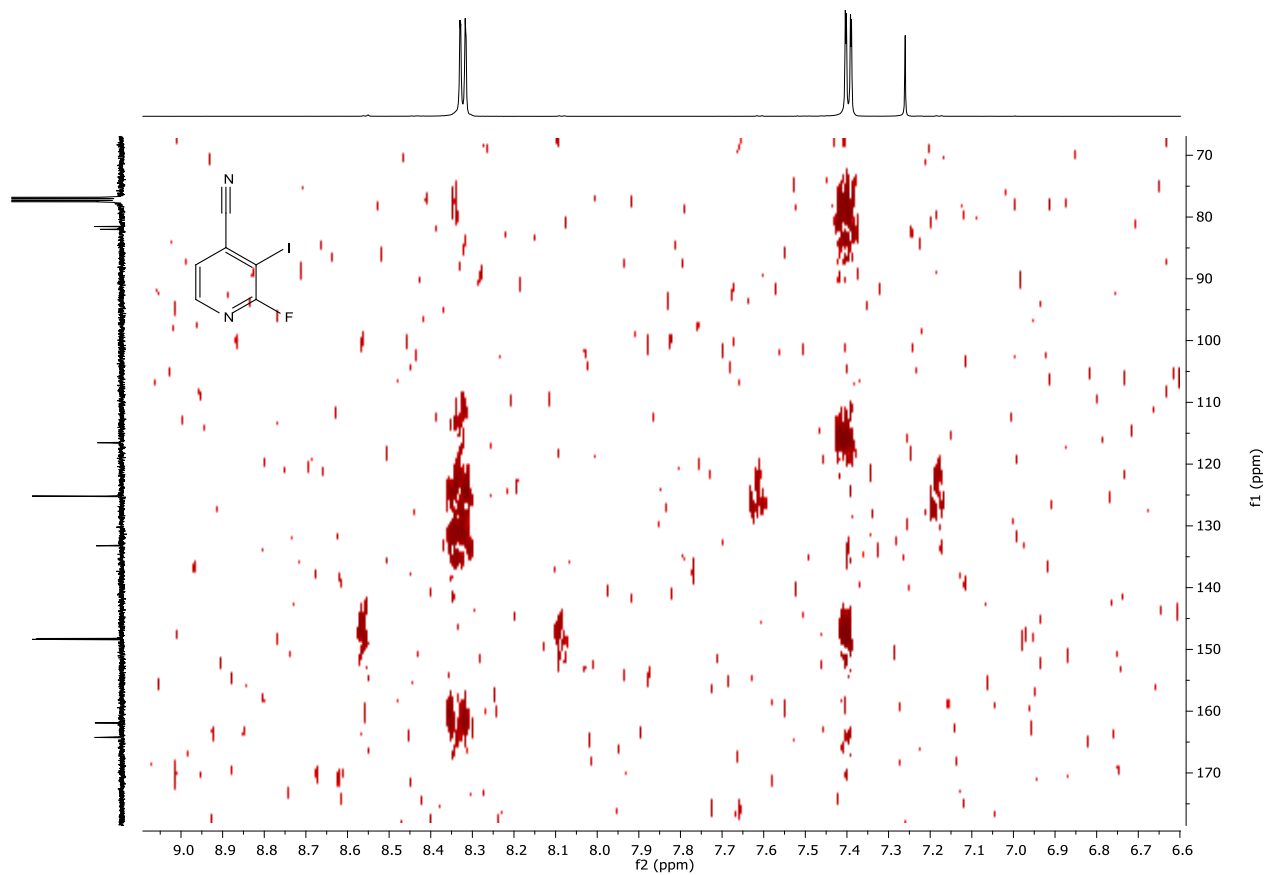


¹⁹F NMR (282 MHz, CDCl₃) spectrum of **125al**.

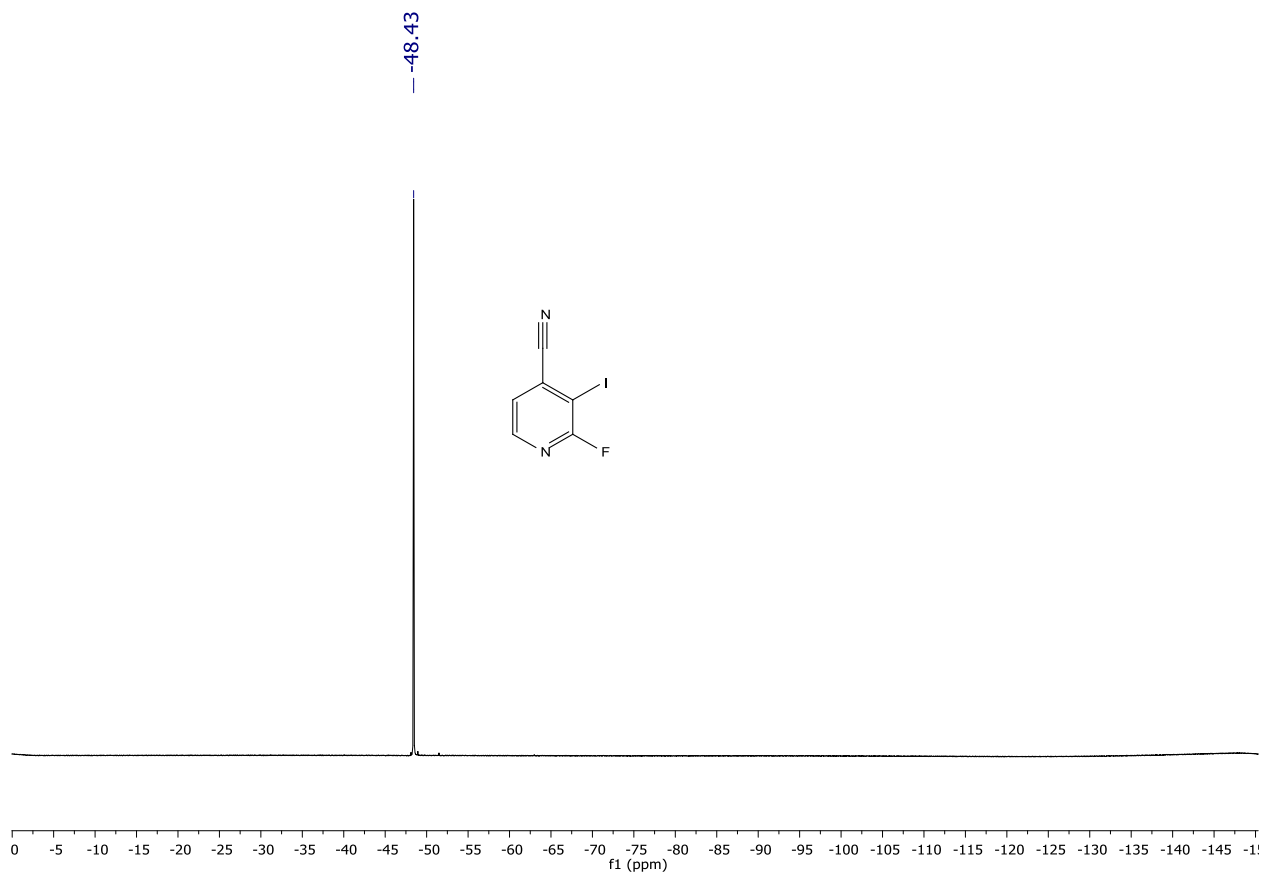




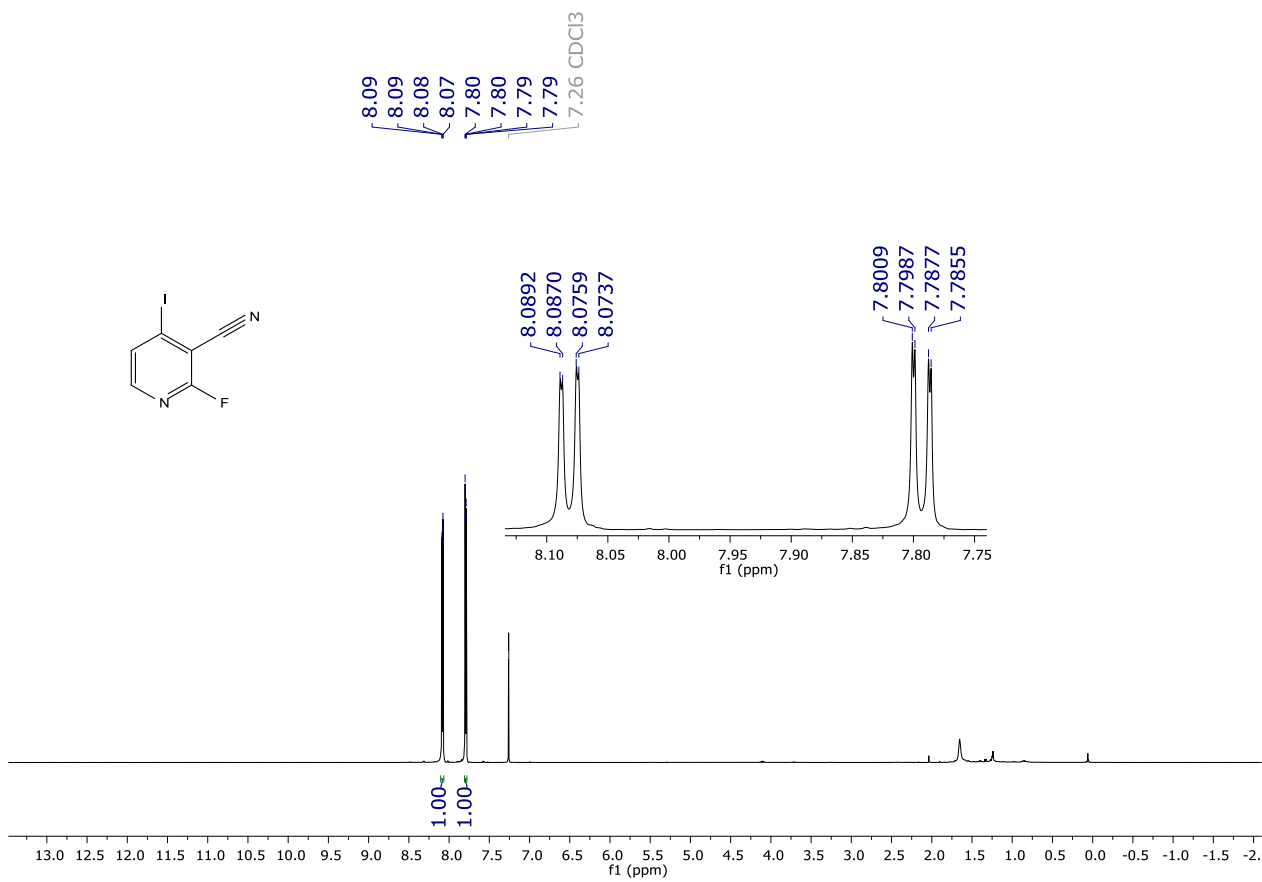
HSQC correlation map of **125am** (400 and 101 MHz, CDCl₃).



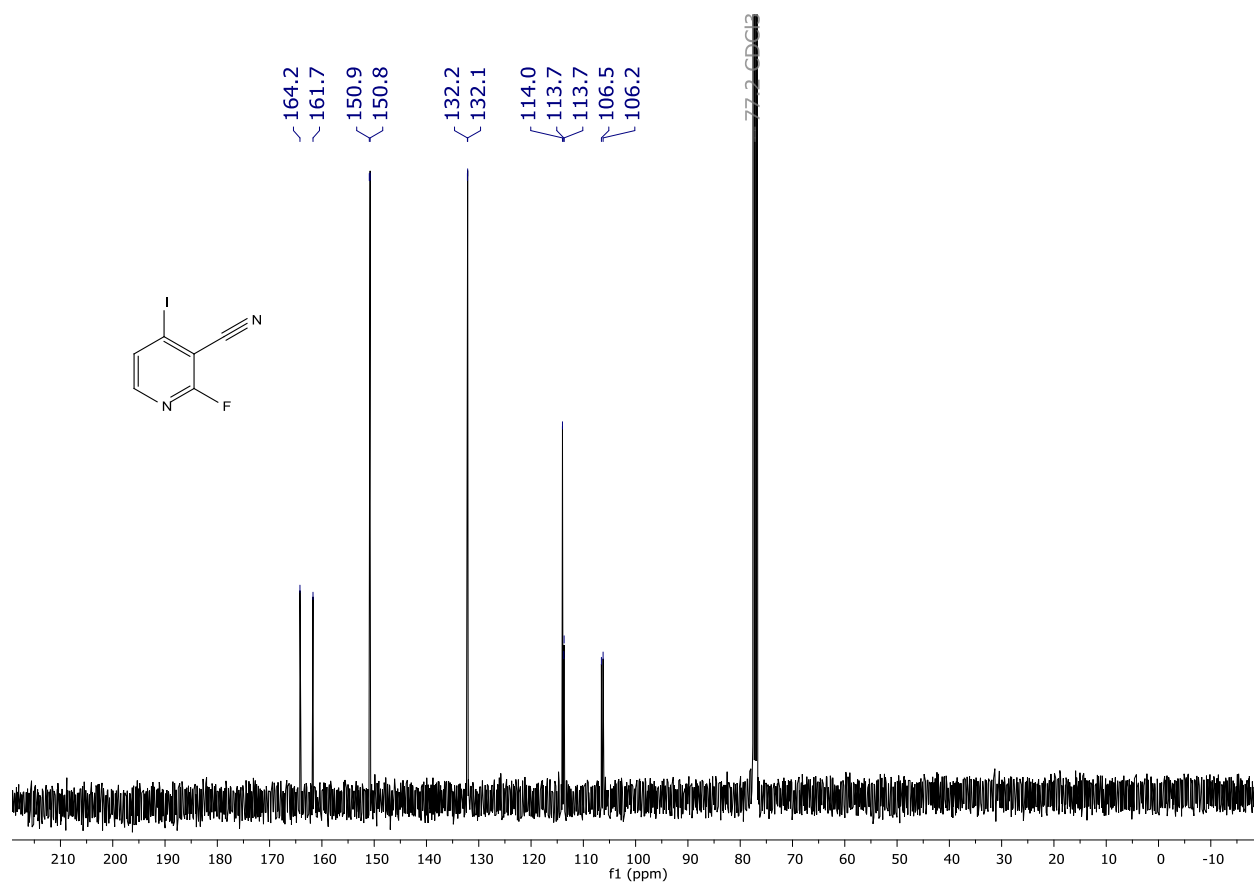
HMBC correlation map of **125am** (400 and 101 MHz, CDCl₃).



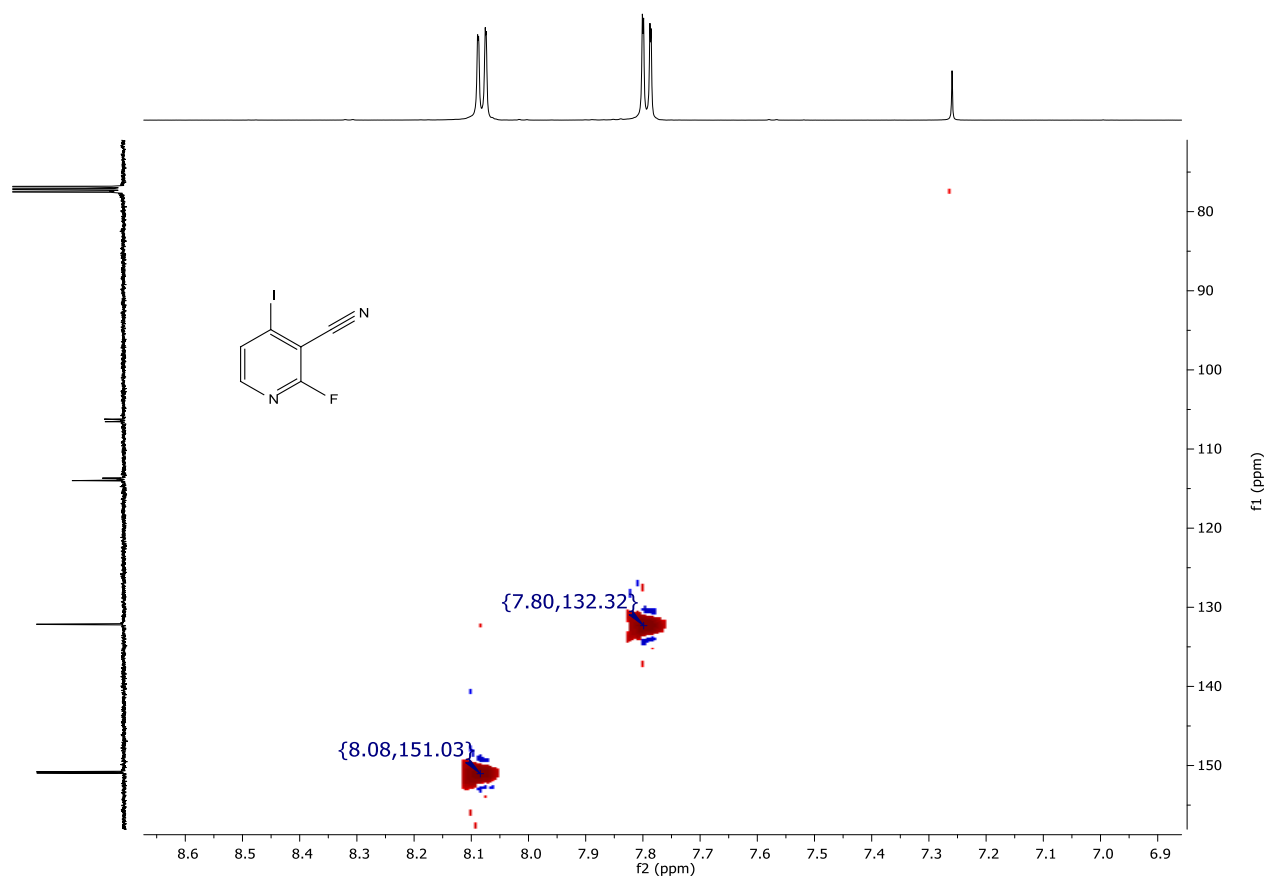
^{19}F NMR (282 MHz, CDCl_3) spectrum of **125an**.



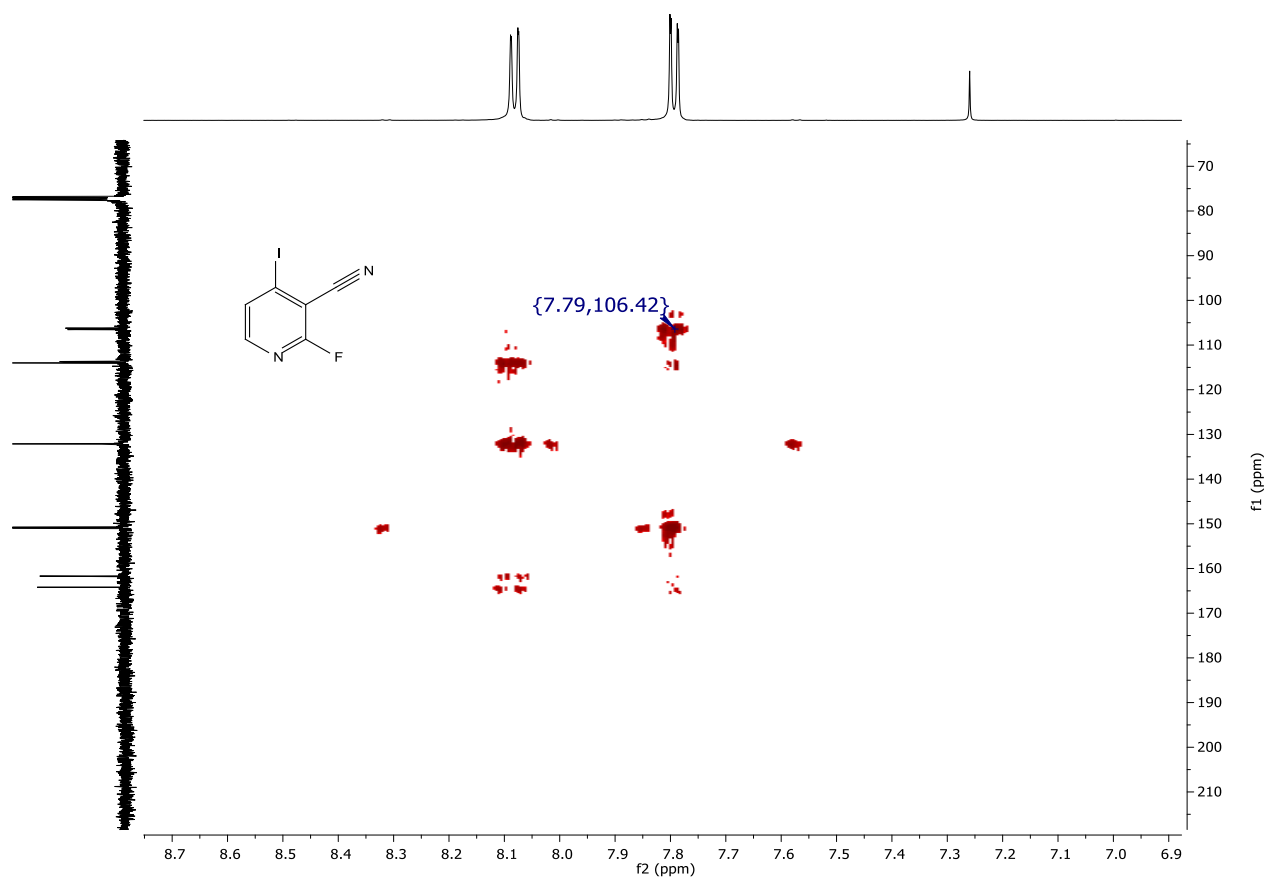
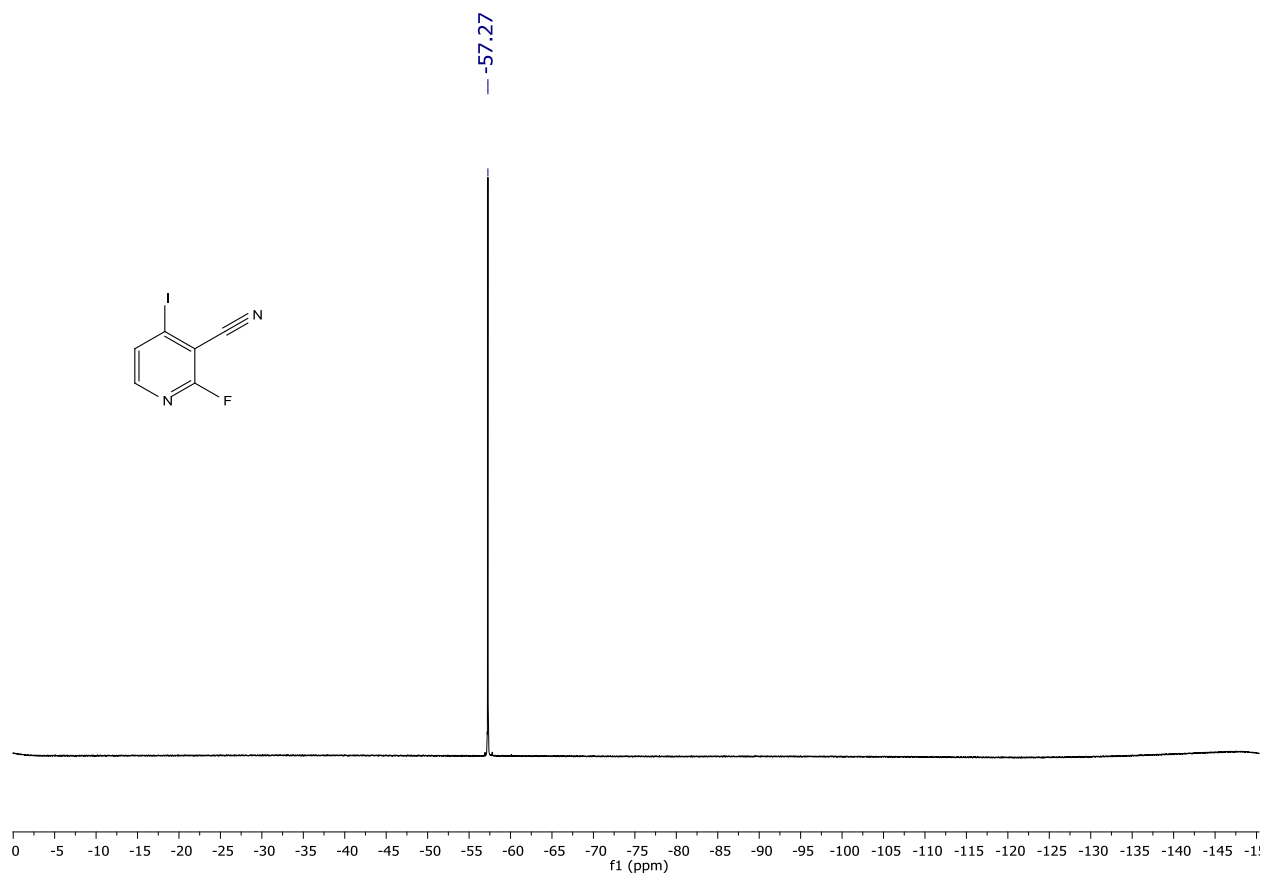
^1H NMR (400 MHz, CDCl_3) spectrum of **125an**.

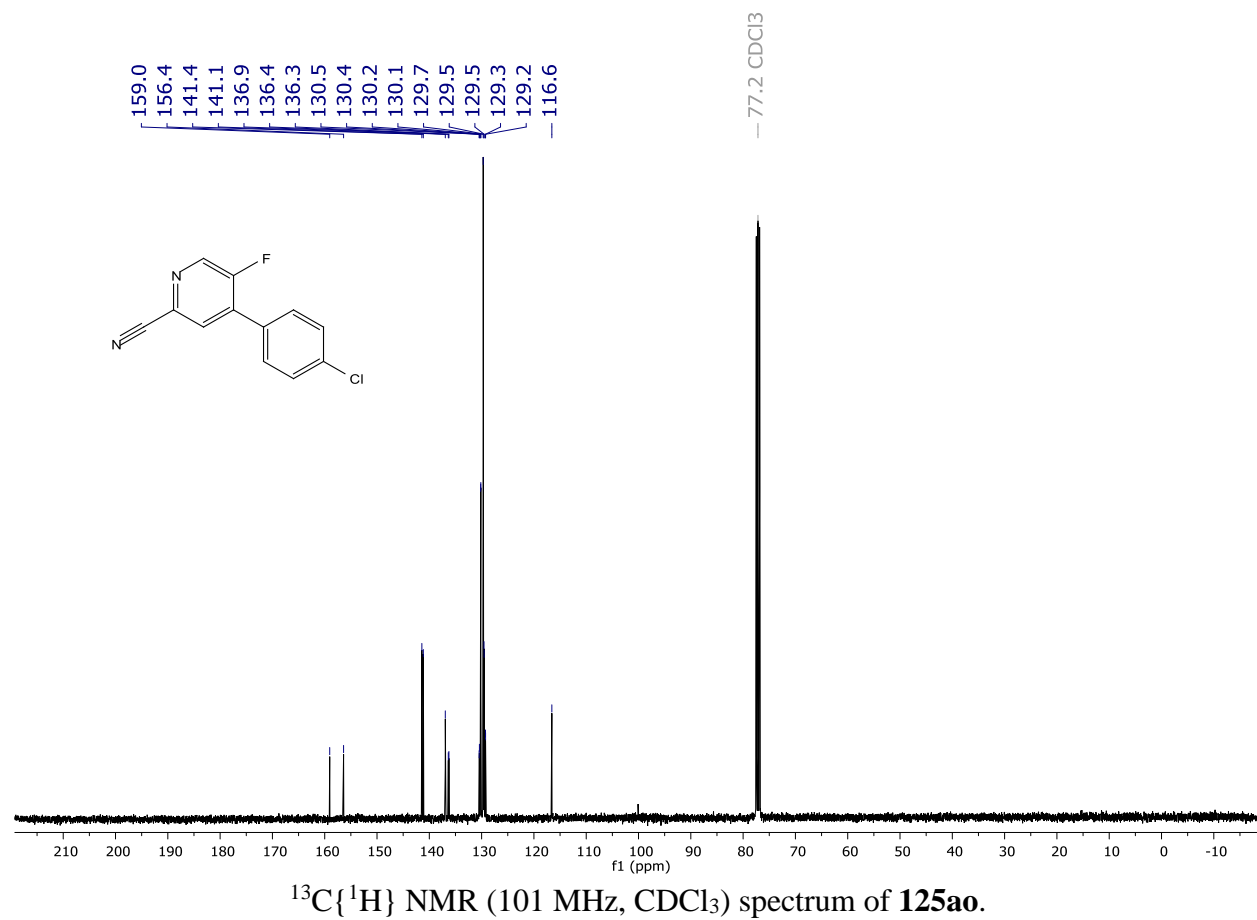
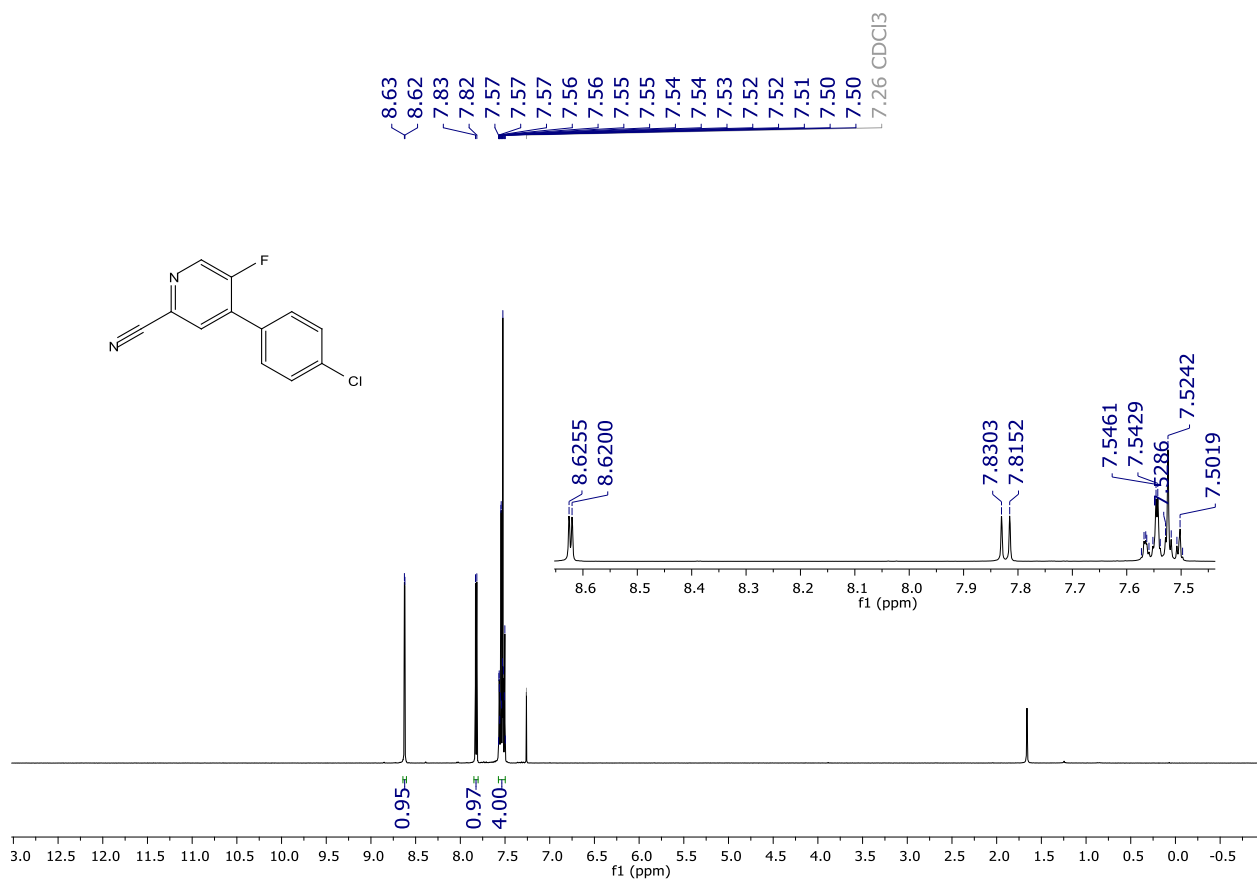


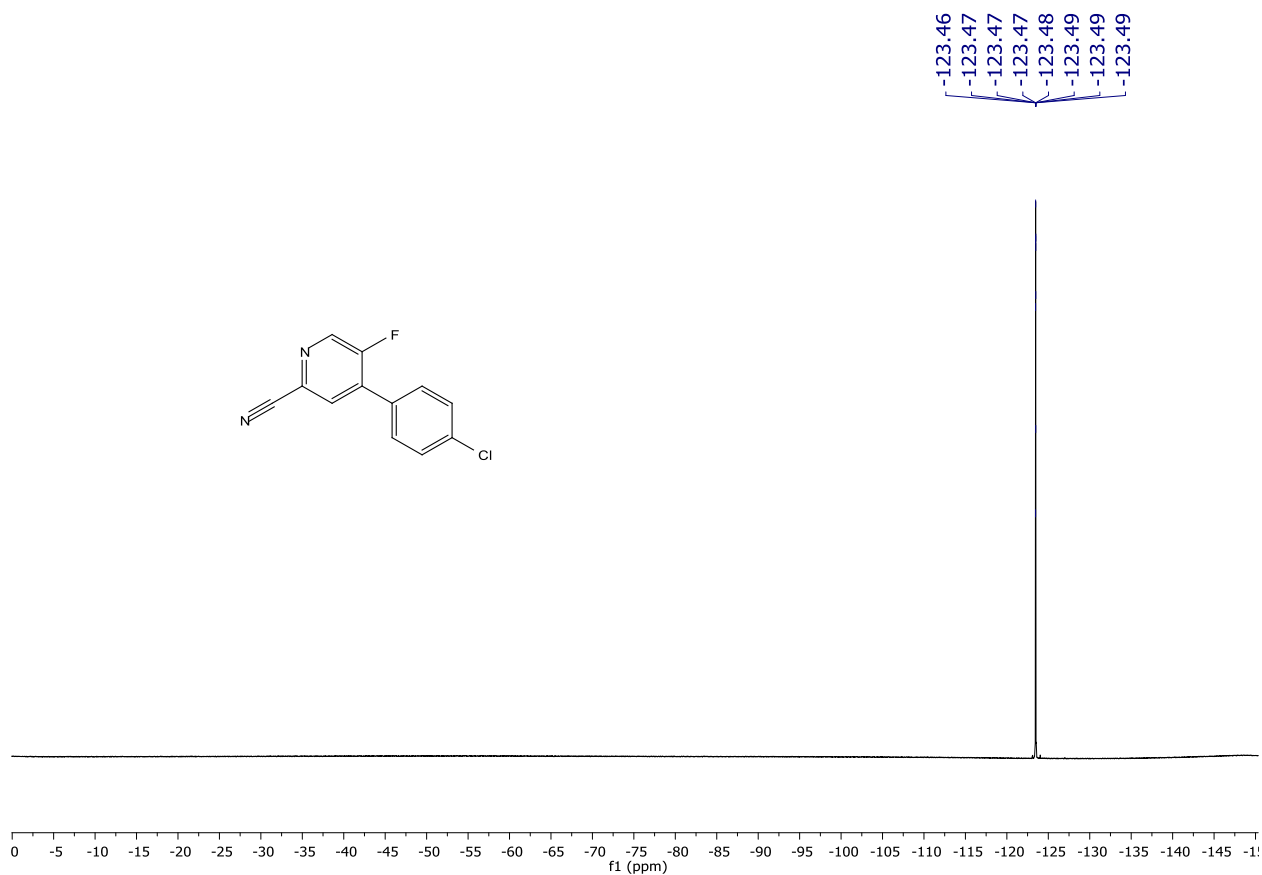
$^{13}\text{C}\{^1\text{H}\}$ NMR (101 MHz, CDCl_3) spectrum of **125an**.



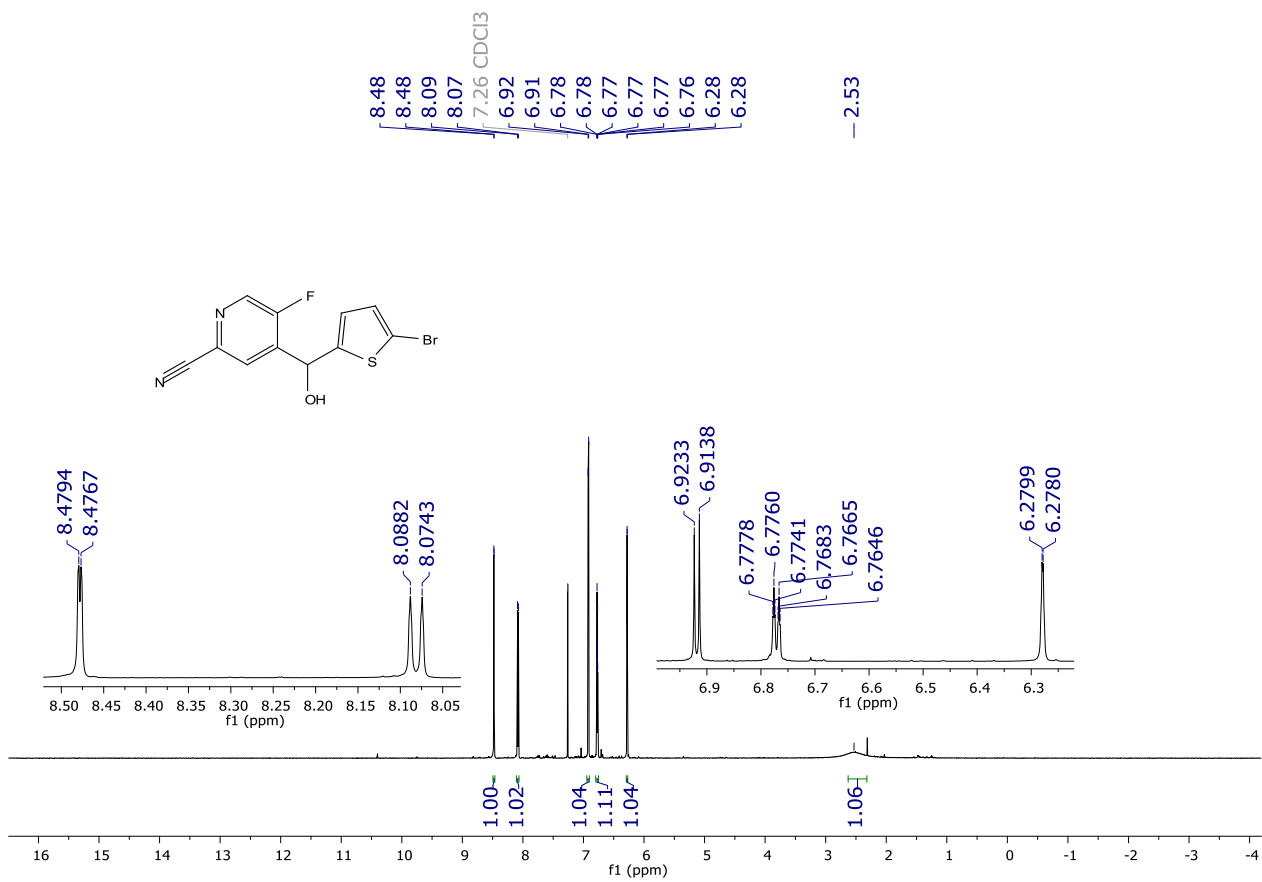
HSQC correlation map of **125an** (400 and 101 MHz, CDCl_3).

HMBC correlation map of **125an** (400 and 101 MHz, CDCl₃).¹⁹F NMR (282 MHz, CDCl₃) spectrum of **125an**.

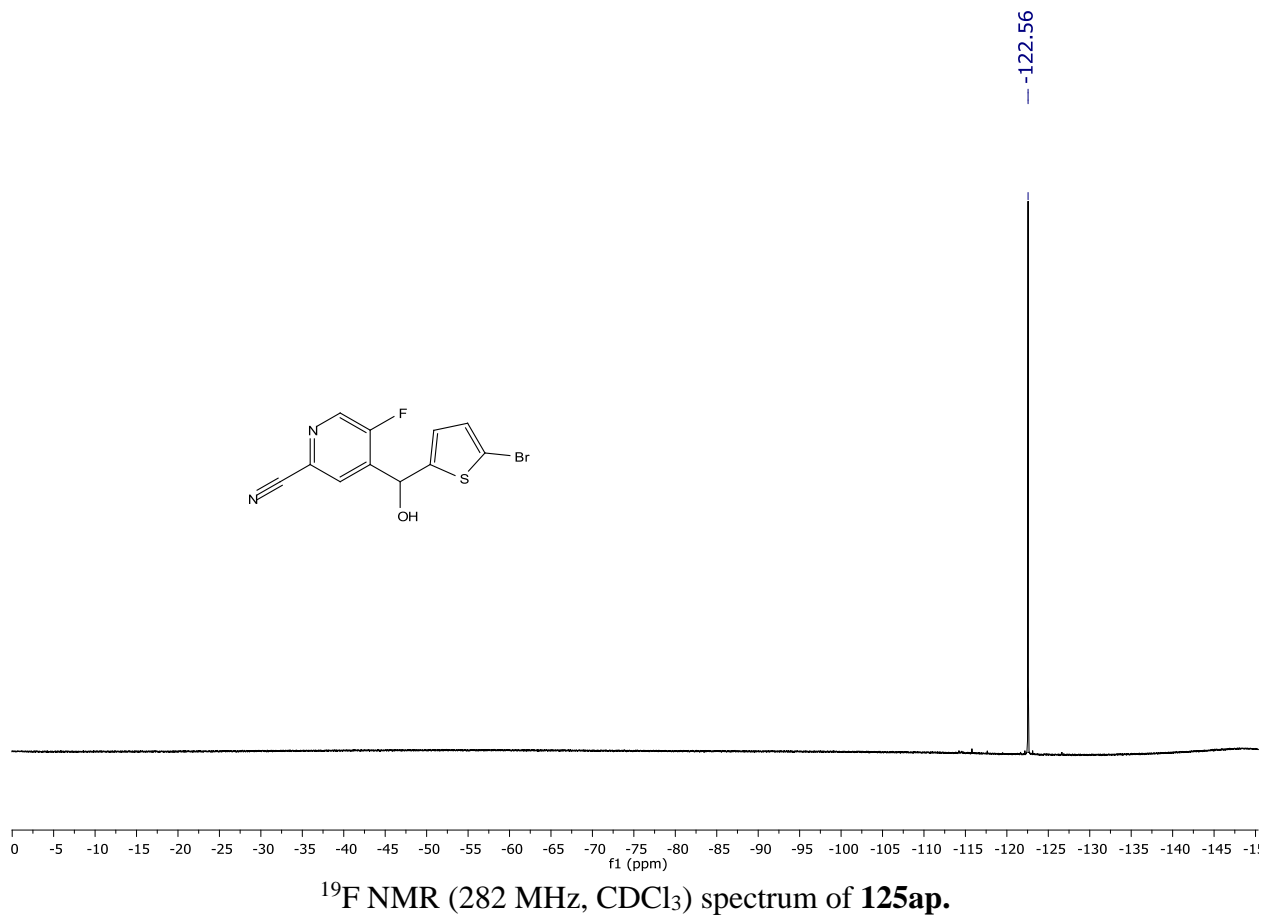
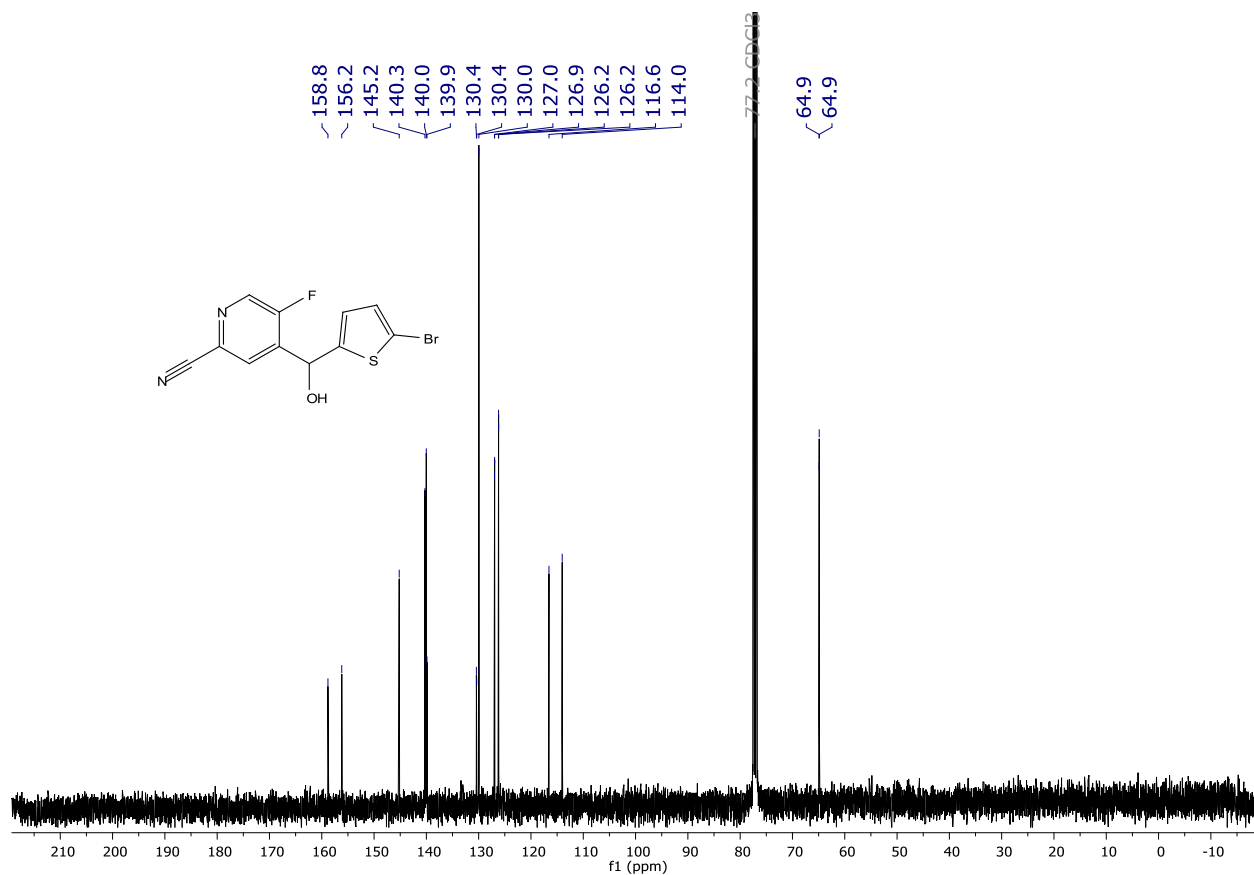


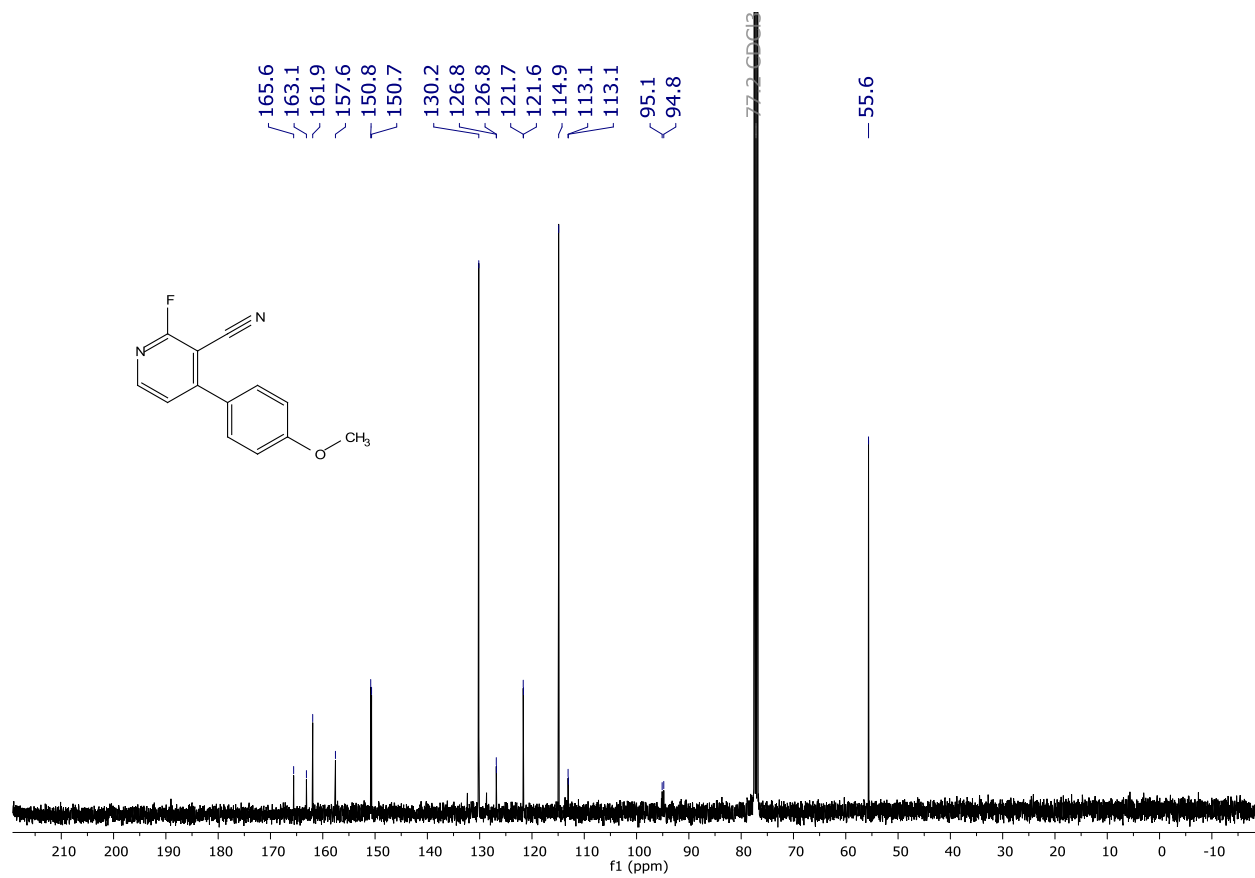
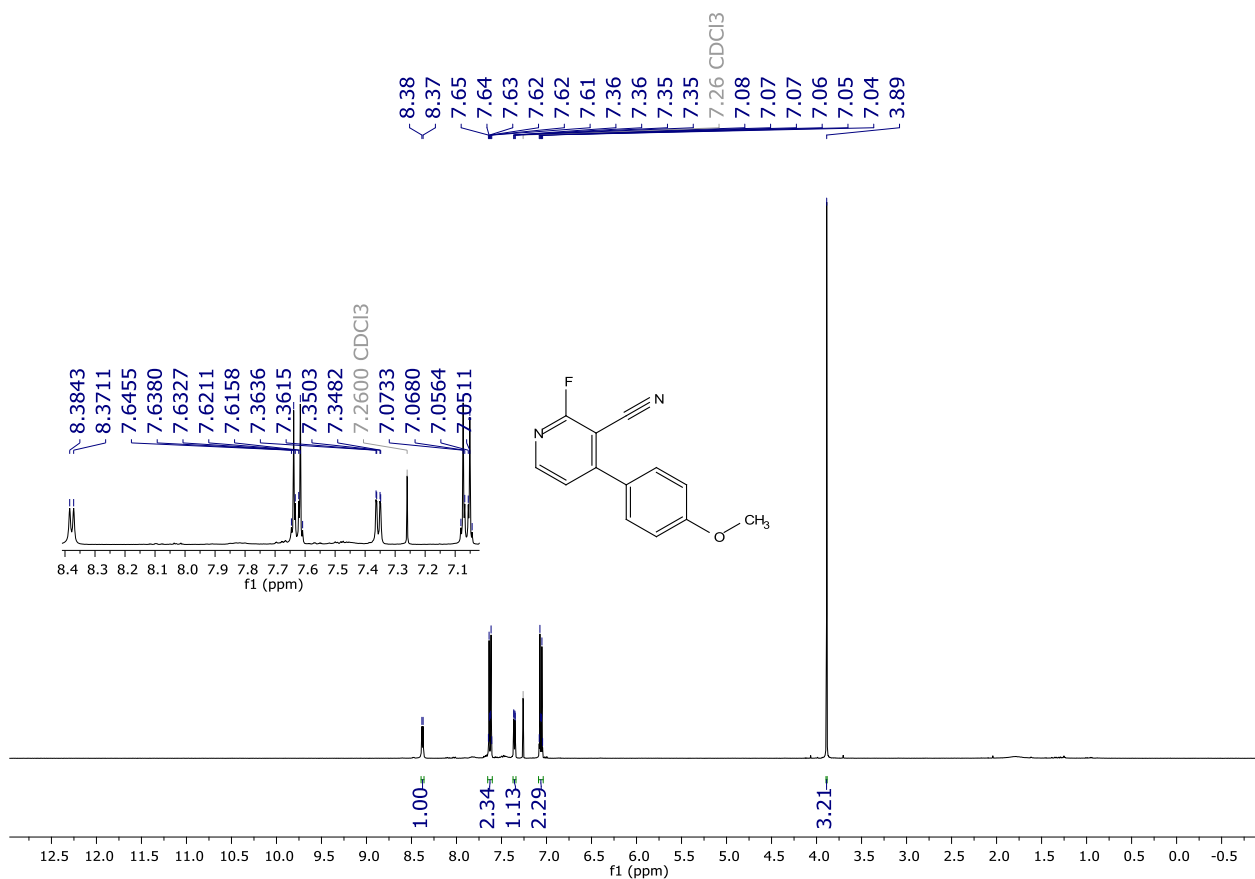


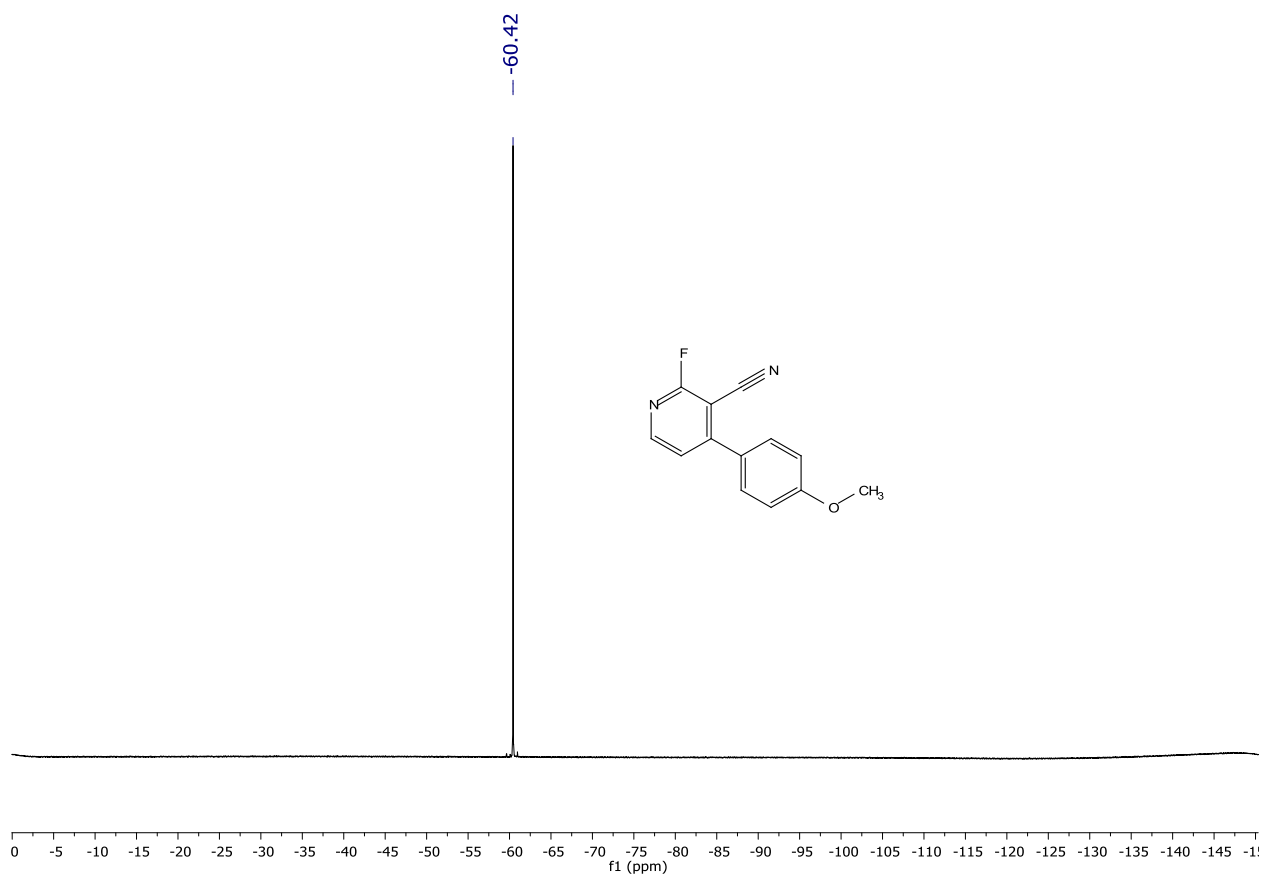
^{19}F NMR (282 MHz, CDCl_3) spectrum of **125ao**.



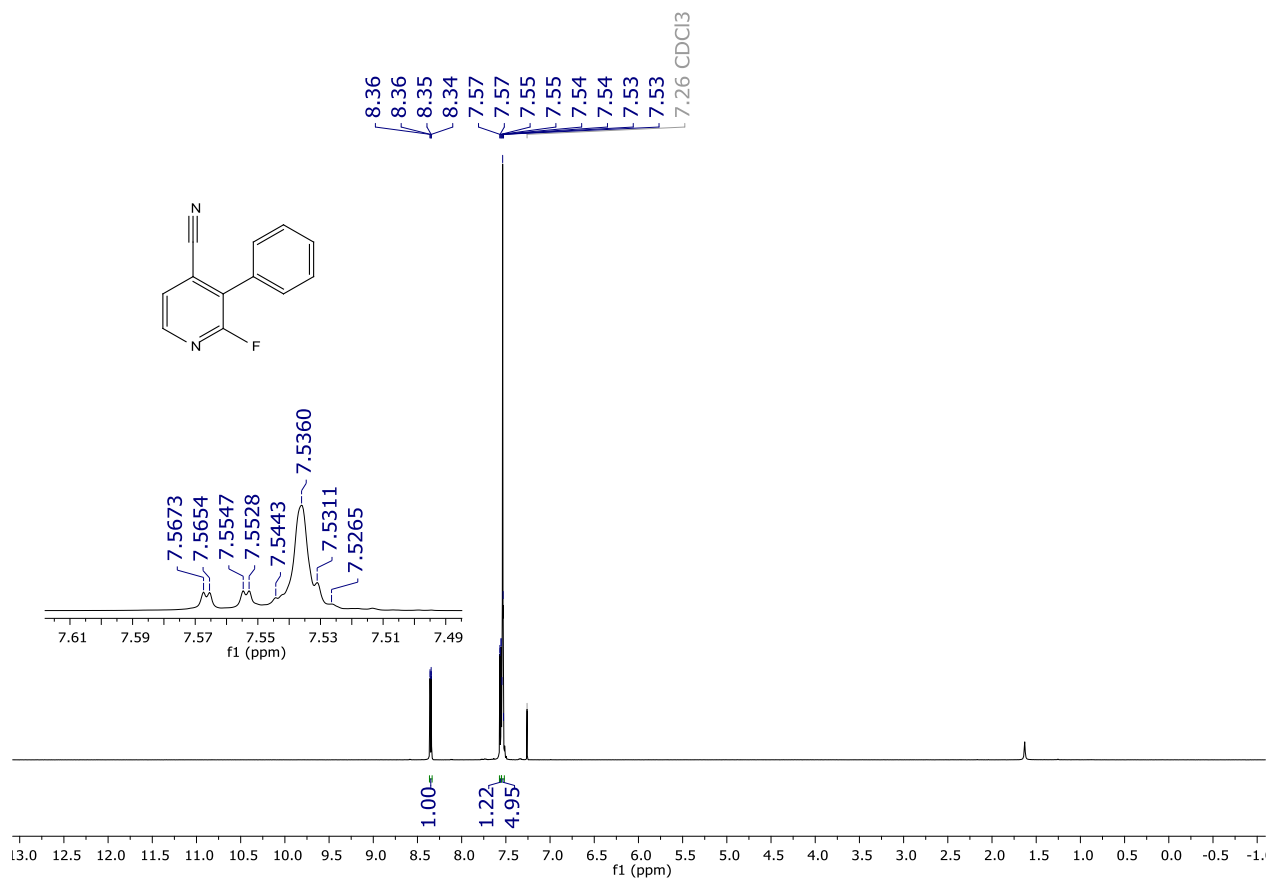
^1H NMR (400 MHz, CDCl_3) spectrum of **125ap**.



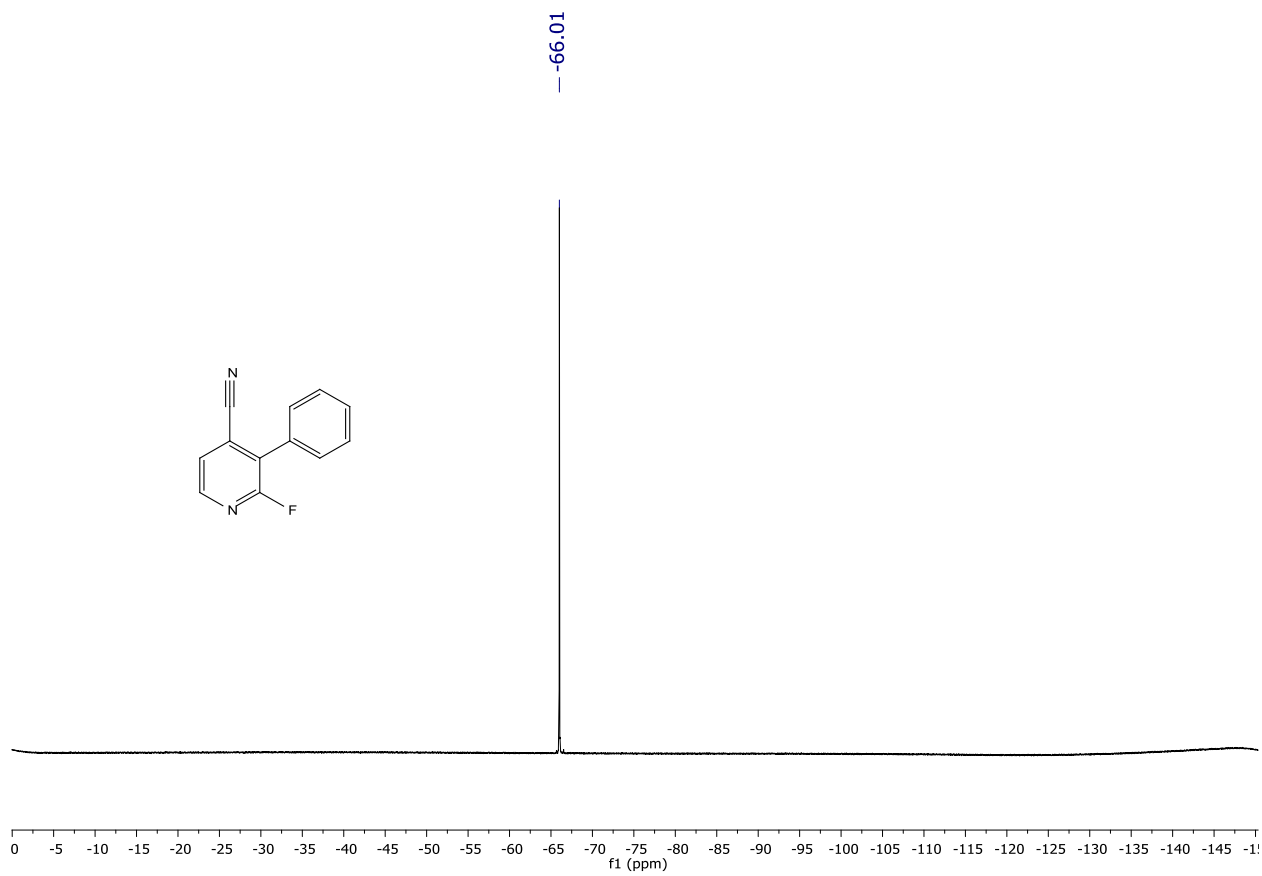
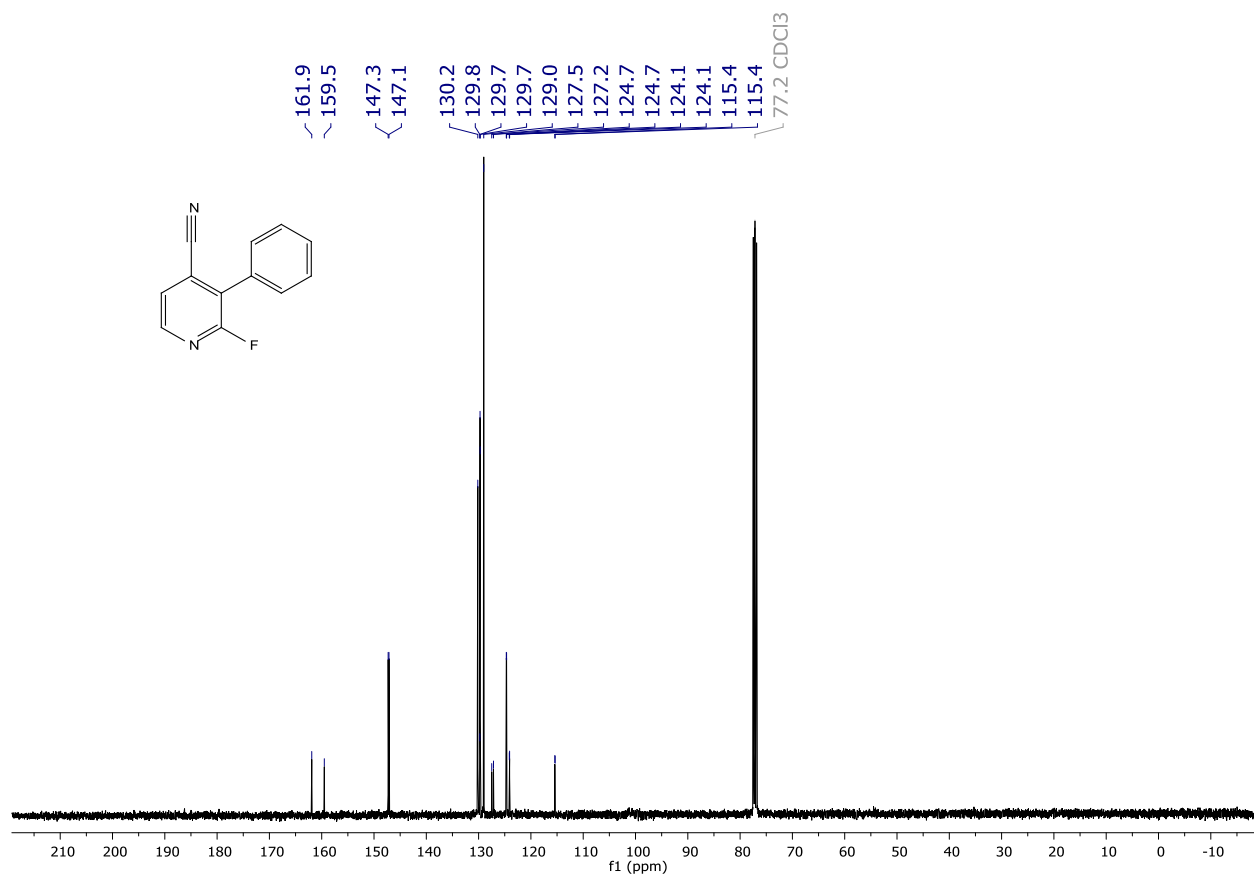




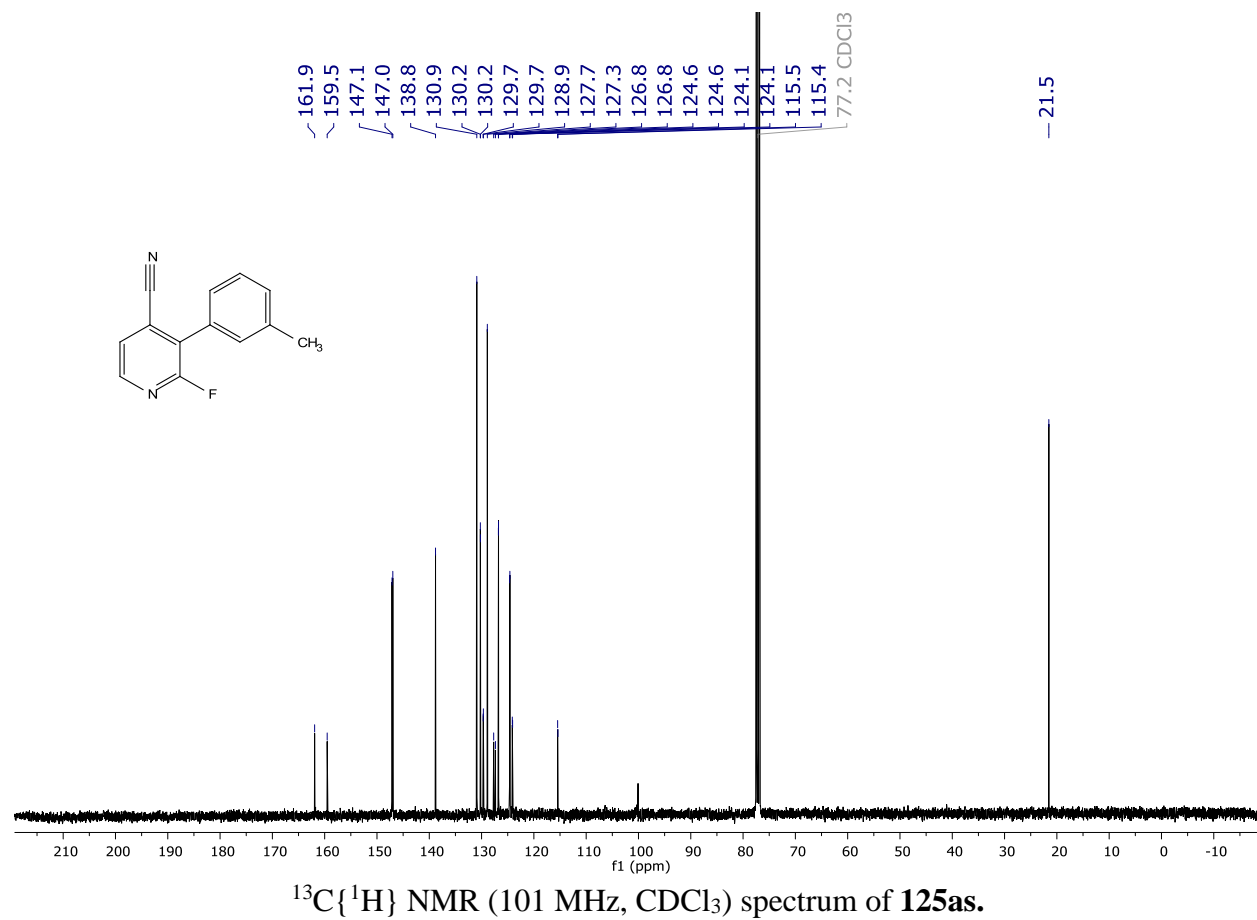
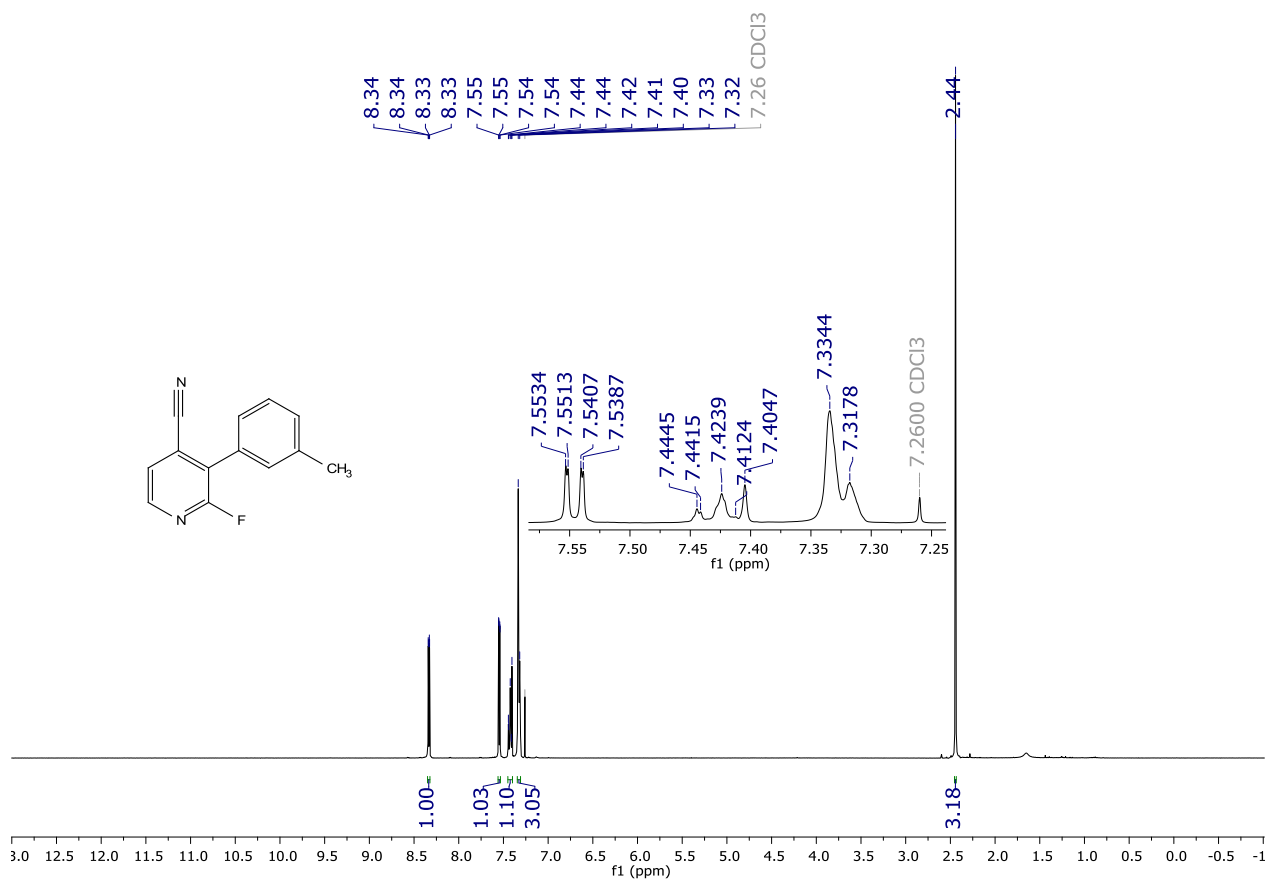
¹⁹F NMR (282 MHz, CDCl₃) spectrum of **125aq**.

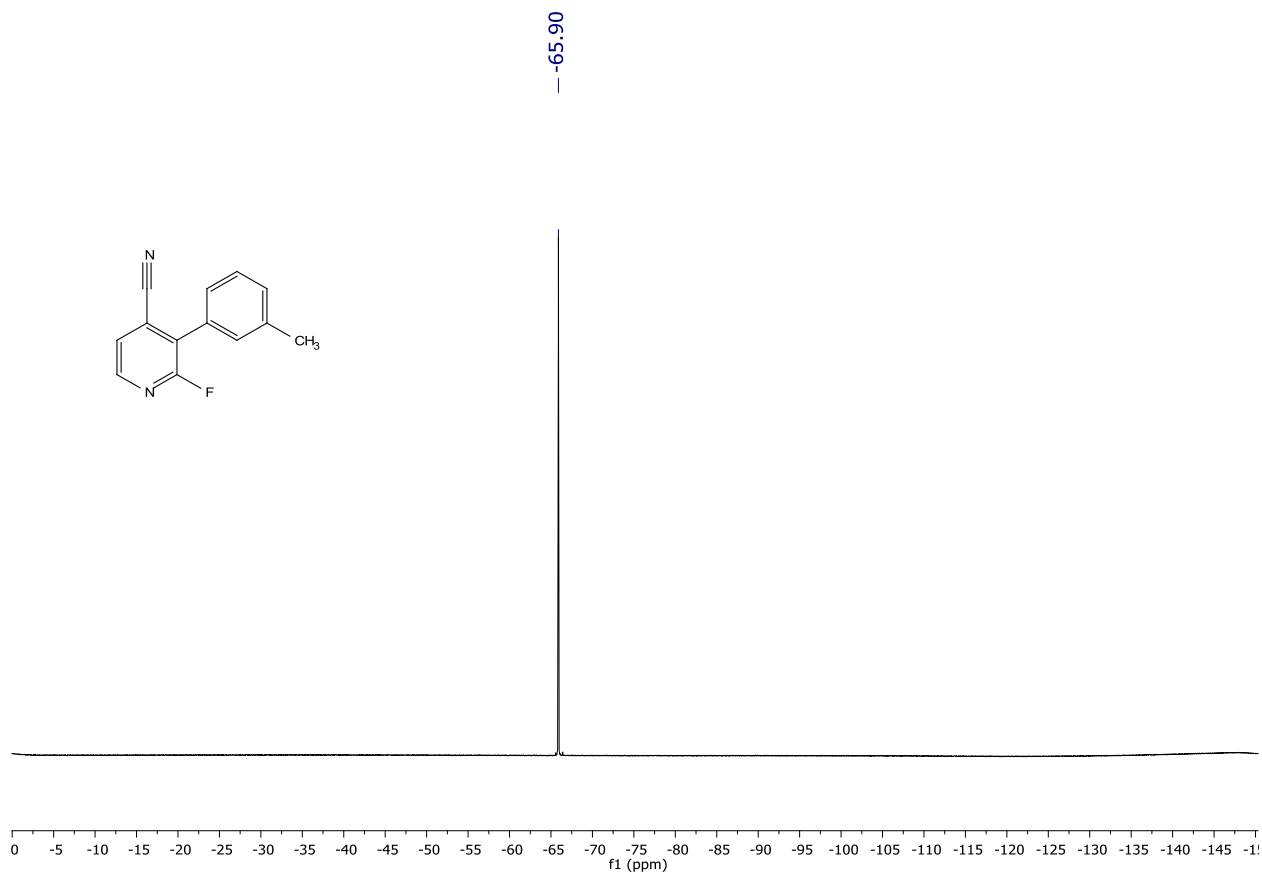


¹H NMR (400 MHz, CDCl₃) spectrum of **125ar**.

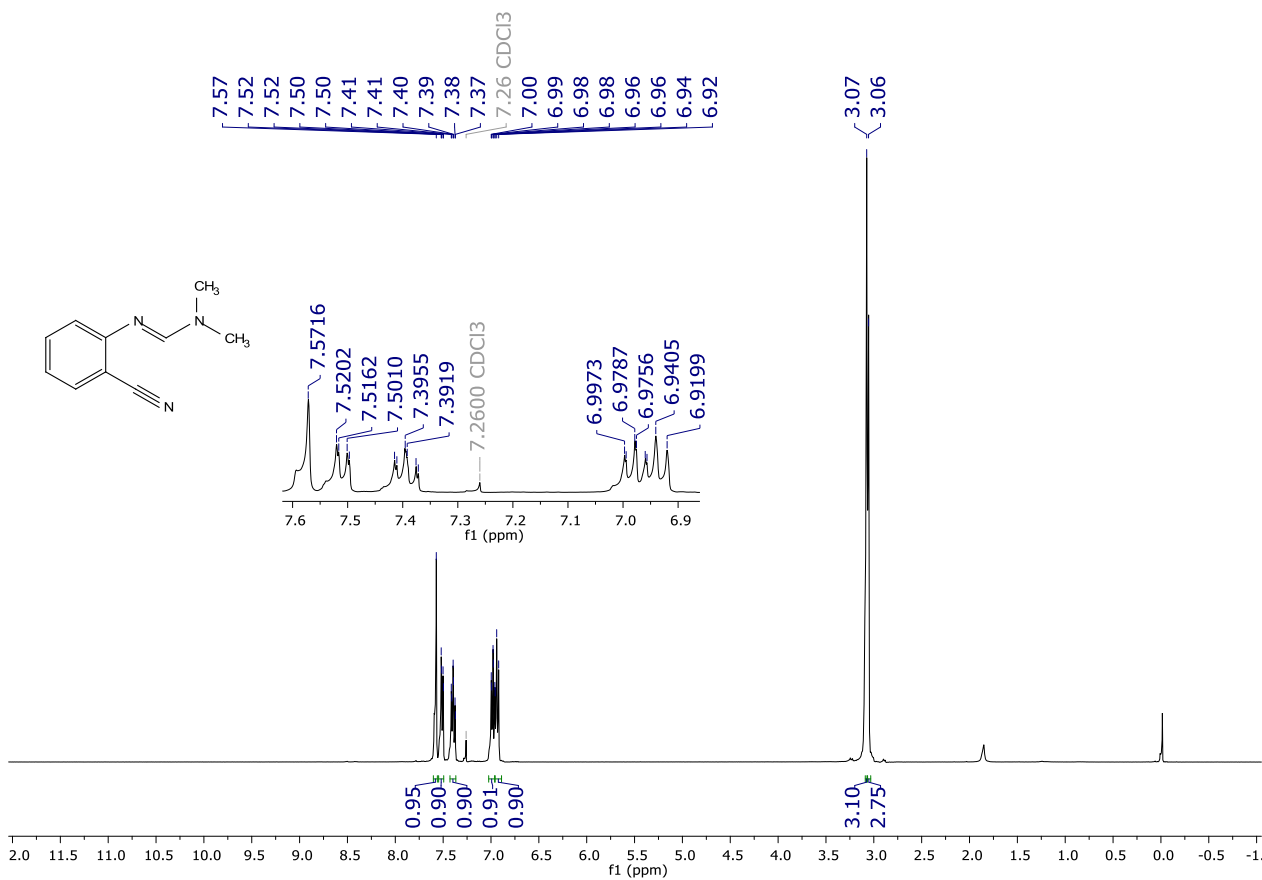


^{19}F NMR (282 MHz, CDCl_3) spectrum of **125ar**.

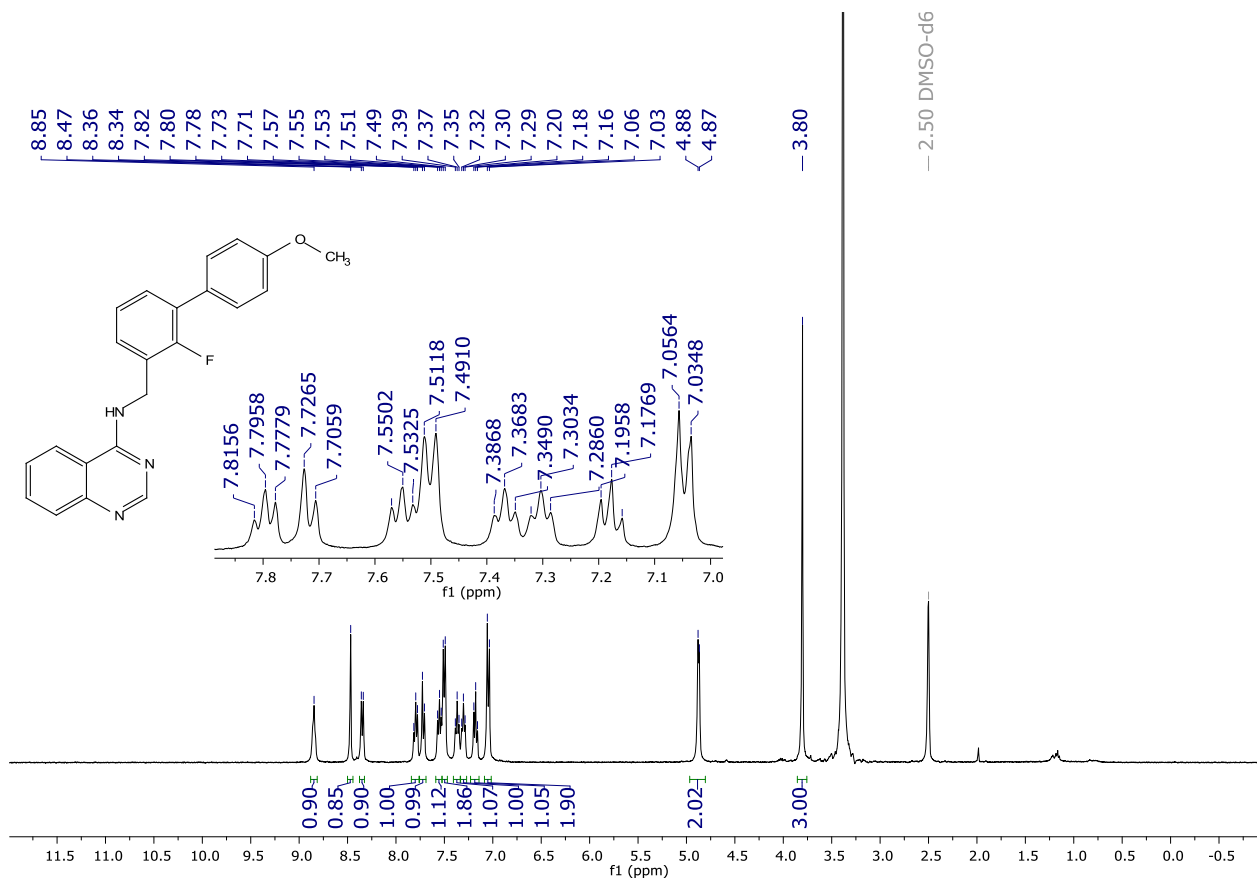
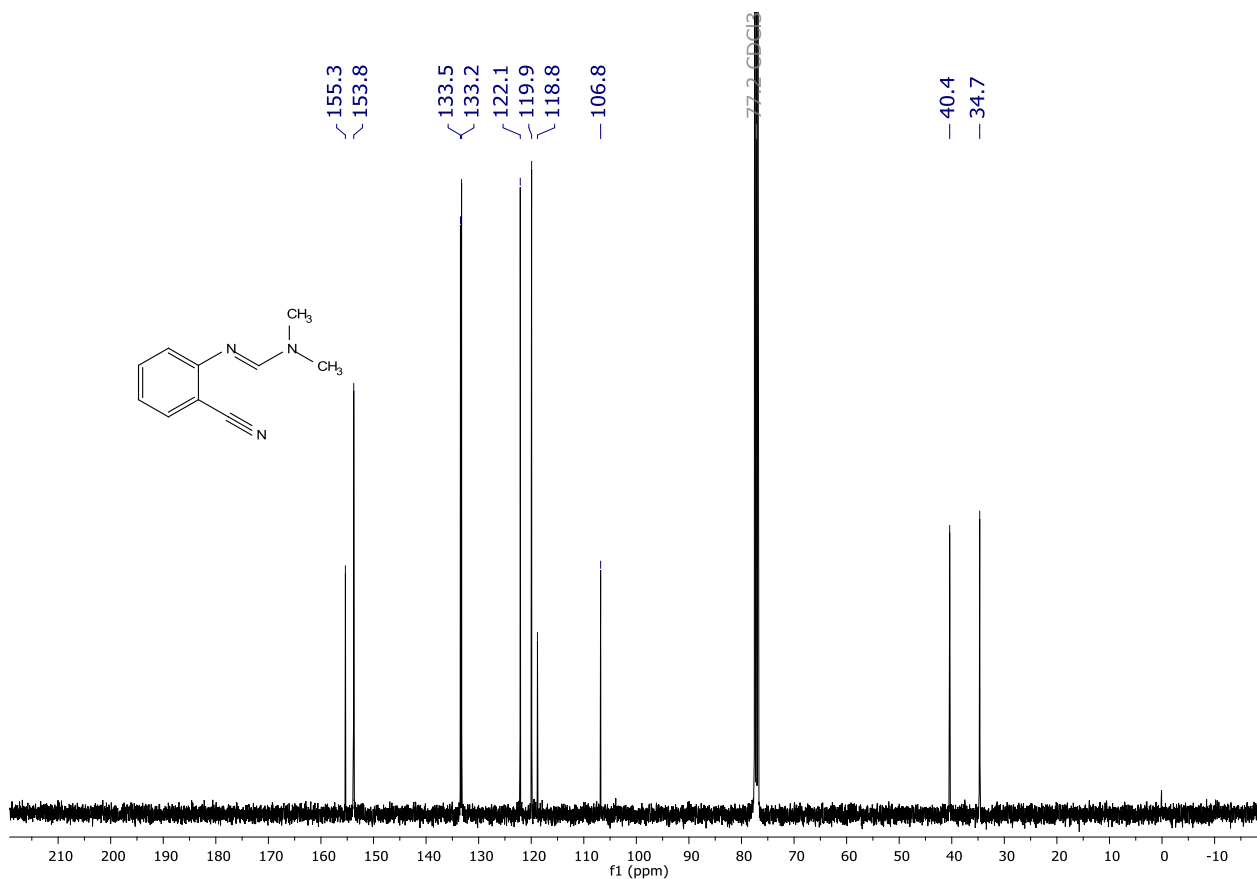


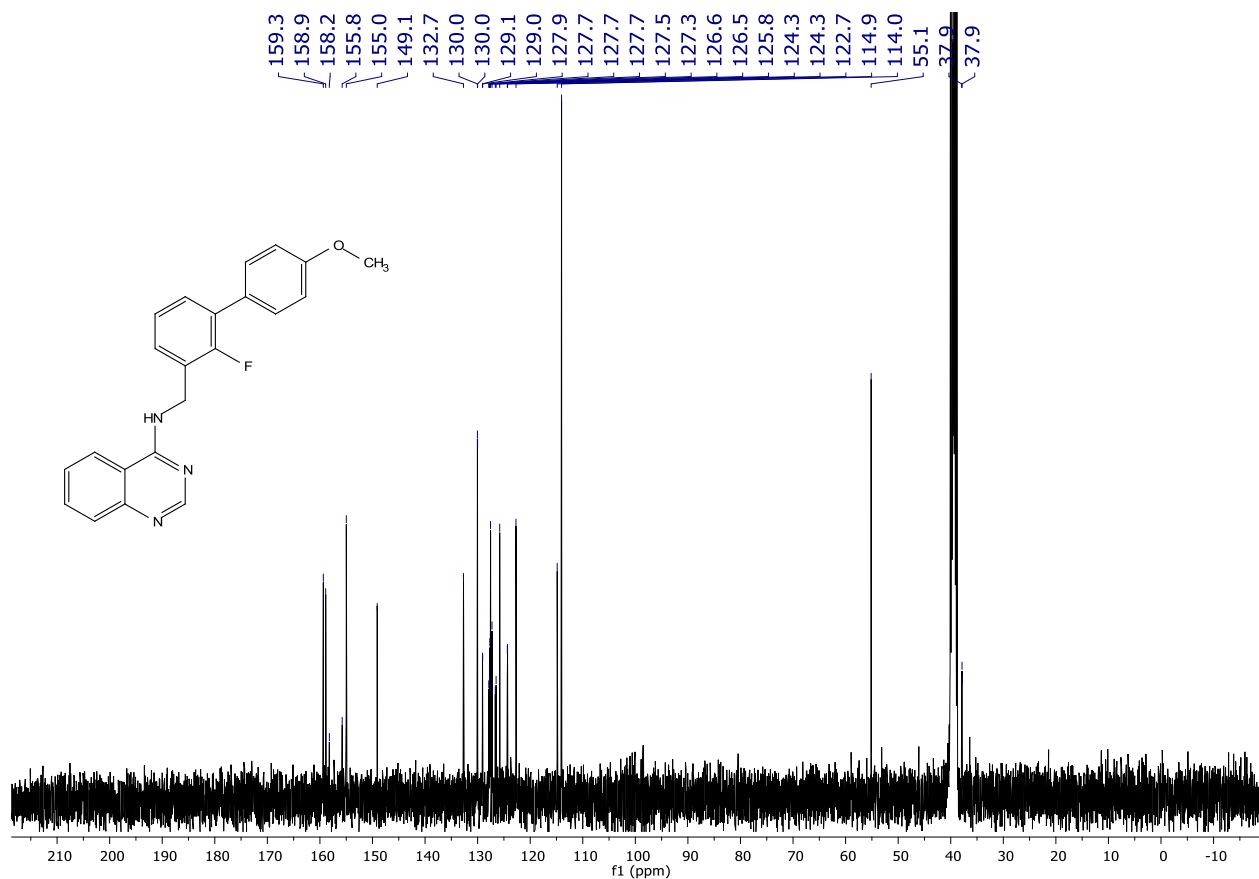


^{19}F NMR (282 MHz, CDCl_3) spectrum of **125as**.

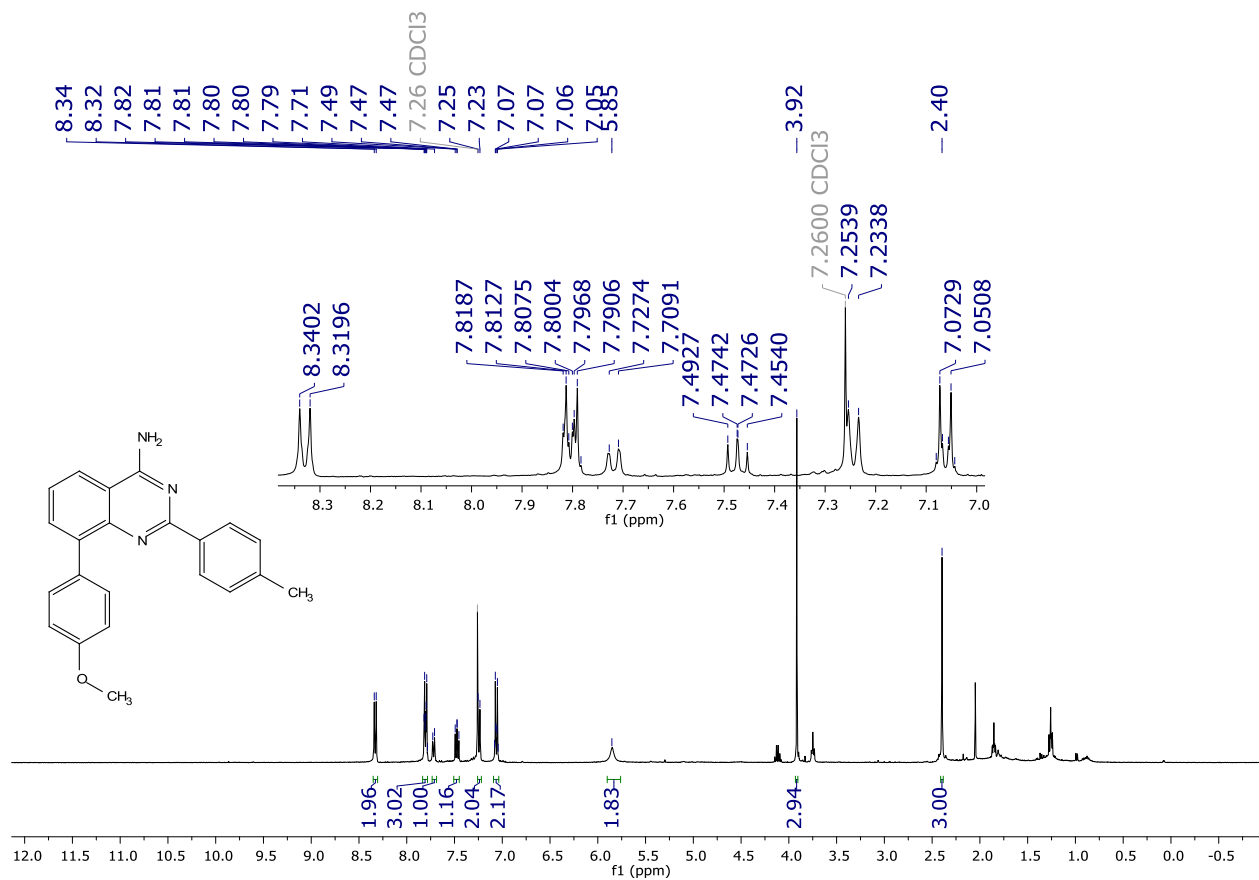


^1H NMR (400 MHz, CDCl_3) spectrum of **132**.

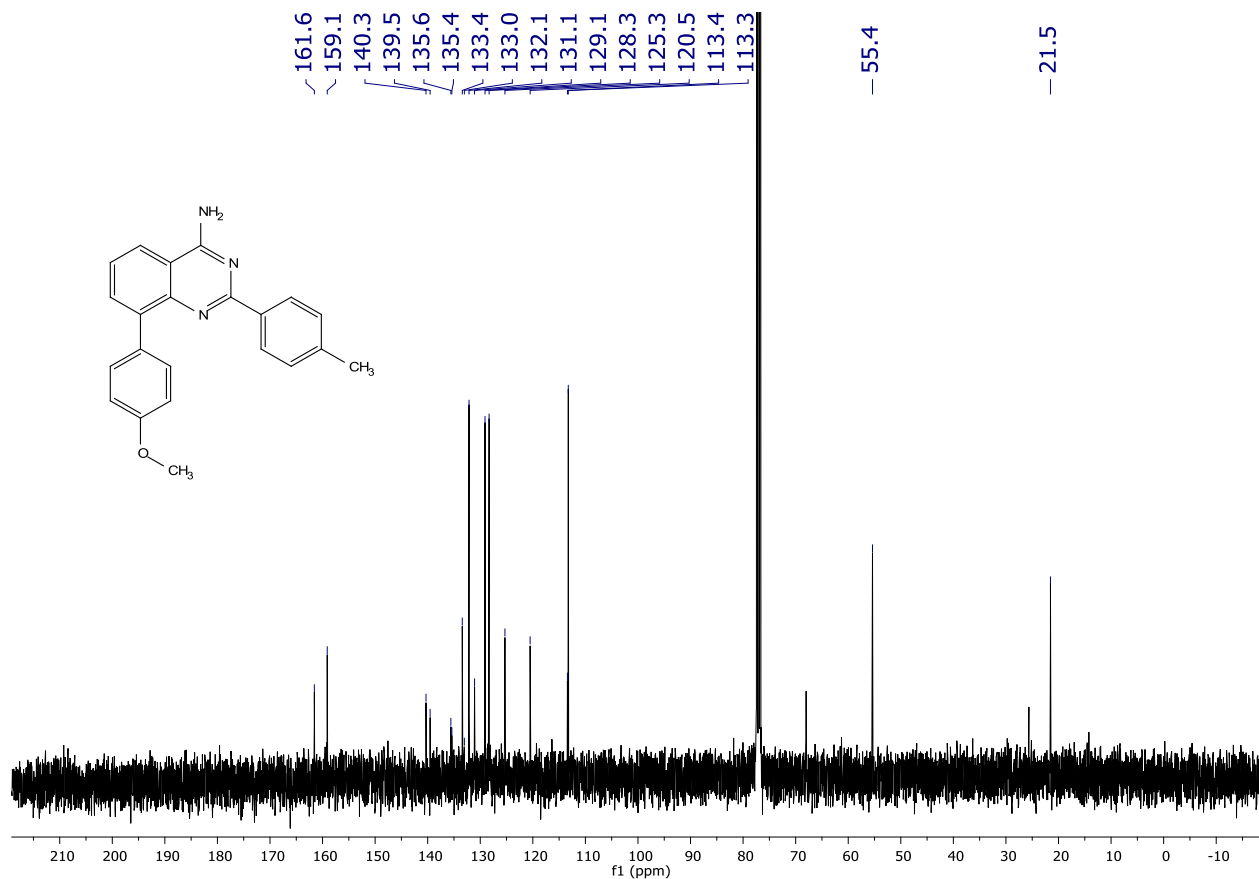




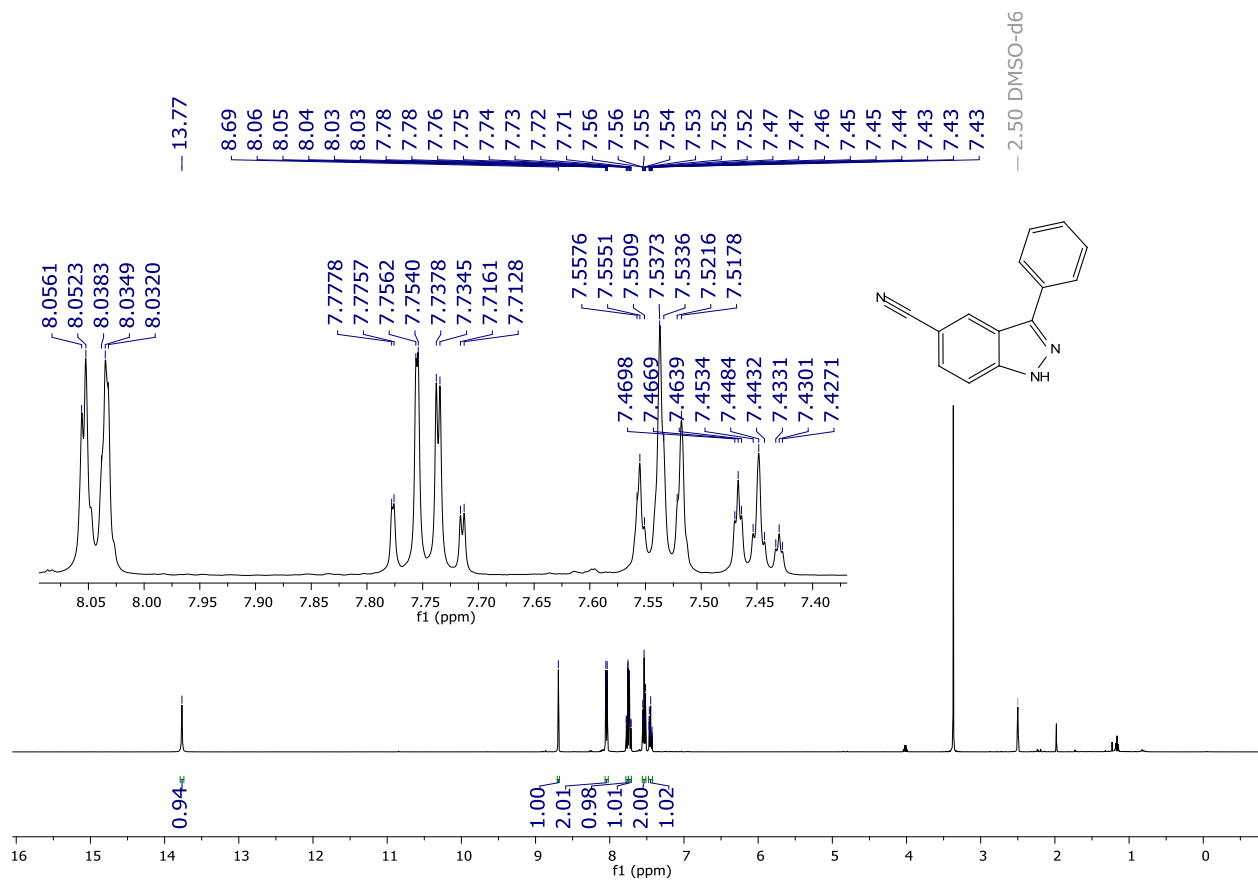
$^{13}\text{C}\{^1\text{H}\}$ NMR (101 MHz, DMSO- d_6) spectrum of **134**.



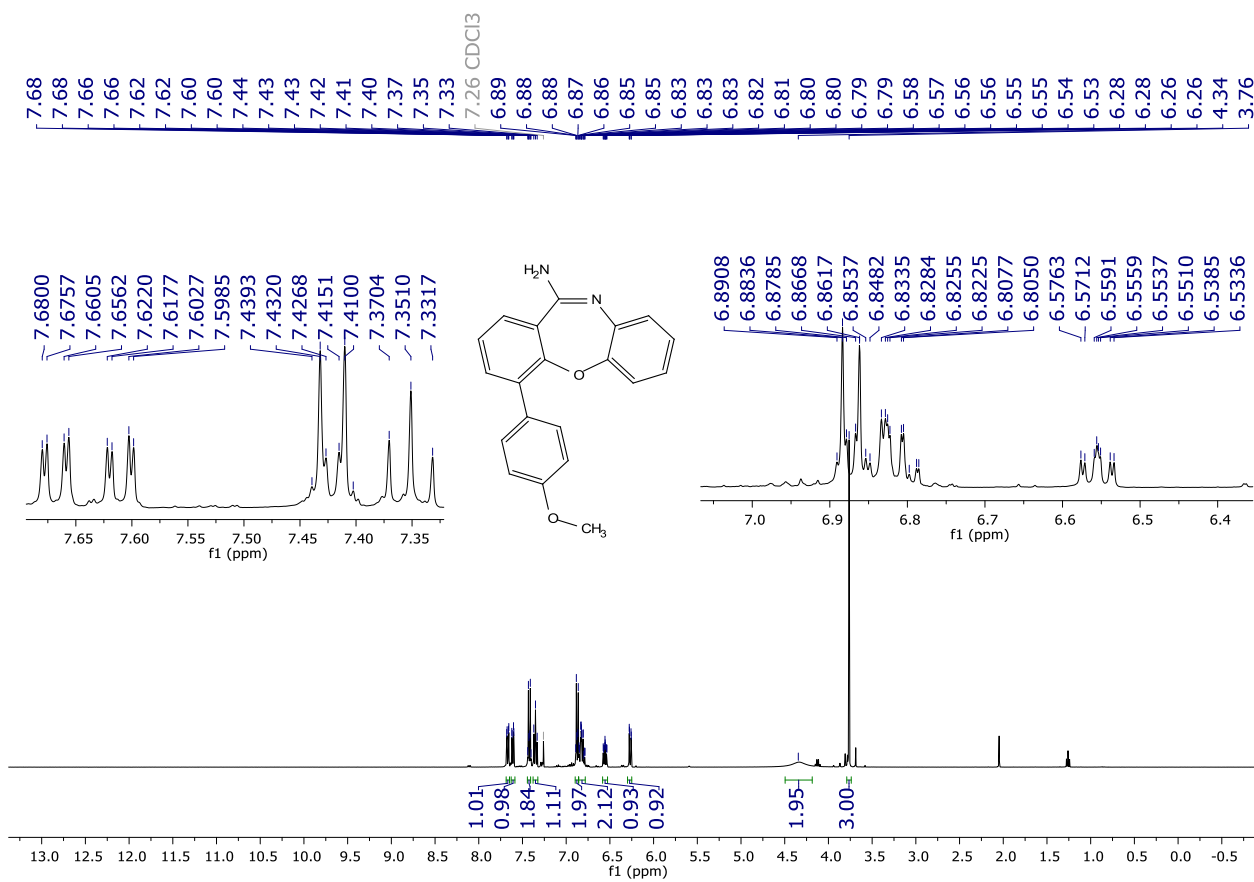
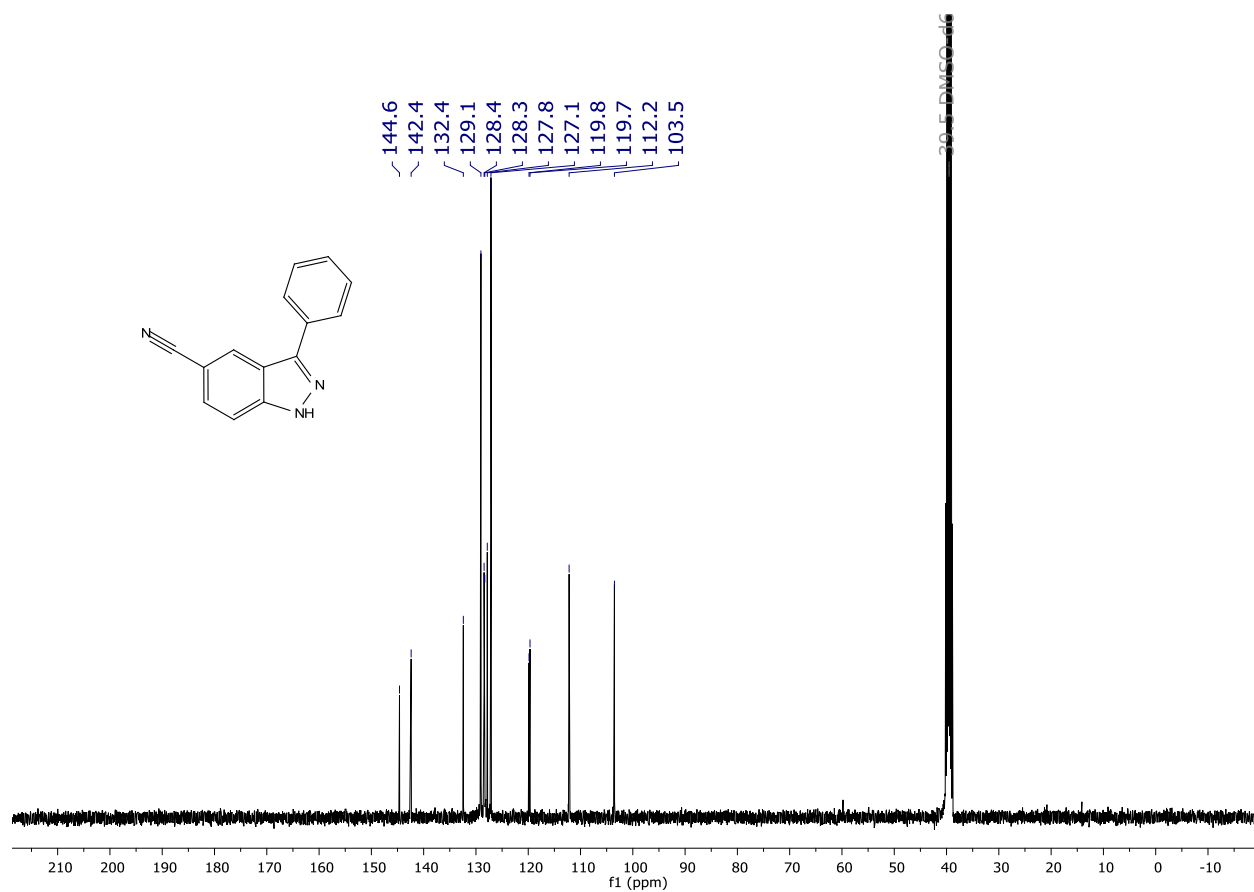
^1H NMR (400 MHz, CDCl_3) spectrum of **135**.

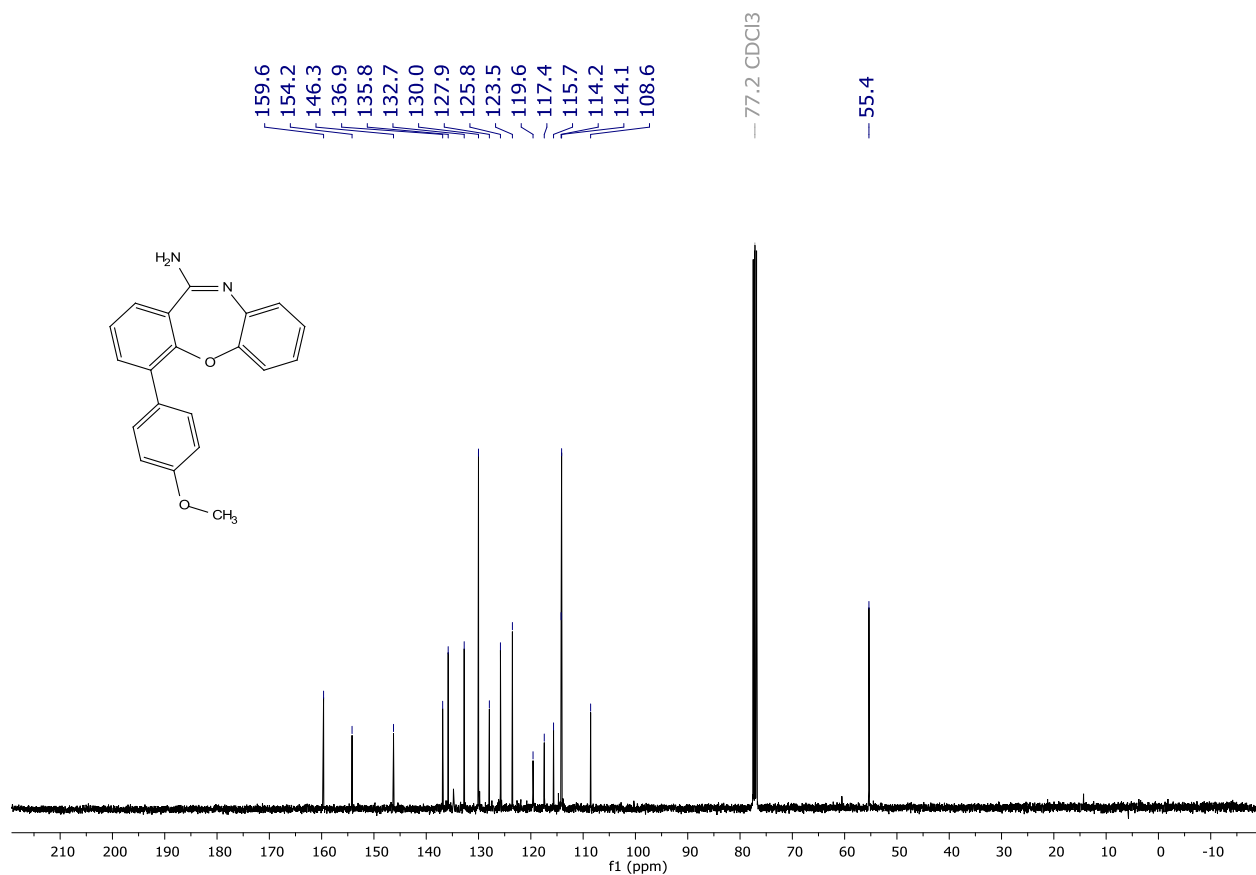


$^{13}\text{C}\{^1\text{H}\}$ NMR (101 MHz, CDCl_3) spectrum of 135.

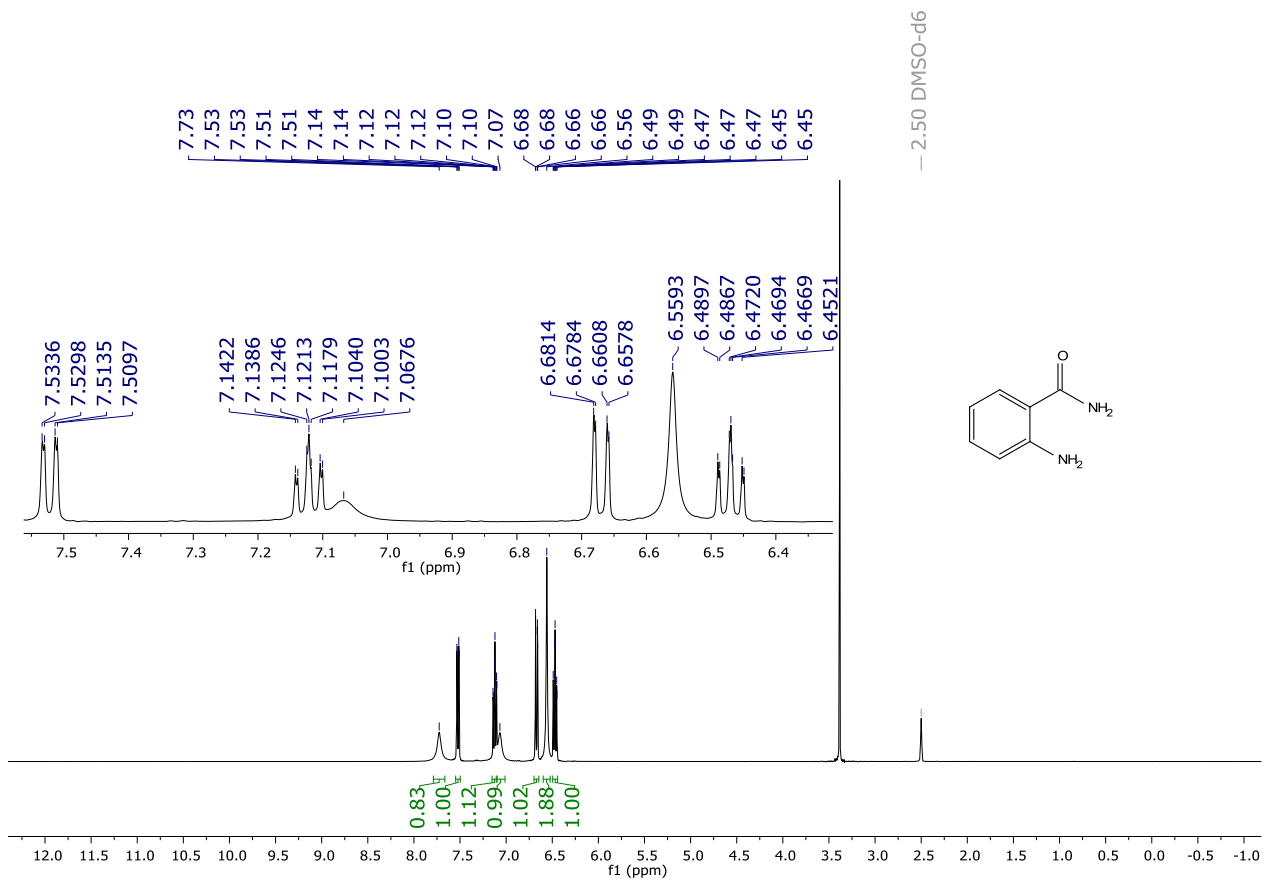


^1H NMR (400 MHz, $\text{DMSO}-d_6$) spectrum of 137.

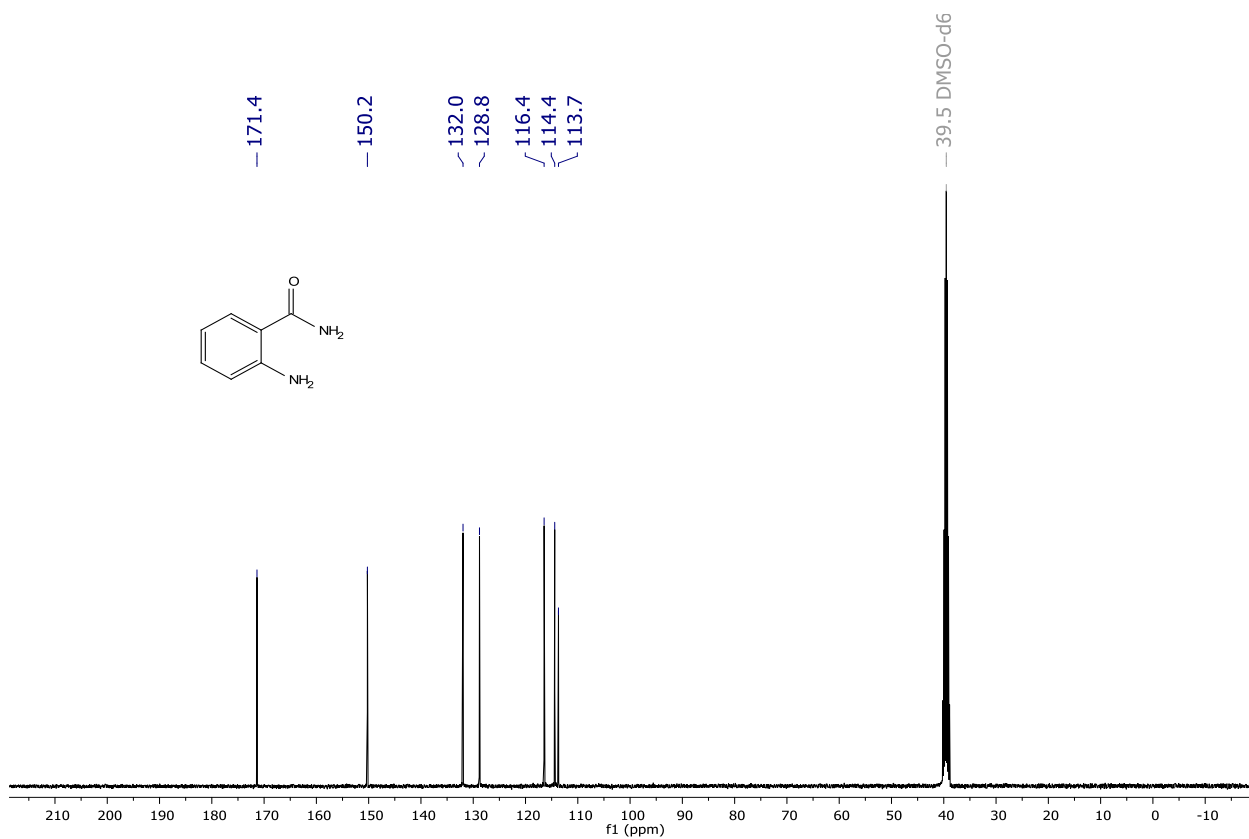




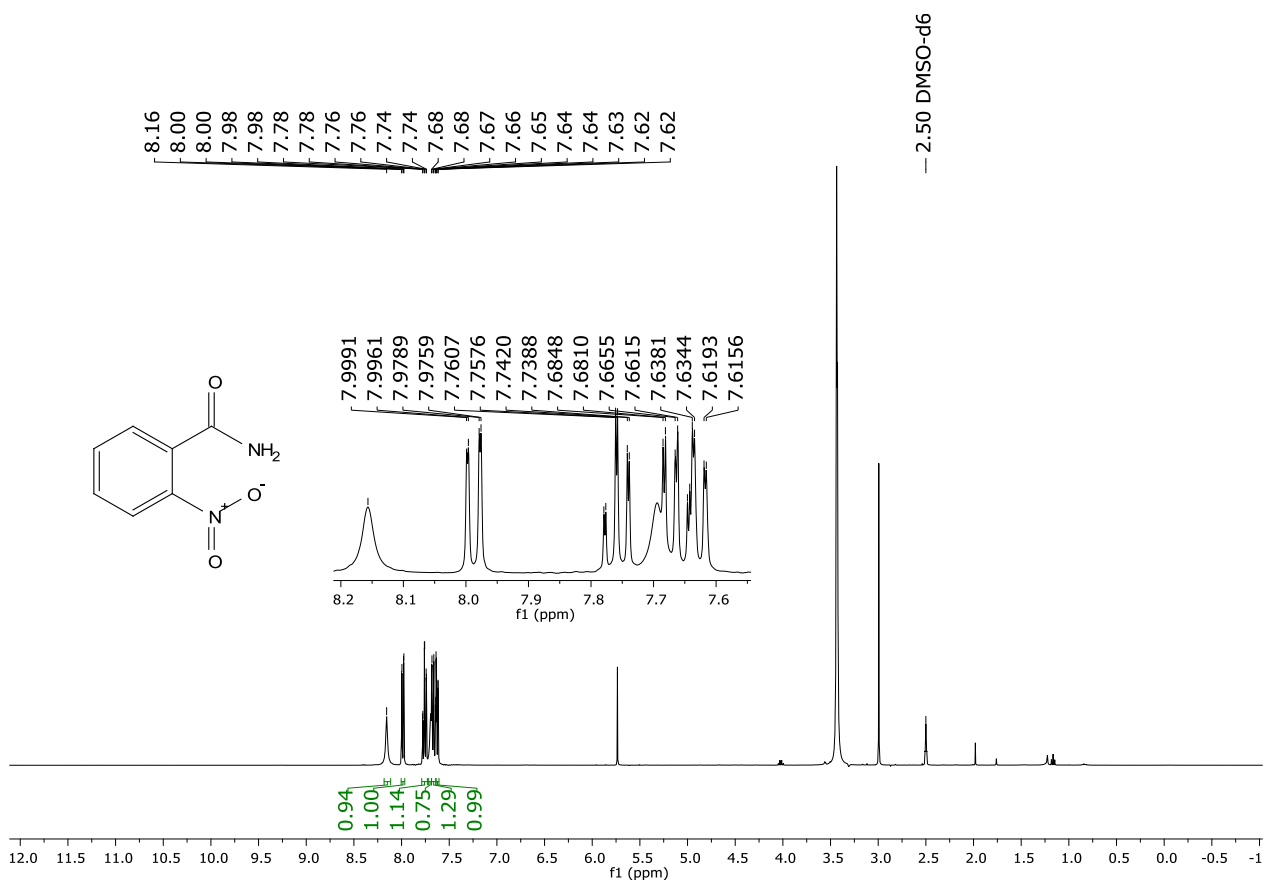
$^{13}\text{C}\{^1\text{H}\}$ NMR (101 MHz, CDCl_3) spectrum of **138**.



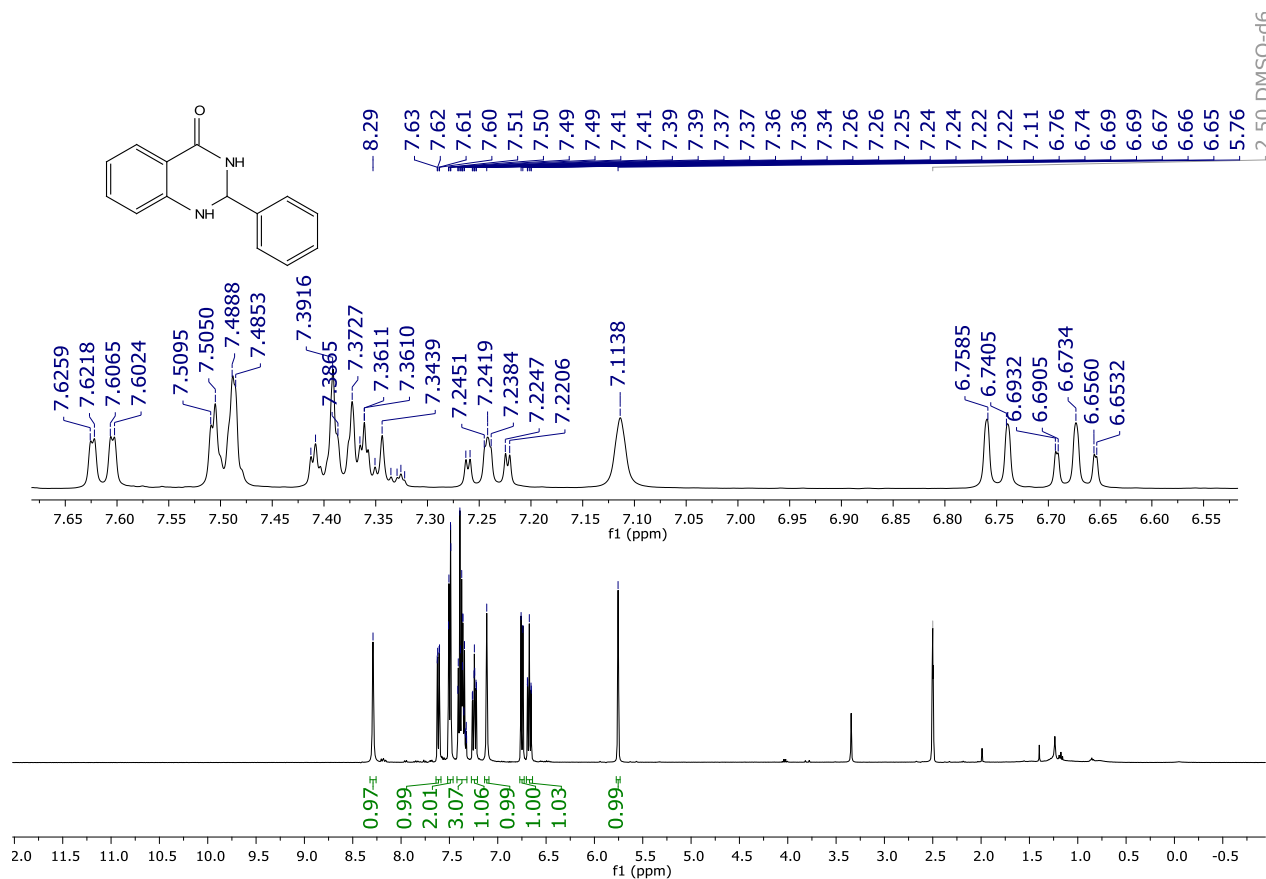
^1H NMR (400 MHz, $\text{DMSO-}d_6$) spectrum of **103**.



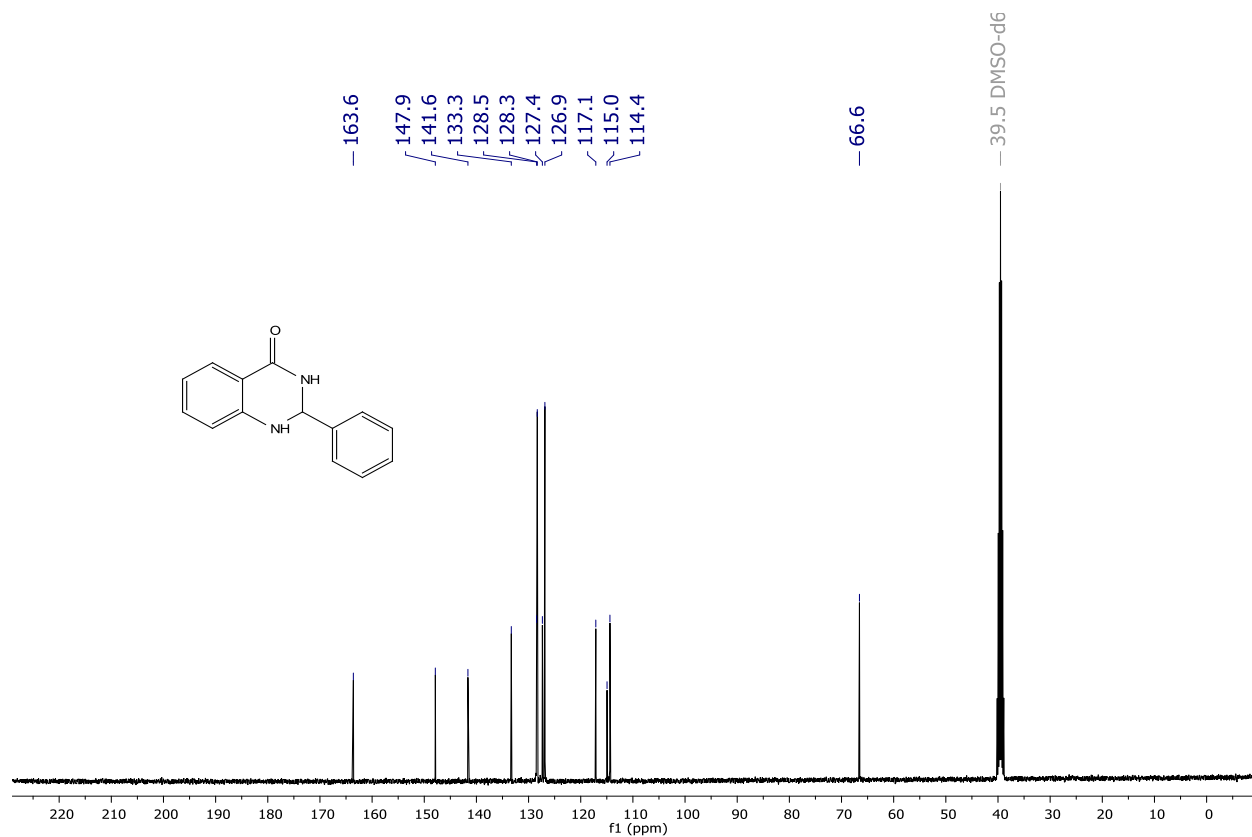
¹³C NMR (101 MHz, DMSO-d₆) spectrum of **103**.



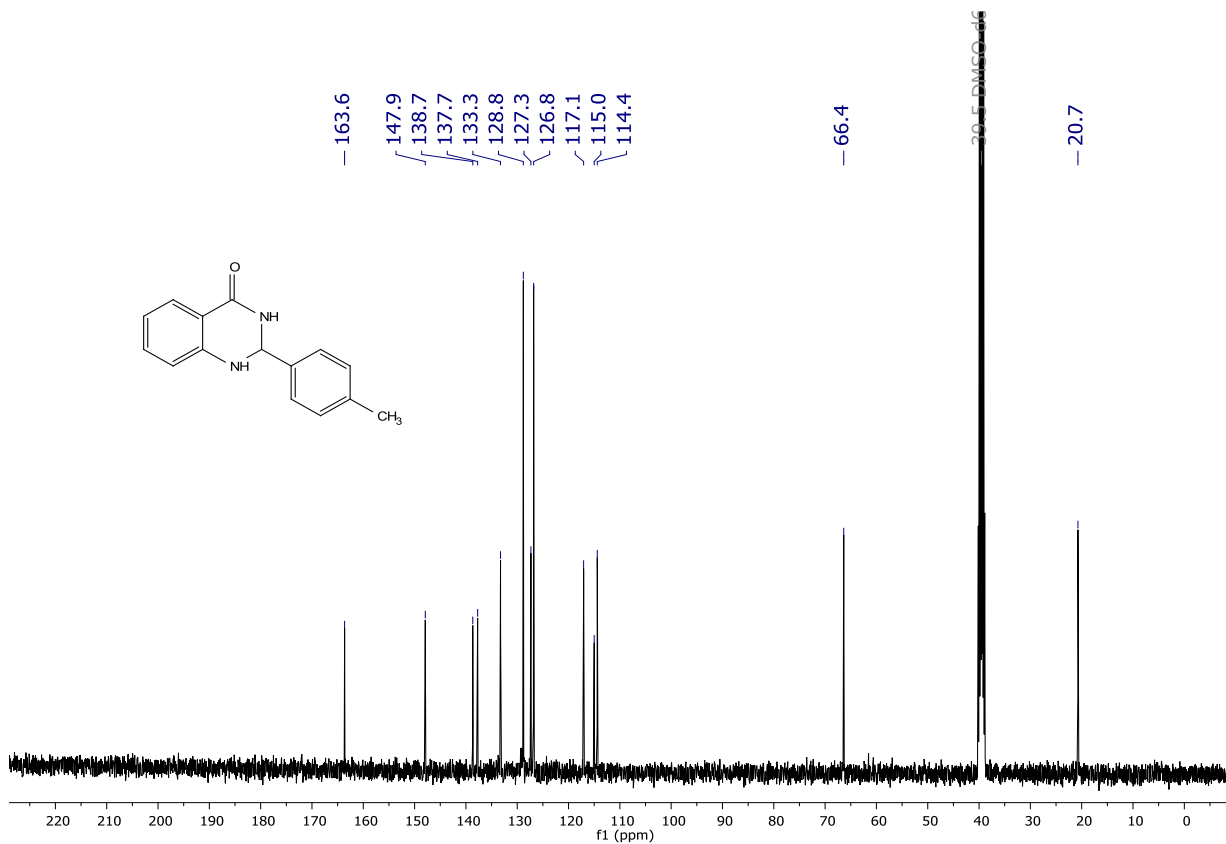
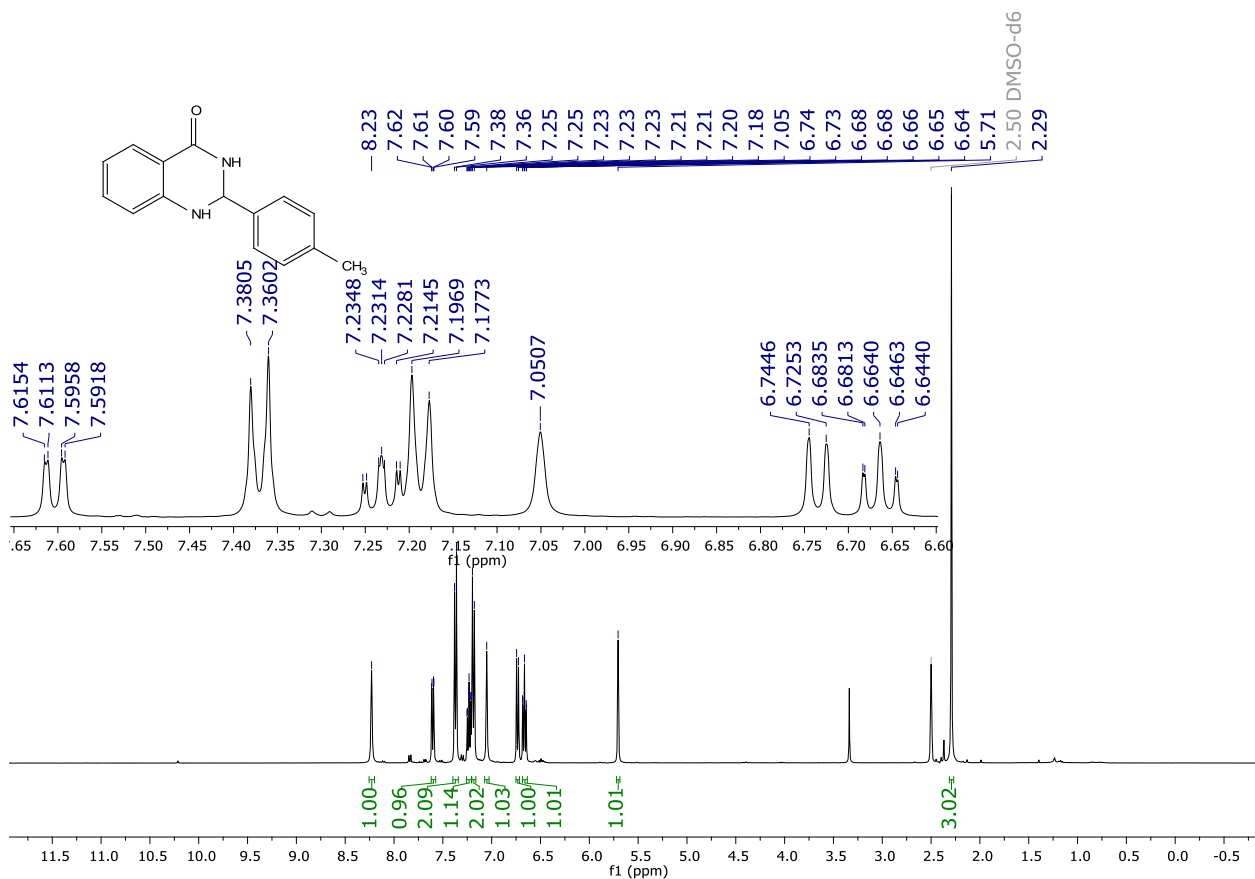
¹H NMR (400 MHz, DMSO-d₆) spectrum of **146**.

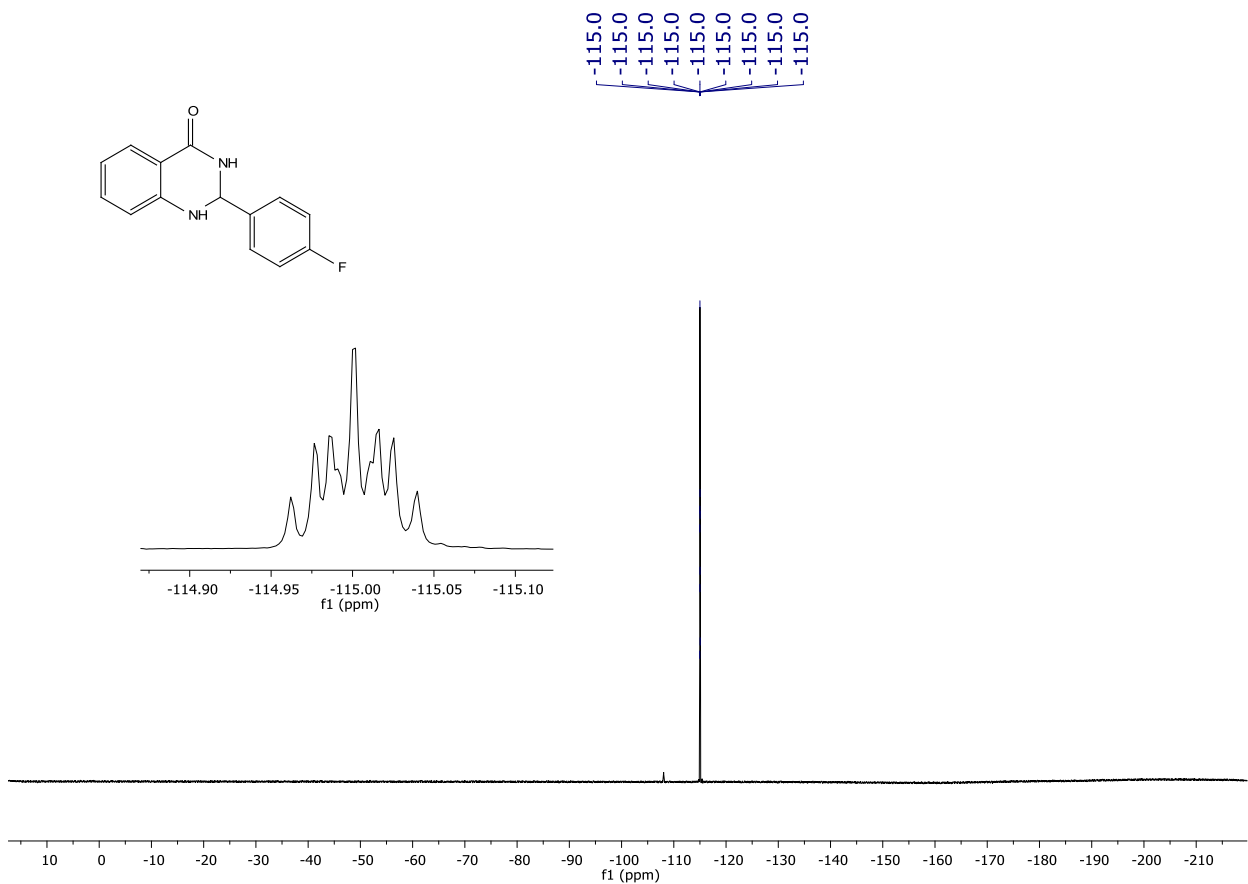


¹H NMR (400 MHz, DMSO-*d*₆) spectrum of 120a.

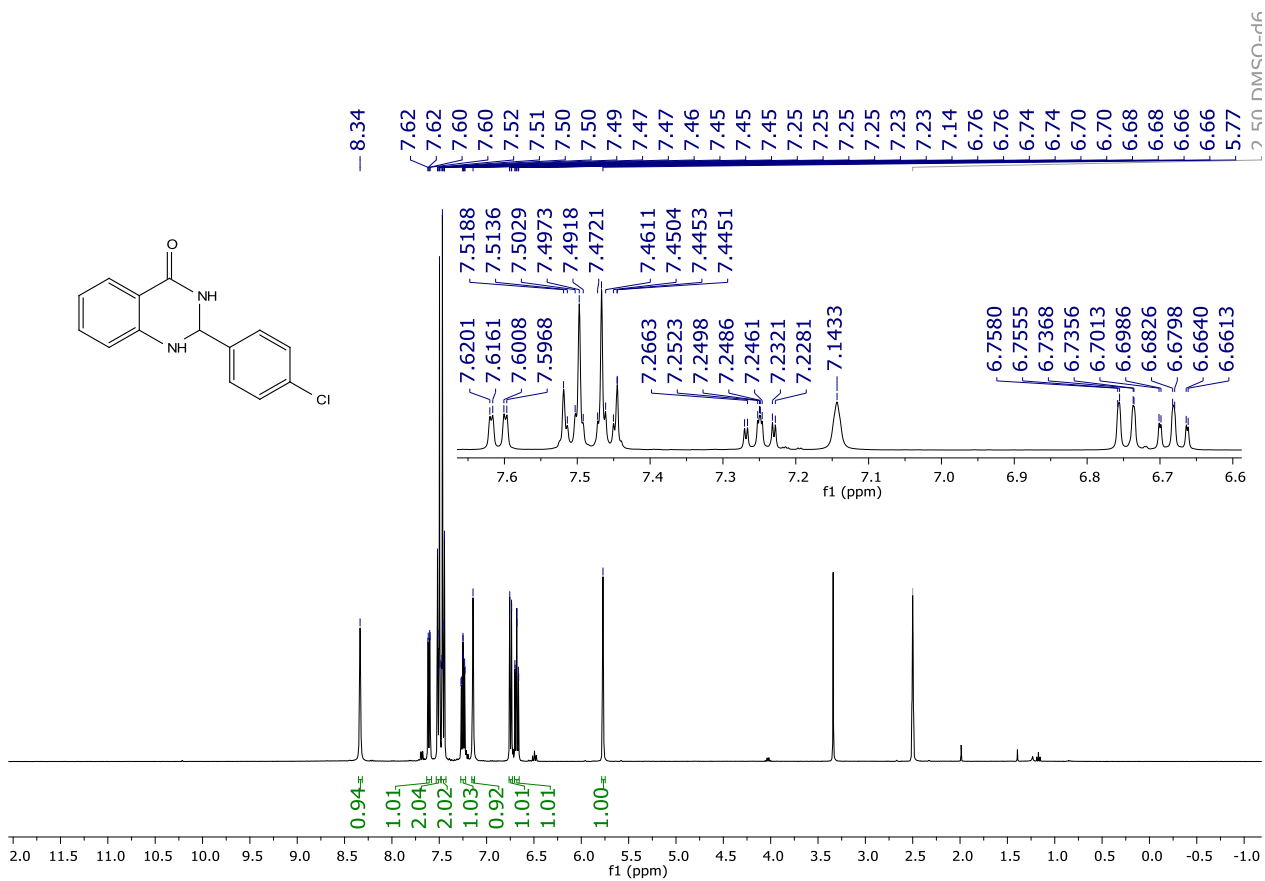


¹³C NMR (101 MHz, DMSO-*d*₆) spectrum of 120a.

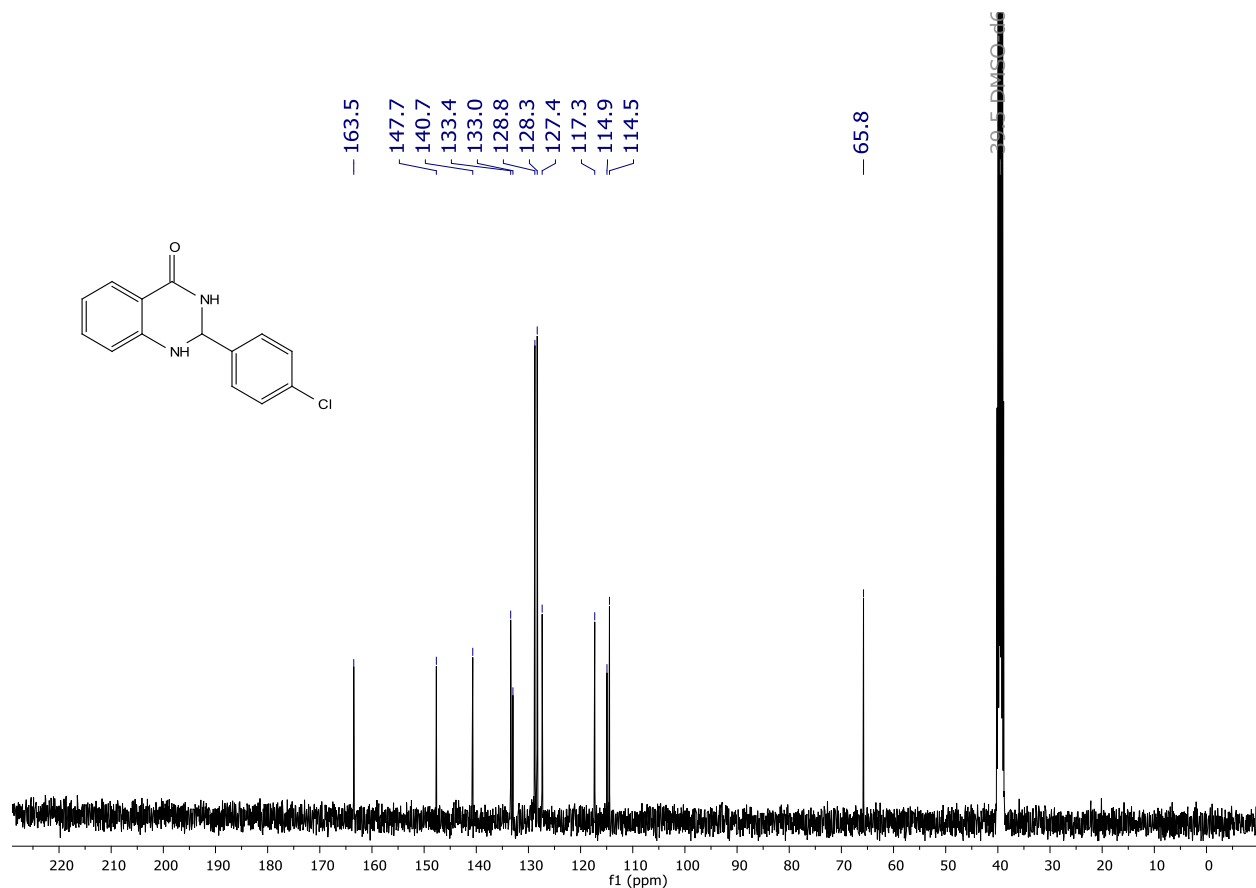




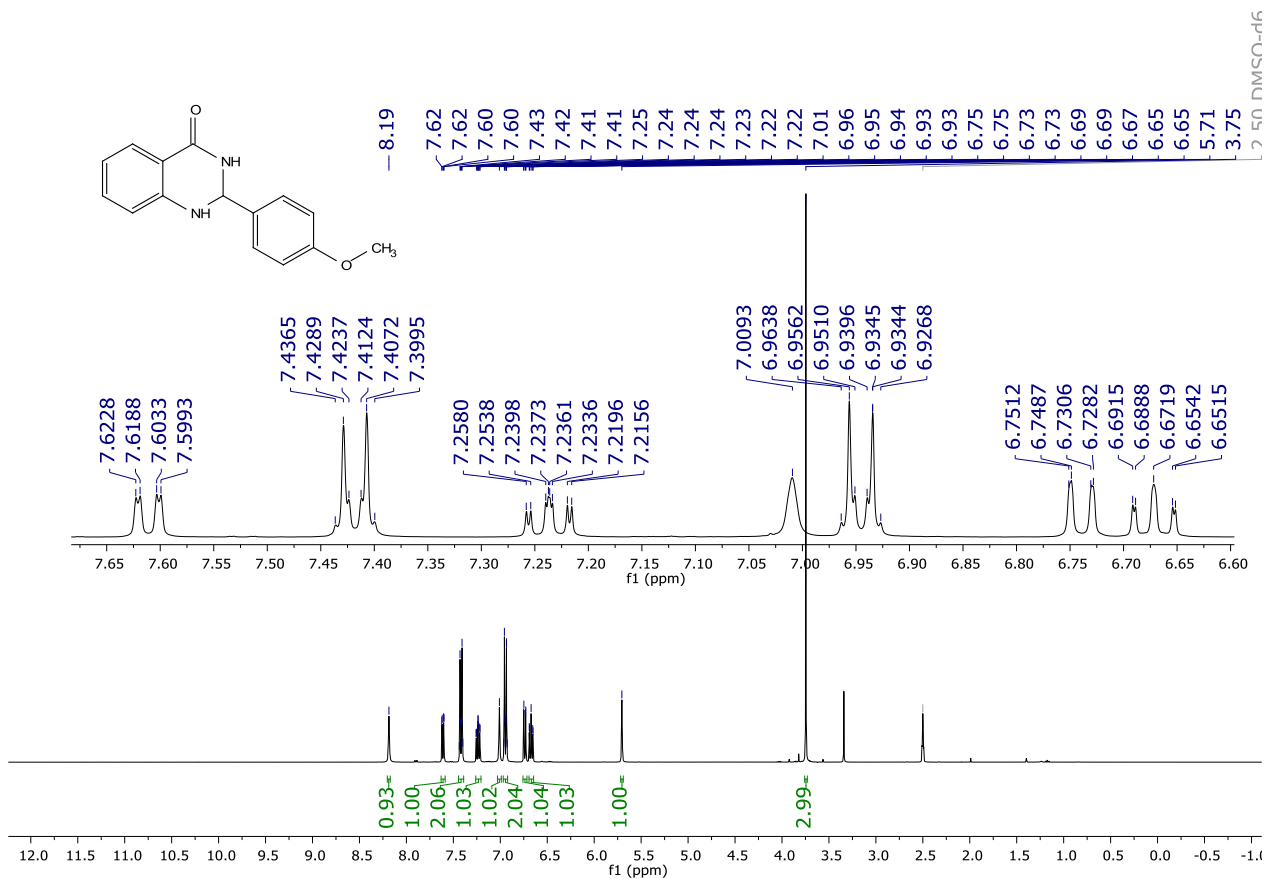
^{19}F NMR (376 MHz, DMSO- d_6) spectrum of **120c**.



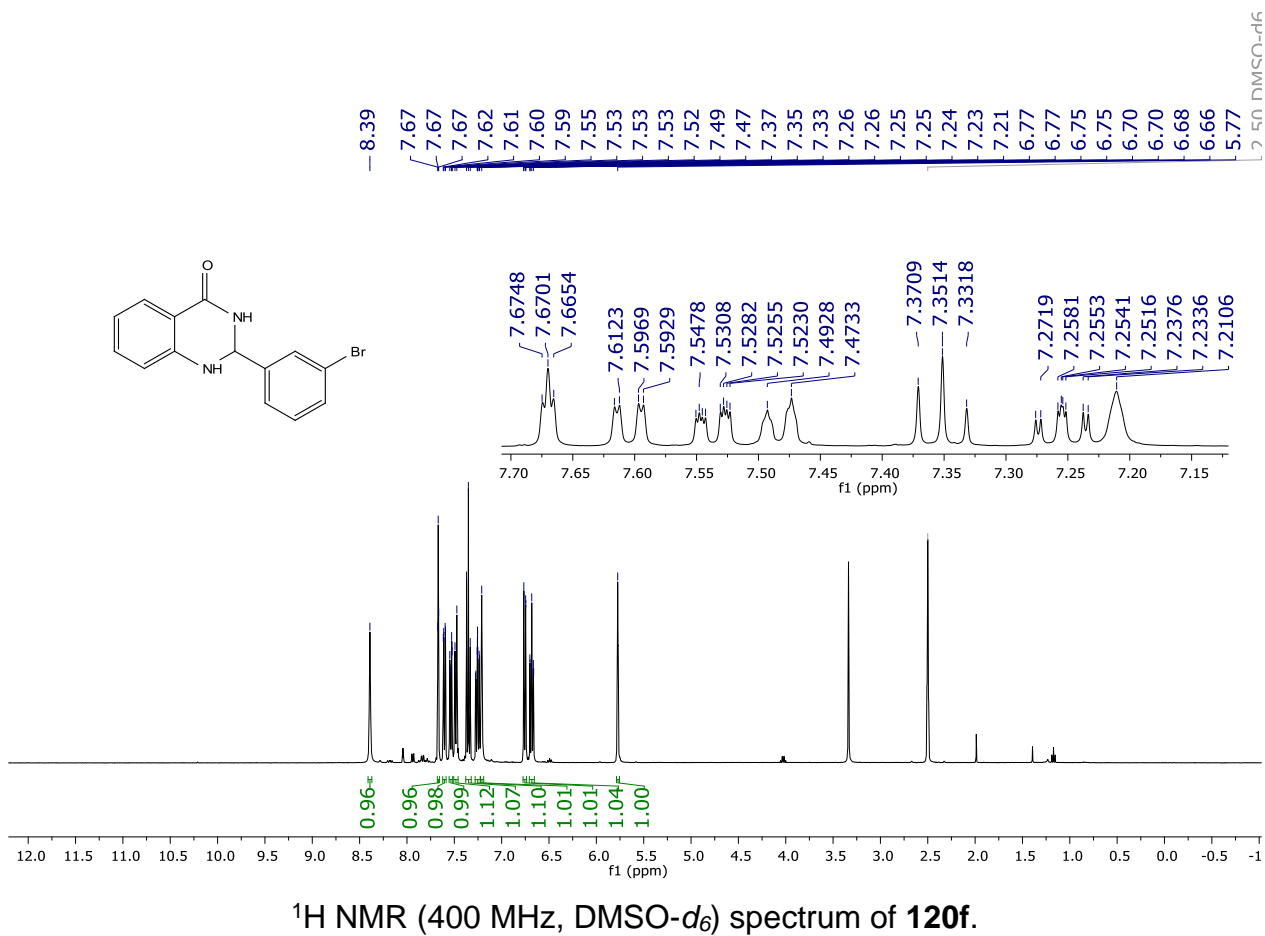
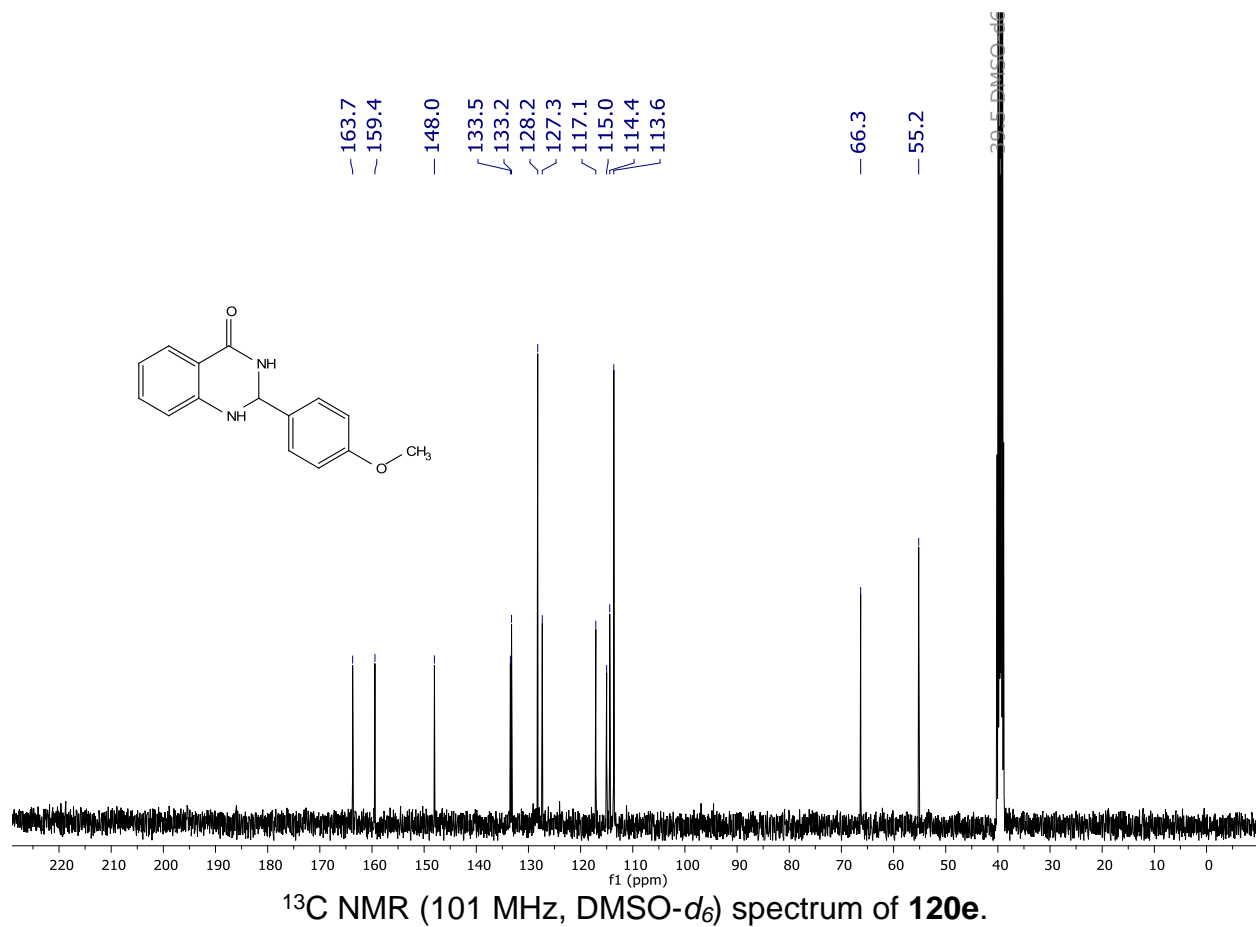
^1H NMR (400 MHz, DMSO- d_6) spectrum of **120d**.

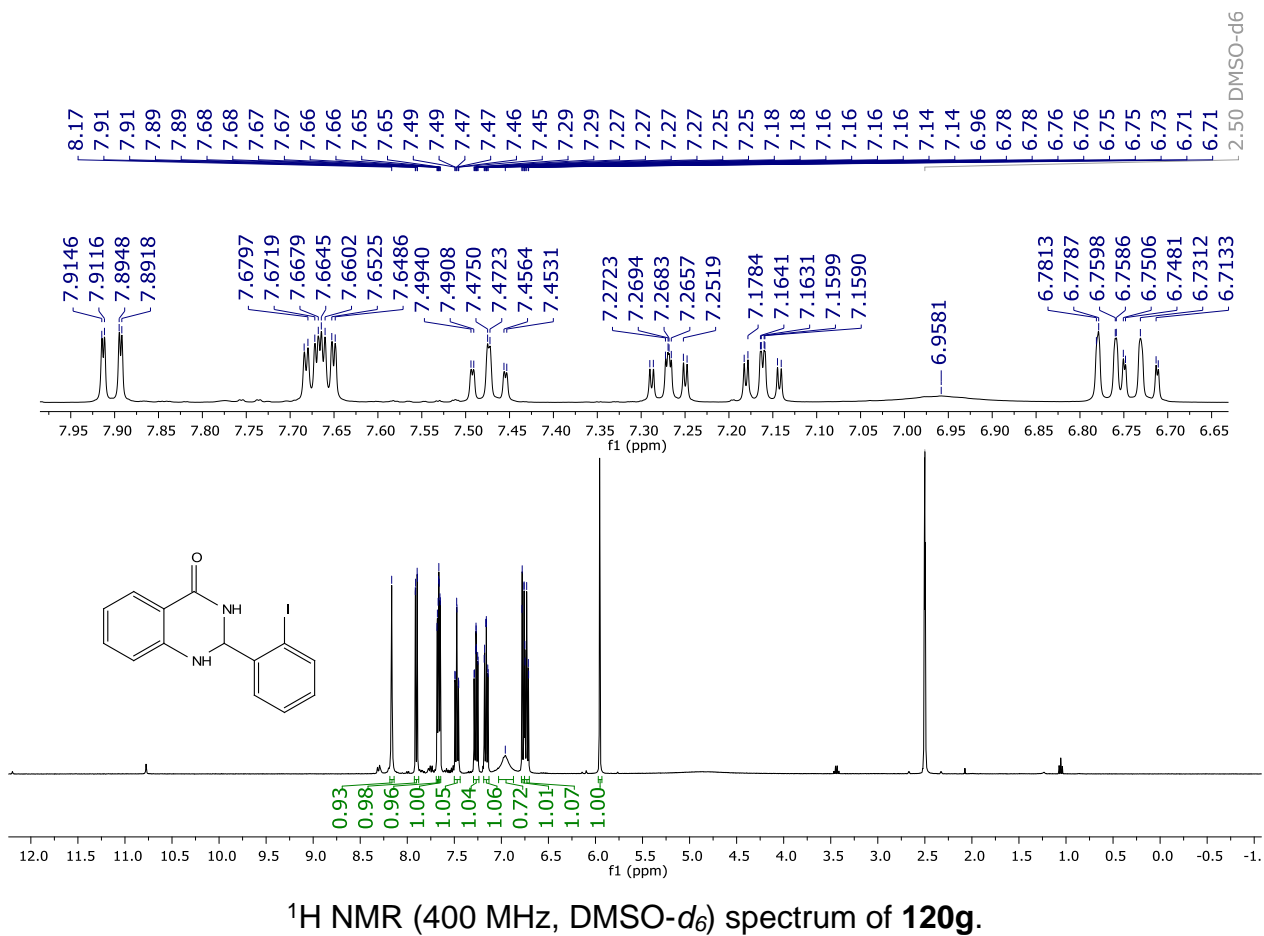
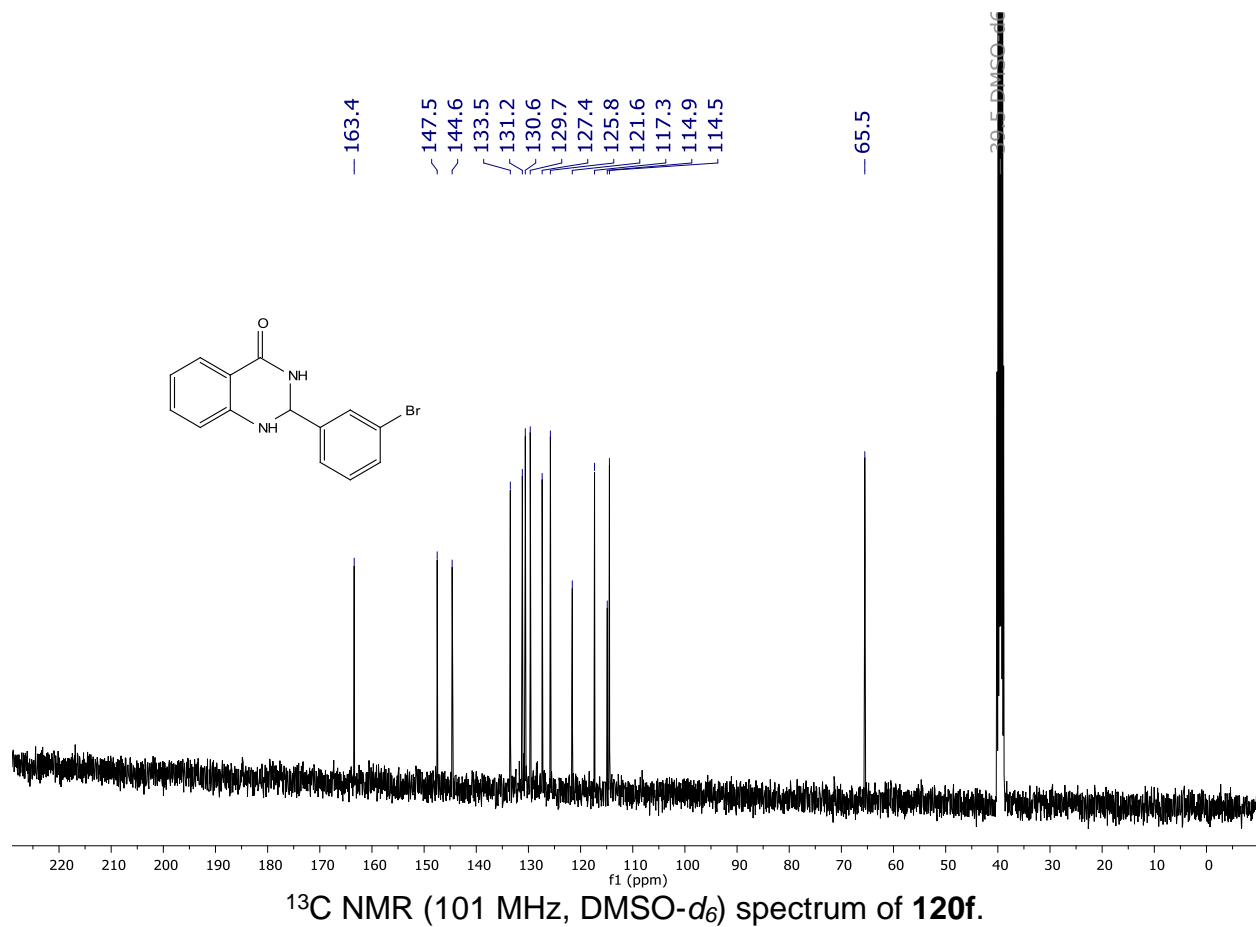


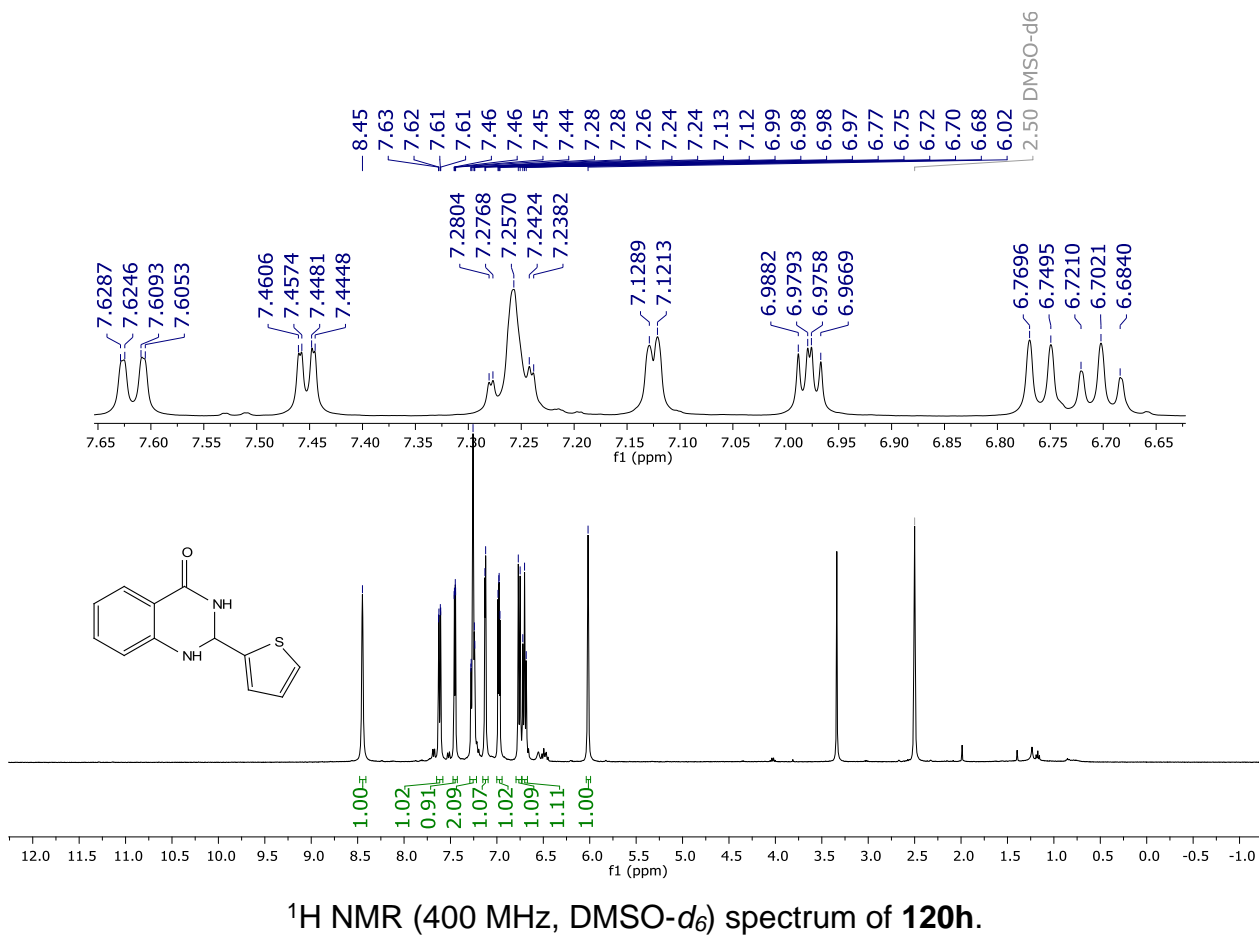
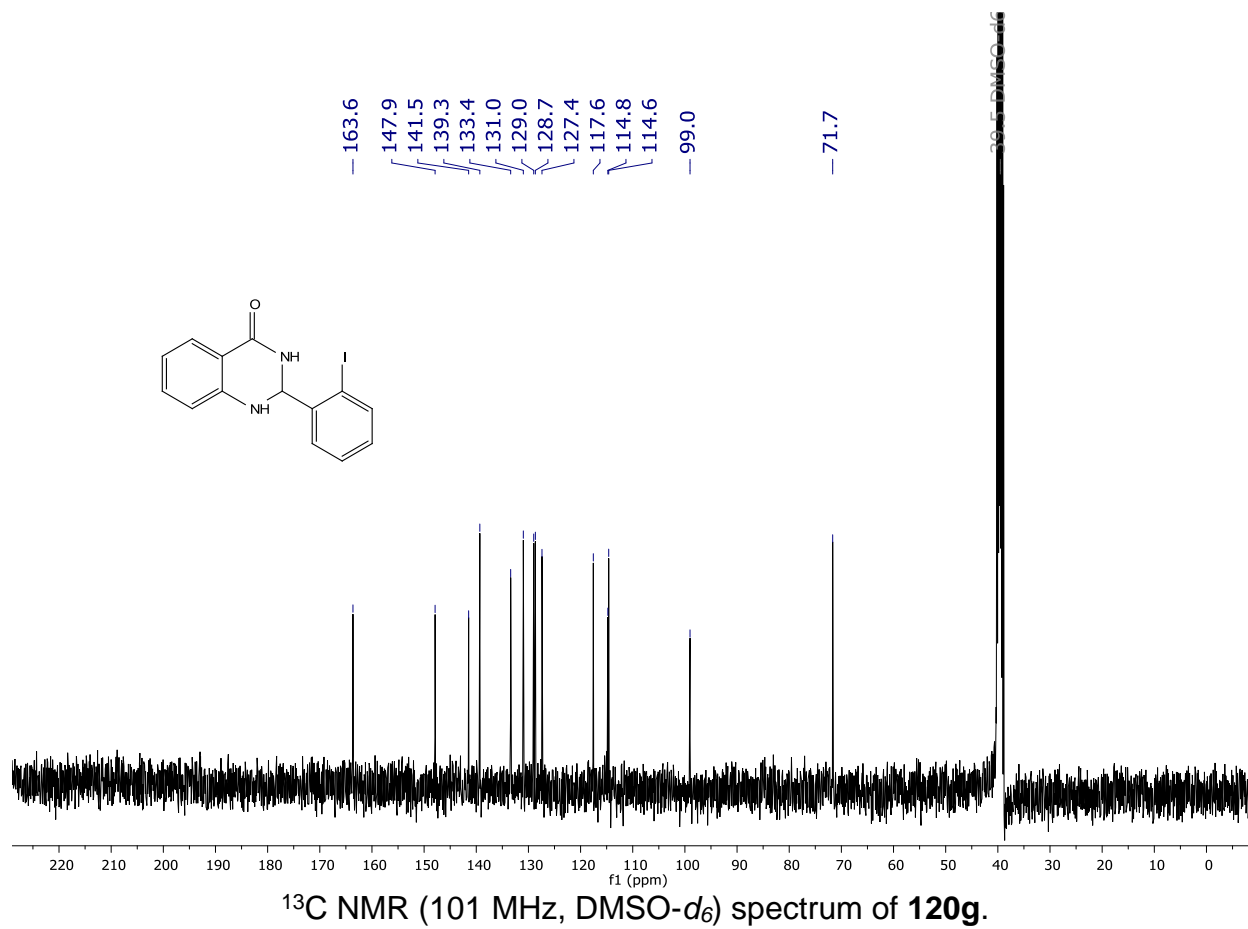
¹³C NMR (101 MHz, DMSO-*d*₆) spectrum of 120d.

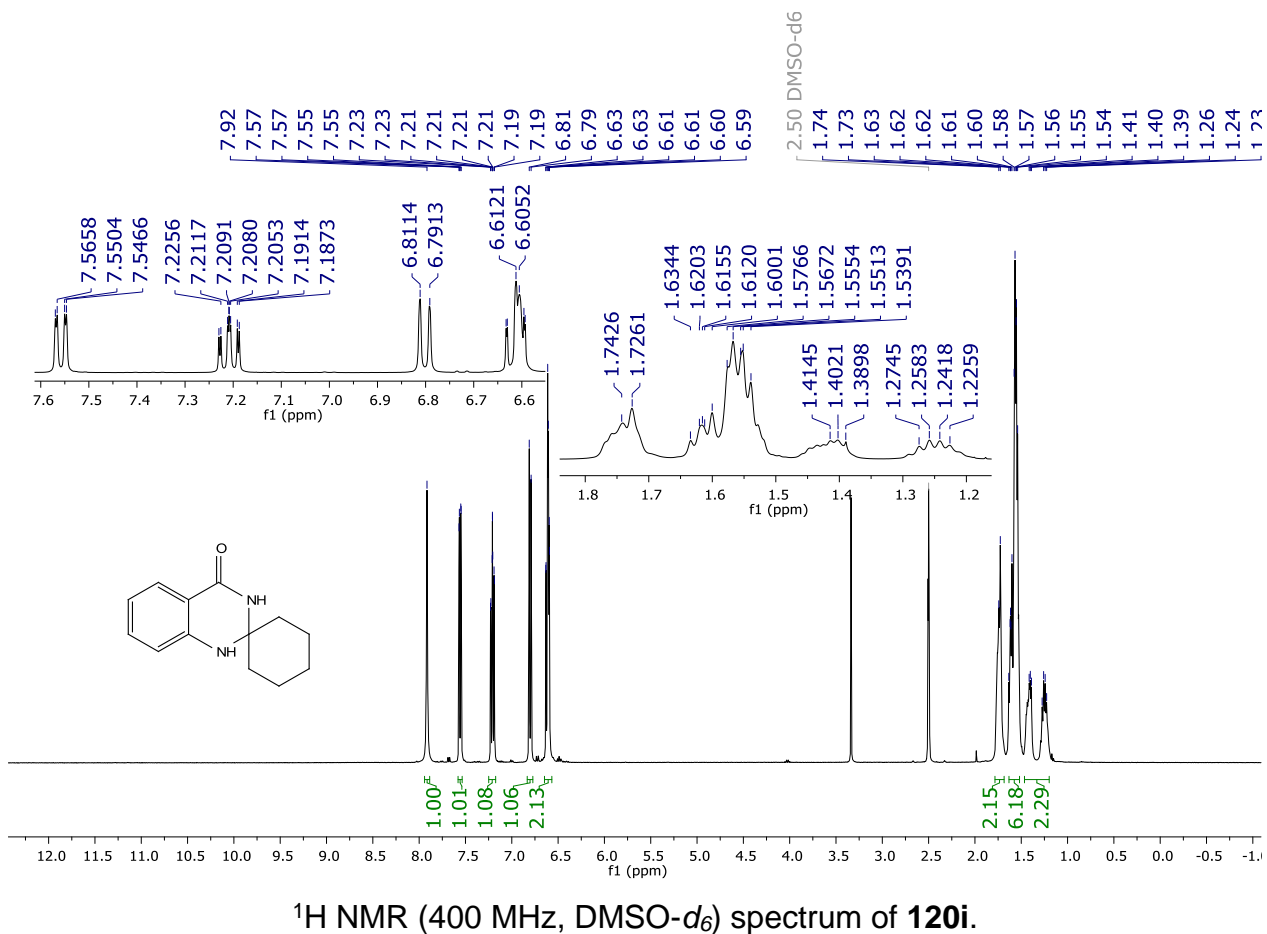
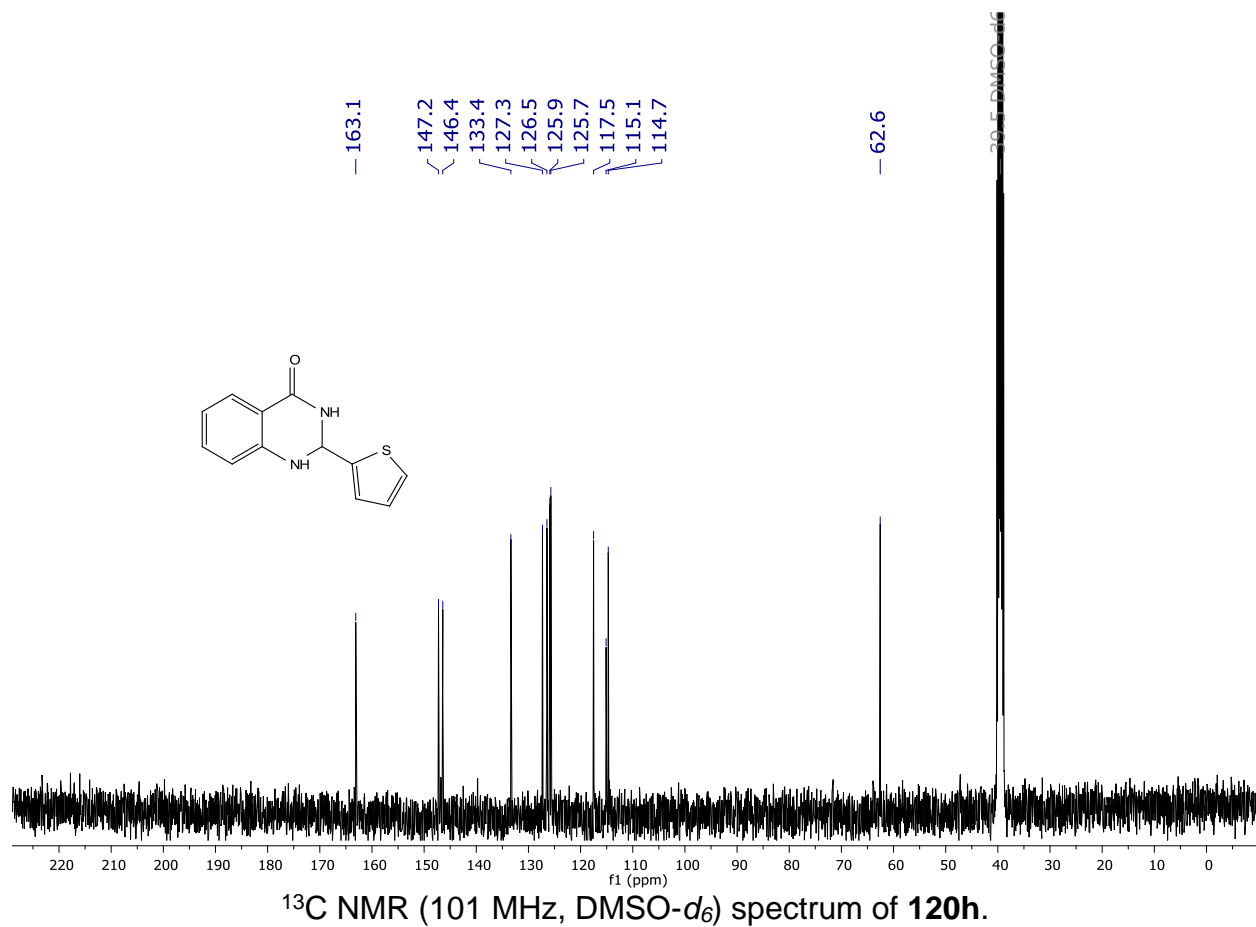


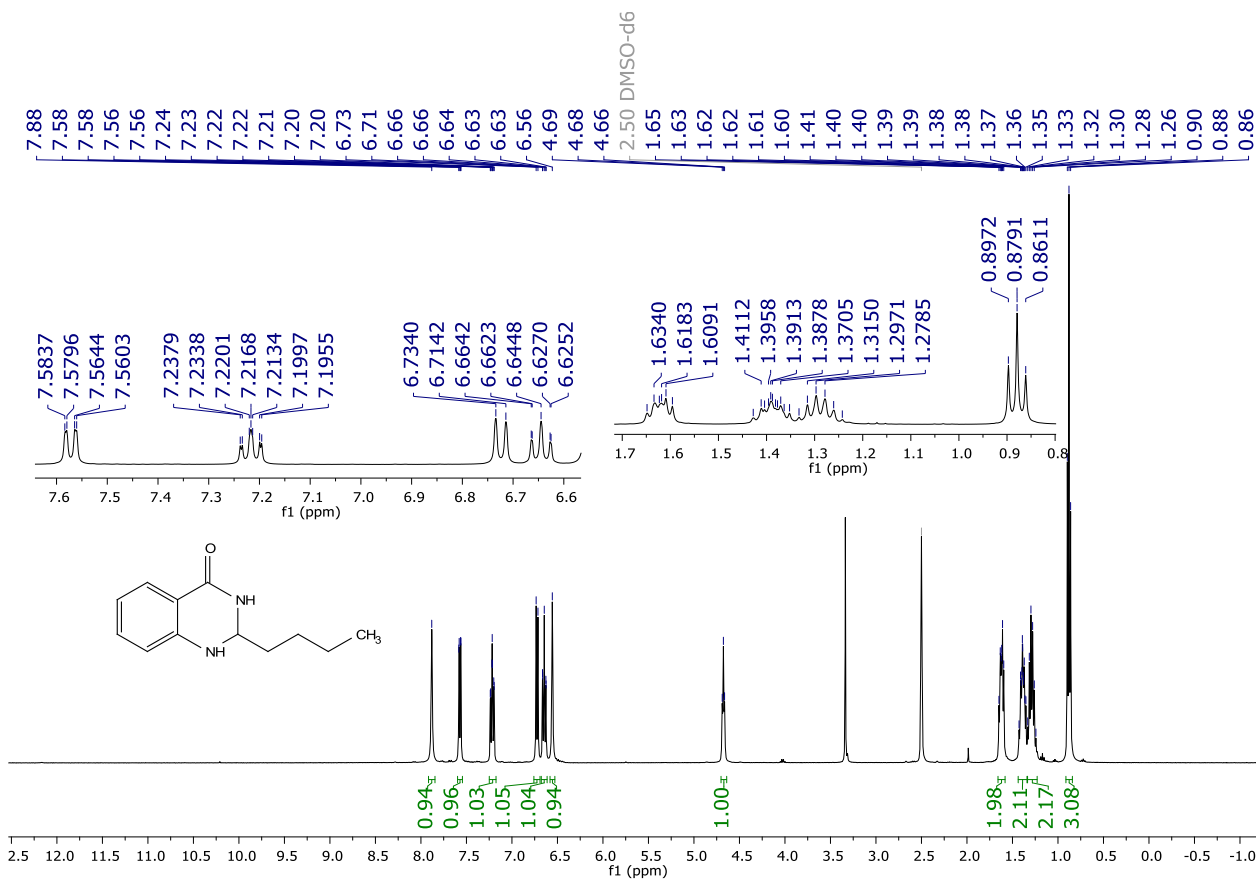
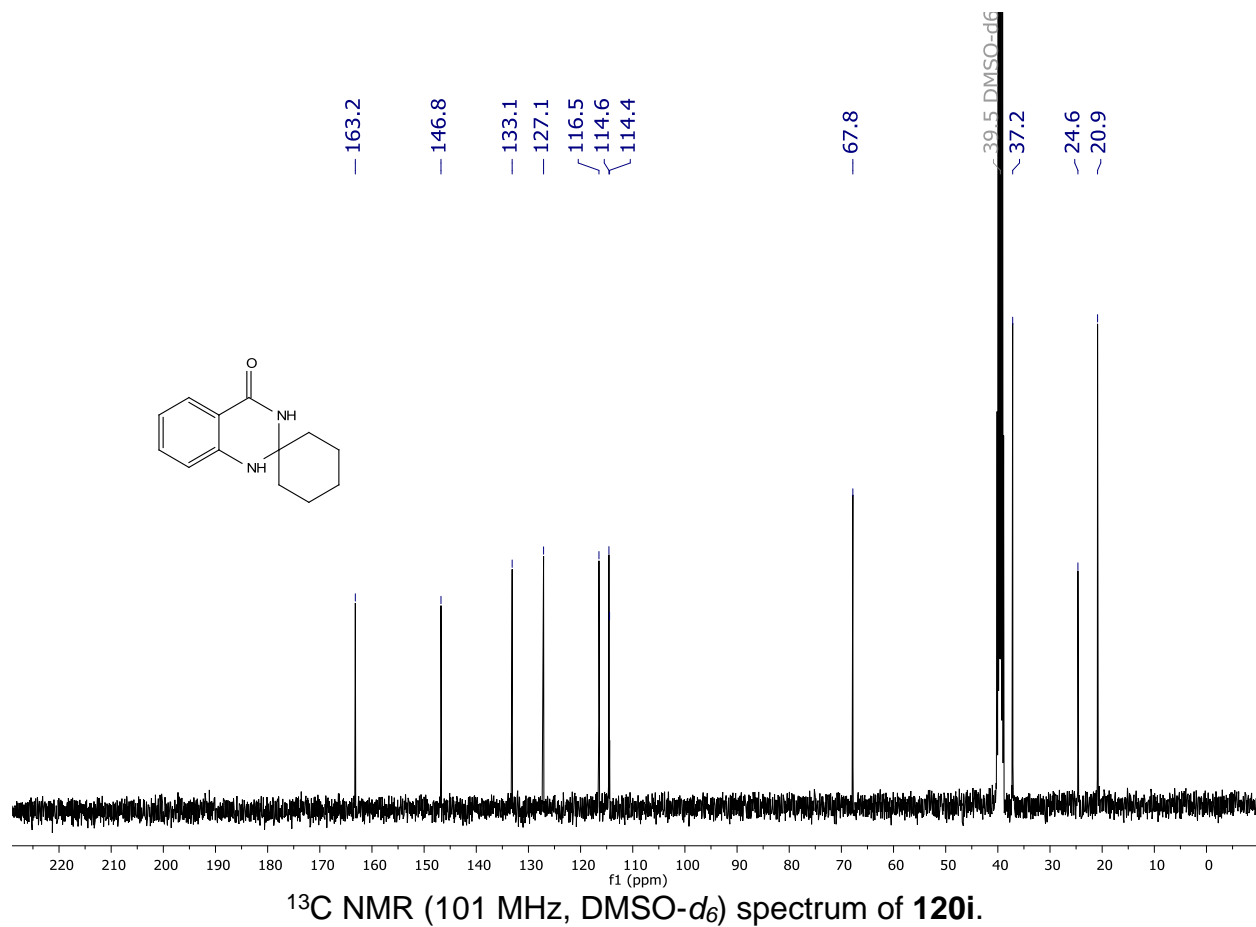
¹H NMR (400 MHz, DMSO-*d*₆) spectrum of 120e.

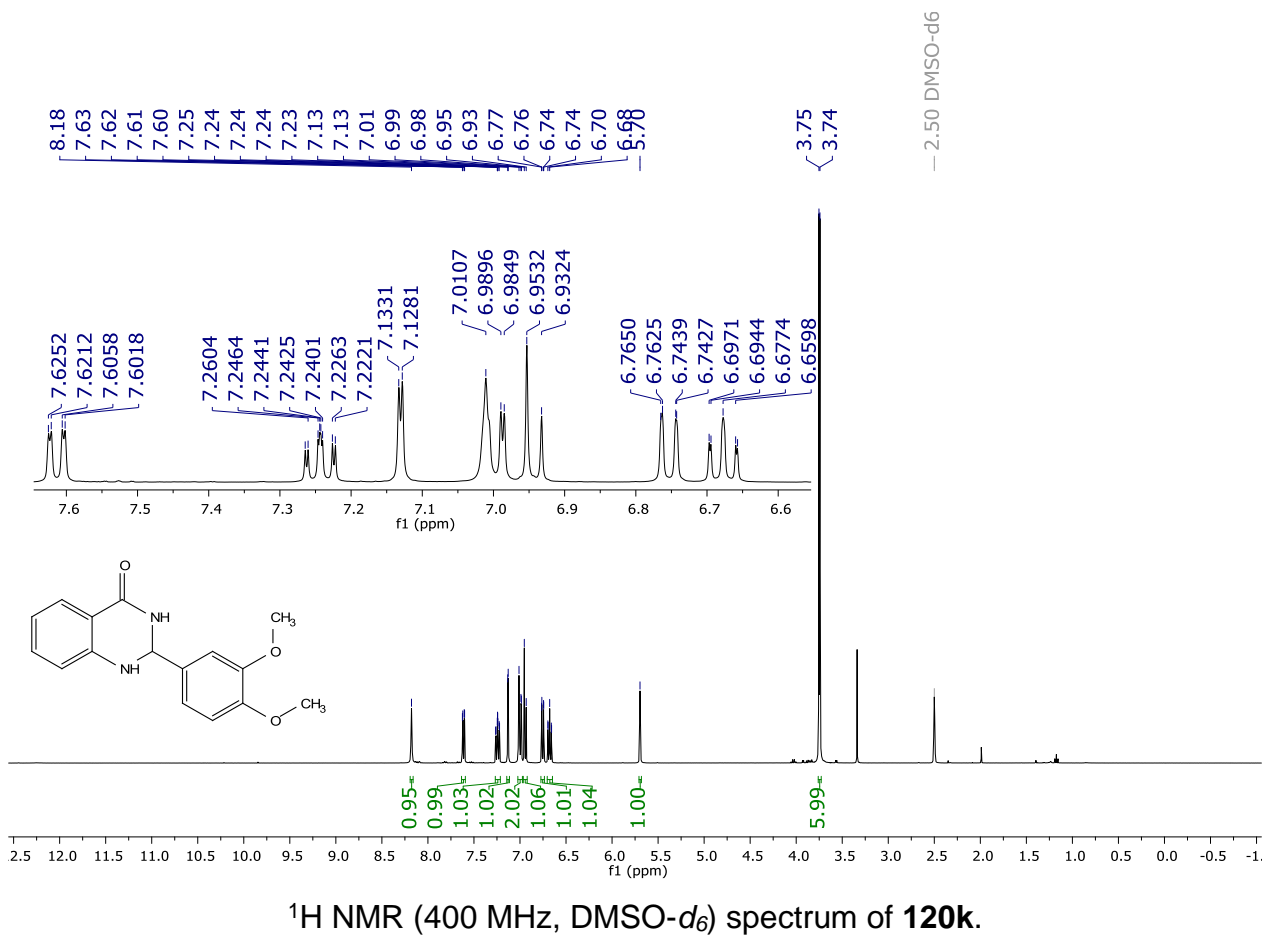
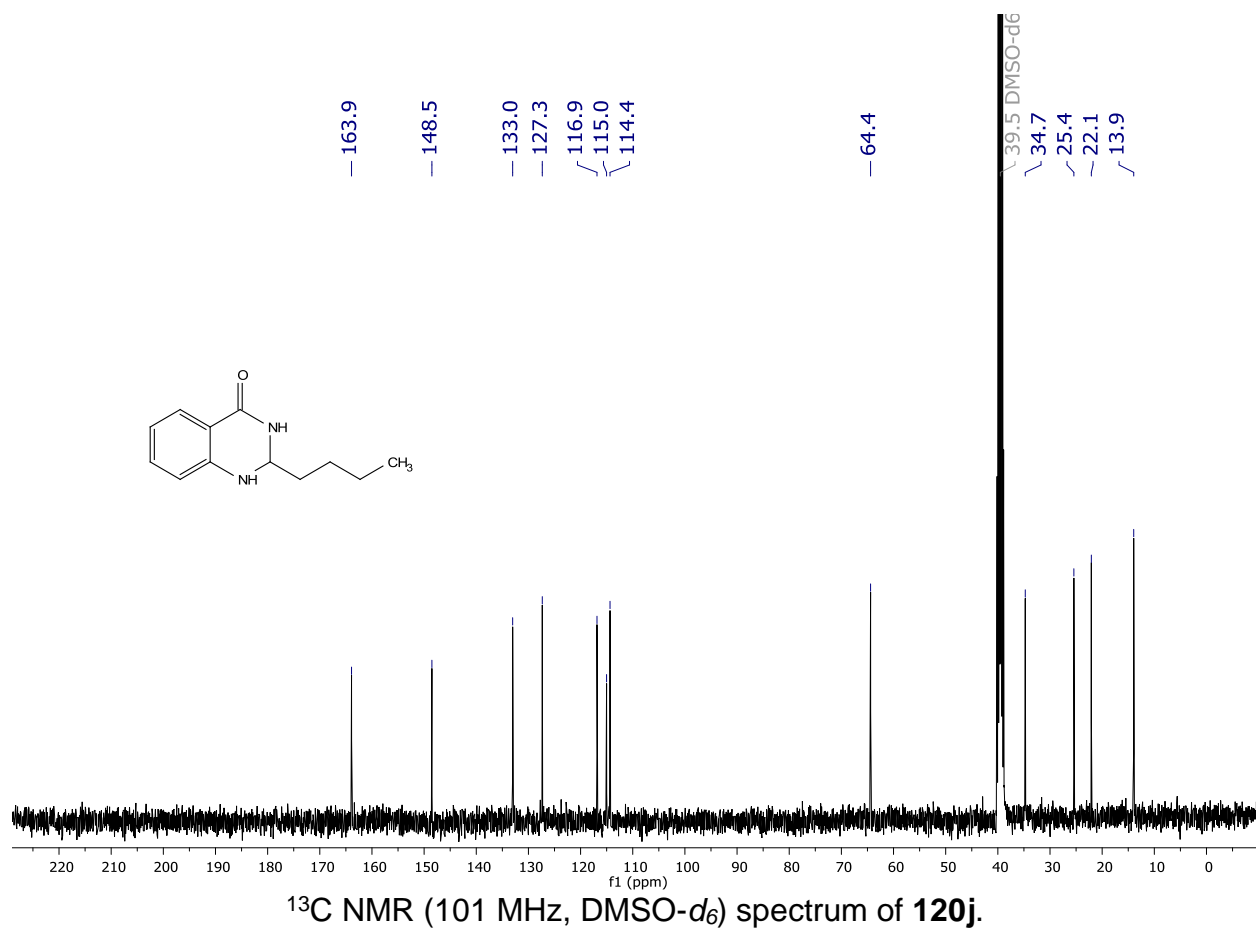


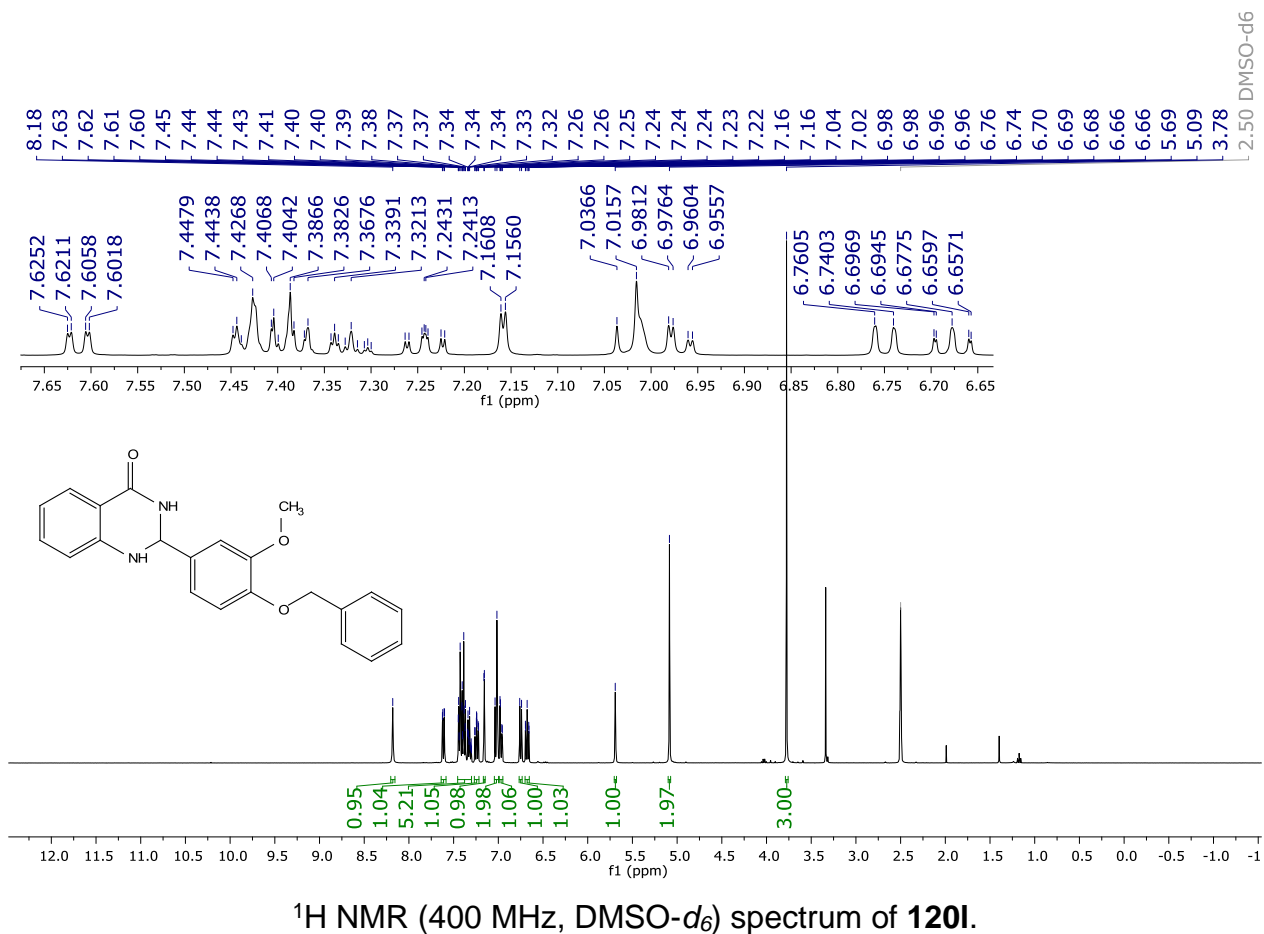
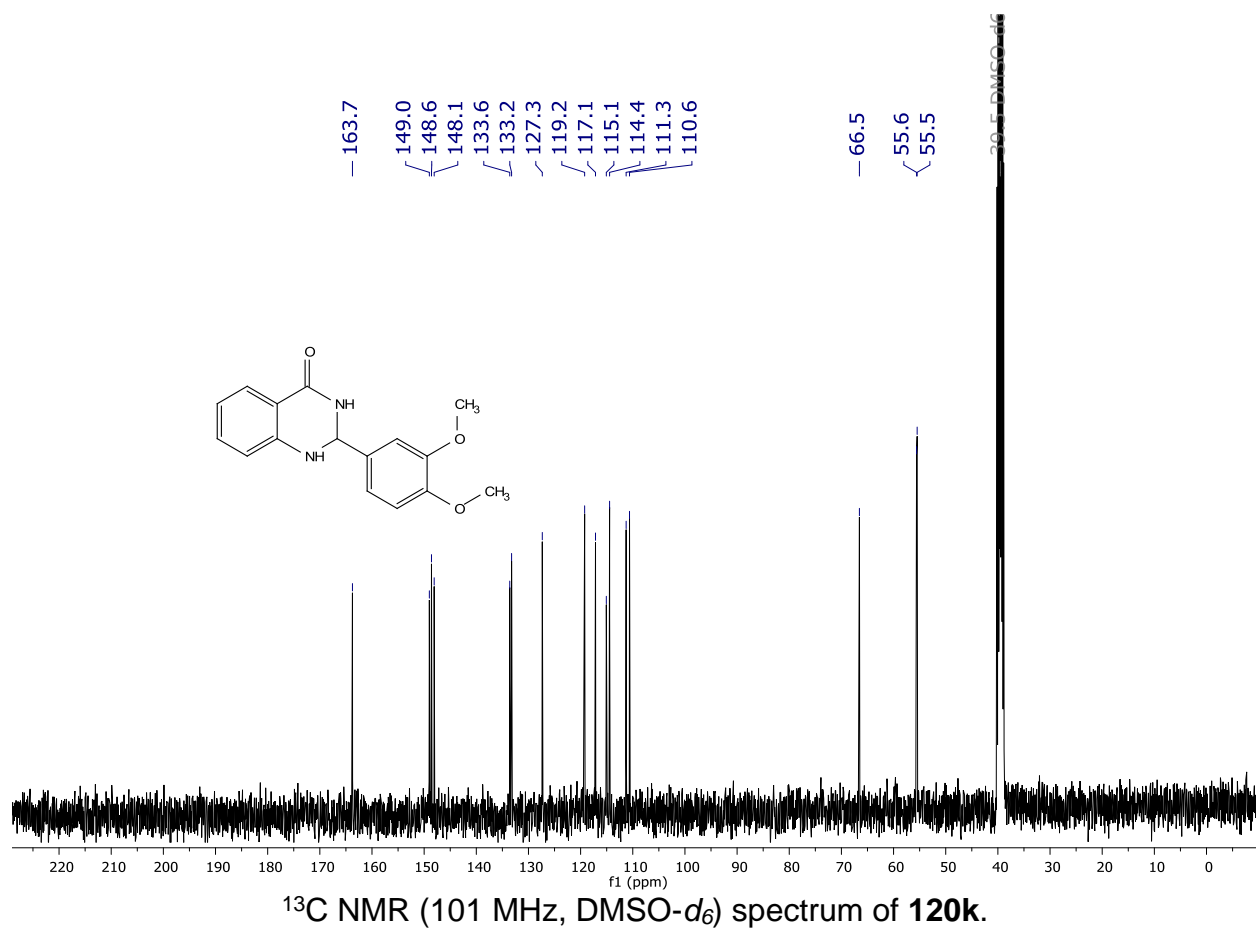


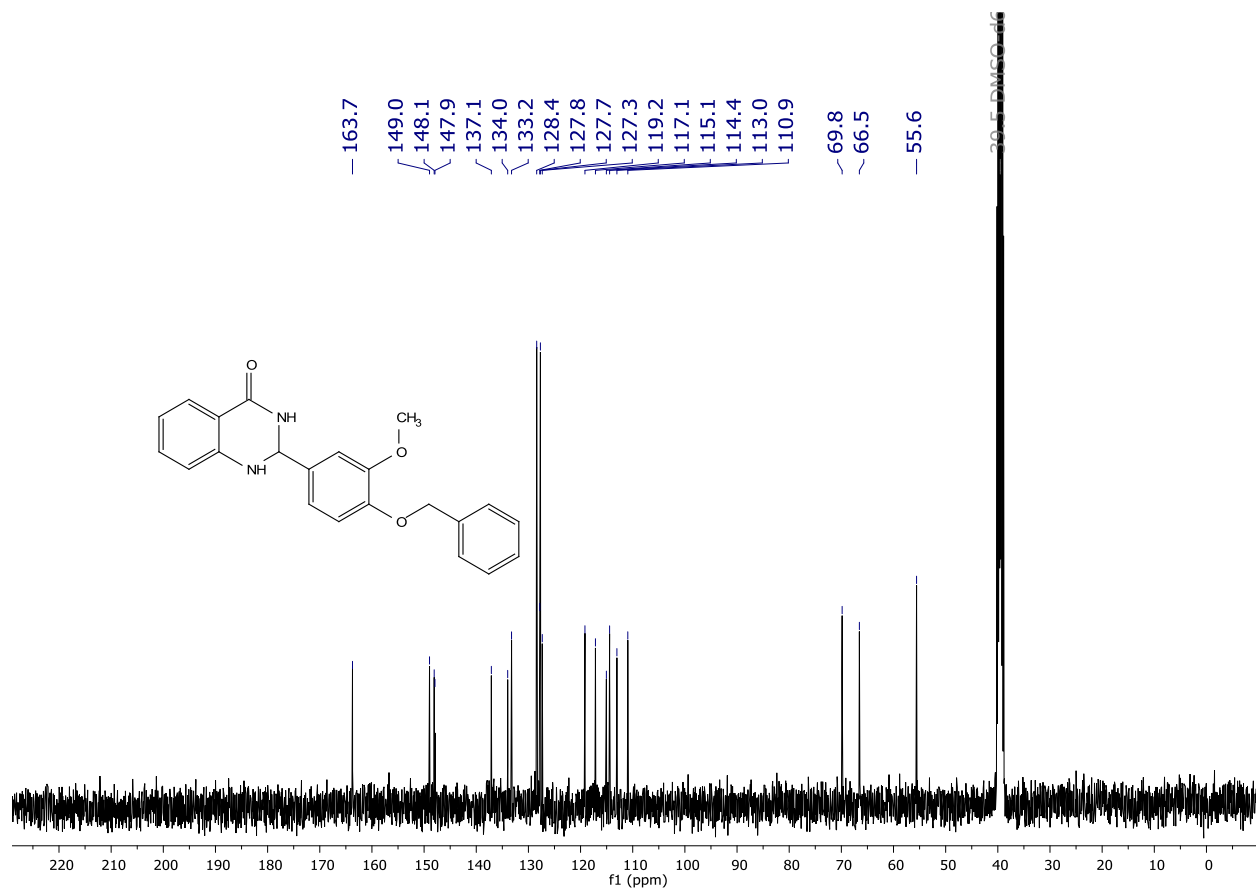




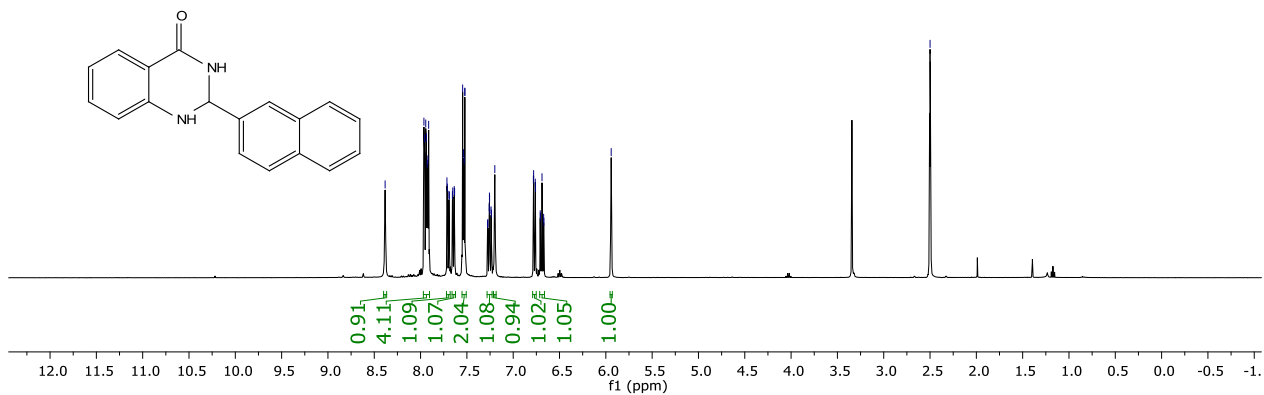
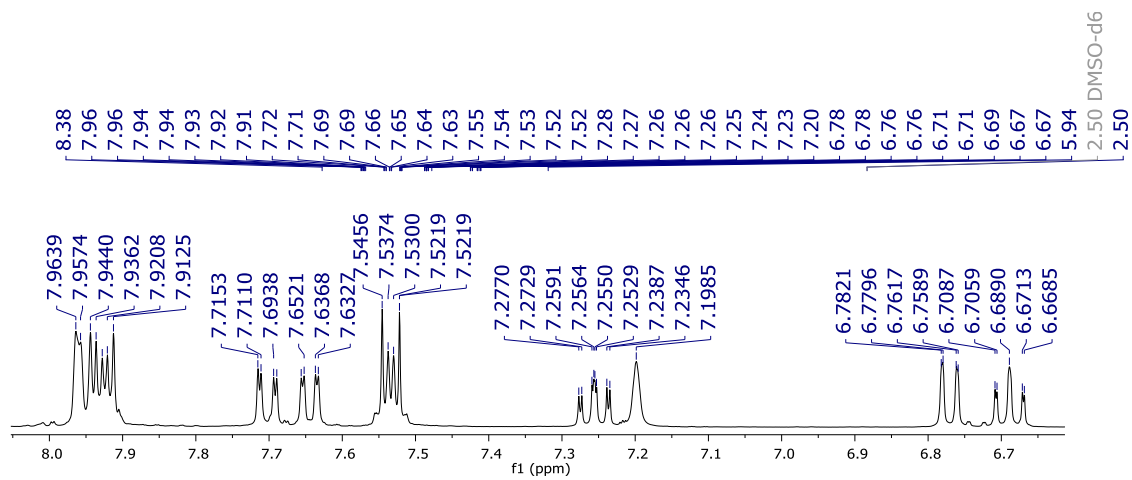








¹³C NMR (101 MHz, DMSO-d₆) spectrum of 120l.



¹H NMR (400 MHz, DMSO-d₆) spectrum of 120m.

